EMERGING INFECTIOUS DISEASES®

CDC Centers for Disease Control and Prevention

Vectorborne Infections

April 2023

Attributed to O Grin (active 1919), *The typhus louse shaking hands with Death*, 1919. Color lithograph, image and border 42.5 in x 28.8 in/100 x 73.2 cm. Wellcome Collection, London, United Kingdom. Permanent link: https://wellcomecollection.org/works/gx47fn2a

EMERGING INFECTIOUS DISEASES®

EDITOR-IN-CHIEF
D. Peter Drotman

ASSOCIATE EDITORS

Charles Ben Beard, Fort Collins, Colorado, USA
Ermias Belay, Atlanta, Georgia, USA
Sharon Bloom, Atlanta, Georgia, USA
Richard Bradbury, Melbourne, Victoria, Australia
Corrie Brown, Athens, Georgia, USA
Benjamin J. Cowling, Hong Kong, China
Michel Drancourt, Marseille, France
Paul V. Effler, Perth, Western Australia, Australia
Anthony Fiore, Atlanta, Georgia, USA
David O. Freedman, Birmingham, Alabama, USA
Isaac Chun-Hai Fung, Statesboro, Georgia, USA
Peter Gerner-Smidt, Atlanta, Georgia, USA
Stephen Hadler, Atlanta, Georgia, USA
Shawn Lockhart, Atlanta, Georgia, USA
Nina Marano, Atlanta, Georgia, USA
Martin I. Meltzer, Atlanta, Georgia, USA
David Morens, Bethesda, Maryland, USA
J. Glenn Morris, Jr., Gainesville, Florida, USA
Patrice Nordmann, Fribourg, Switzerland
Johann D.D. Pitout, Calgary, Alberta, Canada
Ann Powers, Fort Collins, Colorado, USA
Didier Raoult, Marseille, France
Pierre E. Rollin, Atlanta, Georgia, USA
Frederic E. Shaw, Atlanta, Georgia, USA
Neil M. Vora, New York, New York, USA
David H. Walker, Galveston, Texas, USA
J. Scott Weese, Guelph, Ontario, Canada

Deputy Editor-in-Chief
Matthew J. Kuehnert, Westfield, New Jersey, USA

Managing Editor
Byron Breedlove, Atlanta, Georgia, USA

Technical Writer-Editors Shannon O'Connor, Team Lead; Dana Dolan, Thomas Gryczan, Amy Guinn, Tony Pearson-Clarke, Jill Russell, Jude Rutledge, Cheryl Salerno, P. Lynne Stockton, Susan Zunino

Production, Graphics, and Information Technology Staff
Reginald Tucker, Team Lead; William Hale, Barbara Segal, Hu Yang

Journal Administrators J. McLean Boggess, Susan Richardson

Editorial Assistants Letitia Carelock, Alexandria Myrick

Communications/Social Media Sarah Logan Gregory, Team Lead; Heidi Floyd

Associate Editor Emeritus
Charles H. Calisher, Fort Collins, Colorado, USA

Founding Editor
Joseph E. McDade, Rome, Georgia, USA

EDITORIAL BOARD

Barry J. Beaty, Fort Collins, Colorado, USA
David M. Bell, Atlanta, Georgia, USA
Martin J. Blaser, New York, New York, USA
Andrea Boggild, Toronto, Ontario, Canada
Christopher Braden, Atlanta, Georgia, USA
Arturo Casadevall, New York, New York, USA
Kenneth G. Castro, Atlanta, Georgia, USA
Gerardo Chowell, Atlanta, Georgia, USA
Christian Drosten, Berlin, Germany
Clare A. Dykewicz, Atlanta, Georgia, USA
Kathleen Gensheimer, College Park, Maryland, USA
Rachel Gorwitz, Atlanta, Georgia, USA
Duane J. Gubler, Singapore
Scott Halstead, Westwood, Massachusetts, USA
David L. Heymann, London, UK
Keith Klugman, Seattle, Washington, USA
S.K. Lam, Kuala Lumpur, Malaysia
John S. Mackenzie, Perth, Western Australia, Australia
Jennifer H. McQuiston, Atlanta, Georgia, USA
Nkuchia M. M'ikanatha, Harrisburg, Pennsylvania, USA
Frederick A. Murphy, Bethesda, Maryland, USA
Barbara E. Murray, Houston, Texas, USA
Stephen M. Ostroff, Silver Spring, Maryland, USA
W. Clyde Partin, Jr., Atlanta, Georgia, USA
David A. Pegues, Philadelphia, Pennsylvania
Mario Raviglione, Milan, Italy, and Geneva, Switzerland
David Relman, Palo Alto, California, USA
Connie Schmaljohn, Frederick, Maryland, USA
Tom Schwan, Hamilton, Montana, USA
Wun-Ju Shieh, Taipei, Taiwan
Rosemary Soave, New York, New York, USA
Robert Swanepoel, Pretoria, South Africa
David E. Swayne, Athens, Georgia, USA
Kathrine R. Tan, Atlanta, Georgia, USA
Phillip Tarr, St. Louis, Missouri, USA
Duc Vugia, Richmond, California, USA
J. Todd Weber, Atlanta, Georgia, USA
Mary Edythe Wilson, Iowa City, Iowa, USA

Emerging Infectious Diseases is published monthly by the Centers for Disease Control and Prevention, 1600 Clifton Rd NE, Mailstop H16-2, Atlanta, GA 30329-4027, USA. Telephone 404-639-1960; email, eideditor@cdc.gov

The conclusions, findings, and opinions expressed by authors contributing to this journal do not necessarily reflect the official position of the U.S. Department of Health and Human Services, the Public Health Service, the Centers for Disease Control and Prevention, or the authors' affiliated institutions. Use of trade names is for identification only and does not imply endorsement by any of the groups named above.

All material published in *Emerging Infectious Diseases* is in the public domain and may be used and reprinted without special permission; proper citation, however, is required.

Use of trade names is for identification only and does not imply endorsement by the Public Health Service or by the U.S. Department of Health and Human Services.

EMERGING INFECTIOUS DISEASES is a registered service mark of the U.S. Department of Health & Human Services (HHS).

EMERGING INFECTIOUS DISEASES®

Vectorborne Infections **April 2023**

On the Cover

Attributed to O Grin (active 1919), *The typhus louse shaking hands with Death,* 1919. Color lithograph, image and border 42.5 in x 28.8 in/100 x 73.2 cm. Wellcome Collection, London, United Kingdom. Permanent link: https://wellcomecollection.org/works/gx47fn2a

About the Cover p. 871

Perspective

Synopses

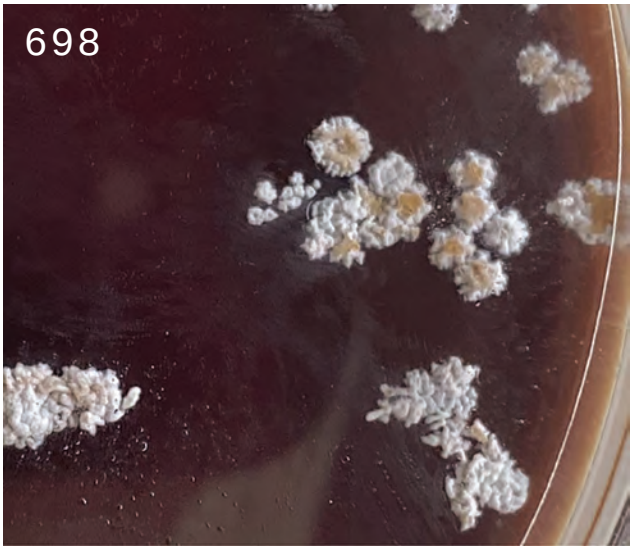

EMERGING INFECTIOUS DISEASES®
April 2023

Research

Dispatches

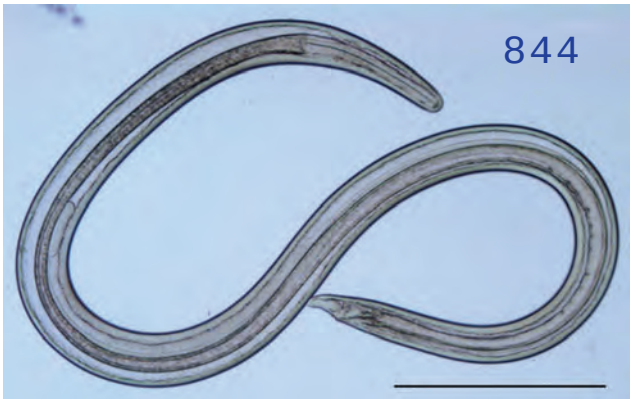

EMERGING INFECTIOUS DISEASES®
April 2023

Research Letters

Books and Media

About the Cover

Etymologia

Online Report

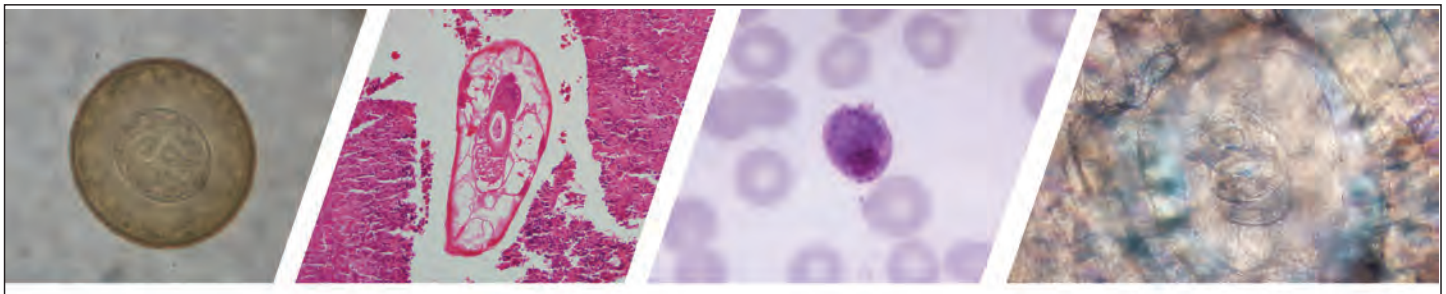

DPDx

Diagnostic Assistance and Training in Laboratory Identification of Parasites

A free service of CDC available to laboratorians, pathologists, and other health professionals in the United States and abroad

- Diagnosis from photographs of worms, histological sections, fecal, blood, and other specimen types
- Expert diagnostic review
- Formal diagnostic laboratory report
- Submission of samples via secure file share

Visit the DPDx website for information on laboratory diagnosis, geographic distribution, clinical features, parasite life cycles, and training via Monthly Case Studies of parasitic diseases.

www.cdc.gov/dpdx
dpdx@cdc.gov

U.S. Department of Health and Human Services
Centers for Disease Control and Prevention

CS272346-DE

Challenges in Forecasting Antimicrobial Resistance

Sen Pei, Seth Blumberg, Jaime Cascante Vega, Tal Robin, Yue Zhang, Richard J. Medford, Bijaya Adhikari, Jeffrey Shaman, for the CDC MIND-Healthcare Program

Antimicrobial resistance is a major threat to human health. Since the 2000s, computational tools for predicting infectious diseases have been greatly advanced; however, efforts to develop real-time forecasting models for antimicrobial-resistant organisms (AMROs) have been absent. In this perspective, we discuss the utility of AMRO forecasting at different scales, highlight the challenges in this field, and suggest future research priorities. We also discuss challenges in scientific understanding, access to high-quality data, model calibration, and implementation and evaluation of forecasting models. We further highlight the need to initiate research on AMRO forecasting using currently available data and resources to galvanize the research community and address initial practical questions.

Antimicrobial resistance (AMR) is a leading threat to global health (*1*). An estimated 4.95 million deaths were associated with bacterial AMR in 2019 worldwide (*2*), mostly caused by 6 pathogens: *Escherichia coli*, *Staphylococcus aureus*, *Klebsiella pneumoniae*, *Streptococcus pneumoniae*, *Acinetobacter baumannii*, and *Pseudomonas aeruginosa*. To limit the spread of antimicrobial-resistant organisms (AMROs) and reduce AMR-related disease burden, improved predictive intelligence is required to better estimate the emergence and spread of AMR within populations and healthcare facilities. However, efforts to operationally forecast the burden of AMROs (i.e., for real settings in real time) are not active as of January 2023.

Author affiliations: Columbia University, New York, New York, USA (S. Pei, J. Cascante Vega, T. Robin, J. Shaman); University of California, San Francisco, California, USA (S. Blumberg); University of Utah, Salt Lake City, Utah, USA (Y. Zhang); University of Texas Southwestern Medical Center, Dallas, Texas, USA (R.J. Medford); University of Iowa, Iowa City, Iowa, USA (B. Adhikari)

DOI: https://doi.org/10.3201/eid2904.221552

Real-time infectious disease forecasting aims to generate estimations of future disease incidence at the population or community level, which can be subsequently evaluated using the observed outcomes. During 2010–2020, predictive models for viral and acute infectious diseases such as influenza (*3*), dengue (*4*), and COVID-19 (*5*) have been put in place and tested in the real world. In contrast, no predictions have been generated and validated for AMROs. Here, we discuss the potential for AMRO forecasting at the population and facility scales, highlight challenges for this field, and suggest future research priorities.

Mathematical Modeling of AMR

Mathematical and statistical models have contributed to the fight against AMR (*6*) and may enable predictions of AMR at different scales. Modeling studies of AMROs have been undertaken to clarify the factors associated with AMR at the population scale. For example, time series analyses have been used to quantify the association between antimicrobial use and prevalence of resistance in populations (*7*,*8*). Such analyses are valuable because they typically result in a set of coefficients representing the effect of antimicrobial use on future AMR outcomes; however, those models do not project AMR prevalence forward and rigorously evaluate future predictive accuracy. In parallel, process-based mathematical models have been developed to study the transmission of AMROs (*9*–*11*), simulate the competition between resistant and sensitive strains (*12*–*16*), and evaluate the effects of various policies (*17*–*22*). More recently, detailed individual-level models informed by historical patient movement or contact with healthcare workers have been used to represent transmission networks and heterogeneity in healthcare facilities (*23*–*26*). Those modeling studies have enriched understanding of the evolutionary dynamics of resistance and AMRO transmission dynamics but have not been used to produce operational AMR predictions.

Forecasting AMROs at Different Scales

Operational forecasting of AMR could have implications for public health and patient care. Depending on the intended use, AMRO forecasting can be done at population-level and facility-level scales. Forecasting at the population level aims to predict the trend of infection or carriage prevalence in the general population for relatively long periods of months to years. For AMR pathogens, the forecast target might be the number of AMR infections or the proportion of isolates exhibiting resistance. Those predictions would estimate future AMR burden (e.g., deaths, hospitalization, days of work lost, or direct and indirect economic costs) and the evolution of resistance. If used in real time, those predictions would support situational awareness and inform public health policies such as antimicrobial drug stewardship and more targeted antimicrobial prescription guidelines to slow down AMR spread.

At the facility level, the forecast target of interest might be the number of AMR infections with clinical symptoms within a hospital or hospital system. Such predictions would support control of nosocomial AMRO transmission and resource planning for equipment, medications, staffing, and space in response to potential patient surges. Depending on the clinical relevance, the forecast horizon might be days or months. Of note, predictive models connecting multiple healthcare facilities in a region could elucidate the risk for AMR introduction through interhospital patient transfer and support decision making for preemptive measures in facilities without ongoing transmission.

Challenges in AMRO Forecasting

Although models and data differ considerably for forecasts at various scales, some common challenges impede the development and operational use of predictive models for AMR. Here we summarize these issues and highlight several research priorities to address these challenges in future studies.

Scientific Understanding

For forecasting using mathematical and statistical models, it is critical to understand the key processes affecting AMR spread. Those processes are often represented as nonlinear effects in forecasting models and, if not properly specified, will produce forecasts that quickly diverge from the truth. As of 2023, many questions on AMR remain open (*27*). For instance, the role of antibiotic use in driving AMR is not fully understood, particularly the effects of coselection (i.e., selection of resistance that is broader than the specific target of an antimicrobial prescription) (*28*) and the relationship between outpatient use of antimicrobial drugs and resistant infections of hospitalized patients. More generally, it is not yet known which type of antimicrobial drug use (e.g., community use, hospital use, or veterinary use) has the greatest effect on AMR emergence (*29*). After the emergence of AMROs, it is unclear how competition with susceptible strains affects the incidence of resistant strains and how to explain their coexistence over long time periods (*30*). Likewise, the issue of spillover (i.e., transmission of AMR across locations) is arguably a substantial challenge for forecasting that has not been addressed (*31*).

In healthcare facilities, it is unknown how contact networks and heterogeneity of exposure to antibiotics shape the spread of AMR; it is hard to disentangle the roles of community importation and nosocomial transmission; and it is difficult to quantify the relative transmissibility among classes of persons (patients, healthcare workers) and the environment. In addition, individual-level causal relationships between the type and duration of therapy and resistance emergence remain unknown in most instances. The human microbiome serves as a reservoir of antimicrobial resistance (*32*–*34*); however, many outstanding scientific questions on microbiome effects are still under active research as of January 2023. Further studies are needed to examine the role of bystander selection (i.e., selection of resistance on microbes that are not the target pathogen) in AMR emergence (*35*,*36*), the reason treatment with cephalosporins is a risk factor for vancomycin-resistant *Enterococcus* colonization (*37*), and the difference between detectable colonization and high-level colonization.

To date, infectious disease forecasting has primarily focused on acute viral infections for which the pathogen and its disease or clinical outcome can be directly linked. For instance, viral load is generally correlated with infectivity and disease phenotype (mild to severe) and, therefore, with illness and death rates. Those correlations make definition of the forecasting target (e.g., incident rates of cases, hospital admissions, or deaths) relatively straightforward. However, for bacterial or fungal species, relationships between pathogen load and clinical outcomes are unclear. Because many bacterial species are commensal with their human host and have varying probabilities of presence across body sites, it is challenging to definitively determine whether a person is colonized. Without accurate observation of colonization, AMR burden is not well resolved and, consequentially, is more difficult to forecast.

Accessing High-Quality Data

Forecasting is fundamentally a data-driven task. Without sufficient data, predictive models cannot be properly trained and evaluated. As of 2023, data that can inform operationally useful forecasts of AMR remain scarce. At the population level, several surveillance systems do exist. For instance, the US National Antimicrobial Resistance Monitoring System for Enteric Bacteria tracks changes in antimicrobial susceptibility for certain enteric bacteria in ill persons, retail meats, and food animals (*38*). However, consistent long-term records of AMR pathogen profiles are lacking in most countries, particularly in low- and middle-income countries and for emerging AMROs with limited cases (*39*). In addition, several major pathogens responsible for healthcare-associated infections have not been included in surveillance.

At the facility level, AMR data from EHR have become increasingly available to researchers in recent years. In healthcare settings, more attention has been given to infected patients with clinical manifestations. Surveillance for asymptomatic AMRO carriage is not prioritized because it is not of immediate clinical interest, although such carriers play an important role in onward transmission (*20*). Such incomplete observation hinders estimation of overall AMRO prevalence and may lead to biased prediction targets. In addition, data on nonbiologic processes driving AMR pathogen transmission, such as patient behavior and interactions with healthcare workers, are difficult to collect. In cases for which relevant data are available, data quality may be poor because records can include errors and misclassification. Even for structured EHR data, both predictive variables and outcomes (e.g., colonization) can suffer from missing data.

Model Calibration

Model calibration is the process by which a mathematical model is tuned to reproduce empirical observations. Although this process does not guarantee accurate prediction, model calibration provides an initial check that the model can closely replicate historical data. Studies that calibrate AMR models to empirical data have been published (*23*,*24*,*40*–*42*). However, as the structure of AMR models becomes increasingly complex, computational difficulties arise in fitting these models to observations of different types and at various scales. For instance, population-level prevalence, individual-level test results, and genomic sequences of pathogens convey different pieces of information on AMRO transmission, and calibrating AMR models to these observations simultaneously is a challenge. AMRO transmission is intrinsically stochastic with large uncertainty. Quantifying the uncertainty of predictions generated by complex AMR models is difficult, especially for models that track individual persons and their contacts. Calibration approaches, and their success, usually depend on the specific model construct and the form of observations.

Implementation and Evaluation

One prominent challenge for AMRO forecasting is the operational implementation and prospective evaluation of predictive models (i.e., generating forecasts in real time and evaluating those forecasts once prediction targets are observed). There are no guidelines on such implementation for AMRO forecasting, such as appropriate data collection and forecast targets. Questions remain open on the proper time scale of forecast horizon, the frequency at which models need to be updated, and the fundamental limit of predictability of models. For long-lead forecasting, evaluation requires data collection in a consistent manner over a long time period. In healthcare facilities, the practice of testing and reporting AMR infections may change over time, which further complicates using such data records and forecast evaluation. A collaborative effort that standardizes training datasets, forecast targets, forecast horizons, and proper scoring rules for evaluating forecast performance (e.g., the FluSight influenza forecasting challenge [*43*–*45*], the dengue forecasting challenge [*4*], and the RAPIDD Ebola forecasting challenge [*46*] can potentially stimulate advances in operational AMR forecasting.

A particular challenge for implementing AMRO forecasting is to handle uncertainty in predictions; uncertainty exists because of imperfect data and a notable degree of variability in many AMR-related processes. Quantifying such uncertainty is critical in other predictive fields, such as numerical weather prediction. For AMROs, whether at the facility level (e.g., determining which patients need to be on contact precautions) or the community level (e.g., public health officials making recommendations for prescribing guidelines because of AMR), decision makers must make decisions that leverage uncertain information. This truism holds for observations as well as forecasts. Designing optimal decision frameworks and architectures that best use forecasts, given their uncertainty, is a needed long-term goal.

Effective communications between modelers and stakeholders such as public health officials, healthcare institutions, and individual practitioners are critical to learn their practical needs from AMR modeling. However, formal reports recording such

communications are lacking in scientific journals, which is another factor limiting the generation and use of operational forecasts in real-world settings.

To illustrate the interconnected challenges faced by AMRO forecasting across scales, we use methicillin-resistant *Staphylococcus aureus* (MRSA) as a concrete example (Figure). Several key issues on MRSA forecasting at the facility scale and population scale and across scales are unresolved; one is that the specific data needed for modeling at those different scales are unknown, as is the role of co-selection and competition with methicillin-susceptible *S. aureus* (MSSA) in affecting the dynamics of MRSA. Answering those questions would improve methods to reduce MRSA burden in both community and hospital settings.

In this perspective, we focus on real-time forecasting of AMROs. A parallel line of research is scenario-based simulations that project AMR infections conditional on postulated changes in prescribed interventions or expected conditions. Previous studies for HIV and tuberculosis control show that such scenario-based projections can substantially affect health policies and save lives (*47*,*48*). For AMR, scenario-based projections should be designed to address practical questions in public health and inform operational policy decision-making in real time, possibly using ensemble approaches that combine multiple models to reflect cross-model variation. Real-time forecasting and scenario-based projections complement each other and should be developed in tandem to control AMR burden and improve human health.

What Can Be Done Now?

Despite all those challenges, research can still be conducted using currently available data and resources. For instance, the feasibility and utility of real-time forecasting of population-level AMR prevalence could be tested using existing surveillance data. Such an exercise might galvanize the research community to address initial practical questions on forecast design (e.g., What variables should be included? What is an appropriate forecast horizon? How forecast skill be evaluated?).

Increasing the availability of existing data could also accelerate progress. Electronic health records contain a wealth of AMR data, each of which reflects a certain aspect of AMR-related processes. Synthesizing previously siloed datasets into mathematical models can potentially answer scientific questions that are otherwise challenging to address using each dataset separately. Privacy-preserved data sharing across facilities can increase the amount of data for modeling and support the development of generalizable methods.

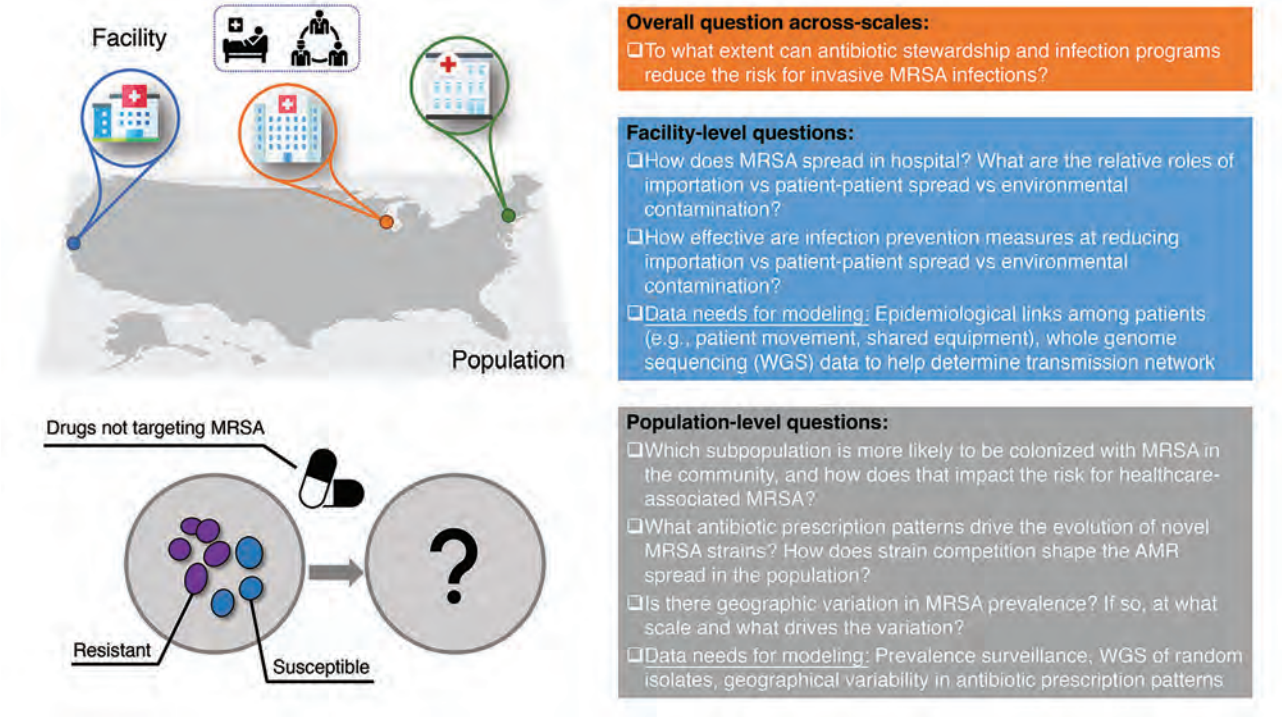

Figure. Open questions for predictive modeling of MRSA. Example questions at the facility level, the population level, and across scales are listed. The upper left panel depicts population-level and facility-level MRSA transmission. The lower left panel represents the uncertainty about the roles of co-selection and competition with MSSA in affecting the dynamics of MRSA. MRSA, methicillin-resistant *Staphylococcus aureus*; MSSA, methicillin-susceptible *S. aureus*.

When data sharing is not practical, models and algorithms can be shared, trained, and implemented with defined standards and quality control.

Future Opportunities

Given existing gaps in forecasting AMR, predictive models are still not mature enough for operational application. To push forward advances in this burgeoning area, several research directions should be prioritized. First, better communication among multiple sectors and stakeholders, including academic researchers, public health agencies, healthcare providers, and the public, will help identify key questions and the needs of end users of predictive models. Developing and applying AMR forecasting will be a collective effort that should address real-world questions in public health and patient care. Second, studies should make better use of existing data and guide the collection of new data that are essential to understand AMR. Investing in consistent surveillance and data collection is of utmost importance for improving understanding of the emergence, spread, and outcomes of AMR. Third, more effective, computationally efficient algorithms are needed to calibrate complex AMR models to multitype and multiscale data. Better interpretability of models can infuse confidence in clinicians when using those tools. Further, research on computational methods that are tailored to AMR prediction could help bridge theoretical models and real-world applications. Fourth, predictive AMR models should be implemented in real-world settings in real time so that operational utility can be assessed by validating real-time operational predictions, as is done for numerical weather predictions. Forecasting skill, including forecast accuracy and uncertainty, should be evaluated to confirm that predictive models can produce useful predictions despite noisy and incomplete data.

In summary, despite lessons learned from recent advances in forecasting for other acute infectious diseases, AMRO prediction has its own set of challenges, including wide and prolonged asymptomatic carriage, longer time scales, continuing evolution due to strain competition and antimicrobial drug use, and poorly observed disease burden. It will be critical to set appropriate expectations for the performance of AMRO predictions and establish sensible criteria for successful forecasting.

This study was supported by the US Centers for Disease Control and Prevention, grant nos. U01CK000592 (J.S. and S.P.), 75D30122C14289 (J.S. and S.P.), U01CK000590 (S.B. and R.J.M.), U01CK000538 (Y.Z.), U01CK000531 (B.A.), and U01CK000594 (B.A.).

R.J.M. served on the advisory committee of Infectious Diseases Society of America—Digital Strategy Advisory Group and the editorial board of Applied Clinical Informatics during the conduct of this study. J.S. and Columbia University disclose partial ownership of SK Analytics. J.S. discloses consulting for BNI. All other authors declare no competing interests.

About the Author

Dr. Pei is an assistant professor in the Department of Environmental Health Sciences at Mailman School of Public Health, Columbia University. His research interests include forecasting, prevention, and control of infectious disease outbreaks.

References

1. World Health Organization. Antimicrobial resistance. 2021 [cited 2022 Jul 18]. https://www.who.int/news-room/fact-sheets/detail/antimicrobial-resistance
2. Murray CJL, Ikuta KS, Sharara F, Swetschinski L, Robles Aguilar G, Gray A, et al.; Antimicrobial Resistance Collaborators. Global burden of bacterial antimicrobial resistance in 2019: a systematic analysis. Lancet. 2022; 399:629–55. https://doi.org/10.1016/S0140-6736(21)02724-0
3. Reich NG, Brooks LC, Fox SJ, Kandula S, McGowan CJ, Moore E, et al. A collaborative multiyear, multimodel assessment of seasonal influenza forecasting in the United States. Proc Natl Acad Sci U S A. 2019;116:3146–54. https://doi.org/10.1073/pnas.1812594116
4. Johansson MA, Apfeldorf KM, Dobson S, Devita J, Buczak AL, Baugher B, et al. An open challenge to advance probabilistic forecasting for dengue epidemics. Proc Natl Acad Sci U S A. 2019;116:24268–74. https://doi.org/10.1073/pnas.1909865116
5. Cramer EY, Ray EL, Lopez VK, Bracher J, Brennen A, Castro Rivadeneira AJ, et al. Evaluation of individual and ensemble probabilistic forecasts of COVID-19 mortality in the United States. Proc Natl Acad Sci U S A. 2022;119:e2113561119. https://doi.org/10.1073/pnas.2113561119
6. Opatowski L, Guillemot D, Boëlle PY, Temime L. Contribution of mathematical modeling to the fight against bacterial antibiotic resistance. Curr Opin Infect Dis. 2011; 24:279–87. https://doi.org/10.1097/QCO.0b013e3283462362
7. López-Lozano JM, Lawes T, Nebot C, Beyaert A, Bertrand X, Hocquet D, et al.; THRESHOLDS Study Group. A nonlinear time-series analysis approach to identify thresholds in associations between population antibiotic use and rates of resistance. Nat Microbiol. 2019;4:1160–72. https://doi.org/10.1038/s41564-019-0410-0
8. Lawes T, Lopez-Lozano JM, Nebot CA, Macartney G, Subbarao-Sharma R, Dare CR, et al. Effects of national antibiotic stewardship and infection control strategies on hospital-associated and community-associated methicillin-resistant *Staphylococcus aureus* infections across a region of Scotland: a non-linear time-series study. Lancet Infect Dis. 2015;15:1438–49. https://doi.org/10.1016/S1473-3099(15)00315-1
9. Niewiadomska AM, Jayabalasingham B, Seidman JC, Willem L, Grenfell B, Spiro D, et al. Population-level mathematical modeling of antimicrobial resistance: a systematic review. BMC Med. 2019;17:81. https://doi.org/10.1186/s12916-019-1314-9

10. Weinstein RA, Bonten MJ Austin DJ, Lipsitch M, Lipsitch M. Understanding the spread of antibiotic resistant pathogens in hospitals: mathematical models as tools for control. Clin Infect Dis. 2001;33:1739–46. https://doi.org/10.1086/323761
11. Doan TN, Kong DCM, Kirkpatrick CMJ, McBryde ES. Optimizing hospital infection control: the role of mathematical modeling. Infect Control Hosp Epidemiol. 2014;35:1521–30. https://doi.org/10.1086/678596
12. Blanquart F. Evolutionary epidemiology models to predict the dynamics of antibiotic resistance. Evol Appl. 2019; 12:365–83. https://doi.org/10.1111/eva.12753
13. Davies NG, Flasche S, Jit M, Atkins KE. Within-host dynamics shape antibiotic resistance in commensal bacteria. Nat Ecol Evol. 2019;3:440–9. https://doi.org/10.1038/s41559-018-0786-x
14. Colijn C, Cohen T, Fraser C, Hanage W, Goldstein E, Givon-Lavi N, et al. What is the mechanism for persistent coexistence of drug-susceptible and drug-resistant strains of *Streptococcus pneumoniae*? J R Soc Interface. 2010;7:905–19. https://doi.org/10.1098/rsif.2009.0400
15. Lehtinen S, Blanquart F, Lipsitch M, Fraser C; with the Maela Pneumococcal Collaboration. On the evolutionary ecology of multidrug resistance in bacteria. PLoS Pathog. 2019; 15:e1007763. https://doi.org/10.1371/journal.ppat.1007763
16. Blanquart F, Lehtinen S, Lipsitch M, Fraser C. The evolution of antibiotic resistance in a structured host population. J R Soc Interface. 2018;15:20180040. https://doi.org/10.1098/rsif.2018.0040
17. Slayton RB, Toth D, Lee BY, Tanner W, Bartsch SM, Khader K, et al. Vital Signs: estimated effects of a coordinated approach for action to reduce antibiotic-resistant infections in health care facilities—United States. MMWR Morb Mortal Wkly Rep. 2015;64:826–31. https://doi.org/10.15585/mmwr.mm6430a4
18. Smith DL, Levin SA, Laxminarayan R. Strategic interactions in multi-institutional epidemics of antibiotic resistance. Proc Natl Acad Sci U S A. 2005;102:3153–8. https://doi.org/10.1073/pnas.0409523102
19. Paul P, Slayton RB, Kallen AJ, Walters MS, Jernigan JA. Modeling regional transmission and containment of a healthcare-associated multidrug-resistant organism. Clin Infect Dis. 2020;70:388–94.
20. Worby CJ, Jeyaratnam D, Robotham JV, Kypraios T, O'Neill PD, De Angelis D, et al. Estimating the effectiveness of isolation and decolonization measures in reducing transmission of methicillin-resistant *Staphylococcus aureus* in hospital general wards. Am J Epidemiol. 2013;177:1306–13. https://doi.org/10.1093/aje/kws380
21. Cooper BS, Medley GF, Stone SP, Kibbler CC, Cookson BD, Roberts JA, et al. Methicillin-resistant *Staphylococcus aureus* in hospitals and the community: stealth dynamics and control catastrophes. Proc Natl Acad Sci U S A. 2004;101:10223–8. https://doi.org/10.1073/pnas.0401324101
22. Bootsma MCJ, Diekmann O, Bonten MJM. Controlling methicillin-resistant *Staphylococcus aureus*: quantifying the effects of interventions and rapid diagnostic testing. Proc Natl Acad Sci U S A. 2006;103:5620–5. https://doi.org/10.1073/pnas.0510077103
23. Pei S, Morone F, Liljeros F, Makse H, Shaman JL. Inference and control of the nosocomial transmission of methicillin-resistant *Staphylococcus aureus*. eLife. 2018;7:e40977.
24. Pei S, Liljeros F, Shaman J. Identifying asymptomatic spreaders of antimicrobial-resistant pathogens in hospital settings. Proc Natl Acad Sci U S A. 2021;118:e2111190118. https://doi.org/10.1073/pnas.2111190118
25. Lee BY, McGlone SM, Wong KF, Yilmaz SL, Avery TR, Song Y, et al. Modeling the spread of methicillin-resistant *Staphylococcus aureus* (MRSA) outbreaks throughout the hospitals in Orange County, California. Infect Control Hosp Epidemiol. 2011;32:562–72. https://doi.org/10.1086/660014
26. Toth DJA, Khader K, Slayton RB, Kallen AJ, Gundlapalli AV, O'Hagan JJ, et al. The potential for interventions in a long-term acute care hospital to reduce transmission of carbapenem-resistant Enterobacteriaceae in affiliated healthcare facilities. Clin Infect Dis. 2017;65:581–7. https://doi.org/10.1093/cid/cix370
27. Knight GM, Davies NG, Colijn C, Coll F, Donker T, Gifford DR, et al. Mathematical modelling for antibiotic resistance control policy: do we know enough? BMC Infect Dis. 2019;19:1011. https://doi.org/10.1186/s12879-019-4630-y
28. Pouwels KB, Muller-Pebody B, Smieszek T, Hopkins S, Robotham JV. Selection and co-selection of antibiotic resistances among *Escherichia coli* by antibiotic use in primary care: an ecological analysis. PLoS One. 2019;14:e0218134. https://doi.org/10.1371/journal.pone.0218134
29. Olesen SW, Barnett ML, MacFadden DR, Brownstein JS, Hernández-Díaz S, Lipsitch M, et al. The distribution of antibiotic use and its association with antibiotic resistance. eLife. 2018;7:e39435. https://doi.org/10.7554/eLife.39435
30. Lehtinen S, Blanquart F, Croucher NJ, Turner P, Lipsitch M, Fraser C. Evolution of antibiotic resistance is linked to any genetic mechanism affecting bacterial duration of carriage. Proc Natl Acad Sci U S A. 2017;114:1075–80. https://doi.org/10.1073/pnas.1617849114
31. Olesen SW, Lipsitch M, Grad YH. The role of "spillover" in antibiotic resistance. Proc Natl Acad Sci U S A. 2020 Nov 2 [Epub ahead of print]. https://doi.org/10.1073/pnas.2013694117
32. Penders J, Stobberingh EE, Savelkoul PH, Wolffs PF. The human microbiome as a reservoir of antimicrobial resistance. Front Microbiol. 2013;4:87. https://doi.org/10.3389/fmicb.2013.00087
33. Anthony WE, Burnham CD, Dantas G, Kwon JH. The gut microbiome as a reservoir for antimicrobial resistance. J Infect Dis. 2021;223(Suppl 3):S209–13. https://doi.org/10.1093/infdis/jiaa497
34. Relman DA, Lipsitch M. Microbiome as a tool and a target in the effort to address antimicrobial resistance. Proc Natl Acad Sci U S A. 2018;115:12902–10. https://doi.org/10.1073/pnas.1717163115
35. Morley VJ, Woods RJ, Read AF. Bystander selection for antimicrobial resistance: implications for patient health. Trends Microbiol. 2019;27:864–77. https://doi.org/10.1016/j.tim.2019.06.004
36. Tedijanto C, Olesen SW, Grad YH, Lipsitch M. Estimating the proportion of bystander selection for antibiotic resistance among potentially pathogenic bacterial flora. Proc Natl Acad Sci U S A. 2018;115:E11988–95. https://doi.org/10.1073/pnas.1810840115
37. Dahms RA, Johnson EM, Statz CL, Lee JT, Dunn DL, Beilman GJ. Third-generation cephalosporins and vancomycin as risk factors for postoperative vancomycin-resistant enterococcus infection. Arch Surg. 1998;133:1343–6. https://doi.org/10.1001/archsurg.133.12.1343
38. National Antimicrobial Resistance Monitoring System for Enteric Bacteria (NARMS). 2020 [cited 2022 Jun 23]. https://www.cdc.gov/narms/index.html
39. Iskandar K, Molinier L, Hallit S, Sartelli M, Hardcastle TC, Haque M, et al. Surveillance of antimicrobial resistance in low- and middle-income countries: a scattered picture. Anti-

microb Resist Infect Control. 2021;10:63. https://doi.org/10.1186/s13756-021-00931-w
40. Cooper BS, Medley GF, Bradley SJ, Scott GM. An augmented data method for the analysis of nosocomial infection data. Am J Epidemiol. 2008;168:548–57. https://doi.org/10.1093/aje/kwn176
41. Thomas A, Redd A, Khader K, Leecaster M, Greene T, Samore M. Efficient parameter estimation for models of healthcare-associated pathogen transmission in discrete and continuous time. Math Med Biol. 2015;32:81–100. https://doi.org/10.1093/imammb/dqt021
42. Eyre DW, Laager M, Walker AS, Cooper BS, Wilson DJ; CDC Modeling Infectious Diseases in Healthcare Program (MInD-Healthcare). Probabilistic transmission models incorporating sequencing data for healthcare-associated *Clostridioides difficile* outperform heuristic rules and identify strain-specific differences in transmission. PLOS Comput Biol. 2021;17:e1008417. https://doi.org/10.1371/ journal.pcbi.1008417
43. Biggerstaff M, Alper D, Dredze M, Fox S, Fung ICH, Hickmann KS, et al.; Influenza Forecasting Contest Working Group. Results from the Centers for Disease Control and Prevention's Predict the 2013–2014 Influenza Season challenge. BMC Infect Dis. 2016;16:357. https://doi.org/10.1186/s12879-016-1669-x
44. Biggerstaff M, Johansson M, Alper D, Brooks LC, Chakraborty P, Farrow DC, et al. Results from the second year of a collaborative effort to forecast influenza seasons in the United States. Epidemics. 2018;24:26–33. https://doi.org/10.1016/j.epidem.2018.02.003
45. McGowan CJ, Biggerstaff M, Johansson M, Apfeldorf KM, Ben-Nun M, Brooks L, et al.; Influenza Forecasting Working Group. Collaborative efforts to forecast seasonal influenza in the United States, 2015–2016. Sci Rep. 2019;9:683. https://doi.org/10.1038/s41598-018-36361-9
46. Viboud C, Sun K, Gaffey R, Ajelli M, Fumanelli L, Merler S, et al.; RAPIDD Ebola Forecasting Challenge group. The RAPIDD Ebola forecasting challenge: synthesis and lessons learnt. Epidemics. 2018;22:13–21. https://doi.org/10.1016/j.epidem.2017.08.002
47. Blower SM, Gershengorn HB, Grant RM. A tale of two futures: HIV and antiretroviral therapy in San Francisco. Science. 2000;287:650–4. https://doi.org/10.1126/cience.287.5453.650
48. Blower SM, Small PM, Hopewell PC. Control strategies for tuberculosis epidemics: new models for old problems. Science. 1996;273:497–500. https://doi.org/10.1126/science.273.5274.497

Address for correspondence: Sen Pei, Columbia University, 722 W 168th St, New York, NY 10032, USA; email: sp3449@cumc.columbia.edu

etymologia revisited

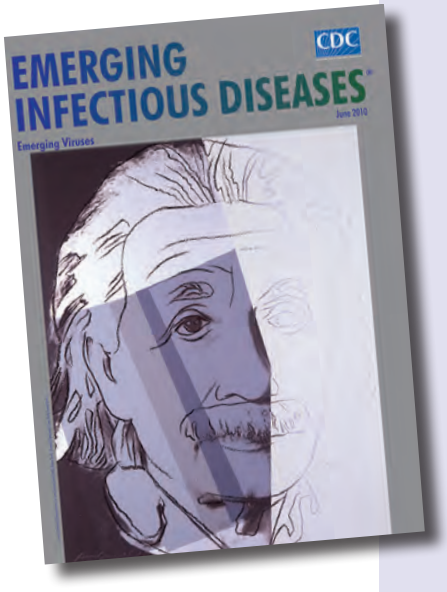

Lassa Virus
[lah sə] virus

This virus was named after the town of Lassa at the southern end of Lake Chad in northeastern Nigeria, where the first known patient, a nurse in a mission hospital, had lived and worked when she contracted this infection in 1969. The virus was discovered as part of a plan to identify unknown viruses from Africa by collecting serum specimens from patients with fevers of unknown origin. Lassa virus, transmitted by field rats, is endemic in West Africa, where it causes up to 300,000 infections and 5,000 deaths each year.

Sources:

1 Frame JD, Baldwin JM Jr, Gocke DJ, Troup JM. Lassa fever, a new virus disease of man from West Africa. I. Clinical description and pathological findings. Am J Trop Med Hyg. 1970;19:670–6.
2. Mahy BW. The dictionary of virology, 4th ed. Burlington (MA): Elsevier; 2009.

Originally published in June 2010

https://wwwnc.cdc.gov/eid/article/16/6/et-1606_article

Pediatric Invasive Meningococcal Disease, Auckland, New Zealand (Aotearoa), 2004–2020

Cameron Burton, Emma Best, Matthew Broom, Helen Heffernan, Simon Briggs, Rachel Webb

Medscape CME Activity

In support of improving patient care, this activity has been planned and implemented by Medscape, LLC and Emerging Infectious Diseases. Medscape, LLC is jointly accredited with commendation by the Accreditation Council for Continuing Medical Education (ACCME), the Accreditation Council for Pharmacy Education (ACPE), and the American Nurses Credentialing Center (ANCC), to provide continuing education for the healthcare team.

Medscape, LLC designates this Journal-based CME activity for a maximum of 1.00 ***AMA PRA Category 1 Credit(s)™***. Physicians should claim only the credit commensurate with the extent of their participation in the activity.

Successful completion of this CME activity, which includes participation in the evaluation component, enables the participant to earn up to 1.0 MOC points in the American Board of Internal Medicine's (ABIM) Maintenance of Certification (MOC) program. Participants will earn MOC points equivalent to the amount of CME credits claimed for the activity. It is the CME activity provider's responsibility to submit participant completion information to ACCME for the purpose of granting ABIM MOC credit.

All other clinicians completing this activity will be issued a certificate of participation. To participate in this journal CME activity: (1) review the learning objectives and author disclosures; (2) study the education content; (3) take the post-test with a 75% minimum passing score and complete the evaluation at http://www.medscape.org/journal/eid; and (4) view/print certificate. For CME questions, see page 874.

Release date: March 16, 2023; Expiration date: March 16, 2024

Learning Objectives

Upon completion of this activity, participants will be able to:

- Assess the global epidemiology of invasive meningococcal disease
- Analyze the epidemiology of invasive meningococcal disease among children in Aotearoa New Zealand
- Evaluate clinical features of invasive meningococcal disease in the current study.
- Distinguish outcomes of invasive meningococcal disease in the current study

CME Editor

Cheryl Salerno, BA, Technical Writer/Editor, Emerging Infectious Diseases. *Disclosure: Cheryl Salerno, BA, has no relevant financial relationships.*

CME Author

Charles P. Vega, MD, Health Sciences Clinical Professor of Family Medicine, University of California, Irvine School of Medicine, Irvine, California. *Disclosure: Charles P. Vega, MD, has the following relevant financial relationships: consultant or advisor for GlaxoSmithKline; Johnson & Johnson Pharmaceutical Research & Development, L.L.C.*

Authors

Cameron Burton, MBChB; Emma Best, MBChB; Matthew Broom, MBChB; Helen Heffernan, BSc (Hons 1); Simon Briggs, MBChB; and ***Rachel Webb, MD.***

Author affiliations: The University of Auckland, Auckland, New Zealand (C. Burton, E. Best, R. Webb); Te Whatu Ora Counties Manukau, Auckland (C. Burton, R. Webb); Te Whatu Ora Te Toka Tumai Auckland, Auckland (E. Best, S. Briggs, R. Webb); Te Whatu Ora Waitematā, Auckland (M. Broom); Institute of Environmental Science and Research, Wellington, New Zealand (H. Heffernan).

DOI: http://doi.org/10.3201/eid2904.221397

New Zealand (Aotearoa) experienced a *Neisseria meningitidis* serogroup B epidemic during 1991–2006, and incidence remains twice that of other high-income countries. We reviewed clinical, laboratory, and immunization data for children <15 years of age with laboratory-confirmed invasive meningococcal disease in Auckland, New Zealand, during January 1, 2004–December 31, 2020. Of 319 cases in 318 children, 4.1% died, and 23.6% with follow-up data experienced sequelae. Children of Māori and Pacific ethnicity and those living in the most deprived areas were overrepresented. Eighty-one percent were positive for *N. meningitidis* serogroup B, 8.6% for serogroup W, 6.3% for serogroup C, and 3.7% for serogroup Y. Seventy-nine percent had bacteremia, and 63.9% had meningitis. In New Zealand, Māori and Pacific children are disproportionately affected by this preventable disease. *N. meningitidis* serogroup B vaccine should be included in the New Zealand National Immunization Schedule to address this persistent health inequity.

Invasive meningococcal disease (IMD) is a bacterial infection with typically rapid onset. In children, infection is associated with high (7%–9%) case-fatality rates (CFRs) and serious long-term sequelae (*1*,*2*). Infants and young children have the highest incidence of disease; a second peak occurs during adolescence (*3*). IMD inequitably affects Indigenous populations and persons living in areas of deprivation (*3*,*4*).

The bacterium *Neisseria meningitidis* is categorized into serogroups based on its polysaccharide capsule; 6 serogroups (A, B, C, W, X, and Y) are responsible for nearly all IMD cases worldwide (*5*). The major clinical manifestations of IMD are meningitis and sepsis. Early recognition is critical because sepsis can rapidly progress to multiorgan dysfunction and death (*6*). A leading cause of admission to pediatric intensive care units (ICUs) throughout Australasia (*7*), IMD can lead to disabling, long-term sequelae for approximately one third of surviving children, including hearing loss, neurodevelopmental impairment, limb or digit loss, and scarring (*2*,*8*,*9*). Those sequelae heavily affect healthcare resources and the quality of life of affected children and their families (*2*,*9*).

Epidemiology of IMD Globally and in New Zealand

The global incidence of IMD has declined over the past 20 years, partly because of the availability of safe, effective vaccines for all major disease-causing serogroups and successful vaccination programs (*5*). Overall incidence of IMD in most high-income countries is well under 1.5 per 100,000 per year (*5*). In contrast, New Zealand (Aotearoa) reports the highest rate of *N. meningitidis* serogroup B (MenB) disease in the world (*3*,*5*,*10*). During 1991–2006, New Zealand experienced a prolonged MenB epidemic caused by the B:P1.7–2,4 strain (*11*). The epidemic peaked in 2001, with an incidence of 17.4 cases/100,000 persons in the overall population and 212 cases/100,000 infants (*11*). In response, MeNZB, a strain-specific outer membrane vesicle (OMV) vaccine, was developed and delivered nationally in 3 doses to persons <20 years of age during 2004–2006 and in 4 doses to infants during 2006–2008 (*11*). Overall vaccination coverage was 80%, and coverage was higher among Pacific peoples compared with those of other ethnicities. The vaccine effectiveness of MeNZB against the epidemic strain was estimated at 68%–77% and was associated with the waning of the epidemic (*4*,*11*).

Since that time, regional outbreaks of *N. meningitidis* serogroup C (MenC) and serogroup W (MenW) disease have been associated with high CFRs, prompting emergency targeted vaccination programs in 2011 and 2018 (*12*,*13*). However, since 2014, the incidence of IMD in NZ has been increasing, up to an overall rate of 2.8 cases/100,000 persons in 2019 (*3*). Almost half of cases in 2019 occurred in children <15 years of age, and the highest rates in infants <1 year of age (51.5/100,000 infants). As observed internationally, an increasing proportion of IMD caused by MenW has occurred in New Zealand, accounting for 30% of the country's cases in 2019 (*3*,*5*). Auckland, New Zealand's largest city, has a pediatric (<15 years of age) population of ≈320,000, which makes up 34% of the total New Zealand pediatric population (*14*). Ethnic groups in Auckland include Māori (18%), Pacific peoples (19%), and those of Asian (25%) and European (34%) heritage.

Meningococcal Vaccines

A 4-component MenB vaccine, 4CMenB (Bexsero; GlaxoSmithKline), was developed using 3 subcapsular antigens and the NZ MeNZB OMV vaccine (*15*). Vaccine effectiveness data from Australia, Canada, Italy, and the United Kingdom show reductions in MenB of 71%–100% in eligible cohorts 2–5 years after 4CMenB was introduced (*15*). Although there is no evidence that 4CMenB reduces *N. meningitidis* carriage (*16*), OMV meningococcal vaccines appear to provide some protection against IMD caused by non-MenB serogroups, as well as against *N. gonorrhoeae* (*17*,*18*). Although 4CMenB and MenACWY vaccines are funded in New Zealand for a small number of persons with high-risk medical

conditions and, recently, for adolescents in certain collective residences, no meningococcal vaccines are universally funded in the National Immunization Schedule. We aimed to describe the experience of pediatric IMD in Auckland during 2004–2020—including demographic factors; clinical, microbiological, and laboratory features; treatment; and outcomes—to demonstrate the impact of IMD on children in New Zealand and to highlight the need for funding of meningococcal vaccines.

Methods

Study Design and Collection of Data

We conducted a retrospective, observational study in Auckland. Eligible cases were those in children <15 years of age who contracted IMD while residing within the Auckland region during January 1, 2004–December 31, 2020. We included cases where *N. meningitidis* was identified by culture or PCR from a normally sterile site (i.e., blood, cerebrospinal fluid [CSF], synovial fluid).

All persons who test positive for *N. meningitidis* in New Zealand are actively notified as part of public health surveillance; isolates and DNA extracted from sterile site specimens are forwarded to the Meningococcal Reference Laboratory at the Institute of Environmental Science and Research (*3*). The institute provided all cases confirmed by *N. meningitidis* culture or PCR. We collected data by using National Health Index numbers (a unique identifier for medical care for all persons residing in New Zealand) (*19*) from clinical and laboratory records and the National Immunization Register (an electronic record of vaccination events for New Zealand children) (*20*).

Case Definitions and Variables

We categorized clinical manifestations according to the presence of bacteremia, meningitis, and septic arthritis. We defined bacteremia as a positive *N. meningitidis* culture or PCR from blood. We defined meningitis as a positive *N. meningitidis* culture or PCR from CSF or an alternative sterile site positive for *N. meningitidis* with a CSF leukocytosis or with clinical signs of meningitis if CSF was not obtained. We defined septic arthritis as a positive *N. meningitidis* culture or PCR from synovial fluid or an alternative sterile site positive for *N. meningitidis* with clinical signs of septic arthritis. We defined sepsis by Pediatric Sepsis Consensus Congress criteria (*21*). We calculated CFR as the number of children who died divided by the total number of cases. For survivors, we classified outcomes as cure, cure with sequelae, and unknown. We used a composite outcome of death and cure with sequelae in our outcome analysis.

We obtained population denominators from Statistics New Zealand (*22*) and recorded prioritized ethnicity using New Zealand ethnicity data protocols (*23*). We measured socioeconomic deprivation using the New Zealand Index of Deprivation (NZDep) quintiles for 2013 and 2018 (*24*). NZDep stratifies small geographic areas into equal-sized groups based on multiple measures of socioeconomic deprivation. We identified serogroup by serological means or by PCR. DNA sequence analysis of the porA gene determined the subtype. We defined the epidemic strain as MenB with the P1.7–2,4 subtype and defined vaccine subtype IMD as any serogroup with the P1.7–2,4 subtype. We determined MICs by using Etest (bioMérieux). We categorized isolates with penicillin MICs of >0.06 mg/L as having reduced penicillin susceptibility and interpreted ceftriaxone, ciprofloxacin, and rifampin MICs according to standardized breakpoints (*25*). We defined MeNZB vaccination status as fully vaccinated (received all approved doses for age), partially vaccinated (received less than approved doses for age), unvaccinated (received no doses), or ineligible (born outside of the MeNZB program period). We obtained approval for the study from the Health and Disability Ethics Committees (18/NTA/86/AM02).

Statistical Methods

We performed calculations using R (The R Foundation for Statistical Computing, https://www.r-project.org) and OpenEpi (Open Source Epidemiologic Statistics for Public Health, https://www.openepi.com). We included only cases with available data in the analysis of each variable. We employed a 2-tailed test to determine p values, using a significance level of 0.05, and used a Poisson model to investigate temporal trends in IMD and the epidemic strain. We used univariate logistic regression to investigate factors associated with an increased risk of death or sequelae and χ^2 test to compare rates and calculate 95% CIs. We compared MeNZB vaccination status with timing of IMD illness by using analysis of variance and independent samples t-tests.

Results

Case Numbers

We reviewed data from 331 cases, excluding 12 cases (6 in nonresidents, 5 that were noninvasive disease, and 1 that lacked sufficient data). The remaining 319 cases of laboratory-confirmed IMD occurred in 318

children. One child had 2 unrelated episodes of IMD that occurred in 2006 and 2017. There were no documented relapses after treatment in the cohort. The average annual incidence of IMD across the study period was 5.9/100,000 population. Incidence rates declined from the tail end of the epidemic in 2004 to a nadir in 2014, then increased to a second peak in 2019 (Figure 1). Overall, we found a trend toward reduced incidence over the study period (Poisson coefficient −0.07 [95% CI −0.14 to −0.01; p<0.01]; rate ratio 0.92 [95% CI 0.90–0.95]). Cases were more common in winter (135/319, 42.3%), followed by spring (87/319, 27.3%), autumn (52/319, 16.3%), and summer (45/319, 14.1%) (p<0.0001).

Demographic Factors

Median age at time of diagnosis was 18 months (interquartile range [IQR] 7–60 months). The highest average incidence rates were among infants <1 year of age (31.5/100,000 population/year), followed by those 1–4 years of age (8.2/100,000 population/year), 5–9 years of age (2.6/100,000 population/year), and 10–14 years of age (2.0/100,000 population/year) (Table 1; Figure 2, panel A). Average incidence rates by ethnic group were highest in Pacific peoples (13.4/100,000 population/year), followed by Māori (11.6/100,000 population/year) and those who were neither Māori or Pacific (1.9/100,000 population/year) (Table 1; Figure 2, panel B). Based on census data and compared with non-Māori and non-Pacific groups, the unadjusted relative risk of IMD was 5.9 (95% CI 4.4–8.1) for Māori (p<0.0001) and 6.9 (95% CI 5.1–9.3) for Pacific peoples (p<0.0001). Most children (189/317, 59.6%) lived in NZDep quintile 5 (most deprived 20%) areas. The unadjusted relative risk of IMD for children living in NZDep quintile 5 areas compared with quintile 1 areas was 17.2 (95% CI 9.7–33.2; p<0.0001).

Microbiology and Laboratory Features

Of the 319 cases, we confirmed a microbiological diagnosis by both culture and PCR for 81 (25.4%), on culture alone for 114 (35.7%), and on PCR alone for 124 (38.9%). We compared *N. meningitidis* culture and PCR from blood and from CSF (Appendix Table 1, https://wwwnc.cdc.gov/EID/article/29/4/22-1397-App1.pdf). Blood culture was negative for 56 (78.9%) of 71 cases in children who received antibiotics before hospital admission (odds ratio 5.1 [95% CI 2.7–9.5]) compared with no prehospital antibiotics (p<0.0001). Of those 56 cases, *N. meningitidis* blood PCR was positive in all 50 cases tested. CSF analysis was performed in 138 (67.6%) of the 204 cases classified as meningitis (Appendix Table 2). CSF leukocytosis for age was present in 130 (97.7%) of 133 cases of meningitis where a CSF leukocyte count was performed. The serogroup was identified for 301 (94.4%) of the 319 cases: 245 (81.4%) were MenB, 26 (8.6%) MenW, 19 (6.3%) MenC, and 11 (3.7%) serogroup Y. Beginning in 2017, there was an increase in disease caused by MenW, which accounted for 8 (29.6%) of the 27 cases serogrouped in 2019; MenB was the remaining predominant serogroup (Figure 1). The epidemic B:P1.7–2,4 strain accounted for 135 cases (44.9%), waning over time, from 42 cases (14.0/100,000 population) in 2004 to 3 cases (0.90/100,000 population) in 2020 (Poisson coefficient −0.20 [95% CI −0.28 to −0.11]; p<0.01; rate ratio 0.82 [95% CI 0.78–0.85]). The proportion of isolates with reduced penicillin susceptibility increased during the study period. A MIC of >0.06 mg/L was identified in 28 (22.6%) of 124 isolates in 2004–2012 and 47 (66.2%) of 71 isolates in 2013–2020 (p<0.0001). Reduced penicillin susceptibility was identified in 20 (76.9%) of 26 MenW isolates compared with 55 (32.5%) of 169 non-MenW isolates (p = 0.012). All isolates were susceptible to ceftriaxone, ciprofloxacin, and rifampin.

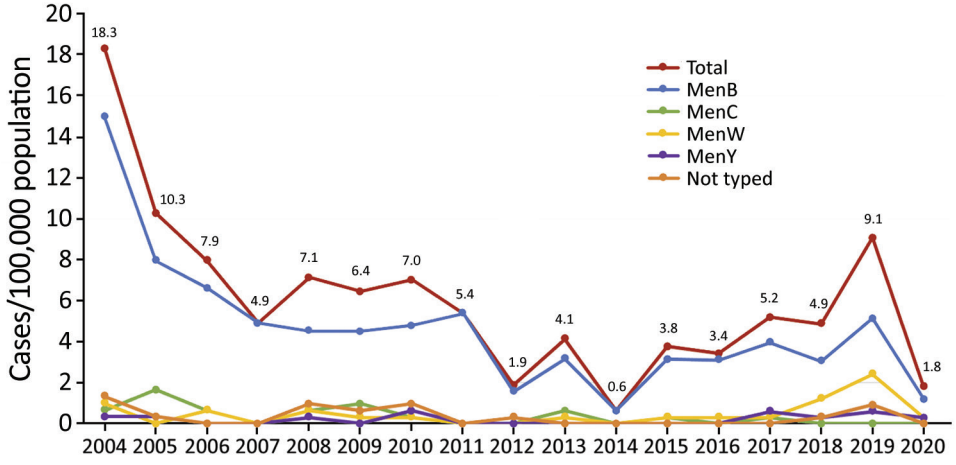

Figure 1. Timeline of 319 cases of confirmed invasive meningococcal disease in children <15 year of age, by serogroup, reported by year, Auckland, New Zealand, 2004–2020. Numbers along data line indicate exact rates for all cases by year. Men, *Neisseria meningitidis* serogroup.

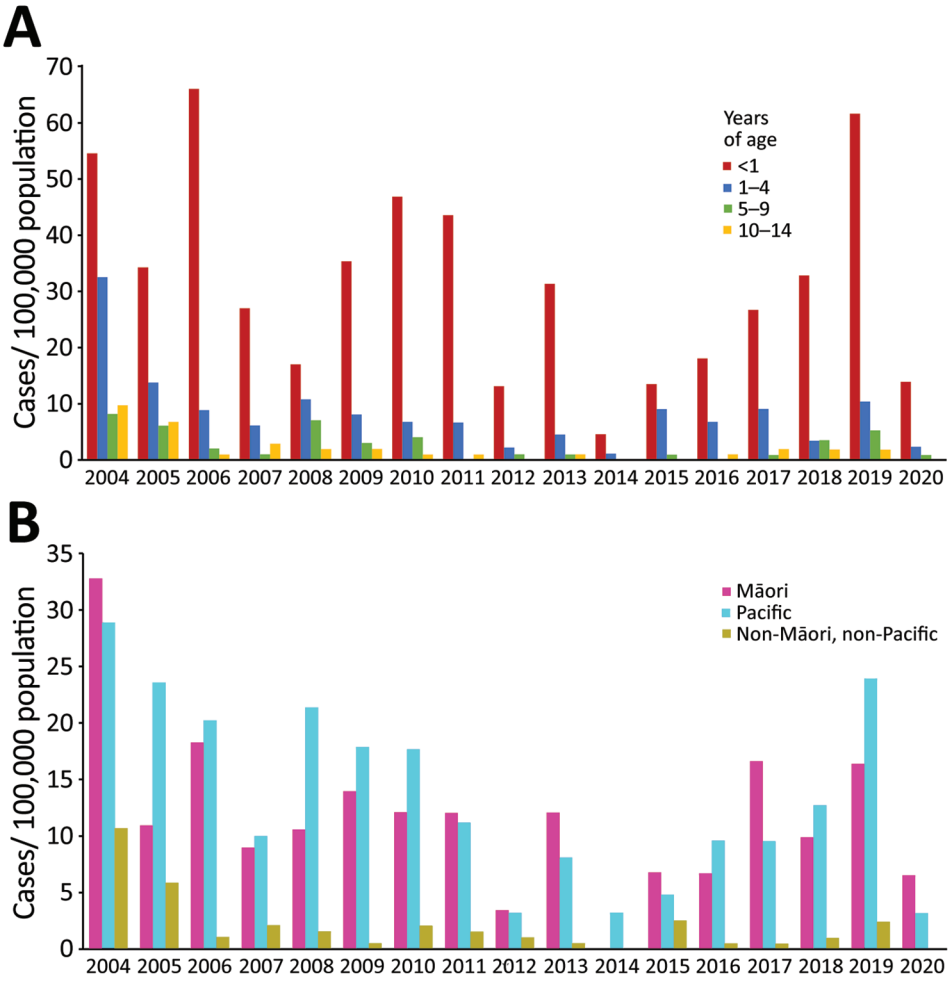

Figure 2. Timeline of 319 cases of confirmed invasive meningococcal disease in children <15 years of age by age group (A) and prioritized ethnicity (B), reported by year, Auckland, New Zealand, 2004–2020.

Clinical Features

The median duration of illness before care was sought was 1 day (IQR 1–3 days). Bacteremia was present in 251 cases (78.7%), meningitis in 204 (63.9%), and septic arthritis in 10 (3.1%) (Table 1). Concomitant bacteremia and meningitis occurred in 141 (44.2%) cases. No cases of chronic meningococcemia were recorded. Sepsis occurred in 172 (80.8%) of the 213 cases with complete systemic inflammatory response syndrome data.

Treatment

Of the 319 cases, 317 (99%) were treated in a hospital; 2 children (0.6%) died before arrival. The median duration of hospitalization was 5 nights (IQR 3–7 nights). Prehospital parenteral antibiotics were administered in 52 (16.3%) cases. In the hospital, empiric antibiotics included a third-generation cephalosporin in 294 (92.7%) cases. There were 303 children who completed a full targeted treatment course of antibiotics, which included a third-generation cephalosporin in 230 cases (75.9%), benzylpenicillin in 67 cases (22.1%), amoxicillin in 8 cases (2.6%), and another antibiotic in 4 cases (1.3%). The median duration of antibiotic treatment was 5 days (IQR 5–7 days). Dexamethasone was administered in 47 (23%) of the 204 meningitis cases. Of the 100 (31.3%) children who were admitted to an ICU (median duration of stay 1 night [IQR 1–3 nights]), 55 received ≥1 life-saving measure: 46 received invasive ventilation, 44 received inotropic/vasopressor support, and 7 received renal replacement therapy. Plastic surgical procedures were performed in 12 (3.8%) cases, orthopedic procedures in 12 (3.8%), and neurosurgical procedures in 6 (1.9%).

Outcomes

Thirteen children died, resulting in a CFR of 4.1% (Table 2). The average death rate over the study period was 0.24/100,000 population/year. Of the 13 children who died(Appendix Table 3), 12 (92.3%) were Māori or Pacific peoples, 11 (84.6%) were living in NZDep quintile 5 areas, and 9 (69.2%) were infants <1 year of age. Ten deaths (76.9%) occurred

in the community or within the first 48 hours of hospitalization. Of the 306 survivors, outcome data were complete for 258 cases (84.3%): cure without sequelae occurred in 197 (76.4%) and cure with sequelae in 61 (23.6%). We classified outcome as unknown in 48 cases; all had meningitis with no available audiometry results (none had other sequelae identified on follow-up). Documented audiologic assessment occurred in 143 (72.6%) of 197 cases after meningitis. Of the 142 cases with audiometry results available, 32 (22.5%) had sensorineural impairment. Māori children with IMD had 2.5 (95% CI 1.1–6.4) times the odds for death or sequelae compared with non-Māori, non-Pacific peoples (p = 0.0366) (Table 3). Pacific peoples with IMD had 2.9 (95% CI 1.3–7.2) times the odds for death or sequelae compared with non-Māori, non-Pacific peoples p = 0.0128). Results of univariate comparisons of age, sex, NZDep quintile, season, MeNZB vaccination status, sepsis criteria, serogroup, reduced penicillin susceptibility, and prehospital parenteral antibiotics were not significant.

MeNZB Vaccination

Of the 163 children with complete vaccination records who were eligible for MeNZB, 114 (69.9%) had received ≥1 dose and 64 (39.3%) were fully vaccinated at time of hospital admission. For the 97 eligible children with vaccine subtype IMD, 55 (56.7%) had received ≥1 dose and 31 (32%) were fully vaccinated at time of hospital admission. The mean number of days between the date of last MeNZB vaccine and IMD onset increased with the number of doses received (p<0.00027) (Appendix Table 4).

Table 1. Demographic and clinical factors of 319 confirmed cases of invasive meningococcal disease in children <15 years of age, Auckland, New Zealand, 2004–2020*

Variable	Total no. (missing data)	No. (%) cases	Average incidence, cases/100,000 population/y
Age, y	319 (0)		
<1 y		118 (37.0)	31.5
1–4		120 (37.6)	8.2
5–9		46 (14.4)	2.6
10–14		35 (11.0)	2.0
Sex	319 (0)		
F		125 (39.2)	4.8
M		194 (60.8)	7.0
Ethnicity, prioritized	319 (0)		
Māori		114 (35.7)	11.6
Pacific		140 (43.9)	13.4
Non-Māori, non-Pacific		65 (20.4)	1.9
New Zealand Index of Deprivation Quintile†	317‡		
1		11 (3.5)	NA
2		21 (6.6)	NA
3		42 (13.2)	NA
4		54 (17.0)	NA
5		189 (59.6)	NA
Clinical manifestations	319 (0)		
Bacteremia only		108 (33.9)	NA
Meningitis only		63 (19.7)	NA
Meningitis with bacteremia		138 (42.3)	NA
Septic arthritis only		5 (1.6)	NA
Septic arthritis with bacteremia		2 (0.6)	NA
Meningitis and septic arthritis with bacteremia		3 (0.9)	NA
Vital signs on first presentation			
Temperature >38·5°C or <36°C	314 (5)	150 (47.7)	NA
Systolic hypotension for age	218 (101)	84 (38.5)	NA
Impaired level of consciousness	291 (28)	99 (34.0)	NA
Clinical signs at first presentation			
Rash in cases with bacteremia	248 (3)	213 (85.9)	NA
Includes purpura	213 (3)	108 (50.7)	NA
Includes petechiae without purpura	213 (3)	86 (40.4)	NA
Blanching only	213 (3)	19 (8.9)	NA
Meningism in cases with meningitis	184 (20)	111 (60.3)	NA
Bulging fontanelle in infants with meningitis	43 (39)	19 (44.2)	NA
Arthritis during admission	314 (5)	19 (6.1)	NA
Arthralgia during admission	314 (5)	23 (7.3)	NA

*NA, not applicable.
†Each NZDep quintile contains ≈20% of the population. 1 = least deprived; 5 = most deprived.
‡Two overseas cases were excluded.

Table 2. Outcomes of 319 confirmed cases of invasive meningococcal disease in children <15 years of age, Auckland, New Zealand, 2004–2020

Outcome	No. cases/total no. (%)
Died	13/319 (4.1)
Cure, complete outcome data	258/306 (84.3)
Cure, incomplete outcome data	48/306 (15.6)
Cure without sequelae	197/258 (76.4)
Cure with sequelae	61/258 (23.6)
Sequelae	
Neurodevelopmental	35/258 (13.6)
Sensorineural hearing loss	32/258 (12.4)
Skin scarring	16/258 (6.2)
Loss of limbs or digits	7/258 (2.7)
Chronic kidney disease	1/258 (0.4)
Other sequelae*	5/258 (1.9)
Neurodevelopmental sequelae	
Delayed development	20/258 (7.8)
Cerebral ischemia	13/258 (5)
Epilepsy	8/258 (3.1)
Learning, concentration, behavior, psychological	8/258 (3.1)
Other†	10/258 (3.9)

*Other: bone growth arrest 2/258 (0.8%); cardiomyopathy 1/258 (0.4%); gastrointestinal hemorrhage 1/258 (0.4%); panniculitis 1/258 (0.4%).
†Other neurodevelopmental: chronic hydrocephalus 2/258 (0.8%); autism spectrum disorder 1/258 (0.4%); ataxia 1/258 (0.4%); carotid artery narrowing 1/258 (0.4%); chronic headache 1/258 (0·4%); cranial nerve palsy 1/258 (0.4%); encephalomalacia 1/258 (0.4%); hypertonia 1/258 (0.4%); syringomyelia 1/258 (0.4%).

Discussion

Despite a reduction in the number of cases of IMD since the MenB epidemic, the incidence of IMD in New Zealand remains double that of other high-income countries (*3*,*5*). Although MenB remains the most common serogroup in children, the epidemic B:P1.7–2,4 strain no longer dominates in the Auckland region. Rates of pediatric IMD increased in Auckland and nationally in 2014–2019, partly because of an observed global increase in MenW (*3*,*5*). Mirroring international trends in invasive bacterial disease during the COVID-19 pandemic (*26*–*28*), there was a sharp decrease in cases of pediatric IMD in NZ in 2020 after national COVID-19 control measures began, and that decrease continued through 2021 (*29*). Future patterns of pediatric IMD remain uncertain; however, there is a risk of resurgent disease exacerbated by rising poverty and socioeconomic inequity (*30*).

Our findings highlight the severity of IMD. One third of the cases we studied included admission to an ICU, comparable with data for international cohorts (*8*,*31*). Over half of those cases required invasive ventilation or inotropic/vasopressor support. The CFR in our cohort was 4.1%, which compares to rates for other high-income settings of 2%–12% (*1*). Sequelae occurred in 23.6% of survivors. Because outcome was classified as unknown for 48 cases that lacked audiologic data but had no other reported sequelae, we might have overestimated the proportion of survivors with sequelae. Our study revealed that 1 in 4 children did not receive an audiology assessment after meningococcal meningitis. Given this finding, we strongly recommend that children in New Zealand who are diagnosed with meningococcal meningitis receive audiology assessment before hospital discharge. Active follow-up for survivors of IMD should focus on confirming audiology assessment and screening for neurologic, developmental, and psychological effects (*2*,*9*). Our lack of access to mental health and

Table 3. Univariate logistic regression for combined outcome of death or sequelae in 271 confirmed cases of invasive meningococcal disease in children <15 years of age, Auckland, New Zealand, 2004–2020*

Variable	No. cases (%)	OR (95% CI)	p value
Ethnicity, compared with non-Māori, non-Pacific population			
Pacific	38/118 (32.2)	2.91 (1.31–7.18)	0.0128
Māori	28/96 (29.2)	2.52 (1.10–6.35)	0.0366
Reduced penicillin susceptibility	12/64 (18.8)	0.548 (0.25–1.14)	0.117
NZDep quintile†	271	1.21 (0.95–1.58)	0.142
Age, mo†	271	0.996 (0.99–1.00)	0.157
Serogroup, compared with MenB			
MenC	7/18 (38.9)	1.80 (0.64–4.82)	0.247
MenW	6/25 (24.0)	0.89 (0.31–2.24)	0.822
MenY	3/8 (37.5)	1.70 (0.34–7.16)	0.478
Male sex, compared with female	50/168 (29.8)	1.39 (0.80–2.48)	0.248
Season, compared with autumn			
Spring	23/76 (30.3)	1.47 (0.64–3.60)	0.374
Summer	11/35 (31.4)	1.56 (0.57–4.31)	0.386
Winter	30/116 (25.9)	1.19 (0.54–2.79)	0.683
MeNZB vaccination, compared with fully vaccinated			
Unvaccinated	43/166 (25.9)	0.76 (0.39–1.51)	0.425
Partially vaccinated	12/41 (29.3)	0.90 (0.37–2.17)	0.817
Prehospital parenteral antibiotic treatment	10/44 (22.7)	0.79 (0.35–1.64)	0.537
Sepsis criteria	39/145 (26.9)	1.14 (0.51–2.77)	0.751

*Men, *Neisseria meningitidis* serogroup; OR, odds ratio; NZDep, New Zealand Index of Deprivation
†Continuous variable; OR represents increase in odds for each unit increase in variable.

educational data and shorter follow-up durations of ≥3 months might have underestimated the prevalence of long-term neurocognitive and psychological effects. Our data demonstrate the usefulness of PCR for diagnosing culture-negative IMD (*32*,*33*). Blood culture results were negative in 79% of children who received prehospital antibiotics. However, when performed, *N. meningitidis* blood PCR was positive in all those cases. Drew et al. similarly reported positive blood PCR in 25 of 28 IMD cases that had a negative blood culture after intramuscular penicillin (*32*). We suggest that clinicians consider using *N. meningitidis* PCR testing, especially in the context of prior antibiotic administration. We found no statistically significant differences in clinical outcomes between children who received prehospital parenteral antibiotics and those who did not; however, our study was not powered to detect a difference in those outcomes.

In our cohort, bacteremia and meningitis coexisted in 44.2% of cases; we propose that CSF testing be carefully considered for those with proven meningococcal bacteremia, especially in infants. In cases with bacteremia, 85.9% had a rash at first examination; rash characteristics included purpura (50.7%), petechiae without purpura (40.4%), and blanching only (8.9%), findings similar to those reported for a pediatric cohort in Ireland (*9*). Whereas a classic purpuric or petechial rash can suggest IMD, rash at presentation might be nonspecific or absent. It is therefore important for clinicians to maintain a high index of suspicion of IMD in children with suspected sepsis without rash.

In our cohort, we noted an increase over time in the proportion of isolates with reduced penicillin susceptibility. Similar trends have been reported among adults in Auckland, as well as in Spain and Australia (*34*–*36*). Earlier literature reported an association between reduced penicillin susceptibility and increased complications (*37*); however, no difference in outcomes were noted for our pediatric cohort or for the Auckland adult cohort (*34*). New Zealand guidelines recommend a third-generation cephalosporin for empiric treatment of sepsis in children (*38*). Because all isolates we studied were ceftriaxone-susceptible, reduced penicillin susceptibility is unlikely to have clinical significance for empiric therapy in New Zealand.

Our study illustrates the considerable inequity of IMD in the Auckland region of New Zealand. Māori and Pacific children had disproportionately higher rates of IMD and were more likely to experience complications. All but 1 death occurred in Māori or Pacific children. Children living in Auckland's most deprived 20% of neighborhoods had rates of IMD 17 times higher than those in the least deprived 20% of neighborhoods. The relationship between ethnicity, socioeconomic deprivation, and the risk of severe childhood infections is not well understood but is likely rooted in the ongoing effects of colonization and structural racism (*39*). Recent findings from a nationally representative longitudinal study, Growing Up in New Zealand (*40*), indicate that disparities in infectious disease hospitalizations among infants of Māori or Pacific peoples can be only partly explained by socioeconomic deprivation factors. Nonetheless, household crowding has been shown to be strongly associated with epidemic IMD in New Zealand (*41*). Urgent action is needed to honor the nation's commitment to Te Tiriti o Waitangi, the 1840 founding document that established bicultural partnership between indigenous Māori and the British Crown.

Addressing the upstream determinants of health is important, but vaccination remains the best strategy to control IMD and is a key method for reducing inequity (*4*,*5*,*42*). Although New Zealand's universal vaccination programs have not yet resulted in equitable uptake, prioritizing delivery and implementation might improve coverage and outcomes for those most at risk (*43*). Despite having the highest rate of MenB in the world and some prior success with MeNZB immunization, New Zealand has not yet included 4CMenB in the National Immunization Schedule nor funded vaccine for children at highest risk of disease. The real-world evidence for 4CMenB is clear and demonstrates that control of IMD in New Zealand is within reach (*15*).

In conclusion, IMD remains a severe, life-threatening disease in young children in New Zealand; Māori and Pacific infants and those living in areas of socioeconomic deprivation are at greatest risk.The recent increase in incidence of MenB IMD highlights the urgent case for inclusion of 4CMenB in the National Immunization Schedule. Using *N. meningitidis* PCR to aid diagnosis of culture-negative, clinically suspected IMD, along with routine inpatient audiology assessment after cases of meningococcal meningitis, may improve clinical outcomes.

Acknowledgments

We thank Sara Johansson and Maria Hansen for their contribution to data collection during their elective attachment in New Zealand, Heather Davies and Kristin Dyet for provision and advice on case details, Sharon Arrol for provision and advice on population statistics, Andrew Anglemyer for assistance with statistical methods, Andrew Lavery for technical editing, and the Stevenson Foundation for providing support for a research fellow position at Te Whatu Ora Counties Manukau.

This work is sincerely dedicated to our tamariki, rangatahi, and whānau who have been affected by meningococcal disease. It has been an honor to tell your stories. *He waka eke noa.*

C.B. completed a portion of this research while employed as a research fellow by Te Whatu Ora Counties Manukau in 2019, through a charitable grant through the Stevenson Foundation. A payment of $2,000 USD was received from the University of Gothenburg, Sweden, to cover supervision costs for the elective medical students S.J. and M.H.. The New Zealand Ministry of Health funds E.S.R.'s national IMD surveillance, including epidemiological typing and antimicrobial susceptibility testing. The remaining authors report no conflicts of interest.

About the Author

Dr. Burton is a general pediatrician and PhD student at the University of Auckland who works part-time as a pediatrician at Kidz First Hospital, Te Whatu Ora Counties Manukau.

References

1. Wang B, Santoreneos R, Giles L, Haji Ali Afzali H, Marshall H. Case fatality rates of invasive meningococcal disease by serogroup and age: A systematic review and meta-analysis. Vaccine. 2019;37:2768–82. https://doi.org/10.1016/j.vaccine.2019.04.020
2. Olbrich KJ, Müller D, Schumacher S, Beck E, Meszaros K, Koerber F. Systematic review of invasive meningococcal disease: sequelae and quality of life impact on patients and their caregivers. Infect Dis Ther. 2018;7:421–38. https://doi.org/10.1007/s40121-018-0213-2
3. Institute of Environmental Science and Research. Invasive meningococcal disease quarterly report: January–December 2019. 2020 [cited 2022 Feb 26]. https://surv.esr.cri.nz/PDF_surveillance/MeningococcalDisease/2019/MeningococcalDisease_Q4_2019.pdf
4. Lennon D, Reid S, Stewart J, Jackson C, Crengle S, Percival T. Reducing inequalities with vaccines: New Zealand's MeNZB vaccine initiative to control an epidemic. J Paediatr Child Health. 2012;48:193–201. https://doi.org/10.1111/j.1440-1754.2010.01969.x
5. Parikh SR, Campbell H, Bettinger JA, Harrison LH, Marshall HS, Martinon-Torres F, et al. The everchanging epidemiology of meningococcal disease worldwide and the potential for prevention through vaccination. J Infect. 2020;81:483–98. https://doi.org/10.1016/j.jinf.2020.05.079
6. Nadel S. Treatment of meningococcal disease. J Adolesc Health. 2016;59(suppl):S21–8. https://doi.org/10.1016/j.jadohealth.2016.04.013
7. Schlapbach LJ, Straney L, Alexander J, MacLaren G, Festa M, Schibler A, et al.; ANZICS Paediatric Study Group. Mortality related to invasive infections, sepsis, and septic shock in critically ill children in Australia and New Zealand, 2002–13: a multicentre retrospective cohort study. Lancet Infect Dis. 2015;15:46–54. https://doi.org/10.1016/S1473-3099(14)71003-5
8. Ó Maoldomhnaigh C, Drew RJ, Gavin P, Cafferkey M, Butler KM. Invasive meningococcal disease in children in Ireland, 2001–2011. Arch Dis Child. 2016;101:1125–9. https://doi.org/10.1136/archdischild-2015-310215
9. Vyse A, Anonychuk A, Jäkel A, Wieffer H, Nadel S. The burden and impact of severe and long-term sequelae of meningococcal disease. Expert Rev Anti Infect Ther. 2013;11:597–604. https://doi.org/10.1586/eri.13.42
10. Sridhar S, Greenwood B, Head C, Plotkin SA, Sáfadi MA, Saha S, et al. Global incidence of serogroup B invasive meningococcal disease: a systematic review. Lancet Infect Dis. 2015;15:1334–46. https://doi.org/10.1016/S1473-3099(15)00217-0
11. Arnold R, Galloway Y, McNicholas A, O'Hallahan J. Effectiveness of a vaccination programme for an epidemic of meningococcal B in New Zealand. Vaccine. 2011;29:7100–6. https://doi.org/10.1016/j.vaccine.2011.06.120
12. Mills C, Penney L. The Northland emergency meningococcal C vaccination programme. N Z Med J. 2013;126:30–9.
13. New Zealand Ministry of Health. Meningococcal W information release. 2019 [cited 2022 Dec 8]. https://www.health.govt.nz/about-ministry/information-releases/general-information-releases/meningococcal-w-information-release
14. Statistics New Zealand. NZ.Stat [cited 2022 Dec 8]. https://www.stats.govt.nz/tools/nz-dot-stat
15. Martinón-Torres F, Banzhoff A, Azzari C, De Wals P, Marlow R, Marshall H, et al. Recent advances in meningococcal B disease prevention: real-world evidence from 4CMenB vaccination. J Infect. 2021;83:17–26. https://doi.org/10.1016/j.jinf.2021.04.031
16. Marshall HS, McMillan M, Koehler AP, Lawrence A, Sullivan TR, MacLennan JM, et al. Meningococcal B vaccine and meningococcal carriage in adolescents in Australia. N Engl J Med. 2020;382:318–27. https://doi.org/10.1056/NEJMoa1900236
17. Ladhani SN, Campbell H, Andrews N, Parikh SR, White J, Edelstein M, et al. First real world evidence of meningococcal group B vaccine, 4CMenB, protection against meningococcal group W disease: prospective enhanced national surveillance, England. Clin Infect Dis. 2021;73:e1661–8. https://doi.org/10.1093/cid/ciaa1244
18. Petousis-Harris H, Paynter J, Morgan J, Saxton P, McArdle B, Goodyear-Smith F, et al. Effectiveness of a group B outer membrane vesicle meningococcal vaccine against gonorrhoea in New Zealand: a retrospective case-control study. Lancet. 2017;390:1603–10. https://doi.org/10.1016/S0140-6736(17)31449-6
19. Ministry of Health New Zealand. National Health Index [cited 2022 Dec 8]. https://www.health.govt.nz/our-work/health-identity/national-health-index
20. Ministry of Health New Zealand. National Immunisation Register [cited 2022 Dec 8]. https://www.health.govt.nz/our-work/preventative-health-wellness/immunisation/national-immunisation-register
21. Mathias B, Mira JC, Larson SD. Pediatric sepsis. Curr Opin Pediatr. 2016;28:380–7. https://doi.org/10.1097/MOP.0000000000000337
22. Statistics New Zealand. Stats NZ population projections (projections produced by Statistics New Zealand according to assumptions specified by the Ministry of Health). New Zealand: Statistics New Zealand; 2020 [cited 2022 May 13]. https://www.stats.govt.nz
23. New Zealand Ministry of Health. HISO 10001:2017 ethnicity data protocols. 2017 [cited 2022 May 13]. https://www.health.govt.nz/publication/hiso-100012017-ethnicity-data-protocols
24. Environmental Health Intelligence New Zealand. Socioeconomic deprivation profile [cited 2022 May 13].

https://www.ehinz.ac.nz/indicators/population-vulnerability/socioeconomic-deprivation-profile
25. Clinical and Laboratory Standards Institute. Performance standards for antimicrobial susceptibility testing. 27th ed. CLSI supplement M100. Wayne (PA): The Institute; 2017.
26. Brueggemann AB, Jansen van Rensburg MJ, Shaw D, McCarthy ND, Jolley KA, Maiden MCJ, et al. Changes in the incidence of invasive disease due to *Streptococcus pneumoniae*, *Haemophilus influenzae*, and *Neisseria meningitidis* during the COVID-19 pandemic in 26 countries and territories in the Invasive Respiratory Infection Surveillance Initiative: a prospective analysis of surveillance data. Lancet Digit Health. 2021;3:e360–70. https://doi.org/10.1016/S2589-7500(21)00077-7
27. Kadambari S, Goldacre R, Morris E, Goldacre MJ, Pollard AJ. Indirect effects of the covid-19 pandemic on childhood infection in England: population based observational study. BMJ. 2022;376:e067519. https://doi.org/10.1136/bmj-2021-067519
28. Deghmane AE, Taha MK. Changes in invasive *Neisseria meningitidis* and *Haemophilus influenzae* infections in France during the COVID-19 pandemic. Microorganisms.2022; 10:907. https://doi.org/10.3390/microorganisms10050907
29. Institute of Environmental Science and Research. Invasive meningococcal disease monthly report: October 2022 [cited 2022 Dec 8]. https://surv.esr.cri.nz/PDF_surveillance/MeningococcalDisease/2022/Meningococcal_disease_monthly_report_October2022.pdf
30. Duncanson M, Roy M, van Asten H, Oben G, Wicken A, Tustin K, et al. Child poverty monitor 2022 technical report. NZ Child and Youth Epidemiology Service University of Otago, Dunedin [cited 2022 Dec 8]. https://nzchildren.co.nz
31. Parikh SR, Campbell H, Gray SJ, Beebeejaun K, Ribeiro S, Borrow R, et al. Epidemiology, clinical presentation, risk factors, intensive care admission and outcomes of invasive meningococcal disease in England, 2010–2015. Vaccine. 2018;36:3876–81. https://doi.org/10.1016/j.vaccine.2018.02.038
32. Drew RJ, Ó Maoldomhnaigh C, Gavin PJ, O'Sullivan N, Butler KM, Cafferkey M. The impact of meningococcal polymerase chain reaction testing on laboratory confirmation of invasive meningococcal disease. Pediatr Infect Dis J. 2012;31:316–8. https://doi.org/10.1097/INF.0b013e318241f824
33. Heinsbroek E, Ladhani S, Gray S, Guiver M, Kaczmarski E, Borrow R, et al. Added value of PCR-testing for confirmation of invasive meningococcal disease in England. J Infect. 2013;67:385–90. https://doi.org/10.1016/j.jinf.2013.06.007
34. Broom M, Best E, Heffernan H, Svensson S, Hansen Hygstedt M, Webb R, et al. Outcomes of adults with invasive meningococcal disease with reduced penicillin susceptibility in Auckland 2004–2017. Infection. 2022. https://doi.org/10.1007/s15010-022-01897-6
35. Latorre C, Gené A, Juncosa T, Muñoz C, González-Cuevas A. *Neisseria meningitidis*: evolution of penicillin resistance and phenotype in a children's hospital in Barcelona, Spain. Acta Paediatr. 2000;89:661–5. https://doi.org/10.1111/j.1651-2227.2000.tb00360.x
36. Lahra MM, Hogan TR. Australian Meningococcal Surveillance Programme annual report, 2019. Commun Dis Intell. 2018;2020:44. [
37. Pérez-Trallero E, Aldamiz-Echeverria L, Pérez-Yarza EG. Meningococci with increased resistance to penicillin. Lancet. 1990;335:1096. https://doi.org/10.1016/0140-6736(90)92668-8
38. Shepherd M, McCarthy B, Fong MS. Starship Clinical Guidelines: Sepsis [cited 2022 Dec 8]. https://starship.org.nz/guidelines/sepsis
39. Hobbs M, Ahuriri-Driscoll A, Marek L, Campbell M, Tomintz M, Kingham S. Reducing health inequity for Māori people in New Zealand. Lancet. 2019;394:1613–4. https://doi.org/10.1016/S0140-6736(19)30044-3
40. Hobbs MR, Morton SM, Atatoa-Carr P, Ritchie SR, Thomas MG, Saraf R, et al. Ethnic disparities in infectious disease hospitalisations in the first year of life in New Zealand. J Paediatr Child Health. 2017;53:223–31. https://doi.org/10.1111/jpc.13377
41. Baker M, McNicholas A, Garrett N, Jones N, Stewart J, Koberstein V, et al. Household crowding a major risk factor for epidemic meningococcal disease in Auckland children. Pediatr Infect Dis J. 2000;19:983–90. https://doi.org/10.1097/00006454-200010000-00009
42. Petousis-Harris H, Howe AS, Paynter J, Turner N, Griffin J. Pneumococcal conjugate vaccines turning the tide on inequity: a retrospective cohort study of New Zealand children born 2006–2015. Clin Infect Dis. 2019;68:818–26. https://doi.org/10.1093/cid/ciy570
43. Sinclair O, Russell J, de Lore D, Andersen E, Percival T, Wiles S. The urgent need for an equitable COVID-19 paediatric vaccine roll-out to protect tamariki Māori. N Z Med J. 2021;134:8–15.

Address for correspondence: Cameron Burton, Kidz First Children's Hospital, 100 Hospital Rd, Auckland, New Zealand; email: cameron.burton@auckland.ac.nz

Nocardia pseudobrasiliensis Co-infection in SARS-CoV-2 Patients

Daniel Beau Stamos, Aldo Barajas-Ochoa, Jillian E. Raybould

Medscape CME Activity

In support of improving patient care, this activity has been planned and implemented by Medscape, LLC and Emerging Infectious Diseases. Medscape, LLC is jointly accredited with commendation by the Accreditation Council for Continuing Medical Education (ACCME), the Accreditation Council for Pharmacy Education (ACPE), and the American Nurses Credentialing Center (ANCC), to provide continuing education for the healthcare team.

Medscape, LLC designates this Journal-based CME activity for a maximum of 1.00 ***AMA PRA Category 1 Credit(s)™***. Physicians should claim only the credit commensurate with the extent of their participation in the activity.

Successful completion of this CME activity, which includes participation in the evaluation component, enables the participant to earn up to 1.0 MOC points in the American Board of Internal Medicine's (ABIM) Maintenance of Certification (MOC) program. Participants will earn MOC points equivalent to the amount of CME credits claimed for the activity. It is the CME activity provider's responsibility to submit participant completion information to ACCME for the purpose of granting ABIM MOC credit.

All other clinicians completing this activity will be issued a certificate of participation. To participate in this journal CME activity: (1) review the learning objectives and author disclosures; (2) study the education content; (3) take the post-test with a 75% minimum passing score and complete the evaluation at http://www.medscape.org/journal/eid; and (4) view/print certificate. For CME questions, see page 875.

Release date: March 22, 2023; Expiration date: March 22, 2024

Learning Objectives

Upon completion of this activity, participants will be able to:

- Determine the clinical features and predisposing factors for nocardiosis and COVID-19 coinfection, based on a case report of SARS-CoV-2 coinfection with pulmonary *Nocardia pseudobrasiliensis* and a literature review
- Assess the course and treatment of nocardiosis and COVID-19 coinfection, based on a case report of SARS-CoV-2 coinfection with pulmonary *Nocardia pseudobrasiliensis* and a literature review
- Evaluate the clinical implications of the features, course, treatment, and predisposing factors for nocardiosis and COVID-19 coinfection, based on a case report of SARS-CoV-2 coinfection with pulmonary *Nocardia pseudobrasiliensis* and a literature review

CME Editor

Dana C. Dolan, BS, Technical Writer/Editor, Emerging Infectious Diseases. *Disclosure: Dana C. Dolan, BS, has no relevant financial relationships.*

CME Author

Laurie Barclay, MD, freelance writer and reviewer, Medscape, LLC. *Disclosure: Laurie Barclay, MD, has no relevant financial relationships.*

Authors

Daniel Beau Stamos, BS; Aldo Barajas-Ochoa, MD; and ***Jillian E. Raybould, MD***.

Author affiliation: Virginia Commonwealth University Health System, Richmond, Virginia, USA.

DOI: https://doi.org/10.3201/eid2904.221439

During the SARS-CoV-2 pandemic, few cases of Nocardia spp. co-infection have been reported during or after a COVID-19 infection. Nocardia spp. are gram-positive aerobic actinomycetes that stain partially acid-fast, can infect immunocompromised patients, and may cause disseminated disease. We present the case of a 52-year-old immunocompromised man who developed Nocardia pseudobrasiliensis pneumonia after a SARS-CoV-2 infection, and we summarize the current literature for nocardiosis and SARS-CoV-2 co-infections. Nocardia spp. infection should remain on the differential diagnosis of pneumonia in immunocompromised hosts, regardless of other co-infections. Sulfonamide–carbapenem combinations are used as empiric therapy for nocardiosis; species identification and susceptibility testing are required to select the optimal treatment for each patient.

Nocardia pseudobrasiliensis are gram-positive aerobic actinomycetes; stains of *N. pseudobrasiliensis* are partially acid fast (*1*). As with other *Nocardia* species, *N. pseudobrasiliensis* can infect immunocompromised patients and may cause disseminated disease (*2*). Risk factors for nocardiosis include immunosuppression caused by solid organ or hematopoietic cell transplantation, glucocorticoid therapy, chronic lung disease, diabetes, AIDS, and malignancy (*3*,*4*). Infection by other pathogens during or after SARS-CoV-2 infection is a known but relatively uncommon occurrence. Nocardiosis co-infection with SARS-CoV-2 is rarely reported. We describe a case of SARS-CoV-2 co-infection with pulmonary *Nocardia pseudobrasiliensis* and summarize the literature on nocardiosis and COVID-19 co-infection.

Case Report

A 52-year-old man sought care at the emergency department at Virginia Commonwealth University Health System (Richmond, Virginia, USA) in July 2022 because of increased work of breathing after a positive home COVID-19 test. The patient's symptoms began 10 days before admission. He reported that he had not experienced fevers, chills, sore throat, abdominal pain, or diarrhea. He was admitted for the management of hypoxia caused by COVID-19 pneumonia. His medical history included type 2 diabetes mellitus treated with empagliflozin, bronchiectasis, and multisystem sarcoidosis. His sarcoidosis was first diagnosed in 2011 by lung biopsy and had progressed to stage IV pulmonary sarcoidosis by 2019. An implantable cardioverter defibrillator was placed in 2019 to address cardiac sarcoidosis. For his sarcoidosis, the patient received oral hydroxychloroquine (200 mg 2×/d) and intravenous (IV) infliximab (800 mg every 8 wk). He was a former smoker who stopped 30 years earlier; he had a job as an apartment maintenance worker.

At the time of admission, the patient was hemodynamically stable and afebrile. Pertinent physical examination findings included increased work of breathing and wheezing. Cardiac and pulmonary examination were otherwise unremarkable. Chest radiograph showed findings related to sarcoidosis without acute cardiopulmonary disease. On hospital day 1, he started COVID-19 treatment with intravenous remdesivir (200 mg/d) and dexamethasone (6 mg/d). However, his hypoxia progressed; by hospitalization day 2, he required 5 L/min of oxygen delivered by face mask. Remdesivir was discontinued because of gastrointestinal side effects. Laboratory testing revealed a leukocyte count of 10.1×10^9 cells/L, a C-reactive protein concentration of 15.0 mg/dL, and a positive COVID-19 PCR test.

Because the patient's hypoxia continued to worsen, we obtained a chest computed tomography scan without IV contrast on hospital day 5. Imaging revealed progressive consolidative opacities bilaterally, most pronounced in the lung bases without a ground glass appearance (Figure 1, panel B). We obtained sputum cultures and started the patient on intravenous piperacillin/tazobactam (3.375 g every 6 h) to treat suspected bacterial pneumonia.

On hospital day 7, sputum Gram stain revealed beaded, gram-positive rods concerning for *Nocardia* spp. (Figure 2, panel A). The patient's antimicrobial treatments were transitioned to intravenous trimethoprim/sulfamethoxazole (TMP/SMX) (5 mg/kg every 8 h) and imipenem (500 mg every 6 h) pending confirmation of suspected *Nocardia* spp. Despite dual therapy, the patient's hypoxia persisted; a repeat chest CT without IV contrast on hospital day 12 showed progression of a consolidative nodular opacity in the left lung base (Figure 1, panel C). Because the patient was not responding to treatment, we added oral linezolid (600 mg every 12 h) to his antimicrobial regimen.

After initiation of linezolid with continued imipenem and TMP/SMX therapy, the patient demonstrated gradual improvement; his hypoxia eventually resolved. On hospital day 16, species identification with matrix-assisted laser desorption/ionization time-of-flight mass spectrometry confirmed *N. pseudobrasiliensis*. Colonies from the *Nocardia* culture plate had the characteristic chalky white appearance and orange pigmentation (Figure 2, panel B). The susceptibility profile (conducted using broth dilution by LabCorp) demonstrated imipenem resistance (Table 1). Because the resistance to imipenem and hyperkalemia was likely caused by TMP/SMX, the patient was discharged on hospital day 20 on linezolid (600 mg 2×/d) and ciprofloxacin (500 mg 2×/d) with plans to continue dual therapy

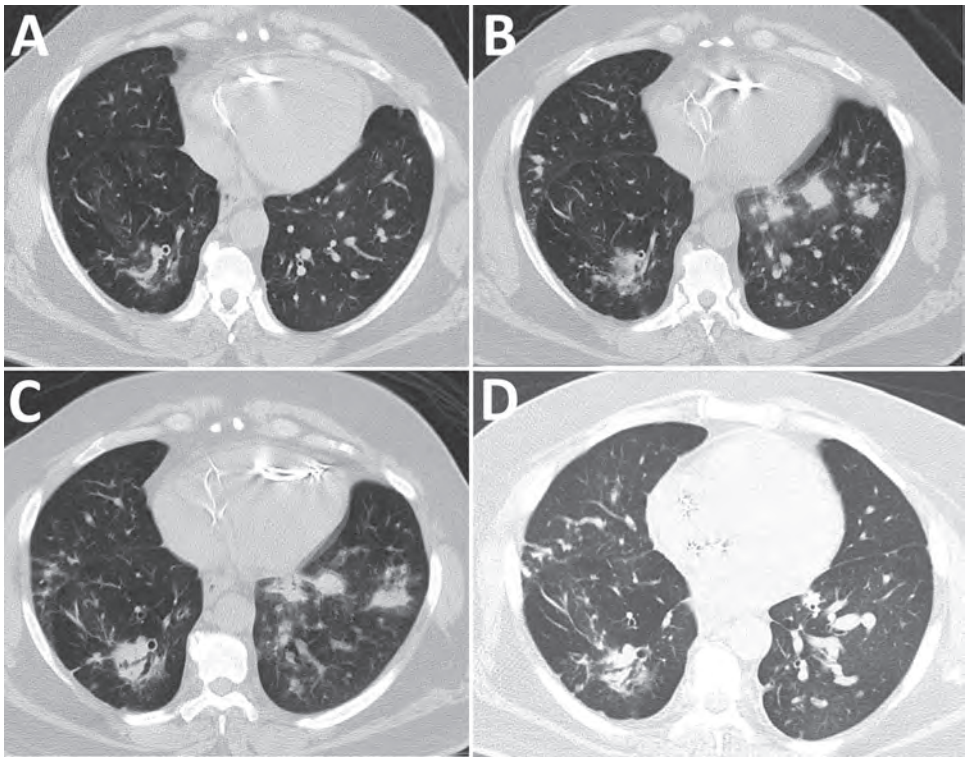

Figure 1. Computed tomography of the chest without contrast showing progression of illness in a 52-year-old immunocompromised man who experienced *Nocardia pseudobrasiliensis* pneumonia after a SARS-CoV-2 infection. A) Scan obtained 4 months before patient sought care. B) Scan on hospitalization day 5 shows development of lung nodules without ground-glass opacities in both lungs. C) Scan on hospitalization day 12 shows progression of nodules on the left lung. D) Scan obtained 28 days after discharge shows improvement of pulmonary nodules.

for ≥6 weeks after discharge. Of note, a magnetic resonance image of the brain with contrast, which we performed before discharge, did not show ring-enhancing lesions or signs of central nervous system nocardiosis. At the 2-week follow-up visit, the patient's shortness of breath improved and he no longer needed supplemental oxygen at rest but did intermittently require supplemental oxygen on exertion. Imaging at 28 days after discharge showed improvement of the pulmonary nodules (Figure 1, panel D). After a month of outpatient treatment, the patient's symptoms continued to improve, but he experienced a break in therapy for 2 weeks because of financial constraints, after which the linezolid was switched to TMP/SMX (2 double-strength tablets of 160 mg TMP and 800 SMX every 8 h) and oral ciprofloxacin (500 mg 2×/d). After discussion with the patient, we decided to continue dual antimicrobial therapy because of his need to continue taking glucocorticoids for his sarcoidosis. At follow-up 4 months after discharge, the patient reported dyspnea only with heavy exertion and no medication side effects. He would undergo repeat imaging of the chest with plans to transition to TMP/SMX monotherapy if the imaging shows significant improvement of the pulmonary nodules.

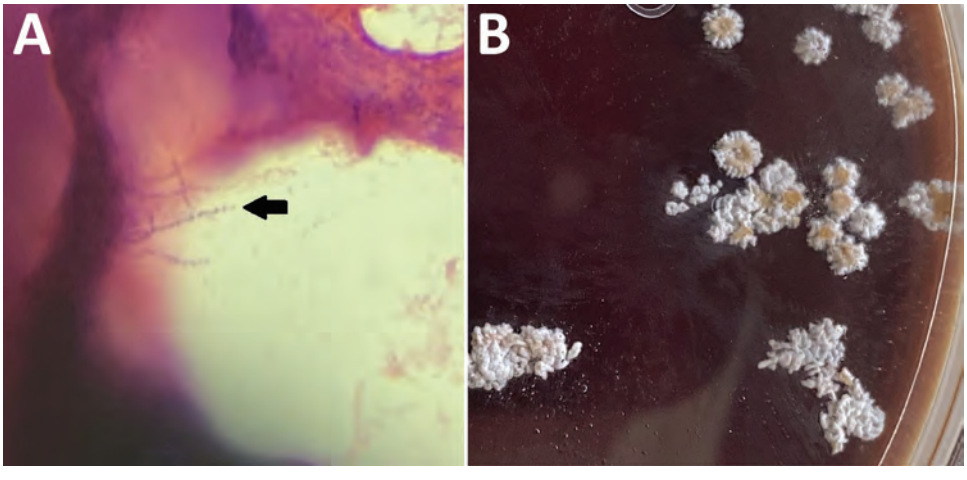

Figure 2. Histopathology of samples from a 52-year-old immunocompromised man who experienced *Nocardia pseudobrasiliensis* pneumonia after a SARS-CoV-2 infection. A) Branching gram-positive rods (arrow) seen in Gram stain of *Nocardia* culture plate. Original magnification ×100. B) *N. pseudobrasiliensis* colonies seen on a *Nocardia* culture plate with characteristic chalky white and orange pigmentation.

Table 1. Reported susceptibility of *Nocardia pseudobrasiliensis* bacteria to antimicrobial drugs*

Antimicrobial drug	This study	Case 1†	Case 2†	Case 3†	Case 4†	Case 5†	Case 6†	Case 7‡
Amikacin	S	R	S	II	S	S	S	VSR or II
Amoxi-clav	R	R	II	S	R	R	R	R
Ceftriaxone	I	R	R	II	S	S	R	VSR or II
Ciprofloxacin	S	S	S	S	S	S	S	II
Clarithromycin	S	S	II	S	S	S	S	S
Doxycycline	R	R	II	II	II	R	R	II
Imipenem	R	R	R	R	II	R	R	VSR or II
Linezolid	S	S	S	II	II	S	S	S
Minocycline	R	R	II	II	M	R	R	II
Moxifloxacin	S	S	II	II	II	S	II	II
Tobramycin	S	II	II	II	II	II	II	II
TMP/SMX	S	R	R	II	S§	R	S	S

*Amoxi-clav, amoxicillin/clavulanic acid; I, intermediate; II, insufficient information; M, moderate; R, resistant; S, susceptible; TMP/SMX, trimethoprim/sulfamethoxazole; VSR, variable susceptibility results.
†Veerappan Kandasamy et al. (*2*).
‡Wilson et al. (*3*).
§This specimen was susceptible to SMX only.

Discussion

This patient had a previous COVID-19 infection and multiple other risk factors for pulmonary nocardiosis, including diabetes mellitus, bronchiectasis, and immunosuppression caused by sarcoidosis treatment. To date, 10 cases of nocardiosis during or shortly after COVID-19 infection have been reported (Table 2, https://wwwnc.cdc.gov/EID/article/29/4/22-1439-T2.htm). All patients had risk factors that predisposed them to infection with *Nocardia* spp. (*2*–*4*). Most patients experienced nocardiosis 5–50 days after their SARS-CoV-2 diagnosis; average time to co-infection identification was 17 days. One immunosuppressed patient experienced brain nocardiosis 200 days after their initial COVID-19 diagnosis but had persistently tested positive by reverse transcription PCR for SARS-CoV-2 during that time. Of note, all patients received glucocorticoids during their hospitalizations.

Pulmonary nocardiosis was the most common site of infection, occurring in 7 patients. Central nervous system nocardiosis occurred in 4 patients. Five different species of *Nocardia* were identified, but *N. farcinica* was the most frequently isolated species. This heterogeneity likely explains why each patient was ultimately discharged on a different antimicrobial regimen (Table 2); *Nocardia* species have unique susceptibilities (*2*,*3*,*14*). Our patient's delayed clinical improvement until the addition of linezolid highlights the clinical importance of *Nocardia* species identification and susceptibilities. Ciprofloxacin, clarithromycin, and linezolid are typically effective against *N. pseudobrasiliensis*, whereas TMP/SMX susceptibility varies between cases (Table 1).

The overall risk for all-cause co-infection in patients with COVID-19 appears to be low. A cohort study by Garcia-Vidal et al. (*15*) analyzed 989 patients admitted to the hospital with COVID-19 and found that only 31 patients had a community-acquired co-infection at the time of COVID-19 diagnosis; 25/31 patients had bacterial co-infections. Garcia-Vidal et al. also observed 51 total cases of hospital-acquired co-infections diagnosed in 43 patients; 44/51 cases were bacterial co-infections. However, when focusing on COVID-19 patients requiring invasive mechanical ventilation, the incidence of co-infection appears to be higher. Søvik et al. (*16*) reviewed 156 patients who required mechanical ventilation while infected with COVID-19 and evaluated those patients for co-infection. A total of 67 patients experienced 90 co-infections, 78% of which involved the lower airways; no *Nocardia* spp. infections were reported. Co-infection was strongly associated with dexamethasone use, underlying autoimmune disease, and length of intensive care stay (*16*). Despite these findings, mechanical ventilation was unlikely to be an independent predisposing factor for pulmonary nocardiosis; 1 patient required mechanical ventilation during their hospitalization.

Analytical epidemiologic studies are needed to assess whether SARS-CoV-2 infection is an independent risk factor for nocardiosis. However, mechanical and immune mechanisms after COVID-19 infection may play a role in *Nocardia* spp. co-infection. Paget and Trottein (*17*) recently described how influenza virus infection can cause direct or indirect damage to the respiratory barrier, creating conditions for bacterial attachment and translocation, and lead to macrophage, neutrophil, and natural killer cell dysfunction which result in poor bacterial control. COVID-19 infection might promote co-infections by opportunistic pathogens such as *Nocardia* spp. although these mechanisms are not well studied. Because nocardiosis is rarely transmitted in the nosocomial setting (*4*), the patients identified in this series were likely colonized with *Nocardia* spp. before admission; all of the patients had factors that made them immunocompromised and received steroids before

receiving their *Nocardia* diagnosis (Table 2). It is possible that a COVID-19 infection and the glucocorticoid therapy used to treat it synergistically trigger *Nocardia* spp. co-infection in patients who are already chronically immunocompromised because of the combination of additional immunosuppression and permissive parenchymal conditions. Although a synergistic relationship between COVID-19 and glucocorticoid use is plausible, the data in this study are observational; analytical studies would further clarify the association.

In summary, *Nocardia* bacteria can be a cause of co-infection in patients with COVID-19 pneumonia that may present as further respiratory deterioration. However, *Nocardia* spp. has not been reported in reviews as a cause of co-infection in patients with COVID-19 pneumonia (*16*,*18*,*19*). Immunocompromised patients, such as those on glucocorticoid therapy, those who have received solid organ or hematopoietic cell transplantation, and those positive for HIV, are at higher risk for nocardiosis. Clinicians should include nocardiosis in the differential diagnosis for immunosuppressed patients with severe pneumonia and assess for disseminated disease and central nervous system involvement, especially in the context of potent steroid use to treat immunocompromised patients with COVID-19. Sulfonamide–carbapenem combinations are used as empiric therapy for nocardiosis, but species identification and susceptibility testing are required to select optimal treatment.

About the Author

Mr. Stamos is a fourth-year medical student at Virginia Commonwealth University. His clinical interests include hematology/oncology, autoimmunity, and opportunistic infections.

References

1. Wallace RJ Jr, Brown BA, Blacklock Z, Ulrich R, Jost K, Brown JM, et al. New Nocardia taxon among isolates of *Nocardia brasiliensis* associated with invasive disease. J Clin Microbiol. 1995;33:1528–33. https://doi.org/10.1128/jcm.33.6.1528-1533.1995
2. Veerappan Kandasamy V, Nagabandi A, Horowitz EA, Vivekanandan R. Multidrug-resistant *Nocardia pseudobrasiliensis* presenting as multiple muscle abscesses. BMJ Case Rep. 2015;2015:bcr2014205262. https://doi.org/10.1136/bcr-2014-205262
3. Wilson JW. Nocardiosis: updates and clinical overview. Mayo Clin Proc. 2012;87:403–7. https://doi.org/10.1016/j.mayocp.2011.11.016
4. Saubolle MA, Sussland D. Nocardiosis. J Clin Microbiol. 2003;41:4497–501. https://doi.org/10.1128/JCM.41.10.4497-4501.2003
5. Colaneri M, Lupi M, Sachs M, Ludovisi S, Di Matteo A, Pagnucco L, et al. A challenging case of SARS-CoV-2- AIDS and nocardiosis coinfection from the SMatteo COvid19 REgistry (SMACORE). New Microbiol. 2021;44:129–34.
6. Arif M, Talon A, Sarma H, Munoz J, Charley E. Nocardia after COVID-19 infection. Chest. 2021;160(Supplement):A429. https://doi.org/10.1016/j.chest.2021.07.424
7. Atemnkeng F, Ducey J, Khalil A, Elemam A, Diaz K. Diagnosing disseminated nocardiosis in a patient with COVID-19 pneumonia. J Med Cases. 2021;12:319–24. https://doi.org/10.14740/jmc3716
8. Kaur T, Bhatti W. Complications of high-dose steroids in COVID-19. Chest. 2021;160(Supplement):A490. https://doi.org/10.1016/j.chest.2021.07.480
9. Driscoll S, Carroll WD, Nichani S, Fishwick R, Bakewell K, Gilchrist FJ. COVID-19 infection and nocardiosis causing the death of an adolescent with cystic fibrosis. Pediatr Pulmonol. 2022;57:1823–5. https://doi.org/10.1002/ppul.25954
10. Cicero MN, Memmo AI, Piccionello IR, Seminara G, Benfante A, Scichilone N. A 79-year-old-man with SARS-CoV-2 pneumonia and unusual pulmonary coinfection. Minerva Respir Med. 2022;61:86–91. https://doi.org/10.23736/S2784-8477.21.01993-8
11. Veličković J, Vukičević TA, Spurnić AR, Lazić I, Popović B, Bogdanović I, et al. Case report: nocardial brain abscess in a persistently SARS-CoV-2 PCR positive patient with systemic lupus erythematosus. Front Med (Lausanne). 2022;9:973817. https://doi.org/10.3389/fmed.2022.973817
12. DiMeglio M, Shaikh H, Newman J, Vazsquez Rubio G. Nocardiosis of the central nervous system: a rare complication of COVID management? IDCases. 2022;29:e01599. https://doi.org/10.1016/j.idcr.2022.e01599
13. Laplace M, Flamand T, Ion C, Gravier S, Mohseni-Zadeh M, Debriel D, et al. Pulmonary nocardiosis as an opportunistic infection in COVID-19. Eur J Case Rep Intern Med. 2022;9:003477. https://doi.org/10.12890/2022_003477
14. Toyokawa M, Ohana N, Ueda A, Imai M, Tanno D, Honda M, et al. Identification and antimicrobial susceptibility profiles of *Nocardia* species clinically isolated in Japan. Sci Rep. 2021;11:16742. https://doi.org/10.1038/s41598-021-95870-2
15. Garcia-Vidal C, Sanjuan G, Moreno-García E, Puerta-Alcalde P, Garcia-Pouton N, Chumbita M, et al.; COVID-19 Researchers Group. Incidence of co-infections and superinfections in hospitalized patients with COVID-19: a retrospective cohort study. Clin Microbiol Infect. 2021;27:83–8. https://doi.org/10.1016/j.cmi.2020.07.041
16. Søvik S, Barratt-Due A, Kåsine T, Olasveengen T, Strand MW, Tveita AA, et al. Corticosteroids and superinfections in COVID-19 patients on invasive mechanical ventilation. J Infect. 2022;85:57–63. https://doi.org/10.1016/j.jinf.2022.05.015
17. Paget C, Trottein F. Mechanisms of bacterial superinfection post-influenza: a role for unconventional T cells. Front Immunol. 2019;10:336. https://doi.org/10.3389/fimmu.2019.00336
18. Chong WH, Saha BK, Ramani A, Chopra A. State-of-the-art review of secondary pulmonary infections in patients with COVID-19 pneumonia. Infection. 2021;49:591–605. https://doi.org/10.1007/s15010-021-01602-z
19. Russell CD, Fairfield CJ, Drake TM, Turtle L, Seaton RA, Wootton DG, et al.; ISARIC4C investigators. Co-infections, secondary infections, and antimicrobial use in patients hospitalised with COVID-19 during the first pandemic wave from the ISARIC WHO CCP-UK study: a multicentre, prospective cohort study. Lancet Microbe. 2021;2:e354–65. https://doi.org/10.1016/S2666-5247(21)00090-2

Address for correspondence: Jillian E. Raybould, Virginia Commonwealth University Health System, 1200 E Broad St, Richmond, VA 23219, USA: email: jillian.raybould@vcuhealth.org

Bacterial Agents Detected in 418 Ticks Removed from Humans during 2014–2021, France

Marie Jumpertz, Jacques Sevestre, Léa Luciani, Linda Houhamdi, Pierre-Edouard Fournier, Philippe Parola

Monitoring of tickborne diseases is critical for prevention and management. We analyzed 418 ticks removed from 359 patients during 2014–2021 in Marseille, France, for identification and bacteria detection. Using morphology, molecular methods, or matrix-assisted laser desorption/ionization time-of-flight mass spectrometry, we identified 197 (47%) *Ixodes*, 136 (33%) *Dermacentor*, 67 (16%) *Rhipicephalus*, 8 (2%) *Hyalomma*, 6 (1%) *Amblyomma*, 2 (0.5%) *Argas*, and 2 (0.5%) *Haemaphysalis* tick species. We also detected bacterial DNA in 241 (58%) ticks. The most frequent bacterial pathogens were *Rickettsia raoultii* (17%) and *R. slovaca* (13%) in *Dermacentor* ticks, *Borrelia* spp. (9%) in *Ixodes* ticks, and *R. massiliae* (16%) in *Rhipicephalus* ticks. Among patients who were bitten, 107 had symptoms, and tickborne diseases were diagnosed in 26, including scalp eschar and neck lymphadenopathy after tick bite and Lyme borrelioses. Rapid tick and bacteria identification using a combination of methods can substantially contribute to clinical diagnosis, treatment, and surveillance of tickborne diseases.

Ticks are obligate hematophagous arthropods that are the second most prevalent vectors of human zoonotic pathogens after mosquitoes (*1*). Ticks harbor a vast number of pathogenic bacteria, viruses, and protozoa (*2*). Emerging tickborne disease (TBD) agents that cause human infections, such as *Borrelia miyamotoi* and *Rickettsia tamurae*, have been reported (*3*). In Europe, ticks most frequently implicated in human infectious diseases are *Ixodes*, *Rhipicephalus*, and *Dermacentor* spp. (*4*). Tularemia, Crimean-Congo hemorrhagic fever, and tick-borne encephalitis are the 3 TBDs under specific surveillance by the European Centre for Disease Prevention and Control (*5*). Surveillance of other TBDs relies mainly on national reference centers, reports, literature analysis, and serologic surveys. Most TBDs have geographic disease patterns, and distribution evolves with climatic conditions and human behavioral modifications. Monitoring TBDs is critical for developing optimal prevention and management strategies (*6*).

The Institut Hospitalo-Universitaire Méditerranée Infection (IHU-MI) in Marseille, France (*7*) includes the National Reference Centre for rickettsioses and bartonelloses and Southern Reference Center for tickborne diseases. The laboratory receives ticks collected from the field, animals, and patients in France and worldwide. Analyses include species-level tick identification and detection of tickborne human bacterial pathogens. Clinicians or patients are contacted to use this information for surveillance, medical advice, and treatment.

In 2016, a study of tickborne bacteria and ticks removed from humans during 2002–2013 was conducted at the Aix-Marseille University (*8*). Innovative entomologic and microbiologic techniques were used for identification of ticks and bacteria, including molecular methods and matrix-assisted laser desorption/ionization time-of-flight (MALDI-TOF) mass spectrometry. The principle of MALDI-TOF mass spectrometry identification resides in acquisition of species-specific mass spectra from a study sample. Spectra are secondarily queried against a reference mass spectral database, enabling identification on the basis of the spectra's similarity profile (*9*). This identification technique revolutionized everyday practices in clinical microbiology laboratories and has proven to be a robust, reproducible, and time-effective method for identifying arthropod vectors, notably ticks (*9*). We analyzed 418 ticks removed from humans and sent to the IHU-MI during 2014–2021, using MALDI-TOF mass spectrometry to identify the ticks and molecular methods and serology to identify tickborne pathogenic bacteria.

Author affiliations: Aix-Marseille University, Marseille, France; IHU-Méditerranée Infection, Marseille

DOI: https://doi.org/10.3201/eid2904.221572

Material and Methods

Tick Identification

We included all ticks removed from humans and analyzed at the IHU-MI during January 2014–March 2021. When possible, the tick was first identified morphologically by an entomologist by using morphologic identification keys applicable to the specimen's geographic location (*10*,*11*). When available, we used 4 legs of each tick to identify the tick species by using MALDI-TOF mass spectrometry (*9*). We obtained protein mass profiles for each sample by using the Microflex LT MALDI-TOF instrument (Bruker, https://www.bruker.com) as described (*12*). We compared protein spectra to those in our in-house arthropod MALDI-TOF mass spectrometry database. For molecular identification of ticks, we extracted DNA from half of the tick body by using the EZ1 DNA Tissue Kit (QIAGEN, https://www.qiagen.com) (*12*) and performed Sanger sequencing of a 360-bp PCR amplification product from the 12S rRNA gene (*13*).

Detecting and Identifying Bacteria in Ticks

We identified tickborne bacteria by using the same DNA extracts used for molecular identification of ticks. We used DNA samples extracted from uninfected laboratory-reared *Rhipicephalus sanguineus* s.l. ticks as negative controls. We screened ticks for *Rickettsia* spp., *Bartonella* spp., *Borrelia* spp., *Francisella tularensis*, *Coxiella burnetii*, *Coxiella*-like bacteria, and Anaplasmataceae bacteria by using quantitative real-time or standard PCR (Table 1; Appendix Table, https://wwwnc.cdc.gov/EID/article/29/4/22-1572-App1.pdf).

Patients

For each tick received, we collected clinical and epidemiologic data for the patient who was bitten. We collected information on sex, age, date, geographic origin of exposure, symptoms, and antimicrobial drug treatment. The seasonality of tick bites was described only for ticks from metropolitan France, also known as European France, the area of France which is geographically in Europe and includes the Mediterranean island of Corsica. For symptomatic patients, medical consultation and laboratory testing for TBDs was offered to patients who were within a reasonable geographic distance, and advice was given to the patient's clinician, when they could be reached.

For laboratory testing, we screened 100 µL of acute-phase serum and, when possible, convalescent serum collected ≥2 weeks later by using indirect immunofluorescence assays for antigens of spotted fever group *Rickettsia* spp., *Bartonella quintana*, *B. henselae*, *Borrelia* spp., *F. tularensis*, *C. burnetii* phase I and II, and *Anaplasma phagocytophilum* (*8*). We performed an ELISA for *Borrelia burgdorferi* sensu lato and then Western blot if the ELISA was positive (*14*). For acute Q fever (*C. burnetii*), we used cutoff titers of 1:200 for phase II IgG and 1:50 for phase II IgM (*15*). For other bacteria, cutoff values were 1:64 for IgG and 1:32 for IgM (*8*). For some patients, we analyzed blood (collected in EDTA tubes, 200 µL), skin biopsy, or eschar swab samples for tickborne pathogens. We extracted DNA from those patient samples and performed quantitative or standard PCR for tickborne pathogens by using the same primers described for ticks (Appendix Table).

Results

Tick Identification

We analyzed a total of 418 ticks removed from 359 patients. The number of tick bites per patient ranged from 1–16. The most frequent tick species identified were *Ixodes* (197 specimens, 47%), *Dermacentor* (136 specimens, 33%), and *Rhipicephalus* (67 specimens, 16%). (Table 1).

We identified 247/254 (92%) ticks by using MALDI-TOF mass spectrometry and 165/179 (92.2%) ticks by using molecular methods at the species level. We did not observe identification discrepancies between MALDI-TOF mass spectrometry and molecular methods. Morphologic identification was performed for 86 (20%) ticks, and we observed congruent species level identification with either MALDI-TOF mass spectrometry or molecular methods, when performed.

Tick Distribution and Seasonality

In metropolitan France, 78% of tick bites occurred in March through August during 2014–2021. Bites from *Ixodes* spp. were more frequent during the summer, bites from *Rhipicephalus* spp. occurred mainly at the end of spring, and bites from *Dermacentor* spp. occurred mainly in spring and autumn (Figure 1).

In metropolitan France, *Ixodes* spp. were the most frequently observed ticks, except in southern France, where *Dermacentor* spp. were most frequent (Table 1). *Rhipicephalus* spp. ticks originated from southern and eastern France, and 4 *Hyalomma* spp. ticks were received from southern France. Three *Amblyomma* spp. ticks were received from an overseas territory (Guadeloupe) of France, and 28 ticks were received from other countries.

Bacteria Identified in Ticks

We detected bacterial DNA in 242/418 (58%) ticks received (Table 1). Co-infections were frequent; 78 ticks

were simultaneously infected by 2 bacteria species, and 3 ticks were simultaneously infected by 3 bacteria species. Most co-infections were caused by *Rickettsia* spp. and *Coxiella*-like bacteria (77 ticks). We analyzed the geographic distribution of bacteria found in ticks from metropolitan France (Figure 2).

For ticks from other countries in Europe, 1 tick was infected with *R. africae* (Greece), 1 with *Wolbachia* sp. (United Kingdom), 1 with *Borrelia* sp. (Switzerland), and 1 with *Coxiella*-like bacteria (Belgium). In Guadeloupe, an island of France in the West Indies, 1 *Amblyomma variegatum* tick was infected with *R. africae*. In Cuba, 1 *Amblyomma mixtum* tick was infected with both *R. amblyommatis* and *Coxiella*-like bacteria. Ticks received from Asia and Africa were negative for all tested bacteria (Table 1).

Patient Characteristics

Of the 359 patients who had been bitten by ticks, 137 (38%) were men and 222 (62%) were women. Ages ranged from 1 month to 86 years, and most children (43%, 155) were <10 years of age. We obtained clinical data for 217 (60%) patients; 110 (51%) were asymptomatic and 107 (49%) experienced various symptoms (Figure 3). The most prevalent symptoms were local erythema (37 patients), inoculation eschar (33 patients), lymphadenopathy (27 patients), fever (17 patients), and cutaneous rash (15 patients).

Table 1. Tick identification and number of bacterial agents detected in 418 ticks removed from humans during 2014–2021 in France and their geographic origin*

Tick species	No. ticks	Tick origin	Bacteria from ticks					
			Rickettsia sp.	CLB	*Coxiella burnetii*	*Borrelia* sp.	Anaplasmataceae	*Bartonella* sp.
Ixodes ricinus	183	MF, n = 169; Switzerland n = 4; UK, n = 2; Italy, Russia, Croatia, the Netherlands, Sweden, Spain, Latvia, or Germany, n = 1	*R. helvetica*, n = 2; *R. monacensis*, n = 1; *Rickettsia* sp., n = 7	10	0	*B. afzelii*, n = 3; *B. miyamotoi*, n = 2; *Borrelia* sp., n = 11	*Wolbachia* sp., n = 2; *Anaplasma phagocytophilum*, n = 1; undetermined, n = 7	0
I. hexagonus	4	MF, n = 4	0	2	0	0	0	0
I. frontalis	1	MF, n = 1	0	1	0	0	0	0
Ixodes sp.	9	MF, n = 3; UK, n = 2; Switzerland, n = 4	*Rickettsia sp.* 1	3	0	*Borrelia sp.* 1	0	0
Dermacentor marginatus	113	MF, n = 113	*R. raoultii*, n = 21; *R. slovaca*, n = 17; *Rickettsia* sp., n = 11	95	1	0	0	0
D. reticulatus	5	MF, n = 5	*R. raoutlii*, n = 1	1	0	0	0	0
Dermacentor sp.	18	MF, n = 18	*R. raoultii*, n = 1; *Rickettsia* sp., n = 7	16	1	0	0	0
Rhipicephalus sanguineus	52	MF, n = 51; Egypt, n = 1	*R. massiliae*, n = 8; *Rickettsia* sp., n = 3	49	1	0	*Ehrlichia canis*, n = 1	0
R. pusillus	9	MF, n = 9	*R. sibirica mongolitimoniae*, n = 6; *R. massiliae*, n = 3	5	3	0	0	0
R. bursa	4	MF, n = 4	*R. barbariae*, n = 1	3	0	0	0	0
Rhipicephalus sp.	2	MF, n = 2	*Rickettsia* sp., n = 1	2	0	0	0	0
Hyalomma marginatum	2	MF, n = 2	*Rickettsia* sp., n = 1	0	0	0	0	0
H. aegyptium	1	Turkey, n = 1	0	0	0	0	0	0
Hyalomma sp.	5	MF, n = 2; Greece, n = 3	*R. africae*, n = 1	1	0	0	0	0
Amblyomma variegatum	3	Guadeloupe, n = 3	*Rickettsia* sp., n = 1, *R. africae*, n = 1	2	0	0	0	0
A. hebraeum	1	South Africa, n = 1	0	0	0	0	0	0
A. mixtum	1	Cuba, n = 1	*R. amblyommatis*, n = 1	1	0	0	0	0
A. oblongoguttatum	1	Guadeloupe, n = 1	0	0	0	0	0	0
Argas reflexus	2	MF, n = 2	0	2	0	0	0	0
Haemaphysalis concinna	1	Belgium, n = 1	0	1	0	0	0	0
H. punctata	1	MF, n = 1	0	1	0	0	0	0

*Ticks (n = 418) were sent to the Institut Hospitalo-Universitaire Méditerranée Infection in Marseille, France, during 2014–2021 for identification of tick and bacteria species by using mass spectrometry (ticks) and molecular and serologic methods (bacteria). CLB, *Coxiella*-like bacteria; MF, metropolitan France.

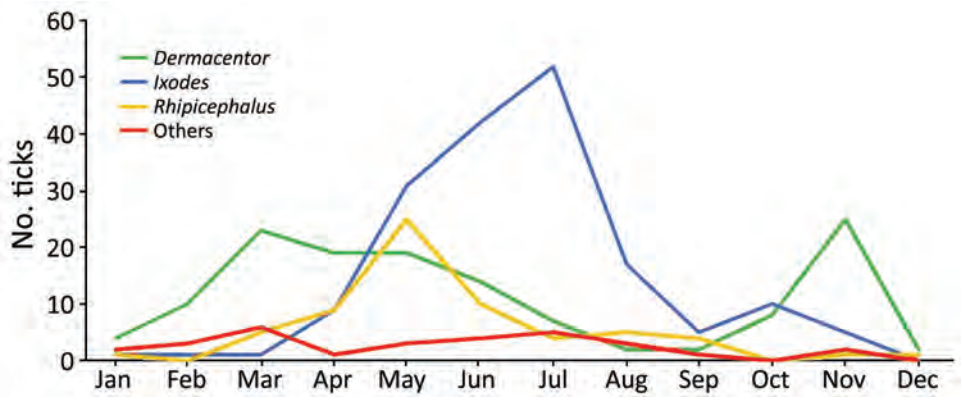

Figure 1. Tick seasonality in study of bacterial agents detected in 418 ticks removed from humans during 2014–2021, France. Overall prevalence of *Dermacentor*, *Ixodes*, *Rhipicephalus*, and other tick species in metropolitan France (n = 387), which includes Corsica, during January–December is indicated. The ticks were among those sent to the Institut Hospitalo-Universitaire Méditerranée Infection in Marseille, France, and identified by using matrix-assisted laser desorption/ionization time-of-flight mass spectrometry or sequencing PCR products.

We tested human blood and tissue samples for tickborne pathogenic bacteria (Table 2), and TBD was diagnosed for 26 patients after clinical and biologic investigations (Figure 3). Lyme borreliosis was diagnosed for 9 patients; 6 of those cases had been clinically diagnosed by the original clinician because the patients had typical erythema migrans and were treated with doxycycline. One patient had a skin biopsy that was PCR positive for *Borrelia* sp. and received doxycycline treatment. Lyme borreliosis was diagnosed for the last 2 patients on the basis of seroconversion between acute and follow-up serum samples. We observed cephalic or cervical inoculation eschar and cervical lymphadenopathy corresponding to scalp eschar and neck lymphadenopathy syndrome (SENLAT) after tick bites in 15 patients. Acute hepatitis developed in 1 patient who had positive serologic results (1:400 phase II IgG, 1:50 phase II IgM) and positive blood PCR results for *C. burnetii*; acute Q fever was diagnosed, and the patient was treated with doxycycline. One patient had a skin biopsy that was PCR-positive for *Coxiella*-like bacteria and was treated with doxycycline. All patients with a TBD diagnosis had been bitten by ticks that carried pathogenic bacteria. The remaining symptomatic patients did not meet clinical or biologic criteria for a TBD diagnosis.

We collected data on antimicrobial drug treatment received by 80 patients, 12 of whom were treated at the IHU-MI. In addition to the patient treated for Q fever, patients at the IHU-MI were treated with doxycycline after being bitten by *Dermacentor* ticks positive for *R. raoultii* (2 patients) or *R. slovaca* (2 patients) that caused SENLAT. For the 68 patients treated outside the IHU-MI, when a TBD diagnosis was suspected, the managing clinician sometimes began probabilistic antimicrobial drug treatment, which could be continued or suspended according to tick analysis results. The most frequently used antimicrobial drugs after tick bites were doxycycline (26 patients), azithromycin (21 patients), and amoxicillin (18 patients). Other antimicrobial drugs used were pristinamycin, vancomycin, amoxicillin/clavulanic acid, and topical fucidic acid ointment.

Discussion

We identified 418 ticks that were removed from 359 patients in France by using various methods and emerging tools, such as MALDI-TOF mass spectrometry. Rapid identification of ticks has major clinical implications because different tick species carry different pathogens. Arthropods have historically been identified morphologically and, more recently, by using molecular methods (*16*). Morphologic identification of ticks during routine clinical practice is limited by the availability of appropriate documentation, trained entomologists, and might also be impeded if the arthropod specimen's preservation state is poor (*17*). MALDI-TOF mass spectrometry has been used for identification of microorganisms since ≈2003. MALDI-TOF mass spectrometry has also been shown to be a robust, reproducible, and time-effective method for identifying arthropod vectors, notably ticks (*9*,*12*); advantages are low running costs and time efficiency compared with molecular methods. Moreover, no specific expertise is required, in contrast to morphologic approaches. In our study, we identified ticks by MALDI-TOF mass spectrometry and successfully applied results to routine diagnoses. Limitations of this method are the need to obtain good quality spectra and availability of an extensive database for reliable identification (*18*). Biomolecular methods also identified tick species efficiently, but those methods can

be affected by PCR inhibitors in the ticks (*19*). The combination of MALDI-TOF mass spectrometry, molecular, and morphologic identification methods enabled the complete identification of 92% of ticks in our study. The remaining 8% were only identified at the genus level, often because of insufficient tick material (which limited the number of analyses that could be performed) and limitations of the various diagnostic methods.

Data on tick engorgement status or attachment duration were not available and, thus, not analyzed in our study. Acquisition of those data is needed because engorgement indicates an efficient blood meal, which is more likely to result in bacterial transmission (*20*). Transmission of microorganisms is linked to attachment duration. During the first hours, the tick mainly injects the cement that will enable firm attachment to the host's skin; transmission of bacterial agents usually occurs 20–24 hours after attachment (*21*).

Ixodes spp. ticks are present in every region of France. *I. ricinus,* the known vector of Lyme disease in Europe, mostly lives in temperate humid regions and forested areas but can also be found in specific biotopes within the Mediterranean area (*22*). *Ixodes* spp. tick bites can occur throughout the year but have a higher prevalence in summer when tick populations, especially biting nymphs, are at their peak, which is also associated with the highest occurrence of Lyme disease (*23*). We observed that *I. ricinus* ticks were frequently infected by *Borrelia* sp. (9%). Nine patients had documented Lyme borreliosis after bites from *I. ricinus* ticks infected with *Borrelia* sp., mostly acute infections confirmed either clinically (6 patients with erythema migrans) or by PCR (1 cutaneous specimen) or serology (2 positive follow-up serum samples). The seroconversion period for Lyme borreliosis is 2–4 weeks, and, in early Lyme disease, the diagnosis can be made by the

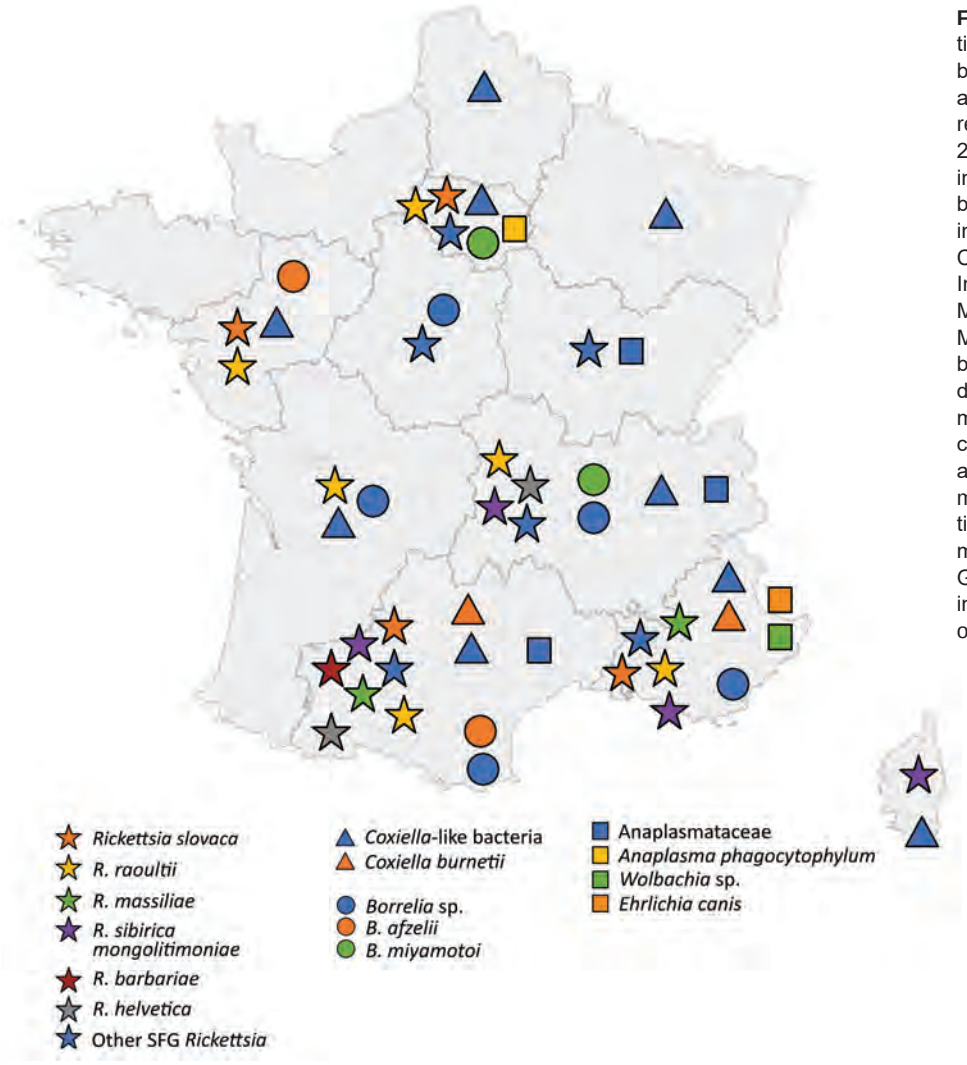

Figure 2. Geographic origin of ticks and identification of tickborne bacteria in study of bacterial agents detected in 418 ticks removed from humans during 2014–2021, France. Symbols indicate tick species and tickborne bacteria identified from locations in metropolitan France, including Corsica. Ticks were sent to the Institut Hospitalo-Universitaire Méditerranée Infection in Marseille, France, and identified by using matrix-assisted laser desorption ionization time-of-flight mass spectrometry. Bacteria carried by the ticks were isolated and identified by PCR or serologic methods at the institute. Of the ticks evaluated, 387 were from metropolitan France; 3 from Guadeloupe, a territory of France in the West Indies; and 28 from other countries.

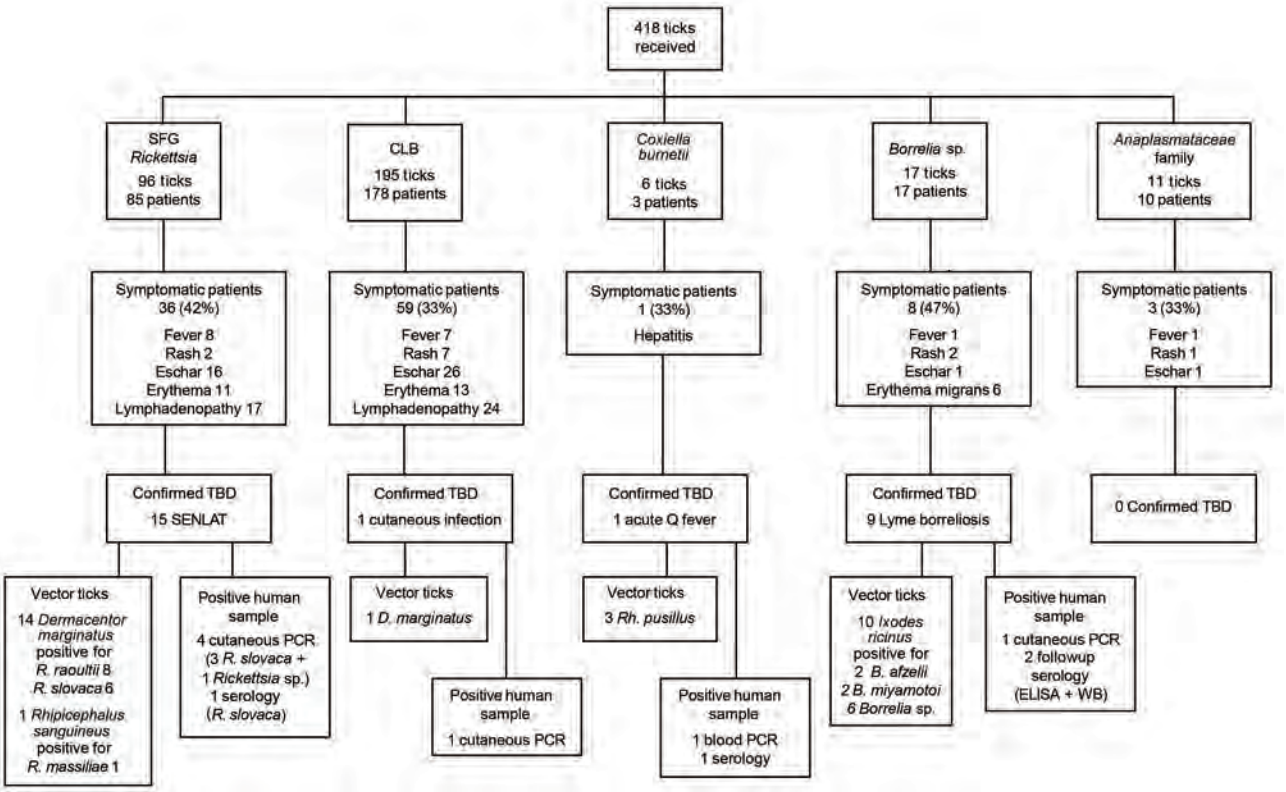

Figure 3. Flow chart of bacteria and tick identification and patient signs/symptoms in study of bacterial agents detected in 418 ticks removed from humans during 2014–2021, France. Ticks were removed from 359 patients and sent to the Institut Hospitalo-Universitaire Méditerranée Infection in Marseille, France, where they were identified by using matrix-assisted laser desorption/ionization time-of-flight mass spectrometry or sequencing PCR products. Bacteria carried by ticks were isolated and identified by PCR or serologic methods at the institute. CLB, *Coxiella*-like bacteria; SENLAT, scalp eschar and neck lymphadenopathy syndrome; SFG, spotted fever group; TBD, tickborne disease; WB, Western blot.

presence of erythema migrans alone without positive serology; serology is frequently negative in the early stage of Lyme disease (*24*). Identifying *Borrelia* sp. DNA in the tick can guide the patient's treatment and surveillance before seroconversion. Furthermore, 8% of *Ixodes* spp. ticks were infected with spotted fever group *Rickettsia*, including *R. helvetica* and *R. monacensis,* both emerging pathogens associated with those ticks (*25*). We found *Ixodes* spp. ticks (2 ticks) carried *Wolbachia* sp. bacteria, endosymbionts of many arthropods including ticks (*26*) and not known to be human pathogens. In 1 *I. ricinus* tick, we found *A. phagocytophilum* bacteria, the cause of human granulocytic anaplasmosis, which can induce fever, cytopenia, and elevated levels of transaminases in the blood. Granulocytic anaplasmosis is diagnosed by using PCR, blood smears, or retrospectively by serology (*27*).

Dermacentor spp. ticks are found in various habitats and have high tolerance to temperature variations. In Europe, *D. marginatus*, the ornate sheep tick, is most frequently found in Mediterranean areas. *D. reticulatus,* the ornate dog tick, is most frequently found in colder northern areas that have high humidity and mild winters. We observed *Dermacentor* tick bite peaks in early spring and autumn and a decrease in summer activity, which is frequently described in temperate Europe (*28*). *Dermacentor* ticks are potential vectors for various human pathogens (*29*) and were associated with SENLAT in 14 cases after bites from *D. marginatus* ticks infected with either *R. raoultii* or *R. slovaca*. *R. slovaca* infection was first referred to as TIBOLA (tick-borne lymphadenopathy) (*30*); lymphadenopathy is the most frequent symptom. After a role for *Dermacentor* ticks was found, the name DEBONEL (*Dermacentor*-borne necrosis erythema lymphadenopathy) was proposed (*31*). *R. raoultii* was identified as another frequent etiologic agent of lymphadenopathy (*32*), which is caused by local control of infection within the lymph node but is not pathogen-specific. Lymphadenopathy can be caused by other tickborne

bacteria, including *C. burnetii*, *B. burgdorferi*, *B. henselae*, and *F. tularensis* (*33*). The acronym SENLAT was proposed to provide an accurate clinical description of lymphadenopathy after tick bite (*34*), and diagnosis is based on typical symptoms. In our study, SENLAT occurred in 1 patient after a bite from a *Rh. sanguineus* s.l. tick infected with *R. massiliae.* SENLAT etiology is determined by detecting bacterial DNA in vector ticks or from eschar swab samples (*35*) because serology sensitivity might be low (12% for *R. slovaca*) and seroconversion might occur only during late stages of infection (*36*).

We also detected a high (83%) prevalence of *Coxiella*-like bacteria in *Dermacentor* ticks. One patient, who was bitten by a *D. marginatus* tick and had a cutaneous rash and an eschar, was PCR-positive for *Coxiella*-like bacteria in a cutaneous specimen; the bacteria were also found in the tick. However, pathogenic potential of *Coxiella*-like bacteria in humans remains unclear.

Rh, sanguineus s.l. ticks (brown dog ticks) are found in proximity to dogs, which are their primary feeding hosts (*37*). In our study, we identified *Rh. sanguineus* s.l. ticks mostly in southern France, where they are endemic. *Rhipicephalus* ticks were more frequently found at the end of spring, although previous studies have described peak activity during the summer months, potentially because of warmer temperatures during spring months in recent years. Although *Rhipicephalus* ticks are active during May–November, human bites are reported more frequently during the warmer months, most likely because warmer weather increases their propensity to bite other hosts, including humans (*38*). *Rh. sanguineus* s.l. ticks are vectors for *R. conorii conorii,* the agent causing Mediterranean spotted fever (*39*). None of the 418 ticks in our study was positive for *R. conorii conorii*, in line with a study from Spain, where 2,229 *Rh. sanguineus* ticks were negative for that bacteria (*40*). *R. conorii conorii* infections of *Rh. sanguineus* s.l. ticks might vary in the wild from 1 specific setting to another and have a small focus, low propensity for diffusion, and potentially understudied vertebrate reservoir and environmental requirements (*39*).

Several species of *Rhipicephalus* ticks can carry *R. massiliae* (*41*). In our study, we found *R. massiliae* in 8 *Rh. sanguineus* s.l. and 3 *Rh. pusillus* ticks from southern France. Since the first case reported in Italy in 2005, only a few human cases of *R. massiliae* infection have been reported, which causes symptoms similar to those of Mediterranean spotted fever or SENLAT (*25*). We found *R. sibirica mongolitimonae*, which was associated with lymphangitis-associated rickettsiosis (*42*), in 5 *Rh. pusillus* ticks, occurring more frequently in the spring and summer in France (*25*). We found *Candidatus* Rickettsia barbariae in 1 *Rhipicephalus* sp. tick, which has been detected previously in ticks in France and elsewhere, but its pathogenicity is unknown (*13*). *Rhipicephalus* ticks were also frequent (88%) carriers of *Coxiella*-like bacteria. Those endosymbionts are part of the microbiome of *Rhipicephalus* and other ticks and might promote tick development and fertility (*43*).

We report 1 patient who had acute Q fever that was documented by seroconversion and PCR of a blood sample and complicated by hepatitis; the patient was bitten by 3 *Rh. pusillus* ticks, all of which were infected with *C. burnetii*. Ticks are competent vectors for *C. burnetii* in experimental models, but only a few cases of Q fever caused by tick bites have been reported. The main route of human infection is through exposure to infected ruminants and their products via aerosols or direct contact (*44*). The clinical manifestations of Q fever can vary from influenza-like symptoms in acute disease to persistent focalized infections, such as endocarditis and vascular infections (*16*).

Hyalomma ticks can be found in Asia, Africa, and Europe and are of medical and veterinary significance in tropical regions (*45*). In our study, 1 patient was bitten in Greece by a *Hyalomma* sp. tick that was positive for *R. africae*, the etiologic agent of African tick bite fever, known to be endemic in sub-Saharan Africa and the West Indies. *Hyalomma* ticks have been reported to carry *R. africae* (*46*), but no proof

Table 2. Bacterial species identified in different patient samples in study of bacterial agents detected in 418 ticks removed from humans during 2014–2021, France*

Patient sample	Total	Identified bacteria	Bacteria found in tick	Negative samples
Blood†	31	*Coxiella burnetii*, n = 1	Yes	30
Cutaneous‡	39	*Rickettsia slovaca*, n = 3; *Borrelia* sp., n = 1; *Rickettsia* sp., n = 1; *Coxiella*-like bacteria, n = 1	Yes	30
Serum, acute	47	*Borrelia* sp., n = 3	No	44
Serum, followup	30	*Borrelia* sp., n = 2; *Coxiella burnetii*, n = 1; *R. slovaca*, n = 1	Yes	26

*Different types of patient samples for which at least 1 tick was also identified were tested for bacteria by using serologic and molecular methods at the Institut Hospitalo-Universitaire Méditerranée Infection, Marseille, France.
†Collected in tubes with EDTA.
‡Samples from 33 biopsies and 6 cutaneous swab specimens.

exists for their vectorial competence for African tick bite fever. Indeed, the main recognized vectors of the disease are *Amblyomma* spp. ticks, such as *A. variegatum* (*25*,*47*). We found that 1 *A. variegatum* tick from a patient in Guadeloupe carried *R. africae*. All tick bites by *Amblyomma* spp. reported in our study occurred in tropical territories, but no cases of related diseases were diagnosed. Of note, we detected *R. amblyommatis* in an *A. mixtum* tick from Cuba; this spotted fever group rickettsia is known to infect *Amblyomma* ticks, but its pathogenicity in humans is unknown (*25*).

In conclusion, our study underscores the large number of tick species that can bite humans and bacteria species that ticks can carry, including recognized and unknown pathogens. Furthermore, MALDI-TOF mass spectrometry is an efficient technique for identifying ticks in diagnostic settings and has recently been evaluated in terms of its ability to detect the infectious status of ticks (*48*). Our study enabled the reorganization of our laboratory for optimal specimen analysis. Currently, ticks are photographed first by laboratory technicians in accordance with specific guidelines if an entomologist is unavailable. Ticks are then identified by using MALDI-TOF mass spectrometry. If the quality of the mass spectrometry spectrum is low or identification is doubtful, the tick is identified by using PCR and then sequencing. Detection of bacteria by PCR is conducted simultaneously. Most ticks are known vectors of various TBDs, and identification of the tick species and bacteria they carry is a first step in disease diagnosis for the patient who has been bitten. Of note, transmission of a bacterial agent through the bite of an infected tick does not occur systematically, because transmission of bacteria is dependent on the duration of tick attachment. In nonexpert settings, such as local laboratories, rapid identification of ticks and the pathogens they carry can lead to expedited decisions to treat patients if the tick is infected. In addition, knowledge of local tick and bacteria ecology might influence patient care strategies. Knowing that a specific TBD is prevalent in a region where tick bites occurs necessitates close surveillance of the patient for disease symptoms, and, in TBD hyperendemic areas, patients might benefit from preventive antimicrobial drug treatment after a tick bite (*49*). Rapid detection and identification of ticks and tickborne bacteria by using a combination of MALDI-TOF mass spectrometry, molecular methods, and serology can substantially contribute to early TBD diagnoses and treatment.

About the Author

Dr. Jumpertz is a medical doctor and infectious disease specialist at IHU-Méditerranée Infection and Aix Marseille University, France. Her research interests focus on vector-borne diseases and antimicrobial drug treatments.

References

1. Parola P, Raoult D. Ticks and tickborne bacterial diseases in humans: an emerging infectious threat. Clin Infect Dis. 2001;32:897–928. https://doi.org/10.1086/319347
2. Estrada-Peña A. Ticks as vectors: taxonomy, biology and ecology. Rev Sci Tech. 2015;34:53–65. https://doi.org/10.20506/rst.34.1.2345
3. Kernif T, Leulmi H, Raoult D, Parola P. Emerging tick-borne bacterial pathogens. Microbiol Spectr. 2016;4. https://doi.org/10.1128/microbiolspec.EI10-0012-2016
4. Heyman P, Cochez C, Hofhuis A, van der Giessen J, Sprong H, Porter SR, et al. A clear and present danger: tick-borne diseases in Europe. Expert Rev Anti Infect Ther. 2010;8:33–50. https://doi.org/10.1586/eri.09.118
5. European Centre for Disease Prevention and Control. ECDC activities on surveillance [cited 2023 Feb 23]. https://www.ecdc.europa.eu/en/all-topics-z/surveillance-and-disease-data/diseases-and-special-health-issues-under-eu-surveillance
6. Estrada-Peña A, Venzal JM. Climate niches of tick species in the Mediterranean region: modeling of occurrence data, distributional constraints, and impact of climate change. J Med Entomol. 2007;44:1130–8. https://doi.org/10.1603/0022-2585(2007)44[1130:CNOTSI]2.0.CO;2
7. Bataille J, Brouqui P. Building an intelligent hospital to fight contagion. Clin Infect Dis. 2017;65:S4–11. https://doi.org/10.1093/cid/cix402
8. Aubry C, Socolovschi C, Raoult D, Parola P. Bacterial agents in 248 ticks removed from people from 2002 to 2013. Ticks Tick Borne Dis. 2016;7:475–81. https://doi.org/10.1016/j.ttbdis.2016.02.003
9. Sevestre J, Diarra AZ, Laroche M, Almeras L, Parola P. Matrix-assisted laser desorption/ionization time-of-flight mass spectrometry: an emerging tool for studying the vectors of human infectious diseases. Future Microbiol. 2021;16:323–40. https://doi.org/10.2217/fmb-2020-0145
10. Pérez-Eid C. Les tiques. Identification, biologie, importance médicale et vétérinaire. Coll. Monographies de microbiologie. Paris: Lavoisier; 2007.
11. Ticks of Europe and North Africa. A guide to species identification. In: Estrada-Peña A, Mihalca AD, Petney TN, editors. Cham (Switzerland): Springer Cham; 2017.
12. Huynh LN, Diarra AZ, Pham QL, Le-Viet N, Berenger JM, Ho VH, et al. Morphological, molecular and MALDI-TOF MS identification of ticks and tick-associated pathogens in Vietnam. PLoS Negl Trop Dis. 2021;15:e0009813. https://doi.org/10.1371/journal.pntd.0009813
13. Socolovschi C, Reynaud P, Kernif T, Raoult D, Parola P. Rickettsiae of spotted fever group, *Borrelia valaisiana*, and *Coxiella burnetii* in ticks on passerine birds and mammals from the Camargue in the south of France. Ticks Tick Borne Dis. 2012;3:355–60. https://doi.org/10.1016/j.ttbdis.2012.10.019
14. Figoni J, Chirouze C, Hansmann Y, Lemogne C, Hentgen V, Saunier A, et al.; endorsed by scientific societies. Lyme borreliosis and other tick-borne diseases. Guidelines from the French Scientific Societies (I): prevention,

epidemiology, diagnosis. Med Mal Infect. 2019;49:318–34. https://doi.org/10.1016/j.medmal.2019.04.381
15. Eldin C, Mélenotte C, Mediannikov O, Ghigo E, Million M, Edouard S, et al. From Q fever to *Coxiella burnetii* infection: a paradigm change. Clin Microbiol Rev. 2017;30:115–90. https://doi.org/10.1128/CMR.00045-16
16. Yssouf A, Almeras L, Raoult D, Parola P. Emerging tools for identification of arthropod vectors. Future Microbiol. 2016;11:549–66. https://doi.org/10.2217/fmb.16.5
17. Cuisance D, Antoine Rioux J. Current status of medical and veterinary entomology in France: endangered discipline or promising science? Comp Immunol Microbiol Infect Dis. 2004;27:377–92. https://doi.org/10.1016/j.cimid.2004.03.007
18. Diarra AZ, Almeras L, Laroche M, Berenger JM, Koné AK, Bocoum Z, et al. Molecular and MALDI-TOF identification of ticks and tick-associated bacteria in Mali. PLoS Negl Trop Dis. 2017;11:e0005762. https://doi.org/10.1371/journal.pntd.0005762
19. Socolovschi C, Huynh TP, Davoust B, Gomez J, Raoult D, Parola P. Transovarial and trans-stadial transmission of *Rickettsiae africae* in *Amblyomma variegatum* ticks. Clin Microbiol Infect. 2009;15:317–8. https://doi.org/10.1111/j.1469-0691.2008.02278.x
20. Nadelman RB, Nowakowski J, Fish D, Falco RC, Freeman K, McKenna D, et al.; Tick Bite Study Group. Prophylaxis with single-dose doxycycline for the prevention of Lyme disease after an *Ixodes scapularis* tick bite. N Engl J Med. 2001;345:79–84. https://doi.org/10.1056/NEJM200107123450201
21. Eisen L. Pathogen transmission in relation to duration of attachment by *Ixodes scapularis* ticks. Ticks Tick Borne Dis. 2018;9:535–42. https://doi.org/10.1016/j.ttbdis.2018.01.002
22. Sevestre J, Diarra AZ, Oumarou HA, Durant J, Delaunay P, Parola P. Detection of emerging tick-borne disease agents in the Alpes-Maritimes region, southeastern France. Ticks Tick Borne Dis. 2021;12:101800. https://doi.org/10.1016/j.ttbdis.2021.101800
23. Hartemink N, van Vliet AJH, Gort G, Gassner F, Jacobs F, Fonville M, et al. Seasonal patterns and spatial variation of *Borrelia burgdorferi* (sensu lato) infections in *Ixodes ricinus* in the Netherlands. Parasit Vectors. 2021;14:121. https://doi.org/10.1186/s13071-021-04607-7
24. Kullberg BJ, Vrijmoeth HD, van de Schoor F, Hovius JW. Lyme borreliosis: diagnosis and management. BMJ. 2020;369:m1041. https://doi.org/10.1136/bmj.m1041
25. Parola P, Paddock CD, Socolovschi C, Labruna MB, Mediannikov O, Kernif T, et al. Update on tick-borne rickettsioses around the world: a geographic approach. Clin Microbiol Rev. 2013;26:657–702. https://doi.org/10.1128/CMR.00032-13
26. Hussain S, Perveen N, Hussain A, Song B, Aziz MU, Zeb J, et al. The symbiotic continuum within ticks: opportunities for disease control. Front Microbiol. 2022;13:854803. https://doi.org/10.3389/fmicb.2022.854803
27. Sanchez E, Vannier E, Wormser GP, Hu LT. Diagnosis, treatment, and prevention of Lyme disease, human granulocytic anaplasmosis, and nabesiosis: a review. JAMA. 2016;315:1767–77. https://doi.org/10.1001/jama.2016.2884
28. Zając Z, Kulisz J, Woźniak A, Bartosik K, Khan A. Seasonal activity of *Dermacentor reticulatus* ticks in the era of progressive climate change in eastern Poland. Sci Rep. 2021;11:20382. https://doi.org/10.1038/s41598-021-99929-y
29. Földvári G, Široký P, Szekeres S, Majoros G, Sprong H. *Dermacentor reticulatus*: a vector on the rise. Parasit Vectors. 2016;9:314. https://doi.org/10.1186/s13071-016-1599-x
30. Lakos A. TIBOLA—a new tick-borne infection [in Hungarian]. Orv Hetil. 1997;138:3229–32.
31. Raoult D, Lakos A, Fenollar F, Beytout J, Brouqui P, Fournier PE. Spotless rickettsiosis caused by *Rickettsia slovaca* and associated with *Dermacentor* ticks. Clin Infect Dis. 2002;34:1331–6. https://doi.org/10.1086/340100
32. Parola P, Rovery C, Rolain JM, Brouqui P, Davoust B, Raoult D. *Rickettsia slovaca* and *R. raoultii* in tick-borne rickettsioses. Emerg Infect Dis. 2009;15:1105–8. https://doi.org/10.3201/eid1507.081449
33. Dubourg G, Socolovschi C, Del Giudice P, Fournier PE, Raoult D. Scalp eschar and neck lymphadenopathy after tick bite: an emerging syndrome with multiple causes. Eur J Clin Microbiol Infect Dis. 2014;33:1449–56. https://doi.org/10.1007/s10096-014-2090-2
34. Angelakis E, Pulcini C, Waton J, Imbert P, Socolovschi C, Edouard S, et al. Scalp eschar and neck lymphadenopathy caused by *Bartonella henselae* after tick bite. Clin Infect Dis. 2010;50:549–51. https://doi.org/10.1086/650172
35. Hocquart M, Drouet H, Levet P, Raoult D, Parola P, Eldin C. Cellulitis of the face associated with SENLAT caused by *Rickettsia slovaca* detected by qPCR on scalp eschar swab sample: an unusual case report and review of literature. Ticks Tick Borne Dis. 2019;10:1142–5. https://doi.org/10.1016/j.ttbdis.2019.06.010
36. Foissac M, Socolovschi C, Raoult D. Update on SENLAT syndrome: scalp eschar and neck lymph adenopathy after a tick bite [in French]. Ann Dermatol Venereol. 2013;140:598–609. https://doi.org/10.1016/j.annder.2013.07.014
37. Gray J, Dantas-Torres F, Estrada-Peña A, Levin M. Systematics and ecology of the brown dog tick, *Rhipicephalus sanguineus*. Ticks Tick Borne Dis. 2013;4:171–80. https://doi.org/10.1016/j.ttbdis.2012.12.003
38. Parola P, Socolovschi C, Jeanjean L, Bitam I, Fournier PE, Sotto A, et al. Warmer weather linked to tick attack and emergence of severe rickettsioses. PLoS Negl Trop Dis. 2008;2:e338. https://doi.org/10.1371/journal.pntd.0000338
39. Parola P, Socolovschi C, Raoult D. Deciphering the relationships between *Rickettsia conorii conorii* and *Rhipicephalus sanguineus* in the ecology and epidemiology of Mediterranean spotted fever. Ann N Y Acad Sci. 2009;1166:49–54. https://doi.org/10.1111/j.1749-6632.2009.04518.x
40. Márquez FJ, Rodríguez-Liébana JJ, Soriguer RC, Muniaín MA, Bernabeu-Wittel M, Caruz A, et al. Spotted fever group Rickettsia in brown dog ticks *Rhipicephalus sanguineus* in southwestern Spain. Parasitol Res. 2008;103:119–22. https://doi.org/10.1007/s00436-008-0938-z
41. Olivieri E, Wijnveld M, Bonga M, Berger L, Manfredi MT, Veronesi F, et al. Transmission of *Rickettsia raoultii* and *Rickettsia massiliae* DNA by *Dermacentor reticulatus* and *Rhipicephalus sanguineus* (s.l.) ticks during artificial feeding. Parasit Vectors. 2018;11:494. https://doi.org/10.1186/s13071-018-3075-2
42. Edouard S, Parola P, Socolovschi C, Davoust B, La Scola B, Raoult D. Clustered cases of *Rickettsia sibirica mongolitimonae* infection, France. Emerg Infect Dis. 2013;19:337–8. https://doi.org/10.3201/eid1902.120863
43. Ben-Yosef M, Rot A, Mahagna M, Kapri E, Behar A, Gottlieb Y. *Coxiella*-like endosymbiont of *Rhipicephalus sanguineus* is required for physiological processes during ontogeny. Front Microbiol. 2020;11:493. https://doi.org/10.3389/fmicb.2020.00493
44. Raoult D. Treatment of Q fever. Antimicrob Agents Chemother. 1993;37:1733–6. https://doi.org/10.1128/AAC.37.9.1733
45. Kumar B, Manjunathachar HV, Ghosh S. A review on *Hyalomma* species infestations on human and animals and progress on management strategies. Heliyon. 2020;6:e05675. https://doi.org/10.1016/j.heliyon.2020.e05675

46. Wallménius K, Barboutis C, Fransson T, Jaenson TGT, Lindgren PE, Nyström F, et al. Spotted fever *Rickettsia* species in *Hyalomma* and *Ixodes* ticks infesting migratory birds in the European Mediterranean area. Parasit Vectors. 2014;7:318. https://doi.org/10.1186/1756-3305-7-318
47. Mazhetese E, Magaia V, Taviani E, Neves L, Morar-Leather D. *Rickettsia africae*: identifying gaps in the current knowledge on vector-pathogen-host interactions. J Infect Dev Ctries. 2021;15:1039–47. https://doi.org/10.3855/jidc.13291
48. Yssouf A, Almeras L, Terras J, Socolovschi C, Raoult D, Parola P. Detection of *Rickettsia* spp in ticks by MALDI-TOF MS. PLoS Negl Trop Dis. 2015;9:e0003473. https://doi.org/10.1371/journal.pntd.0003473
49. Zhou G, Xu X, Zhang Y, Yue P, Luo S, Fan Y, et al. Antibiotic prophylaxis for prevention against Lyme disease following tick bite: an updated systematic review and meta-analysis. BMC Infect Dis. 2021;21:1141. https://doi.org/10.1186/s12879-021-06837-7

Address for correspondence: Prof. Philippe Parola, Institut Hospitalo-Universitaire Méditerranée Infection, 19–21 Blvd Jean Moulin, 13005 Marseille, France; email: philippe.parola@univ-amu.fr

etymologia

Haematospirillum jordaniae [Hae.ma.to.spi.ril'lum jor.da'ni.ae]

Clyde Partin

For the sesquipedalian term Haematospirillum, Haema is derived from the Greek *haima*, meaning blood. Spirillum is derived from Medieval Latin in the mid-13th century Latin (*spiralis*), French in the 1550s (*spiral*), and Greek (*speira*). All suggest a winding or coil. A New Latin reference book entry in 1875 implied a little coil.

Isolated from human blood, *Haematospirillum jordaniae* was reported as a novel genus and species in 2016 by Centers for Disease Control and Prevention (CDC) scientist Ben W. Humrighouse and his laboratory team, which included Jean G. Jordan, a microbiologist. This gram-negative bacterium was isolated 14 times in 10 states during 2003–2012 before its identification in 2016.

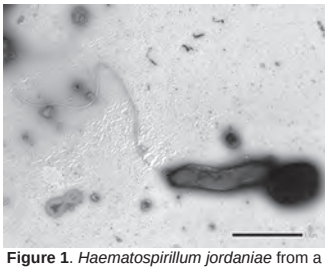

Figure 1. *Haematospirillum jordaniae* from a human blood sample. Scale bar indicates 1 μm. Source: (5).

H. jordaniae was previously considered an environmental bacterium with limited pathogenicity, but increasing numbers of isolates indicated a possible emerging pathogen. All cases occurred in male patients, and the pathogen showed a predilection for infecting lower leg injuries. In 2018, Hovan and Hollinger reported a case of infection in a Delaware man who, in 2016, had sepsis from a lower leg wound. The organism isolated was identified at the CDC Special Bacteriology Reference Laboratory (SBRL) in the Division of High-Consequence Pathogens and Pathology, National Center for Emerging and Zoonotic Infectious Diseases.

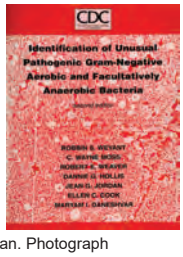

Figure 2. Jean G. Jordan. Photograph provided by the Special Bacteriology Reference Laboratory, Division of High-Consequence Pathogens and Pathology, National Center for Emerging and Zoonotic Infectious Diseases, Centers for Disease Control and Prevention.
Figure 3. The Orange Book (7). Jean G. Jordan was one of the original authors.

Jordan, who helped identify an *H. jordaniae* sample in 2010, was honored by having the species named after her. She spent 52 years at CDC and was one of the authors of the "The Orange Book," the standard reference for bacterial special pathogens, more formally known as "Identification of Unusual Pathogenic Gram-Negative Aerobic and Facultatively Anaerobic Bacteria." Her colleagues fondly recall Jordan, noting, "Jean was an integral part of SBRL's founding. Although not necessarily a well-known person, she was the behind the scenes expert who never wanted any special credit."

Sources:

1. Hovan G, Hollinger A. Clinical isolation and identification of H*aematospirillum jordaniae*. Emerg Infect Dis. 2018;24:1955–6. https://doi.org/10.3201/eid2410.180548
2. Humrighouse BW, Emery BD, Kelly AJ, Metcalfe MG, Mbizo J, McQuiston JR. *Haematospirillum jordaniae* gen. nov., sp. nov., isolated from human blood samples. Antonie van Leeuwenhoek. 2016;109:493–500. https://doi.org/10.1007/s10482-016-0654-0
3. LPSN. List of prokaryotic names with standing in nomenclature. Species *Haematospirillum jordaniae* [cited 2022 May 21]. https://lpsn.dsmz.de/species/haematospirillum-jordaniae
4. Jean Jordan obituary. Published by the Atlanta Journal-Constitution on May 28, 2014. [cited 2022 Oct 17]. https://www.legacy.com/us/obituaries/atlanta/name/jean-jordan94 obituary?id=23964116
5. Pal E, Štrumbelj I, Kišek TC, Kolenc M, Pirš M, Rus KR, et al. *Haematospirillum jordaniae* cellulitis and bacteremia. Emerg Infect Dis. 2022;28:2116–9. https://doi.org/10.3201/eid2810.220326
6. Persiana (1875) (Latin Edition): Heckmanns, Alexius. *Spirillum* (n.) [cited 2022 May 21]. https://www.etymoline.com/word/spirillum
7. Weyant RS, Moss CW, Weaver RE. Hollis, Jordan JG, Cook E, et al.; Centers for Disease Control and Prevention. Identification of unusual pathogenic gram-negative aerobic and facultatively anaerobic bacteria. The Orange Book, 2nd ed. Philadelphia: Lippincott Williams and Wilkins; 1996.

Author affiliation: Emory University, Atlanta, Georgia, USA

DOI: https://doi.org/10.3201/eid2904.220831

Address for correspondence: Clyde Partin, Department of Internal Medicine, Emory University, 1365 Clifton Rd NE, Atlanta, GA 30322-1007, USA; email: wpart01@emory.edu

Association of Scrub Typhus in Children with Acute Encephalitis Syndrome and Meningoencephalitis, Southern India

Tina Damodar, Bhagteshwar Singh, Namratha Prabhu,[1] Srilatha Marate,[1] Vykuntaraju K. Gowda, A.V. Lalitha, Fulton Sebastian Dsouza, Sushma Veeranna Sajjan, Mallesh Kariyappa, Uddhava V. Kinhal, P.V. Prathyusha, Anita Desai, Kandavel Thennarasu, Tom Solomon, Vasanthapuram Ravi, Ravi Yadav

Scrub typhus is an established cause of acute encephalitis syndrome (AES) in northern states of India. We systematically investigated 376 children with AES in southern India, using a stepwise diagnostic strategy for the causative agent of scrub typhus, *Orientia tsutsugamushi*, including IgM and PCR testing of blood and cerebrospinal fluid (CSF) to grade its association with AES. We diagnosed scrub typhus in 87 (23%) children; of those, association with AES was confirmed in 16 (18%) cases, probable in 55 (63%), and possible in 16 (18%). IgM detection in CSF had a sensitivity of 93% and specificity of 82% compared with PCR. Our findings suggest scrub typhus as an emerging common treatable cause of AES in children in southern India and highlight the importance of routine testing for scrub typhus in diagnostic algorithms. Our results also suggest the potential promise of IgM screening of CSF for diagnosis of AES resulting from scrub typhus.

Scrub typhus is an acute febrile illness caused by an obligate intracellular gram-negative bacterium, *Orientia tsutsugamushi*. It is transmitted through chigger mites and is considered endemic to the tsutsugamushi triangle (covering Asia, northern Australia, and islands in the Indian and Pacific Oceans), although scrub typhus caused by other *Orientia* species has also been reported in Africa, France, the Middle East, and South America (*1*). A recent systematic review from hospital-based studies in India reported 25% of acute undifferentiated febrile illness was caused by scrub typhus. Most studies included were from southern India, but only 20% of included patients were ≤15 years of age (*2*). Although scrub typhus illness is typically self-limiting, neurologic complications are seen in 20%–25% of patients admitted to the hospital and are associated with high mortality rates (*3*,*4*). Scrub typhus can result in myriad neurologic manifestations, including meningitis, meningoencephalitis, encephalopathy, seizures, stroke, neuropathy, optic neuritis, myositis, myelitis, involuntary movements, and Guillain-Barré syndrome, all of which are well recognized in adults (*3*,*4*).

Recent studies in India have identified *O. tsutsugamushi* as a major cause of acute encephalitis syndrome (AES) outbreaks, especially in northern states of the country, such as Uttar Pradesh, Bihar, West Bengal, and Assam (*5*–*7*). Outbreaks of AES pose a major public health problem in India, predominantly affecting children (*8*). The definition of AES used for syndromic surveillance is broad and includes all patients experiencing acute onset of fever and altered mental state (*9*,*10*). The clinical manifestation might be caused by encephalitis or meningitis (direct invasion of the

Author affiliations: National Institute of Mental Health and Neurosciences, Bangalore, India (T. Damodar, N. Prabhu, S. Marate, P.V. Prathyusha, A. Desai, K. Thennarasu, V. Ravi, R. Yadav); Christian Medical College, Vellore, India (B. Singh); University of Liverpool, Liverpool, UK (B. Singh, T. Solomon); Liverpool University Hospitals NHS Foundation Trust, Liverpool (B. Singh, T. Solomon); Indira Gandhi Institute of Child Health, Bangalore (V.K. Gowda, U.V. Kinhal); St. John's Medical College and Hospital, Bangalore (A.V. Lalitha, F.S. Dsouza); Vani Vilas Women and Children's Hospital, Bangalore Medical College and Research Institute, Bangalore (S.V. Sajjan, M. Kariyappa); The Walton Centre NHS Foundation Trust, Liverpool (T. Solomon); The Pandemic Institute, Liverpool (T. Solomon)

DOI: https://doi.org/10.3201/eid2904.221157

[1]These authors contributed equally to this article.

central nervous system [CNS] by the pathogen) or encephalopathy without CNS invasion, such as in the case of severe systemic infection, metabolic derangement, or other neurologic complications after the infection (*10*,*11*). Identifying the pathogenesis could inform management and prognosis (*10*,*12*).

Early diagnosis is key to initiating prompt specific treatment, which can reduce complications and fatality rates of scrub typhus (*2*,*13*). Clinical diagnosis can be challenging because of the overlap of symptoms with other tropical infections endemic to the area that can also cause AES (*5*), such as dengue, chikungunya, malaria, and leptospirosis (*14*). Current microbiological diagnostics for scrub typhus, which are usually based on detecting IgM in serum samples or nucleic acid by PCR, have limitations. IgM appears in serum 5–6 days after onset of illness, can persist long after acute illness, and might cross-react with IgM of other cocirculating pathogens (*14*,*15*). Therefore, in AES patients with simultaneous microbiological evidence for another potential pathogen and *O. tsutsugamushi*, confirming *O. tsutsugamushi* as the cause is difficult. Detection of IgM in cerebrospinal fluid (CSF) is yet to be used widely in patients with suspected neurologic scrub typhus. Immunofluorescence assay has long been considered the reference standard serologic test, but its use is limited by expense and challenges in interpretation. PCR might help overcome shortcomings of serologic tests with respect to cross-reacting and persisting antibodies, but a positive result is only likely during the bacteremia phase of infection (*16*). Moreover, the recommended samples for *O. tsutsugamushi* PCR are blood or eschar material, whereas the sensitivity of PCR on CSF remains unclear (*7*,*16*,*17*). Therefore, a diagnostic approach using accessible tests to determine the association of scrub typhus with AES is urgently needed.

We present preliminary findings of an ongoing multicenter prospective cohort study suggesting scrub typhus as a cause of AES in children in southern India. We used a diagnostic strategy to investigate the association of scrub typhus with AES. We describe the clinical spectrum, epidemiology, and laboratory findings of children with scrub typhus manifesting as AES. We then identify patients demonstrating evidence of meningoencephalitis or encephalitis and explore the value of performing IgM ELISA on CSF samples.

Methods

Patients and Study Sites

We prospectively enrolled pediatric patients from 1 month to 18 years of age who fulfilled the Indian National Vector Borne Disease Control Programme (NVBDCP) and World Health Organization case definition of AES (*8*) (Appendix Table 1, https://wwwnc.cdc.gov/EID/article/29/4/22-1157-App1.pdf) and with illness duration of <30 days at the time of hospital admission. Patients were those treated at 3 tertiary-care hospitals in Bangalore, Karnataka state, India (Indira Gandhi Institute of Child Health, St. John's Medical College and Hospital, and Vani Vilas Hospital), during March 2019–March 2022.

Ethics Statement

The study was approved by the institutional ethics and review boards of the hospitals and the coordinating center, National Institute of Mental Health and Neurosciences. Full informed consent was taken by the study team, who were trained specifically in taking consent from caregivers, and assent from older children, using procedures and forms approved by the institutional ethics committees.

Clinical Assessment and Data Collection

Clinical coinvestigators (V.K.G., L.A.V., F.S.D., S.S., M.K.) from the 3 centers performed clinical and neurologic examination of patients. After obtaining consent, we entered detailed clinical history and examination findings on an electronic clinical proforma. Results of routine laboratory tests and patient demographics were collected and entered online by N.P., S.M., or T.D. We determined the normal range of routine laboratory tests according to the age of the patient (*18*) and defined single-organ dysfunction and multiorgan dysfunction syndrome according to established criteria (*19*).

Microbiological Testing

Blood and CSF specimens of enrolled patients were tested at the Department of Neurovirology, National Institute of Mental Health and Neurosciences, by using a laboratory algorithm designed by Ravi et al. (*5*) with some modifications (Figure 1). First-line tests included serum IgM ELISA for various pathogens. CSF samples of patients with IgM-positive ELISA serum samples were diluted in 1:10 proportion for detection of IgM. We performed confirmatory tests on IgM-positive patients, including real-time PCR for *O. tsutsugamushi* on CSF and blood samples. For PCR, we extracted DNA from samples by using the QIAamp DNA mini kit (QIAGEN, https://www.qiagen.com) and performed real-time PCR targeting the 47kDa protein gene using the protocol described by Jiang et al. (*20*). In

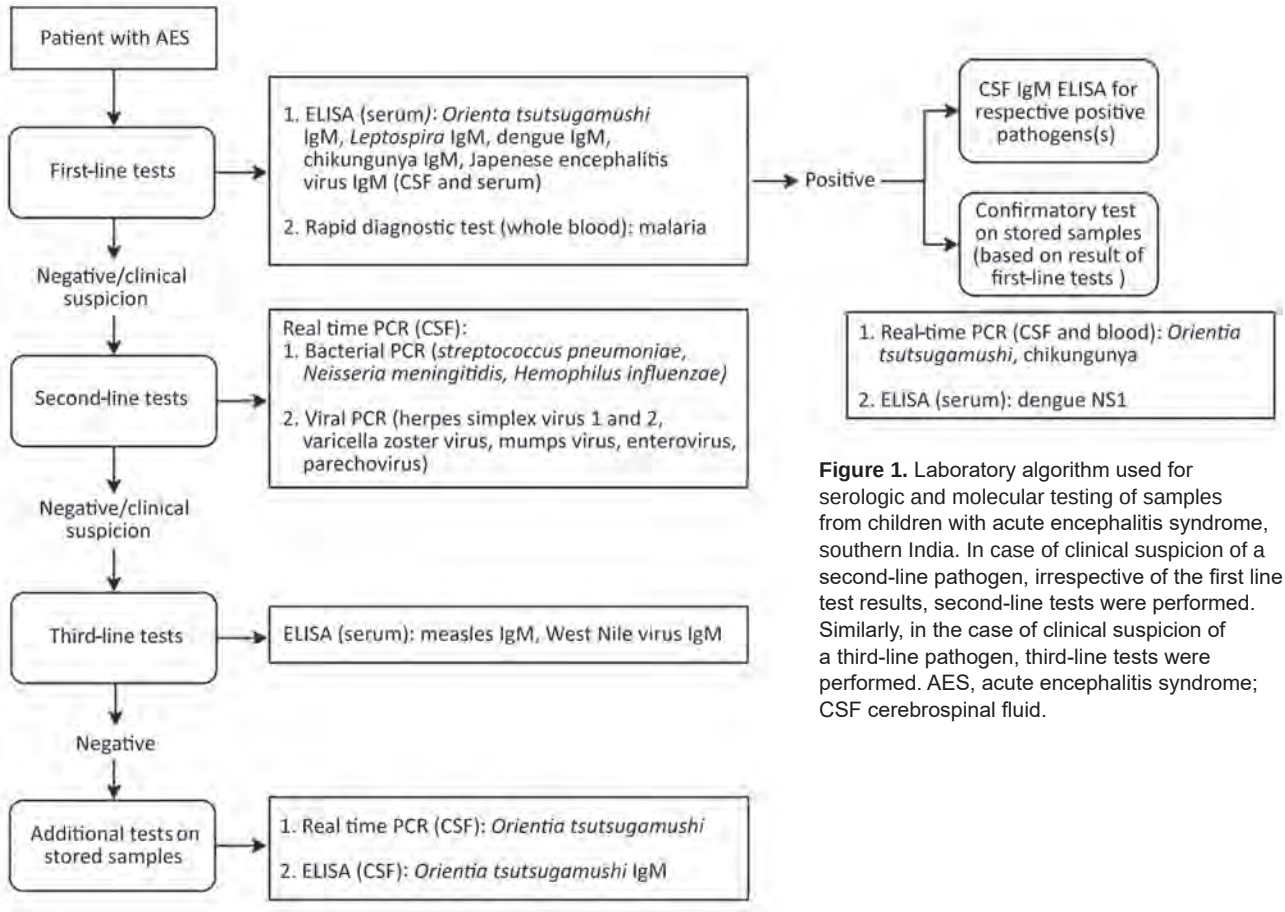

Figure 1. Laboratory algorithm used for serologic and molecular testing of samples from children with acute encephalitis syndrome, southern India. In case of clinical suspicion of a second-line pathogen, irrespective of the first line test results, second-line tests were performed. Similarly, in the case of clinical suspicion of a third-line pathogen, third-line tests were performed. AES, acute encephalitis syndrome; CSF cerebrospinal fluid.

addition, we also performed real-time PCR and IgM ELISA for *O. tsutsugamushi* on stored CSF samples of patients with a negative result after third-line tests. We used the Scrub Typhus Detect IgM ELISA kit (InBios International, http://inbios.com) and considered an optical density (OD) cutoff of 0.8 in serum (*15*) and 0.5 in CSF (*21*) samples to be positive. Scrub typhus was diagnosed in patients with IgM-positive real-time PCR or ELISA.

The level of certainty of association of scrub typhus with AES in cases positive for ≥1 microbiological test(s) for *O. tsutsugamushi* was determined by using criteria determined by Granerod et al. (*11*) with modifications (Tables 1, 2). We identified patients with meningoencephalitis/encephalitis (ME) and scrub typhus ME as those demonstrating clinical signs of either encephalitis or meningoencephalitis (Table 2).

Statistical Analysis

We performed statistical analysis by using R version 3.6.3 (The R Project for Statistical Computing, https://www.r-project.org). We presented descriptive data for categorical variables as frequencies, percentages, or both and described continuous variables using mean ±SD or median and interquartile range (IQR). To describe the diagnostic accuracy of CSF IgM, we compared results against CSF PCR to calculate the sensitivity, specificity, positive predictive value (PPV), and negative predictive value (NPV) of CSF IgM with 95% CI. We also calculated those values for patients with scrub typhus ME.

Table 1. Diagnostic criteria for certainty in the association of AES with scrub typhus in children, southern India*

Association of AES with scrub typhus	Real-time PCR	Serum IgM ELISA	CSF IgM ELISA	Simultaneous evidence of another pathogen(s)
Confirmed	+	+/−	+/−	+/−
Probable, single†	–	+	+/−	–
Probable, co-positive‡	–	+	+	+
Possible	–	+	–	+

*AES, acute encephalitis syndrome; CSF, cerebrospinal fluid.
†Without evidence of another potentially causative pathogen.
‡With evidence of another potentially causative pathogen.

Table 2. Definitions used for diagnostic association of AES with scrub typhus, ME, and scrub typhus ME in study of association of AES with scrub typhus in children, southern India*

Condition	Definition
Diagnostic association of AES with scrub typhus	Confirmed: Detection of *Orientia tsutsugamushi* DNA by PCR in CSF or blood Probable (single): Positive serum IgM ELISA with or without positive CSF IgM ELISA for *Orientia tsutsugamushi* and no other explanatory pathogen or cause Probable (co-positive): Positive serum IgM ELISA and positive CSF IgM ELISA for *Orientia tsutsugamushi* with evidence of another pathogen(s) Possible: Positive serum IgM ELISA and negative CSF IgM ELISA for *Orientia tsutsugamushi* with evidence of another pathogen(s)
Meningoencephalitis (22)	Presence of ≥1 of the following findings: CSF pleocytosis, meningeal enhancement or parenchymal inflammation on contrast enhanced CT or MRI of brain, positive real time PCR in CSF
Scrub typhus ME	Patients with meningoencephalitis AND positive real-time PCR or serum IgM ELISA for *Orientia tsutsugamushi* (and no other explanatory pathogen or cause) (i.e, patients with confirmed or probable [single] diagnostic association of AES with scrub typhus)

*AES, acute encephalitis syndrome; CSF, cerebrospinal fluid; CT, computed tomography; ME, meningoencephalitis; MRI, magnetic resonance imaging.

Results

We included a total of 376 children with AES in the study (Appendix Figure 1). Of those, scrub typhus was diagnosed in 87 patients by using the laboratory algorithm described.

Microbiological Testing

We collected samples for microbiological testing a median of 11 (IQR 8–14) days from onset of symptoms and median of 4 (IQR 2–6) days after hospitalization. Serum samples were positive for *O. tsutsugamushi* IgM in 86/376 (22.8%) patients. Of those 86 patients, 39 (45.4%) had a positive microbiological test result for another pathogen (referred to as copositive) (Appendix Table 2); 47 (54.6%) were positive for *O. tsutsugamushi* IgM alone (referred to as single-positive).

CSF samples were available for 82/86 patients with *O. tsutsugamushi* IgM–positive serum samples and all 184 patients who had no etiologic diagnosis after use of the laboratory algorithm. CSF samples were IgM-positive in 58/82 (71%) patients (23/36 of copositive patients and 35/45 of single-positive patients). All 184 serum IgM-seronegative patients were negative for CSF IgM by ELISA.

Real-time PCR results were positive in 15/86 (17%) patients with IgM-positive serum (real-time PCR of both CSF and blood was positive in 2 patients; 11 were positive by CSF PCR only and 2 by blood PCR only). Of the 184 CSF samples of patients with no etiologic diagnosis after first-line and second-line tests, 1 was positive by real-time PCR for *O. tsutsugamushi*. In total, 16 patients were positive for *O. tsutsugamushi* by PCR. Therefore, of 376 patients with AES, 87 (23%) had a positive microbiological test for scrub typhus (AES–scrub typhus) (Figure 2).

Diagnostic Association of Scrub Typhus with AES

On the basis of serum IgM results, the association of scrub typhus with AES was probable in 47/87 (54%) patients and possible in 39/87 (45%) patients. Further, on performing IgM ELISA on CSF samples, the association was probable (single-positive) in 47 (58.8%) persons, probable (copositive) in 23 (26.4%) persons, and possible in 16 (18%) persons. Finally, on the basis of real-time PCR results, the association was confirmed in 16 (18%) patients, probable (single-positive) in 38 (43.7%) patients, probable (co-positive) in 17 (19.5%) patients, and possible in 16 (18.4%) patients (Figure 2).

ME and Scrub Typhus ME

Of the 87 patients, 65 (74.7%) had findings suggestive of ME (Appendix Tables 3, 4). The diagnostic association of ME with scrub typhus was confirmed or probable (single-positive) in 54 (62%) patients (Figure 2), and of those patients, 43 had ME. Therefore, among all 87 patients, 49.4% had scrub typhus ME (Figure 3).

Diagnostic Accuracy of CSF IgM Testing

We performed IgM ELISA and real-time PCR on CSF samples of 266 patients (i.e., 82/86 patients with IgM-positive serum samples and 184/184 patients with no etiology after tests were performed per the laboratory algorithm). We created a 2×2 table to compare the performance of CSF IgM with CSF PCR. The sensitivity of CSF IgM ELISA was 92.9% (95% CI 66.1%–99.8%), specificity 82.1% (95% CI 76.8%–86.6%), PPV 22.4% (12.5%–35.2%), and NPV 99.5% (97.3%–100%) (Table 3).

CSF samples were available for 53/54 patients with confirmed or probable (single-positive) scrub typhus.

CSF IgM was positive in 36/42 (85.7%) patients with ME and 5/11 (45.5%) patients without ME. Sensitivity of CSF IgM in patients with ME was 85.7% (95% CI 71.4–94.5%) and specificity was 54.5% (95% CI 23.3%–83.2%); the corresponding PPV was 87.8% (78.8%–93.3%) and NPV was 50.0% (28.6%–71.4%) (Figure 3).

Demographic and Clinical Profile

The male:female ratio of children with scrub typhus was 1.5:1. Ages ranged from 2 months to 17 years; the mean age was 8.5 (SD ±4) years (Table 4). Proportions of AES-scrub typhus cases were highest in the months of August and September. In addition, the number of

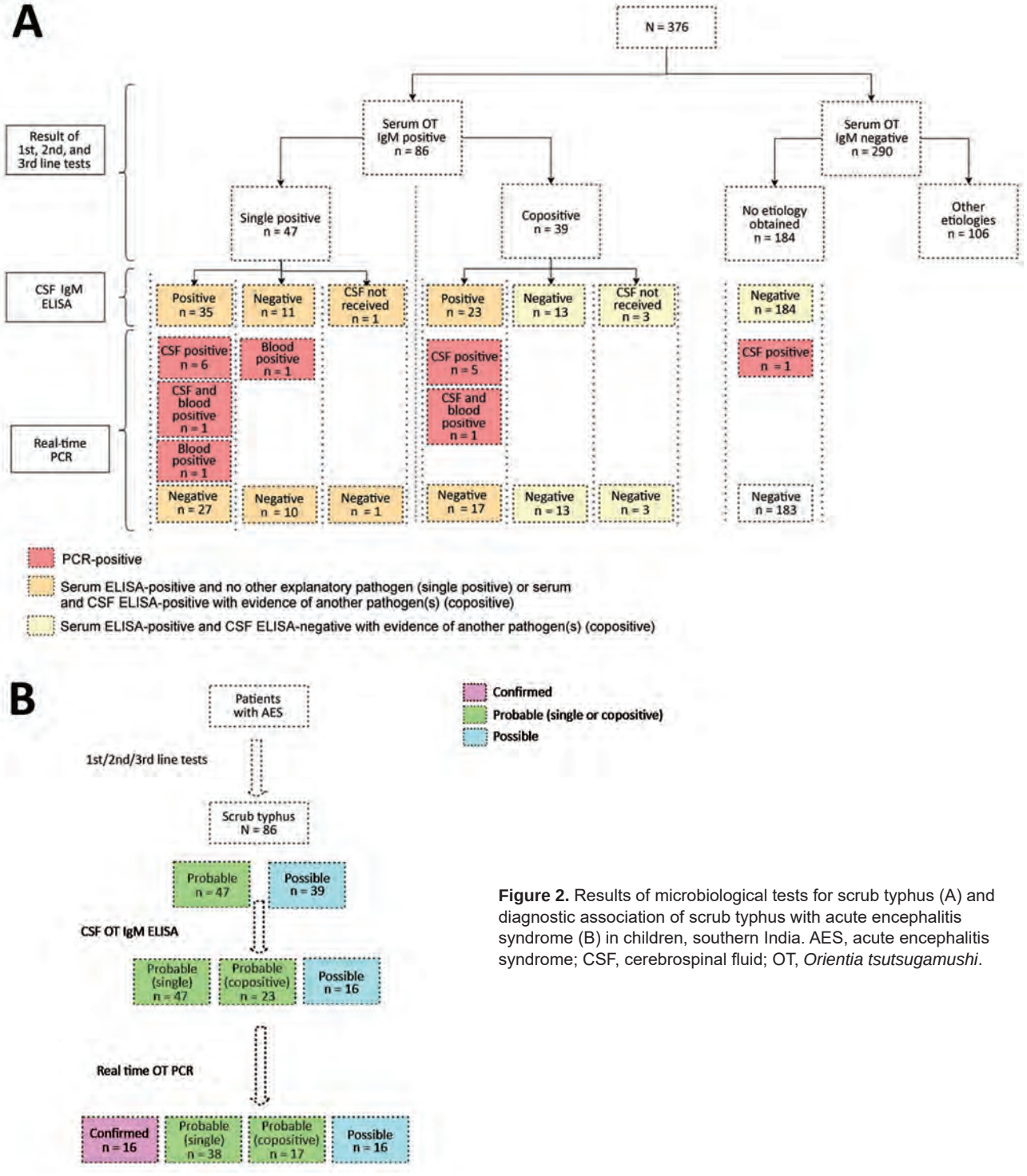

Figure 2. Results of microbiological tests for scrub typhus (A) and diagnostic association of scrub typhus with acute encephalitis syndrome (B) in children, southern India. AES, acute encephalitis syndrome; CSF, cerebrospinal fluid; OT, *Orientia tsutsugamushi*.

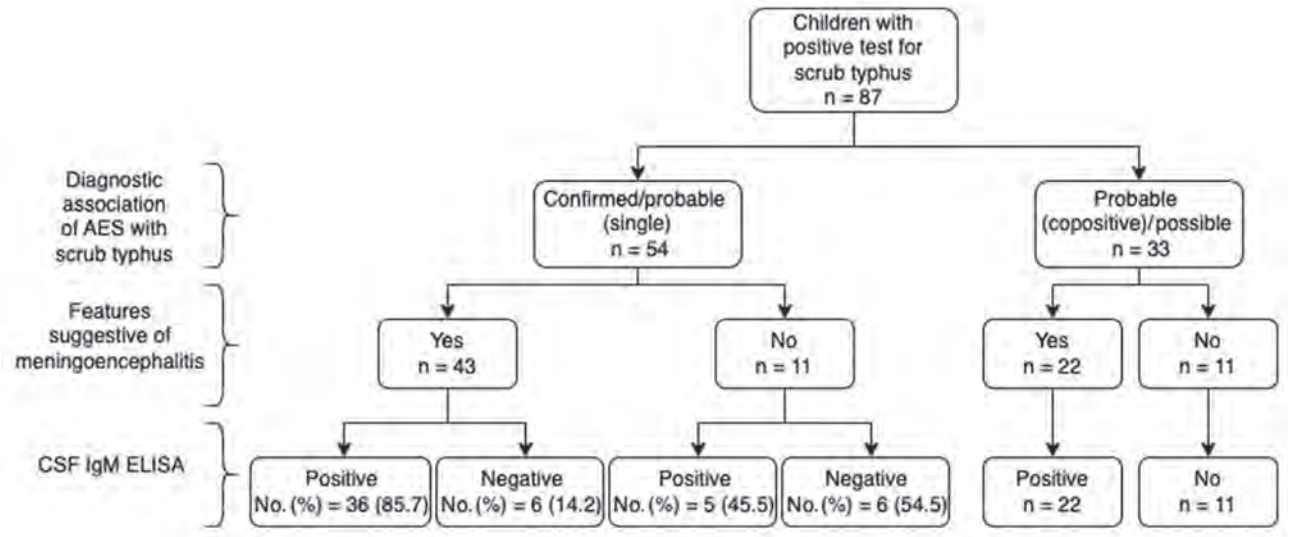

Figure 3. CSF IgM ELISA results of children with scrub typhus ME, southern India. CSF samples were available in 42/43 children with ME of which CSF IgM was positive in 85.7% children. AES, acute encephalitis syndrome; CSF, cerebrospinal fluid; ME, meningoencephalitis.

AES-scrub typhus patients and their proportion of total AES patients followed the same pattern as the total number of AES cases (Appendix Figures 2, 3). The largest percentage of children (37%) were from Anantapur district in Andhra Pradesh state, followed by 17% from Tumkur district in Karnataka state (Figure 4). Nearly 48% of patients were referred from another hospital, and 34% received anti-infective medications before being admitted to the study hospital. The median duration of illness before admission to the study hospital was 6 (IQR 4–9.5) days.

All 87 children experienced fever and change in mental state; fever was the first symptom in 95% of cases. Around 62% of children had seizures; generalized tonic-clonic seizures were the most common type (74%), and some patients also had focal, tonic, or absence seizures. Upon examination at the time of hospital admission, 55 (64%) patients had altered mental state. The Glasgow Coma Scale at admission ranged from 3 to 15; the median was 13 (IQR 10–15) (Table 5). Signs of meningeal irritation were detected in 48% of patients, cerebellar signs in 21%, and papilledema in 20%. Other neurologic findings were cranial nerve abnormalities (6%), involuntary movements (9%) and photophobia (9%), abnormal tone (50%), decreased power (19%), and abnormal plantar reflexes (24%) (Table 5). Approximately 39% of the patients met criteria for multiorgan dysfunction syndrome (Appendix Table 5).

Laboratory Findings

Anemia, leukocytosis, thrombocytopenia, transaminitis, hypoalbuminemia, and uremia were each present in >50% of patients (Table 6). CSF results revealed lymphocytic pleocytosis and elevated protein concentration in most patients (Appendix Table 6).

Treatment

Of the patients with scrub typhus, 44 (51%) required care in the intensive care unit during their hospitalization, and 26 of those required ventilatory support. All patients except 1 were prescribed doxycycline (100 mg 2×/d for 10 days). One patient died during hospitalization.

Discussion

Our findings suggest that scrub typhus is a major cause of AES in children in southern India. Of 193 (51%) patients with a known etiology, a microbiological test for *O. tsutsugamushi* was positive in 87 (45%)

Table 3. Performance of cerebrospinal fluid IgM ELISA compared with cerebrospinal fluid real-time PCR for scrub typhus in children with acute encephalitis syndrome and meningoencephalitis, southern India

	Cerebrospinal fluid PCR		
Cerebrospinal fluid IgM	No. (%) positive	No. (%) negative	Total
Positive	13 (92.8)	45 (17.8)	58
Negative	1 (7.1)	207 (82.1)	208
Total	14	252	266

patients, making it the most common etiology obtained in the study. An increasing number of studies in Asia have reported the contribution of *O. tsutsugamushi* to the burden of acute febrile illness in the continent, including South Korea, Japan, China, Taiwan, Thailand, and Bhutan, countries where scrub typhus is a notifiable disease (*24*). Studies including screening for *O. tsutsugamushi* as part of systematic surveillance of childhood CNS infections in Cambodia, Vietnam, Laos, Myanmar, and Thailand report its presence in 1%–4.7% of children (*17*,*25*–*28*). Although studies in India have documented meningoencephalitis as a manifestation of scrub typhus in children (*2*,*29*,*30*), our study highlights the importance of systematic screening for scrub typhus in children with AES in southern India. Scrub typhus is a well-recognized cause of acute febrile illness in the major southern Indian states of Andhra Pradesh and Karnataka (*31*–*33*), but we report scrub typhus is also a common cause of AES in children from these states.

Given the challenges in clinical diagnosis (*10*,*14*,*15*) and complexity of defining the causal relationship of scrub typhus with AES on the basis of serum IgM ELISA, the most widely used test for scrub typhus (*15*), we used a causality strategy. This diagnostic strategy helped in differentiating the certainty of association of 87 AES–scrub typhus cases into 16 cases with confirmed association, 55 with probable association, and 16 with possible association. Real-time PCR, which is confirmatory for scrub typhus, was positive in 6/39 (15%) cases with microbiological evidence of another pathogen and increased the diagnostic association from possible to confirmed. We were able to diagnose scrub typhus in 1 extra case in which

Table 4. Demographic details of children with scrub typhus manifesting as acute encephalitis syndrome, southern India

Variable	No. (%) patients
Age, y, n = 87	
<2	2 (2.3)
2–9	50 (57.5)
10–18 y	35 (40.2)
Sex, n = 87	
M	52 (59.8)
F	35 (40.2)
State, n = 81	
Karnataka	44 (54.3)
Andhra Pradesh	36 (44.4)
Tamil Nadu	1 (1.2)
Setting, n = 82	
Rural	64 (78)
Urban	18 (22)
Risk factors, n = 78*	
Contact with shrubs, vegetation, or agricultural farms	49 (62.8)
Contact with animals, birds, or pets	47 (60.3)
Proximity to forest	14 (17.9)

*Based on response to a structured questionnaire in the form of Yes or No.

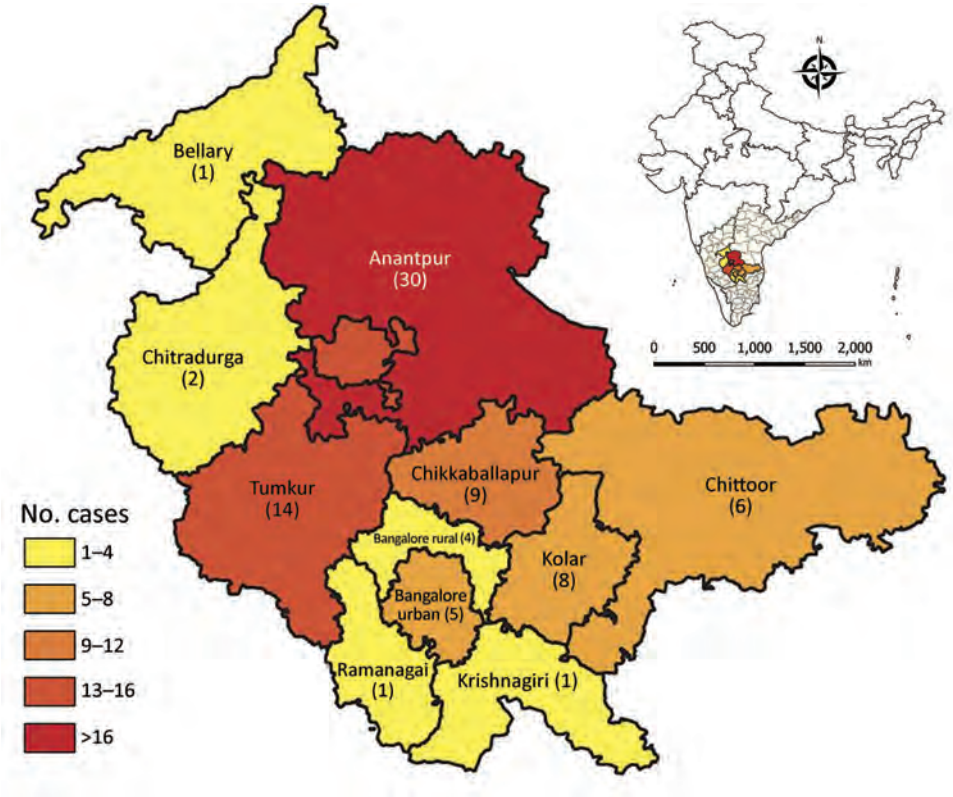

Figure 4. District-wise distribution of children with scrub typhus manifesting as acute encephalitis syndrome, southern India. Number of children from each district with scrub typhus manifesting as acute encephalitis syndrome is indicated. The 3 recruiting hospitals and the coordinating center are located in Bangalore urban. Inset shows location of study area in India.

IgM ELISA for *O. tsutsugamushi* and tests for other pathogens were negative. Despite systematic testing, the prevalence of positive real-time PCR in children with AES caused by scrub typhus was low in our study (16 [18%] children), although still higher than in other studies (*7*,*34*). PCR positivity might be maximized by collecting clinical samples sooner after illness onset and using whole blood or buffy coat instead of serum to capture intracellular bacteria (*14*,*16*). In this study, patients with a positive PCR had a median duration of illness of 9 (IQR 5.75–12.25) days before clinical specimen sampling versus 11 (IQR 8.5–14.5) days for patients with a negative PCR result.

Because IgM does not ordinarily cross the blood–CSF barrier, presence of those antibodies in CSF implies their production within the CNS (*35*) and higher certainty of association with the infection compared to serum IgM. Using CSF IgM ELISA increased the certainty of association from possible to probable in 23 patients who had simultaneous evidence of another pathogen. Although the kit is recommended for

Table 5. Clinical findings of children with scrub typhus manifesting as acute encephalitis syndrome, southern India

Clinical features, n = 86*	No. (%) patients
Duration of illness, d	
≤5	38 (44)
>5	48 (56)
Clinical signs and symptoms	
Fever	87 (100)
Change in mental status†	87 (100)
Seizure	53 (61.6)
Vomiting	46 (53.5)
Headache	32 (37.2)
New abnormal speech (e.g., slurred) including the inability to speak	24 (27.9)
Change in personality or behavior	18 (20.9)
Limb weakness	11 (12.8)
Arthralgia or myalgia	7 (8.1)
Respiratory symptoms‡	8 (9.3)
Gastrointestinal symptoms§	29 (33.7)
Urinary symptoms: decreased urine output, burning micturition	3 (3.5)
General and systemic examination findings	
Pallor	23 (26.7)
Icterus	6 (7)
Lymphadenopathy: cervical, inguinal, axillary, mesenteric	16 (18.6)
Edema: periorbital, facial, lower limbs, upper limbs	17 (19.8)
Conjunctivitis/subconjunctival hemorrhage	17 (19.8)
Skin rash	12 (14)
Eschar: axilla, groin, dorsal aspect of penis	4 (4.7)
Abnormal bleeding: nasal, anal, gums	3 (3.5)
Respiratory system findings¶	21 (24.4)
Gastrointestinal system findings#	50 (58.1)
Cardiac system abnormalities: abnormal heart sounds, abnormal pulse	4 (4.7)
Neurologic findings	
Cranial nerve abnormality: 6th and 7th	5 (5.7)**
Sign of meningeal irritation: nuchal rigidity, Kernig's sign, Brudzinski sign, bulging of anterior fontanelle in infants	41 (47.7)
Photophobia	8 (9.3)
Papilledema	17 (19.8)
Abnormal tone	43 (50)
Paresis/paralysis: decreased power in ≥1 limbs	16 (18.6)
Exaggerated reflexes	4 (4.7)
Abnormal Plantar reflex	21 (24.4)
Involuntary movements††	8 (9.3)
Cerebellar sign(s)‡‡	18 (20.9)

*All 87 children had fever and change in mental status, but detailed clinical findings of just 86 children were recorded.
†Change in mental status was defined as ≥1 of the following: change in cognition (such as confusion or disorientation), drowsiness, coma, lethargy, irritability, reduced activity, poor feeding, irrelevant/abnormal talk.
‡Includes cough and/or difficulty breathing. Both were present in 5 patients each.
§Includes ≥1 of the following symptoms: abdominal pain, abdominal distension, and diarrhea. Individually, abdominal pain was a symptom in 19 (22%), abdominal distention in 12 (14%), and diarrhea in 3 (3.5%) patients.
¶Signs of respiratory distress occurred in 16 (19%) patients; reduced air entry or abnormal respiratory sounds occurred in 5 (5%) patients.
#Hepatomegaly was present in 47 (54.7%) patients, splenomegaly was present in 16 (18.6%) patients, and ascites was present in 4 (4.7%) patients.
**Four persons had abnormalities in 6th cranial nerve, and 1 in 7th cranial nerve.
††Opsoclonus and myoclonus, choreoathetoid movements and hemiballismus, abnormal perioral movements, lip smacking, teeth grinding, and rapid eye blinking occurred in 1 patient each; tremors occurred in 2 patients.
‡‡Includes ≥1 of the following: truncal ataxia, gait abnormality, finger-nose incoordination, nystagmus, dysdiadochokinesis, and dysarthria.

detecting IgM in serum samples only, Murhekar et al. (*6*) observed good correlation between OD values for *O. tsutsugamushi* IgM in serum and CSF. They determined a cutoff OD value of 0.22 after testing CSF samples from 374 children <14 years of age with AES in Gorakhpur, Uttar Pradesh state, India (*35*). A cutoff OD value for IgM in CSF has not been determined in the southern states in India, so we used a higher cutoff (0.5), as used by Behera et al. (*21*) for CSF of children with scrub typhus ME in eastern India.

Our results demonstrate that, compared with PCR, IgM ELISA of CSF had a sensitivity of 92.9%, but with a wide 95% CI, suggesting the estimate is less precise. Although the comparison is indirect, that sensitivity is similar to that of serum IgM by the same ELISA kit (92.4%) used for patients with acute febrile illness caused by scrub typhus in southern India (*14*). The specificity of CSF IgM ELISA was moderate compared to PCR at 82%. That finding might be because PCR positivity was less common in our study, which could be explained by delayed sampling during the course of illness, resulting in a higher likelihood of detection of IgM than DNA. In addition, the use of a single reference standard (PCR) in our study could result in a low PPV of IgM ELISA of CSF. The sensitivity of CSF IgM in patients with scrub typhus ME was 85.7%. Because only 11 patients did not have features suggestive of ME, ascertaining the true specificity is difficult.

Almost three quarters of the patients with AES-scrub typhus had meningoencephalitis. Distinguishing patients with scrub typhus ME from patients with encephalopathy with other causes is crucial. Therapeutic failure of doxycycline, the drug of choice for scrub typhus, has been reported in patients with scrub typhus ME (*36*). This failure could be caused by inadequate concentration of doxycycline in CSF at conventional doses and might indicate the need for increased dosages, intravenous administration, or administration of other antimicrobial agents such as rifampin that have good penetration to the CNS. However, the efficacy of this treatment is yet to be proven (*37*,*38*).

The neurologic manifestations in children with scrub typhus that meet the broader epidemiologic definition of AES are rarely reported (*13*,*25*,*39*,*40*), and no data from southern India have been published. Of all children with scrub typhus in our study, 8 (9%) had involuntary hyperkinetic movements that are rare neurologic manifestations of scrub typhus more often reported in adults than children (*41*). Opsoclonus-myoclonus, best recognized as part of opsoclonus-myoclonus-ataxia syndrome associated with neuroblastoma in children, is rarely caused by infections (*13*,*41*). Only 2 such cases of scrub typhus associated with pediatric opsoclonus-myoclonus-ataxia syndrome have been reported from India (*42*,*43*). Cerebellar signs, which are uncommon in children with scrub typhus (*3*,*13*), were noted in almost one fifth of the children in our study. As reported by Vishwanath et al. (*30*), the sixth cranial nerve was the most affected cranial nerve. Papilledema was detected in 20% of children in our study. Few studies have reported direct retinal involvement and isolated optic disc edema in the absence of raised intracranial pressure in scrub typhus (*29*,*44*,*45*); however, findings in this area remain inconclusive in our study. Presence of eschar typically occurs in 4%–46% of patients with scrub typhus; therefore, while specific, eschar is not a sensitive marker (*30*), and it was found in only 5% of patients in this study.

The first limitation of our study is that, whereas serum IgM ELISA is the most widely used specific test for *O. tsutsugamushi*, we used a single-positive IgM result as a criterion for diagnosis of scrub typhus. Obtaining serial blood samples and performing immunofluorescence or similar assays to demonstrate a 4-fold rise in antibody titers would have enabled more certainty in the diagnosis, especially in cases in which antibodies to another pathogen were detected. However, we defined those patients as having possible scrub typhus to allow for this uncertainty, and they comprised only 18% of the scrub

Table 6. Laboratory results of children with scrub typhus manifesting as acute encephalitis syndrome, southern India

Sample type and variables	No. (%) patients
Peripheral blood, n = 87 unless stated otherwise	
Anemia	79 (90.8)
Leukocytosis	45 (51.7)
Leukopenia	4 (4.6)
Relative neutrophilia	31 (35.6)
Relative neutropenia	40 (46)
Relative lymphocytosis	43 (49.4)
Relative lymphopenia	26 (29.9)
Thrombocytopenia	45 (51.7)
Hyperbilirubinemia, n = 75	21 (28)
Elevated transaminases, n = 85*	72 (84.7)
Hypoalbuminemia, n = 80	66 (82.5)
Elevated urea, n = 80	56 (70)
Elevated creatinine, n = 86	6 (7)
Cerebrospinal fluid, n = 85 unless stated otherwise	
Pleocytosis†	59 (69.4)
Lymphocytic pleocytosis‡	54 (63.5)
Neutrophilic pleocytosis§	5 (5.8)
Elevated protein, n = 83	51 (61.4)

*Includes elevated levels of aspartate transaminase or alanine transaminase.
†Cerebrospinal fluid pleocytosis was recorded if white blood cell counts were >10 cells/μL in infants (1 mo–12 mo of age) and >4 cells/μL in older children (22).
‡Cerebrospinal fluid lymphocytic pleocytosis was defined as >50% mononuclear cells in cerebrospinal fluid of patients with pleocytosis (23).
§Cerebrospinal fluid neutrophilic pleocytosis was defined as a neutrophil count >50% of total leukocytes in patients with cerebrospinal fluid pleocytosis (23).

typhus patients in this study. Also, for IgM detection in CSF, we relied on a cutoff value widely used for serum IgM, because a cutoff value for CSF has not been determined in this region. Furthermore, we could not perform sequencing of the PCR-amplified nucleic acid or characterization of surface antigen because of limited resources.

In this study, despite limited accessibility and shortcomings of reference standard tests, we present a stepwise approach to identify scrub typhus as a probable or confirmed etiology by using tests that are relatively easy to access and perform. Our findings highlight the importance of systematic routine testing for the treatable and common pathogen *O. tsutsugamushi* in all patients with AES in southern India, as is practiced in several states in northern India. This testing could have a notable effect on the approach to clinical management and public health interventions for patients with AES. Apart from reinforcing common clinical, epidemiologic, and laboratory findings reported by other studies (*13*,*29*,*39*,*40*,*46*), we report insights into the neurologic spectrum of scrub typhus in children, which appears to be broad and underreported.

Finally, CSF IgM ELISA is a promising test for patients with AES caused by scrub typhus, which requires evaluation in a larger population and determination of a region-specific cutoff OD value. Combining CSF PCR with CSF IgM ELISA wherever feasible might increase the certainty of association between AES and scrub typhus.

Acknowledgment

We thank Manisha Biswal and Jasleen Kaur for providing us with positive control and technical advice to standardize real-time PCR for *Orientia tsutsugamushi*. We thank Reeta Mani for standardizing bacterial and chikungunya real-time PCR used as part of the laboratory algorithm.

This work was supported by DBT/Wellcome Trust India Alliance Fellowship IA/E/15/1/503960 awarded to T.D. The funders had no role in study design, data collection and analysis, decision to publish, or preparation of the manuscript.

About the Author

Dr. Damodar is an India Alliance DBT/Wellcome Trust early career fellow (Clinical and Public Health) in the Department of Neurovirology, National Institute of Mental Health and Neurosciences (Bangalore, India). Her research interests include strengthening diagnostics for infectious diseases of international public health concern.

References

1. Jiang J, Richards AL. Scrub typhus: no longer restricted to the tsutsugamushi triangle. Trop Med Infect Dis. 2018;3:11. https://doi.org/10.3390/tropicalmed3010011
2. Devasagayam E, Dayanand D, Kundu D, Kamath MS, Kirubakaran R, Varghese GM. The burden of scrub typhus in India: a systematic review. PLoS Negl Trop Dis. 2021;15:e0009619. https://doi.org/10.1371/journal.pntd.0009619
3. Garg D, Manesh A. Neurological facets of scrub typhus: a comprehensive narrative review. Ann Indian Acad Neurol. 2021;24:849–64. https://doi.org/10.4103/aian.aian_739_21
4. Varghese GM, Trowbridge P, Janardhanan J, Thomas K, Peter JV, Mathews P, et al. Clinical profile and improving mortality trend of scrub typhus in South India. Int J Infect Dis. 2014;23:39–43. https://doi.org/10.1016/j.ijid.2014.02.009
5. Ravi V, Hameed SKS, Desai A, Mani RS, Reddy V, Velayudhan A, et al. An algorithmic approach to identifying the aetiology of acute encephalitis syndrome in India: results of a 4-year enhanced surveillance study. Lancet Glob Health. 2022;10:e685–93. https://doi.org/10.1016/S2214-109X(22)00079-1
6. Murhekar MV, Vivian Thangaraj JW, Sadanandane C, Mittal M, Gupta N, Rose W, et al. Investigations of seasonal outbreaks of acute encephalitis syndrome due to *Orientia tsutsugamushi* in Gorakhpur region, India: a One Health case study. Indian J Med Res. 2021;153:375–81. https://doi.org/10.4103/ijmr.IJMR_625_21
7. Jain P, Prakash S, Tripathi PK, Chauhan A, Gupta S, Sharma U, et al. Emergence of *Orientia tsutsugamushi* as an important cause of acute encephalitis syndrome in India. PLoS Negl Trop Dis. 2018;12:e0006346. https://doi.org/10.1371/journal.pntd.0006346
8. Sen PK, Dhariwal AC, Jaiswal RK, Lal S, Raina VK, Rastogi A. Epidemiology of acute encephalitis syndrome in India: changing paradigm and implication for control. J Commun Dis. 2014;46:4–11.
9. Government of India. Guidelines for surveillance of acute encephalitis syndrome (with special reference to Japanese encephalitis). November 2006 [cited 2022 Jul 1]. http://nvbdcp.gov.in/WriteReadData/l892s/AES_guidelines.pdf
10. John TJ, Verghese VP, Arunkumar G, Gupta N, Swaminathan S. The syndrome of acute encephalitis in children in India: need for new thinking. Indian J Med Res. 2017;146:158–61. https://doi.org/10.4103/ijmr.IJMR_1497_16
11. Granerod J, Cunningham R, Zuckerman M, Mutton K, Davies NWS, Walsh AL, et al. Causality in acute encephalitis: defining aetiologies. Epidemiol Infect. 2010;138:783–800. https://doi.org/10.1017/S0950268810000725
12. Venkatesan A, Geocadin RG. Diagnosis and management of acute encephalitis: a practical approach. Neurol Clin Pract. 2014;4:206–15. https://doi.org/10.1212/CPJ.0000000000000036
13. Misra UK, Kalita J, Mani VE. Neurological manifestations of scrub typhus. J Neurol Neurosurg Psychiatry. 2015;86:761–6. https://doi.org/10.1136/jnnp-2014-308722
14. Kannan K, John R, Kundu D, Dayanand D, Abhilash KPP, Mathuram AJ, et al. Performance of molecular and serologic tests for the diagnosis of scrub typhus. PLoS Negl Trop Dis. 2020;14:e0008747. https://doi.org/10.1371/journal.pntd.0008747
15. Varghese GM, Rajagopal VM, Trowbridge P, Purushothaman D, Martin SJ. Kinetics of IgM and IgG

antibodies after scrub typhus infection and the clinical implications. Int J Infect Dis. 2018;71:53–5. https://doi.org/10.1016/j.ijid.2018.03.018
16. Koh GC, Maude RJ, Paris DH, Newton PN, Blacksell SD. Diagnosis of scrub typhus. Am J Trop Med Hyg. 2010; 82:368–70. https://doi.org/10.4269/ajtmh.2010.09-0233
17. Pommier JD, Gorman C, Crabol Y, Bleakley K, Sothy H, Santy K, et al.; SEAe Consortium. Childhood encephalitis in the Greater Mekong region (the SouthEast Asia Encephalitis Project): a multicentre prospective study. Lancet Glob Health. 2022;10:e989–1002. https://doi.org/10.1016/S2214-109X(22)00174-7
18. Lo Stanley F. Reference intervals for laboratory tests and procedures. In: Kleigman RM, Behrman RE, Jenson HB, Stanton BP, editors. Nelson textbook of pediatrics. 20th ed. Philadelphia: Saunders Elsevier; 2011. p. 3464–3472.
19. Goldstein B, Giroir B, Randolph A; International Consensus Conference on Pediatric Sepsis. International pediatric sepsis consensus conference: definitions for sepsis and organ dysfunction in pediatrics. Pediatr Crit Care Med. 2005;6:2–8. https://doi.org/10.1097/01.PCC.0000149131.72248.E6
20. Jiang J, Chan TC, Temenak JJ, Dasch GA, Ching WM, Richards AL. Development of a quantitative real-time polymerase chain reaction assay specific for *Orientia tsutsugamushi*. Am J Trop Med Hyg. 2004;70:351–6. https://doi.org/10.4269/ajtmh.2004.70.351
21. Behera B, Satapathy AK, Ranjan J, Chandrasekar S, Patel S, Mishra B, et al. Profile of scrub typhus meningitis/meningoencephalitis in children with and without scrub typhus IgM antibody in CSF. J Neurosci Rural Pract. 2021;12:786–91. https://doi.org/10.1055/s-0041-1734003
22. Granerod J, Ambrose HE, Davies NW, Clewley JP, Walsh AL, Morgan D, et al.; UK Health Protection Agency (HPA) Aetiology of Encephalitis Study Group. Causes of encephalitis and differences in their clinical presentations in England: a multicentre, population-based prospective study. Lancet Infect Dis. 2010;10:835–44. https://doi.org/10.1016/S1473-3099(10)70222-X
23. Jaijakul S, Salazar L, Wootton SH, Aguilera E, Hasbun R. The clinical significance of neutrophilic pleocytosis in cerebrospinal fluid in patients with viral central nervous system infections. Int J Infect Dis. 2017;59:77–81. https://doi.org/10.1016/j.ijid.2017.04.010
24. Bonell A, Lubell Y, Newton PN, Crump JA, Paris DH. Estimating the burden of scrub typhus: a systematic review. PLoS Negl Trop Dis. 2017;11:e0005838. https://doi.org/10.1371/journal.pntd.0005838
25. Horwood PF, Duong V, Laurent D, Mey C, Sothy H, Santy K, et al. Aetiology of acute meningoencephalitis in Cambodian children, 2010–2013. Emerg Microbes Infect. 2017;6:e35. https://doi.org/10.1038/emi.2017.15
26. Olsen SJ, Campbell AP, Supawat K, Liamsuwan S, Chotpitayasunondh T, Laptikulthum S, et al.; Thailand Encephalitis Surveillance Team. Infectious causes of encephalitis and meningoencephalitis in Thailand, 2003–2005. Emerg Infect Dis. 2015;21:280–9. https://doi.org/10.3201/eid2102.140291
27. Dittrich S, Rattanavong S, Lee SJ, Panyanivong P, Craig SB, Tulsiani SM, et al. Orientia, rickettsia, and leptospira pathogens as causes of CNS infections in Laos: a prospective study. Lancet Glob Health. 2015;3:e104–12. https://doi.org/10.1016/S2214-109X(14)70289-X
28. Dubot-Pérès A, Mayxay M, Phetsouvanh R, Lee SJ, Rattanavong S, Vongsouvath M, et al. Management of central nervous system infections, Vientiane, Laos, 2003–2011. Emerg Infect Dis. 2019;25:898–910. https://doi.org/10.3201/eid2505.180914
29. Dinesh Kumar N, Arun Babu T, Vijayadevagaran V, Ananthakrishnan S, Kittu D. Clinical profile of scrub typhus meningoencephalitis among South Indian children. J Trop Pediatr. 2018;64:472–8.
30. Viswanathan S, Muthu V, Iqbal N, Remalayam B, George T. Scrub typhus meningitis in South India—a retrospective study. PLoS One. 2013;8:e66595. https://doi.org/10.1371/journal.pone.0066595
31. Subbalaxmi MV, Madisetty MK, Prasad AK, Teja VD, Swaroopa K, Chandra N, et al. Outbreak of scrub typhus in Andhra Pradesh—experience at a tertiary care hospital. J Assoc Physicians India. 2014;62:490–6.
32. Usha K, Kumar E, Kalawat U, Kumar BS, Chaudhury A, Gopal DV. Molecular characterization of *Orientia tsutsugamushi* serotypes causing scrub typhus outbreak in southern region of Andhra Pradesh, India. Indian J Med Res. 2016;144:597–603.
33. Mørch K, Manoharan A, Chandy S, Chacko N, Alvarez-Uria G, Patil S, et al. Acute undifferentiated fever in India: a multicentre study of aetiology and diagnostic accuracy. BMC Infect Dis. 2017;17:665. https://doi.org/10.1186/s12879-017-2764-3
34. Khan SA, Bora T, Laskar B, Khan AM, Dutta P. Scrub typhus leading to acute encephalitis syndrome, Assam, India. Emerg Infect Dis. 2017;23:148–50. https://doi.org/10.3201/eid2301.161038
35. Gupte MD, Gupte M, Kamble S, Mane A, Sane S, Bondre V, et al. Detection of immunoglobulin m and immunoglobulin g antibodies against *Orientia tsutsugamushi* for scrub typhus diagnosis and serosurvey in endemic regions. Indian Pediatr. 2020;57:1131–4. https://doi.org/10.1007/s13312-020-2067-4
36. Kim DM, Chung JH, Yun NR, Kim SW, Lee JY, Han MA, et al. Scrub typhus meningitis or meningoencephalitis. Am J Trop Med Hyg. 2013;89:1206–11. https://doi.org/10.4269/ajtmh.13-0224
37. Peter JV, Sudarsan TI, Prakash JA, Varghese GM. Severe scrub typhus infection: clinical features, diagnostic challenges and management. World J Crit Care Med. 2015;4:244–50. https://doi.org/10.5492/wjccm.v4.i3.244
38. Varghese GM, Mathew A, Kumar S, Abraham OC, Trowbridge P, Mathai E. Differential diagnosis of scrub typhus meningitis from bacterial meningitis using clinical and laboratory features. Neurol India. 2013;61:17–20. https://doi.org/10.4103/0028-3886.107919
39. Pan S, Islam K, Datta A. Orientia tsutsugamushi: an emerging major cause of acute encephalitis syndrome in south Asian children. In: Abstracts of the British Paediatric Allergy Immunity and Infection Group; 2021. Abstract 989. Archives of Disease in Childhood, 2021 [cited 2022 Jul 1]. https://adc.bmj.com/content/archdischild/106/Suppl_1/A185.full.pdf
40. Kaur P, Jain R, Kumar P, Randev S, Guglani V. Clinical spectrum and outcome of acute encephalitis syndrome in children with scrub typhus: a series of eight cases from India. Indian J Crit Care Med. 2020;24:885–7. https://doi.org/10.5005/jp-journals-10071-23590
41. Ralph R, Prabhakar AT, Sathyendra S, Carey R, Jude J, Varghese GM. Scrub typhus-associated opsoclonus: clinical course and longitudinal outcomes in an Indian cohort. Ann Indian Acad Neurol. 2019;22:153–8.
42. Saini L, Dhawan SR, Madaan P, Suthar R, Saini AG, Sahu JK, et al. Infection-associated opsoclonus: a retrospective case record analysis and review of literature. J Child Neurol. 2020;35:480–4. https://doi.org/10.1177/0883073820911327

43. Nandi M, Maity D. Opsoclonus myoclonus syndrome: a presenting feature of scrub typhus in a child. The Child and Newborn. 2018;22:8–9.
44. Cho HJ, Choi JH, Sung SM, Jung DS, Choi KD. Bilateral optic neuritis associated with scrub typhus. Eur J Neurol. 2013;20:e129–30. https://doi.org/10.1111/ene.12268
45. Jessani LG, Gopalakrishnan R, Kumaran M, Devaraj V, Vishwanathan L. Scrub typhus causing unilateral optic neuritis. Indian J Pediatr. 2016;83:1359–60. https://doi.org/10.1007/s12098-016-2169-0
46. Sood AK, Chauhan L, Gupta H. CNS manifestations in *Orientia tsutsugamushi* disease (scrub typhus) in North India. Indian J Pediatr. 2016;83:634–9. https://doi.org/10.1007/s12098-015-2001-2

Address for correspondence: Tina Damodar, Department of Neurovirology, National Institute of Mental Health & Neurosciences, Bangalore 560029, India; email: tinadamodar86@gmail.com; Ravi Yadav, Department of Neurology, National Institute of Mental Health & Neurosciences, Bangalore 560029, India; email: docravi20@yahoo.com

etymologia revisited

Tularemia

[t-lə-rē-mē-ə]

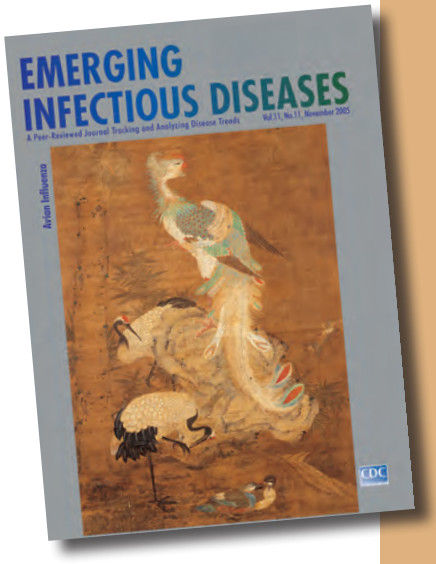

Originally published in November 2007

An infectious, plaguelike, zoonotic disease caused by the bacillus *Francisella tularensis*. The agent was named after Tulare County, California, where the agent was first isolated in 1910, and Edward Francis, an Officer of the US Public Health Service, who investigated the disease. Dr. Francis first contracted deer fly fever from a patient he visited in Utah in the early 1900s. He kept a careful record of his 3-month il ness and later discovered that a single attack confers permanent immunity. He was exposed to the bacterium for 16 years and even deliberately reinfected himself 4 times.

Tularemia occurs throughout North America, many parts of Europe, the former Soviet Union, the Peoples Republic of China, and Japan, primarily in rabbits, rodents, and humans. The disease is transmitted by the bites of deerflies, fleas, and ticks; by contact with contaminated animals; and by ingestion of contaminated food or water.

Clinical manifestations vary depending on the route of introduction and the virulence of the agent. Most often, an ulcer is exhibited at the site of introduction, together with swelling of the regional lymph nodes and abrupt onset of fever, chills, weakness, headache, backache, and malaise.

Source:

1. Dorland's illustrated medical dictionary, 31st edition. Philadelphia: Saunders; 2007; Benenson AS, editor. Control of communicable diseases manual. Washington: American Public Health Association; 1995; www.whonamedit.com

https://wwwnc.cdc.gov/eid/article/13/11/e1-1311_article

Monitoring Temporal Changes in SARS-CoV-2 Spike Antibody Levels and Variant-Specific Risk for Infection, Dominican Republic, March 2021–August 2022

Eric J. Nilles, Michael de St. Aubin, Devan Dumas, William Duke, Marie Caroline Etienne, Gabriela Abdalla, Petr Jarolim, Timothy Oasan, Salome Garnier, Naomi Iihoshi, Beatriz Lopez, Lucia de la Cruz, Yosanly Cornelio Puello, Margaret Baldwin, Kathryn W. Roberts, Farah Peña, Kara Durski, Isaac Miguel Sanchez, Sarah M. Gunter, Alexander R. Kneubehl, Kristy O. Murray, Allison Lino, Sarah Strobel, Amado Alejandro Baez, Colleen L. Lau, Adam Kucharski, Emily Zielinski Gutiérrez, Ronald Skewes-Ramm, Marietta Vasquez,[1] Cecilia Then Paulino[1]

To assess changes in SARS-CoV-2 spike binding antibody prevalence in the Dominican Republic and implications for immunologic protection against variants of concern, we prospectively enrolled 2,300 patients with undifferentiated febrile illnesses in a study during March 2021–August 2022. We tested serum samples for spike antibodies and tested nasopharyngeal samples for acute SARS-CoV-2 infection using a reverse transcription PCR nucleic acid amplification test. Geometric mean spike antibody titers increased from 6.6 (95% CI 5.1–8.7) binding antibody units (BAU)/mL during March–June 2021 to 1,332 (95% CI 1,055–1,682) BAU/mL during May–August 2022. Multivariable binomial odds ratios for acute infection were 0.55 (95% CI 0.40–0.74), 0.38 (95% CI 0.27–0.55), and 0.27 (95% CI 0.18–0.40) for the second, third, and fourth versus the first anti-spike quartile; findings were similar by viral strain. Combining serologic and virologic screening might enable monitoring of discrete population immunologic markers and their implications for emergent variant transmission.

Given widespread unreported SARS-CoV-2 infections, variable immunologic response based on host immunogenicity, vaccine type, viral strain, timing and sequence of vaccine or viral exposure, and humoral waning, the global SARS-CoV-2 immune landscape is largely unknown. Most countries launched national COVID-19 vaccination campaigns during early 2021, but few studies have characterized population-level immunologic responses to SARS-CoV-2, and fewer have aimed to translate findings to immunologic protection. Many large national seroepidemiologic studies were conducted in the pre–COVID-19 vaccine era and before emerging variants of concern, focusing primarily on seroprevalence (i.e., the presence or absence of SARS-CoV-2 antibodies) but not antibody levels (*1*–*4*). This focus was largely

Author affiliations: Brigham and Women's Hospital, Boston, Massachusetts, USA (E.J. Nilles, M. de St. Aubin, D. Dumas, M.C. Etienne, G. Abdalla, P. Jarolim, T. Oasan, S. Garnier, N. Iihoshi, M. Baldwin, K.W. Roberts, K. Durski); Harvard Humanitarian Initiative, Cambridge, Massachusetts, USA (E.J. Nilles, M. de St. Aubin, D. Dumas, S. Garnier, M. Baldwin, K.W. Roberts, K. Durski); Harvard Medical School, Boston (E.J. Nilles, P. Jarolim); Pedro Henríquez Ureña National University, Santo Domingo, Dominican Republic (W. Duke); US Centers for Disease Control and Prevention, Central America Regional Office, Guatemala City, Guatemala (B. Lopez, E. Zielinski Gutiérrez); Ministry of Health and Social Assistance, Santo Domingo (L. de la Cruz, Y. Cornelio Puello, F. Peña, I.M. Sanchez, R. Skewes-Ramm, C. Then Paulino); Baylor College of Medicine and Texas Children's Hospital, Houston, Texas, USA (S.M. Gunter, A.R. Kneubehl, K.O. Murray, A. Lino, S. Strobel); Dominican Republic Office of the Presidency, Santo Domingo (A.A. Baez); University of Queensland, Brisbane, Queensland, Australia (C.L. Lau); London School of Hygiene and Tropical Medicine, London, England, UK (A. Kucharski); Yale School of Medicine, New Haven, Connecticut, USA (M. Vasquez)

DOI: https://doi.org/10.3201/eid2904.221628

[1]These authors contributed equally to this article.

because of an urgent need to understand population-level transmission and transmission risks, but it was also the result of limited understanding of what binding antibody levels mean for immunologic protection and whether quantification of binding antibodies translate into actionable or otherwise useful data. Although neutralizing antibodies are the generally accepted standard correlate of protection against symptomatic infection (*5*–*7*), measuring neutralizing activity is slow and resource intensive and therefore impractical for most population-based studies, particularly in low- and middle-income countries. Recent approaches have combined screening subsets of populations for neutralizing activity and applying machine learning methods to estimate population-level immunologic protection (*8*), but those approaches still require neutralization testing of a certain fraction of samples in addition to applying machine learning methods. The direct use of binding antibodies to estimate immunologic protection is, therefore, attractive, at least for population-based studies, where the tolerance for imprecision may be higher than vaccine efficacy trials. Although global health authorities including the World Health Organization previously cautioned against using binding antibodies to assess immunologic protection, several large studies subsequently demonstrated that SARS-CoV-2 spike binding antibodies (hereafter S antibodies) largely track with protection against infection (*5*–*7*). However, those studies were conducted in the setting of controlled vaccine efficacy studies and before emergence of highly immune evasive viral variants, so the utility of S antibodies for understanding immunologic protection in a real-world setting, in which transmission is driven by Omicron-derived strains, is unknown.

Given those knowledge gaps, which we believe are essential to address in order to inform and prioritize public health activities moving forward, we conducted a study using a novel methodologic approach to first characterize temporal changes in S antibody titers across a discrete population. In addition, we evaluated the utility of S antibodies for assessing risk for acute SARS-CoV-2 infection across viral variants and strains.

Methods

Setting

The Dominican Republic is an upper-middle-income Latin American country that shares the island of Hispaniola with Haiti. With ≈11 million residents, it is the second most populous country in the Caribbean (*9*,*10*). The first laboratory-confirmed case of SARS-CoV-2 infection was reported in the Dominican Republic on March 1, 2020, and strict public health measures commensurate with those in most countries of the region were implemented (*11*). Six discrete waves of SARS-CoV-2 transmission were observed during March 2020–August 2022; the last 3 waves were predominantly attributable to B.1.617.2 Delta (October–November 2021); BA.1 Omicron (January–February 2022); and post–BA.1 Omicron variants, including BA.2, BA.4, and BA.5 (June–August 2022). Peak national cases reported per day were 4–5 times higher during the BA.1 wave (≈6,000 cases/day) than during the other waves (≈1,100–1,300 cases/day) (*6*). A national COVID-19 vaccination campaign was launched in late February 2021, and by March 22, 2021 (the start of our study), ≈7.4% of the national population had received 1 COVID-19 vaccine dose (*12*). The principal COVID-19 vaccines administered were inactivated viral CoronaVac (Sinovac, https://www.sinovac.com), adenovirus vector ChAdOx1-S (Oxford/AstraZeneca, https://www.astrazeneca.com), and mRNA BNT162b2 (Pfizer/BioNTech, https://www.pfizer.com) vaccines.

Latin America emerged as a global SARS-CoV-2 hotspot early in the COVID-19 pandemic; model estimates suggested that by November 2021 the regional cumulative population infected was 57.4% (95% CI 51.7%–63.1%) (*13*). A national cross-sectional household serologic survey in the Dominican Republic estimated that by August 2021, 85.0% (95% CI 82.1%–88.0%) of the ≥5-year-old population had been immunologically exposed through vaccination, infection, or both, and 77.5% (95% CI 71.3%–83.0%) had been previously infected (*8*).

Study Design, Study Sites, and Participant Selection

We conducted prospective enrollment across 2 study sites: Hospital Dr. Antonio Musa, located in San Pedro de Macoris Province in the southeast of the country, and Dr. Toribio Bencosme Hospital in Espaillat Province in the northwest of the country. Those study sites are part of a longitudinal US Centers for Disease Control and Prevention (CDC)–funded acute febrile infection enhanced surveillance platform, which, in collaboration with the Ministry of Health and Social Assistance, aims to better characterize the epidemiology and transmission of acute febrile infection pathogens, including SARS-CoV-2. Patients >2 years of age who arrived at the study sites with an undifferentiated fever, either measured (>38.0°C) or by history, or with new onset anosmia or ageusia were invited to participate. Study staff (all of whom were medical doctors) conducted enrollment 5 days/week

from 8 A.M. to 5 P.M. We administered questionnaires by using the KoBo Toolbox data collection platform (https://www.kobotoolbox.org) on electronic tablets to collect individual-level covariates, including demographic data (e.g., age, sex, race, and ethnicity); underlying medical conditions (e.g., hypertension, coronary heart disease, diabetes, active cancer, chronic kidney disease, stroke, asthma, and chronic obstructive pulmonary disease); weight and height; primary occupation; symptom onset date; and number, date, and type of COVID-19 vaccines received. We collected nasopharyngeal swab and venous blood samples from all participants at the time of enrollment. We processed blood as serum samples and stored biologic samples at −80°C.

To assess the association between S antibody levels at the time of SARS-CoV-2 diagnosis (peri-infection) and risk for SARS-CoV-2 infection, we used a test-negative approach that first assigned study participants into 2 groups based on SARS-CoV-2 virologic test result. We then assessed crude S antibody levels between groups and subsequently performed univariable and multivariable binomial logistic regression with S antibody levels categorized by quartile. We considered peri-infection antibody levels to reflect antibody levels at the time of infection.

Ethical Considerations

We obtained written consent for all participants. For children <18 years of age, except emancipated minors, we obtained consent from the legal guardian. Written assent was provided by adolescents 14–17 years of age and verbal assent by children 7–13 years of age. The study was reviewed and approved by the National Council of Bioethics in Health, Santo Domingo (approval no. 013–2019), the Institutional Review Board of Pedro Henríquez Ureña National University, Santo Domingo, and the Massachusetts General Brigham Human Research Committee, Boston, Massachusetts, USA (approval no. 2019P000094). Study procedures and reporting adhere to STROBE criteria for observational studies.

Immunoassay Characteristics

We measured serum pan-Ig against the SARS-CoV-2 S glycoprotein at Brigham and Women's Hospital (Boston, Massachusetts, USA) on the Roche Elecsys SARS-CoV-2 electrochemiluminescence immunoassay that uses a recombinant protein–modified double-antigen sandwich format (Roche Diagnostics, https://www.roche.com). We calibrated the assay with positive (wild-type) and negative quality controls before analyses. We quantified values ranging from 0.40 to 250 U/mL representing the primary measurement range; we reported values <0.40 U/mL as 0.40 U/mL. Samples with measured values >250 U/mL underwent automated 1:50 dilution with further 1:10 dilution for samples >12,500 U/mL, representing an upper limit of detection of 125,000 U/mL. We considered samples to be reactive according to the manufacturer cutoff index (≥0.8 U/mL). We report values as binding antibody units (BAU) that equal Elecsys SARS-CoV-2 S antibody U/mL in accordance with manufacturer's recommendations and the World Health Organization's international standard and international reference panel for SARS-CoV-2 Ig (*14*). Assay performance measures reported by a largest, non–manufacturer-sponsored study registered a specificity of 99.8% (95% CI 99.3%–100%) and sensitivity of 98.2% (95% CI 96.5%–99.2%) (*15*).

Virologic Assays

We assessed acute SARS-CoV-2 infection by using a real-time reverse transcription PCR nucleic acid amplification test (NAAT) on nasopharyngeal specimens using the Allplex SARS-CoV-2 kit (Seegene, https://www.seegene.com), which amplifies the envelope, nucleocapsid, and RNA dependent RNA polymerase genes. Conditions for amplifications were 50°C for 20 min, 95°C for 15 min, followed by 45 cycles of 95°C for 10 s and 60°C for 15 s and 72°C for 10 s. We considered samples to be positive according to the manufacturer recommendations (i.e., with a cycle threshold value <37). We defined a cycle threshold value ≥38 as a negative. We performed genomic sequencing on a subset of NAAT-positive samples (Appendix, https://wwwnc.cdc.gov/EID/article/29/4/22-1628-App1.pdf).

Classification and Statistical Analysis

We analyzed mean SARS-CoV-2 seroprevalence and number of COVID-19 vaccines received by 7-day intervals, starting on the first day of the study period. We defined viral strain transmission phases according to the predominant circulating viral strain based on genome sequencing of 237 SARS-CoV-2 NAAT–positive study samples: March 22, 2021–August 15, 2021 (pre-Delta), August 16, 2021–December 23, 2021 (Delta), December 24, 2021–April 30, 2022 (BA.1 [Omicron]), and May 1, 2022–August 17, 2022 (post-BA.1). Because phases varied in duration, we created a second date partition that captured largely similar 3- to 4-month time intervals: March–June 2021 (March 22–June 30, 2021), July–September 2021, October–December 2021, January–April 2022, and May–August 2022 (May 1–August 17, 2022). We analyzed data by date of participant enrollment. We calculated days

post–symptom onset (DPSO) by subtracting the symptom onset date from the date of enrollment. For 10 participants without symptom onset date, we imputed DPSO as the DPSO mode for all other participants. We aggregated age into 3 groups (2–17, 18–54, and ≥55 years) and selected cutoffs to capture groups with documented differences in seroprevalence in the Dominican Republic while minimizing data sparsity among older adults. Because our study was an observational study of prospectively enrolled patients, we included all eligible participants with required data and performed no sample size power calculation.

We conducted analyses by using the R statistical programming language (R version 4.1.3) with finalfit (glm) for univariable and multivariable logistic regression (*16*). We performed data visualization by using visreg and ggplot2 (*17,18*).

Data Sources

We obtained national SARS-CoV-2 cases, deaths, and vaccination data from the COVID-19 GitHub repository (*6*). We enumerated other data during the study.

Results

During March 22, 2021–August 17, 2022, we invited 2,814 eligible patients to participate in our study, of whom 2,502 (89.0%) were enrolled. Of those, 2,300 (91.9%) had complete virologic, serologic, and demographic data and were included in analyses (Appendix Figure 1). The median age of participants was 31 years (interquartile range 7–55 years); 1,422/2,300 (61.8%) were women and girls (Table 1). The mean interval between symptom onset and enrollment was 4.0 days (mean absolute difference 2.5 days) for all participants and 3.7 days (mean absolute difference 2.1 days) for

Table 1. Population characteristics of participants in study of SARS-CoV-2 spike antibody levels, by SARS-CoV-2 NAAT status, Dominican Republic, March 2021–August 2022*

Variable	NAAT-positive, n = 517	NAAT-negative, n = 1,783	Total, N = 2,300
Sex			
F	327 (63.2)	1,095 (61.4)	1,422 (61.8)
M	189 (36.6)	688 (38.6)	877 (38.1)
Median age (IQR), y	36 (10–62)	30 (5.5–54.5)	31 (7–55)
Age group, y			
2–17	43 (8.3)	376 (21.1)	419 (18.2)
18–54	368 (71.2)	1,189 (66.7)	1,557 (67.7)
≥55	106 (20.5)	218 (12.2)	324 (14.1)
Area of residence			
Rural or semirural	366 (70.8)	1,245 (69.8)	1,611 (70.0)
Urban	147 (28.4)	514 (28.8)	661 (28.7)
Unclassified	4 (0.8)	24 (1.3)	28 (1.2)
No. household residents			
1–2	104 (20.1)	377 (21.1)	481 (20.9)
3–4	245 (47.4)	838 (47.0)	1,083 (47.1)
5–6	130 (25.1)	430 (24.1)	560 (24.4)
≥7	38 (7.4)	135 (7.6)	173 (7.5)
Enrollment site			
San Pedro de Macoris Province	243 (47.0)	802 (45.0)	1,045 (45.4)
Espaillat Province	274 (53.0)	981 (55.0)	1,255 (54.6)
Underlying condition†			
Respiratory disease	52 (10.1)	245 (13.7)	297 (12.9)
Cardiovascular disease	105 (20.3)	277 (15.5)	382 (16.6)
Diabetes	44 (8.5)	114 (6.4)	158 (6.9)
BMI ≥30	89 (17.2)	332 (18.6)	421 (18.3)
Pregnancy	18 (3.5)	57 (3.2)	75 (3.3)
No. COVID-19 vaccine doses			
0	150 (29.0)	604 (33.9)	754 (32.8)
1	61 (11.8)	177 (9.9)	238 (10.3)
2	262 (50.7)	766 (43.0)	1,028 (44.7)
3	44 (8.5)	230 (12.9)	274 (11.9)
4	0 (0.0)	6 (0.3)	6 (0.3)
Study period interval			
Mar–Jun 2021	99 (19.1)	335 (18.8)	434 (18.9)
Jul–Sep 2021	126 (24.4)	271 (15.2)	397 (17.3)
Oct–Dec 2021	137 (26.5)	442 (24.8)	579 (25.2)
Jan–Apr 2022	61 (11.8)	403 (22.6)	464 (20.2)
May–Aug 2022	94 (18.2)	332 (18.6)	426 (18.5)

*Values are no. (%) except as indicated. Number of household residents missing for 3 participants. One participant reported 'other' for sex and was not included in analyses. BMI, body mass index; IQR, interquartile range; NAAT, nucleic acid amplification test.
†Respiratory disease includes chronic obstructive pulmonary disease, asthma, other chronic respiratory diseases. Cardiovascular disease includes hypertension and coronary artery disease. BMI calculated by dividing weight in pounds by height in inches squared and multiplied by a conversion factor of 703.

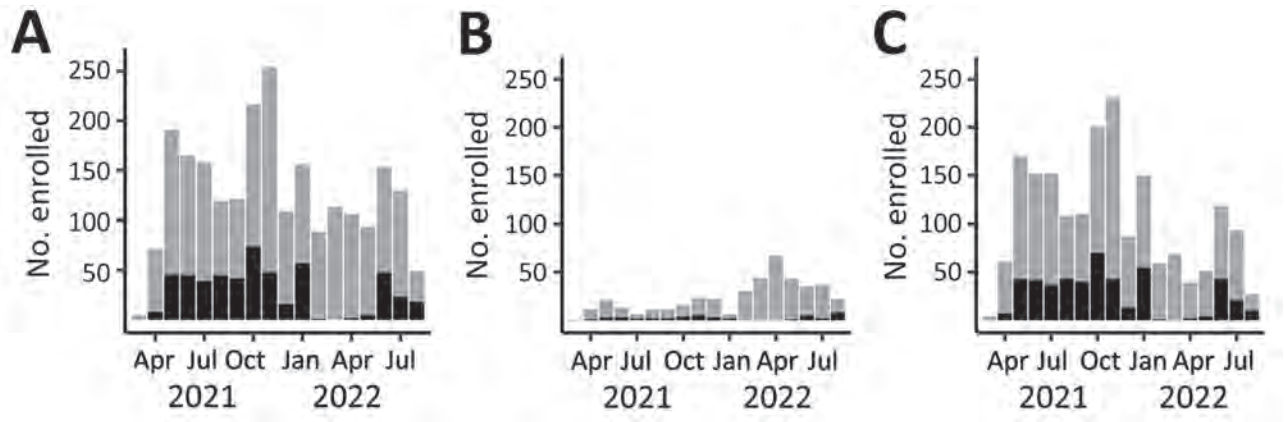

Figure 1. Number of participants (N = 2,300) enrolled per month, by age group, in a study of SARS-CoV-2 spike antibody levels, Dominican Republic, March 2021–August 2022. A) All ages; B) 2–17 years of age; C) ≥18 years of age. Gray bar sections indicates SARS-CoV-2 NAAT–negative participants; black bar sections indicate SARS-CoV-2 NAAT–positive participants. Labels on x-axis indicate complete months, except March 2021, which represents enrollment starting March 22, 2021, and August 2022, which represents enrollment through August 17, 2022.

SARS-CoV-2 NAAT–positive participants (Appendix Table 1). Overall SARS-CoV-2 NAAT test positivity was 22.4% (517/2,300) (Figure 1).

Changes in COVID-19 Vaccination Rates

After the launch of the national COVID-19 vaccination campaign in late February 2021, coverage among the study population increased rapidly, consistent with nationally reported data. By December 2021, approximately 75% of study participants had completed a 2-dose primary series (Figure 2). Unexpectedly, overall vaccination rates declined after December 2021, a finding attributable to an increase in younger pediatric patients who were ineligible for COVID-19 vaccines at the time, a finding consistent across study sites (Appendix Figure 2, 3). Vaccination coverage among adults remained high through the remainder of the study, and by June–August 2022, approximately 80% of adults had completed a primary vaccine series and about 35% had received a third vaccine dose. Vaccination coverage among adult study participants appeared to be modestly higher than national reported COVID-19 data (*7*), but without age-stratified national vaccination data, which were not available, we could not make direct comparisons.

Temporal Changes in S Antibody Seropositivity and Levels

During the March–June 2021 and May–August 2022 study periods, the proportion of participants testing positive for S antibodies increased from 61.1% to 95.8%. Geometric mean titer (GMT) values increased 202-fold, median titer values increased 757-fold (Table 2; Figure 3, panel A), and near–log linear increases occurred across the study population through January 2022, when overall GMT flattened. We visualized the trend in overall antibody titers during the study period (Figure 3, panel A) and further stratified those trends by age group (Figure 3, panel B), and vaccination status (Figure 3, panel C). We observed progressive increases in S antibody titers over time across all age groups and within each vaccine dose category. For example, among recipients of 2 vaccine doses, GMT increased from 72.1 BAU/mL (95% CI 40.1–129.7 BAU/mL) during March–June 2021 to 2,153.2 BAU/mL (95% CI 1,684.7–2,752.1 BAU/mL) during May–August 2022; we observed similar trends across recipients of 1 vaccine dose (Figure 2, panel C; Appendix Table 3). We observed a less pronounced increase across recipients of 3 vaccine doses, who demonstrated high titers, measured on a logarithmic scale, across all study periods. Increases in GMT over time within vaccine dose categories probably represent ongoing immunologic exposure attributable to SARS-CoV-2 infections and transition from the less immunogenic Sinovac vaccine early in the national vaccination campaign to the mRNA BNT162b2 vaccine in late 2021. As evidenced by progressively increasing S antibody titers over time among unvaccinated study participants, and consistent with nationally reported data, substantial SARS-CoV-2 transmission continued through most of the study period. However, despite ongoing transmission, S antibody titers remained substantially lower in unvaccinated participants than in vaccinated participants. For example, during May–August 2022, GMTs among unvaccinated participants represented 25.7% of S antibody GMT among recipients of 1 vaccine dose, 13.1% among recipients

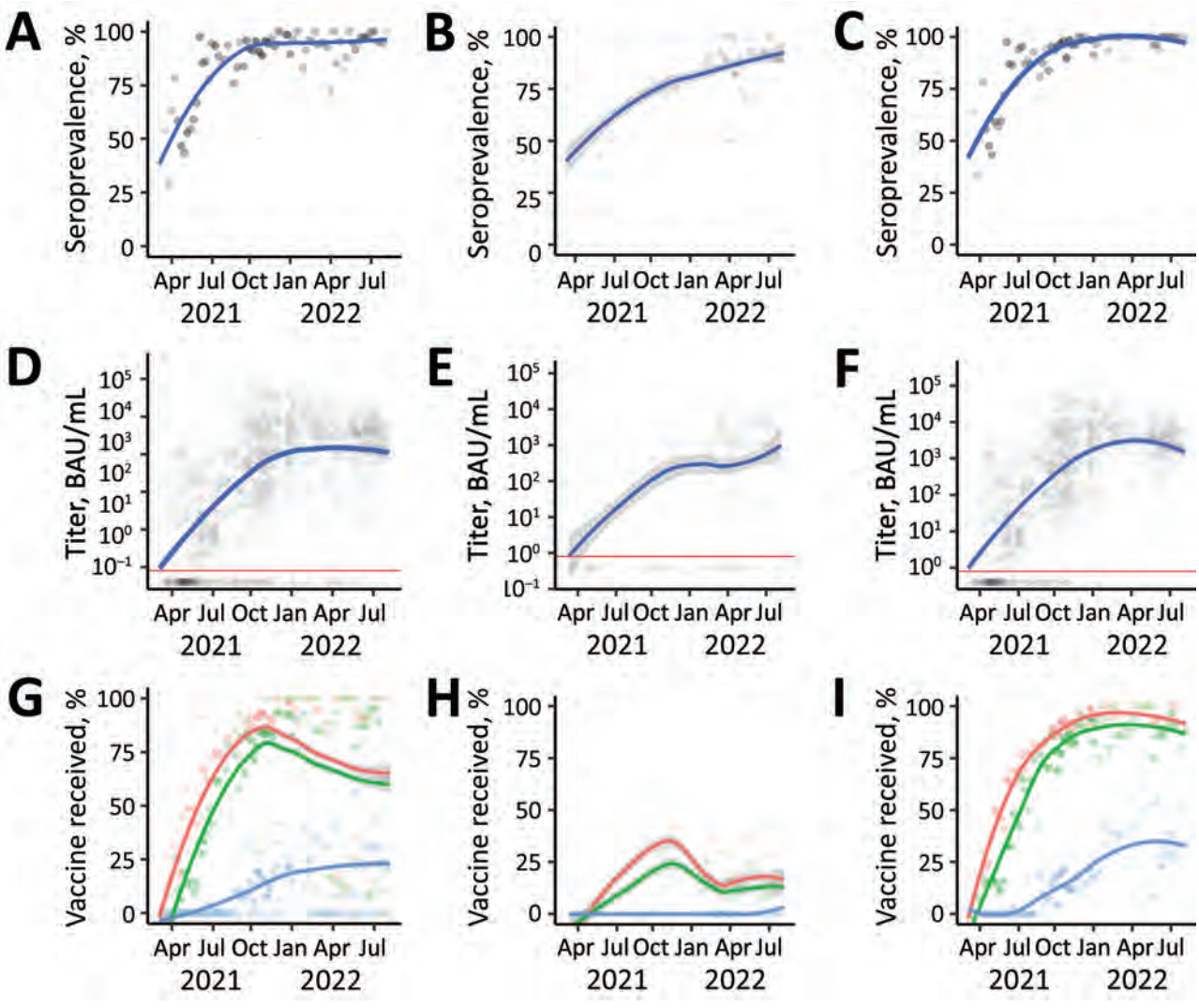

Figure 2. SARS-CoV-2 S antibody seroprevalence, titers, and vaccine doses of participants enrolled (N = 2,300) in a study of SARS-CoV-2 S antibody levels, by age group, Dominican Republic, March 2021–May 2022. A–C) Seroprevalence among study participants of all ages (A), 2–17 years of age (B), and ≥18 years of age (C). Gray dots indicate weekly mean values; increased dot intensity reflected more observations. Blue line indicates locally estimated scatterplot smoothing (LOESS) smoothed seroprevalence; gray shading indicates 95% CI around the smoothed estimate. D–F) Titers among study participants of all ages (D), 2–17 years of age (E), and ≥18 years of age (F), by week, plotted on a log scale. Each gray dot indicates a unique study participant (n = 1,910). Blue lines indicate LOESS smoothed antibody levels; gray shading indicates 95% CI around the smoothed estimate. Horizontal red line indicates manufacturer recommended cutoff index (≥0.800 BAU /mL); values above the line represent a positive result and values below the line a negative result. G–I) Percentage of weekly enrolled participants of all ages (G), 2–17 years of age (H), and ≥18 years of age (I) who had received ≥1 (red dots), ≥2 (green dots), or ≥3 (blue dots) COVID-19 vaccine doses; increased dot intensity reflects more observations. Colored lines indicate LOESS smoothed percentage; gray shading indicates 95% CI around smoothed percentage. BAU, binding antibody units; S, spike.

of 2 vaccine doses, and 6.3% among recipients of 3 vaccine doses (Figure 2, panel C; Appendix Table 3).

Association between S Antibody Titers and SARS-CoV-2 NAAT Status

Although we observed a substantial increase in S antibody levels across all demographic groups during the study period, the implications for immunologic protection were unclear. Therefore, we used a test-negative approach to assess whether simple unadjusted S antibody levels were associated with the NAAT test result. We identified a consistent inverse association across all phases of transmission (Table 3), observing broadly similar ratios when we compared S antibody levels between NAAT-positive and NAAT-negative participants across viral strains.

Using multivariable analyses, we again identified an inverse association between S antibody quartile

and odds ratio (OR) for a positive NAAT; results demonstrated a clear biologic gradient (Table 4). Younger age (2–17 years) was associated with a lower OR (0.45 [95% CI 0.29–0.68]; p<0.001) and older age (≥55 years) with higher OR (1.58 [95% CI 1.19–2.07]; p = 0.001) for a positive NAAT test compared with the 18–54 year age group; we observed similar but largely nonsignificant trends when these data were stratified by phase (Appendix Tables 4–8). We observed no consistent association between NAAT status and sex or number of COVID-19 vaccine doses received after controlling for S antibody levels (Appendix Tables 4–8).

We examined whether antibody levels trended higher based on the number of days between symptom onset and sample collection but were unable to detect a clear trend, even after stratifying by number of vaccine doses received (Appendix Figure 4), potentially because 50% of NAAT-positive case-patients had samples collected within 3 days of symptom onset and 90% within 6 days (Appendix Table 1). We also performed sensitivity analyses comparing samples collected 0–4 DPSO versus ≥5 DPSO and observed broadly similar findings, although the biologic gradient observed for samples collected 0–4 DPSO was less clearly defined for samples collected >5 DPSO (Appendix Table 9).

Discussion

We report on the temporal change in SARS-CoV-2 S antibody prevalence levels over 18 months among patients enrolled through a longitudinal acute febrile illness surveillance platform in the Dominican Republic. The study period aligned with the beginning of the national COVID-19 vaccination campaign in late February 2021, providing a unique opportunity to characterize the evolution of S antibody levels in this setting and across a population that was largely COVID-19 vaccine–naive early in the study period. We observed a progressive increase in S antibody seroprevalence (from 61% to 96%), reflecting vaccination, infection, or both. Strikingly, during the study period, GMT increased ≈200-fold, and median titers increased 760-fold. To determine the implications of those findings for public health, we used a test-negative approach to assess antibody levels between NAAT-positive and NAAT-negative case-patients. We identified a consistent inverse association between S antibody titers and the likelihood of testing positive for SARS-CoV-2 by NAAT and extended those findings to phases of predominantly pre-Delta, Delta, Omicron BA.1, and Omicron-derivative strain waves of transmission.

S antibody levels were lower among those who tested positive versus negative for acute SARS-CoV-2 infection, a trend that was consistent across strains and after adjustment for potential confounders. When compared with the first quartile, the likelihood of testing positive was reduced by ≈45% for the second quartile, ≈60% for the third quartile and ≈75% for the fourth quartile. This finding aligns with several correlates of protection studies that reported S antibody levels track with risk for SARS-CoV-2 infection (*5*–*7*,*19*). We built on the findings from those prior studies, which were conducted before widespread transmission of variants of concern, to include transmission waves that were primarily driven by Delta, Omicron BA.1 and subsequent Omicron strains (BA.2, BA.4, and BA.5), and documented similar predictive utility of S antibody levels against those strains. These findings suggest that binding antibodies, at least total S antibody levels as measured in this study, track with functional measures of immunologic protection, such as viral neutralization, Fc-function, and potentially T-cell responses, as previously reported (*19*–*21*). Our findings suggest that, although total S antibody levels are probably inappropriate for adjudicating vaccine efficacy and vaccine approval, they are reasonable surrogate markers of immunologic protection against infection, including infection by emerging strains with substantial immune-evasion capacity. Given the relative simplicity, high-throughput capacity, and cost-effectiveness of measuring S antibody versus live or pseudoviral neutralizing activity, this approach may be suitable for characterizing population-level immunologic protection, creating transmission and prediction models, and informing national and regional public health policy.

Table 2. SARS-CoV-2 spike binding antibody serostatus, geometric mean titers, and median titers of participants in study of SARS-CoV-2 spike antibody levels, by study period interval, Dominican Republic, March 2021–August 2022*

Study period interval	No. patients	Seropositive, no. (%)†	GMT (95% CI)	Median titer, BAU/mL (Q1–Q3)
Mar–Jun 2021	434	265 (61.1)	6.6 (5.1–8.7)	3.8 (0.4–57.5)
Jul–Sep 2021	397	344 (86.6)	62.8 (45.8–86.0)	62.5 (6.0–581.8)
Oct–Dec 2021	579	543 (93.8)	559.4 (439.8–711.5)	781.7 (104.9–4,813.5)
Jan–Apr 2022	463	434 (93.7)	1,180.3 (906.3–1,537.2)	2,578 (390.8–8,137.5)
May–Aug 2022	427	409 (95.8)	1,332.4 (1,055.3–1,682.3)	2,876 (775.8–5,483.5)

*N = 2,300. Study periods indicate complete months except March 2021, which represents enrollment starting March 22, 2021, and August 2022, which represents enrollment through August 17, 2022. BAU, binding antibody units; GMT, geometric mean titer.
†Seropositive defined as SARS-CoV-2 spike binding antibodies above the test manufacturer's cutoff index (≥0.8 BAU/mL).

For our analyses, we assumed a priori that S antibody levels measured at the time that a patient seeks care is a reasonable surrogate measure of levels at the time of infection, including among NAAT-positive case-patients, an approach that is not well-characterized but has been previously described (*22*). Most of the SARS-CoV-2 NAAT–positive case-patients can be assumed to have been mounting a humoral response to the acute infection at the time of sample collection, and persons previously exposed to SARS-CoV-2 antigens would be expected to mount a more rapid and robust anamnestic response. However, whether this response would obscure differences in antibody levels between groups, if present, was unclear before our study. Although we did identify a clear difference in risk for testing positive by S antibody levels, our observed differences in levels by NAAT status were probably attenuated.

Among the strengths of our study is that dedicated study staff prospectively enrolled study participants

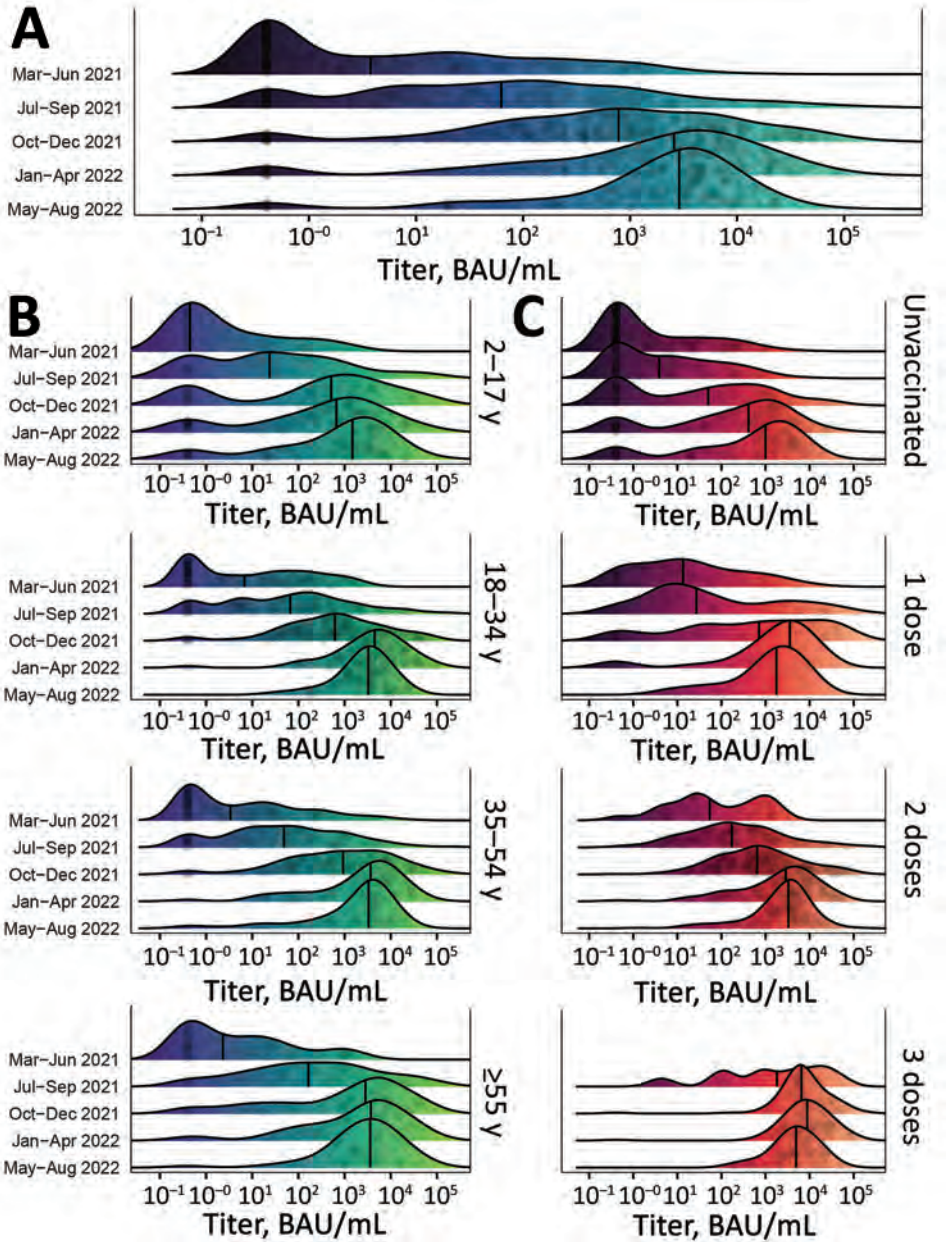

Figure 3. Distribution of SARS-CoV-2 S antibody titers among participants in a study of SARS-CoV-2 S antibody levels, Dominican Republic, March 2021–August 2022. A) Smoothed density plot demonstrates log-adjusted distribution of anti-S antibody titers among all study participants (N = 2,300), stratified by date interval when study participants were enrolled from earliest (March–June 2021, upper) to latest (May–August 2022, lower). Study interval labels indicate complete months except March 2021, which represents enrollment starting March 22, 2021, and August 2022, which represents enrollment through August 17, 2022. B) Smoothed density plot demonstrates log-adjusted distribution of S antibody titers among study participants (n = 2,300) stratified by age group. Dark purple shading indicates lower S titers and light green higher titers. C) Smoothed density plot demonstrates log-adjusted distribution of S antibody titers among participants (n = 2,293), stratified by number of COVID-19 vaccine doses received from none (unvaccinated, top plot) to 3 (bottom plot). Darker red shading indicates lower S titers and light orange higher titers. Six participants who received 4 COVID-19 vaccine doses not included. Values for 3 vaccine doses for March–June 2021 period plot not shown given sparsity of datapoints (n = 1). For all plots, gray circles represent titer adjusted individual study participant values. Narrow vertical black lines indicates median values. Lower limit of assay measurement is 0.4 BAU/mL, and values <0.4 BAU/mL are represented as 0.4 BAU/mL, with smoothing extending curves below the lower measurement limit. Therefore, density plot shading is used for illustrative purposes. Table 2 and Appendix Tables 2, 3 (https://wwwnc.cdc.gov/EID/article/29/4/22-1628-App1.pdf) summarize data used for plots. BAU, binding antibody units; S, spike.

Table 3. Geometric mean and median spike binding antibody titers of participants in study of SARS-CoV-2 spike antibody levels, by SARS-CoV-2 NAAT status and phase of predominant circulating viral strain, Dominican Republic, March 2021–August 2022*

Phase†	SARS-COV-2 NAAT result	No. (%) participants	GMT, BAU/mL (95% CI)	Fold difference in GMT‡	Median titer, BAU/mL (Q1–Q3)	Fold difference in median titer
Pre-Delta	Negative	495 (76.6)	14.1 (10.9–18.2)	**3.4**	13.3 (0.8–132.8)	5.5
	Positive	151 (23.4)	4.1 (2.6–6.5)		2.4 (0.4–24.4)	
Delta	Negative	553 (72.4)	604.8 (475.3–769.7)	**3.9**	792.3 (127.8–4,805)	4.5
	Positive	211 (27.6)	154.7 (97.8–244.7)		176.2 (24.7–1,638.5)	
Omicron BA.1	Negative	403 (86.9)	1,288.3 (965.4–1,719.2)	**1.8**	2,822 (511.1–8,656)	3.4
	Positive	61 (13.1)	713.8 (375.1–1,358.5)		837.2 (126.8–5,739)	
Omicron BA.2/4/5	Negative	332 (77.9)	1,541.4 (1,183.4–2,007.6)	**2.0**	3,202 (1,011–6,173)	1.7
	Positive	94 (22.1)	759.6 (468.1–1,232.6)		1,835 (197.7–3,882.2)	
Total	Negative	1,783 (77.5)	300.6 (256.5–352.4)	**3.5**	725 (31.6–4,351.5)	6.0
	Positive	517 (22.5)	85.8 (62.9–117.1)		121.2 (4.6–1,905)	

*N = 2,300. BAU, binding antibody units; GMT, geometric mean titer; NAAT, nucleic acid amplification test.
†Phases based on dominant circulating strain: March 22–August 15, 2021 (pre-Delta, primarily Mu, Gamma, Iota, and Lambda strains), August 16–December 23, 2021 (Delta), December 24, 2021–April 30, 2022 (Omicron, BA.1), and May 1–August 17, 2022 (Omicron, BA.2, BA.4, BA.5). Appendix Figure 5 (https://wwwnc.cdc.gov/EID/article/29/4/22-1628-App1.pdf) shows sequence-confirmed variant by week.
‡Fold difference is GMT or median titer of NAAT-negative participants divided by the titer of NAAT-positive participants. Bolded type indicates statistical significant result (p<0.001, by t test for GMT difference between NAAT-negative and positive-study participants).

using well-defined procedures, administered standardized survey questionnaires, and simultaneously collected respiratory and blood samples. Enrollment of eligible patients was high (89%) for this type of surveillance study. Serum samples were tested with a widely used and validated immunoassay, and antibody titers were reported as internationally standardized units, so our findings can be compared across other settings. We developed an approach to understand temporal changes in population-level SARS-CoV-2 antibodies, methods that may be applicable to other settings. We performed genomic sequencing of a relatively large number of samples from among the current study population, and therefore were able to characterize timing of predominant SARS-CoV-2 strain transmission. Furthermore, we enrolled participants across geographically discrete settings, limiting the potential for study-site specific biases, and producing findings consistent across sites (Appendix Figure 2–3).

The first limitation of our study is that ≈8% of enrolled study participants did not have serologic or NAAT data and were excluded from analyses, but the demographic profile of those persons largely reflected the final study population. Second, demographic information, underlying conditions, and COVID-19 vaccination status were self-reported, which may introduce recall or social-desirability biases, potentially affecting our findings in either direction. Third, we used a total S antibody immunoassay, and findings may be different for other assays that measure binding or neutralizing antibodies. Fourth, the immunoassay used in our study was designed to measure antibodies against the wild-type SARS-CoV-2 virus, and quantitative antibody measures may be different for highly immune-evasive variants (*23*). Fifth, sensitivity of NAAT for the detection of acute symptomatic SARS-CoV-2 infection is estimated to be 70%–95% (*24*); therefore, some infections may have been misclassified as non-infections, which would attenuate the differences in S

Table 4. Multivariable odds ratios for a SARS-CoV-2 NAAT-positive test result in participants in study of SARS-CoV-2 spike antibody levels, by phase of predominant circulating viral strain, Dominican Republic, March 2021–August 2022*

S antibody titer quartile	OR (95% CI)†				
	Total, N = 2,300	Pre-Delta, n = 646	Delta, n = 764	Omicron (BA.1), n = 464	Omicron (BA.2/4/5), n = 426
Q1	Referent	Referent	Referent	Referent	Referent
Q2	0.55 (0.40–0.74)§	0.25 (0.14–0.44)§	0.38 (0.23–0.62)§	0.69 (0.27–1.76)	0.60 (0.30–1.17)
Q3	0.38 (0.27–0.55)§	0.13 (0.07–0.25)§	0.31 (0.19–0.51)§	0.46 (0.16–1.27)	0.30 (0.14–0.60)¶
Q4	0.27 (0.18–0.40)§	0.13 (0.06–0.25)§	0.31 (0.18–0.54)§	0.14 (0.04–0.42)¶	0.22 (0.09–0.50)§

*Phases based on dominant circulating strain: March 22–August 15, 2021 (pre-Delta, primarily Mu, Gamma, Iota, and Lambda strains), August 16–December 23, 2021 (Delta), December 24, 2021–April 30, 2022 (Omicron, BA.1), and May 1–August 17, 2022 (Omicron, BA.2, BA.4, BA.5). Anti-S, SARS-CoV-2 spike binding antibody.
†Odds ratios with 95% CIs calculated using binomial multivariable logistic regression models with data presented for log-adjusted anti-S titers stratified by quartile. Quartiles calculated using the quantile function in R (*16*) and are specific to each phase. Appendix Table 10 (https://wwwnc.cdc.gov/EID/article/29/4/22-1628-App1.pdf) shows phase and quartile anti-S geometric mean titers and median titers Model covariates include, in addition to anti-S titer quartile, number of COVID-19 vaccine doses received, days since last COVID-19 vaccine dose, sex, age, and month of sample collection. Appendix Tables 4–8 show full univariable and multivariable models, underlying data, predictor variables, and model performance measures.
§p<0.001.
¶p<0.01.

antibody levels between cases and noncases reported in this study. Sixth, the study was conducted among a discrete population of patients seeking healthcare for undifferentiated fever; therefore, changes in antibody levels may not reflect the broader population, which would limit generalizability of our findings. However, as previously stated, findings were similar across our 2 geographically discrete study sites, suggesting that our findings are comparable across similar healthcare settings in the country.

In summary, we believe there are 3 broad findings from this study. First, we provide documentation of longitudinal changes in SARS-CoV-2 antibody titers after the launch of a national vaccination campaign. Second, we document that total S antibody levels track closely with risk for infection across multiple viral strains, including strains with highly effective immune-evasion capacity, suggesting that this test-negative approach may be valuable to model correlates of protection, while noting potential limitations as described previously. Third, we present a novel approach to monitoring changes in immune biomarkers among discrete populations, an approach that is relatively simple and can leverage existing surveillance infrastructure. Because future SARS-CoV-2 variants of concern and other emerging pathogens will occur, establishing pragmatic and sustainable methods to estimate population immune markers while simultaneously assessing strain-specific risks for infection may prove a valuable complement to existing surveillance infrastructure.

Acknowledgments

We thank the many participants who volunteered to participate in this study. We also thank the study staff who collected the field data and the Dominican Republic Ministry of Health and Social Assistance and the Pedro Henriquez Ureña National University for their commitment and support for the study. CDC staff supported the design, interpretation, and manuscript editing.

This study was funded through a CDC-funded U01 award (awarded to principal investigator E.J.N.). C.L.L., A.K., D.D., M.dS.A., S.G., M.C.E., W.D., N.I., G.A., M.B., K.W.R., K.D., and M.V. received salary support, consultancy fees, or travel paid through this award. E.Z.G. and B.L. are employees of CDC. C.T., L.C., I.M.S., F.P., and R.S.R. are employees of the Ministry of Health and Social Assistance, Dominican Republic, that was subcontracted with funds from the CDC award. A.K. is supported by the Welcome Trust, UK. We declare no other competing interests.

The first 9 and last 4 authors had full access to all the data. E.J.N., R.S.M., E.Z.G., and C.T.P. had final responsibility for the decision to submit for publication.

About the Author

Dr. Nilles is a clinician and medical epidemiologist at the Brigham and Women's Hospital and Harvard Medical School and the director of the Program on Infectious Diseases and Epidemics at the Harvard Humanitarian Initiative. His primary research interests include the surveillance and seroepidemiology of emerging and reemerging epidemic pathogens in lower- and middle-income settings, interdisciplinary approaches to characterizing pathogen epidemiology and transmission, and translating field research to policy.

References

1. Hallal PC, Hartwig FP, Horta BL, Silveira MF, Struchiner CJ, Vidaletti LP, et al. SARS-CoV-2 antibody prevalence in Brazil: results from two successive nationwide serological household surveys. Lancet Glob Health. 2020;8:e1390–8. https://doi.org/10.1016/S2214-109X(20)30387-9
2. Le Vu S, Jones G, Anna F, Rose T, Richard JB, Bernard-Stoecklin S, et al. Prevalence of SARS-CoV-2 antibodies in France: results from nationwide serological surveillance. Nat Commun. 2021;12:3025. https://doi.org/10.1038/s41467-021-23233-6
3. Anand S, Montez-Rath M, Han J, Cadden L, Hunsader P, Kerschmann R, et al. Estimated SARS-CoV-2 seroprevalence in US patients receiving dialysis 1 year after the beginning of the COVID-19 pandemic. JAMA Netw Open. 2021; 4:e2116572. https://doi.org/10.1001/jamanetworkopen.2021.16572
4. Pollán M, Pérez-Gómez B, Pastor-Barriuso R, Oteo J, Hernán MA, Pérez-Olmeda M, et al.; ENE-COVID Study Group. Prevalence of SARS-CoV-2 in Spain (ENE-COVID): a nationwide, population-based seroepidemiological study. Lancet. 2020;396:535–44. https://doi.org/10.1016/S0140-6736(20)31483-5
5. Feng S, Phillips DJ, White T, Sayal H, Aley PK, Bibi S, et al.; Oxford COVID Vaccine Trial Group. Correlates of protection against symptomatic and asymptomatic SARS-CoV-2 infection. Nat Med. 2021;27:2032–40. https://doi.org/10.1038/s41591-021-01540-1
6. Gilbert PB, Montefiori DC, McDermott AB, Fong Y, Benkeser D, Deng W, et al.; Immune Assays Team; Moderna, Inc. Team; Coronavirus Vaccine Prevention Network (CoVPN)/Coronavirus Efficacy (COVE) Team; United States Government (USG)/CoVPN Biostatistics Team. Immune correlates analysis of the mRNA-1273 COVID-19 vaccine efficacy clinical trial. Science. 2022; 375:43–50. https://doi.org/10.1126/science.abm3425
7. Khoury DS, Cromer D, Reynaldi A, Schlub TE, Wheatley AK, Juno JA, et al. Neutralizing antibody levels are highly predictive of immune protection from symptomatic SARS-CoV-2 infection. Nat Med. 2021;27:1205–11. https://doi.org/10.1038/s41591-021-01377-8
8. Nilles EJ, Paulino CT, de St Aubin M, Restrepo AC, Mayfield H, Dumas D, et al. SARS-CoV-2 seroprevalence, cumulative infections, and immunity to symptomatic infection—a multistage national household survey and modelling study, Dominican Republic, June–October 2021. Lancet Reg Health Am. 2022;16:100390. https://doi.org/10.1016/j.lana.2022.100390
9. Oficina Nacional de Estadistica (República Dominicana). Inicio [cited 2021 Sep 13]. https://www.one.gob.do

10. United Nations Statistic Division. Global demographics. Population by age, sex and urban/rural residence: latest available year, 2008–2017. 2017 [cited 2021 Sep 24]. https://unstats.un.org/unsd/demographic-social/products/dyb/documents/dyb2017/table07.pdf
11. Charles PWD. COVID-19, GitHub repository. 2013 [cited 2022 May 16]. https://github.com/govex/COVID-19/tree/master/data_tables/vaccine_data/global_data
12. Ritchie H, Mathieu E, Rodés-Guirao L, et al. Coronavirus pandemic (COVID-19). 2020 [cited 2022 Sep 14]. https://ourworldindata.org/coronavirus
13. Barber RM, Sorensen RJD, Pigott DM, Bisignano C, Carter A, Amlag JO, et al.; COVID-19 Cumulative Infection Collaborators. Estimating global, regional, and national daily and cumulative infections with SARS-CoV-2 through Nov 14, 2021: a statistical analysis. Lancet. 2022;399:2351–80. https://doi.org/10.1016/S0140-6736(22)00484-6
14. Kristiansen PA, Page M, Bernasconi V, Mattiuzzo G, Dull P, Makar K, et al. WHO international standard for anti-SARS-CoV-2 immunoglobulin. Lancet. 2021;397:1347–8. https://doi.org/10.1016/S0140-6736(21)00527-4
15. Ainsworth M, Andersson M, Auckland K, Baillie JK, Barnes E, Beer S, et al.; National SARS-CoV-2 Serology Assay Evaluation Group. Performance characteristics of five immunoassays for SARS-CoV-2: a head-to-head benchmark comparison. Lancet Infect Dis. 2020;20:1390–400. https://doi.org/10.1016/S1473-3099(20)30634-4
16. Harrison E, Drake T, Ots R. finalfit: quickly create elegant regression results tables and plots when modelling. 2021 [cited 2021 Oct 9]. https://cran.r-project.org/package=finalfit
17. Breheny PBW, Burchett W. Visualization of regression models using visreg. R J. 2017;9:56–71. https://doi.org/10.32614/RJ-2017-046
18. Wickham H. Ggplot2: elegant graphics for data analysis. Second edition. New York: Springer–Verlag; 2016.
19. Molodtsov IA, Kegeles E, Mitin AN, Mityaeva O, Musatova OE, Panova AE, et al. Severe acute respiratory syndrome coronavirus 2 (SARS-CoV-2)–specific T cells and antibodies in coronavirus disease 2019 (COVID-19) protection: a prospective study. Clin Infect Dis. 2022;75:e1–9. https://doi.org/10.1093/cid/ciac278
20. Bartsch YC, Fischinger S, Siddiqui SM, Chen Z, Yu J, Gebre M, et al. Discrete SARS-CoV-2 antibody titers track with functional humoral stability. Nat Commun. 2021;12:1018. https://doi.org/10.1038/s41467-021-21336-8
21. Finch E, Lowe R, Fischinger S, de St Aubin M, Siddiqui SM, Dayal D, et al.; CMMID COVID-19 Working Group and the SpaceX COVID-19 Cohort Collaborative. SARS-CoV-2 antibodies protect against reinfection for at least 6 months in a multicentre seroepidemiological workplace cohort. PLoS Biol. 2022;20:e3001531. https://doi.org/10.1371/journal.pbio.3001531
22. Bergwerk M, Gonen T, Lustig Y, Amit S, Lipsitch M, Cohen C, et al. Covid-19 breakthrough infections in vaccinated health care workers. N Engl J Med. 2021;385:1474–84. https://doi.org/10.1056/NEJMoa2109072
23. Asamoah-Boaheng M, Goldfarb DM, Karim ME, O'Brien SF, Wall N, Drews SJ, et al. The relationship between anti-spike SARS-CoV-2 antibody levels and risk of breakthrough COVID-19 among fully vaccinated adults. J Infect Dis. 2022;2022:1–5. https://doi.org/10.1093/infdis/jiac403
24. Arevalo-Rodriguez I, Buitrago-Garcia D, Simancas-Racines D, Zambrano-Achig P, Del Campo R, Ciapponi A, et al. False-negative results of initial RT-PCR assays for COVID-19: a systematic review. PLoS One. 2020;15:e0242958. https://doi.org/10.1371/journal.pone.0242958

Address for correspondence: Eric J. Nilles, Brigham and Women's Hospital, 75 Francis St, Boston, MA 02115, USA; email: enilles@bwh.harvard.edu

Extensive Spread of SARS-CoV-2 Delta Variant among Vaccinated Persons during 7-Day River Cruise, the Netherlands

Thijs Veenstra, Patrick D. van Schelven, Yvonne M. ten Have, Corien M. Swaan, Willem M. R. van den Akker

We investigated a large outbreak of SARS-CoV-2 infections among passengers and crew members (60 cases in 132 persons) on a cruise ship sailing for 7 days on rivers in the Netherlands. Whole-genome analyses suggested a single or limited number of viral introductions consistent with the epidemiologic course of infections. Although some precautionary measures were taken, no social distancing was exercised, and air circulation and ventilation were suboptimal. The most plausible explanation for introduction of the virus is by persons (crew members and 2 passengers) infected during a previous cruise, in which a case of COVID-19 had occurred. The crew was insufficiently prepared on how to handle the situation, and efforts to contact public health authorities was inadequate. We recommend installing clear handling protocols, direct contacts with public health organizations, training of crew members to recognize outbreaks, and awareness of air quality on river-cruise ships, as is customary for most seafaring cruises.

Cruise ships have long been associated with an increased risk for outbreaks of infectious diseases, illustrated by transmissions of respiratory pathogens and pathogenic microorganisms spreading by the fecal–oral route (*1*–*5*). The special circumstances on a cruise ship with crowded, confined spaces, where fresh air supply is sometimes limited, contributes to the risk for spreading airborne pathogens (*6*–*9*). An additional factor is that the passengers on cruise ships are in general of older age and therefore more susceptible to infections (*10*).

The consequences of an outbreak of an infectious disease on a seafaring cruise can be massive (*11*–*13*). At every port, exchange of passengers occurs, leading to a new risk for introduction of a contagious disease. Besides the financial and commercial consequences, the distance to medical facilities is sometimes considerable, which hinders medical consultation and eventual hospitalization. Therefore, companies organizing seafaring cruises take extensive measures to reduce risks by appointing medically trained personnel, installing care facilities on board, and training personnel to be vigilant about presence of symptomatic passengers that might point to infectious diseases. In addition, prevention plans, outbreak protocols, and procedures for early contact with port health authorities, consistent with provisions of the Maritime Declaration of Health, Annex 8 of the World Health Organization International Health Regulations (*14*), should be installed (*15*,*16*).

In contrast to the preparedness for seafaring cruises, only limited attention is given to those risks on river cruise ships (*17*), although there are many characteristics in common with the larger seafaring cruise ships. In general, river cruises are subject to less regulation concerning medical preparedness (expertise and facilities) because of proximity of shore-based facilities. It has been reported that the number of (river) cruises was increasing worldwide before the pandemic (*18*). Therefore, closer attention is justified.

The outbreak of infection with SARS-CoV-2 on the seafaring cruise ship Diamond Princess in early 2020 gained worldwide attention (*19*), and many studies were directed at conditions on the ship and handling of viral spread among passengers (*20*–*24*). During the COVID-19 pandemic, additional outbreaks on boats and seagoing cruise ships were reported (*12*,*17*,*25*). Sekizuka et al. (*26*) reported a SARS-CoV-2 outbreak at a river-cruise ship sailing the Nile. However, there is only limited awareness of the risk for spread and handling of airborne pathogens on river cruise ships (*27*).

Author affiliations: National Institute for Public Health and the Environment, Bilthoven, the Netherlands (T. Veenstra, Y.M. ten Have, C.M. Swaan, W.M.R. van den Akker); Municipal Health Services Gelderland-Midden, Arnhem, the Netherlands (P.D. van Schelven)

DOI: https://doi.org/10.3201/eid2904.221433

We investigated a large outbreak of infection with SARS-CoV-2 on a river cruise ship sailing in the Netherlands. We focused on virus introduction and spread among passengers and crew members, as well as conditions on the ship that might have contributed to transmission of the virus. Using epidemiologic investigation and genomic sequence analyses, we present a plausible chronicle of spread of the virus among passengers and crew members. We identified some serious issues concerning preparedness of the crew and company. On the basis of this study, we propose several feasible prevention and intervention strategies to mitigate the chance of introduction and (further) transmission of airborne pathogens in a river cruise setting.

Methods

Description of Cruise Ship and Demographics of Virus-Positive Passengers

The outbreak of COVID-19 among crew and passengers took place on a 91-m long, 3-deck cruise ship that has capacity for 124 passengers. The ship contains 65 cabins. During the 7-day cruise over rivers in the Netherlands during October 2021, 90% of the cabins were occupied. The exact itinerary and dates are not given because doing so would enable identification of the ship; this anonymity enabled company owners and employees to speak freely to us and to provide valuable insights. We compiled demographics of the persons who tested positive (Table 1). No permission was obtained to contact persons who were not tested or who tested negative for further inquiries.

Epidemiologic Investigation of SARS-CoV-2–Positive Persons

To investigate and control SARS-CoV-2 infection outbreaks in the Netherlands, the Municipal Health Services (MHS) perform SARS-CoV-2 laboratory testing, collect patient information (date of birth, sex, vaccination status, date of first symptoms, and date of testing) and perform contact tracing. Because participants of the cruise lived throughout the Netherlands, the coordinating MHS sent a questionnaire to all 15 involved MHS locations to collect outbreak-related information from exposed passengers and crew. Anonymized data of persons who had positive results during this outbreak were made available by the MHS (data for virus-negative tested persons were not available), as well as conclusions from the contact-tracing investigation concerning possible transmissions between passengers during the cruise.

Genetic Characterization and Comparison of Viral Strains

We used nanopore sequencing (Oxford Nanopore Technologies, https://nanoporetech.com) to determine the genomic sequence of the SARS-CoV-2 isolates (*28*). The MHS made a random selection of 20 samples for whole-genome sequencing based on the lowest day of birth in a month. Several of those samples had already been destroyed in the different testing facilities involved, which resulted in the availability of 11 specimens for sequencing. To determine the prevalence and spread of SARS-CoV-2 lineages within the Netherlands, we used the GISAID database (https://www.gisaid.org) and used the Audacity/Instant tool to query for most similar sequences.

Table 1. Characteristics of passengers and crew who had positive PCR or rapid antigen (self) test results for severe acute respiratory syndrome coronavirus-2 during 7-day river cruise, the Netherlands

Characteristic	Result
All persons	60
Passengers	49 (44% of total passengers)
Crew*	11 (52% of total crew members)
Sex	22 male (37%), 38 female (63%)
Passengers	16 male (33%), 33 female (67%)
Crew	6 male (55%), 5 female (45%)
Age distribution, y	
0–20	2 (3%)
21–40	4 (7%)
41–60	2 (3%)
61–80	33 (54%)
≥81	15 (25%)
Missing data	4 (7%)
Symptomatic	52 (87%), 3 missing data (5%)
Passengers	47 (96%)
Crew	6 (55%), 3 missing data (27%)
Vaccinated	56 (93%)
Passengers	49 (100%)
Crew	7 (64%)

*The child of a crew member was included in the crew statistics.

Investigation of Cruise Ship and Circumstances during the Cruise

We collected information about the ship and the conditions during the cruise from the shipping company. Some authors visited the ship and conducted interviews with the owner, the captain, and 3 crew members. A ship sanitation inspector accompanied the interviewers and reviewed the ventilation systems of the ship.

Results

SARS-CoV-2 Infections on River Cruise Ship

In October 2021, a local MHS was contacted indirectly by a shipping company, reporting that 2 passengers on their ship had tested positive for SARS-CoV-2 by using rapid antigen self-test. The rapid-antigen tests were available on the ship for crew members and symptomatic passengers. Because the ship was on the 6th day of a 7-day voyage, the municipal health authorities advised reverse transcription PCR testing of all symptomatic persons as soon as possible after disembarking. When the number of identified cases increased strongly after the cruise, all passengers and crew members were encouraged to be voluntarily tested, regardless of symptoms, at the MHS reverse transcription PCR testing facility near their location (free of charge).

One week after the cruise, 60 cases were detected and reported to the MHS, which indicated that at least 49 (44%) of 111 passengers and 11 (52%) of 21 crew members had tested positive for SARS-CoV-2. It is unknown how many passengers and crew members tested negative. All infected passengers and 64% of the crew members were vaccinated (Table 1). This finding raised the question of how SARS-CoV-2 could have been introduced massively onto the ship or alternatively, how the virus could have spread so extensively among passengers and crew members during the cruise; a combination of these 2 factors is also possible.

Time Line and Epidemiologic Analysis

On the basis of information from the municipal health authorities, the crew members, and the questionnaires, we constructed a timeline of the events before, during, and after the river cruise (Figure 1). All crew members, who were the same crew members as on a previous cruise, tested negative for SARS-CoV-2 by using rapid antigen self-tests before departure of the cruise ship. The passengers had to show a document of being vaccinated or proof of a laboratory-confirmed recent infection (or a recent negative test result) and were asked if they had any symptoms before they were allowed to participate in the cruise. Vaccinated at the time consisted of a full series of European Union–approved vaccines, meaning 2 doses of Pfizer-BioNTech (https://www.pfizer.com), Moderna (https://www.modernatx.com), or AstraZeneca (https://www.astrazeneca.com) vaccines or a single dose of Janssen https://www.janssen.com) vaccine.

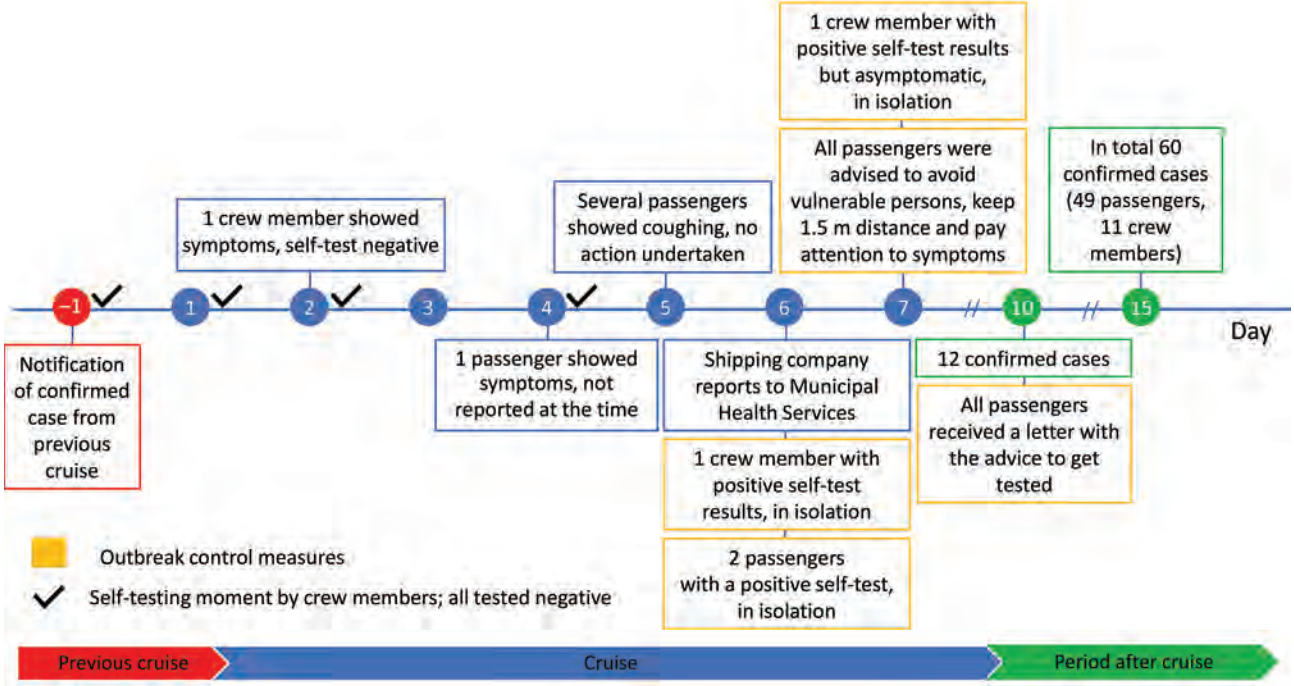

Figure 1. Timeline for COVID-19–related conditions as part of extensive spread of SARS-CoV-2 Delta variant among vaccinated persons during 7-day river cruise, the Netherlands.

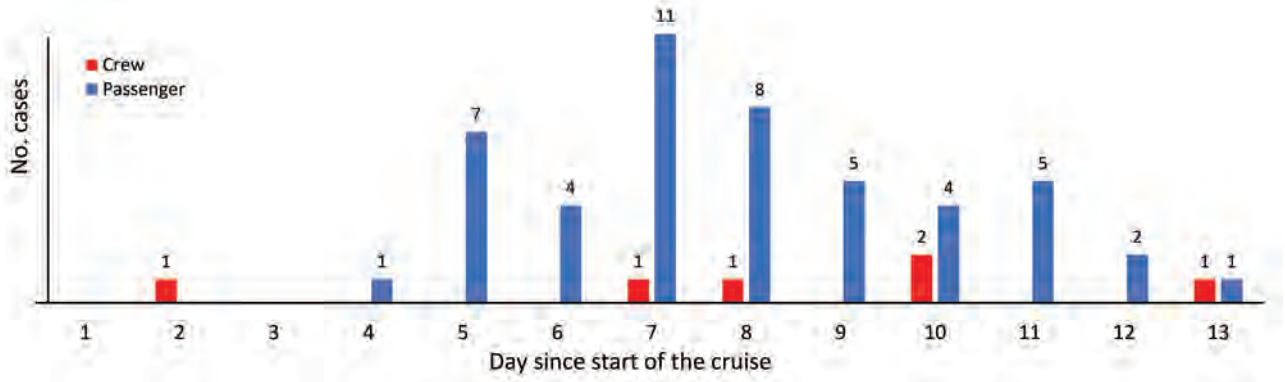

Figure 2. Day of first symptoms for COVID-19–conditions as part of extensive spread of SARS-CoV-2 Delta variant among vaccinated persons during 7-day river cruise, the Netherlands. Infections were later confirmed by using reverse transcription PCR. The day for first symptoms is unknown for 3 crew members. The cruise ended on day 7.

At the time of the cruise, no boosters were registered in the Netherlands. Two passengers from the previous cruise stayed on board and were not tested or asked about having symptoms at the start of their second journey. On the day before departure, the company was informed that another passenger from the previous cruise had tested positive for SARS-CoV-2. The 2 passengers and 1 crew member from the previous cruise showed symptoms and tested positive on the 6th day of their second cruise. Although there were facemasks on board, use was not encouraged, even after identification of these positive persons, as was revealed in interviews with passengers.

After the positive cases were identified, the company searched for advice and had difficulties reaching the appropriate authority. Eventually, contact was established with the MHS, which started a contact-tracing investigation. Passengers and members of the crew who had positive results were isolated in their cabins until disembarking. The only 2 passengers who tested positive in a rapid-antigen test on board also shared a cabin. They were isolated together in their cabin until disembarking that night. Crew members who tested positive were isolated individually.

Because of the infected persons, entertainment on the last evening of the cruise was limited and social distancing between families was encouraged. On the 7th day, a second member of the crew who had a positive test result was isolated. When 12 cases were confirmed 3 days after disembarking, all other passengers and crew members were advised to be tested at the MHS, regardless of symptoms, which resulted in identification of 60 infected persons total. We constructed an epidemiologic curve showing the days of first symptoms for all 60 cases (Figure 2). From the 5th day of the cruise on, larger numbers of persons had symptoms, which reached a peak at the end of the 7-day cruise and gradually decreased in the days thereafter.

During the contact-tracing investigation, passengers reported to have noticed limited COVID-19–related measurements. Social distancing was barely practiced, and the use of face masks was not applied. The shipping company confirmed the lack of additional measurements and stated that these measurements were not mandatory at that point during the pandemic.

Retrospectively, a few participants reported that several passengers had serious coughing. During the cruise, several recreational activities took place outside the ship, including a museum visit, an excursion with a tour boat, and a bus trip. There were multiple city walks, combined with visiting restaurants and terraces. Throughout these activities, the passengers primarily remained in groups, and only limited mixing with the public occurred.

Genomic SARS-CoV-2 Analyses

We sequenced the SARS-CoV-2 genomes of available isolates from 8 passengers and 3 crew members. All samples were successfully sequenced except for the sample from 1 passenger, for which sequencing of the first 340 nt of the genome was not successful. The 11 strains belonged to the Delta variant of concern (B.1.617.2) and were closely related, with a maximum difference of 2 nt (Figure 3). Of the 723 sequenced isolates in the 4 provinces that were visited during the cruise and the following week, only 2 isolates showed close relatedness (3-nt and 4-nt genomic differences). The SARS-CoV-2 incidence was 24.4 cases/100,000 persons in the Netherlands at that time (https://coronadashboard.rijksoverheid.nl/landelijk/positief-geteste-mensen).

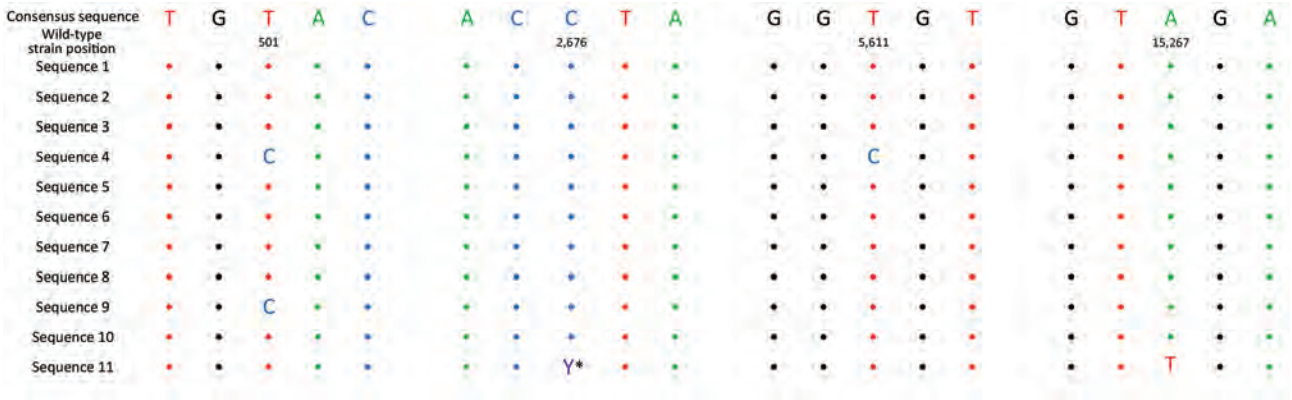

Figure 3. Comparison of whole-genome SARS-CoV-2 sequences obtained from cruise participants during 7-day river cruise, the Netherlands. Only the regions with different nucleotides from the consensus sequence are displayed. Colored circles indicate sequences identity. Sequences classified as the Delta variant of concern were subtyped as AY.126. *Indicates C and T in the same person, possibly co-infection with 2 strains or a mutation that occurred in that person.

Use of Ship Facilities during River Cruise

The cruise ship was occupied by 21 crew members and 111 passengers throughout the 7-day river cruise. We provide the sizes of various areas of the ship and their occupancy during the cruise (Table 2). Because the weather was chilly and rainy, the passengers stayed inside, and mostly the interior spaces of the ship were used. The restaurant area was at times crowded because all passengers used the area at the same time for ≈3 hours/day. This location was the only common area where seats were assigned to individual passengers, and this plan had not changed throughout the journey.

The seating plan showed no clear clustering of persons who had positive results. Also, no clustering was observed in the layout of the cabins (conclusions from contact-tracing investigation). Available data showed that for 16 cases, both passengers sharing a cabin were infected, whereas for 9 cases, only 1 of the 2 passengers sharing a cabin was infected. Throughout the day, the reception area, including lounge and bar, was used by small groups of passengers. Passengers in this area were mostly involved in conversations. The crew reported limited crowding during the day, but in the evening the lounge area was used extensively for multiple group activities, including a quiz, bingo, and a music performance. Other potential areas of close contact were the narrow corridors, but the crew did not observe crowding there.

The ventilation mechanisms on board established recirculation of air in the restaurant, reception area, and lounge bar (Table 2). In the reception area and lounge bar, the crew had modified the air outlets, mainly situated in the windowsills, to prevent recirculation. The cabins received air from the corridors. The ventilation systems contained elementary filters, but they were not of the quality of high-efficiency particulate air filters (*29*,*30*). In intensively used areas, a fresh air supply was not guaranteed. In the restaurant area, air was only recirculated.

Discussion

Seafaring cruise ships and river cruise ships have many characteristics in common regarding the use of confined spaces, air quality control, a high occupation level, a similar age group of passengers, duration of voyages, and similar responsibilities of the crew. However, the preparedness for outbreaks of contagious diseases differ considerably between the 2 types of cruises (*27*).

In our study, we investigated an extensive outbreak of SARS-CoV-2 infections among passengers and crew members on a river cruise ship, which affected 60 persons. However, we cannot exclude that some infections might have occurred directly after disembarking. Another limitation of our study is that we do not have insight into the number of persons who tested negative or were not tested at all. The

Table 2. Ventilation systems and maximum occupancy of the various areas of the cruise ship during 7-Day River Cruise

Area	Volume, m^3 (area × height)	Ventilation system	Maximum occupancy
Cabin	21 (10 × 2.1)	Air supply from corridor and extrusion through the bathroom	2
Corridors	105 (50 × 2.1)	Air from common areas leading to cabins	15
Restaurant	262 (125 × 2.1)	Mechanical recirculation	110
Lounge	440 (200 × 2.2)	Mechanical ventilation, mixing recirculated and fresh air	110
Reception hall	80 (36 × 2.2)	Mechanical ventilation, mixing recirculated and fresh air	50

epidemic pattern is consistent with an early introduction of the virus at the cruise and the incubation time of the SARS-CoV-2 Delta variant (peak ≈4–6 days (*31*).

On the basis of combined epidemiologic and genetic analyses, we conclude that the virus was probably introduced to the cruise by persons (crew or the 2 passengers) from the previous cruise. Because genetic information was not available for all persons who had positive results, we cannot exclude that multiple SARS-CoV-2 introductions had taken place. All passengers were fully vaccinated, and this factor probably contributed to mildness of the symptoms but less so to preventing infections (*32*). Most information about the role of the vaccines to protect from disease and reduction of transmissibility of the Delta variant is derived from large-scale surveillance programs and not from specified crowded conditions. The COVID-19 measures taken on the cruise ship did not prevent extensive spread of the virus.

Because pathogens causing respiratory infections are spreading between persons mostly through droplets and aerosols, air flows and air filtering are major parameters, especially when accommodations are cramped and used by many persons simultaneously (*9*). A systematic review of studies on long-distance airborne transmission of SARS-CoV-2 in indoor community settings provides insight into factors contributing to such transmission (*33*); that review identified insufficient air replacement as a critical determinant of transmission. Installation of high-efficiency particulate air filters can be an effective measure to reduce recirculation of airborne pathogens (*34*).

There are no general regulations concerning ventilation in river cruise ships, and regulations for buildings do not apply to those ships in the Netherlands. In this outbreak, the cruise ship had an inferior air circulation and filtering system. Continuous refreshment of the air in all areas on a ship, preferably using fresh outside air, might lower the spread of airborne pathogens. Air recirculation is only an option in combination with proper filtering. The design stage of a cruise ship should take into consideration the risk for spread of microorganisms by air movements within the ship. Later adjustments are in many situations more difficult and sometimes provisional, as was the instance on the ship in this outbreak. The crew should be well aware of the air climate and install clear instructions for refreshing the air in areas of the ship. The COVID-19 pandemic has demonstrated the effectiveness of wearing a face mask in reducing the number of cases (*35*,*36*). As a simple preventive measure, we recommend that face masks be made available for all persons on board so that they can be used without delay when a risk for infection is suspected.

Multiple passengers on the river cruise reported retrospectively that some of the passengers were regularly coughing at the beginning of the cruise. Because it cannot be expected that passengers ask fellow passengers about their health, crew members can be instructed to be attentive to symptoms of passengers that might indicate an infectious disease and address the situation.

A major problem is that not all symptoms, such as coughing, general malaise, and fever, can be exclusively ascribed to an infectious cause and that the decision to take additional action is a difficult one. The crew can be trained to recognize potential symptoms of infectious diseases and handle these symptoms accordingly. A solution can be that in instances of doubt, the crew seek advice from an appropriate health agency. For the cruise we describe, crew members made contact with public health authorities indirectly, even using private telephone numbers of health officials. Prearranged points of contact provided by health authorities would increase efficiency and effectivity in an outbreak situation. Thus, the combination of well-instructed crew members and the initiative to handle a suspicious situation, including contacting health officials, is a crucial issue.

This outbreak shows the need for preventive measures and vigilance for infectious diseases in river cruise operations. Although full prevention of the spread of infectious agents during a cruise is hard to achieve because passengers can embark during their incubation period and (subclinical) carriership, several simple and effective measures can be taken. Compared with those for seagoing cruises, only minimal requirements for the prevention of spread of infectious diseases on river cruises are available (*37*). Standardized preventive measures would support companies in reducing risk for infectious disease outbreaks, and vigilance on board and the involvement of health authorities could support early detection and response in case of an outbreak. Awareness, training of staff, presence of face masks, and an infrastructure for direct contact with health authorities should be part of a general standard for river cruise operations.

Acknowledgments

We thank employees of the shipping company for their hospitality and information, colleagues at the Municipal Health Services for their efforts and cooperation, team members of the sequencing and bioinformatic groups at the Dutch National Institute for Public Health and the Environment for their efforts, Tanja Hartog for accompanying the visit of the ship and sharing her knowledge of ship ventilation systems, and Lance Presser for critically reading the manuscript.

About the Author

Mr. Veenstra is a senior advisor at the Center for Infectious Disease Control and coordinator of the Infection Prevention Unit at the National Institute for Public Health and the Environment, Bilthoven, the Netherlands. His primary research interest is public health response to infectious diseases in the maritime and transportation sectors.

References

1. Brotherton JM, Delpech VC, Gilbert GL, Hatzi S, Paraskevopoulos PD, McAnulty JM; Cruise Ship Outbreak Investigation Team. A large outbreak of influenza A and B on a cruise ship causing widespread morbidity. Epidemiol Infect. 2003;130:263–71. https://doi.org/10.1017/S0950268802008166
2. Kak V. Infections on cruise ships. Microbiol Spectr. 2015; 3:3.4.24. https://doi.org/10.1128/microbiolspec.IOL5-0007-2015
3. Pavli A, Maltezou HC, Papadakis A, Katerelos P, Saroglou G, Tsakris A, et al. Respiratory infections and gastrointestinal illness on a cruise ship: a three-year prospective study. Travel Med Infect Dis. 2016;14:389–97. https://doi.org/10.1016/j.tmaid.2016.05.019
4. Ward KA, Armstrong P, McAnulty JM, Iwasenko JM, Dwyer DE. Outbreaks of pandemic (H1N1) 2009 and seasonal influenza A (H3N2) on cruise ship. Emerg Infect Dis. 2010;16:1731–7. https://doi.org/10.3201/eid1611.100477
5. Isakbaeva ET, Widdowson MA, Beard RS, Bulens SN, Mullins J, Monroe SS, et al. Norovirus transmission on cruise ship. Emerg Infect Dis. 2005;11:154–8. https://doi.org/10.3201/eid1101.040434
6. Kak V. Infections in confined spaces: cruise ships, military barracks, and college dormitories. Infect Dis Clin North Am. 2007;21:773–84, ix–x. https://doi.org/10.1016/j.idc.2007.06.004
7. Melikov AK. COVID-19: Reduction of airborne transmission needs paradigm shift in ventilation. Build Environ. 2020; 186:107336. https://doi.org/10.1016/j.buildenv.2020.107336
8. Sun C, Zhai Z. The efficacy of social distance and ventilation effectiveness in preventing COVID-19 transmission. Sustain Cities Soc. 2020;62:102390. https://doi.org/10.1016/j.scs.2020.102390
9. Moon J, Ryu BH. Transmission risks of respiratory infectious diseases in various confined spaces: a meta-analysis for future pandemics. Environ Res. 2021; 202:111679. https://doi.org/10.1016/j.envres.2021.111679
10. Kobayashi T, Yoshii K, Linton NM, Suzuki M, Nishiura H. Age dependence of the natural history of infection with severe acute respiratory syndrome coronavirus 2 (SARS-CoV-2): an analysis of Diamond Princess data. Int J Infect Dis. 2022;115:109–15. https://doi.org/10.1016/j.ijid.2021.12.319
11. Moriarty LF, Plucinski MM, Marston BJ, Kurbatova EV, Knust B, Murray EL, et al.; CDC Cruise Ship Response Team; California Department of Public Health COVID-19 Team; Solano County COVID-19 Team. Public health responses to COVID-19 outbreaks on cruise ships—worldwide, February–March 2020. MMWR Morb Mortal Wkly Rep. 2020;69:347–52. https://doi.org/10.15585/mmwr.mm6912e3
12. Ito H, Hanaoka S, Kawasaki T. The cruise industry and the COVID-19 outbreak. Transp Res Interdiscip Perspect. 2020;5:100136. https://doi.org/10.1016/j.trip.2020.100136
13. Muritala BA, Hernández-Lara AB, Sánchez-Rebull MV, Perera-Lluna A. #CoronavirusCruise: impact and implications of the COVID-19 outbreaks on the perception of cruise tourism. Tour Manag Perspect. 2022;41:100948. https://doi.org/10.1016/j.tmp.2022.100948
14. World Health Organization. International Health Regulations, 2005. 3rd edition. 2016 [cited 2023 Feb 2]. https://www.who.int/publications/i/item/9789241580496
15. Centers for Disease Control and Prevention. CDC issues framework for resuming safe and responsible cruise ship passenger operations. 2020 Oct 30 [cited 2023 Feb 2]. https://www.cdc.gov/media/releases/2020/s1030-safe-responsible-ship-passenger-operations.html
16. Chowell G, Dahal S, Bono R, Mizumoto K. Harnessing testing strategies and public health measures to avert COVID-19 outbreaks during ocean cruises. Sci Rep. 2021;11:15482. https://doi.org/10.1038/s41598-021-95032-4
17. Kordsmeyer AC, Mojtahedzadeh N, Heidrich J, Militzer K, von Münster T, Belz L, et al. Systematic review on outbreaks of SARS-CoV-2 on cruise, navy and cargo Ships. Int J Environ Res Public Health. 2021;18:5195. https://doi.org/10.3390/ijerph18105195
18. Cruise Lines International Association. Ocean & river cruise review 2018. 2019 Jun [cited 2023 Feb 2]. https://cruising.org/-/media/eu-resources/pdfs/CLIA-Cruise-Review-2018-Published-2019
19. Baraniuk C. What the Diamond Princess taught the world about COVID-19. BMJ. 2020;369:m1632. https://doi.org/10.1136/bmj.m1632
20. Azimi P, Keshavarz Z, Cedeno Laurent JG, Stephens B, Allen JG. Mechanistic transmission modeling of COVID-19 on the *Diamond Princess* cruise ship demonstrates the importance of aerosol transmission. Proc Natl Acad Sci U S A. 2021;118:e2015482118. https://doi.org/10.1073/pnas.2015482118
21. Plucinski MM, Wallace M, Uehara A, Kurbatova EV, Tobolowsky FA, Schneider ZD, et al. Coronavirus disease 2019 (COVID-19) in Americans aboard the Diamond Princess cruise ship. Clin Infect Dis. 2021;72:e448–57. https://doi.org/10.1093/cid/ciaa1180
22. Rocklöv J, Sjödin H, Wilder-Smith A. COVID-19 outbreak on the Diamond Princess cruise ship: estimating the epidemic potential and effectiveness of public health countermeasures. J Travel Med. 2020;27:taaa030. https://doi.org/10.1093/jtm/taaa030
23. Sekizuka T, Itokawa K, Kageyama T, Saito S, Takayama I, Asanuma H, et al. Haplotype networks of SARS-CoV-2 infections in the *Diamond Princess* cruise ship outbreak. Proc Natl Acad Sci U S A. 2020;117:20198–201. https://doi.org/10.1073/pnas.2006824117
24. Walker LJ, Codreanu TA, Armstrong PK, Goodwin S, Trewin A, Spencer E, et al. SARS-CoV-2 infections among Australian passengers on the Diamond Princess cruise ship: a retrospective cohort study. PLoS One. 2021;16:e0255401. https://doi.org/10.1371/journal.pone.0255401
25. Hatzianastasiou S, Mouchtouri VA, Pavli A, Tseroni M, Sapounas S, Vasileiou C, et al. COVID-19 outbreak on a passenger ship and assessment of response measures, Greece, 2020. Emerg Infect Dis. 2021;27:1927–30. https://doi.org/10.3201/eid2707.210398
26. Sekizuka T, Kuramoto S, Nariai E, Taira M, Hachisu Y, Tokaji A, et al. SARS-CoV-2 genome analysis of Japanese travelers in Nile River cruise. Front Microbiol. 2020;11:1316. https://doi.org/10.3389/fmicb.2020.01316
27. Verhoef L, Boxman IL, Duizer E, Rutjes SA, Vennema H, Friesema IH, et al. Multiple exposures during a norovirus

outbreak on a river-cruise sailing through Europe, 2006. Euro Surveill. 2008;13:18899. https://doi.org/10.2807/ese.13.24.18899-en
28. Andeweg SP, Vennema H, Veldhuijzen I, Smorenburg N, Schmitz D, Zwagemaker F, et al.; SeqNeth Molecular surveillance group; RIVM COVID-19 Molecular epidemiology group. Elevated risk of infection with SARS-CoV-2 Beta, Gamma, and Delta variant compared to Alpha variant in vaccinated individuals. Sci Transl Med. 2022;Jul 21:eabn4338. https://doi.org/10.1126/scitranslmed.abn4338
29. Landry SA, Subedi D, Barr JJ, MacDonald MI, Dix S, Kutey DM, et al. Fit-tested N95 masks combined with portable HEPA filtration can protect against high aerosolized viral loads over prolonged periods at close range. J Infect Dis. 2022;226:199–207. https://doi.org/10.1093/infdis/jiac195
30. Mousavi ES, Godri Pollitt KJ, Sherman J, Martinello RA. Performance analysis of portable HEPA filters and temporary plastic anterooms on the spread of surrogate coronavirus. Build Environ. 2020;183:107186. https://doi.org/10.1016/j.buildenv.2020.107186
31. Kang M, Xin H, Yuan J, Ali ST, Liang Z, Zhang J, et al. Transmission dynamics and epidemiological characteristics of SARS-CoV-2 Delta variant infections in Guangdong, China, May to June 2021. Euro Surveill. 2022;27:2100815. https://doi.org/10.2807/1560-7917.ES.2022.27.10.2100815
32. Eyre DW, Taylor D, Purver M, Chapman D, Fowler T, Pouwels KB, et al. Effect of COVID-19 vaccination on transmission of Alpha and Delta variants. N Engl J Med. 2022;386:744–56. https://doi.org/10.1056/NEJMoa2116597
33. Duval D, Palmer JC, Tudge I, Pearce-Smith N, O'Connell E, Bennett A, et al. Long distance airborne transmission of SARS-CoV-2: rapid systematic review. BMJ. 2022;377:e068743. https://doi.org/10.1136/bmj-2021-068743
34. Coyle JP, Derk RC, Lindsley WG, Blachere FM, Boots T, Lemons AR, et al. Efficacy of ventilation, HEPA air cleaners, universal masking, and physical distancing for reducing exposure to simulated exhaled aerosols in a meeting room. Viruses. 2021;13:2536. https://doi.org/10.3390/v13122536
35. Cheng Y, Ma N, Witt C, Rapp S, Wild PS, Andreae MO, et al. Face masks effectively limit the probability of SARS-CoV-2 transmission. Science. 2021;372:1439–43. https://doi.org/10.1126/science.abg6296
36. Asadi S, Cappa CD, Barreda S, Wexler AS, Bouvier NM, Ristenpart WD. Efficacy of masks and face coverings in controlling outward aerosol particle emission from expiratory activities. Sci Rep. 2020;10:15665. https://doi.org/10.1038/s41598-020-72798-7
37. Centers for Disease Control and Prevention. Vessel sanitation program, 2022 [cited 2023 Feb 2]. https://www.cdc.gov/nceh/vsp/default.htm

Address for correspondence: Willem M.R van den Akker, National Institute for Public Health and the Environment, Antoni van Leeuwenhoeklaan 9, 3721 MA Bilthoven, the Netherlands, email: vandenakkerwillem@gmail.com

Mapping Global Bushmeat Activities to Improve Zoonotic Spillover Surveillance by Using Geospatial Modeling

Soushieta Jagadesh, Cheng Zhao, Ranya Mulchandani, Thomas P. Van Boeckel

Human populations that hunt, butcher, and sell bushmeat (bushmeat activities) are at increased risk for zoonotic pathogen spillover. Despite associations with global epidemics of severe illnesses, such as Ebola and mpox, quantitative assessments of bushmeat activities are lacking. However, such assessments could help prioritize pandemic prevention and preparedness efforts. We used geospatial models that combined published data on bushmeat activities and ecologic and demographic drivers to map the distribution of bushmeat activities in rural regions globally. The resulting map had high predictive capacity for bushmeat activities (true skill statistic = 0.94). The model showed that mammal species richness and deforestation were principal drivers of the geographic distribution of bushmeat activities and that countries in West and Central Africa had the highest proportion of land area associated with bushmeat activities. These findings could help prioritize future surveillance of bushmeat activities and forecast emerging zoonoses at a global scale.

Bushmeat or wild meat refers to the meat of terrestrial wild mammals hunted primarily for human consumption in tropical and subtropical regions (*1*). Terrestrial wild mammals represent just 1.8% (≈0.003 gigatons of carbon [GtC]) of the global biomass of mammals (≈0.17 GtC) but are vastly outweighed by the biomass of domestic mammals raised for food (≈0.1 GtC) (*2*). However, >70% of zoonotic disease spillover events have been associated with wildlife and bushmeat (*3*,*4*). Hunting, preparing, and selling bushmeat (hereafter referred to as bushmeat activities) has been associated with high risk for zoonotic pathogen spillover due to contact with infectious materials from animals. Bushmeat activities provide opportunities for repeated pathogen transmission between animals and humans, leading to outbreaks, epidemics, and pandemics (*5*,*6*). For instance, Ebola virus spillover events and subsequent outbreaks in the Congo Basin have been traced back to hunters who were exposed to ape carcasses (*7*,*8*).

Bushmeat remains a staple source of protein among low-economic rural communities, where alternative proteins can be scarce (*9*,*10*). However, geographic distribution of bushmeat activities in rural areas remains insufficiently documented (*11*). The urban demand for bushmeat from rural areas is inconsistent and dependent on various reasons, including low cost compared with domestic meat, taste preferences, or social prestige (*12*). The hunted animal is often butchered and consumed immediately in rural areas (*13*). In regions where the urban demand is high, the animals are transported either live-caged or butchered and smoked to urban markets (*13*). Bushmeat activities pose a risk for zoonotic disease transmission regardless of setting (*14*), and the geographic and anthropologic heterogeneities in bushmeat activities renders surveillance for spillover risk challenging.

A recent study used the geographic range of endangered mammals to map mammal hunting for bushmeat and traditional medicine (*15*). Other mapping efforts, although accurate in capturing the market dynamics, have been restricted to local or regional settings (*16*,*17*). Research on bushmeat has been either biocentric, based on wildlife conservation (*18*), or anthropocentric, related to food security (*19*). Because zoonotic diseases known to be transmitted from wild mammals, such as mpox and Ebola, continue to emerge and expand geographically, an urgent need exists to integrate bushmeat activities into the epidemiology of

Author affiliations: Eidgenössische Technische Hochschule Zürich, Zurich, Switzerland (S. Jagadesh, C. Zhao, R. Mulchandani, T.P. Van Boeckel); Sahlgrenska Academy, University of Gothenburg, Gothenburg, Sweden; One Health Trust, Washington, DC, USA (T.P. Van Boeckel)

DOI: https://doi.org/10.3201/eid2904.221022

emerging zoonoses. Efforts to document bushmeat activities have been sporadic and have not been synthesized geographically to enable objective prioritization and targeting of epidemiologic surveillance resources. However, to sustainably and effectively monitor at-risk areas for outbreak prevention and preparedness, bushmeat activity hotspots need to be identified on a global scale.

We mapped bushmeat activities in tropical and subtropical rural areas. We trained geospatial models that we calibrated by using published data and environmental and demographic covariates of bushmeat activities. We validated the capacity of the bushmeat activities map in predicting zoonotic disease emergence by using 2 established models of Ebola virus disease (EVD) (*20*,*21*). In addition, we identified 100 urban locations that could most benefit from increased surveillance for bushmeat activities.

Methods

We used a multistep procedure to model the distribution of bushmeat activities. We modeled activities by using the following steps: collate datapoints from systematic literature search; prepare environmental and demographic covariates; fit model; conduct ensemble modeling; calculate the geographic area associated with bushmeat activities; and perform post hoc validation (Appendix, https://wwwnc.cdc.gov/EID/article/29/4/22-1022-App1.pdf).

Data Collection

We searched for peer-reviewed reports on bushmeat hunting, handling, butchering, and selling by reviewing 3 electronic databases: Web of Science (https://www.webofscience.com), PubMed (https://pubmed.ncbi.nlm.nih.gov), and Google Scholar (https://scholar.google.com). We also searched websites for nongovernmental agencies, including International Union for Conservation of Nature (https://www.iucn.org), TRAFFIC (https://www.traffic.org), and the Center for International Forestry Research (CIFOR; https://www.cifor.org). We included studies with locations of bushmeat activities during January 1, 2000–February 1, 2022, and restricted the search to literature in English and French.

We identified 2,113 articles from all databases, of which 130 articles included geographic coordinates and precise locations of bushmeat activities. Among those 130 articles, we identified and included in the study 76 articles that were based in rural sites (defined as human settlements of <50,000 persons) (Figure 1). We excluded the other 54 articles because the locations included were urban sites (n = 28) or national parks without precise geographic coordinates of bushmeat activities (n = 26) (i.e., bushmeat was hunted or sold within the park). We excluded urban sites because different covariates could be associated with bushmeat activities between urban and rural sites, precise geographic coordinates were not given, and model prediction based on population density might be overestimated if a single pooled model was used for rural and urban sites (Appendix).

We extracted 221 unique locations from the included studies and reports and georeferenced location latitude and longitude coordinates in decimal degrees. We used village or town centroids unless the exact

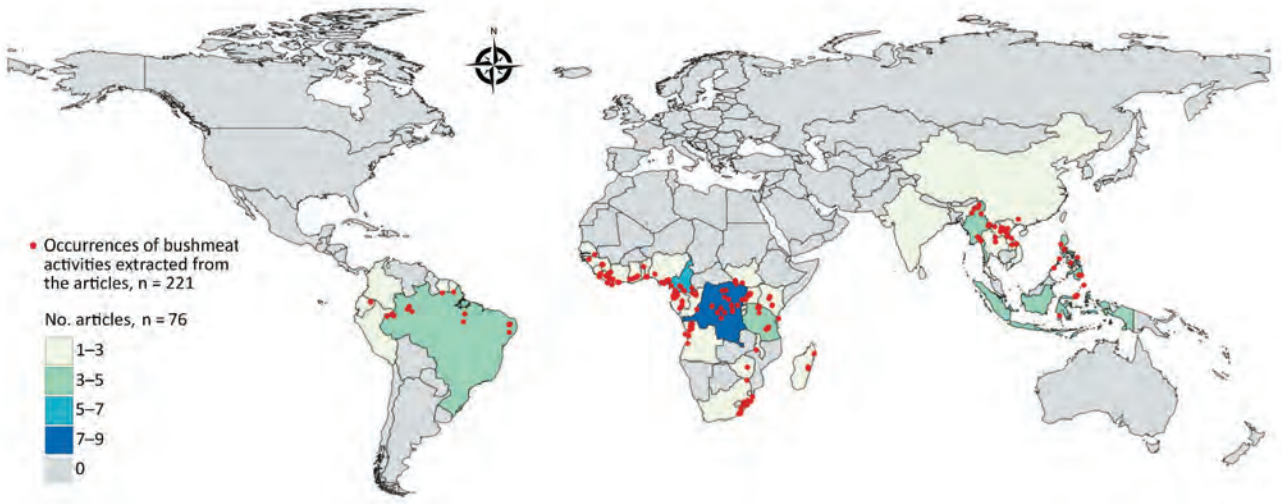

Figure 1. Geographic distribution of articles from the literature used to model a map of global bushmeat activities (hunting, preparing, and selling bushmeat) to improve zoonotic spillover surveillance. We extracted data from 76 articles. Red dots indicate occurrences of bushmeat activities (n = 221) in 38 countries, and colored shading indicated the number of articles extracted per country.

location of markets were mentioned in the articles (Appendix). We created a search string and used PRISMA (https://www.prisma-statement.org) to create a flowchart of data extraction (Appendix Figure 1).

Environmental and Demographic Covariates

We extracted data from potential environmental and demographic covariates of bushmeat activities based on previous analyses (Appendix Table 1). Among those covariates, we developed 2 raster layers that we considered essential for predicting bushmeat prevalence. First, we developed a bushmeat species diversity raster from terrestrial mammal distribution data (*22*) and a list of mammals hunted and sold for commercial purposes for consumption, excluding mammals hunted as pests and trophies (*15*) (Appendix). We extracted a polygon layer of the distribution of 128 mammal species selected from the International Union for Conservation of Nature database of terrestrial wild mammals by using the species identification and then rasterized to 0.00833 degrees. Second, we constructed a raster of the distance to protected areas, such as natural parks, forest reserves, and wilderness areas (Appendix). We used data from World Geodetic System version 84 (GISGeography, https://gisgeography.com) to project all covariates and resampled by using a pixel resolution of 2.5 minutes of arc (0.04166 degrees), equating to ≈5 × 5 km resolution.

Model Fitting and Evaluation

We selected 8 covariates with a recommended variance inflation factor (VIF) <10 (*23*) to account for potential collinearity among the covariates (Appendix Table 2). We used data on bushmeat activity extracted from the literature search datapoints, along with 1,000 randomly generated background points biased toward more populous areas as a proxy for reporting bias across the study area (*24*). We mapped bushmeat activities by using 4 models: MaxENT, random forest (RF), boosted regression tree (BRT), and Bayesian additive regression tree (BART). For each model, we used 80% of the datapoints (observed and background) for the training dataset; we used the remaining 20% of datapoints as the validation dataset (Appendix Figure 4). We fit and evaluated the base models by using area under the curve (AUC) and true skill statistic (maxTSS).

We used 2 cross-validation (CV) methods and input covariates from R (The R Foundation for Statistical Computing, https://www.r-project.org) to prevent model overfitting: k-fold CV based on covariates from the SDMtune package (*25*) and environmental CV (EnvCV) with covariates from the blockCV package (*26*). We split the training data into 4-folds (k = 4) for both approaches. We only chose models with an AUC and maxTSS >0.5 after CV for hyperparameter tuning and to develop an ensemble model. The MaxENT model performed poorly (maxTSS = 0.47) in EnvCV, and we excluded it from further analysis. We also compared the models with a geographic null model to assess the predictive power of covariates (*27*).

Model Optimization and Ensemble Modeling

We split data into training, validation, and testing sets for model optimization by tuning the appropriate hyperparameters for each model. We used the entire dataset in the optimized models to predict the global distribution of bushmeat activities. We stacked the model predictions from RF, BRT, and BART and used those as metacovariates for developing an ensemble model. We used a binomial logistic regression model in a hierarchical Bayesian framework with an intrinsic conditional autoregressive model (iCAR) (*28*) to assemble the model predictions. We validated the output ensemble prediction by using maxTSS and comparing deviance with a geographic null model. We generated the final 5 × 5 km resolution bushmeat activities raster from the mean probability from each pixel of the ensemble model. We took the SD of each pixel as an uncertainty metric. We used Pearson correlation between the mean probability and uncertainty raster to assess collinearity between the 2 metrics. To ensure that the prediction was focused in rural areas, we masked the urban centers by using an urban built-up area raster (*29*).

Calculation of Area Associated with Bushmeat Activities

We reclassified the probability of bushmeat activities into 4 categories: very low probability (<0.2), low (0.2–0.5), intermediate (0.5–0.8), and high (>0.8). We then calculated the number of pixels per country in each category. For each country, we derived the proportion of area belonging to the high probability category by dividing the cumulative surface of those pixels by the area of the country.

Post Hoc Validation

To evaluate the added value of the bushmeat activities raster map, we used it as a covariate in 2 established infectious disease risk mapping models and measured how the performance of these models improved. We chose 2 models of EVD (*20*,*21*), a zoonotic disease known to be transmitted through bushmeat. To reproduce the models, we used the dataset, predictors, and R code (if available) from the original published articles. To ensure the same number of predictor variables were used, we ran each model twice. We first used

the MaxENT version 3.41 EVD model (*20*). We used a mask raster as the control in the first run of the MaxENT model, then compared its results with the bushmeat raster as a predictor covariate in the second run. We then used a BRT EVD model (*21*). For the first run, we used a randomly permuted bushmeat predictor as the control; for the second run, we used the extracted bushmeat covariate. We used a jackknife (leave-one-out) approach to determine the variable importance and AUC to compare the model performance without and with the bushmeat predictor layer (Appendix).

Identifying Urban Locations for Future Bushmeat Activity Surveillance

We identified 100 urban locations across the study area where we could conduct hypothetical surveys to maximize information gained from bushmeat activity surveillance. We quantified the necessity for additional surveillance (NS), a previously described measure (*30*), as the product of the uncertainty on bushmeat activity predictions and population density (Figure 2). We identified and placed a hypothetical survey on the pixel with the highest NS value, then gradually reduced NS around this first hypothetical survey by a 50-km radius (Appendix). We used the same procedure to add consecutive surveys by using the pixels with the highest NS until we identified 100 locations that could benefit from additional surveillance.

Results

We conducted a systematic literature search and identified 2,113 studies reporting bushmeat activities (Appendix). To calibrate our model, we extracted 221 unique rural locations where bushmeat activities

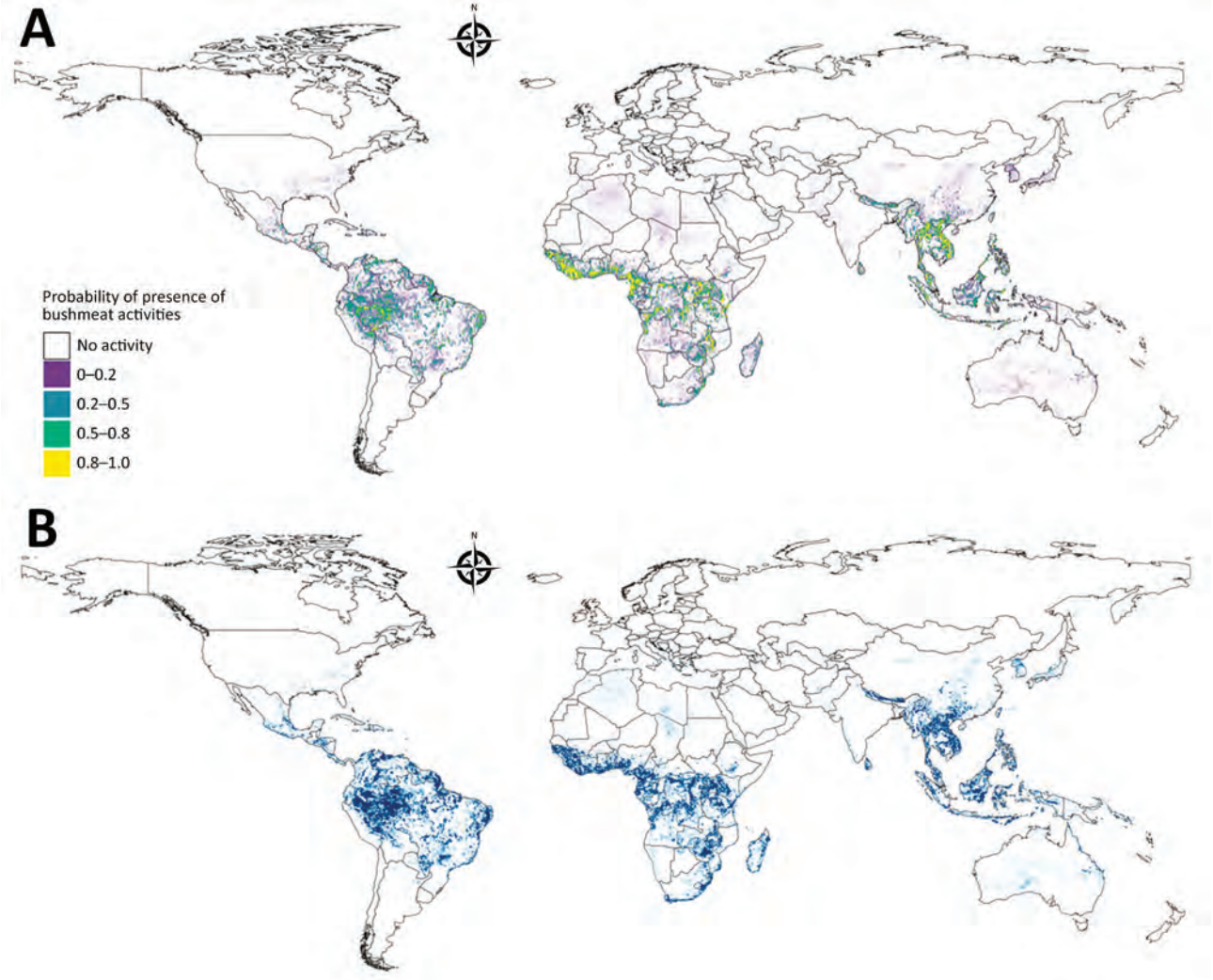

Figure 2. Model prediction and uncertainty maps for model of global bushmeat activities (hunting, preparing, and selling bushmeat) to improve zoonotic spillover surveillance. A) Distribution of bushmeat activities in the tropical and subtropical regions from an ensemble of 3 model predictions using a hierarchical binomial model with spatial autocorrelation. B) Map illustrating the uncertainty of predicted bushmeat activities represented by the SD of each pixel. Each pixel represents a 5 × 5 km area.

were reported from 76 articles (Figure 1). We extracted data on the taxonomic groups of bushmeat species from 59.2% (45/76) of the included articles. Even-toed ungulates (31%) were the most reported taxonomic group, followed by primates (28%), bats (15%), and rodents (15%) (Appendix Figure 3).

We modeled the geographic distribution of bushmeat activities by using the extracted occurrences and predictions of 3 geospatial models, RF, BRT, and BART (Figure 2). The resulting ensemble raster had a high maxTSS of 0.94 and was able to predict presence and absence of bushmeat activities. We identified an 859,765 km^2 area, a superficial area ≈3.5 times the land area of the United Kingdom, as having a high probability (0.8–1) of bushmeat activities. Globally, the 3 countries with the largest proportion of their territory associated with bushmeat activities were Equatorial Guinea, Guinea-Bissau, and Liberia (Table 1). In Asia, Laos and Vietnam had the highest risk areas. The largest region, as classified by the United Nations geoscheme (https://www.un.org/geospatial), with bushmeat activities was in Central Africa (216,863 km^2); the next highest was Southeast Asia (205,367 km^2) (Appendix Table 18).

Of the optimized RF, BRT, and BART models, the AUC and maxTSS were high and performed well against the geographic null model (average AUC 0.97 vs. 0.63; maxTSS 0.76 vs. 0.47) (Table 2). In both the RF and BRT models, the distribution of bushmeat activities was affected most by mammal richness, 42.2% in RF and 28.8% in BRT, and deforestation, 25.9% in RF and 17.2% in BRT. However, mean precipitation and mammal richness contributed most in the BART model (Appendix).

For the ensemble model, the hierarchical binomial model with iCAR performed better than the model without spatial autocorrelation and the geographic null model when we compared the deviance (Table 3). We calculated the global distribution of bushmeat activities from the mean value of the posterior distributions of probability per pixel of the ensemble model, and generated the uncertainty raster from the SD of the probability (Figure 2, panel A). We found no collinearity between the mean probability and the uncertainty per pixel (Appendix Figure 22).

We conducted a post hoc validation by assessing the added value of the resulting map on the predictive performance of 2 established Ebola risk mapping models (*21*,*22*). Despite the negligible increase (<0.01) in AUCs of models with the bushmeat raster (Table 4), using bushmeat activities as a covariate contributed greatly to the distribution of EVD (Table 4; Appendix).

We used uncertainty levels on the map to identify 100 urban locations that could most benefit from future bushmeat surveillance efforts (Figure 3). The model predicted the largest number of surveys per country for Brazil (17 surveys) and the Democratic Republic of Congo (DRC; 15 surveys), the next highest was Colombia (8 surveys). South America (34 surveys) had the highest NS compared with South Asia (1 survey) and Central America (2 surveys) (Appendix Table 19). We provide model data in GitHub (https://github.com/soushie13/Bushmeat-related_activities) (Appendix).

Discussion

We developed a global map of bushmeat activities in rural tropical and subtropical regions by using an ensemble geospatial modeling approach combined with 221 occurrence points extracted from previously published reports. The resulting map of 5 × 5 km pixels was consistent with published data on occurrence of local bushmeat activities (*16*,*17*), and with previous global mapping of efforts that focused on bushmeat hunting (*15*). We assessed the predictive capacity of our map by using 2 complementary approaches. First, we compared our model with a geographic null model, then we measured the improvement of existing risk mapping models for the occurrence of Ebola, after excluding our map in the model training

Table 1. Countries with high bushmeat activities in a study to map global bushmeat activities to improve zoonotic spillover surveillance by using geospatial modeling*

Country	Area with high probability for bushmeat activities, km^2	Land surface area, km^2	Percentage of country with high probability for bushmeat activities	Region
Equatorial Guinea	13,570	28,050	48.4	Central Africa
Guinea-Bissau	11,064	28,120	39.3	Central Africa
Liberia	28,955	96,320	30.1	West Africa
Malawi	25,498	94,280	27.0	East Africa
Sierra Leone	18,929	72,180	26.2	West Africa
Laos	49,354	230,800	21.4	Southeast Asia
Uganda	34,487	200,520	17.2	East Africa
Vietnam	48,230	310,070	15.6	Southeast Asia
Côte d'Ivoire	43,736	318,000	13.8	West Africa
Cameroon	56,355	472,710	11.9	West Africa

*High bushmeat activities (hunting, preparing, and selling bushmeat) are based on the proportion of high probability (>80%) areas in the ensemble raster.

process. Because we excluded urban areas from this study, we created an additional surveillance map to identify urban areas with the highest uncertainty of bushmeat activities and prioritized 100 urban locations for future surveillance.

Our results suggest that the largest areas associated with bushmeat activities were in Central Africa, Southeast Asia, and West Africa (Appendix Table 18). In most countries of Central Africa, the domestic livestock sector is negligible (Gabon, DRC, Congo) or limited (Cameroon, Central African Republic), leading bushmeat to be a crucial component of food security (*12*). Our results show that Equatorial Guinea in Central Africa had the highest proportion of land area associated with bushmeat activities. Equatorial Guinea is also home to the largest bushmeat market in Africa, Malabo Market on Bioko Island, where recent efforts to limit bushmeat sales through bans have been largely ineffective (*31*). Notable zoonotic diseases such as EVD and mpox have established origins from Central Africa in the 1970s and are believed to have been transmitted through bushmeat (*32*,*33*), demonstrating the significance of active surveillance of bushmeat activities in this region.

In Asia, Laos and Vietnam were the countries most associated with bushmeat activity (Table 1). A high volume of wildlife trade and established trade routes previously have been reported between Vietnam, Laos, and China (*34*,*35*). Studies have linked the origin of infectious reservoir sources of 2002–2004 SARS-CoV-1 outbreak that arrived at Guangdong markets and restaurants to Vietnam or Laos through a regional network (*36*,*37*).

Our study shows that data on bushmeat harvest in the Americas remain limited (10/76 studies included in data extraction), and only 10% of the predicted area was linked to bushmeat activities. Bushmeat commercialization was restricted to hidden markets in the Amazon Basin. Consumption in urban areas of the Americas has been unevenly studied (*12*) and is highly variable but not negligible, as previously thought because of large livestock production systems in South America (*38*,*39*). Our study also identified 34 urban sites in South America that would benefit from additional surveillance for bushmeat activities, highlighting that bushmeat activities remain underreported and understudied in that region (Figure 3).

As the risks of zoonotic spillover directly from wildlife are increasing, increased surveillance measures, including identifying and monitoring bushmeat hotspots, are urgently needed to predict spillover risk and enable early intervention (*5*,*40*). Virologic sampling and seroprevalence surveys that can be used to monitor spillover risk are costly and time consuming; thus, to optimize resources, those surveys require targeting locations where bushmeat is prevalent (*41*). Our approach to map the global distribution of bushmeat activities aims to help prioritize these efforts. Moreover, we validated this map for predicting the risk for EVD from previously established models (*20*,*21*) and found bushmeat activity was a major covariate in the distribution of EVD in Africa. Local governments and agencies could apply the necessity for additional surveillance map (Figure 3) to effectively monitor bushmeat activity sites that are often unreported, potentially unregulated, and previously unknown.

In this analysis, we used 8 environmental and demographic covariates to predict the geographic distribution of bushmeat activities. Mammal richness, deforestation, and precipitation had the greatest influence on the model distributions. Deforestation associated with development of logging roads enables easier access to the deeper forest and provides faster transportation of hunted meat to villages and towns (*42*). Control of deforestation and logging is urgently needed and could have far-reaching benefits for preventing bushmeat-associated zoonoses, as already established with EVD (*43*). In addition, studies show that precipitation effects bushmeat activities (*44*). In most areas, hunting pressure increases during the dry season when the water sources dry up, but in other areas, bushmeat hunting is preferred in periods of increased rainfall because the hunting sites become inaccessible to conservation patrols (*44*).

Table 2. Model predictive performance of a model map of global bushmeat activities to improve zoonotic spillover surveillance*

Model	AUC	maxTSS
Random forest	0.945	0.741
Boosted regression trees	0.945	0.758
Bayesian additive regression trees	0.952	0.775
Geographic null	0.633	0.472

*Predictive performance measured by AUC and maxTSS. Bushmeat activities are hunting, preparing, and selling bushmeat. AUC, area under the curve; maxTSS, maximum true skill statistic.

Table 3. Comparison of model deviance and the percentage of deviance explained by the predictor covariates for model of global bushmeat activities to improve zoonotic spillover surveillance*

Model	Deviance	% Deviance explained	Covariates
Null	1153.835	0	None
Binomial	373.936	85	3 metacovariates†
Binomial iCAR	235.874	100	Addition of spatial autocorrelation

*Bushmeat activities are hunting, preparing, and selling bushmeat. iCAR, intrinsic conditional autoregressive.
†Covariates included random forest, boosted regression tree, and Bayesian additive regression tree.

Table 4. Comparison performance for a map of global bushmeat activities to improve zoonotic spillover surveillance*

Model	Area under the curve		% Relative contribution of bushmeat activity
	Without bushmeat activity raster	With bushmeat activity raster	
EVD MaxENT	0.893	0.899	44.23
EVD BRT	0.880	0.887	17.06

*We compared area under the curve with and without bushmeat activities (hunting, preparing, and selling bushmeat) as predictor variable for EVD. BRT, boosted regression tree; EVD, Ebola virus disease.

The first limitation of our study is that data on geographic sites of bushmeat hunting and selling are limited. Collecting reliable information on bushmeat-related activities is challenging because many species are protected under national laws, deterring informants from discussing their involvement to avoid incriminating themselves (*45*). Second, we did not independently collect data for this analysis, but that limitation is inherent to any modeling study attempting to map burden or risk by using passive surveillance data. Third, restriction of the spatial extent of the study area to the tropical and subtropical parts of the world might be considered an implicit bias; however, our intent was to focus on these regions as per the definition of bushmeat (*1*). Fourth, we did not quantify the distribution of zoonotic risk based on the taxonomic group of the mammal reservoir species as in other studies (*46*,*47*). However, the data we extracted from the literature search were insufficient to categorize the bushmeat by taxonomic groups because the species of bushmeat hunted was not consistently mentioned in the studies (*45*). Finally, we chose to exclude the urban sites for model calibration because they contained few locations (28 sites) with geographic coordinates of wet markets and chop shops, because different covariates may be associated with bushmeat activities between urban and rural sites, and because of overestimation of model prediction based on population density. However, we mitigated the exclusion of the urban sites by developing the necessity for additional surveillance map that detects urban areas that would benefit from future surveillance efforts (Figure 3; Appendix Table 19). A limitation of this map is that it is dependent on a single demographic variable, population density, and does not consider other factors, such as accessibility to the nearest city of population size.

Although geographic bushmeat data are limited, we attempted to characterize the distribution of bushmeat activities at a global scale to help identify priorities for action. Our study illustrates how environmental covariates, such as mammal richness, deforestation, and precipitation, affect bushmeat activities. Our findings highlight the increased need for conservation efforts, including prevention of habitat fragmentation and action against climate change. In addition to driving the bushmeat crisis, those factors also play a major role in the transmission of zoonoses (*48*).

In conclusion, our findings contribute to the modeling and prediction of emerging zoonoses at global scale. The modeled findings can help target surveillance of bushmeat and bushmeat-related zoonotic spillovers by local reference laboratories established

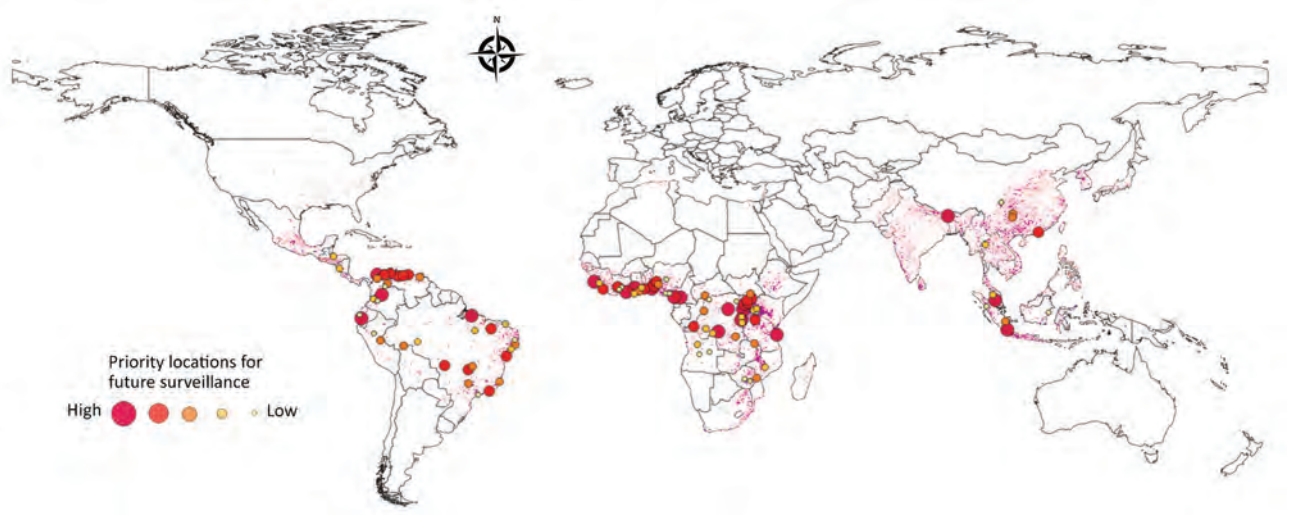

Figure 3. Predicted priority regions for future survey efforts in urban areas as determined by a model of global bushmeat activities (hunting, preparing, and selling bushmeat) to improve zoonotic spillover surveillance. The 100 priority locations identified are indicated by the necessity for surveillance, a previously described measure (*30*). Color and size and color of the dots indicate high to low priority on the background of the necessity for surveillance, a previously described measure (*30*).

by the World Organization for Animal Health (*49*) and global outbreak prevention and preparedness initiatives like the Global Health Security Agenda (*50*). Our efforts to geographically synthesize bushmeat-related data could help prioritize future surveillance of bushmeat activities and forecast emerging zoonoses at a global scale.

Acknowledgments

We thank David Pigott and Nick Golding for sharing data and code to reproduce their models.

S.J. was supported by the NRP78 program for the Swiss National Science Foundation (grant no. 4078P0_198428); C.Z. was supported by the Branco Weiss Foundation; R.M. was supported by the EU Horizon 2020 grant for MOOD (grant no. 874850); and T.P.V.B. was supported by the Eccellenza Fellowship of the Swiss National Science Foundation (grant no. PCEFP3_181248).

About the Author

Dr. Jagadesh is a postdoctoral researcher at Eidgenössische Technische Hochschule Zürich, Zürich, Switzerland. Her primary research interests include spatial modeling of zoonoses and emerging infectious diseases.

References

1. Milner-Gulland EJ, Bennett EL. Wild meat: the bigger picture. Trends Ecol Evol. 2003;18:351–7. https://doi.org/10.1016/S0169-5347(03)00123-X
2. Bar-On YM, Phillips R, Milo R. The biomass distribution on Earth. Proc Natl Acad Sci U S A. 2018;115:6506–11. https://doi.org/10.1073/pnas.1711842115
3. Jones KE, Patel NG, Levy MA, Storeygard A, Balk D, Gittleman JL, et al. Global trends in emerging infectious diseases. Nature. 2008;451:990–3. https://doi.org/10.1007/978-3-540-70962-6_5
4. Cleaveland S, Haydon DT, Taylor L. Overviews of pathogen emergence: which pathogens emerge, when and why? Curr Top Microbiol Immunol. 2007;315:85–111. https://doi.org/10.1038/nature06536
5. Milbank C, Vira B. Wildmeat consumption and zoonotic spillover: contextualising disease emergence and policy responses. Lancet Planet Health. 2022;6:e439–48. https://doi.org/10.1016/S2542-5196(22)00064-X
6. Plowright RK, Parrish CR, McCallum H, Hudson PJ, Ko AI, Graham AL, et al. Pathways to zoonotic spillover. Nat Rev Microbiol. 2017;15:502–10. https://doi.org/10.1038/nrmicro.2017.45
7. Georges-Courbot MC, Sanchez A, Lu CY, Baize S, Leroy E, Lansout-Soukate J, et al. Isolation and phylogenetic characterization of Ebola viruses causing different outbreaks in Gabon. Emerg Infect Dis. 1997;3:59–62. https://doi.org/10.3201/eid0301.970107
8. Leroy EM, Rouquet P, Formenty P, Souquière S, Kilbourne A, Froment JM, et al. Multiple Ebola virus transmission events and rapid decline of central African wildlife. Science. 2004;303:387–90. https://doi.org/10.1126/science.1092528
9. Coad L, Abernethy K, Balmford A, Manica A, Airey L, Milner-Gulland EJ. Distribution and use of income from bushmeat in a rural village, central Gabon. Conserv Biol. 2010;24:1510–8. https://doi.org/10.1111/j.1523-1739.2010.01525.x
10. Schulte-Herbrüggen B, Cowlishaw G, Homewood K, Rowcliffe JM. The importance of bushmeat in the livelihoods of West African cash-crop farmers living in a faunally-depleted landscape. PLoS One. 2013;8:e72807. https://doi.org/10.1371/journal.pone.0072807
11. Martins V, Shackleton CM. Bushmeat use is widespread but under-researched in rural communities of South Africa. Glob Ecol Conserv. 2019;17:e00583. https://doi.org/10.1016/j.gecco.2019.e00583
12. Nasi R, Taber A, Van Vliet N. Empty forests, empty stomachs? Bushmeat and livelihoods in the Congo and Amazon Basins. Int For Rev. 2011;13:355–68. https://doi.org/10.1505/146554811798293872
13. Zhou W, Orrick K, Lim A, Dove M. Reframing conservation and development perspectives on bushmeat. Environ Res Lett. 2022;17:011001. https://doi.org/10.1088/1748-9326/ac3db1
14. Friant S, Ayambem WA, Alobi AO, Ifebueme NM, Otukpa OM, Ogar DA, et al. Eating bushmeat improves food security in a biodiversity and infectious disease "hotspot". EcoHealth. 2020;17:125–38. https://doi.org/10.1007/s10393-020-01473-0
15. Ripple WJ, Abernethy K, Betts MG, Chapron G, Dirzo R, Galetti M, et al. Bushmeat hunting and extinction risk to the world's mammals. R Soc Open Sci. 2016;3:160498. https://doi.org/10.1098/rsos.160498
16. Fa JE, Wright JH, Funk SM, Márquez AL, Olivero J, Farfán MÁ, et al. Mapping the availability of bushmeat for consumption in Central African cities. Environ Res Lett. 2019;14:094002. https://doi.org/10.1088/1748-9326/ab36fa
17. Deith MCM, Brodie JF. Predicting defaunation: accurately mapping bushmeat hunting pressure over large areas. Proc Biol Sci. 2020;287(1922):20192677. https://doi.org/10.1098/rspb.2019.2677
18. Brashares JS, Golden CD, Weinbaum KZ, Barrett CB, Okello GV. Economic and geographic drivers of wildlife consumption in rural Africa. Proc Natl Acad Sci U S A. 2011;108:13931–6. https://doi.org/10.1073/pnas.1011526108
19. Cawthorn DM, Hoffman LC. The bushmeat and food security nexus: A global account of the contributions, conundrums and ethical collisions. Food Res Int. 2015;76:906–25. https://doi.org/10.1016/j.foodres.2015.03.025
20. Nyakarahuka L, Ayebare S, Mosomtai G, Kankya C, Lutwama J, Mwiine FN, et al. Ecological niche modeling for filoviruses: a risk map for Ebola and Marburg virus disease outbreaks in Uganda. PLoS Curr. 2017;9:ecurrents.outbreaks.07992a87522e1f229c7cb023270a2af1. https://doi.org/10.1371/currents.outbreaks.07992a87522e1f229c7cb023270a2af1
21. Pigott DM, Golding N, Mylne A, Huang Z, Henry AJ, Weiss DJ, et al. Mapping the zoonotic niche of Ebola virus disease in Africa. eLife. 2014;3:e04395–e04395. https://doi.org/10.7554/eLife.04395
22. International Union for Conservation of Nature and Natural Resources. IUCN red list of threatened species [cited 2022 Mar 30]. https://www.iucnredlist.org
23. Marcoulides KM, Raykov T. Evaluation of variance inflation factors in regression models using latent variable modeling methods. Educ Psychol Meas. 2019;79:874–82. https://doi.org/10.1177/0013164418817803

24. Phillips SJ, Dudík M, Elith J, Graham CH, Lehmann A, Leathwick J, et al. Sample selection bias and presence-only distribution models: implications for background and pseudo-absence data. Ecol Appl. 2009;19:181–97. https://doi.org/10.1890/07-2153.1
25. Vignali S, Barras AG, Arlettaz R, Braunisch V. SDMtune: An R package to tune and evaluate species distribution models. Ecol Evol. 2020;10:11488–506. https://doi.org/10.1002/ece3.6786
26. Valavi R, Elith J, Lahoz-Monfort JJ, Guillera-Arroita G. blockCV: An r package for generating spatially or environmentally separated folds for k-fold cross-validation of species distribution models. Methods Ecol Evol. 2019;10:225–32. https://doi.org/10.1111/2041-210X.13107
27. Raes N, ter Steege H. A null-model for significance testing of presence-only species distribution models. Ecography. 2007;30:727–36. https://doi.org/10.1111/j.2007.0906-7590.05041.x
28. Vieilledent G, Merow C, Guélat J, Latimer A, Kéry M, Gelfand AE, et al. hSDM: hierarchical Bayesian species distribution models [cited 2022 May 10]. https://cran.r-project.org/web/packages/hSDM/index.html
29. Joint Research Centre European Commission; Center for International Earth Science Information Network Columbia University. Global human settlement layer: population and built-up estimates, and degree of urbanization settlement model grid. Palisades (NY): NASA Socioeconomic Data and Applications Center (SEDAC); 2021 [cited 2022 May 10]. https://doi.org/10.7927/h4154f0w
30. Zhao C, Wang Y, Tiseo K, Pires J, Criscuolo NG, Van Boeckel TP. Geographically targeted surveillance of livestock could help prioritize intervention against antimicrobial resistance in China. Nature Food. 2021;2:596–602. https://doi.org/10.1038/s43016-021-00320-x
31. Cronin DT, Woloszynek S, Morra WA, Honarvar S, Linder JM, Gonder MK, et al. Long-term urban market dynamics reveal increased bushmeat carcass volume despite economic growth and proactive environmental legislation on Bioko Island, Equatorial Guinea. PLoS One. 2015;10:e0134464. https://doi.org/10.1371/journal.pone.0134464
32. Breman JG, Heymann DL, Lloyd G, McCormick JB, Miatudila M, Murphy FA, et al. Discovery and description of Ebola Zaire virus in 1976 and relevance to the West African epidemic during 2013–2016. J Infect Dis. 2016;214(suppl 3):S93–101. https://doi.org/10.1093/infdis/jiw207
33. Rezza G. Emergence of human monkeypox in west Africa. Lancet Infect Dis. 2019;19:797–9. https://doi.org/10.1016/S1473-3099(19)30281-6
34. Jiao Y, Yeophantong P, Lee TM. Strengthening international legal cooperation to combat the illegal wildlife trade between Southeast Asia and China. Front Ecol Evol. 2021;9:645427. https://doi.org/10.3389/fevo.2021.645427
35. Lee TM, Sigouin A, Pinedo-Vasquez M, Nasi R. The harvest of wildlife for bushmeat and traditional medicine in East, South and Southeast Asia: current knowledge base, challenges, opportunities and areas for future research. Center for International Forestry Research (CIFOR); 2014 [cited 2022 May 21]. https://doi.org/10.17528/cifor/005135
36. Bell D, Roberton S, Hunter PR. Animal origins of SARS coronavirus: possible links with the international trade in small carnivores. Philos Trans R Soc Lond B Biol Sci. 2004;359:1107–14. https://doi.org/10.1098/rstb.2004.1492
37. Centers for Disease Control and Prevention. Prevalence of IgG antibody to SARS-associated coronavirus in animal traders—Guangdong Province, China, 2003. MMWR Morb Mortal Wkly Rep. 2003;52:986–7.
38. van Vliet N, Quiceno MP, Cruz D, de Aquino LJN, Yagüe B, Schor T, et al. Bushmeat networks link the forest to urban areas in the Trifrontier region between Brazil, Colombia, and Peru. Ecol Soc. 2015;20:art21. https://doi.org/10.5751/ES-07782-200321
39. Rushton J, Viscarra R, Viscarra C, Basset F, Baptista R, Brown D. How important is bushmeat consumption in South America: now and in the future? ODI Wildlife Policy Briefings. 2005;11:1–4.
40. Kurpiers LA, Schulte-Herbrüggen B, Ejotre I, Reeder DM. Bushmeat and emerging infectious diseases: lessons from Africa. In: Angelici FM, editor. Problematic wildlife: a cross-disciplinary approach. Cham: Springer International Publishing; 2016. p. 507–51 [cited 2022 May 12]. https://doi.org/10.1007/978-3-319-22246-2_24
41. Mulangu S, Borchert M, Paweska J, Tshomba A, Afounde A, Kulidri A, et al. High prevalence of IgG antibodies to Ebola virus in the Efé pygmy population in the Watsa region, Democratic Republic of the Congo. BMC Infect Dis. 2016;16:263. https://doi.org/10.1186/s12879-016-1607-y
42. Mayor P, Pérez-Peña P, Bowler M, Puertas PE, Kirkland M, Bodmer R. Effects of selective logging on large mammal populations in a remote indigenous territory in the northern Peruvian Amazon. Ecol Soc. 2015;20:art36. https://doi.org/10.5751/ES-08023-200436
43. Olivero J, Fa JE, Real R, Márquez AL, Farfán MA, Vargas JM, et al. Recent loss of closed forests is associated with Ebola virus disease outbreaks. Sci Rep. 2017;7:14291. https://doi.org/10.1038/s41598-017-14727-9
44. Martin A, Caro T, Mulder MB. Bushmeat consumption in western Tanzania: a comparative analysis from the same ecosystem. Trop Conserv Sci. 2012;5:352–64. https://doi.org/10.1177/194008291200500309
45. St. John FAV, Edwards-Jones G, Gibbons JM, Jones JPG. Testing novel methods for assessing rule breaking in conservation. Biol Conserv. 2010;143:1025–30. https://doi.org/10.1016/j.biocon.2010.01.018
46. Brierley L, Vonhof MJ, Olival KJ, Daszak P, Jones KE. Quantifying global drivers of zoonotic bat viruses: a process-based perspective. Am Nat. 2016;187:E53–64. https://doi.org/10.1086/684391
47. Olival KJ, Hosseini PR, Zambrana-Torrelio C, Ross N, Bogich TL, Daszak P. Host and viral traits predict zoonotic spillover from mammals. Nature. 2017;546:646–50. https://doi.org/10.1038/nature22975
48. Loh EH, Zambrana-Torrelio C, Olival KJ, Bogich TL, Johnson CK, Mazet JAK, et al. Targeting transmission pathways for emerging zoonotic disease surveillance and control. Vector Borne Zoonotic Dis. 2015;15:432–7. https://doi.org/10.1089/vbz.2013.1563
49. Caceres P, Awada L, Barboza P, Lopez-Gatell H, Tizzani P. The World Organisation for Animal Health and the World Health Organization: intergovernmental disease information and reporting systems and their role in early warning. Rev Sci Tech. 2017;36:539–48. https://doi.org/10.20506/rst.36.2.2672
50. Belay ED, Kile JC, Hall AJ, Barton-Behravesh C, Parsons MB, Salyer S, et al. Zoonotic disease programs for enhancing global health security. Emerg Infect Dis. 2017;23(Suppl 1):S65–70. https://doi.org/10.3201/eid2313.170544

Address for correspondence: Soushieta Jagadesh, Eidgenössische Technische Hochschule Zürich, Sonneggstrasse 33, Zurich 8092, Switzerland; email: soushieta.jagadesh@usys.ethz.ch and thomas.van.boeckel@gmail.com

Adeno-Associated Virus 2 and Human Adenovirus F41 in Wastewater during Outbreak of Severe Acute Hepatitis in Children, Ireland

Niamh A. Martin, Gabriel Gonzalez, Liam J. Reynolds, Charlene Bennett, Christine Campbell, Tristan M. Nolan, Alannah Byrne, Sanne Fennema, Niamh Holohan, Sailusha Ratnam Kuntamukkula, Natasha Sarwar, Laura Sala-Comorera, Jonathan Dean, Jose Maria Urtasun-Elizari, Daniel Hare, Emer Liddy, Eadaoin Joyce, John J. O'Sullivan, John M. Cuddihy, Angeline M. McIntyre, Eve P. Robinson, Darren Dahly, Nicola F. Fletcher, Suzanne Cotter, Emer Fitzpatrick, Michael J. Carr, Cillian F. De Gascun, Wim G. Meijer

During April–July 2022, outbreaks of severe acute hepatitis of unknown etiology (SAHUE) were reported in 35 countries. Five percent of cases required liver transplantation, and 22 patients died. Viral metagenomic studies of clinical samples from SAHUE cases showed a correlation with human adenovirus F type 41 (HAdV-F41) and adeno-associated virus type 2 (AAV2). To explore the association between those DNA viruses and SAHUE in children in Ireland, we quantified HAdV-F41 and AAV2 in samples collected from a wastewater treatment plant serving 40% of Ireland's population. We noted a high correlation between HAdV-F41 and AAV2 circulation in the community and SAHUE clinical cases. Next-generation sequencing of the adenovirus hexon in wastewater demonstrated HAdV-F41 was the predominant HAdV type circulating. Our environmental analysis showed increased HAdV-F41 and AAV2 prevalence in the community during the SAHUE outbreak. Our findings highlight how wastewater sampling could aid in surveillance for respiratory adenovirus species.

During April 5–July 8, 2022, the World Health Organization (WHO) received reports of 1,010 probable cases of severe acute hepatitis of unknown etiology (SAHUE) in young children from 35 countries (*1*). Many cases resulted in severe clinical outcomes; ≈5% of patients required liver transplants, and 22 died. Most (48%) cases were reported from the WHO European Region, and 484 cases were reported in previously healthy children from 21 countries (*1*). Ireland reported 28 probable cases of SAHUE in non-A–E hepatitis, including 2 patients who received liver transplants and 1 who died but did not receive a transplant (*2*).

The causes of SAHUE remain unclear. A possible connection with SARS-CoV-2 has been suggested (*3*), but SARS-CoV-2 RNA was detected in only 16% of SAHUE cases reported in the WHO European Region (*1*). Recent studies suggest a possible association between SAHUE and human adenovirus (HAdV) species F type 41 (HAdV-F41) and adeno-associated virus 2 (AAV2) infections (*4*,*5*; A. Ho et al., unpub. data, https://doi.org/10.1101/2022.07.19.22277425).

HAdVs are double-stranded DNA viruses that cause a wide range of self-limiting illnesses, including upper respiratory infections, conjunctivitis, and gastroenteritis. HAdV infections are particularly common in children because of a lack of humoral

Author affiliations: University College Dublin, Dublin, Ireland (N.A. Martin, G. Gonzalez, L.J. Reynolds, C. Bennett, C. Campbell, T.M. Nolan, A. Byrne, S. Fennema, N. Holohan, S.R. Kuntamukkula, N. Sarwar, L. Sala-Comorera, J. Dean, J.M. Urtasun-Elizari, D. Hare, J.J. O'Sullivan, N.F. Fletcher, M.J. Carr, C.F. De Gascun, W.G. Meijer); Hokkaido University, Sapporo, Japan (G. Gonzalez, M.J. Carr); Health Protection Surveillance Centre, Dublin, Ireland (E. Liddy, J.M. Cuddihy, A.M McIntyre, E.P. Robinson, S. Cotter); Irish Water, Dublin, Ireland (E. Joyce); University College Cork, Cork, Ireland (D. Dahly); Children's Health Ireland at Crumlin, Crumlin, Ireland (E. Fitzpatrick)

DOI: https://doi.org/10.3201/eid2904.221878

immunity, and rare manifestations of HAdV illnesses involving hepatitis and liver failure have been reported, mainly in immunocompromised patients (*6*). To date, HAdV is the most frequently detected pathogen (52%) among SAHUE cases where data are available in Europe (*1*). Furthermore, clinical signs and symptoms of SAHUE can occur several weeks after an acute gastrointestinal episode (A. Ho et al., unpub. data). HAdV-F41 and HAdV-F40 are leading causes of diarrhea worldwide, behind only rotavirus (*7*,*8*). Phylogenetic analysis of specimens taken from SAHUE patients in the United States identified 3 distinct enteric HAdV-F41 variants (*4*). In Europe, HAdV-F41 was also identified in SAHUE cases where sequencing data were available (*1*).

In addition, 2 independent studies in the United Kingdom, identified AAV2 from probable cases (A. Ho et al., unpub. data; S. Morfopoulou et al., unpub. data, https://doi.org/10.1101/2022.07.28.22277963). High detection rates of AAV2 DNA have been reported in whole blood, plasma, and explanted liver tissue in SAHUE cases and, of note, AAV2 was not detected in controls of HAdV-negative and severe hepatitis cases not meeting the SAHUE case definition (A. Ho et al., unpub. data; S. Morfopoulou et al., unpub. data). AAV2 possesses a single-stranded DNA genome of 4.7 kb and requires co-infection with a helper virus, most frequently HAdV but also human herpesvirus (e.g., HHV-6/7) or human papillomavirus, to enable productive replication. AAVs are not known to be associated with human pathology and are intensively studied as gene-delivery vectors although transient hepatitis has been reported in clinical trials (*9*). Subclinical seroconversion occurs early in life, and >90% of adults have antibodies to AAV, showing that the virus is common and widely distributed (*10*,*11*).

AAV2 could represent the primary pathogen in SAHUE cases or serve as a valuable biomarker for HAdV infection (A. Ho et al., unpub. data). Alternatively, the pathology of SAHUE could be the result of co-infection with HAdV-F41 and AAV2, where AAV2 might replicate within HAdV-F41–infected cells outside the liver before causing an abortive infection of hepatocytes (*12*). A recent study identified a possible immunogenetic association on the basis of high frequency of the class II HLA-DRB1*04:01 allele associated with the UK SAHUE cases (A. Ho et al., unpub. data). This allele is more frequently detected in populations in northwestern Europe (*13*), suggesting that children in Ireland could be particularly vulnerable to SAHUE. Nonetheless, because the precise cause of this outbreak has not been identified, monitoring for changes in the prevalence of potential pathogens in the community is increasingly pertinent. Studies have shown that HAdV and AAV2 are detectable in stool samples from persons infected with those viruses (*14*,*15*), suggesting that both viruses could be quantified by using wastewater surveillance.

Wastewater-based epidemiology is a valuable tool for monitoring the prevalence of viral pathogens circulating at the population level (*16*,*17*). During the COVID-19 pandemic, wastewater-based surveillance proved to be an efficient tool for monitoring SARS-CoV-2 infections and identifying circulating variants of concern in Ireland and elsewhere (*18*–*20*). A recent study reported SAHUE clinical cases increased concomitant with an increase the levels of HAdV-F40 and HAdV-F41 detected in wastewater in Northern Ireland (*21*). We hypothesized that HAdV-F and AAV2 could be directly or indirectly associated with the SAHUE outbreak; thus, levels of these viruses in wastewater should positively correlate with the onset of the SAHUE outbreak. We used molecular approaches and next-generation sequencing (NGS) to quantify HAdV-F, AAV2, and SARS-CoV-2 in wastewater and identify HAdV types circulating before and during the peak of SAHUE cases in Ireland.

Materials and Methods

Wastewater Sample Collection and Concentration

The Ringsend Wastewater Treatment Plant (WWTP) in Dublin, Ireland, has a capacity of 1.98 million population equivalents and serves the greater Dublin area, which is home to ≈40% of the population of Ireland. Eighty-five 24-hour composite wastewater samples were collected during June 2020–August 2022 and concentrated as previously described (*18*).

Nucleic Acid Extraction

We extracted DNA and RNA from 250 µL of wastewater concentrate by using QIAcube Connect (QIAGEN, https://www.qiagen.com). We used the DNeasy PowerSoil Pro Kit (QIAGEN) to extract DNA, and the RNeasy PowerMicrobiome Kit (QIAGEN) to extract RNA, according to the manufacturer's guidelines.

PCR Quantification of HAdV-F and SARS-CoV-2 in Wastewater

We used TaqMan probe assays and conducted quantitative PCR (qPCR) on the Lightcycler 96 platform (Roche Diagnostics, https://www.roche.com) to quantify DNA from HAdV-F and the human biomarker crAss_2 DNA in wastewater. We selected the HAdV-F species assay to specifically detect HAdV-F40 and HAdV-F41 serotypes by targeting the long-fiber

coding gene (*22*). We quantified the crAss_2 bacteriophage as a DNA extraction control in all samples (*23*). We conducted amplification by using FastStart Essential DNA Probes Master (Roche Diagnostics) in a total volume of 20 µL according to manufacturer's recommendations. We quantified SARS-CoV-2 RNA on the same platform by using LightCycler Multiplex RNA Virus Master (Roche Diagnostics) for reverse transcription qPCR (qRT-PCR), as previously published (*18*). We analyzed all samples in triplicate along with positive and negative controls. We quantified gene targets by a standard curve, which we generated by using a 10-fold serial dilution of gBlock Gene Fragment (Integrated DNA Technologies, https://www.idtdna.com) for the HAdV-F assay (*22*) and targeting HAdV-F41 (GenBank accession no. AB728839), and the control plasmid for the SARS-CoV-2 nucleocapsid 1 (N1) assay from the US Centers for Disease Control and Prevention (*24*,*25*). We provide information on thermocycler conditions and final oligonucleotide primer and probe concentrations (Appendix Table 1, https://wwwnc.cdc.gov/EID/article/29/4/22-1878-App1.pdf).

Digital PCR Quantification of AAV2 in Wastewater

We quantified AAV2 DNA in wastewater by using digital PCR (dPCR) on the QIAcuity Four Platform System (QIAGEN) by using 2 separate assays targeting the capsid protein viral protein (VP) 1 and nonstructural protein (NSP) genes (Appendix Table 1). We analyzed samples in duplicate on 26K 24-well Nanoplates (QIAGEN) by using the QIAcuity OneStep Advanced Probe Kit (QIAGEN). We conducted amplification in 40 µL reactions containing 5 µL DNA template and 10 µL master mix (Appendix Table 1). We included positive and negative controls on each nanoplate to determine the fluorescence intensity threshold (Appendix Figure 1). We used AAV2-positive samples as positive controls and nuclease-free water as a negative control. We analyzed results by using QIAcuity Suite software version 2.1 (QIAGEN).

Nanopore Sequencing of the HAdV Hexon from Wastewater

We further analyzed 12 wastewater samples and 1 clinical stool sample from an HAdV-F41 gastrointestinal case by targeting an ≈800-bp subgenomic fragment from the HAdV hexon-coding gene, which contains type-specific epitopes within variable loop 1, which enables molecular typing. We amplified the fragments by using an established pan-adenovirus endpoint PCR (*26*) and deep sequenced amplicons by using the GridION nanopore device (Oxford Nanopore Technologies, https://nanoporetech.com) on genomic DNA by using the Ligation Sequencing Kit (Oxford Nanopore Technologies) and Native Barcodes (Oxford Nanopore Technologies) (Appendix). We published the raw sequence data in the National Center for Biotechnology Information Sequence Reads Archive (https://www.ncbi.nlm.nih.gov/sra) under BioProject no. PRJNA885073.

Sequence Analysis

We assessed HAdV types in each sample by aligning the reads against a database of hexon proteins of known types by using Diamond version 2.0.14.152 (*27*) (Appendix Table 2). We used genome sequences from the most frequently aligned types (>5% of reads per sample) as references to assemble consensus sequences for the target fragment by using minimap2 version 2.23 (*28*) and polished contig sequences by using medaka version 1.5.0 (Oxford Nanopore Technologies). We used MAFFT (*29*) for multiple sequence alignment of consensus sequences and refer-

Table 1. Clinicodemographic characteristics of probable SAHUE cases in children during time in which AAV2 and HAdV-F41 were detected in wastewater, Ireland*

Characteristics	No. (%) cases
Age, y	
<1	2
1–4	15
5–11	10
12–16	1
Sex	
M	13
F	15
Ethnicity	
White Irish	27
Other	1
Liver transplant	
Y	2
N	26
International travel	
Y	6
N	18
Unknown	4
SARS-CoV-2 vaccination status	
Vaccinated	2
Unvaccinated	19
Unknown	7
Hospitalization status	
Non-ICU	21
ICU	6
Not hospitalized	1
Positive cases	
HAdV	27 (52)
AAV2	22 (63.6)
SARS-CoV-2†	25 (60)

*Information obtained from Health Protection Surveillance Centre public website on September 23, 2022 (https://www.hpsc.ie/a-z/hepatitis/acutehepatitisofunknownaetiology/title-22079-en.html). AAV2, adeno-associated virus type 2; HAdV, human adenovirus; HAdV-F41, human adenovirus type F41; ICU, intensive care unit; SAHUE, severe acute hepatitis of unknown etiology.
†Positive for SARS-CoV-2 antibodies.

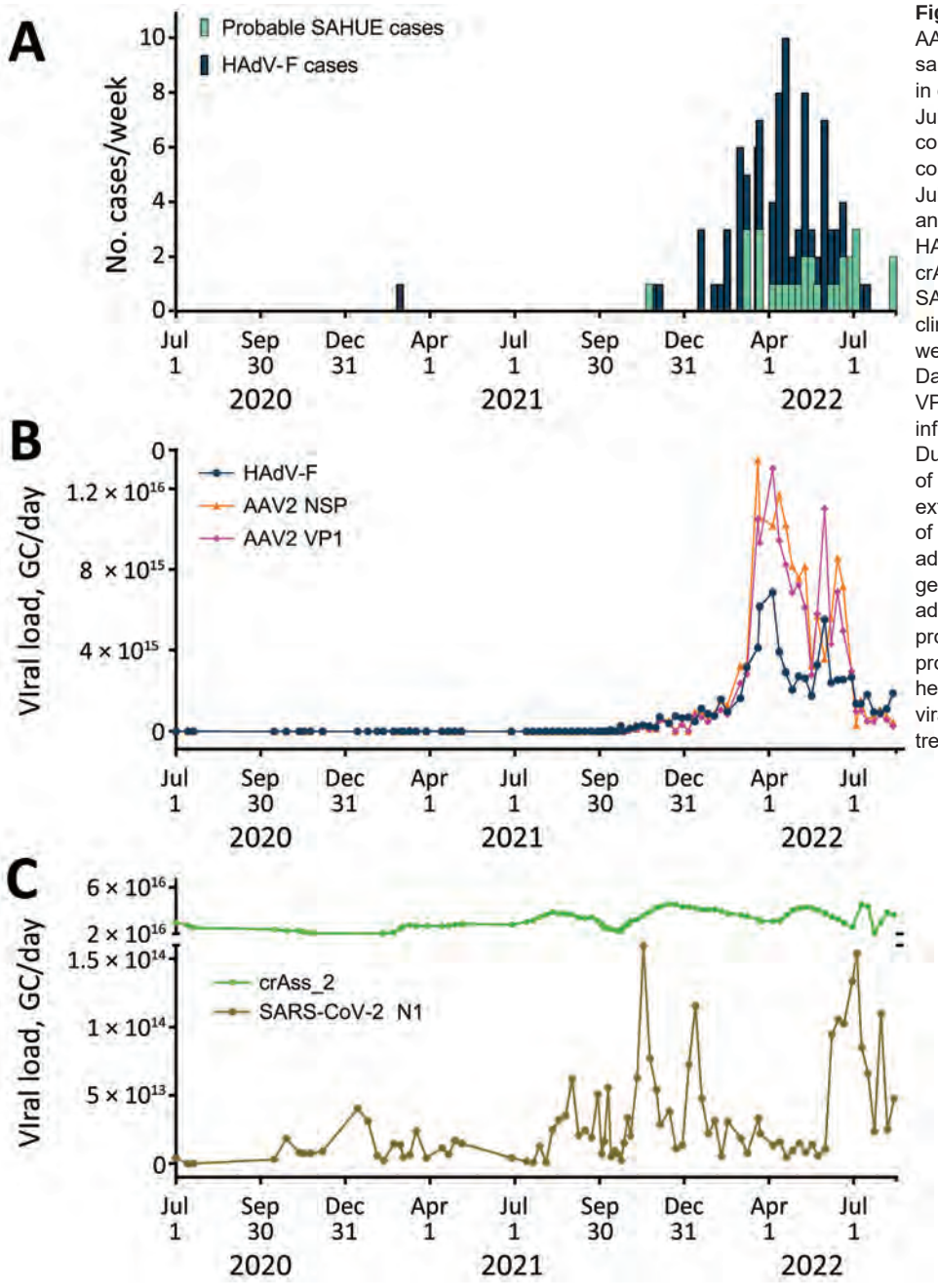

Figure 1. Relationship between AAV2 and HAdV-F in wastewater samples and SAHUE clinical cases in children, Ireland, July 1, 2020–July 30, 2022. Eighty-five 24-h composite wastewater samples collected during July 1, 2020–July 30, 2022, were retroactively analyzed for SARS-CoV-2, AAV2, HAdV-F, and the human biomarker crAss-2. A) Number of probable SAHUE cases and HAdV-F–positive clinical samples reported per week during the study period. B) Daily viral load of HAdV-F, AAV2 VP1, and AAV2 NSP detected in influent of the Ringsend WWTP, Dublin, Ireland. C) Daily viral load of SARS-CoV-2 RNA N1 and DNA extraction crAss_2 control in influent of the Ringsend WWTP. AAV2, adeno-associated virus type 2; GC, genome copies; HAdV-F, human adenovirus type F; N1, nucleocapsid protein 1; NSP, nonstructural protein; SAHUE, severe acute hepatitis of unknown etiology; VP, viral protein; WWTP, wastewater treatment plant.

ence sequences. We inferred a phylogenetic tree by using RAxML (*30*) and estimated topology support by using a bootstrap approach with 100 repetitions. In addition, we assessed detectable SNPs in each sample by using loFreq version 2 (*31*). We deposited the assembled sequences in GenBank (accession nos. OP554817–910).

Clinical Data

We obtained publicly available SAHUE probable case data from the Health Protection Surveillance Centre (HPSC) via an HPSC report on acute hepatitis of unknown etiology (*2*). The HPSC defined probable cases as cases in persons ≤16 years of age with signs and symptoms of SAHUE, including acute hepatitis of unknown etiology (non–hepatitis A–E) with no other likely cause identified, and with serum transaminases (aspartate transaminase or alanine aminotransferase) >500 U/L, who were identified after October 1, 2021 and notified under Infectious Disease (Amendment) (No. 3) Regulations 2003 (regulation 14) (*32*). The National Virus Reference Laboratory provided clinical

data from all HAdV-F–positive cases tested as part of routine gastroenteritis screening during July 2020–July 2022. Routine screening is conducted on all samples received from persons with viral gastrointestinal symptoms. Routine screening is standard in Ireland and is applied to all age groups but predominantly represents pediatric gastrointestinal cases.

Data Analysis

We determined the daily HAdV-F, AAV2, SARS-CoV-2, and crAssphage load flowing through the Ringsend WWTP by using the concentration of each viral marker in genome copies per 100 milliliter (GC/100 mL) and the daily WWTP flow rate of cubic meters per second (m^3/s); thus, flow rate (m^3/day) × GC/100 mL × 10^4 = GC/day. Irish Water (https://www.water.ie) provided WWTP flow rate data. We used $\log_{10}$ transformed qPCR and dPCR data and Spearman correlation (r_s) analysis on Prism 9.4.1 (GraphPad Software Inc., https://www.graphpad.com) to examine the correlation between variables over time and considered $p \leq 0.001$ statistically significant.

Results

SAHUE Clinical and Demographic Data

During October 2021–August 2022, Ireland reported 28 probable SAHUE cases in children ≤12 years of age (Table 1). Among case-patients, 1 death and 2 liver transplants were reported for 3 patients. Overall, 52% (14/27) of tested patients had evidence of HAdV infection and 63.6% (14/22) had evidence of AAV2 infection. Among 25 case-patients tested, 15 (60%) had reports of current or past SARS-CoV-2 infection (*2*).

HAdV-F and AAV2 Wastewater Surveillance Over Time

We retrospectively screened 85 wastewater samples to determine HAdV-F and AAV2 viral load in wastewater in the greater Dublin area during June 2020–August 2022. We detected HAdV-F in wastewater collected on October 13, 2021, at 7.6 × 10^{13} GC/day. HAdV-F levels remained low, but on April 6, 2022, levels increased by 2 orders of magnitude and peaked at 6.86 × 10^{15} GC/day. Of note, AAV2 followed a similar trend, also peaking on April 6, 2022, for VP1 at 1.3 × 10^{16} GC/day; NSP peaked on March 21, 2022, at 1.34 × 10^{16} GC/day (Figure 1, panel B). HAdV-F levels in wastewater significantly correlated with both AAV2 VP1 (r_s = 0.91; p = 0) and NSP (r_s = 0.88; p = 0) genes in wastewater (Figure 2).

The daily concentration of SARS-CoV-2 RNA was quantified in wastewater throughout the sampling period (*18*). SARS-CoV-2 levels in wastewater fluctuated over time, peaking in November 2021 and January 2022, during the 4th and 5th waves of the SARS-CoV-2 pandemic, then decreased in February 2022. A 3rd peak was observed in July 2022. We observed no significant correlation between SARS-CoV-2 and HAdV-F (r_s = –0.21, p>0.001) (Figure 2, panel C) or AAV2 (VP1 r_s = 0.28, p>0.001; NSP r_s = 0.28, p>0.001) over time (Table 2).

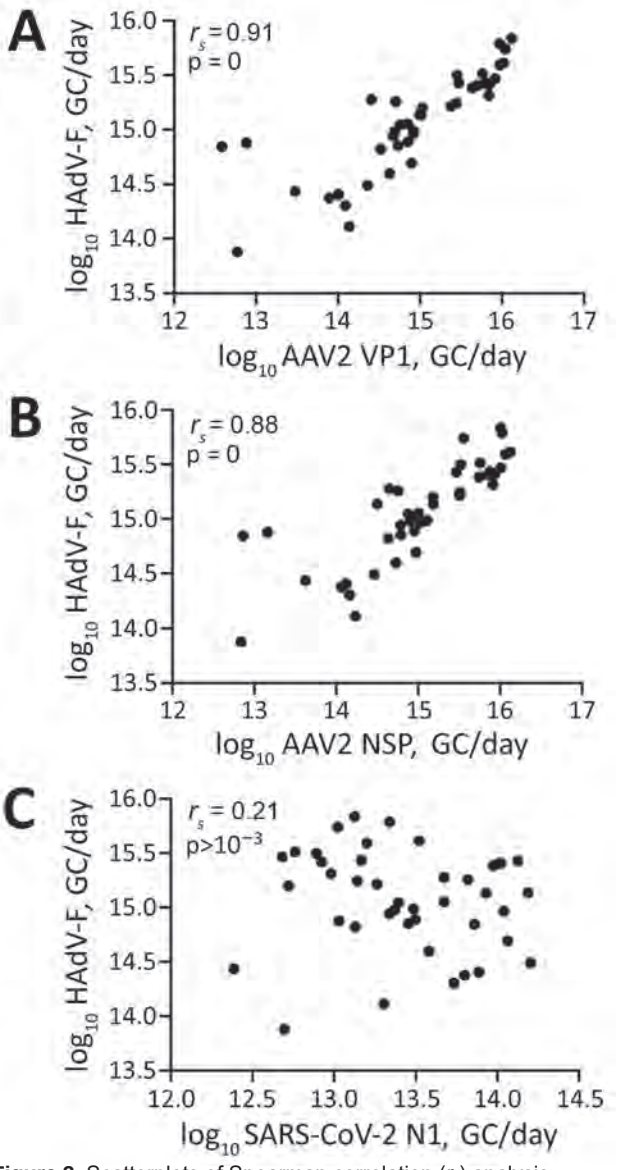

Figure 2. Scatterplots of Spearman correlation (r_s) analysis between HAdV-F, AAV2, and SARS-CoV-2 detected in wastewater samples during outbreak of SAHUE in children, Ireland. Plots depict Spearman correlations between the $\log_{10}$ transformed daily HAdV viral load and AAV2 VP1 (A), AAV2 NSP (B), and SARS-CoV-2 N1 (C) in wastewater. AAV2, adeno-associated virus type 2; GC, genome copies; HAdV-F, human adenovirus type F; N1, nucleocapsid protein 1; NSP, nonstructural protein; SAHUE, severe acute hepatitis of unknown etiology.

Table 2. Spearman correlations between clinical SAHUE cases in children and daily viral loads of AAV2, HAdV, and SARS-CoV-2 in wastewater, Ireland*

Correlations between detected viruses	Spearman r_s (95% CI)
No. SAHUE probable cases/week	
HAdV-F GC/day	**0.62** (0.382–0.781)
AAV2 VP1 GC/day	**0.57** (0.323–0.740)
AAV2 NSP GC/day	**0.55** (0.297–0.727)
SARS-CoV-2 N1 GC/day	0.006 (−0.291 to 0.303)
No. HAdV-F clinical cases/week	
HAdV-F GC/day	**0.85** (0.719–0.920)
AAV2 VP1 GC/day	**0.82** (0.723–0.884)
AAV2 NSP GC/day	**0.81** (0.713–0.880)
SARS-CoV-2 N1 GC/day	0.206 (−0.022 to 0.414)
HAdV-F GC/day	
AAV2 VP1 GC/day	**0.91** (0.833–0.951)
AAV2 NSP GC/day	**0.88** (0.787–0.937)
SARS-CoV-2 N1 GC/day	
HAdV-F GC/day	−0.21 (−0.494 to 0.105)
AAV2 VP1 GC/day	0.28 (0.055–0.483)
AAV2 NSP GC/day	0.29 (0.063–0.492)

*Bold text indicates statistical significance (p≤0.001). AAV2, adeno-associated virus type 2; GC, genome copies; HAdV-F, human adenovirus species F; N1, nucleocapsid protein 1; NSP, nonstructural protein; SAHUE, severe acute hepatitis of unknown etiology; VP, viral protein.

HAdV Types in Wastewater

The hexon genomic fragment we targeted for deep sequencing encompasses the region between nt positions 17921 and 18661 relative to the HAdV-F41 prototype (GenBank accession no. ON442316), including variable loop 1 of the hexon protein (*26*) (Figure 3, panel A). That fragment enables HAdV type classification based on similarity to other characterized types. The number of aligned reads varied among samples from 111,000–274,000 reads (Figure 3, panel B); however, we detected HAdV-F41 in all samples, supporting the real-time qPCR results we described. Few (<1%) reads aligned with HAdV-F40. Samples collected from week 41 of 2021 (October 13) to week 22 of 2022 (June 1) showed >30% of sequenced reads belonged to HAdV-F41, peaking on week 12 of 2022 (March 23). In contrast, by week 27 (July 5) the proportion of HAdV-F41 fell to 10%. Of note, besides HAdV-F41, the NGS protocol detected other HAdV types circulating in the community, such as HAdV-B3, -B7, -C1, -C2, and C5, which are usually related to respiratory infections (*6*,*33*), and even detected changes in the progression of the proportion among these types.

We assembled the reads into consensus sequences to assess their genetic relationships. We compared consensus sequences against HAdV type reference sequences in a maximum-likelihood phylogenetic tree that showed well-supported separation among types and consensus sequence clustering that corresponded to different sampling dates (Figure 4). We noted some divergence among consensus sequences in the HAdV-F41 clade, which prompted us to assess single-nucleotide variants (SNVs) in different samples (Appendix Figure 2). Despite finding 46–59 SNVs in samples with a frequency >10%, we observed that 44 SNVs remained constant for all 12 samples, suggesting a rather homogenous population of HAdV-F41 variants circulating in Ireland during the SAHUE outbreak. Nevertheless, the frequency of variants in samples were not constant and we observed some genetic drift over time. For instance, A603G and T604C, relative to the sequenced fragment, increased from a frequency of <25% in week 41 (2021) to >70% by week 33 (2022).

Correlation of SAHUE and Viral Nucleic Acids in Wastewater Over Time

The clinical reports of SAHUE showed a significant correlation with the HAdV-F viral load detected in wastewater samples collected during October 13, 2021–August 14, 2022 (r_s = 0.62; p<0.001) (Table 2). Similarly, we observed a significant correlation between SAHUE cases and detection of both AAV2 gene targets in wastewater, VP1 (r_s = 0.57; p<0.001) and NSP (r_s = 0.55; p<0.001). In contrast, SAHUE cases showed no correlation to SARS-CoV-2 detection in wastewater samples during the same period (r_s = 0.006; p = 0.97) (Table 2).

Correlation of HAdV-F Gastrointestinal Cases and HAdV-F DNA in Wastewater Over Time

We evaluated the relationship between the number of reported HAdV-F gastrointestinal cases and HAdV-F DNA levels in wastewater (Table 2; Figure 1). We observed a significant correlation, inferring that HAdV-F DNA levels in wastewater reflect the prevalence of HAdV-F in the community (r_s = 0.85; p<0.001) (Table 2). We also observed a significant correlation between clinical HAdV-F cases and AAV2 VP1 (r_s = 0.82; p<0.001) and AAV2 NSP (r_s = 0.81; p<0.001) (Table 2). In contrast, we detected no significant correlation between HAdV-F and AAV2 and the levels of SARS-CoV-2 N1 in wastewater (r_s = 0.206; p>0.1).

Discussion

We examined associations between the number of pediatric SAHUE cases reported and the levels of HAdV-F and AAV2 in wastewater influent taken from the Ringsend WWTP in Dublin, Ireland. By September 8, 2022, Ireland had 28 probable SAHUE cases reported (*2*). Probable cases were geographically spread broadly throughout Ireland, but most cases occurred in Dublin, an area served by the Ringsend WWTP, which captures ≈40% of the population of Ireland.

Our results showed a positive temporal correlation between the number of SAHUE cases and the daily viral load of both HAdV-F and AAV2 in wastewater during the outbreak period, consistent with the hypothesis that these 2 viruses could be directly or indirectly involved with the etiopathogenesis of SAHUE. Of 27 probable cases tested for HAdV in Ireland, 14 (52%) tested positive (*2*), which is comparable to other SAHUE cases reported in Europe during that time (*1*). Furthermore, 64% (14/22) of cases analyzed for AAV2 also tested positive.

Our results showed that HAdV-F levels in wastewater corresponded with the trends in the number of HAdV-positive cases reported weekly throughout the study period. A similar robust correlation was seen between the levels of AAV2 in wastewater and clinical HAdV cases reported. Correlation between AAV2 and HAdV-F is expected because of the adenovirus-dependent nature of AAV2.

In addition to AAV2 and HAdV-F, our results showed other respiratory adenoviruses were circulating in the community. Sequencing results showed a high prevalence of HAdV-F41 and low prevalence of HAdV-F40 in wastewater, suggesting that HAdV-F41 was the dominant F species circulating in the community during the study period. In addition, a large number (52%) of hexon loop 1 reads derived from HAdV species A–E enabled identification of other HAdV species associated with respiratory disease. This finding highlights that wastewater sampling could be used for surveillance of respiratory adenoviral species, just as for surveillance for other respiratory viruses, such as SARS-CoV-2 and influenza (*18*,*34*).

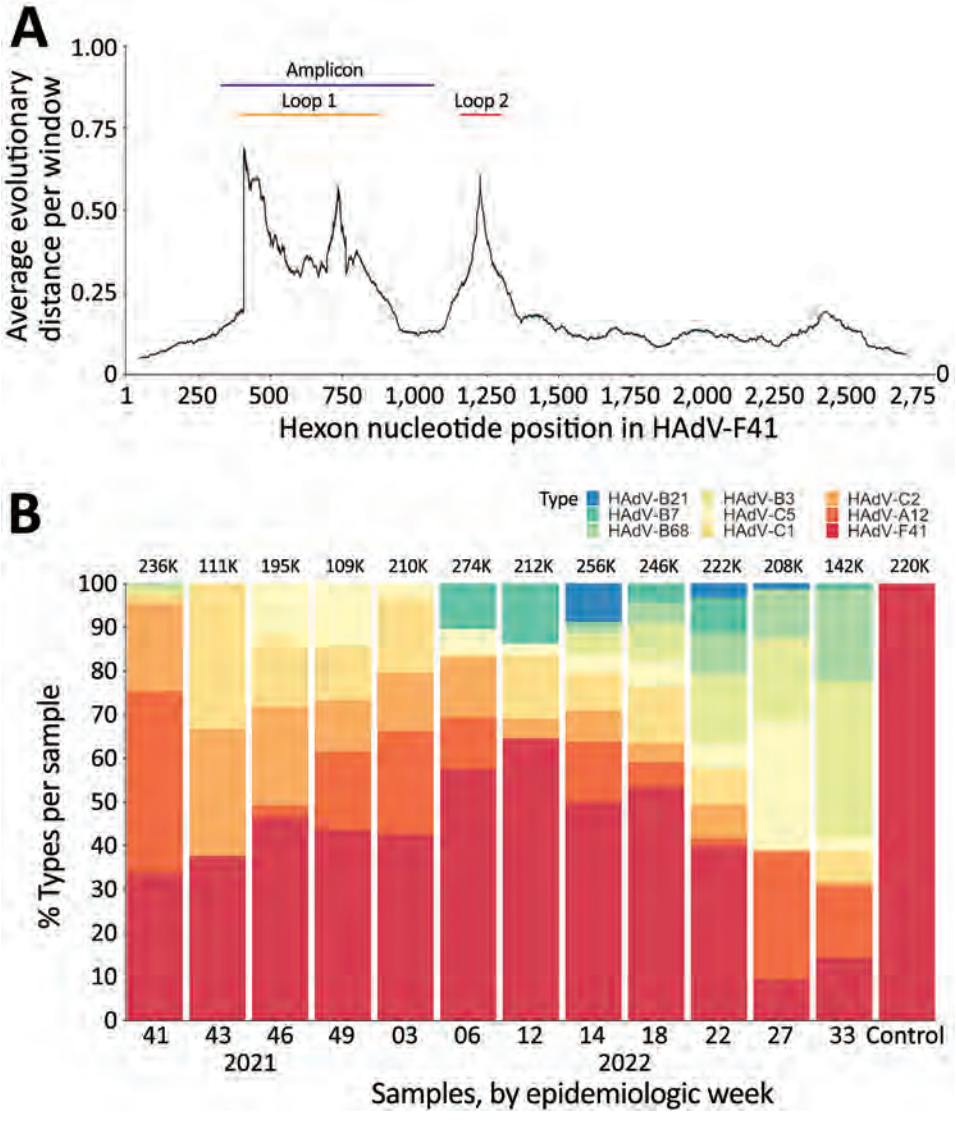

Figure 3. Hexon fragment sequencing for HAdV typing in wastewater, Ireland. A) Diagram of the average nucleotide evolutionary distance among all known HAdV types across the hexon-coding gene. The positions of the variable loops 1 and 2 have been annotated relative to positions in HAdV-F41. The amplicon target used for typing is annotated in blue. B) Type classification of reads in each sample, shown as the percentage of the total of aligned reads per sample, shown at the top of each bar. HAdV, human adenovirus.

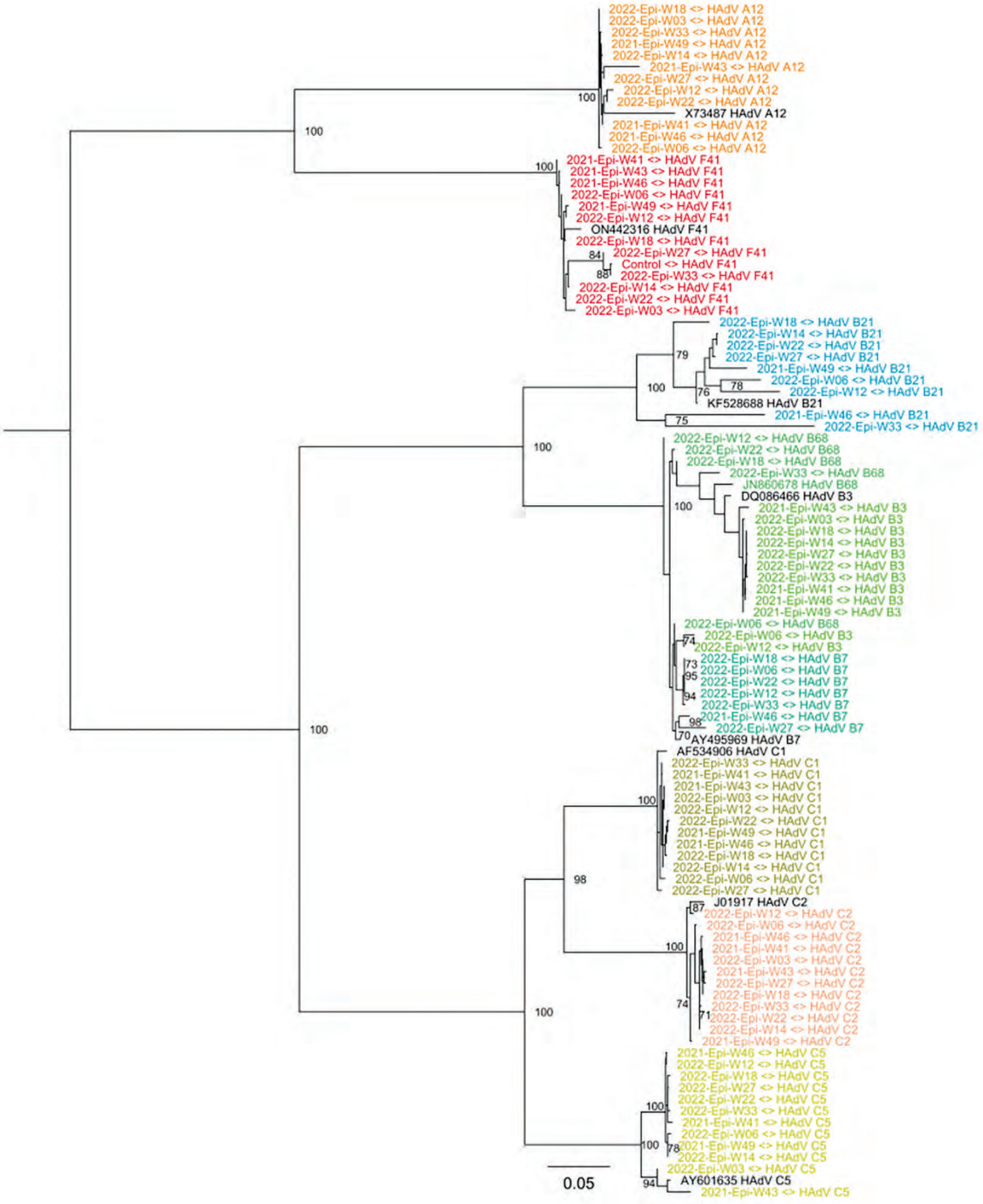

Figure 4. Maximum-likelihood phylogenetic tree of HAdV genetic diversity in wastewater samples collected during SAHUE outbreak in children, Ireland. The tree was inferred by using RAxML (https://github.com/stamatak/standard-RAxML). Branch support was estimated by using the bootstrap method with 100 repetitions and is shown next to the branches that have >70% support. Black text indicates reference sequences, identified by GenBank accession number. Colors indicate HAdV species and types. Scale bar indicates nucleotide substitutions per site. Epi-W, epidemiologic week; HAdV, human adenovirus; SAHUE, severe acute hepatitis of unknown etiology.

Our results showed no statistically significant relationship between SARS-CoV-2 levels and either HAdV-F and AAV2 in wastewater, suggesting that the epidemiology of the viruses is different. Of note, SARS-CoV-2 was detectable throughout the SAHUE outbreak period. Although we did not observe an association between SARS-CoV-2 levels in wastewater and the number of SAHUE cases, the relationship of SARS-CoV-2 infections with the SAHUE cases remains to be explored. In Ireland, 60% of SAHUE cases also tested positive for SARS-CoV-2 antibodies, indicating a current or past SARS-CoV-2 infection.

Throughout the COVID-19 pandemic, nonpharmaceutical interventions (NPIs), such as mandatory face coverings and social distancing, played a crucial role in reducing SARS-CoV-2 transmission rates. Studies have shown that COVID-19 NPIs were associated with reduced transmission of other viruses, such as HAdV and influenza (*35*–*37*). Our results support those findings; HAdV-F was not detectable in wastewater during July 2020–October 2021, when mandatory NPIs were in place in Ireland. Wastewater samples from before the SARS-CoV-2 pandemic are not available; therefore, the level of HAdV in wastewater before March 2020 remains unknown.

Similarly, AAV2 persisted at lower levels throughout the pandemic before increasing toward the end of 2021. The intensity of the SAHUE outbreak might be a result of the immunologically naive status of young children who had limited exposure to HAdV species and AAV2 during the preceding 2 years.

After February 28, 2022, public health measures such as social distancing and pods were abolished in schools and early learning settings in Ireland; beginning on April 1, 2022, all COVID-19 restrictions ended in the wider community (*38*). Those dates coincide with the sharp increase in the number of weekly HAdV-positive cases and HAdV-F and AAV2 DNA levels in wastewater, indicative of an increase in the transmission of both viruses and a higher number of infections in the community. Furthermore, NGS data showed that the proportion of sequenced reads belonging to HAdV-F41 peaked around that time, suggesting that HAdV-F41 was one of the dominant HAdV serotypes circulating during the study period.

In conclusion, the observed increases in prevalence of HAdV-F41 and AAV2 DNA in wastewater correlated with clinical SAHUE cases in Ireland, supporting the hypothesis that these viruses could be involved in SAHUE outbreaks. Although such correlations are associative and are not direct evidence of causation, our results showing the identity and changes in prevalence of HAdV-F41 and AAV2, provide compelling arguments for further clinical characterization of SAHUE cases. Clinical characterization of SAHUE could reveal conditions relating HAdV and AAV2 viruses to the observed incidence of acute hepatitis. In addition, wastewater sampling could aid in surveillance for HAdV-F, AAV2, and other respiratory adenovirus species that might be involved in SAHUE outbreaks.

This work was funded by grants from Science Foundation Ireland (grants nos. 20-COV-0159 and 20-COV-8460), the European Regional Development Fund through the Ireland Wales Cooperation Programme (Acclimatize), the Health Service Executive, and the European Commission DG Environment (grant no. 060701/2021/864480/SUB/ENV.C2).

About the Author

Dr. Martin is a scientist in the School of Biomolecular and Biomedical Science at University College Dublin, Dublin, Ireland. Her research interests include wastewater-based epidemiology and waterborne pathogens.

References

1. World Health Organization. Severe acute hepatitis of unknown aetiology in children—multi-country. 2022 Jul 12 [cited 2022 Sep 27]. https://www.who.int/emergencies/disease-outbreak-news/item/2022-DON400
2. Health Protection Surveillance Centre. Acute hepatitis of unknown cause in children. 2022 Dec 14 [cited 2022 Sep 27]. https://www.hpsc.ie/a-z/hepatitis/acutehepatitisofunknownaetiology/title-22079-en.html
3. Mücke MM, Zeuzem S. The recent outbreak of acute severe hepatitis in children of unknown origin—what is known so far. J Hepatol. 2022;77:237–42. https://doi.org/10.1016/j.jhep.2022.05.001
4. Gutierrez Sanchez LH, Shiau H, Baker JM, Saaybi S, Buchfellner M, Britt W, et al. A case series of children with acute hepatitis and human adenovirus infection. N Engl J Med. 2022;387:620–30. https://doi.org/10.1056/NEJMoa2206294
5. UK Health Security Agency. Investigation into acute hepatitis of unknown aetiology in children in England, technical briefing 2022 April 25 [cited 2022 October 13]. https://assets.publishing.service.gov.uk/government/uploads/system/uploads/attachment_data/file/1071198/acute-hepatitis-technical-briefing-1_4_.pdf
6. Lynch JP III, Kajon AE. Adenovirus: epidemiology, global spread of novel serotypes, and advances in treatment and prevention. Semin Respir Crit Care Med. 2016;37:586–602. https://doi.org/10.1055/s-0036-1584923
7. Zlateva KT, Maes P, Rahman M, Van Ranst M. Chromatography paper strip sampling of enteric adenoviruses type 40 and 41 positive stool specimens. Virol J. 2005;2:6. https://doi.org/10.1186/1743-422X-2-6
8. Rafie K, Lenman A, Fuchs J, Rajan A, Arnberg N, Carlson LA. The structure of enteric human adenovirus 41-A leading cause of diarrhea in children. Sci Adv. 2021;7:eabe0974. https://doi.org/10.1126/sciadv.abe0974
9. Büning H, Schmidt M. Adeno-associated vector toxicity–to be or not to be? Mol Ther. 2015;23:1673–5. https://doi.org/10.1038/mt.2015.182

10. Srivastava A, Carter BJ. AAV infection: protection from cancer. Hum Gene Ther. 2017;28:323–7. https://doi.org/10.1089/hum.2016.147
11. Li C, Narkbunnam N, Samulski RJ, Asokan A, Hu G, Jacobson LJ, et al.; Joint Outcome Study Investigators. Neutralizing antibodies against adeno-associated virus examined prospectively in pediatric patients with hemophilia. Gene Ther. 2012;19:288–94. https://doi.org/10.1038/gt.2011.90
12. Götting J, Cordes AK, Steinbrück L, Heim A. Molecular phylogeny of human adenovirus type 41 lineages. Virus Evol. 2022;8:veac098. PubMed https://doi.org/10.1093/ve/veac098
13. Leen G, Stein JE, Robinson J, Maldonado Torres H, Marsh SGE. The HLA diversity of the Anthony Nolan register. HLA. 2021;97:15–29. https://doi.org/10.1111/tan.14127
14. Primo D, Pacheco GT, Timenetsky MDCST, Luchs A. Surveillance and molecular characterization of human adenovirus in patients with acute gastroenteritis in the era of rotavirus vaccine, Brazil, 2012–2017. J Clin Virol. 2018;109:35–40. https://doi.org/10.1016/j.jcv.2018.10.010
15. Aiemjoy K, Altan E, Aragie S, Fry DM, Phan TG, Deng X, et al. Viral species richness and composition in young children with loose or watery stool in Ethiopia. BMC Infect Dis. 2019;19:53. https://doi.org/10.1186/s12879-019-3674-3
16. Hellmér M, Paxéus N, Magnius L, Enache L, Arnholm B, Johansson A, et al. Detection of pathogenic viruses in sewage provided early warnings of hepatitis A virus and norovirus outbreaks. Appl Environ Microbiol. 2014;80:6771–81. https://doi.org/10.1128/AEM.01981-14
17. Daughton CG. Wastewater surveillance for population-wide Covid-19: The present and future. Sci Total Environ. 2020; 736:139631. https://doi.org/10.1016/j.scitotenv.2020.139631
18. Reynolds LJ, Gonzalez G, Sala-Comorera L, Martin NA, Byrne A, Fennema S, et al. SARS-CoV-2 variant trends in Ireland: wastewater-based epidemiology and clinical surveillance. Sci Total Environ. 2022;838:155828. https://doi.org/10.1016/j.scitotenv.2022.155828
19. Ahmed W, Simpson SL, Bertsch PM, Bibby K, Bivins A, Blackall LL, et al. Minimizing errors in RT-PCR detection and quantification of SARS-CoV-2 RNA for wastewater surveillance. Sci Total Environ. 2022;805:149877. https://doi.org/10.1016/j.scitotenv.2021.149877
20. Amman F, Markt R, Endler L, Hupfauf S, Agerer B, Schedl A, et al. Viral variant-resolved wastewater surveillance of SARS-CoV-2 at national scale. Nat Biotechnol. 2022;40:1814–22. https://doi.org/10.1038/s41587-022-01387-y
21. Reyne MI, Allen DM, Levickas A, Allingham P, Lock J, Fitzgerald A, et al. Detection of human adenovirus F41 in wastewater and its relationship to clinical cases of acute hepatitis of unknown aetiology. Sci Total Environ. 2023; 857:159579. https://doi.org/10.1016/j.scitotenv.2022.159579
22. Tiemessen CT, Nel MJ. Detection and typing of subgroup F adenoviruses using the polymerase chain reaction. J Virol Methods. 1996;59:73–82. https://doi.org/10.1016/0166-0934(96)02015-0
23. García-Aljaro C, Ballesté E, Muniesa M, Jofre J. Determination of crAssphage in water samples and applicability for tracking human faecal pollution. Microb Biotechnol. 2017;10:1775–80. https://doi.org/10.1111/1751-7915.12841
24. Lu X, Wang L, Sakthivel SK, Whitaker B, Murray J, Kamili S, et al. US CDC real-time reverse transcription PCR panel for detection of severe acute respiratory syndrome coronavirus 2. Emerg Infect Dis. 2020;26:1654–65. https://doi.org/10.3201/eid2608.201246
25. Centers for Disease Control and Prevention. 2019-novel coronavirus (2019-nCoV) real-time rRT-PCR panel primers and probes [cited 2022 Sep 29]. https://www.cdc.gov/coronavirus/2019-ncov/downloads/rt-pcr-panel-primer-probes.pdf
26. Lu X, Erdman DD. Molecular typing of human adenoviruses by PCR and sequencing of a partial region of the hexon gene. Arch Virol. 2006;151:1587–602. https://doi.org/10.1007/s00705-005-0722-7
27. Buchfink B, Reuter K, Drost H-G. Sensitive protein alignments at tree-of-life scale using DIAMOND. Nature Methods. 2021;18:366–8. https://doi.org/10.1038/s41592-021-01101-x
28. Li H. Minimap2: pairwise alignment for nucleotide sequences. Bioinformatics. 2018;34:3094–100. https://doi.org/10.1093/bioinformatics/bty191
29. Yamada KD, Tomii K, Katoh K. Application of the MAFFT sequence alignment program to large data-reexamination of the usefulness of chained guide trees. Bioinformatics. 2016;32:3246–51. https://doi.org/10.1093/bioinformatics/btw412
30. Stamatakis A. RAxML version 8: a tool for phylogenetic analysis and post-analysis of large phylogenies. Bioinformatics. 2014;30:1312–3. https://doi.org/10.1093/bioinformatics/btu033
31. Wilm A, Aw PP, Bertrand D, Yeo GH, Ong SH, Wong CH, et al. LoFreq: a sequence-quality aware, ultra-sensitive variant caller for uncovering cell-population heterogeneity from high-throughput sequencing datasets. Nucleic Acids Res. 2012;40:11189–201. https://doi.org/10.1093/nar/gks918
32. Irish Statute Book. Infectious Diseases (Amendment) (No. 3) Regulations 2003, S.I. no. 707/2003 [cited 2022 Sep 27]. https://www.irishstatutebook.ie/eli/2003/si/707/made/en/print
33. Yoshitomi H, Sera N, Gonzalez G, Hanaoka N, Fujimoto T. First isolation of a new type of human adenovirus (genotype 79), species human mastadenovirus B (B2) from sewage water in Japan. J Med Virol. 2017;89:1192–200. https://doi.org/10.1002/jmv.24749
34. Mercier E, D'Aoust PM, Thakali O, Hegazy N, Jia JJ, Zhang Z, et al. Municipal and neighbourhood level wastewater surveillance and subtyping of an influenza virus outbreak. Sci Rep. 2022;12:15777. https://doi.org/10.1038/s41598-022-20076-z
35. Cowling BJ, Ali ST, Ng TWY, Tsang TK, Li JCM, Fong MW, et al. Impact assessment of non-pharmaceutical interventions against coronavirus disease 2019 and influenza in Hong Kong: an observational study. Lancet Public Health. 2020;5:e279–88. https://doi.org/10.1016/S2468-2667(20)30090-6
36. Shi HJ, Kim NY, Eom SA, Kim-Jeon MD, Oh SS, Moon BS, et al. Effects of non-pharmacological interventions on respiratory viruses other than SARS-CoV-2: analysis of laboratory surveillance and literature review from 2018 to 2021. J Korean Med Sci. 2022;37:e172. https://doi.org/10.3346/jkms.2022.37.e172
37. Quan C, Zhang Z, Ding G, Sun F, Zhao H, Liu Q, et al. Seroprevalence of influenza viruses in Shandong, northern China during the COVID-19 pandemic. Front Med. 2022;16:984–90. https://doi.org/10.1007/s11684-022-0930-5
38. Citizens Information. Public health measures for COVID-19. 2022 Apr 4 [cited 2022 Oct 4]. https://www.citizensinformation.ie/en/health/covid19/public_health_measures_for_covid19.html

Address for correspondence: Wim G. Meijer, UCD School of Biomolecular and Biomedical Science, Rm H1.38, O'Brien Centre for Science, University College Dublin, Belfield, Dublin 4, Ireland D04 V1W8; email: wim.meijer@ucd.ie

Outbreaks of SARS-CoV-2 Infections in Nursing Homes during Periods of Delta and Omicron Predominance, United States, July 2021–March 2022

W. Wyatt Wilson, Amelia A. Keaton, Lucas G. Ochoa, Kelly M. Hatfield, Paige Gable, Kelly A. Walblay, Richard A. Teran, Meghan Shea, Urooj Khan, Ginger Stringer, Meenalochani Ganesan, Jordan Gilbert, Joanne G. Colletti, Erin M. Grogan, Carly Calabrese, Andrew Hennenfent, Rebecca Perlmutter, Katherine A. Janiszewski, Christina Brandeburg, Ishrat Kamal-Ahmed, Kyle Strand, Matthew Donahue, M. Salman Ashraf, Emily Berns, Jennifer MacFarquhar, Meghan L. Linder, Dat J. Tran, Patricia Kopp, Rebecca M. Walker, Rebekah Ess, James Baggs, John A. Jernigan, Alex Kallen, Jennifer C. Hunter; Monitoring Outbreaks of Variants in Nursing Homes (MOVIN) Surveillance Team[1]

SARS-CoV-2 infections among vaccinated nursing home residents increased after the Omicron variant emerged. Data on booster dose effectiveness in this population are limited. During July 2021–March 2022, nursing home outbreaks in 11 US jurisdictions involving ≥3 infections within 14 days among residents who had received at least the primary COVID-19 vaccine(s) were monitored. Among 2,188 nursing homes, 1,247 outbreaks were reported in the periods of Delta (n = 356, 29%), mixed Delta/Omicron (n = 354, 28%), and Omicron (n = 536, 43%) predominance. During the Omicron-predominant period, the risk for infection within 14 days of an outbreak start was lower among boosted residents than among residents who had received the primary vaccine series alone (risk ratio [RR] 0.25, 95% CI 0.19–0.33). Once infected, boosted residents were at lower risk for all-cause hospitalization (RR 0.48, 95% CI 0.40–0.49) and death (RR 0.45, 95% CI 0.34–0.59) than primary vaccine–only residents.

After its detection in November 2021, the SARS-CoV-2 B.1.1.529 (Omicron) variant was labeled a variant of concern by the World Health Organization (*1*). Compared with previous variants, Omicron had at least 37 mutations identified in the spike gene, raising concerns about reduced antibody binding affinity and the potential for immune escape (*2*,*3*). Among the US adult population, studies demonstrated that the odds of symptomatic infection are higher for the Omicron variant than Delta (*4*). Conversely, the odds of a subsequent severe outcome, such as COVID-19 hospitalization

Author affiliations: Centers for Disease Control and Prevention, Atlanta, Georgia, USA (W.W. Wilson, A.A. Keaton, L.G. Ochoa, K.M. Hatfield, P. Gable, R.A. Teran, J. MacFarquhar, J. Baggs, J.A. Jernigan, A. Kallen, J.C. Hunter); Chicago Department of Public Health, Chicago, Illinois, USA (K.A. Walblay, R.A. Teran); Colorado Department of Public Health and Environment, Denver, Colorado, USA (M. Shea, U. Khan, G. Stringer, M. Ganesan, J. Gilbert); Connecticut Department of Public Health, Hartford, Connecticut, USA (J.G. Colletti, E.M. Grogan); Iowa Department Health and Human Services, Des Moines, Iowa, USA (C. Calabrese, A. Hennenfent); Maryland Department of Health, Baltimore, Maryland, USA (R. Perlmutter); Massachusetts Department of Public Health, Jamaica Plain, Massachusetts, USA (K.A. Janiszewski, C. Brandeburg); Nebraska Department of Health and Human Services, Lincoln, Nebraska, USA (I. Kamal-Ahmed, K. Strand, M. Donahue, M.S. Ashraf); North Carolina Department of Health and Human Services, Raleigh, North Carolina, USA (E. Berns, J. MacFarquhar); Oregon Health Authority, Portland, Oregon, USA (M.L. Linder, D.J. Tran); South Carolina Department of Health and Environmental Control, Columbia, South Carolina, USA (P. Kopp, R.M. Walker); Utah Department of Health, Salt Lake City, Utah, USA (R. Ess).

DOI: https://doi.org/10.3201/eid2904.221605

[1]Additional members of the MOVIN Surveillance Team are listed at the end of this article.

and death, have been lower among Omicron infections than Delta infections (*5*).

In the United States, nursing home residents have been disproportionately affected by COVID-19 (*6*,*7*). Most nursing home residents are older adults with chronic comorbidities who live in congregate settings where infection control strategies are difficult to implement but vital to preventing facility transmission (*8*). As a result, nursing home residents were prioritized to receive the primary COVID-19 vaccine series (*9*), as well as vaccine booster doses (*10*,*11*). During September–October 2021, the Centers for Disease Control and Prevention (CDC) recommended use of a single COVID-19 vaccine booster dose for all persons ≥18 years of age, to be given 6 months after receipt of a primary mRNA vaccination series or 2 months after receipt of a primary Johnson & Johnson/Janssen (https://www.jnj.com) vaccine dose. In January 2022, CDC updated booster recommendations to shorten the interval to 5 months for receiving an mRNA booster after primary mRNA vaccination series (*12*). However, data on SARS-CoV-2 infections and outcomes among nursing home residents during the Omicron-predominant period of the COVID-19 pandemic have been limited. One study from long-term care facilities in England found reduced risk for severe outcomes among SARS-CoV-2–positive residents during the Omicron period compared with the pre-Omicron period (*13*). An analysis of nursing home data from the US National Healthcare Safety Network (NHSN) found that a COVID-19 booster dose provided greater protection against infection (relative vaccine effectiveness = 46.9%) than the primary vaccine series alone during the Omicron period (*14*). However, NHSN data are limited to aggregate reporting at the facility level; few studies have examined resident outcomes within the context of facility outbreaks.

As part of a surveillance effort to monitor SARS-CoV-2 outbreaks in nursing homes (*15*), CDC partnered with a subset of US public health jurisdictions to prospectively monitor COVID-19 outbreaks in nursing homes. We targeted outbreaks beginning July 26, 2021–January 31, 2022, in which ≥3 SARS-CoV-2 infections occurred within 14 days among residents who had completed at least a primary COVID-19 vaccination series. We describe outbreak characteristics during periods of Delta, mixed Delta/Omicron, and Omicron variant predominance; compare the risk for resident outcomes such as infection, all-cause hospitalization, and all-cause death in the Omicron and Delta periods; and examine risk for those outcomes by booster status during the Omicron period.

Methods

Overview of Health Department Recruitment and NH Outbreak Surveillance

We invited CDC-funded healthcare-associated infections programs in health departments to participate in the surveillance project. Participating health departments provided the number of facilities under surveillance and collected outbreak, facility, and resident information from facilities with eligible outbreaks, which were defined as those with ≥3 SARS-CoV-2 infections within a 14-day period in residents who received at least a primary COVID-19 vaccine series. Outbreaks were identified using data reported to NHSN and other state-based surveillance systems.

Infection in a resident who had received a primary vaccine series alone was defined as a positive SARS-CoV-2 viral nucleic acid amplification or antigen test result collected from a respiratory specimen in a resident who had completed a primary vaccination series (2 doses of the Pfizer-BioNTech [https://www.pfizer.com] or Moderna [https://www.modernatx.com] mRNA vaccine or 1 dose of the Johnson & Johnson/Janssen vaccine) at least 14 days earlier. For this analysis, residents were considered boosted 14 days after receipt of an additional primary series dose or booster dose (*9*). Surveillance data could not distinguish between immunocompromised nursing home residents who received an additional primary vaccine and residents who received a booster dose. As such, the category of residents who were vaccinated with an additional or booster dose and are designated as boosted in this analysis included residents who received 2 primary mRNA doses followed by a booster dose; 3 primary mRNA doses; 3 primary mRNA doses followed by a booster dose (i.e., 4 total doses); 1 primary Janssen dose followed by a booster dose; 1 primary Janssen dose and an additional primary mRNA vaccine dose; or 1 primary Janssen dose and an additional primary mRNA vaccine dose followed by a booster dose (*12*). The surveillance definition of boosted used for this study was defined before CDC released the recommendation for when to consider an individual up to date, which is immediately after getting all recommended boosters (*16*). Staff with a positive SARS-CoV-2 test result were not counted toward the infection criteria for an eligible outbreak.

Surveillance Data Collection

Health departments reported facility-level resident census stratified by vaccination status at the date of outbreak onset, defined as the date of first SARS-CoV-2–positive specimen collection in a resident

or staff member after a period of ≥14 days with no resident or staff infections. Other outbreak information collected included outbreak onset date, outbreak closure date (defined as 14 days after last identified SARS-CoV-2 infection in a resident or staff member), and whether the initial infection was detected in a resident or staff member. Information collected for infected residents included whether they were in the facility on outbreak onset date, vaccination status at time of SARS-CoV-2–positive specimen collection date, all-cause hospitalization, all-cause death, and SARS-CoV-2 variant type (if known). Hospitalization from any cause was monitored and recorded through date of outbreak closure; death from any cause was monitored and recorded through 14 days after outbreak closure date.

Surveillance Period

Jurisdictions reported new outbreaks in which onset occurred during July 26, 2021–January 31, 2022, and continued reporting new resident infections until meeting the outbreak closure definition or the end of the infection surveillance period (February 28, 2022). We excluded outbreaks from analyses if reported by health departments that were unable to participate for the entire surveillance period or if outbreak status was listed as unknown at the end of the surveillance period. Any unclosed outbreaks at the end of the infection surveillance period were classified as still active; for these outbreaks, hospitalization and deaths were monitored and recorded for another 14 days and 28 days from the end of the infection surveillance period (March 14 and 28, 2022). Outbreak duration was the number of days from outbreak onset until closure. Because outbreaks with onset on the last day of the outbreak surveillance period (January 31, 2022) had a maximum of 42 days to close (14 days after last resident infection or 14 days after the end of the infection surveillance period on February 28, whichever was earlier) and because a subset of outbreaks continued beyond the infection surveillance period, outbreak duration was categorized into 3 groups: ≤28 days, 29–41 days, and ≥42 days.

Outbreak Characteristics

We analyzed and described outbreak characteristics including outbreak duration and size, initial infection, and SARS-CoV-2 variant identified by whole-genome sequencing (Appendix, https://wwwnc.cdc.gov/EID/article/29/4/22-1605-App1.pdf) by period based on outbreak onset date: Delta (July 26–November 1, 2021), mixed Delta/Omicron (November 2–December 18, 2021), and Omicron (December 19, 2021–January 31, 2022). Periods were defined as the range of dates when the estimated national prevalence for a specific SARS-CoV-2 variant was >75% (*17*). We compared outbreak characteristics across Delta and Omicron periods by using χ^2 or Wilcoxon rank-sum tests for categorical and nonnormally distributed continuous variables. We did not include the mixed Delta/Omicron period in analytic comparisons.

Resident Outcomes by Delta and Omicron Period

We used a Poisson generalized estimating equation (GEE) model with log links, adjusting for facility-level clustering, to estimate the risk for infection in the first 28 days of the outbreak for residents with a completed primary COVID-19 vaccine series who were present at outbreak onset in the Delta and Omicron periods. To enable comparison across all outbreaks, we restricted our analysis to the first 28 days because outbreaks with onset during the last day of surveillance had a maximum of 28 days to register infections. In addition to general exclusion criteria, we excluded additional outbreaks if available sequencing data indicated the outbreak variant was discordant with the outbreak period (i.e., Delta variant during the Omicron period), if multiple variants were identified in a single outbreak, or if resident census data were incomplete.

We compared the risk for severe outcomes among infected residents who had received a primary vaccine series alone by outbreak period (Delta or Omicron) using a binomial GEE regression model with log links adjusting for facility level clustering. We excluded boosted residents because of their limited number in the Delta period.

Resident Outcomes by Booster Status in the Omicron Period

For Omicron period outbreaks, we compared the risk for resident infection within the first 14 days of an outbreak by booster status at the time of outbreak onset (booster dose vs. primary vaccine series alone) using similar Poisson GEE models along with additional outbreak exclusion criteria as previously described. Because the booster status of residents who did not become infected was available only at outbreak onset, this analysis was restricted to the first 14 days of each outbreak to limit the effect of potential changes in booster status among uninfected residents after outbreak onset.

For the subset of Omicron period outbreaks, we compared the risk for severe outcomes among infected residents by booster status using similar binomial GEE models adjusting for facility clustering. We conducted analyses in SAS version 9.4 (SAS Institute

Inc., https://www.sas.com) and defined statistical significance as α = 0.05. This activity was reviewed by CDC and was conducted consistent with applicable federal law and CDC policy (45 C.F.R. part 46.102(l)(2), 21 C.F.R. part 56; 42 U.S.C. Sect. 241(d); 5 U.S.C. Sect. 552a; 44 U.S.C. Sect. 3501 et seq).

Results

Outbreak Surveillance

During July 26, 2021–January 31, 2022, a total of 1,414 new outbreaks were reported among 16 US jurisdictions (14 state and 2 local health departments). We excluded 167 outbreaks: 125 outbreaks reported by 5 jurisdictions that did not participate for the duration of the surveillance project period, 21 outbreaks with unknown status at the end of the surveillance period (e.g., closed or still active), and 21 outbreaks with <3 infections among residents who had completed at least a primary COVID-19 vaccine series (Figure 1). After excluding outbreaks, we identified 1,247 outbreaks from 11 jurisdictions; the outbreaks occurred in 1,090 (49.8%) of the 2,188 individual facilities represented in the surveillance catchment of the participating US jurisdictions. Overall, the surveillance catchment constituted 84% of the 2,602 licensed nursing homes within participating health department jurisdictions and 14% of the 15,600 nursing homes nationwide (*18*).

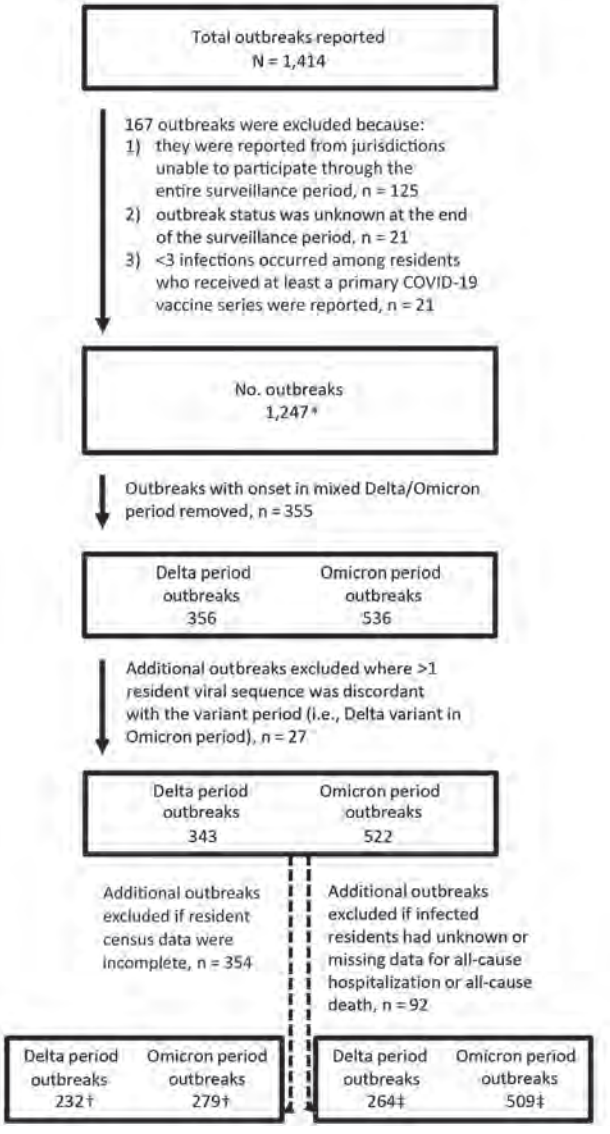

Figure 1. Flow diagram of reported outbreaks included in analysis of SARS-CoV-2 infections in nursing homes during periods of Delta and Omicron variant predominance, United States, July 2021–March 2022. *See Table, Figure 2; †see Figures 3 and 5 for infection attack rate and risk ratio analysis; ‡see Figures 4 and 6 for outcomes attack rate and risk ratio analysis.

Descriptive Characteristics of Outbreaks

Among the 1,247 outbreaks, 356 (29%) began during the Delta-predominant period of the pandemic (July 26–November 1, 2021), 355 (28%) began during the mixed Delta/Omicron period (November 2–December 18, 2021), and 536 (43%) began during the Omicron-predominant period of the pandemic (December 19, 2021–January 31, 2022) (Table). During the Delta period, viral sequences were reported for ≥1 infected resident in 53% (n = 189) of outbreaks; the same was true in the Omicron period for 39% (n = 208) of outbreaks. Among outbreaks with a single variant confirmed by sequence data, Delta was the only variant identified among infected residents in 96% (n = 176/183) of outbreaks during the Delta period; similarly, Omicron was the only variant identified among infected residents in 98% (194/198) of outbreaks during the Omicron period. The mixed Delta/Omicron period had the highest proportion of outbreaks in which multiple SARS-CoV-2 variants were identified in infected residents (22%, n = 31/142).

Median time from initial infection in a staff or resident to next identified resident infection (positive specimen collection date) was 4 days (interquartile range [IQR] 0–11 days) and did not differ between the Delta and Omicron periods. Among closed outbreaks (95.5% in Delta period, 88.4% in Omicron period), 67% of infections occurred during the first 28 days. The median number of residents present at outbreak onset and infected in the first 28 days in Omicron period outbreaks (10, IQR 4–20) was greater than in Delta period outbreaks (4, IQR 0–10) (p<0.001). Half (n = 178) of all outbreaks beginning in the Delta period lasted ≥42 days, compared with 84% (n = 449) during the Omicron period (p<0.001).

New and Active Outbreaks by Calendar Week

The number of new outbreaks per week was highest during the fourth week of December 2021 (n = 217) and lowest during the last week of January 2022 (n = 2), after which surveillance reporting of new outbreaks stopped (Figure 2). The number of active

Table. Descriptive characteristics of eligible nursing home outbreaks (N = 1,247), by period of SARS-CoV-2 variant predominance, United States, July 2021–January 2022*

Characteristic	Outbreaks beginning during Jul 26–Nov 1: Delta period	Outbreaks beginning during Nov 2–Dec 18: mixed Delta/Omicron period	Outbreaks beginning during Dec 19–Jan 31: Omicron period
No. outbreaks (% total)	356 (29)	355 (28)	536 (43)
Individual skilled nursing facilities	347	351	536
Active outbreaks per week, median (IQR)	146 (100–163)	178 (161–237)	697 (470–838)
Jurisdiction			
Chicago	8 (2.2)	51 (14.3)	22 (4.1)
Colorado	63 (17.7)	53 (14.9)	108 (20.1)
Connecticut	33 (9.3)	38 (10.7)	56 (10.5)
Iowa	3 (0.8)	1 (0.3)	1 (0.2)
Maryland	61 (17.1)	92 (25.8)	35 (6.5)
Massachusetts	40 (11.2)	71 (19.9)	184 (34.4)
Nebraska	18 (5.1)	2 (0.6)	2 (0.4)
North Carolina	38 (10.7)	15 (4.2)	21 (3.9)
Oregon	36 (10.1)	10 (2.8)	34 (6.4)
South Carolina	34 (9.6)	12 (3.4)	30 (5.6)
Utah	22 (6.2)	10 (2.8)	43 (8.0)
SARS-CoV-2 outbreak variant identified among ≥1 resident			
Delta, B.1.672 and AY.1-AY.107 lineages	176 (49.4)	60 (16.9)	4 (0.7)
Omicron, B.1.1.529, BA.1, BA.2 lineages	4 (1.1)	50 (14.0)	194 (36.3)
Alpha	1 (0.3)	0	0
Other	2 (0.6)	1 (0.3)	0
Multiple variants identified	6 (1.7)	31 (8.7)	10 (1.9)
No sequencing information available	167 (46.9)	213 (59.8)	328 (61.3)
Initial infection in the outbreak			
Staff	220 (61.8)	226 (63.5)	391 (73.1)
Resident	110 (30.9)	100 (28.1)	77 (14.4)
Both staff and resident infections at onset	26 (7.3)	29 (8.2)	67 (12.5)
Unknown or missing	0	0	1 (0.2)
Days from initial infection to subsequent resident infection in index cluster, median (IQR)	4 (0–11)	5 (0–16)	4 (0–9)
Median resident census at outbreak onset per outbreak†			
Total no. residents (IQR)	89 (59–114)	98 (74–129)	79 (54–106)
Residents with booster dose % (IQR)‡	0.0 (0–0)	55.7 (28–75)	74.0 (56–86)
Residents with primary vaccine series alone, % (IQR)	90.0 (81–96)	38.0 (21–79)	21.0 (11–35)
Residents partially vaccinated, % (IQR)	1.0 (0–3)	1.0 (0–2.3)	0.0 (0–1.8)
Residents unvaccinated, % (IQR)	7.0 (3–13)	5.5 (3–11)	5.0 (2–9)
Median resident infections in first 28 d per outbreak§			
No. infected residents (IQR)	4 (0–10)	6 (1–14)	10 (4–20)
Infected residents with booster dose, % (IQR)‡	0.0 (0–0)	0.0 (0–18)	35.7 (11–59)
Infected residents with primary vaccine series alone, % (IQR)	87.5 (71–100)	75.0 (46–100)	46.2 (27–67)
Infected residents without vaccination, % (IQR)	5.3 (0–25)	8.7 (0–23)	5.0 (0–17)
Outbreak duration			
≤28 d	85 (23.9)	26 (7.3)	16 (3.0)
29–41 d	93 (26.1)	23 (6.5)	71 (13.3)
≥42 d	178 (50.0)	306 (86.2)	449 (83.8)
Outbreak status at end of infection surveillance period¶			
Closed	340 (95.5)	308 (86.8)	474 (88.4)
Still active	16 (4.5)	47 (13.2)	62 (11.6)

*Values are no. (%) except as indicated. Dates of variant predominance were July 26–November 1, 2021 (Delta), November 2–December 18, 2021 (mixed Delta/Omicron), and December 19, 2021–January 31, 2022 (Omicron).
†Resident census data were incomplete for 114 (32%) (Delta period), 133 (37%) (mixed Delta/Omicron period), and 247 (46%) (Omicron period) outbreaks. As a result, denominators used for median resident census at outbreak onset were 242 (Delta), 222 (mixed Delta/Omicron), and 289 (Omicron).
‡Residents who received a booster dose could not be distinguished from residents who received additional vaccine dose.
§Infection attack rates were restricted to resident infections present at outbreak onset and those infected within first 28 days of outbreak; all outbreaks included in this analysis had at least 28 days for case ascertainment.
¶All outbreaks included in analysis began before February 1, 2022. Resident infections were reported through February 28, 2022, making March 14, 2022, the last day for an outbreak to close (2 weeks with no infections among residents or staff).

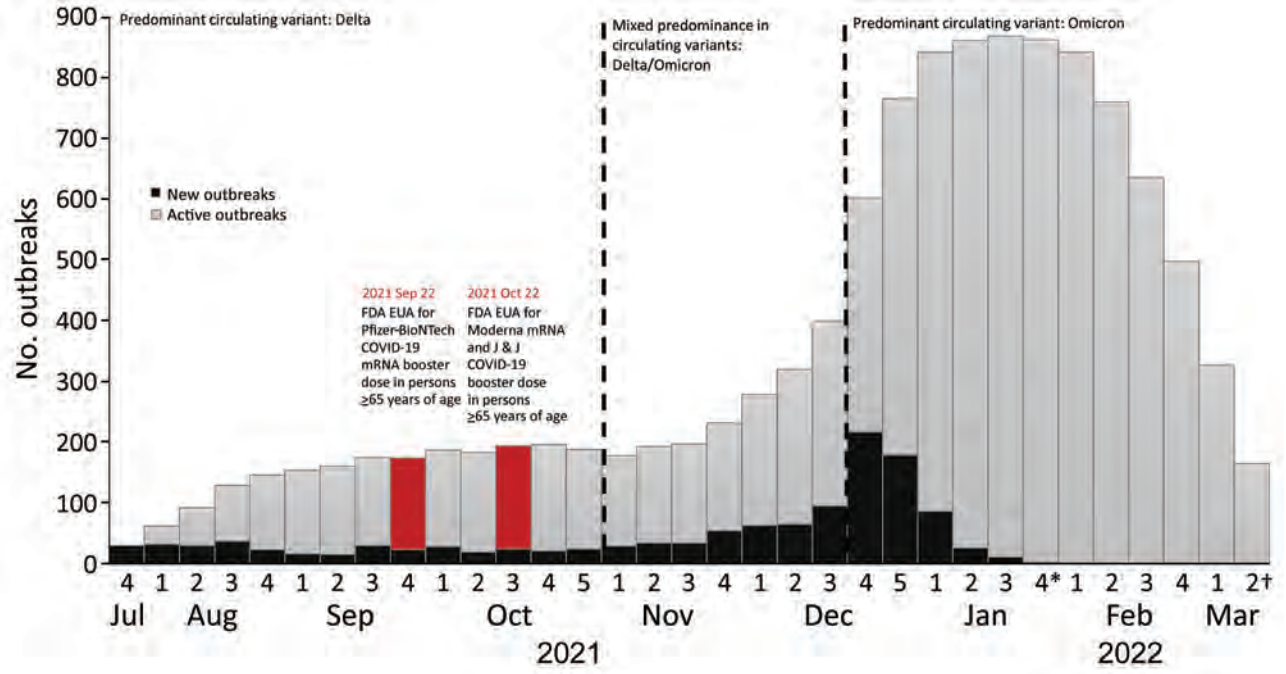

Figure 2. SARS-CoV-2 outbreaks in nursing homes (n = 1,247) by calendar time in weeks, United States, July 2021–March 2022. *January 31, 2022 was the last date for reporting new outbreaks; †resident infections for active outbreaks were reported through February 28, 2022, making March 14, 2022 the last date for an outbreak to close. Outbreaks that were not reported as closed by that date were considered still active. EUA, Emergency Use Authorization; FDA, Food and Drug Administration; J&J, Janssen/Johnson & Johnson, https://www.jnj.com; Pfizer-BioNTech, https://www.pfizer.com.

outbreaks per week in the Omicron period peaked in the fourth week of January 2022 (n = 861) and was 5 times greater than the peak of active outbreaks per week in the Delta period (n = 175), which occurred in the fourth week of October 2021.

Resident Attack Rates and Risk Ratios for Outcomes in Residents Who Received a Primary Vaccine Series Alone by Delta and Omicron Periods

Among residents who had received the primary vaccine series alone, the estimated risk for infection in the first 28 days of an outbreak was significantly higher during the Omicron period (35.0 [95% CI 29.3–40.1]/100 residents) than during the Delta period (7.5 [95% CI 6.2–9.0]/100 residents,) (risk ratio [RR] 4.7, 95% CI 3.6–6.9; p<0.001) (Figure 3). However, the estimated risk for severe outcomes was less than half for infected residents who had received a primary vaccine series alone during the Omicron period, including all-cause hospitalization (RR 0.44, 95% CI 0.35–0.54) and all-cause death (RR 0.38, 95% CI 0.30–0.49), compared with infected residents who had received a primary vaccine series alone during Delta period outbreaks (Figure 4).

Resident Attack Rates and Risk Ratios for Outcomes in the Omicron Period by Booster Status

The estimated risk for infection during the first 14 days of an Omicron-period outbreak was significantly lower among boosted residents (5.6 [95% CI 4.6–6.7]/100 residents) than among residents who had received a primary vaccine series alone (22.2 [95% CI 18.2–26.7]/100 residents) (RR 0.25, 95% CI 0.19–0.33; p<0.001) (Figure 5). Infected

Period of outbreak onset	Infected residents	Residents at risk	Crude AR per 100 residents	Adjusted RR (95% CI)
Delta	1,403	18,640	7.5	Referent
Omicron	2,242	6,351	35.3	4.7 (3.6–6.0)

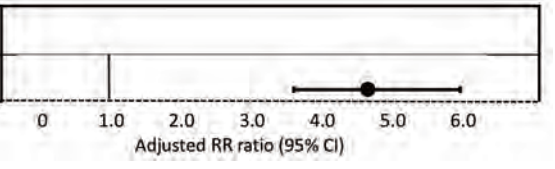

Figure 3. SARS-CoV-2 infection ARs and RRs per 100 nursing home residents by periods of Delta (n = 232) and Omicron (n = 279) variant predominance, United States, July 2021–March 2022. Values are given for residents who had received a primary vaccine series alone, adjusted for facility-level clustering. Resident infections were restricted to the first 28 days of outbreak because all reported outbreaks had at least a 28-day period for case ascertainment. AR, attack rate; RR, risk ratio.

	Outbreak period	Infected residents with outcome	Infected residents at risk	Crude risk	Adjusted RR (95% CI)
All-cause hospitalization	Delta	393	2,806	0.14	Referent
	Omicron	224	3,803	0.06	0.44 (0.35–0.54)
All-cause death	Delta	257	2,806	0.09	Referent
	Omicron	131	3,803	0.03	0.38 (0.30–0.49)

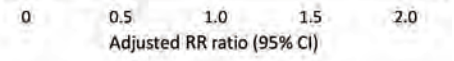

Figure 4. Crude risk and RRs for all-cause hospitalization and all-cause death among SARS-CoV-2–positive nursing home residents who had received a primary COVID-19 vaccine series alone by periods of Delta (n = 264) and Omicron (n = 459) variant predominance, United States, July 2021–March 2022. Values are adjusted for facility-level clustering. RR, risk ratio.

boosted residents were half as likely to have all-cause hospitalization (RR 0.48, 95% CI 0.40–0.59) and all-cause death (RR 0.45, 95% CI 0.34–0.59) than were residents who had received a primary vaccine series alone (Figure 6).

Discussion

By focusing on SARS-CoV-2 outbreaks in nursing homes during the Delta and Omicron periods, this study enables us to describe the effect of these variants within affected facilities and among residents. Five times as many active outbreaks occurred in nursing homes during the peak week of the Omicron period as occurred in the peak of the Delta period. In addition, outbreaks during the Omicron period were significantly larger and longer, and a greater percentage of residents were infected within the first 4 weeks of an outbreak. In contrast, once infected, residents vaccinated with a primary series alone had half the risk of being hospitalized or dying from any cause during the Omicron period than residents vaccinated with a primary series alone in the Delta period. During the Omicron period specifically, 66% (26,992/40,782) of residents had received a booster dose at the time of outbreak onset. Boosted residents in this period were 4 times less likely to get infected in the first 14 days of the outbreak than residents who had received a primary vaccine series alone and, among those infected, they were half as likely to be hospitalized or die from any cause during the follow-up period. In summary, the Omicron period was characterized by an abrupt rise in nursing home outbreak activity, with longer lasting and larger outbreaks compared with the Delta period; fortunately, some of these effects were offset by lower rates of resident hospitalization and death, particularly among persons who received a vaccine booster.

Reported outbreaks in nursing homes increased in December 2021, coinciding with the emergence of the Omicron variant in the United States (*19*). The number of active outbreaks increased over subsequent weeks, mirroring community rates, reflecting the enhanced transmissibility of the Omicron variant and reduced vaccine effectiveness compared with other variants (*4*,*14*). This rise also coincided with worsening staff shortages in nursing homes and increased visitation during the winter holiday season after COVID-19 visitor restrictions were relaxed (*20*). Our data reinforce that persons infected with the Omicron variant are less likely to suffer severe outcomes than are persons with Delta variant infections, both in the general population (*21*) and in nursing homes (*13*). Despite all-cause hospitalization rates being lower during Omicron relative to Delta, the crude number of total hospitalizations among infected residents who had received a booster or primary series during the Omicron period (n = 373) was similar to the number of hospitalizations among infected residents who had received a primary vaccine series alone in the Delta period (n = 393) and, moreover, occurred over a shorter period. Although we were unable to ascertain whether resident hospitalizations resulted from their SARS-CoV-2 infection, our findings indicate that both Delta and Omicron nursing home outbreaks likely placed substantial strains on the US healthcare system.

An analysis of aggregated weekly data from US national surveillance of skilled nursing facilities

Booster status at outbreak onset, Omicron period	Infected residents	Residents at risk	Crude AR per 100 residents	Adjusted RR (95% CI)
Primary series alone	1,412	6,351	22.2	Referent
Boosted	738	13,188	5.6	0.25 (0.19–0.33)

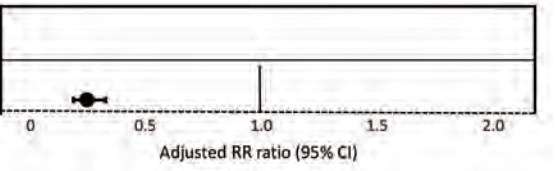

Figure 5. SARS-CoV-2 infection AR and RR per 100 nursing home residents by booster status at outbreak onset during Omicron period outbreaks alone (n = 279), United States, July 2021–March 2022. Values are adjusted for facility-level clustering. AR, attack rate; RR, risk ratio.

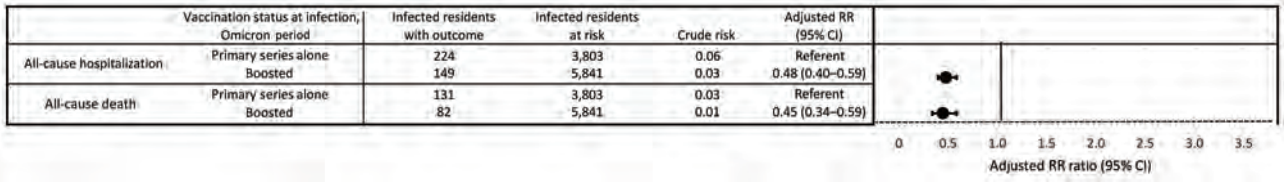

Figure 6. Crude risk and RR for all-cause hospitalization and all-cause death for SARS-CoV-2–positive nursing home residents by vaccination status at time of infection among Omicron period outbreaks alone (n = 509), United States, July 2021–March 2022. Values are adjusted for facility-level clustering. RR, risk ratio.

during February 14–March 27, 2022 (when Omicron was the predominant strain), found that boosted residents were half as likely to be infected (attack rate 2.6, 95% CI 2.5–2.7) than residents with a primary series alone (attack rate 5.0, 95% CI 4.9–5.1) (*14*). Our findings demonstrated similar but greater protection against infection after a booster dose, which was likely caused by several factors, such as a different surveillance period, population, and methodologic approach. Our analysis surveyed outbreaks earlier in the Omicron period, involved a subset of all facilities reporting to NHSN, and used resident-level data (rather than aggregate weekly reporting) to calculate attack rates.

The first limitation of this study is that, without the ability to link US public health and medical records at a national level, we relied on voluntary participation from health departments, which required time-intensive active follow up with facilities and laboratories. As a result, data collection required balancing the burden placed on health departments and nursing home staff with study goals. To ensure collection activities were tenable, we limited reporting of resident census and vaccination status of all residents to one time point (outbreak onset) and did not track resident movements (including discharges, transfers, and admissions). Second, surveillance definitions and recommendations for testing (*22*) were standardized, but investigation practices might have varied by jurisdiction depending on available resources, local policy, and nursing home availability or willingness to share data. That variability could have led to differences in case and outbreak ascertainment, classification of vaccination status at outbreak onset, and verification of hospitalization and death information for cases. Further, it was not feasible to ascertain whether SARS-CoV-2 was the primary reason for hospitalization or cause of death among infected residents. Fourth, the outcome follow-up period was linked to outbreak end date, which led to variations in follow-up times for individual infected residents. Adjusted estimates were not able to account for potential differences in time from infection to outcome by vaccination status or outcomes that occurred beyond the follow-up period. Fifth, specimens with sequence results were only available in ≈50% of all outbreaks because of varying protocols for specimen collection and retention. A sensitivity analysis of attack rates for severe outcomes was restricted to infected residents with confirmed sequencing and demonstrated similar results (Appendix Figure). Sixth, outbreak duration and total infected resident count were likely underestimated in outbreaks that were still active at the end of infection surveillance. As a result, we limited our analysis of outbreak duration and infection attack rates to the minimum number of days collected for all outbreaks.

Residents who received a booster dose might have differed from residents who received a primary vaccine series alone in ways that were not measured, such as medical history, previous SARS-CoV-2 infection and subsequent infection-induced immunity, end-of-life care, or even residing at a facility with enhanced infection prevention practices. In addition, the vaccination status of residents who were not SARS-CoV-2 positive was only reported at outbreak onset. To minimize the effect of unmeasured change in booster status during the course of the outbreak, we focused our comparison of infection attack rates by booster status recorded at outbreak onset and limited it to infections occurring during the first 14 days of the outbreak. Because of those limitations, we did not calculate formal vaccine effectiveness estimates.

Efforts to ensure residents stay up to date with COVID-19 vaccination schedules, which includes additional and booster doses (*23*), are critical to preventing SARS-CoV-2 infection and severe outcomes in nursing home outbreaks. Additional emphasis should be placed on vaccination programs alongside recommended infection prevention and control strategies for long-term care facilities during SARS-CoV-2 outbreaks (*22*), which have the potential to overburden existing nursing home capacities. Continued surveillance of nursing home outbreaks and associated infection attack rates and severe outcomes is warranted as new SARS-CoV-2 variants emerge.

Additional members of the MOVIN Surveillance Team: Joseph F. Perz (Centers for Disease Control and Prevention, Atlanta, Georgia, USA), Daniel Galanto (Chicago Department of Public Health, Chicago, Illinois, USA), Christy Zelinski (Chicago Department of Public Health, Chicago, Illinois, USA), Carly Lipke (Colorado Department of Public Health and Environment, Denver, Colorado, USA), Brooke McCain (Colorado Department of Public Health and Environment, Denver, Colorado, USA), Brandi Tolle (Colorado Department of Public Health and Environment, Denver, Colorado, USA), Wesley Hottel (Iowa Department of Public Health, Des Moines, Iowa, USA), Valérie Reeb (Iowa Department of Public Health, Des Moines, Iowa, USA), Meagan Burns (Massachusetts Department of Public Health, Jamaica Plain, Massachusetts, USA), Melissa Cumming (Massachusetts Department of Public Health, Jamaica Plain, Massachusetts, USA), Matthew Doucette (Massachusetts Department of Public Health, Jamaica Plain, Massachusetts, USA), Glen R. Gallagher (Massachusetts Department of Public Health, Jamaica Plain, Massachusetts, USA), Amanda Slider (Massachusetts Department of Public Health, Jamaica Plain, Massachusetts, USA), Kevin Cueto (Nebraska Department of Health and Human Services, Lincoln, Nebraska, USA), Jonathan Figliomeni (Nebraska Department of Health and Human Services, Lincoln, Nebraska, USA), Shermalyn R. Greene (North Carolina Department of Health and Human Services, Raleigh, North Carolina, USA), Rebecca Pierce (Oregon Health Authority, Portland, Oregon, USA), Amanda E. Faulkner (Oregon Health Authority, Portland, Oregon, USA), Megan Davis (South Carolina Department of Health and Environmental Control, Columbia, South Carolina, USA), Jennifer L. Donehue (South Carolina Department of Health and Environmental Control, Columbia, South Carolina, USA), Terri Hannibal (South Carolina Department of Health and Environmental Control, Columbia, South Carolina, USA), Alison Jamison-Haggwood (South Carolina Department of Health and Environmental Control, Columbia, South Carolina, USA), LaKita D. Johnson (South Carolina Department of Health and Environmental Control, Columbia, South Carolina, USA), Hannah V. Ruegner (South Carolina Department of Health and Environmental Control, Columbia, South Carolina, USA)

Acknowledgments

We thank the Colorado Department of Public Health and Environment COVID-19 Infection Prevention Unit, Colorado Department of Public Health and Environment COVID-19 Regional Epidemiology Response Teams, Colorado Department of Public Health and Environmental COVID-19 Residential Care Epidemiology Team, Colorado State Public Health Laboratory, Brynn Berger, Kaitlin Greenberg, Ramisa Rahman, Tiara Conteh, Summer Shore, Massachusetts State Public Health Molecular Diagnostic and Next Generation Sequencing Laboratory, Saritha Hunter, Claudia J. Crawford, Stephen Rauscher, Justin Albertson, Emily Huseynova, Catherine "Kitty" Chase, North Carolina State Laboratory of Public Health Virology, Molecular Diagnostics and Epidemiology COVID-19 Response Team, Carolina Community Tracing Collaborative – Cluster Outbreak Response Team, Oregon State Public Health Laboratory, and the Oregon COVID-19 Response and Recovery Unit.

About the Author

Dr. Wilson was an Epidemic Intelligence Service Officer for the Division of Healthcare Quality Promotion, National Center for Emerging and Zoonotic Infectious Diseases, Centers for Disease Control and Prevention, stationed in Atlanta, Georgia, during this work. His research interests include public health surveillance and healthcare-associated infections.

References

1. World Health Organization. Update on Omicron. 2021 [cited 2022 Jun 6]. https://www.who.int/news/item/28-11-2021-update-on-omicron
2. Mannar D, Saville JW, Zhu X, Srivastava SS, Berezuk AM, Tuttle KS, et al. SARS-CoV-2 Omicron variant: antibody evasion and cryo-EM structure of spike protein-ACE2 complex. Science. 2022;375:760–4. https://doi.org/10.1126/science.abn7760
3. Wang L, Cheng G. Sequence analysis of the emerging SARS-CoV-2 variant Omicron in South Africa. J Med Virol. 2022;94:1728–33. https://doi.org/10.1002/jmv.27516
4. Accorsi EK, Britton A, Fleming-Dutra KE, Smith ZR, Shang N, Derado G, et al. Association between 3 doses of mRNA COVID-19 vaccine and symptomatic infection caused by the SARS-CoV-2 Omicron and Delta variants. JAMA. 2022;327:639–51. https://doi.org/10.1001/jama.2022.0470
5. Ulloa AC, Buchan SA, Daneman N, Brown KA. Estimates of SARS-CoV-2 Omicron variant severity in Ontario, Canada. JAMA. 2022;327:1286–8. https://doi.org/10.1001/jama.2022.2274
6. Bialek S, Boundy E, Bowen V, Chow N, Cohn A, Dowling N, et al.; CDC COVID-19 Response Team. Severe outcomes among patients with coronavirus disease 2019 (COVID-19)—United States, February 12–March 16, 2020. MMWR Morb Mortal Wkly Rep. 2020;69:343–6. https://doi.org/10.15585/mmwr.mm6912e2
7. Bagchi S, Mak J, Li Q, Sheriff E, Mungai E, Anttila A, et al. Rates of COVID-19 among residents and staff members in nursing homes—United States, May 25–November 22, 2020. MMWR Morb Mortal Wkly Rep. 2021;70:52–5. https://doi.org/10.15585/mmwr.mm7002e2
8. Arons MM, Hatfield KM, Reddy SC, Kimball A, James A, Jacobs JR, et al.; Public Health–Seattle and King County and CDC COVID-19 Investigation Team. Presymptomatic SARS-CoV-2 infections and transmission in a skilled nursing facility. N Engl J Med. 2020;382:2081–90. https://doi.org/10.1056/NEJMoa2008457

9. Food and Drug Administration. FDA takes key action in fight against COVID-19 by issuing Emergency Use Authorization for first COVID-19 vaccine. 2020 [cited 2021 Dec 9]. https://www.fda.gov/news-events/press-announcements/fda-takes-key-action-fight-against-covid-19-issuing-emergency-use-authorization-first-covid-19
10. Food and Drug Administration. Coronavirus (COVID-19) update: FDA authorizes additional vaccine dose for certain immunocompromised individuals. 2021 [updated 2021 Aug 12]. https://www.fda.gov/news-events/press-announcements/coronavirus-covid-19-update-fda-authorizes-additional-vaccine-dose-certain-immunocompromised
11. Food and Drug Administration. Coronavirus (COVID-19) updated: FDA takes additional actions on the use of a booster dose for COVID-19 vaccines. 2021 Oct 20 [cited 2021 Dec 15]. https://www.fda.gov/news-events/press-announcements/coronavirus-covid-19-update-fda-takes-additional-actions-use-booster-dose-covid-19-vaccines
12. Centers for Disease Control and Prevention. Interim clinical consideration: use of COVID-19 vaccines in the United States [cited 2022 Apr 15]. https://www.cdc.gov/vaccines/covid-19/clinical-considerations/covid-19-vaccines-us.html
13. Krutikov M, Stirrup O, Nacer-Laidi H, Azmi B, Fuller C, Tut G, et al.; COVID-19 Genomics UK consortium. Outcomes of SARS-CoV-2 omicron infection in residents of long-term care facilities in England (VIVALDI): a prospective, cohort study. [Erratum in: Lancet Healthy Longev. 2022;3:e587]. Lancet Healthy Longev. 2022;3:e347–55. https://doi.org/10.1016/S2666-7568(22)00093-9
14. Prasad N, Derado G, Nanduri SA, Reses HE, Dubendris H, Wong E, et al. Effectiveness of a COVID-19 additional primary or booster vaccine dose in preventing SARS-CoV-2 infection among nursing home residents during widespread circulation of the Omicron variant—United States, February 14–March 27, 2022. MMWR Morb Mortal Wkly Rep. 2022;71:633–7. https://doi.org/10.15585/mmwr.mm7118a4
15. Wilson WW, Keaton AA, Ochoa LG, Hatfield KM, Gable P, Walblay KA, et al. SARS-CoV-2 outbreaks in nursing homes involving residents who had completed a primary COVID-19 vaccine series—13 U.S. Jurisdictions, July–November 2021. Infect Control Hosp Epidemiol. 2023 Jan 16 [Epub ahead of print].
16. Centers for Disease Control and Prevention. Stay up to date with COVID-19 vaccines including boosters [cited 2022 Apr 15]. https://www.cdc.gov/coronavirus/2019-ncov/vaccines/stay-up-to-date.html
17. Centers for Disease Control and Prevention. COVID data tracker: variant proportions [cited 2022 Mar 1]. https://covid.cdc.gov/covid-data-tracker/#variant-proportions
18. Harris-Kojetin LSM, Lendon JP, Rome V, Valverde R, Caffrey C. Long-term care providers and services users in the United States, 2015–2016. Vital and Health Statistics. 2019;3(43) [cited 2022 May 15]. https://stacks.cdc.gov/view/cdc/76253
19. CDC COVID-19 Response Team. SARS-CoV-2 B.1.1.529 (Omicron) variant—United States, December 1-8, 2021. MMWR Morb Mortal Wkly Rep. 2021;70:1731–4. https://doi.org/10.15585/mmwr.mm7050e1
20. Centers for Medicare and Medicaid Services. Nursing home visitation—COVID-19 (REVISED). 2021 [cited 2021 Jun 14]. https://www.cms.gov/medicareprovider-enrollment-and-certificationsurveycertificationgeninfopolicy-and-memos-states-and/nursing-home-visitation-covid-19-revised
21. Fall A, Eldesouki RE, Sachithanandham J, Morris CP, Norton JM, Gaston DC, et al. The displacement of the SARS-CoV-2 variant Delta with Omicron: an investigation of hospital admissions and upper respiratory viral loads. EBioMedicine. 2022;79:104008. https://doi.org/10.1016/j.ebiom.2022.104008
22. Centers for Disease Control and Prevention. Testing: create a plan for testing residents and hcp for SARS-CoV-2. 2021 [cited 2021]. https://www.cdc.gov/coronavirus/2019-ncov/hcp/long-term-care.html#anchor_1631031062858
23. Centers for Disease Control and Prevention. COVID-19 vaccine boosters [cited 2022 May 16]. https://www.cdc.gov/coronavirus/2019-ncov/vaccines/booster-shot.html

Address for correspondence: W. Wyatt Wilson, Centers for Disease Control and Prevention, 1600 Clifton Rd NE, Mailstop H16-3, Atlanta, GA 30329-4027, USA; email: wuw7@cdc.gov

Effectiveness of BNT162b2 Vaccine against Omicron Variant Infection among Children 5–11 Years of Age, Israel

Aharona Glatman-Freedman, Yael Hershkovitz, Rita Dichtiar, Alina Rosenberg, Lital Keinan-Boker, Michal Bromberg

We assessed effectiveness of the BNT162b2 vaccine against infection with the B.1.1.529 (Omicron) variant (mostly BA.1 subvariant), among children 5–11 years of age in Israel. Using a matched case–control design, we matched SARS-CoV-2–positive children (cases) and SARS-CoV-2–negative children (controls) by age, sex, population group, socioeconomic status, and epidemiologic week. Vaccine effectiveness estimates after the second vaccine dose were 58.1% for days 8–14, 53.9% for days 15–21, 46.7% for days 22–28, 44.8% for days 29–35, and 39.5% for days 36–42. Sensitivity analyses by age group and period demonstrated similar results. Vaccine effectiveness against Omicron infection among children 5–11 years of age was lower than vaccine efficacy and vaccine effectiveness against non-Omicron variants, and effectiveness declined early and rapidly.

Use of the BNT162b2 vaccine (Pfizer-BioNTech, https://www.pfizer.com) among children 5–11 years of age was approved by the US Food and Drug Administration and the European Medicines Agency in October 2021 (*1*,*2*). The approval was given after a randomized clinical trial conducted by the manufacturer found vaccine efficacy of 90.7% (95% CI 67.7%–98.3%) against laboratory-confirmed symptomatic COVID-19 with onset of ≥7 days after the second dose among 2,268 children in this age group who were included in that trial (*3*). In Israel, the vaccine was approved for children 5–11 years of age on November 14, 2021 (*4*), and the vaccination campaign was rolled out on November 22, 2021 (*5*). The BNT162b2 vaccination regimen for children 5–11 years of age consists of two 10-μg doses administered 21 days apart (*3*). By February 15, 2022, a total of 215,707 children had received 2 doses (18.2% of children in this age group in Israel), and 308,813 had received 1 dose (26.1% of children in this age group in Israel.

Shortly after the vaccination campaign among children 5–11 years of age began in Israel, the B.1.1.529 (Omicron) SARS-CoV-2 variant was identified in South Africa (*6*) and rapidly spread throughout the world (*7*). The Omicron variant has been described as having 30 aa substitutions, 3 insertions, and 6 aa deletions within the spike protein (*8*). The first case of infection with the Omicron variant was reported in Israel on November 27, 2021 (*9*), and by January 10, 2022, >90% of the sequenced samples in Israel were identified as the Omicron variant (*10*).

In this study, we evaluated BNT162b2 vaccine effectiveness (VE) against SARS-CoV-2 infection among Israeli children 5–11 years of age during the Omicron-predominant period, which consisted mostly of the BA.1 subvariant. VE represents the degree to which vaccine prevents disease in real-world use, compared with vaccine efficacy, which indicates a controlled trial scenario. Approval for this study was granted by the Israel MOH superior ethics committee (protocol CoR-MOH-081–2021).

Methods

Study Design

After the second vaccine dose was given as part of the vaccine campaign for children 5–11 years of age, we estimated VE among Israel resident children who had

Author affiliations: Israel Center for Disease Control, Israel Ministry of Health, Ramat Gan, Israel (A. Glatman-Freedman, Y. Hershkovitz, R. Dichtiar, A. Rosenberg, L. Keinan-Boker, M. Bromberg); Tel Aviv University School of Public Health, Tel Aviv, Israel (A. Glatman-Freedman, M. Bromberg); Haifa University School of Public Health, Haifa, Israel (L. Keinan-Boker)

DOI: https://doi.org/10.3201/eid2904.221285

not been infected with SARS-CoV-2 (as documented by PCR or official rapid antigen test) before the study period. We applied a matched case–control study design to estimate VE against SARS-CoV-2 infection for days 8–14, 15–21, 22–28, 29–35, and 36–42 after receipt of the second BNT162b2 vaccine dose and compared the vaccination status of children positive for SARS-CoV-2 by PCR (cases) with that of children negative for SARS-CoV-2 by PCR (controls).

During the early stages of the SARS-CoV-2 pandemic, multiple testing sites for SARS-CoV-2 were established throughout Israel. Those sites were operated by health maintenance organizations or by government-appointed operators, and testing was free of charge. During the Omicron wave, both PCR and rapid antigen tests were used, and results were entered into a national SARS-CoV-2 tests database.

To conduct our analyses, we used 2 Ministry of Health (MOH) national databases: the SARS-CoV-2 tests database and the SARS-CoV-2 vaccine database. The data retrieved from the databases included BNT162b2 vaccination status, BNT162b2 vaccination dates, PCR test dates and results, age, sex, population group (ultra-Orthodox Jews, general [which included non–ultra-Orthodox Jews and non-Arab minorities], and Arabs, based on statistical geographic area of a child's residence), socioeconomic status (based on statistical geographic area), hospitalization, and the most severe clinical status (severe/critical disease or death) of hospitalized children. Severity of disease was determined according to the National Institutes of Health guidelines (*11*). For both databases, the unique personal identity numbers were encrypted twice.

We extracted data for January 20–February 15, 2022 (evaluation period). Those dates were selected because of the predominance of the Omicron variant, which exceeded 97% (*10*) and was predominantly BA.1. We excluded from analysis children who were SARS-CoV-2-positive by PCR or rapid antigen test before the evaluation period.

For children who had >1 positive PCR result during the evaluation period, only the first positive test was included in the analysis. For children who had >1 negative PCR result during the evaluation period, only the first negative test was included in the analysis. We excluded from analysis children who had a positive rapid antigen test result before a PCR test during the evaluation period. Each child who became SARS-CoV-2–positive during the evaluation period (case) was matched with 1 SARS-CoV-2–negative child (control) by age group (5–7, 8–9, and 10–11 years of age), sex, population group, socioeconomic status (low, medium, and high), and epidemiologic week of PCR sampling. We developed a flow diagram of the PCR tests included in and excluded from VE analyses (Appendix Figure 1, https://wwwnc.cdc.gov/EID/article/29/4/22-1285-App1.pdf).

We calculated the number and percentage of hospitalizations, severe or critical illnesses, or deaths among the cases who were hospitalized within 14 days of sampling, according to vaccination status. The selection of 14-day follow-up was based on a histogram delineating the time from first SARS-CoV-2 PCR sampling to hospitalization (Appendix Figure 2). Our data did not allow distinction between SARS-CoV-2–positive children hospitalized for COVID-19 or for other reasons.

Statistical Analyses

To estimate the BNT162b2 VE, we used the formula (1 – OR) × 100, in which OR (odds ratio) represents the odds of cases being vaccinated divided by the odds of controls being vaccinated. We used conditional logistic regression for the analyses.

We applied the matching process and the statistical model separately for each week since receipt of the second vaccine dose (i.e., days 8–14, 15–21, 22–28, 29–35, and 36–42 since the second vaccine dose). To evaluate the robustness of the VE estimates, we performed 2 sensitivity analyses. For the first analysis, to determine if age-specific differences in VE estimates existed, we divided the data by age group (5–8 and 9–11 years) and conducted the same analysis for each group separately. For the second sensitivity analysis, to determine if VE estimates varied with the dynamics of infection, we divided the data by period and conducted the same analysis for each period separately. Period 1, which occurred around the peak of the Omicron wave in Israel, lasted from January 20 through February 2, 2022 (14 days). Period 2, which occurred during the decline in new SARS-CoV-2 cases, lasted from February 3 through February 15, 2022 (13 days). We also calculated the mean and median intervals (in days) between the second vaccine dose and the positive SARS-CoV-2 result for study participants in periods 1 and 2. To perform statistical analyses, we used SAS Enterprise Guide 7.1 software (SAS Institute Inc., https://www.sas.com).

Results

Vaccination Campaign

From November 22, 2021, through February 15, 2022, a total of 214,259 children 5–11 years of age received 2 BNT162b2 vaccine doses (Figure 1). That number represents 20.5% of children 5–11 years of age in Israel (*12*).

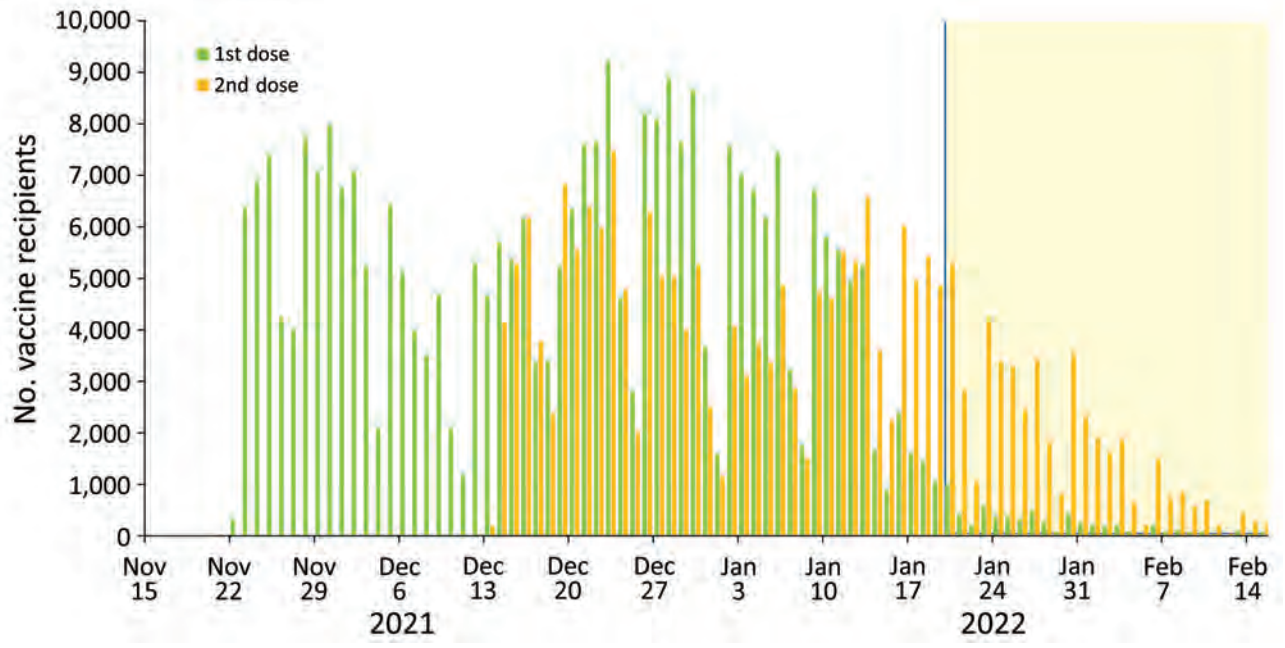

Figure 1. Progress of SARS-CoV-2 vaccination campaign among children 5–11 years of age by daily vaccine recipients, Israel. Green bars represent first-dose recipients; orange bars represent second-dose recipients; yellow highlighting represents the vaccine effectiveness evaluation period.

VE against SARS-CoV-2 Infection

During the evaluation period, we identified 78,541 SARS-CoV-2–positive eligible cases, of which 14,831 were second-dose recipients and 63,710 were unvaccinated. Case characteristics are summarized (Table 1). VE estimates after the second vaccine dose were 58.1% (95% CI 55.5%–60.6%) for days 8–14, 53.9% (95% CI 51.0%–56.5%) for days 15–21, 46.7% (95% CI 43.3%–49.9%) for days 22–28, 44.8% (95% CI 41.9%–47.6%) for days 29–35, and 39.5% (95% CI 36.1%–42.8%) for days 36–42 (Figure 2; Table 2).

Sensitivity Analyses

VE estimates for children in the 5–8- and 9–11-year age groups (Figure 3, panels A, B; Appendix Table) were similar to those found in the primary analysis (Figure 2; Table 2). Specifically, estimates of VE 8–14 days after the second vaccine dose were 60.0% (95% CI 56.5%–63.2%) for the 5–8-year age group and 58.4% (95% CI 54.4%–62.0%) for the 9–11-year age group (Appendix Table), compared with 58.1% (95% CI 55.5%–60.6%) for the primary analysis (Table 2). VE estimates 36–42 after the second vaccine dose were 39.4% (95% CI 34.3%–44.0%) for the 5–8-year age group and 39.6% (95% CI 34.8%–43.9%) for the 9–11-year age group (Appendix Table), compared with 39.5% (95% CI 36.1%–42.8%) for the primary analysis (Table 2).

Sensitivity analysis by period demonstrated that estimates of VE after the second vaccine dose for periods 1 and 2 (Figure 3, panels C, D; Appendix Table) were similar to those of the primary analysis (Figure 2; Table 2). Specifically, estimates of VE 8–14 days after the second vaccine dose were 59.0% (95% CI 56.1%–61.7%) for period 1 and 52.6% (95% CI 45.1%–59.1%) for period 2 (Appendix Table), compared with 58.1% (95% CI 55.5%–60.6%) for the primary analysis (Table 2). VE estimates 36–42 days after the second

Table 1. Characteristics of SARS-CoV-2 cases included in study of effectiveness of BNT162b2 vaccine against Omicron variant infection in children 5–11 years of age, January 20–February 15, 2022, Israel

Variable	Cases, no. (%), n = 78,541
Age, y	
5	9,783 (12.5)
6	11,310 (14.4)
7	11,529 (14.7)
8	11,599 (14.8)
9	11,468 (14.6)
10	11,562 (14.7)
11	11,290 (14.4)
Sex	
F	39,175 (49.9)
M	39,366 (50.1)
Population group	
Ultra-Orthodox Jews	2,194 (2.8)
General*	54,700 (69.6)
Arabs	21,647 (27.6)
Socioeconomic status	
Low	26,048 (33.2)
Medium	36,515 (46.5)
High	15,978 (20.3)

*Includes non–ultra-Orthodox Jews and non-Arab minorities.

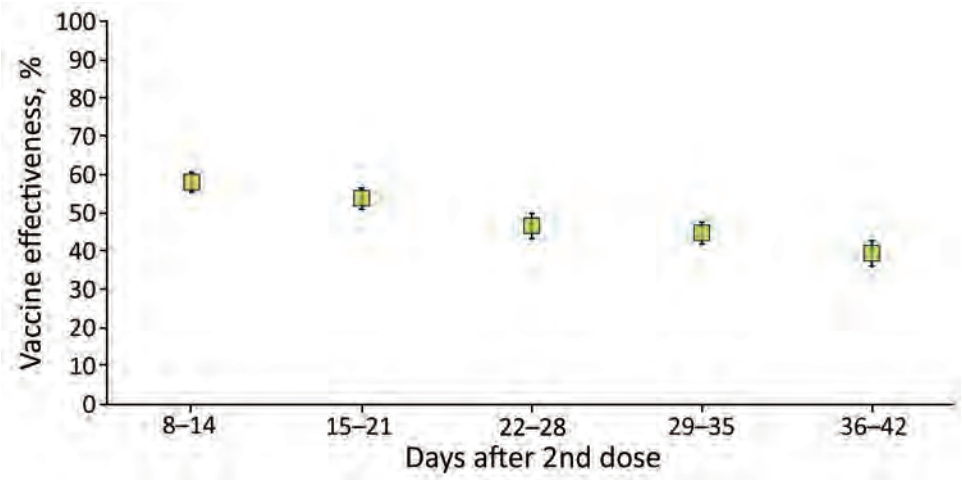

Figure 2. Vaccine effectiveness after second dose of BNT162b2 (Pfizer-BioNTech, https://www.pfizer.com) among children 5–11 years of age, Israel, January 20–February 15, 2022. The center of each symbol is the point estimate; error bars indicate 95% CIs.

vaccine dose were 39.0% (95% CI 35.1%–42.7%) for period 1 and 41.1% (95% CI 34.0%–47.5%) for period 2 (Appendix Table) compared with 39.5% (95% CI 36.1%–42.8%) for the primary analysis (Table 2).

The mean and median days calculated for intervals between the second vaccine dose and the positive SARS-CoV-2 PCR among study participants were similar for both periods. Specifically, the mean (±SD) was 26.5 (±10.1) days for period 1 and 26.5 (±9.3) days for period 2, and the median was 28 days for period 1 and 26 days for period 2. The small difference in medians between periods was not significant (p = 0.53).

Hospitalization, Severe/Critical Disease, and Death

Of the 78,541 SARS-CoV-2–positive children in the study, 102 (0.13%) were hospitalized within 14 days of their swab sample collection date (Table 3). A total of 93 (0.15%) were unvaccinated, and 9 had received 2 vaccine doses (0.06%) (Table 3). The vaccinated children were SARS-CoV-2 positive ≥8 days after the second vaccine dose. A total of 8 hospitalized children were defined as severely/critically ill, and no deaths were reported. All 8 (0.01%) severely/critically ill children were unvaccinated (Table 3).

Discussion

We demonstrated that VE of the BNT162b2 vaccine against SARS-CoV-2 infection with the Omicron variant (predominantly BA.1 subvariant) among children 5–11 years of age was substantially lower than the 90.7% (95% CI 67.7%–98.3%) vaccine efficacy found in a clinical trial conducted before the Omicron variant emerged (*3*). Furthermore, our findings suggest the occurrence of an early decline in VE among children in this age group during the study period. This pattern of VE decline was found in the 5–8- and 9–11-year age groups, both of which received a smaller vaccine dose than that approved for persons ≥12 years of age. A similar decline in VE occurred during 2 time periods of the study, one representing the peak of SARS-CoV-2 cases and the other representing a decline in the number of cases.

VE against Omicron infection among children 5–11 years of age in Israel was also lower than the reported VE against infection with non-Omicron variants for other age groups after the second vaccine dose. Specifically, although reported VE against infection with non-Omicron (mostly Alpha) variants 15–21 days after the second vaccine dose was 96.8% (95% CI 96.1%–97.4%) among persons ≥16 years of age and 91.2% (95% CI 87.4%–93.8%) against infection with the Delta variant among persons 12–15 years of age (*13*,*14*), VE during the equivalent period in our study was 53.9% (95% CI 50.1%–56.5%).

Several groups reported VE estimates against the Omicron variant among children 5–11 years of age that were substantially lower than reported VE estimates

Table 2. VE against SARS-CoV-2 infection among children 5–11 years of age, by time after the second vaccine dose, January 20–February 15, 2022, Israel*

Days since 2nd vaccine dose	Cases		Controls		Total cases, no.	Total controls, no.	VE (95% CI)
	Second-dose recipients, no.	Unvaccinated, no.	Second-dose recipients, no.	Unvaccinated, no.			
8–14	1,655	54,843	3,674	52,824	56,498	56,498	58.1 (55.5–60.6)
15–21	1,814	54,813	3,636	52,991	56,627	56,627	53.9 (51.0–56.5)
22–28	1,732	54,554	3,080	53,206	56,286	56,286	46.7 (43.3–49.9)
29–35	2,778	54,776	4,629	52,925	57,554	57,554	44.8 (41.9–47.6)
36–42	2,435	54,627	3,753	53,309	57,062	57,062	39.5 (36.1–42.8)

*VE, vaccine effectiveness.

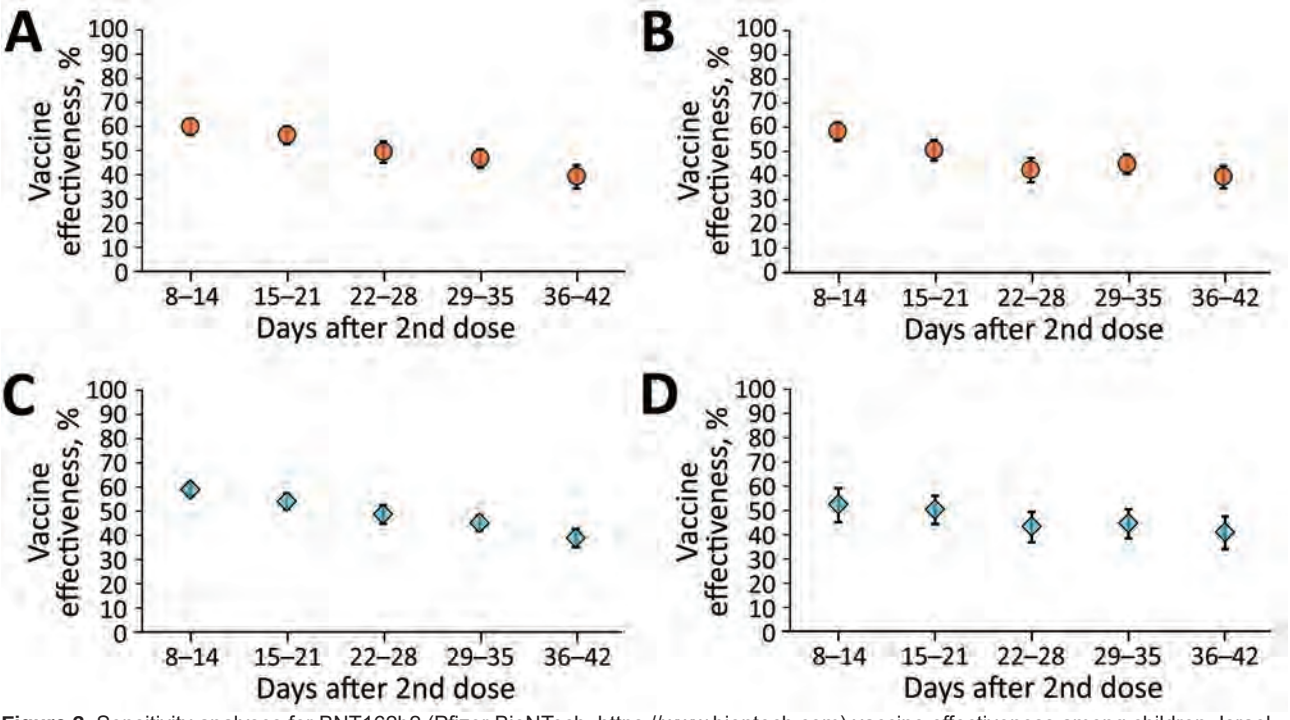

Figure 3. Sensitivity analyses for BNT162b2 (Pfizer BioNTech, https://www.biontech.com) vaccine effectiveness among children, Israel. A) Children 5–8 years of age, January 20–February 15, 2022; B) children 9–11 years of age, January 20–February 15, 2022; C) children 5–11 years of age, period 1 (January 20–February 2, 2022); D) children 5–11 years of age, period 2 (February 3–15, 2022). The center of each symbol is the point estimate; error bars indicate 95% CIs.

against non-Omicron variants. A study from 4 US states demonstrated that the adjusted VE against symptomatic and asymptomatic Omicron infection at 14–82 days after the second BNT162b2 vaccine dose among children 5–11 years of age was 31% (95% CI 9%–48%) (*15*). A study from Singapore demonstrated VE of 36.8% (95% CI 35.3%–38.2%) after 2 BNT162b2 vaccine doses (*16*). A previous study from Israel demonstrated a short-term (7–21 days after the second dose) BNT162b2 VE of 51% (95% CI 39%–61%) against infection and 48% (95% CI 29%–63%) against symptomatic disease (*17*).

However, a possible rapid decline of VE for this age group during an Omicron-predominant period was suggested in studies from 2 countries. A study from the United States demonstrated that VE against symptomatic SARS-CoV-2 infection among children 5–11 years of age was 60.1% (95% CI 54.7%–64.8%) at 2–4 weeks and 28.9% (95% CI 24.5%–33.1%) at 2 months after the second vaccine dose (*18*). A study from New York state also suggested that protection against Omicron infection declined rapidly after the second vaccine dose (*19*). A study from Italy demonstrated that adjusted VE against infection decreased from 38.7% (95% CI 37.7%–39.7%) at 14–28 days after the second BNT162b2 vaccine dose to 21.2% (95% CI 19.7%–22.7%) at 57–97 days after the second dose (the investigators did not consider days 0–14 after the second dose as full vaccination status) (*20*).

Studies that compared VE of 2 doses of mRNA vaccine against the Omicron and the Delta variants in older persons demonstrated that VE against Omicron is lower than VE against Delta. Those VE differences were demonstrated against SARS-CoV-2 infection (C.H. Hansen et al., unpub. data, https://www.medrxiv.org/content/10.1101/2021.12.20.21267966), symptomatic diseases (*21*), emergency department

Table 3. SARS-CoV-2–positive children 5–11 years of age hospitalized within 14 days of sampling, Israel

Variable	Second-dose recipients, no. (%), n = 14,831	Unvaccinated, no. (%), n = 63,710	Total, no. (%), n = 78,541
Hospitalized	9 (0.06)	93 (0.15)	102 (0.13)
Severe/critical illness*	0	8 (0.01)	8 (0.01)
Died	0	0	0

*Severe Illness: oxygen saturation (SpO2) <94% on room air at sea level, a ratio of arterial partial pressure of oxygen to fraction of inspired oxygen (PaO2/FiO2) <300 mm Hg, respiratory rate >30 breaths/min, or lung infiltrates >50% (*11*). Critical Illness: respiratory failure, septic shock, and/or multiple organ dysfunction (*11*).

and acute care visits (*22*), hospitalizations (*23*), and severe outcomes (*24*). Administration of mRNA vaccine booster doses also resulted in lower VE against symptomatic diseases as well as fewer urgent care visits and emergency department visits for infection with Omicron than for infection with Delta (*21*,*22*).

Neutralization titers of the Omicron variant by serum from vaccine recipients and recovered persons who had been infected with non-Omicron variants were considerably reduced, or neutralization failed (*8*). Neutralization titers against the Omicron variant were boosted after the third vaccine dose but to a lesser degree than for other variants (*8*,*25*).

Among the advantages of our study, we provide weekly VE estimates during the evaluation period, whereas 2 other studies of children 5–11 years of age used longer intervals between VE estimates (*18*,*20*). The weekly VE estimates enabled us to demonstrate that the rapid VE waning started soon after the second BNT162b2 vaccine dose. In addition, we evaluated VE during a period when Omicron predominance exceeded 97%, thus minimizing the possibility of a Delta variant effect on estimation of VE.

Our study was limited by being unable to adjust VE estimates for the underlying conditions because of the nature of the MOH databases. We were also unable to estimate VE against symptomatic disease because of paucity of this data. The value of estimating VE against infection cannot be underestimated because the SARS-CoV-2 pandemic unveiled that a substantial portion of the population can be asymptomatic and still transmit the virus (*26*). In that regard, a recent study demonstrated that symptomatic as well as asymptomatic children can carry high amounts of live, replicating virus, which can serve as a potential reservoir for virus transmission (*27*). Another study reported that SARS-CoV-2 RNA loads among children with COVID-19 symptoms were comparable to those among asymptomatic children (*28*). An additional study limitation results from having only small numbers of children who were hospitalized or had severe/critical disease and no deaths, precluding us from estimating VE against those outcomes.

Evaluating VE only among children who were tested by PCR may result in selection bias. As the number of Omicron cases in Israel increased, the Israel MOH recommended PCR testing for persons ≥60 years of age and at high risk and that all other persons be tested by rapid antigen test instead (*29*). However, despite those instructions, which went into effect on January 7, 2022, PCR tests were performed also for residents <60 years of age, including children, in part because of long lines at official rapid antigen test–specific sites. Thus, the daily rate of PCR testing among vaccinated children remained >1.3% during the evaluation period. In that regard, estimating VE against influenza by using the test-negative case–control design has been based on testing only a small fraction of all patients with influenza-related signs/symptoms, and the sampling methods have varied from study to study. Thus, the possibility of selection bias exists also for influenza VE studies. Israel has had very robust national PCR testing for SARS-CoV-2; however, as the pandemic evolved, the number of persons tested (by PCR or antigen) has gradually declined. As such, similar to estimating VE against influenza, future SARS-CoV-2 VE studies will also have to rely on smaller fractions of the population. That the SARS-CoV-2 PCR testing policy in Israel was not strictly adhered to when official rapid antigen testing was introduced and the consistent results of our sensitivity analyses reduce the effect or likelihood of substantial selection bias in our study.

In conclusion, our findings indicate that, after 2 BNT162b2 vaccine doses, protection against infection with the Omicron variant among children 5–11 years of age was lower than protection reported against non-Omicron variants. Our study further suggests that protection against Omicron infection wanes rapidly among children in this age group.

A.G.-F., M.B., and L.K.B. contributed to the study design. Y.H. and R.D. retrieved the data and performed data analysis. A.G.-F. wrote the first draft of the manuscript. A.G.-F., A.R., M.B., and L.K.-B. interpreted the data. Y.H. and R.D. verified the underlying data. All authors reviewed the manuscript critically for important intellectual content, edited, and approved the final manuscript.

About the Author

Dr. Glatman-Freedman is the department director of infectious diseases at the Israel Center for Disease Control. She is affiliated academically with the School of Public Health at Tel Aviv University. Her primary research interests are the epidemiology of respiratory viruses, syndromic surveillance, and vaccine effectiveness.

References

1. Food and Drug Administration. FDA authorizes Pfizer-BioNTech COVID-19 vaccine for emergency use in children 5 through 11 years of age [cited 2021 Dec 27]. https://www.fda.gov/news-events/press-announcements/fda-authorizes-pfizer-biontech-covid-19-vaccine-emergency-use-children-5-through-11-years-age
2. European Medicines Agency. Comirnaty COVID-19 vaccine: EMA recommends approval for children aged 5 to 11 [cited 2021 Dec 27]. https://www.ema.europa.eu/en/news/comirnaty-covid-19-vaccine-ema-recommends-approval-children-aged-5-11

3. Walter EB, Talaat KR, Sabharwal C, Gurtman A, Lockhart S, Paulsen GC, et al.; C4591007 Clinical Trial Group. Evaluation of the BNT162b2 Covid-19 vaccine in children 5 to 11 years of age. N Engl J Med. 2022;386:35–46. https://doi.org/10.1056/NEJMoa2116298
4. Israel Ministry of Health. Ministry of Health Director General accepted the recommendation to vaccinate children 5 to 11 [cited 2021 Dec 27]. https://www.gov.il/en/departments/news/14112021-05
5. Israel Ministry of Health. Vaccination appointments for children now available on HMOs [cited 2021 Dec 27]. https://www.gov.il/en/departments/news/22112021-01
6. Wolter N, Jassat W, Walaza S, Welch R, Moultrie H, Groome M, et al. Early assessment of the clinical severity of the SARS-CoV-2 Omicron variant in South Africa: a data linkage study. Lancet. 2022;399:437–46. https://doi.org/10.1016/S0140-6736(22)00017-4
7. Meo SA, Meo AS, Al-Jassir FF, Klonoff DC. Omicron SARS-CoV-2 new variant: global prevalence and biological and clinical characteristics. Eur Rev Med Pharmacol Sci. 2021;25:8012–8.
8. Dejnirattisai W, Huo J, Zhou D, Zahradník J, Supasa P, Liu C, et al.; OPTIC Consortium; ISARIC4C Consortium. SARS-CoV-2 Omicron-B.1.1.529 leads to widespread escape from neutralizing antibody responses. Cell. 2022;185:467–484.e15. https://doi.org/10.1016/j.cell.2021.12.046
9. Israel Ministry of Health. As of today, 27/11/2021, one confirmed case of the Omicron variant was detected in Israel [cited 2022 Jan 31]. https://www.gov.il/en/departments/news/27112021-01
10. Our World in Data. SARS-CoV-2 variants in analyzed sequences, Israel [cited 2022 Mar 5]. https://ourworldindata.org/grapher/covid-variants-area?country=~ISR
11. National Institutes of Health. Coronavirus disease 2019 (COVID-19) treatment guidelines [cited 2021 Jul 18]. https://www.covid19treatmentguidelines.nih.gov
12. Central Bureau of Statistics. Statistical abstract of Israel 2021—no.72 [cited 2021 Nov 26]. https://www.cbs.gov.il/en/publications/Pages/2021/Population-Statistical-Abstract-of-Israel-2021-No.72.aspx
13. Glatman-Freedman A, Bromberg M, Dichtiar R, Hershkovitz Y, Keinan-Boker L. The BNT162b2 vaccine effectiveness against new COVID-19 cases and complications of breakthrough cases: a nation-wide retrospective longitudinal multiple cohort analysis using individualised data. EBioMedicine. 2021;72:103574. https://doi.org/10.1016/j.ebiom.2021.103574
14. Glatman-Freedman A, Hershkovitz Y, Kaufman Z, Dichtiar R, Keinan-Boker L, Bromberg M. Effectiveness of BNT162b2 vaccine in adolescents during outbreak of SARS-CoV-2 Delta variant infection, Israel, 2021. Emerg Infect Dis. 2021;27:2919–22. https://doi.org/10.3201/eid2711.211886
15. Fowlkes AL, Yoon SK, Lutrick K, Gwynn L, Burns J, Grant L, et al. Effectiveness of 2-dose BNT162b2 (Pfizer BioNTech) mRNA vaccine in preventing SARS-CoV-2 infection among children aged 5-11 years and adolescents aged 12-15 years—PROTECT Cohort, July 202--February 2022. MMWR Morb Mortal Wkly Rep. 2022;71:422–8. https://doi.org/10.15585/mmwr.mm7111e1
16. Tan SHX, Cook AR, Heng D, Ong B, Lye DC, Tan KB. Effectiveness of BNT162b2 vaccine against Omicron in children 5 to 11 years of age. N Engl J Med. 2022;387:525–32. https://doi.org/10.1056/NEJMoa2203209
17. Cohen-Stavi CJ, Magen O, Barda N, Yaron S, Peretz A, Netzer D, et al. BNT162b2 Vaccine effectiveness against Omicron in children 5 to 11 years of age. N Engl J Med. 2022;387:227–36. https://doi.org/10.1056/NEJMoa2205011
18. Fleming-Dutra KE, Britton A, Shang N, Derado G, Link-Gelles R, Accorsi EK, et al. Association of prior BNT162b2 COVID-19 vaccination with symptomatic SARS-CoV-2 infection in children and adolescents during Omicron predominance. JAMA. 2022;327:2210–9. https://doi.org/10.1001/jama.2022.7493
19. Dorabawila V, Hoefer D, Bauer UE, Bassett MT, Lutterloh E, Rosenberg ES. Risk of infection and hospitalization among vaccinated and unvaccinated children and adolescents in New York after the emergence of the Omicron variant. JAMA. 2022;327:2242–4. https://doi.org/10.1001/jama.2022.7319
20. Sacco C, Del Manso M, Mateo-Urdiales A, Rota MC, Petrone D, Riccardo F, et al.; Italian National COVID-19 Integrated Surveillance System and the Italian COVID-19 Vaccines Registry. Effectiveness of BNT162b2 vaccine against SARS-CoV-2 infection and severe COVID-19 in children aged 5–11 years in Italy: a retrospective analysis of January–April, 2022. Lancet. 2022;400:97–103. https://doi.org/10.1016/S0140-6736(22)01185-0
21. Andrews N, Stowe J, Kirsebom F, Toffa S, Rickeard T, Gallagher E, et al. Covid-19 vaccine effectiveness against the Omicron (B.1.1.529) Variant. N Engl J Med. 2022;386:1532–46. https://doi.org/10.1056/NEJMoa2119451
22. Thompson MG, Natarajan K, Irving SA, Rowley EA, Griggs EP, Gaglani M, et al. Effectiveness of a third dose of mRNA vaccines against COVID-19-associated emergency department and urgent care encounters and hospitalizations among adults during periods of Delta and Omicron variant predominance—VISION Network, 10 states, August 2021–January 2022. MMWR Morb Mortal Wkly Rep. 2022;71:139–45. https://doi.org/10.15585/mmwr.mm7104e3
23. Collie S, Champion J, Moultrie H, Bekker LG, Gray G. Effectiveness of BNT162b2 vaccine against Omicron variant in South Africa. N Engl J Med. 2022;386:494–6. https://doi.org/10.1056/NEJMc2119270
24. Buchan SA, Chung H, Brown KA, Austin PC, Fell DB, Gubbay JB, et al. Effectiveness of COVID-19 vaccines against Omicron or Delta symptomatic infection and severe outcomes. JAMA Netw Open. 2022;5:e2232760.
25. Nemet I, Kliker L, Lustig Y, Zuckerman N, Erster O, Cohen C, et al. Third BNT162b2 vaccination neutralization of SARS-CoV-2 Omicron infection. N Engl J Med. 2022;386:492–4. https://doi.org/10.1056/NEJMc2119358
26. Chen X, Huang Z, Wang J, Zhao S, Wong MC, Chong KC, et al. Ratio of asymptomatic COVID-19 cases among ascertained SARS-CoV-2 infections in different regions and population groups in 2020: a systematic review and meta-analysis including 130 123 infections from 241 studies. BMJ Open. 2021;11:e049752. https://doi.org/10.1136/bmjopen-2021-049752
27. Yonker LM, Boucau J, Regan J, Choudhary MC, Burns MD, Young N, et al. Virologic features of severe acute respiratory syndrome coronavirus 2 infection in children. J Infect Dis. 2021;224:1821–9. https://doi.org/10.1093/infdis/jiab509
28. Costa R, Bueno F, Albert E, Torres I, Carbonell-Sahuquillo S, Barrés-Fernández A, et al. Upper respiratory tract SARS-CoV-2 RNA loads in symptomatic and asymptomatic children and adults. Clin Microbiol Infect. 2021;27:1858.e1–7.
29. Israel Ministry of Health. Update of the testing and isolation policy regarding close contacts of a confirmed COVID-19 case, effective 7.1.2022 [cited 2021 Dec 27]. https://www.gov.il/en/departments/news/05012022-01

Address for correspondence: Aharona Glatman-Freedman, The Israel Center for Disease Control, Tel Hashomer, Ramat Gan 5265601, Israel; email: aharona.freedman@moh.gov.il

Monkeypox Virus Infection in 2 Female Travelers Returning to Vietnam from Dubai, United Arab Emirates, 2022

Nguyen Thanh Dung, Le Manh Hung, Huynh Thi Thuy Hoa, Le Hong Nga, Nguyen Thi Thu Hong, Tang Chi Thuong, Nghiem My Ngoc, Nguyen Thi Han Ny, Vo Truong Quy, Vu Thi Kim Thoa, Nguyen Thi Thanh, Phan Vinh Tho, Le Mau Toan, Vo Minh Quang, Dinh Nguyen Huy Man, Nguyen Tan Phat, Tran Thi Lan Phuong, Tran Thi Thanh Tam, Pham Thi Ngoc Thoa, Nguyen Hong Tam, Truong Thi Thanh Lan, Tran Tan Thanh, Sebastian Maurer-Stroh, Le Thuy Thuy Khanh, Lam Minh Yen, Nguyen Huu Hung, Guy Thwaites, Nguyen Le Nhu Tung, Louise Thwaites, Nguyen Van Vinh Chau, Nguyen To Anh, Le Van Tan

Mpox was diagnosed in 2 women returning to Vietnam from the United Arab Emirates. The monkeypox viruses belonged to an emerging sublineage, A.2.1, distinct from B.1, which is responsible for the ongoing multicountry outbreak. Women could contribute to mpox transmission, and enhanced genomic surveillance is needed to clarify pathogen evolution.

By January 12, 2023, more than 84,500 mpox cases and 80 deaths had been reported from 110 countries because of an ongoing multicountry outbreak (*1*). Cases from Europe and Americas accounted for >98% of reported cases, and only 35 cases had been reported from Southeast Asia (*1*). The outbreak has been characterized by involvement of networks of men who have sex with men; women have accounted for only 3.4% of 74,673 reported cases for which gender data were available (*1*). We report virologic, epidemiologic, and clinical features of mpox occurring in 2 women returning to Vietnam from travel to Dubai, United Arab Emirates.

Author affiliations: Hospital for Tropical Diseases, Ho Chi Minh City, Vietnam (N.T. Dung, L.M. Hung, H.T.T. Hoa, N.M. Ngoc, V.T. Quy, V.T.K. Thoa, N.T. Thanh, P.V. Tho, L.M. Toan, V.M. Quang, D.N.H. Man, N.T. Phat, T.T.L. Phuong, T.T.T. Tam, P.T.N. Thoa, N.L.N. Tung); Center for Disease Control, Ho Chi Minh City (L.H. Nga, N.H. Tam, T.T.T. Lan); Oxford University Clinical Research Unit, Ho Chi Minh City (N.T.T. Hong, N.T.H. Ny, T.T. Thanh, L.T.T. Khanh, L.M. Yen, G. Thwaites, L. Thwaites, N.T. Anh, L.V. Tan); Department of Health, Ho Chi Minh City (T.C. Thuong, N.H. Hung, N.V.V. Chau); Agency for Science, Technology and Research, Singapore (S. Maurer-Stroh); University of Oxford, Oxford, England, UK (G. Thwaites, L. Thwaites, L.V. Tan)

DOI: https://doi.org/10.3201/eid2904.221835

The Study

The case-patients were treated at the Hospital for Tropical Diseases (HTD) in Ho Chi Minh City, Vietnam. HTD is a tertiary referral infectious diseases hospital and the designated hospital for receiving and treating mpox patients in Ho Chi Minh City, which has a population of ≈10 million. The study was approved by the HTD Institutional Review Board (approval no. 1066/BVBND-HDDD) and Oxford Tropical Research Ethics Committee (approval no. 1023-13). The patients provided written informed consent for the study.

Patient 1 was a 35-year-old woman who was referred to HTD in September 2022. At admission, she had maculopapular lesions on various parts of her body (Figure 1, panels A–D), including the genital area (not shown). The patient had been in Dubai during July–September 2022 and had sexual contact with 2 male partners during her stay. The most recent contact was in mid-September; 5 days after the contact, she had fever, headache, chills, cough, sore throat, muscle pain, and tiredness, accompanied by a maculopapular rash in the genital area. Her symptoms resolved after 4 days except for the rash, and she returned to HCMC. Upon returning, additional

lesions developed in her mouth and on her back and upper and lower limbs. No information on the clinical status or sexual orientation of her partners was available. Her admission lesion swab tested positive for monkeypox virus (MPXV) by LightMix Modular Monkeypox Virus Kit (TIB Molbiol, https://www.tib-molbiol.de) with a cycle threshold (Ct) value of 18.05 (Appendix Table 1, https://wwwnc.cdc.gov.EID/article/29/4/22-1835-App1.pdf) and for varicella zoster virus (VZV) by VZV Real-TM (Sacace Biotechnologies, https://sacace.com) with a Ct of 30.5.

Patient 2 was a 38-year-old woman who was a friend of patient 1. She reported that she was in Dubai during late September through mid-October 2022 and had a sexual encounter with a male partner at in early October. She noted that the partner had a small rash on his penis and mild fever on the day of the encounter. No information about the partner's other sexual contacts is available. Nine days after the contact, she had fever, tiredness, and vomiting. Although her symptoms resolved after 4 days, a maculopapular rash started to develop on various parts of her body, including her face, a finger of the left hand, the arch of her right foot, and her abdomen (Figure 1, panels E–H). After consulting patient 1, patient 2 decided to fly back to Vietnam for treatment. Before departure she contacted Ho Chi Minh City Center for Disease Control for guidance on the isolation procedure at arrival. Patient 2 was transferred to HTD on arrival. She tested positive for MPXV by PCR at admission via LightMix Modular Monkeypox Virus Kit with a Ct value of 19.40.

At admission to HTD, both patients were afebrile. Except for an elevated alanine aminotransferase in patient 2, all blood test results were unremarkable (Appendix Table 2). All vital signs during hospitalization were measured by using wearable devices (Appendix Figure), as part of an observational study to enable remote patient monitoring (*2*), and measurements were within reference limits (data not shown). Test results for HIV and syphilis were negative. Because of the VZV coinfection, supporting a recent report (*3*), patient 1 was given oral acyclovir (800 mg 5×/d for 5 d). No other specific treatments were given. The patients were isolated, according to local health regulations, and their conditions remained stable without complications. After all lesions were completely healed, they were discharged.

To characterize the virus, we used metagenomics to obtain whole-genome sequences from the admission swab sample from patient 2 and a lesion swab sample with Ct value of 18.19 collected from patient 1 during follow-up (*4*,*5*) (Appendix, Appendix Table 1). We obtained 2 nearly complete MPXV genomes with coverage of 97.7% from patient 1 and 95% from patient 2. We determined viral lineage by using NextClade (*6*). Phylogenetic analysis suggested the sequences belonged to clade IIb, sublineage A.2.1 (Figure 2). Both sequences carried defined mutations of sublineage A.2.1, including C25072T, A140492C, and C179537T (*7*). In addition, we found a novel nonsynonymous substitution from threonine to isoleucine in amino 717 (T717I) of the polymerase protein in the sequence from patient 1. This mutation was not detected in any previously reported MPXV genomes. The estimated time to the most recent common ancestor of lineage A.2, including sublineage A.2.1, was May 27, 2019 (range August 3, 2018–January 23, 2020).

Additional samples were collected from patient 1 for PCR testing during follow up. Of those, 1 rectal (Ct

Figure 1. Monkeypox virus lesions from 2 female travelers returning to Vietnam from Dubai, United Arab Emirates, 2022. A–D) patient 1; E–H) patient 2. Images show lesions sporadically distributed on different body parts, including on patient 1 between 2 fingers (A), right arm (B), right foot (C), and face (D); and for patient 2, on a finger (E), the face (F), the arch of the right foot (G), and abdomen (H).

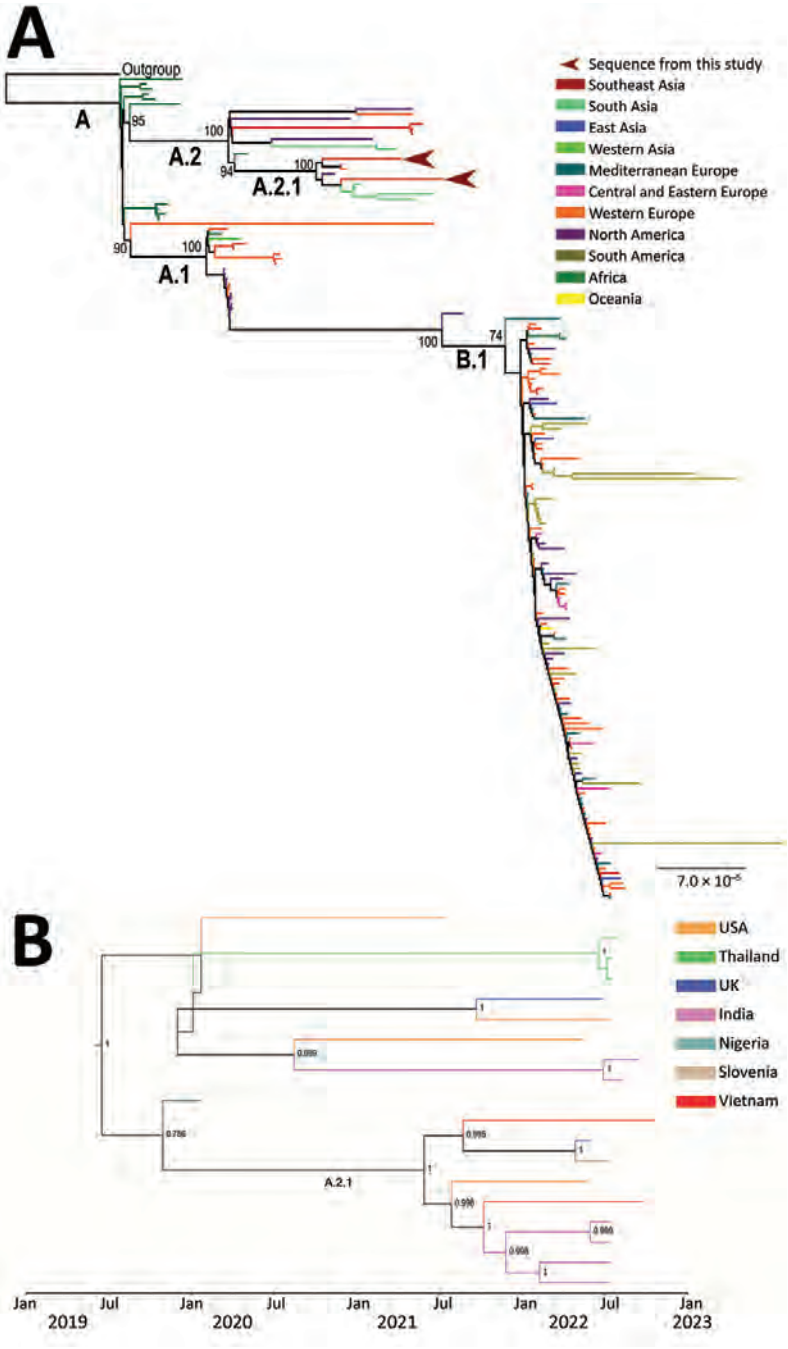

Figure 2. Phylogenetic tree of monkeypox virus infection in 2 female travelers returning to Vietnam from Dubai, United Arab Emirates, 2022. A) Maximum-likelihood phylogenetic tree illustrating the relatedness between virus sequences obtained in this study (Genbank accession nos. OP936000 and OP936001) and reference strains. Most sequences of sublineage A.2.1 from South Asia belong to a cluster from India (green) reported in July 2022 from persons with a travel history to the United Arab Emirates. The remaining sequences of A.2.1 from outside Asia included 1 isolated in the United Kingdom in June 2022, 1 isolated in the United States in May 2022, and 1 isolated in Nigeria in January 2020. Scale bar indicates nucleotide substitutions per site. B) Maximum-clade credibility tree of monkeypox virus lineage A.2. Red branches are sequences from this study.

value 33.30) and 1 pharyngeal lesion (Ct value 33.27) swab sample were also positive for MPXV by PCR (Appendix Table 1). Whole-genome sequencing of follow-up samples was hampered by low viral load (Appendix Table 1). We performed Sanger sequencing of a 531-bp PCR amplicon spanning the nonsynonymous mutation (Appendix Table 3), which confirmed presence of the T717I substitution in both the rectal and pharyngeal lesion swabs (data not shown), suggesting that this mutation was sampling-site independent (*8*).

MPXV consists of 2 main clades, I and II (*9*), and clade II includes subclades IIa and IIb. Clade I is endemic in Central Africa and clade IIa in West Africa. Clade IIb is responsible for the ongoing multicountry outbreak, and B.1 is the predominant virus lineage (*9*). In contrast to lineage B.1, sublineage A.2.1 of clade IIb has only recently been documented in a cluster of persons from India with a travel history to United Arab Emirates (*7*). In addition, 3 other A.2.1 sequences deposited to GISAID

(https://www.gisaid.org) originated in the United Kingdom, the United States, and Nigeria (Figure 1). Because MPXV evolves slowly, the genetic difference between the 2 sequences in this study coupled with the long branches of the A.2.1 cluster on the phylogenetic tree point to the possibility of silent transmission. Alternatively, the current sampling approach might have failed to comprehensively capture the genetic diversity of circulating MPXV strains worldwide. Collectively, these data suggest that lineage A.2, including sublineage A.2.1, likely represents an emerging MPXV lineage, supported by the results of time-scale phylogenetic analysis. Thus, multiple MPXV lineages likely are circulating and causing the ongoing multicountry outbreak.

Conclusions

We report 2 MPXV infections in women returning to Vietnam from Dubai, adding to the few reports of mpox in women (*10*,*11*). The viral strain belonged to sublineage A.2.1 and was phylogenetically distinct from sublineage B.1 circulating and causing the ongoing multicountry outbreak in Europe and Americas (*9*,*12*). Both patients had sexual contacts with male partners in Dubai, 5 and 9 days before symptoms developed. Our findings suggest that contribution of women in MPXV transmission networks might be greater than previously appreciated. Enhanced genomic surveillance is needed to clarify the epidemiology and evolution of MPXV.

Acknowledgments

We thank the patients for participating in our clinical study and our colleagues at the Hospital for Tropical Diseases for providing clinical care for the patients. We also thank Le Kim Thanh and Lam Anh Nguyet for logistic support and Tze Minn Mak for support with data interpretation. We thank all data contributors and their laboratories for obtaining the specimens for this study, and we thank the laboratories that submitted and shared their generated genetic sequence and metadata via GISAID, on which this research is based.

This study was funded by Wellcome of Great Britain (grant nos. 106680/B/14/Z, 222574/Z/21/Z, and 225437/Z/22/Z).

About the Author

Dr. Dung is director of the Hospital for Tropical Diseases in Ho Chi Minh City, Vietnam. His research interests include hepatitis viruses and emerging infections.

References

1. World Health Organization. 2022 Mpox (Monkeypox) outbreak: global trends [cited 2023 Jan 12]. https://worldhealthorg.shinyapps.io/mpx_global
2. Chau NVV, Hai HB, Greeff H, Phan Nguyen Quoc K, Trieu HT, Khoa LDV, et al. Wearable remote monitoring for patients with COVID-19 in low-resource settings: case study. BMJ Innov. 2021;7(Suppl 1):s12–5. https://doi.org/10.1136/bmjinnov-2021-000706
3. Hughes CM, Liu L, Davidson WB, Radford KW, Wilkins K, Monroe B, et al. A Tale of two viruses: coinfections of monkeypox and varicella zoster virus in the Democratic Republic of Congo. Am J Trop Med Hyg. 2020;104:604–11. https://doi.org/10.4269/ajtmh.20-0589
4. Anh NT, Hong NTT, Nhu LNT, Thanh TT, Lau CY, Limmathurotsakul D, et al. Viruses in Vietnamese patients presenting with community-acquired sepsis of unknown cause. J Clin Microbiol. 2019;57:e00386-19. https://doi.org/10.1128/JCM.00386-19
5. Nguyen AT, Tran TT, Hoang VM, Nghiem NM, Le NN, Le TT, et al. Development and evaluation of a non-ribosomal random PCR and next-generation sequencing based assay for detection and sequencing of hand, foot and mouth disease pathogens. Virol J. 2016;13:125. https://doi.org/10.1186/s12985-016-0580-9
6. Aksamentov I, Roemer C, Hodcroft E, Neher R. Nextclade: clade assignment, mutation calling and quality control for viral genomes. J Open Source Softw. 2021;6:3773. https://doi.org/10.21105/joss.03773
7. Shete AM, Yadav PD, Kumar A, Patil S, Patil DY, Joshi Y, et al. Genome characterization of monkeypox cases detected in India: identification of three sub clusters among A.2 lineage. J Infect. 2023;86:66–117. https://doi.org/10.1016/j.jinf.2022.09.024
8. Ulaeto DO, Dunning J, Carroll MW. Evolutionary implications of human transmission of monkeypox: the importance of sequencing multiple lesions. Lancet Microbe. 2022;3:e639–40. https://doi.org/10.1016/S2666-5247(22)00194-X
9. Isidro J, Borges V, Pinto M, Sobral D, Santos JD, Nunes A, et al. Phylogenomic characterization and signs of microevolution in the 2022 multi-country outbreak of monkeypox virus. Nat Med. 2022;28:1569–72. https://doi.org/10.1038/s41591-022-01907-y
10. Zayat N, Huang S, Wafai J, Philadelphia M. Monkeypox virus infection in 22-year-old woman after sexual intercourse, New York, USA. Emerg Infect Dis. 2023;29:222–3. https://doi.org/10.3201/eid2901.221662
11. Vallée A, Chatelain A, Carbonnel M, Racowsky C, Fourn E, Zucman D, et al. Monkeypox virus infection in 18-year-old woman after sexual intercourse, France, September 2022. Emerg Infect Dis. 2023;29:219–22. https://doi.org/10.3201/eid2901.221643
12. Luna N, Ramírez AL, Muñoz M, Ballesteros N, Patiño LH, Castañeda SA, et al. Phylogenomic analysis of the monkeypox virus (MPXV) 2022 outbreak: emergence of a novel viral lineage? Travel Med Infect Dis. 2022;49:102402. https://doi.org/10.1016/j.tmaid.2022.102402

Address for correspondence: Le Van Tan, Oxford University Clinical Research Unit, 764 Vo Van Kiet, ward 1, district 5, Ho Chi Minh 7000, Vietnam; email: tanlv@oucru.org

Experimental Infection and Transmission of SARS-CoV-2 Delta and Omicron Variants among Beagle Dogs

Kwang-Soo Lyoo, Hanbyeul Lee, Sung-Geun Lee, Minjoo Yeom, Joo-Yeon Lee, Kyung-Chang Kim, Jeong-Sun Yang, Daesub Song

We assessed susceptibility of dogs to SARS-COV-2 Delta and Omicron variants by experimentally inoculating beagle dogs. Moreover, we investigated transmissibility of the variants from infected to naive dogs. The dogs were susceptible to infection without clinical signs and transmitted both strains to other dogs through direct contact.

Since COVID-19 was first reported in China in late 2019 and quickly became a worldwide pandemic, zoonotic aspects of SARS-CoV-2 have raised public health concerns (*1*). The first reported case of SARS-CoV-2 infection in a companion animal was in Hong Kong (*2*). Pet dogs living with patients affected by COVID-19 shed low levels of SARS-CoV-2 and show seroconversion without any clinical signs (*2*). Multiple cases of SARS-CoV-2 transmission from humans to dogs have since been reported in several countries (*3*). In experimental infection studies, dogs inoculated with SARS-CoV-2 wild-type strain manifested no clinical signs or seroconversion, shed low titers, or had undetectable viral RNA (*4*,*5*). As companion animals, dogs commonly share living spaces with humans; therefore, more studies are needed to elucidate the susceptibility of dogs to SARS-CoV-2 infection.

SARS-CoV-2 variants Delta, in late 2020, and Omicron, in 2021, emerged and quickly spread worldwide. Those variants have been characterized by more efficient human-to-human transmission than the wild-type strain (*6*). In this study, we assessed susceptibility of beagle dogs to SARS-CoV-2 Delta and Omicron variants and transmissibility of SARS-CoV-2 variants from infected to naive dogs.

Author affiliations: Jeonbuk National University, Iksan, South Korea (K-S. Lyoo, S.-G. Lee); Seoul National University, Seoul, South Korea (H. Lee, M. Yeom, D. Song); Korea Disease Control and Prevention Agency, Cheongju, South Korea (J.-Y. Lee, K.-C. Kim, J.-S. Yang)

DOI: https://doi.org/10.3201/eid2904.221727

The Study

We obtained SARS-CoV-2 Omicron (NCCP 43408, BA.1. lineage) and Delta (NCCP 43390, B.1.617.2 lineage) variants from the National Culture Collection for Pathogens of South Korea. We passaged the viruses twice in Vero E6 cells and titrated the virus stocks on Vero E6 cells using a 50% tissue culture infectious dose ($TCID_{50}$) assay. This study was performed at the Animal Use Biosafety Level 3 facility of the Korea Zoonosis Research Institute. The Institutional Animal Care and Use Committee approved animal experiments (approval number JBNU 2022–033), and the Institutional Biosafety Committee of Jeonbuk National University approved experimental protocols requiring biosafety (approval no. JBNU2022–02–002).

We purchased 9 male beagle dogs, all 9 months of age, from Orient Bio Inc. (http://www.orient.co.kr). We intranasally inoculated 2 dogs with $10^{6.0}$ $TCID_{50}$/mL SARS-CoV-2 Delta variant and 2 others with $10^{6.0}$ $TCID_{50}$/mL SARS-CoV-2 Omicron variant (infected dogs). Twenty-four hours after infection, we housed 2 virus-naive dogs (transmission dogs) each with the infected dogs in separate large animal isolators, 1 for Delta-infected dogs and 1 for Omicron-infected dogs (total 4 dogs in each isolator, 2 infected and 2 naive). We assigned 1 naive dog as the noninfected negative control and kept it separate from the other dogs. We recorded body temperature and weight, and collected blood, nasal swabs, and rectal swabs the day of and 2, 4, 6, 8, and 10 days after infection for the infected dogs or days after cohousing began for the

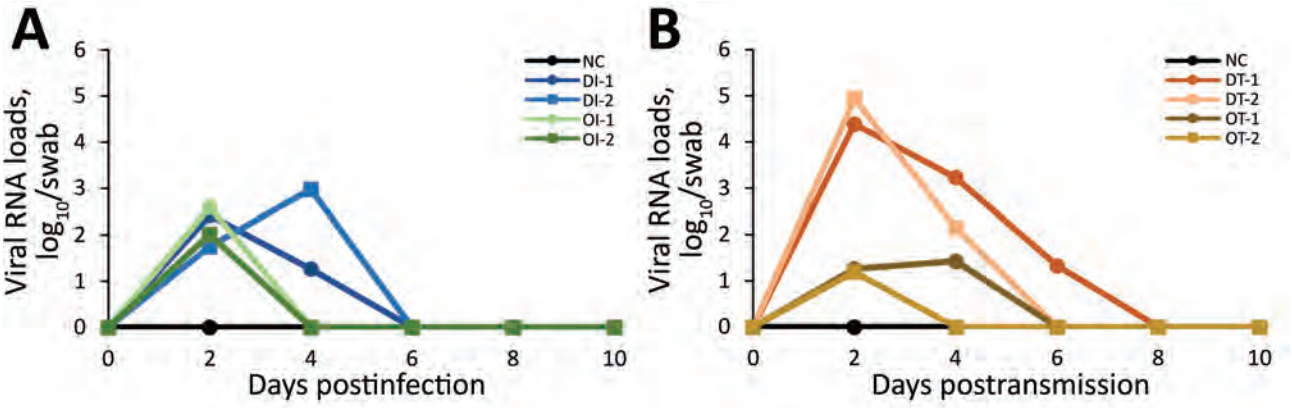

Figure 1. Viral RNA loads of SARS-CoV-2 determined by real-time PCR in animals in study of experimental infection and transmission of SARS-CoV-2 Delta and Omicron variants among beagle dogs. A) Viral loads in nasal swab samples from infected dogs. B) Viral loads in nasal swab samples from naive (transmission) dogs exposed to dogs infected with Delta or Omicron variants. NC, normal control; DI, delta variant infection; OI, omicron variant infection; DT, delta variant transmission; OT, omicron variant transmission.

transmission dogs. All dogs were humanely killed 10 days after infection or cohousing, after which we collected lung tissue for histopathologic examination and viral load measurement.

Using an Exigo C200 automatic analyzer (Boule Medical AB, https://boule.com), we tested for total protein, alkaline phosphatase, alanine aminotransferase, aspartate aminotransferase, lactate dehydrogenase, creatine kinase, creatinine, blood urea nitrogen, blood urea nitrogen/creatinine, and glucose. All results were within reference ranges except creatine kinase which, 4 days after infection or cohousing, was almost 8 times the upper limit of the normal range (0–200 U/L) in 1 infected dog (OI-1, 1,589 U/L) and 1 transmission dog (OT-1, 1,560 U/L) with Omicron variant (Appendix Figure, https://wwwnc.cdc.gov/EID/article/29/4/22-1727-App1.pdf). During the study, none of the dogs showed any clinical signs of illness, including weight loss or fever.

To measure viral RNA loads of SARS-CoV-2 in lung tissues and swab samples, we used real-time quantitative PCR to detect the nucleocapsid gene of SARS-CoV-2 using TaqMan Fast Virus 1-Step Master Mix (Thermo Fisher Scientific, https://www.thermofisher.com), as described elsewhere (*7*,*8*). We cultivated viruses from all nasal swab samples using a $TCID_{50}$ assay with Vero E6 cells. We did not detect viral RNA in lung tissue or rectal swab samples. However, the nasal swab samples taken from all dogs 2 days after infection with Delta or Omicron variants were positive for SARS-CoV-2 RNA; we also detected viral RNA in the swab samples taken from Delta-infected dogs 4 days after infection (Figure 1, panel A). In the SARS-CoV-2 transmission portion of the study, we detected viral RNA in nasal swab samples taken 2 days after transmission from dogs in the Delta and Omicron variant transmission groups; viral RNA loads from the 2 dogs in the Delta variant group (4.4 and 4.9 log_{10} genome copies/swab) were higher than the 2 in the Omicron variant group (1.2 and 1.3 log_{10} genome copies/swab) (Figure 1, panel B). Viral shedding from infected and transmission dogs was revealed by virus cultivation (Table).

Table. Viral titers from nasal swab samples from animals in study of experimental infection and transmission of SARS-CoV-2 Delta and Omicron variants among beagle dogs

		Days after exposure					
Dog group	Dog no.	0	2	4	6	8	10
Control	NA	NA	NA	NA	NA	NA	NA
Infection							
Delta	1	NA	2.5	2.2	NA	NA	NA
	2	NA	3.2	2.7	NA	NA	NA
Omicron	1	NA	2.8	NA	NA	NA	NA
	2	NA	2.2	NA	NA	NA	NA
Transmission							
Delta	1	NA	3.7	2.8	NA	NA	NA
	2	NA	4.3	2.3	NA	NA	NA
Omicron	1	NA	1.8	2.0	NA	NA	NA
	2	NA	2.3	NA	NA	NA	NA

*Values are 50% tissue culture infectious dose/mL. NA, not applicable.

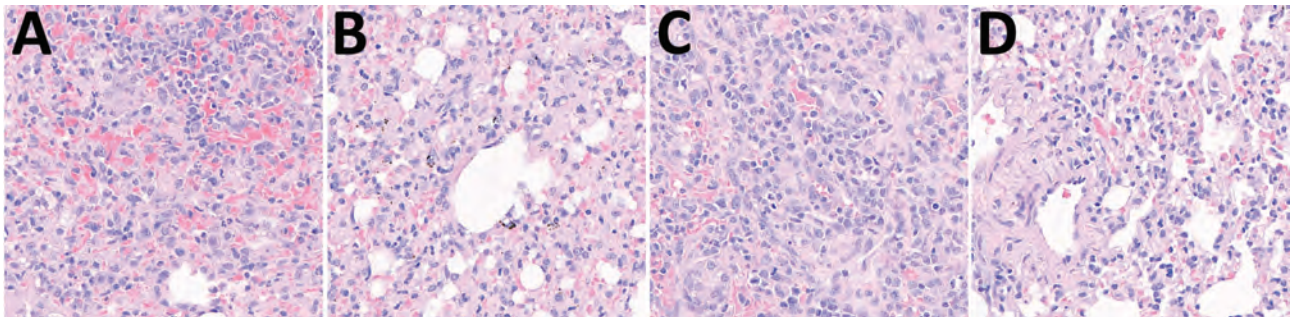

Figure 2. Pathologic changes in the lungs of dogs in study of experimental infection and transmission of SARS-CoV-2 Delta and Omicron variants among beagle dogs. A) Lung tissue from dog experimentally infected with Delta variant shows alveolar septa severely thickened by the infiltration of lymphocytes, macrophages, degenerate neutrophils, and karyorrhectic cellular debris. B) Lung tissue from naive (transmission) dog housed with Delta-infected dog shows alveolar septa thickened by the infiltration of numerous macrophages and lymphocytes, along with collagen accumulation. C) Lung tissue from dog experimentally infected with Omicron variant shows severe interstitial pneumonia and alveolar septal thickening due to the infiltration of lymphocytes, macrophages, and degenerate neutrophils. D) Lung tissue from naive (transmission) dog housed with Omicron-infected dog shows alveolar septa thickened by few macrophages, lymphocytes, and degenerate neutrophils. Original magnification ×400.

During necropsy at the end of the experiment, we found no gross lesions in any organ, but both infected and transmission dogs showed histopathologic changes in the lungs. The alveolar wall was locally thickened by infiltration of lymphocytes and monocytes, including macrophages, and proliferation of the alveolar epithelium (Figure 2).

Conclusions

Continuing emergence of SARS-CoV-2 variant strains presents a threat to public health and challenges the effectiveness of current vaccines. Delta and Omicron variants are more transmissible and resistant to neutralization than other strains in vaccinated persons (*6*). Although the SARS-CoV-2 pandemic has been driven mainly by human-to-human transmission, zoonotic viral infection from companion animals to humans has been reported frequently worldwide (*3*). To examine this dynamic, experimental infection studies have been performed using different animal species, including dogs (*3*,*5*).

For this study, we intranasally infected 9-month-old beagle dogs with SARS-CoV-2 Delta and Omicron variants; our results demonstrate that the dogs were susceptible to infection with and could transmit both strains to other dogs through direct contact. Despite no clinical signs, microscopic lesions were observed in the lungs of both infected and transmission dogs. Among the blood chemistry parameters, creatine kinase levels were markedly increased in Omicron-infected dogs. Creatine kinase is a marker of muscle damage, and elevated levels, such as those found among the Omicron-infected dogs, are associated with worse outcomes in respiratory patients infected with influenza viruses or SARS-CoV-2 (*9*,*10*). However, we could not exclude the possibility that creatine kinase could be elevated by muscle injury caused in an uncontrolled situation such as fighting among dogs instead of by SARS-CoV-2 infection. Therefore, further studies to clarify the role of blood chemistry parameters, such as creatine kinase, in animal models would be valuable.

The higher infectivity of SARS-CoV-2 variants than the wild-type virus strain led us to perform this experimental infection and transmission study in dogs. SARS-CoV-2 variants shed from humans might infect and efficiently circulate among companion animals, such as dogs or cats (*11*,*12*). It has been hypothesized that those companion animals could subsequently zoonotically infect humans. This scenario raises concerns about possible spillover between humans and companion animals, which might require continuous surveillance to monitor SARS-CoV-2 variants in companion animals. In the future, successful vaccination strategies for companion animals might be effective as a public health intervention in protecting animals from infection and preventing zoonotic transmission from infected animals.

Acknowledgments

We thank the National Culture Collection for Pathogens South Korea for providing SARS-CoV-2 Omicron (NCCP 43408, BA.1. lineage) and Delta (NCCP 43390, B.1.617.2 lineage) variants.

Our research was supported by the research program funded by the Korea National Institute of Health & the Korea Disease Control and Prevention Agency (fund codes 2021ER160900 and 2022-NI-043) and National R&D Programs of the National Research Foundation (NRF) funded by the Ministry of Science & ICT (NRF-2021M3E5E3080556).

About the Author

Dr. Lyoo is a deputy research director at Jeonbuk National University. His research interests include pathogenesis of animal viruses and vaccine development.

References

1. Konings F, Perkins MD, Kuhn JH, Pallen MJ, Alm EJ, Archer BN, et al. SARS-CoV-2 variants of interest and concern naming scheme conducive for global discourse. Nat Microbiol. 2021;6:821–3. https://doi.org/10.1038/s41564-021-00932-w
2. Sit THC, Brackman CJ, Ip SM, Tam KWS, Law PYT, To EMW, et al. Infection of dogs with SARS-CoV-2. Nature. 2020;586:776–8. https://doi.org/10.1038/s41586-020-2334-5
3. Cui S, Liu Y, Zhao J, Peng X, Lu G, Shi W, et al. An updated review on SARS-CoV-2 infection in animals. Viruses. 2022;14:1527. https://doi.org/10.3390/v14071527
4. Shi J, Wen Z, Zhong G, Yang H, Wang C, Huang B, et al. Susceptibility of ferrets, cats, dogs, and other domesticated animals to SARS-coronavirus 2. Science. 2020;368:1016–20. https://doi.org/10.1126/science.abb7015
5. Bosco-Lauth AM, Hartwig AE, Porter SM, Gordy PW, Nehring M, Byas AD, et al. Experimental infection of domestic dogs and cats with SARS-CoV-2: pathogenesis, transmission, and response to reexposure in cats. Proc Natl Acad Sci U S A. 2020;117:26382–8. https://doi.org/10.1073/pnas.2013102117
6. Tian D, Sun Y, Zhou J, Ye Q. The global epidemic of SARS-CoV-2 variants and their mutational immune escape. J Med Virol. 2022;94:847–57. https://doi.org/10.1002/jmv.27376
7. Noh JY, Yoon SW, Kim DJ, Lee MS, Kim JH, Na W, et al. Simultaneous detection of severe acute respiratory syndrome, Middle East respiratory syndrome, and related bat coronaviruses by real-time reverse transcription PCR. Arch Virol. 2017;162:1617–23. [Erratum in Arch Virol. 2018;163:819.] https://doi.org/10.1007/s00705-017-3281-9
8. Sia SF, Yan LM, Chin AWH, Fung K, Choy KT, Wong AYL, et al. Pathogenesis and transmission of SARS-CoV-2 in golden hamsters. Nature. 2020;583:834–8. https://doi.org/10.1038/s41586-020-2342-5
9. Borgatta B, Pérez M, Rello J, Vidaur L, Lorente L, Socías L, et al.; pH1N1 GTEI/SEMICYUC. Elevation of creatine kinase is associated with worse outcomes in 2009 pH1N1 influenza A infection. Intensive Care Med. 2012;38:1152–61. [Erratum in Intensive Care Med. 2012;38:1413.] https://doi.org/10.1007/s00134-012-2565-5
10. Akbar MR, Pranata R, Wibowo A, Lim MA, Sihite TA, Martha JW. The prognostic value of elevated creatine kinase to predict poor outcome in patients with COVID-19—a systematic review and meta-analysis. Diabetes Metab Syndr. 2021;15:529–34. https://doi.org/10.1016/j.dsx.2021.02.012
11. Pramod RK, Nair AV, Tambare PK, Chauhan K, Kumar TV, Rajan RA, et al. Reverse zoonosis of coronavirus disease-19: present status and the control by One Health approach. Vet World. 2021;14:2817–26. https://doi.org/10.14202/vetworld.2021.2817-2826
12. Goraichuk IV, Arefiev V, Stegniy BT, Gerilovych AP. Zoonotic and reverse zoonotic transmissibility of SARS-CoV-2. Virus Res. 2021;302:198473. https://doi.org/10.1016/j.virusres.2021.198473

Address for correspondence: Daesub Song, Department of Veterinary Medicine, College of Veterinary Medicine, Seoul National University, Seoul, South Korea; email: sds@snu.ac.kr

EID Podcast: Animal Reservoirs for Emerging Coronaviruses

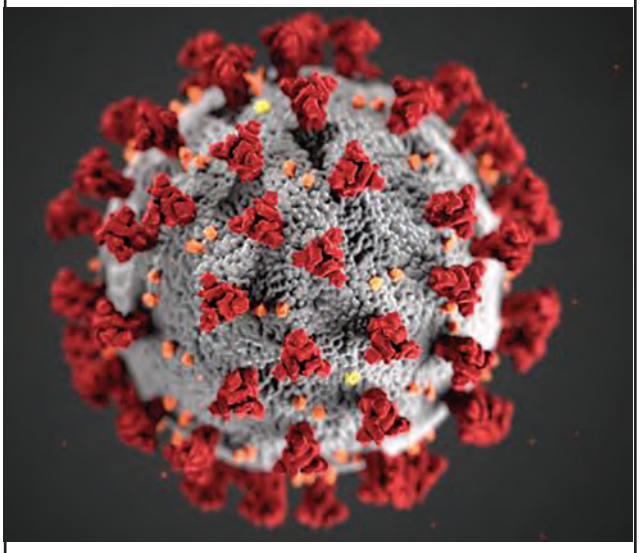

Coronaviruses are nothing new. Discovered in the 1930s, these pathogens have circulated among bats, livestock, and pets for years.

Most coronaviruses never spread to people. However, because this evolutionary branch has given rise to three high-consequence pathogens, researchers must monitor animal populations and find new ways to prevent spillover to humans.

In this EID podcast, Dr. Ria Ghai, an associate service fellow at CDC, describes the many animals known to harbor emerging coronaviruses.

Visit our website to listen: https://go.usa.gov/x6WtY

EMERGING INFECTIOUS DISEASES®

Highly Pathogenic Avian Influenza A(H5N1) Virus Outbreak in New England Seals, United States

Wendy Puryear[1], Kaitlin Sawatzki[1], Nichola Hill, Alexa Foss, Jonathon J. Stone, Lynda Doughty, Dominique Walk, Katie Gilbert, Maureen Murray, Elena Cox, Priya Patel, Zak Mertz, Stephanie Ellis, Jennifer Taylor, Deborah Fauquier, Ainsley Smith, Robert A. DiGiovanni Jr., Adriana van de Guchte, Ana Silvia Gonzalez-Reiche, Zain Khalil, Harm van Bakel, Mia K. Torchetti, Kristina Lantz, Julianna B. Lenoch, Jonathan Runstadler

We report the spillover of highly pathogenic avian influenza A(H5N1) into marine mammals in the northeastern United States, coincident with H5N1 in sympatric wild birds. Our data indicate monitoring both wild coastal birds and marine mammals will be critical to determine pandemic potential of influenza A viruses.

Highly pathogenic avian influenza (HPAI) viruses are of concern because of their pandemic potential, socioeconomic impact during agricultural outbreaks, and risks to wildlife conservation. Since October 2020, HPAI A(H5N1) virus, belonging to the goose/Guangdong H5 2.3.4.4b clade, has been responsible for >70 million poultry deaths and >100 discrete infections in many wild mesocarnivore species (*1*). As of January 2023, H5N1 infections in mammals have been primarily attributed to consuming infected prey, without evidence of further transmission among mammals.

We report an HPAI A(H5N1) virus outbreak among New England harbor and gray seals that was concurrent with a wave of avian infections in the region, resulting in a seal unusual mortality event (UME); evidence of mammal adaptation existed in a small subset of seals. Harbor (*Phoca vitulina*) and gray (*Halichoerus grypus*) seals in the North Atlantic are known to be affected by avian influenza A virus and have experienced previous outbreaks involving seal-to-seal transmission (*2*–*7*). Those seal species represent a pathway for adaptation of avian influenza A virus to mammal hosts that is a recurring event in nature and has implications for human health.

The Study

The first detections of HPAI clade 2.3.4.4b viruses in North America were in wild and domestic birds in November 2021 in Canada and late December 2021 in the United States (*8*–*11*). Starting on January 20, 2022, avian oropharyngeal or cloacal samples were collected from wild birds by personnel in 4 wildlife clinics in Massachusetts. Additional opportunistic samples were collected in Maine and Massachusetts in response to suspicious avian deaths in seabird breeding colonies. We screened samples from 1,079

Author affiliations: Tufts University Cummings School of Veterinary Medicine, North Grafton, Massachusetts, USA (W. Puryear, K. Sawatzki, A. Foss, J.J. Stone, M. Murray, E. Cox, J. Runstadler); University of Massachusetts, Boston, Massachusetts, USA (N. Hill); Marine Mammals of Maine, Brunswick, Maine, USA (L. Doughty, D. Walk, K. Gilbert); New England Wildlife Centers, Barnstable, Massachusetts, USA (P. Patel, Z. Mertz); New England Wildlife Centers, Weymouth, Massachusetts, USA (Z. Mertz); Wild Care, Inc., Eastham, Massachusetts, USA (S. Ellis, J. Taylor); National Oceanic and Atmospheric Administration Fisheries, Silver Spring, Maryland, USA (D. Fauquier); National Oceanic and Atmospheric Administration Fisheries, Gloucester, Massachusetts, USA (A. Smith); Atlantic Marine Conservation Society, Hampton Bays, New York, USA (R.A. DiGiovanni Jr.); Mount Sinai Icahn School of Medicine, New York, New York, USA (A. van de Guchte, A.S. Gonzalez-Reiche, Z. Khalil, H. van Bakel); US Department of Agriculture Animal and Plant Health Inspection Service, Ames, Iowa, USA (M.K. Torchetti, K. Lantz); US Department of Agriculture Animal and Plant Health Inspection Service, Fort Collins, Colorado, USA (J.B. Lenoch)

DOI: https://doi.org/10.3201/eid2904.221538

[1]These first authors contributed equally to this article.

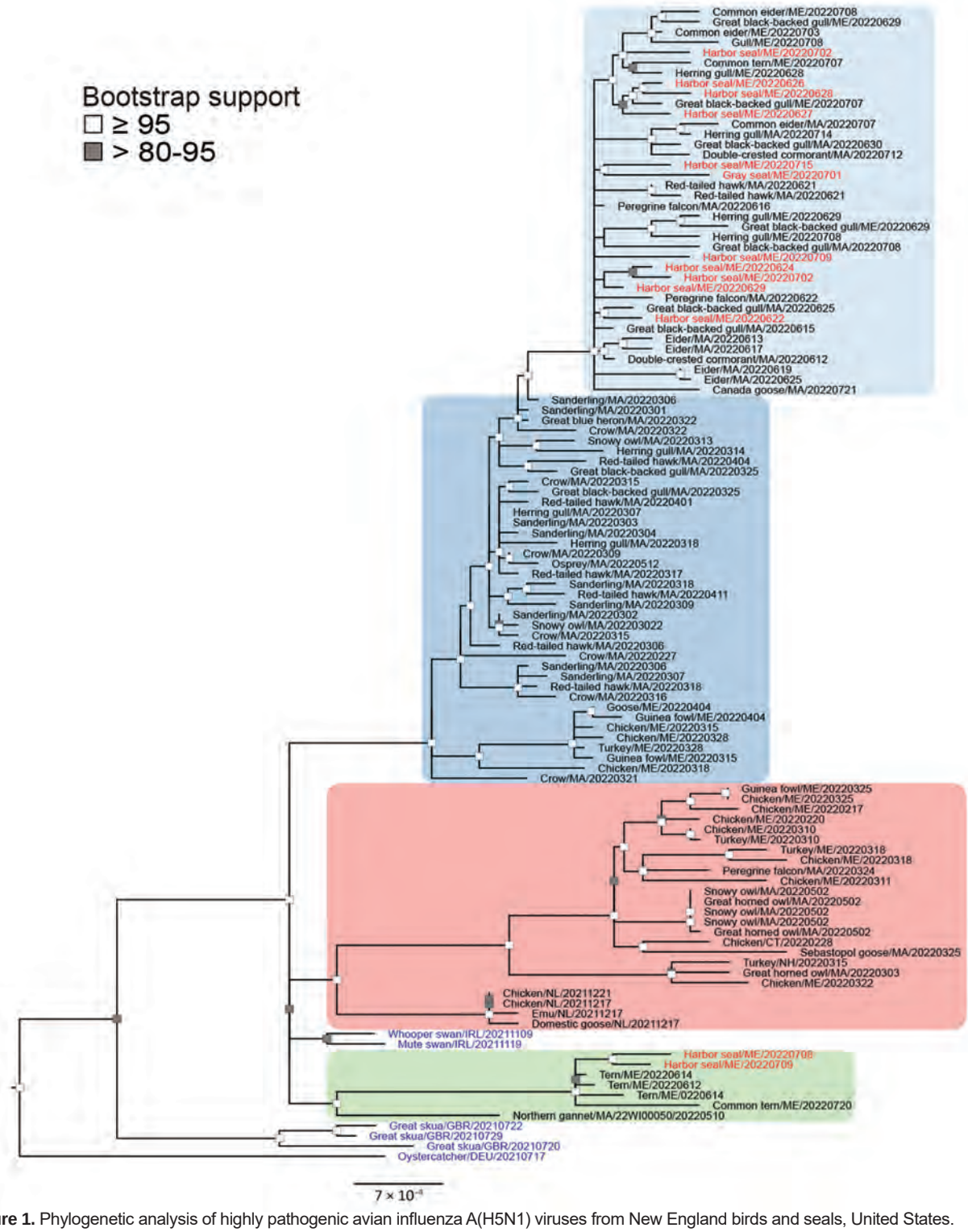

Figure 1. Phylogenetic analysis of highly pathogenic avian influenza A(H5N1) viruses from New England birds and seals, United States. Complete genomes of HPAI H5N1 viruses (GISAID database, https://www.gisaid.org) were compared by using IQ-TREE (https://www.iqtree.org) with the Ultrafast bootstrap (n = 10,000) option and A/chicken/NL/FAV-0033/2021 as a reference. Bootstrap support values >80 are shown at nodes. Red text indicates seal-derived sequences, black text avian-derived sequences from New England and Newfoundland, and blue text indicates avian-derived sequences from Europe . Branches are shaded on the basis of lineage groups: primary lineage from North America, pink; New England–specific lineage A, 1st wave blue, 2nd wave light blue; and New England–specific lineage B, green. All newly reported specimens were collected in the New England region during February–July 2022. Scale bar indicates nucleotide substitutions per site.

individual wild birds representing 78 avian species of concern for H5 influenza and identified 119 infected birds from 21 species (Appendix 1 Figure 1, panel A, https://wwwnc.cdc.gov/EID/article/29/4/22-1538-App1.pdf; Appendix 2, https://wwwnc.cdc.gov/EID/article/29/4/22-1538-App2.xlsx). Wild birds in New England experienced 2 waves of influenza infections during 2022. The first wave peaked in March and was largely represented by raptor deaths (39.1% influenza-positive birds). A second wave began in June; gull (38% influenza-positive) and eider (26.8% influenza-positive) deaths were most frequently reported during the second wave. Mortality events affected seabird breeding colonies throughout the coastal region during the second wave; 8 islands had ≥1 bird test positive for H5 (Appendix 1 Table).

During January 20–July 31, 2022, opportunistic nasal, oral, conjunctival or rectal swab samples were collected from 132 stranded seals along the North Atlantic coast from Maine to Virginia (Appendix 2). HPAI virus was not detected in any of the 82 seals that were sampled through May 31, 2022. Concurrent with the second wave of avian infections, increased seal strandings in Maine led to a National Oceanic and Atmospheric Administration declaration of a UME beginning on June 1, 2022, that included 164 harbor and 11 gray seals in Maine during June and July (*12*). Swab samples were collected from 41 of those animals; 17/35 harbor and 2/6 gray seals were HPAI-positive and were within coastal regions of known and suspected HPAI outbreaks among terns, eiders, cormorants, and gulls (Appendix Figure 1, panel B). Respiratory symptoms were observed with a subset of neurologic cases, although most stranded seals were deceased. The respiratory tract was the most consistent source of reverse transcription PCR–positive samples from affected seals (15/19 nasal, 16/19 oral, 6/19 conjunctiva, and 4/19 rectal samples).

We sequenced influenza A viruses from swab samples, resulting in 71 avian- and 13 seal-derived virus genomes from New England. We performed phylogenetic analysis of sequences from New England and the most closely related available virus sequences by using IQ-TREE (https://www.iqtree.org) (Figure 1; Appendix 1). We classified all but 1 virus as nonreassortant Eurasia 2.3.4.4b viruses and included those in further analyses (Appendix 1 Figures 2, 3). Sequences fell into 4 distinct clusters; 2 lineages were unique to New England. We found single-nucleotide polymorphisms (SNPs) (Appendix 1 Figures 4–7) and amino acid mutations (Figure 2) by using vSNP (https://github.com/USDA-VS/vSNP). Most sequences fell within a dominant New England–specific cluster that spanned the first and second waves (lineage A in this study). All second-wave viruses from lineage A exhibited the acquisition of new, shared mutations. That cluster spanned diverse species, including gulls, geese, eiders, raptors, and seals. A small number of raptor-derived sequences clustered with the primary lineage prevalent in North America at the time of sampling. All but 1 sample from the second wave of avian infections fell into either lineage A or a smaller, unique cluster primarily associated with terns (lineage B in this study).

We inferred that ≥2 spillover events occurred in the seal population during the second wave of avian infections. Of the sequences derived from seals, 11/13 clustered with second wave lineage A (Figure 1). We found 4 aa changes in specific proteins in both birds and seals that were distinct from the first wave of HPAI (polymerase acidic protein, A70V; polymerase acidic X protein, A62V; hemagglutinin protein, P152S; and nonstructural 1 protein, R67Q) (Figure 2). Within second wave lineage A, we found 37 aa changes in ≥1 seal sequence that were infrequent or absent from bird sequences. Most changes were unique; each occurred in only 1 animal. The polymerase basic 2 protein amino acid substitutions, E627K (in seal no. Pv/MME-22–131) and D701N (in seal no. Pv/MME-22–122), previously associated with mammalian adaptation were each present in 1 seal in second wave lineage A. An additional 2/13 seal-derived sequences clustered with lineage B; 10 aa mutations occurred in both bird and seal sequences (Figure 2). Another 10 aa changes occurred in at least 1 seal sequence that were infrequent or absent in the bird sequences. In contrast to lineage A, most amino acid changes were shared between the 2 seals in lineage B and were derived from animals stranded within the same town and sampled 1 day apart. The polymerase basic 2 protein substitution, D701N, was present in 1 seal from lineage B (Figure 2, seal no. PV12, MME-22–195).

Conclusions

Transmission from wild birds to seals was evident for ≥2 distinct HPAI H5N1 lineages in this investigation and likely occurred through environmental transmission of shed virus. Viruses were not likely acquired by seals through predation or scavenging of infected animals, because birds are not a typical food source for harbor or gray seals (*13*). Data do not support

		Lineage A													Lineage B		
Gene	aa change	A1	A2	Pv1	Pv2	Pv3	Pv4	Pv5	Pv6	Hg1	Pv7	Pv8	Pv9	Pv10	B	Pv11	Pv12
PB2	S12L	S					L										
	E627K	E						K									
	D701N	D					N								D		N
PB1	P13S	P			S				S			S					
	R211K	R											K				
	N213K	N														K	K
	N375T	N														T	
	R480K	R													K	K	K
	M523L	M												L			
	V527I	V												I			
	I728V	I									V						
PB1-F2	A56V	A				V		V									
	G70E	G													E	E	E
PA	I38V	I			V							V					
	A70V	A	V	V	V	V	V	V	V	V	V	V	V	V			
	E101G	E											G				
	E252G	E											G				
	T263K	T		K													
	V379M	V								M							
	L425F	L		F													
	T465I	T													I	I	I
	L672F	L														F	
PA-X	I38V	I			V							V					
	A70V	A	V	V	V	V	V	V	V	V	V	V	V	V			
	E101G	E											G				
	K227R	K													R	R	R
	K252E	K												E			
HA	T10I	T													I	I	I
	P152S	P	S	S	S	S	S	S	S	S	S	S	S	S			
	E201K	E												K			
	T226A	T													A	A	A
	S377N	S												N			
	A538S	A											S				
NP	S165P	S		P													
	A181S	A														S	
	V194I	V											I			I	I
	P318Q	P						Q									
	N377S	N											S			S	S
	Q409H	Q														H	
	Q415R	Q										R					
	P419S	P									S						
	M448V/1	M			I					V				V			
	D455N	D								N							
	G485R	G				R											
NA	M23I	M								I							
	A343T	A									T						
	I362T	I													T	T	T
	S439G	S													G	G	G
	K469R	K											R				
M1	F109S	F						S									
M2	I27V	I													V	V	V
NS1	R67Q	R	Q	Q	Q	Q	Q	Q	Q	Q	Q	Q	Q	Q			
	S87T	S								T							
	M98I	M		I													
	N127T	N													T	T	T
	T197N	T														N	N
NS2	L40I	L														I	I
	H85R	H					R										
	I89V	I											V				

Figure 2. Amino acid changes in highly pathogenic avian influenza A(H5N1) viruses from New England birds and seals, United States. Each single-nucleotide polymorphism (SNP) that resulted in an amino acid change within ≧1 seal-derived sequence is shown. SNPs were observed in 12 H5N1 virus genes resulting in amino acid changes in corresponding proteins: PB2, PB1, PB1-F2, PA, PA-X, HA, NP, NA, M1, M2, NS1, and NS2. All avian virus reference sequences are shaded gray. A/Sanderling/MA/CW_22–112 (H5N1) (GISAID database, https://www.gisaid.org) (labeled A1) was used as a reference for first wave lineage A sequences; A/common eider/MA/TW_22–1400 (H5N1) (labeled A2) was used as a reference for second wave lineage A sequences; and A/common tern/MA/20220612_1 (H5N1) (labeled B) was used as a reference for lineage B sequences. Four aa differ between first and second wave lineage A viruses and 10 aa differ between first wave lineage A and lineage B. Second wave lineage A and lineage B seal-derived virus sequences, sampling date, and sampling location in Maine, USA, are indicated for each seal as follows: Pv1, MME22-112, 2022 Jun 22, Wells; Pv2, MME22-117, 2022 Jun 24, Yarmouth; Pv3, MME22-121, 2022 Jun 26, Georgetown; Pv4, MME22-122, 2022 Jun 27, New Harbor; Pv5, MME22-131, 2022 Jun 28, Harpswell; Pv6, MME22-133, 2022 Jun 29, S. Portland; Hg1, MME22-144, 2022 Jul 1, Phippsburg; Pv7, MME22-150, 2022 Jul 2, Westport; Pv8, MME22-155, 2022 Jul 2, Falmouth; Pv9, MME22-198, 2022 Jul 9, Wells; Pv10, MME22-230, 2022 Jul 15, Kennebunkport; Pv11, MME22-191, 2022 Jul 8, Harpswell; Pv12, MME22-195, 2022 Jul 9, Harpswell. HA, hemagglutinin; Hg, gray seal; M, matrix; NA, neuraminidase; NP, nucleoprotein; NS, nonstructural; PA, polymerase acidic; PB, polymerase basic; Pv, harbor seal.

seal-to-seal transmission as a primary route of infection. If individual bird–seal spillover events represent the primary transmission route, the associated seal UME suggests that transmission occurred frequently and had a low seal species barrier. We observed novel amino acid changes throughout the virus genome in seals, including amino acid substitutions associated with mammal adaptation.

In contrast to outbreaks in agricultural settings, outbreaks of HPAI in wild populations can rarely be managed well through biosecurity measures or depopulation, which is particularly true for large, mobile marine species such as seals. Avian and mammalian colonial wildlife might be particularly affected by influenza A viruses, which could enable ongoing circulation between and within species, providing opportunities for reassortments of novel strains and study of mammalian virus adaptation. Migratory animals might further disseminate the viruses over broad geographic regions. Therefore, the interface of wild coastal birds and marine mammals is critical for monitoring the pandemic potential of influenza A viruses.

Acknowledgments

We thank the numerous staff and volunteers at Marine Mammals of Maine, College of the Atlantic, Seacoast Science Center, National Marine Life Center, Marine Mammal Alliance Nantucket, International Fund for Animal Welfare, Atlantic Marine Conservation Society, New York Marine Rescue Center, National Aquarium, Mystic Aquarium, Tufts Wildlife Clinic, New England Wildlife Center, New England Fisheries and Science Center, Wild Care Inc., Cape Wildlife Center, Linda Loring Nature Foundation, Maine Coastal National Wildlife Reservation, Rachel Carson National Wildlife Refuge, University of Massachusetts Nantucket Field Station, US Fish and Wildlife Services, and Massachusetts Audubon Society for providing critical expertise on marine and avian wildlife, obtaining samples from stranded animals, and providing essential insights on ecological contexts from the field; and the authors and originating and submitting laboratories of the sequences from GISAID's EpiFlu Database (https://www.gisaid.org) on which this research is based.

The study was funded by Mount Sinai Center for Research in Influenza Pathogenesis and Transmission, a Center of Excellence in Influenza Research and Response established by the National Institute of Allergy and Infectious Disease, National Institutes of Health, US Department of Health and Human Services (contract no. 75N93021C00014). The scientific results and conclusions and any views or opinions expressed herein are those of the authors and do not necessarily reflect the views or policies of the US Government, its agencies, or any of the included organizations.

All sequencing data are available in the GISAID database (https://www.gisaid.org) (EPI_ISL_14098915, EPI_ISL_14098917–24, EPI_ISL_16632466, EPI_ISL_16632487–8, EPI_ISL_16632494–6, EPI_ISL_16632498–524, EPI_ISL_16632536–42, EPI_ISL_16641764–94, EPI_ISL_16641796–9) or as a single file on GitHub (https://github.com/ksawatzki/H5N1_EID). All additional data are available in the appendices.

About the Author

Dr. Puryear is a virologist at The Cummings School of Veterinary Medicine at Tufts University in the Department of Infectious Disease and Global Health. Her research interests focus on epidemiology, evolution, and adaptation of wildlife diseases.

References

1. World Organisation for Animal Health. World animal health information system [cited 2022 Jul 19]. https://wahis.woah.org/#/dashboards/qd-dashboard
2. Geraci JR, St Aubin DJ, Barker IK, Webster RG, Hinshaw VS, Bean WJ, et al. Mass mortality of harbor seals: pneumonia associated with influenza A virus. Science. 1982;215:1129–31. https://doi.org/10.1126/science.7063847
3. Callan RJ, Early G, Kida H, Hinshaw VS. The appearance of H3 influenza viruses in seals. J Gen Virol. 1995;76:199–203. https://doi.org/10.1099/0022-1317-76-1-199
4. Anthony SJ, St Leger JA, Pugliares K, Ip HS, Chan JM, Carpenter ZW, et al. Emergence of fatal avian influenza in New England harbor seals. mBio. 2012;3:e00166–12. https://doi.org/10.1128/mBio.00166-12
5. Bodewes R, Bestebroer TM, van der Vries E, Verhagen JH, Herfst S, Koopmans MP, et al. Avian influenza A(H10N7) virus-associated mass deaths among harbor seals. Emerg Infect Dis. 2015;21:720–2. https://doi.org/10.3201/eid2104.141675
6. Bodewes R, Zohari S, Krog JS, Hall MD, Harder TC, Bestebroer TM, et al. Spatiotemporal analysis of the genetic diversity of seal influenza A(H10N7) virus, northwestern Europe. J Virol. 2016;90:4269–77. https://doi.org/10.1128/JVI.03046-15
7. Puryear WB, Keogh M, Hill N, Moxley J, Josephson E, Davis KR, et al. Prevalence of influenza A virus in live-captured North Atlantic gray seals: a possible wild reservoir. Emerg Microbes Infect. 2016;5:e81. https://doi.org/10.1038/emi.2016.77
8. Canadian Food Inspection Agency, National Emergency Operation Centre, Geographic Information System Services. Highly pathogenic avian influenza—wild birds [cited 2022 Jul 19]. https://cfia-ncr.maps.arcgis.com/apps/dashboards/89c779e98cdf492c899df23e1c38fdbc
9. United States Department of Agriculture. USDA confirms highly pathogenic avian influenza in a wild bird in South Carolina [cited 2022 Jul 7]. https://www.aphis.usda.gov/aphis/newsroom/stakeholder-info/sa_by_date/sa-2022/hpai-sc

10. Bevins SN, Shriner SA, Cumbee JC Jr, Dilione KE, Douglass KE, Ellis JW, et al. Intercontinental movement of highly pathogenic avian influenza A(H5N1) clade 2.3.4.4 virus to the United States, 2021. Emerg Infect Dis. 2022;28:1006–11. https://doi.org/10.3201/eid2805.220318
11. Caliendo V, Lewis NS, Pohlmann A, Baillie SR, Banyard AC, Beer M, et al. Transatlantic spread of highly pathogenic avian influenza H5N1 by wild birds from Europe to North America in 2021. Sci Rep. 2022;12:11729. https://doi.org/10.1038/s41598-022-13447-z
12. National Oceanic and Atmospheric Administration. 2018–2020 Pinniped unusual mortality event along the Northeast Coast [cited 2022 Jul 19]. https://www.fisheries.noaa.gov/new-england-mid-atlantic/marine-life-distress/2018-2020-pinniped-unusual-mortality-event-along
13. Bowen WD, Harrison GD. Comparison of harbour seal diets in two inshore habitats of Atlantic Canada. Can J Zool. 1996;74:125–35. https://doi.org/10.1139/z96-017

Address for correspondence: Wendy Puryear, Tufts University, 200 Westboro Rd, Bldg 20, North Grafton, MA 01536, USA; email: wendy.puryear@tufts.edu

February 2022

Vectorborne Infections

- Viral Interference between Respiratory Viruses
- Novel Clinical Monitoring Approaches for Reemergence of Diphtheria Myocarditis, Vietnam
- Clinical and Laboratory Characteristics and Outcome of Illness Caused by Tick-Borne Encephalitis Virus without Central Nervous System Involvement
- Role of *Anopheles* Mosquitoes in Cache Valley Virus Lineage Displacement, New York, USA
- Burden of Tick-Borne Encephalitis, Sweden
- Invasive *Burkholderia cepacia* Complex Infections among Persons Who Inject Drugs, Hong Kong, China, 2016–2019
- Comparative Effectiveness of Coronavirus Vaccine in Preventing Breakthrough Infections among Vaccinated Persons Infected with Delta and Alpha Variants
- Effectiveness of mRNA BNT162b2 Vaccine 6 Months after Vaccination among Patients in Large Health Maintenance Organization, Israel
- Comparison of Complications after Coronavirus Disease and Seasonal Influenza, South Korea
- Epidemiology of Hospitalized Patients with Babesiosis, United States, 2010–2016
- Rapid Spread of Severe Fever with Thrombocytopenia Syndrome Virus by Parthenogenetic Asian Longhorned Ticks
- Wild Boars as Reservoir of Highly Virulent Clone of Hybrid Shiga Toxigenic and Enterotoxigenic *Escherichia coli* Responsible for Edema Disease, France

- Public Acceptance of and Willingness to Pay for Mosquito Control, Texas, USA
- Widespread Detection of Multiple Strains of Crimean-Congo Hemorrhagic Fever Virus in Ticks, Spain
- West Nile Virus Transmission by Solid Organ Transplantation and Considerations for Organ Donor Screening Practices, United States
- Serial Interval and Transmission Dynamics during SARS-CoV-2 Delta Variant Predominance, South Korea
- Postvaccination Multisystem Inflammatory Syndrome in Adult with No Evidence of Prior SARS-CoV-2 Infection
- SARS-CoV-2 Circulation, Guinea, March 2020–July 2021
- Postmortem Surveillance for Ebola Virus Using OraQuick Ebola Rapid Diagnostic Tests, Eastern Democratic Republic of the Congo, 2019–2020
- SARS-CoV-2 Seroprevalence before Delta Variant Surge, Chattogram, Bangladesh, March–June 2021
- SARS-CoV-2 B.1.619 and B.1.620 Lineages, South Korea, 2021
- *Neisseria gonorrhoeae* FC428 Subclone, Vietnam, 2019–2020
- Zoonotic Infection with Oz Virus, a Novel Thogotovirus
- SARS-CoV-2 Cross-Reactivity in Prepandemic Serum from Rural Malaria-Infected Persons, Cambodia
- Tonate Virus and Fetal Abnormalities, French Guiana, 2019
- *Babesia crassa*–Like Human Infection Indicating Need for Adapted PCR Diagnosis of Babesiosis, France
- Clinical Features and Neurodevelopmental Outcomes for Infants with Perinatal Vertical Transmission of Zika Virus, Colombia
- Probable Transmission of SARS-CoV-2 Omicron Variant in Quarantine Hotel, Hong Kong, China, November 2021
- Seroprevalence of SARS-Cov-2 Antibodies in Adults, Arkhangelsk, Russia
- Ulceroglandular Infection and Bacteremia Caused by *Francisella salimarina* in Immunocompromised Patient, France
- Surveillance of Rodent Pests for SARS-CoV-2 and Other Coronaviruses, Hong Kong

EMERGING INFECTIOUS DISEASES

To revisit the February 2022 issue, go to:
https://wwwnc.cdc.gov/eid/articles/issue/28/2/table-of-contents

Emergence and Persistent Dominance of SARS-CoV-2 Omicron BA.2.3.7 Variant, Taiwan

Pei-Lan Shao,[1] Hsiao-Chen Tu,[1] Yu-Nong Gong,[1] Hung-Yu Shu, Ralph Kirby, Li-Yun Hsu, Hui-Yee Yeo, Han-Yueh Kuo, Yi-Chia Huang, Yung-Feng Lin, Hui-Ying Weng, Yueh-Lin Wu, Chien-Chih Chen, Tzen-Wen Chen, Kuo-Ming Lee, Chung-Guei Huang, Shin-Ru Shih, Wei J. Chen, Chen-Chi Wu, Chong-Jen Yu, Shih-Feng Tsai

Since April 2022, waves of SARS-CoV-2 Omicron variant cases have surfaced in Taiwan and spread throughout the island. Using high-throughput sequencing of the SARS-CoV-2 genome, we analyzed 2,405 PCR-positive swab samples from 2,339 persons and identified the Omicron BA.2.3.7 variant as a major lineage within recent community outbreaks in Taiwan.

The COVID-19 pandemic, caused by SARS-CoV-2, originated in China in late 2019, probably in the city of Wuhan (*1*,*2*). The outbreak of this unusual respiratory disease led to a wide variety of responses by various countries across the world (*3*–*6*). The response in Taiwan was rapid and based on both its proximity to China and its experiences during the SARS pandemic ≈2 decades earlier (*5*,*7*,*8*). The introduction of strict travel restrictions on incoming air and sea passengers, long compulsory quarantine periods for the few residents allowed to enter Taiwan, and a vast public acceptance of safety measures (e.g., social distancing, temperature checks, mask wearing) resulted in a delay in the emergence of the COVID-19 pandemic in Taiwan compared with other countries (*5*,*9*,*10*). Until April 2022, there were only limited outbreaks, all of which were quickly contained. Taiwan therefore provides a unique opportunity to explore what happened when the Omicron variant finally evaded the controls put in place by the Taiwan government and began to spread through the country's population.

Residents of Taiwan had not been exposed, on a large scale, to any of the virus variants before Omicron. By the time SARS-CoV-2 began to spread widely in Taiwan April 2022, there had been around 17,000 recorded cases of COVID-19 in the country, and most of them were linked to the Alpha variant (almost all cases in our study had not been infected with SARS-CoV-2 before). Vaccination rates of Taiwan's population at that time were 82.7% having received 1 dose, 78% having received 2 doses, and 59.1% having received 3 doses. The vaccines used in Taiwan before May 2022 were the Oxford-AstraZeneca vaccine (https://www.astrazeneca.com), the Pfizer-BioNTech vaccine (https://www.pfizer.com), the Moderna vaccine (https://www.modernatx.com), the Johnson & Johnson/Janssen vaccine (https://www.jandj.com), and The Median vaccine (a protein subunit COVID-19 vaccine made in Taiwan). Most residents of Taiwan received doses of the first 3 vaccines.

Author affiliations: National Taiwan University Hospital Hsin-Chu Branch, Hsin-Chu, Taiwan (P.-L. Shao, L.-Y. Hsu, H.-Y. Yeo, H.-Y. Kuo, Y.-C. Huang, C.-C. Wu, C.-J. Yu); Institute of Molecular and Genomic Medicine, National Health Research Institutes, Miaoli, Taiwan (H.-C. Tu, Y.-F. Lin, S.-F. Tsai); Research Center for Emerging Viral Infections, Chang Gung University College of Medicine, Taoyuan, Taiwan (Y.-N. Gong, K.-M. Lee, C.-G. Huang, S.-R. Shih); Linkou Chang Gung Memorial Hospital, Taoyuan (Y.-N. Gong, K.-M. Lee, C.-G. Huang S.-R. Shih); Chang Gung University College of Medicine, Taoyuan (Y.-N. Gong, K.-M. Lee, C.-G. Huang, S.-R. Shih); Chang Jung Christian University, Tainan, Taiwan (H.-Y. Shu); National Yang Ming Chiao Tung University, Taipei, Taiwan (R. Kirby, H.-Y. Weng, S.-F. Tsai); National Yang-Ming University, Taipei (H.-Y. Weng); TMU Research Center of Urology and Kidney, Taipei Medical University, Taipei, Taiwan (Y.-L. Wu); Wei-Gong Memorial Hospital, Miaoli, Taiwan (Y.-L. Wu, C.-C. Chen, T.-W. Chen,); Center for Neuropsychiatric Research, National Health Research Institutes, Miaoli (W.-J. Chen); Institute of Epidemiology and Preventive Medicine, National Taiwan University College of Public Health, Taipei (W.-J. Chen); National Taiwan University College of Medicine, Taipei (C.-C. Wu)

DOI: http://doi.org/10.3201/eid2904.221497

[1]These authors contributed equally to this article.

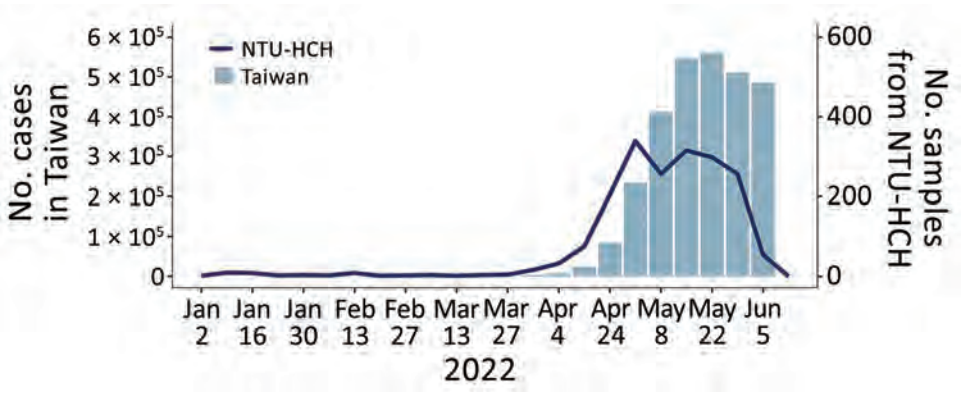

Figure 1. Weekly statistics for confirmed COVID-19 cases in Taiwan and sequenced samples, lineage distribution, and mutation prevalence derived from the NTU-HCH surveillance program, January–June 2022. Graph shows the number of COVID-19 confirmed cases in Taiwan and the sequenced samples from NTU-HCH from January (epidemiologic week 1) to early June (epidemiologic week 23). This figure was constructed using the publicly available data of Taiwan Centers for Disease Control (https://nidss.cdc.gov.tw/nndss/disease?id=19CoV). NTU-HCH, National Taiwan University Hospital–Hsinchu Branch.

Very few COVID-19 cases occurred in Taiwan during 2020 and 2021. Clustered infections were reported in May and June 2021, mainly in northern Taiwan. Even at the peak, only hundreds of positive cases were recorded by Taiwan's Centers for Disease Control. Early in 2022, several Omicron infection clusters were noted, first in northern Taiwan, and new cases quickly followed, soon exceeding 50,000 per day, with outbreaks affecting the entire country (Figure 1) (Infectious Disease Statistics Query System, https://nidss.cdc.gov.tw/nndss/disease?id=19CoV).

The Study

To gain insights into community transmission and to monitor viral evolution, we deployed a genomic surveillance protocol at National Taiwan University Hospital Hsinchu Branch (NTU-HCH) whereby we performed whole-genome sequencing on nasal swab samples detected by PCR to be positive for SARS-CoV-2 (Appendix 1, https://wwwnc.cdc.gov/EID/article/29/4/22-1497-App1.pdf). To ensure data quality, we submitted genomic data to GISAID (https://www.gisaid.org) only on those sequences that had >98% coverage of the 29,903-bp SARS-CoV-2 target genome. We used the same set of high-quality sequences for tracking the signature mutations in the viral samples (Table 1) and for phylogenetic analysis (Figure 2; Appendix 1, Figure 1). We found 2,405 samples among 5 batches that met the above criterion and this generated 2,043 sequences (84.9% pass rate). We selected 1,966 sequences for GISAID submission (Appendix 1 Table 1).

We analyzed the assembled viral genome sequences (Appendix 1 Table 2) and tracked the lineages and nonsynonymous amino acid changes in the Omicron samples collected during 2022 (Appendix 1 Figures 2, 3). Comparing the later 3 datasets (batches 3–5), we discovered that 3 amino acid changes (open reading frame [ORF]1a: L631F; spike (S): K97E; nucleocapsid; M322I) occurred only after the fourth sequencing batch. The percentage of sequences containing the signatures progressed steadily from 62% in batch 4 to 85% in batch 5. All batch-3 isolates belonged to the BA.1 or BA.2 classification, suggesting that the rapid increase of cases in Taiwan in April and May 2022—from 0 cases/day to ≈100,000 cases/day—came from a strain (BA.2.3.7) that might have been involved in a founder effect.

To construct the framework of the phylogenetic tree, we took 1,966 genome sequences from our study and analyzed them in the global context of 881 GISAID reference sequences (Figure 2; Appendix 2, https://wwwnc.cdc.gov/EID/article/29/4/22-1497-App2.xlsx). We then zoomed in and compared the 1,577 Omicron sequences of our study against the 228 Omicron BA.2.3.7 strains from GISAID. Those sequences were reported from 21 countries, including 51 from Taiwan (Table 2). We conducted phylogenetic analysis using the Pango-dynamic nomenclature system (*11*).

We found evidence that this novel lineage BA.2.3.7 with 3 amino acid changes (ORF1a: L631F; S: K97E; and nucleocapsid: M322I) was circulating dominantly in Taiwan over the study period. Of note, the first BA.2.3.7 strain identified in the epidemic in Taiwan was collected on March 27, 2022, and since that time we detected several genomic changes affecting this Omicron lineage. For example, we noted a new mutation, G1251V (Appendix 1 Figure 3, green line) in the S protein, from April onward, and that particular circulating lineage then rapidly spread across Taiwan.

Conclusions

We acknowledge that our study is limited in that we conducted the genomic surveillance in only 1 medical center; therefore, the observed dominance of BA.2.3.7 might be due to clustering of cases. Of note, while this

Table 1. Signature mutations in SARS-CoV-2 BA.2.3.7 sublineages of viral samples from a study of the Omicron BA.2.3.7 variant in community outbreaks, Taiwan

	Accumulated mutations*			
Lineage	BA.2	BA.2.3	BA.2.3.7	Selected mutations†
ORF1a	S135R	S135R	S135R	NA
	NA	NA	NA	A591V
	NA	NA	L631F	L631F
	T842I	T842I	T842I	NA
	NA	NA	NA	I1091T
	G1307S	G1307S	G1307S	NA
	NA	A2909V	A2909V	NA
	L3027F	L3027F	L3027F	NA
	T3090I	T3090I	T3090I	NA
	L3201F	L3201F	L3201F	NA
	NA	NA	NA	T3224A
	T3255I	T3255I	T3255I	NA
	P3395H	P3395H	P3395H	NA
	del3675	del3675	del3675	NA
	del3676	del3676	del3676	NA
	del3677	del3677	del3677	NA
	NA	NA	NA	V3683I
Spike	T19I	T19I	T19I	NA
	L24S	L24S	L24S	NA
	del25	del25	del25	NA
	del26	del26	del26	NA
	del27	del27	del27	NA
	NA	NA	K97E	K97E
	G142D	G142D	G142D	NA
	V213G	V213G	V213G	NA
	G339D	G339D	G339D	NA
	S371F	S371F	S371F	NA
	S373P	S373P	S373P	NA
	S375F	S375F	S375F	NA
	T376A	T376A	T376A	NA
	D405N	D405N	D405N	NA
	R408S	R408S	R408S	NA
	K417N	K417N	K417N	NA
	N440K	N440K	N440K	NA
	S477N	S477N	S477N	NA
	T478K	T478K	T478K	NA
	E484A	E484A	E484A	NA
	Q493R	Q493R	Q493R	NA
	Q498R	Q498R	Q498R	NA
	N501Y	N501Y	N501Y	NA
	Y505H	Y505H	Y505H	NA
	D614G	D614G	D614G	NA
	H655Y	H655Y	H655Y	NA
	N679K	N679K	N679K	NA
	P681H	P681H	P681H	NA
	N764K	N764K	N764K	NA
	D796Y	D796Y	D796Y	NA
	Q954H	Q954H	Q954H	NA
	N969K	N969K	N969K	NA
	NA	NA	NA	G1251V
ORF3a	NA	L140F	L140F	NA
	T223I	T223I	T223I	NA
Nucleocapsid	P13L	P13L	P13L	NA
	del31	del31	del31	NA
	del32	del32	del32	NA
	del33	del33	del33	NA
	R203K	R203K	R203K	NA
	G204R	G204R	G204R	NA
	NA	NA	M322I	M322I
	S413R	S413R	S413R	NA

*Using SARS-CoV-2 Wuhan-Hu-1 (GenBank accession no. MN908947.3) as the reference sequence. Mutations in ORF1b, E, M, ORF6, and ORF8 are not shown as they are identical between BA.2, BA.2.3 and BA.2.3.7. NA, not applicable; ORF, open reading frame.
†Mutations detected in the Omicron lineages are characterized in this study.

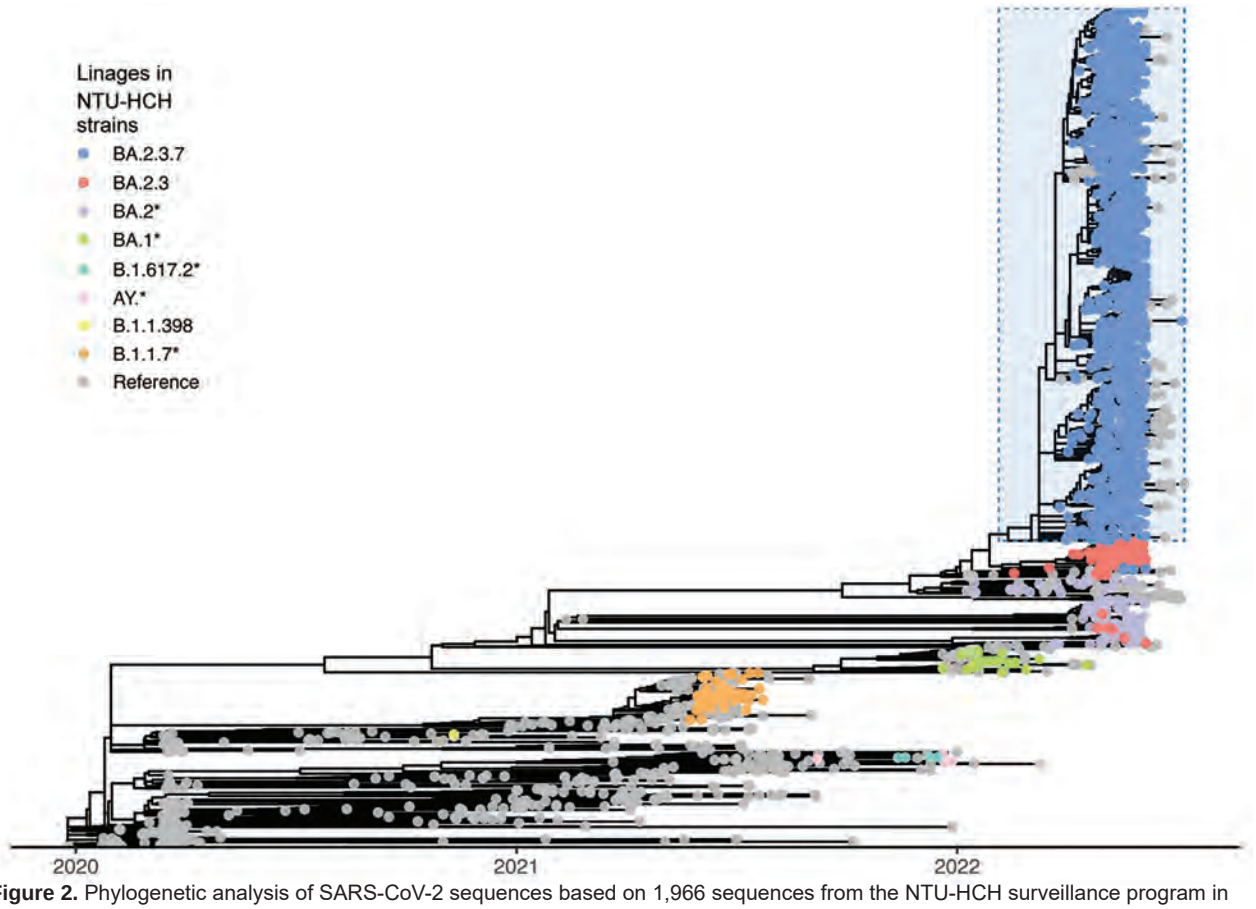

Figure 2. Phylogenetic analysis of SARS-CoV-2 sequences based on 1,966 sequences from the NTU-HCH surveillance program in Taiwan and 881 sequences from GISAID (https://www.gisaid.org). Lineages of NTU-HCH strains are annotated in different colors; asterisks (*) represent the collection of a specific lineage with its sublineage. The BA.2.3.7 strains were dominantly circulating in Taiwan from March 2022, highlighted by light blue in the tree. NTU-HCH, National Taiwan University Hospital–Hsinchu Branch.

paper was in preparation, we became aware that several viral sequences with the same signature mutations had been reported in Taiwan. Although the number of cases was relatively small (51) compared with the number of cases we studied, the 4 locations in Taiwan reporting those cases were different from our collection point at the hospital. Thus, this new lineage appeared to be broadly detectable across Taiwan.

Other Asia-Pacific countries have also recently reported a substantial cumulative prevalence of the BA.2.3.7 variant (Table 2). Among the 44 Omicron BA.2.3.7 strains reported from Japan, 2 of the affected persons had travel history to Vietnam and 41 to Taiwan, suggesting considerable silent outward transmission from Taiwan. In contrast, BA.2.3.7 accounts for <0.5% of the sequences reported in either California, USA, or globally. The emergence of Omicron BA.2.3.7 in Asia is remarkable. Because there are no reliable genomic data from early cases in Malaysia and Vietnam, our phylogenic analysis and the metadata from GISAID suggests that travel between

Table 2. Submitted sequences of SARS-CoV-2 BA2.3.7 from different countries for inclusion in a study of the Omicron BA.2.3.7 variant in community outbreaks, Taiwan

Country	No. sequences
Taiwan	51*
Japan	44
United States	37
Indonesia	27
Hong Kong	22
Australia	7
Denmark	6
Canada	5
Singapore	4
South Korea	4
Philippines	3
Thailand	3
France	3
Cambodia	2
Austria	2
Sweden	2
Germany	2
Spain	1
Vietnam	1
Slovenia	1
New Zealand	1
Total	228

*Number does not include the contributions from this study.

countries in Asia contributed to the rapid spread of this unique Omicron lineage.

In summary, our genomic dataset is uniquely valuable for understanding how a major COVID-19 outbreak occurs in a naive and vaccinated population in Taiwan, a country with a very limited number of entry events. We theorize that the dominant circulation of BA.2.3.7 in Taiwan is likely the result of genetic drift or a founder effect, although it is also possible that increased transmissibility or vaccine evasion played some part. As countries in Asia move from zero tolerance to more open COVID-19 policies, continued surveillance of SARS-CoV-2 using next-generation sequencing is important. Early detection of viral evolution events in endemic areas will help minimize future disruptions caused by a new variant.

Acknowledgments

We extend our thanks to Y. Henry Sun and Hsiao-Hui Tso for critical reading of the manuscript; Yi-Chun Tsai, Shuo-Peng Chou, Jhen-Rong Huang, and Yuan-Yu You for sample collection and nucleic acid preparation; and Tai-Yun Lin, Yu-Chen Huang, and Chiao-Chan Wang for library construction and sequencing operation. We gratefully acknowledge the authors from the originating laboratories responsible for obtaining the specimens as well as the submitting laboratories where the genome data were generated and shared via GISAID and GenBank (Appendix 2).

This work was supported by Ministry of Health and Welfare of Taiwan (MOHW110-TDU-C-222-000010) to S.F.T., by the Research Center for Emerging Viral Infections from The Featured Areas Research Center Program within the framework of the Higher Education Sprout Project by the Ministry of Education of Taiwan, the Ministry of Science and Technology of Taiwan (MOST 111-2321-B-182-001, MOST 111-2634-F-182-001, MOST 110-2222-E-182-004, and MOST 111-2221-E-182-053-MY3), and the National Institute Of Allergy And Infectious Diseases of the National Institutes of Health under Award Number 5U01AI151698-02 to Y.N.G. and S.R.S.

About the Author

Dr. Shao is an assistant professor in the Department of Laboratory Medicine and Pediatrics, National Taiwan University College of Medicine, Taiwan. Her main research interests include infectious disease, clinical virology, clinical microbiology, and vaccines. Dr. Tu is postdoctoral fellow in the Institute of Molecular and Genomic Medicine, National Health Research Institutes, Taiwan. Her research interests include next generation sequencing technology, cancer, and genomic research. Dr. Gong is an assistant professor in Research Center for Emerging Viral Infections and International Master's Degree Program for Molecular Medicine in Emerging Viral Infections, Chang Gung University, Taiwan. His research interests include bioinformatics, phylogenetics, machine learning, and viral evolution.

References

1. World Health Organization. WHO statement regarding cluster of pneumonia cases in Wuhan, China. January 9, 2020 [cited 2023 Jan 26]. https://www.who.int/china/news/detail/09-01-2020-who-statement-regarding-cluster-of-pneumonia-cases-in-wuhan-china
2. Zhu N, Zhang D, Wang W, Li X, Yang B, Song J, et al.; China Novel Coronavirus Investigating and Research Team. A novel coronavirus from patients with pneumonia in China, 2019. N Engl J Med. 2020;382:727–33. https://doi.org/10.1056/NEJMoa2001017
3. Mathieu E, Ritchie H, Rodés-Guirao L, Appel C, Giattino C, Hasell J, et al. Coronavirus pandemic (COVID-19). Our world in data [cited 2023 Jan 26]. https://ourworldindata.org/coronavirus
4. Jung AS, Haldane V, Neill R, Wu S, Jamieson M, Verma M, et al. National responses to covid-19: drivers, complexities, and uncertainties in the first year of the pandemic. BMJ. 2021;375:e068954. https://doi.org/10.1136/bmj-2021-068954
5. Summers J, Cheng HY, Lin HH, Barnard LT, Kvalsvig A, Wilson N, et al. Potential lessons from the Taiwan and New Zealand health responses to the COVID-19 pandemic. Lancet Reg Health West Pac. 2020;4:100044. https://doi.org/10.1016/j.lanwpc.2020.100044
6. Tsou HH, Kuo SC, Lin YH, Hsiung CA, Chiou HY, Chen WJ, et al. A comprehensive evaluation of COVID-19 policies and outcomes in 50 countries and territories. Sci Rep. 2022;12:8802. https://doi.org/10.1038/s41598-022-12853-7
7. Chen SC. Taiwan's experience in fighting COVID-19. Nat Immunol. 2021;22:393–4. https://doi.org/10.1038/s41590-021-00908-2
8. Wang CJ, Ng CY, Brook RH. Response to COVID-19 in Taiwan: Big data analytics, new technology, and proactive testing. JAMA. 2020;323:1341–2. https://doi.org/10.1001/jama.2020.3151
9. Gong YN, Tsao KC, Hsiao MJ, Huang CG, Huang PN, Huang PW, et al. SARS-CoV-2 genomic surveillance in Taiwan revealed novel ORF8-deletion mutant and clade possibly associated with infections in Middle East. Emerg Microbes Infect. 2020;9:1457–66. https://doi.org/10.1080/22221751.2020.1782271
10. Lin C, Braund WE, Auerbach J, Chou JH, Teng JH, Tu P, et al. Policy decisions and use of information technology to fight coronavirus disease, Taiwan. Emerg Infect Dis. 2020;26:1506–12. https://doi.org/10.3201/eid2607.200574
11. Rambaut A, Holmes EC, O'Toole Á, Hill V, McCrone JT, Ruis C, et al. A dynamic nomenclature proposal for SARS-CoV-2 lineages to assist genomic epidemiology. Nature Microbiology. 2020;5:1403-07. https:// doi.org/10.1038/s41564-020-0770-5

Address for correspondence: Chong-Jen Yu, NTUH, Hsin-Chu Branch, Sec. 1 Shengyi Rd, Zhubei, Hsinchu 30261, Taiwan; email: jefferycjyu@ntu.edu.tw; Shih-Feng Tsai, NHRI, 35 Keyan Rd, Zhunan, Miaoli 35053, Taiwan; email: petsai@nhri.edu.tw

Yezo Virus Infection in Tick-Bitten Patient and Ticks, Northeastern China

Xiaolong Lv,[1] Ziyan Liu,[1] Liang Li,[1] Wenbo Xu, Yongxu Yuan, Xiaojie Liang, Li Zhang, Zhengkai Wei, Liyan Sui, Yinghua Zhao, Zhijun Hou, Feng Wei, Shuzhen Han, Quan Liu, Zedong Wang

We identified Yezo virus infection in a febrile patient who had a tick bite in northeastern China, where 0.5% of *Ixodes persulcatus* ticks were positive for viral RNA. Clinicians should be aware of this potential health threat and include this emerging virus in the differential diagnosis for tick-bitten patients in this region.

Tickborne orthonairoviruses have been considered a major public health threat worldwide (*1*). In China, other than Crimean-Congo hemorrhagic fever virus, there are 3 emerging orthonairoviruses: Tacheng tick virus 1 (*2*), Songling virus (*3*), and Beiji nairovirus (*4*). Those viruses have been associated with human febrile illness in northeastern and northwestern China.

Yezo virus (YEZV), a new tickborne orthonairovirus discovered in Japan in 2021, can cause acute febrile illness in humans, whose clinical symptoms include thrombocytopenia and leukopenia (*5*). We report a case of YEZV infection in a tick-bitten patient and provide molecular evidence of YEZV infection in ticks in northeastern China.

The Study

The research protocol was approved by the human bioethics committee of Inner Mongolia General Forestry Hospital and the First Hospital of Jilin University, China. During 2018–2020, a total of 402 blood samples from tick-bitten patients were collected at the Inner Mongolia General Forestry Hospital (164 in 2018, 97 in 2019, and 141 in 2020) for viral detection by using reverse transcription PCR (Appendix Table 1 https://wwwnc.cdc.gov/EID/article/29/4/22-0885-App1.pdf). Results showed that 1 sample collected in 2018 was YEZV positive.

The patient was a 33-year-old man who lived on a farm in the Oroqen Autonomous Banner of Hulunbuir, Inner Mongolia, northeastern China, who had no history of underlying diseases. On June 18, 2018, he noticed a tick embedded on his back after he grazed horses on a mountain. The tick was removed intact by using tweezers in a local clinic and identified as *Ixodes persulcatus*. At that time, no obvious clinical symptoms, such as rash, itching, and discomfort, occurred. However, fever developed, followed by light headache, dizziness, blurred vision, chest distress, shortness of breath, fatigue, and arthralgia in 1 week (Table 1; Figure 1). No gastrointestinal (e.g., nausea, vomit, diarrhea) or hemorrhagic (e.g., melena, petechia, and ecchymosis) symptoms occurred.

Laboratory tests identified lymphocytopenia and neutrophilia, which accounted for 15.0% and 75.9% of the total leukocyte count, respectively. However, leukocyte counts (4,460 cells/mL) and platelet counts (199,000 cells/mL) were within reference ranges. Serum levels of liver aminotransferases were slightly increased (alanine aminotransferase 40 U/L, aspartate aminotransferase 44 U/L, and γ-glutamyltransferase 124 U/L) (Appendix Table 2). The serum level of C-reactive protein increased to 11.1 mg/L.

The patient was hospitalized for 8 days. Headache, dizziness, and arthralgia continued throughout the hospitalization, whereas the clinical signs of fever, blurred vision, chest distress, shortness of breath, and fatigue were relieved or disappeared (Figure 1). Lymphopenia continued until day 5, but counts of leukocytes, platelets, and erythrocytes and the hemoglobin level were all within reference ranges. Evidence of liver damage continued through the discharge date (alanine aminotransferase 56 U/L and γ -glutamyltransferase 181 U/L).

Author affiliations: First Hospital of Jilin University, Changchun, China (Z. Liu, W. Xu, L. Sui, Y. Zhao, Q. Liu, Z. Wang); Inner Mongolia General Forestry Hospital, Yakeshi, China (X. Lv, S. Han); Jilin Agricultural University, Changchun (Z. Liu, Y. Yuan, X. Liang, F. Wei); Chinese Academy of Agricultural Sciences, Changchun (L. Li, L. Zhang, Q. Liu, Z. Wang); Foshan University, Foshan, China (Z. Wei, Q. Liu); Northeast Forestry University, Harbin, China (Z. Hou)

DOI: https://doi.org/10.3201/eid2904.220885

[1]These authors contributed equally to this article.

Table 1. Characteristics of a tick-bitten patient infected with Yezo virus, northeastern China*

Characteristic	Result and treatment
Fever	
Temperature at admission, °C	39.5
Highest temperature, °C	39.6
Complications	
Headache	Yes
Dizziness	Yes
Blurred vision	Yes
Arthralgia	Yes
Chest distress	Yes
Shortness of breath	Yes
Fatigue	Yes
Bacterial co-infection	No
Tickborne pathogen detection	
TBEV	Negative
SFTSV	Negative
Alongshan virus	Negative
Songling virus	Negative
Beiji nairovirus	Negative
Yezo virus	Positive
Borrelia spp.	Negative
Rickettsia spp.	Negative
Anaplasma spp.	Negative
Babesia spp.	Negative
Treatment	
Day 1–4	Ribavirin (1 g IV), azithromycin (0.5 g IV), rocephin (3 g IV) daily
Day 1–8	Glycyrrhizin (3 tablets orally daily)

*IV, intravenous; SFTSV, severe fever with thrombocytopenia syndrome virus; TBEV, tick-borne encephalitis virus.

A blood sample was collected at admission and was negative for the tick-borne pathogens that have been identified in northeastern China (Table 1). The patient was empirically given ribavirin (1 g), azithromycin (0.5 g), and rocephin (3 g) intravenously each day during the first 4 days of hospitalization (Table 1). Glycyrrhizin was used to treat liver injury. The patient was discharged on the 8th day of hospitalization, although some clinical manifestations, such as headache, dizziness, and arthralgia, were still present. Two weeks later, the patient had recovered completely.

During April 2020–July 2021, a total of 2,830 ticks were collected from Heilongjiang, Jilin, and Inner Mongolia in northeastern China (214 *Haemaphysalis japonica*, 431 *H. concinna*, 1,110 *Dermacentor silvarum*, and 1,075 *I. persulcatus*) (Table 2). YEZV RNA was detected in *I. persulcatus* ticks by using reverse transcription PCR; overall prevalence was 0.5% (95% CI 0.2%–1.0%) (Table 2). The prevalence of YZEV infection in *I. persulcatus* ticks in Inner Mongolia, Heilongjiang, and Jilin varied from 0.4% to 0.5%. No positive sample was detected in other tick species.

We obtained complete genomes of 6 YEZV strains (1 from the patient and 5 from *I. persulcatus* ticks) by using specific primers (Appendix Table 1). YEZV has a genomic structure of typical orthonairoviruses (*5*). The complete genome of YEZV identified in this study included large (12,122-nt), medium (4,256-nt) and small (1,697-nt) segments (Appendix Table 3), which encoded a 3,938-aa large protein, a 1,356-aa glycoprotein precursor, and a 502-aa nucleocapsid (Appendix Figure 1). YEZV strain H-IM01 from the patient showed high sequence identities with those detected in ticks (T-HLJ01–03, T-JL01, and T-IM01) and nucleotide identities of 99.6%–100% (Appendix Tables 4, 5). Strains isolated from northeastern China were clustered with strains detected in tick-bitten patients in Japan and showed high nucleotide identities of 97.2%–98.8% (Appendix Tables 4, 5).

The YEZV strains from China were genetically related to Sulina virus discovered in *I. ricinus* ticks in Romania (*6*), showing complete genome nucleotide identities of 59.7%–70.3% and large protein amino acid identities of 82.3%–82.5%; they were grouped into the genogroup Sulina (Figure 2; Appendix Tables 4, 5, Figure 2) (*5*). Phylogenetic analysis indicated that viruses in the genogroup Sulina had a close relationship with Tamdy virus; those viruses showed nucleotide identities of ≈50% and large protein amino acid identities of ≈45% with each other. All viral genome sequences have been submitted to GenBank (Appendix Table 3).

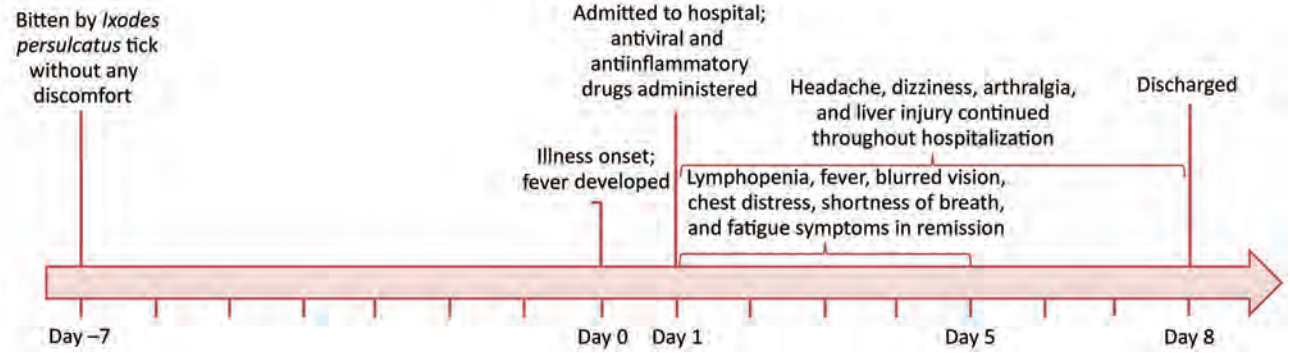

Figure 1. Timeline of the clinical course for a tick-bitten person infected with Yezo virus, northeastern China.

Table 2. Detection of Yezo virus RNA in *Ixodes persulcatus* ticks, northeastern China*

Province	Sampling time	No. pools/no. ticks	No. positive pools	Positive rate (95% CI)
Heilongjiang	2021	63/625	3	0.5 (0.1–1.3)
Jilin	2020–2021	19/192	1	0.5 (0.0–2.5)
Inner Mongolia	2021	26/258	1	0.4 (0.0–1.9)
Total	2020–2021	108/1,075	5	0.5 (0.2–1.0)

*Prevalence of Yezo virus infection in ticks was calculated by using PooledInfRate Excel Add-In version 4.0 (Microsoft, https://www.microsoft.com) and a 1-sample analysis with a bias-corrected maximum likelihood estimation method with 95% CIs and a scale of 100.

Conclusions

Clinical manifestations of the YEZV-infected patient in China were milder than those reported for patients in Japan, where leukopenia, lymphocytopenia, thrombocytopenia, coagulation disorder, and increased levels of liver and heart enzymes have been observed (*5*); only mild lymphocytopenia and mildly increased levels of liver enzymes were

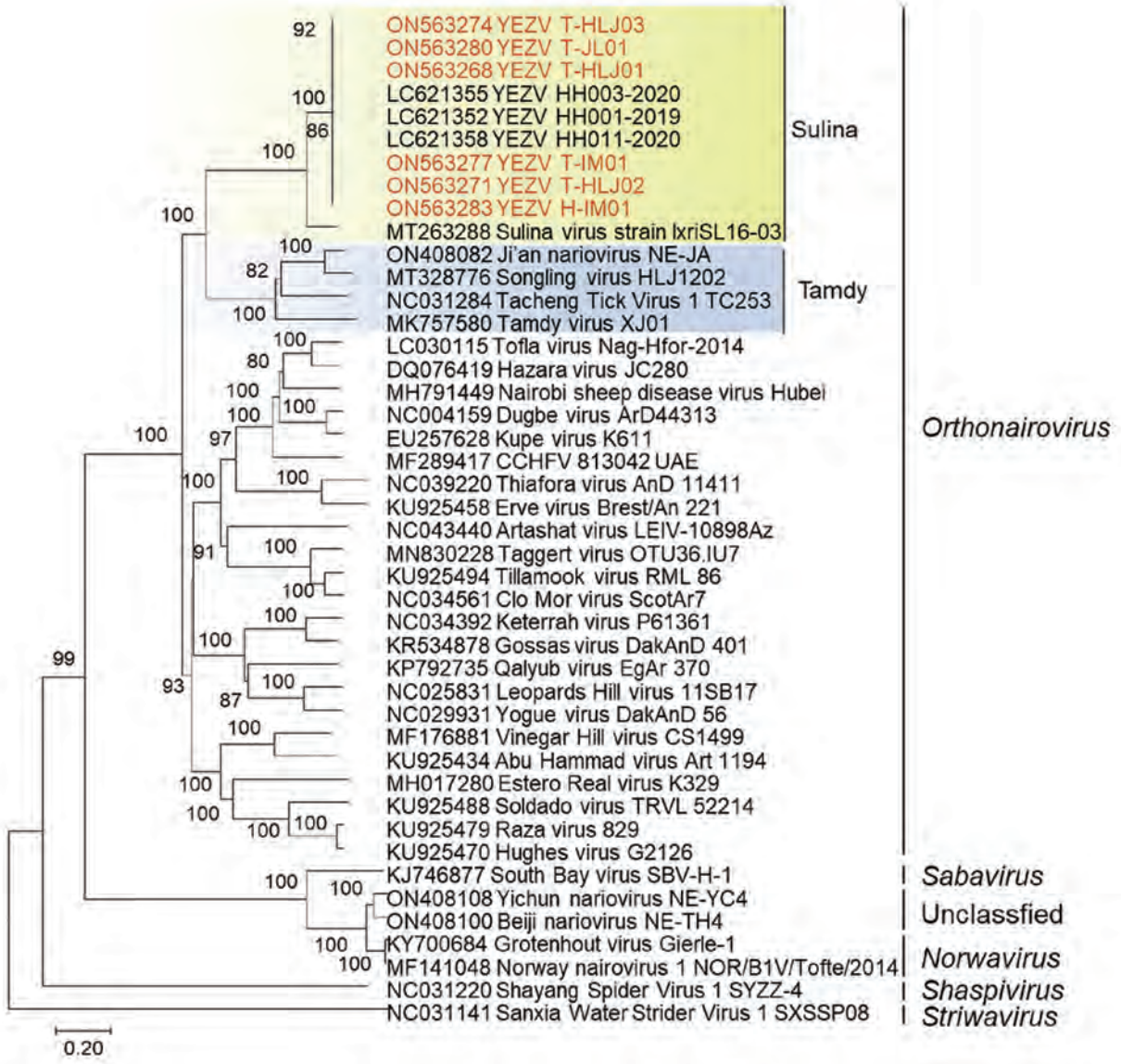

Figure 2. Phylogenetic analyses of Yezo virus from a tick-bitten person and *Ixodes persulcatus* ticks, northeastern China (red text), and references viruses. Sequences of representative viral strains were downloaded from National Center for Biotechnology Information public databases (https://www.ncbi.nlm.nih.gov) and aligned together using MEGA version 7.0 (https://www.megasoftware.net). A bootstrapping analysis of 1,000 replicates were conducted, and values >70 were considered significant and are shown. Shading indicates Sulin virus genogroup strains (green) and Tamdy virus strain (blue). Numbers along branches are bootstrap values. Scale bar indicates amino acid substitutions per site.

found in the patient in this study. The 2 patients in Japan were a 59-year-old man and a 41-year-old man who had medical histories of hyperuricemia and hyperlipidemia, and the patient from China was 33-year-old man who had no underlying disease. The YEZV-infected patient in this study was given ribavirin on days 1–4, but the patients in Japan were not given ribavirin. The clinical signs of YEZV infection might be related to age, medical history, and medication. No gastrointestinal symptoms, such as nausea, vomiting, and diarrhea, or hemorrhagic symptoms, such as melena, petechia, and ecchymosis, occurred in any of the YEZV-infected patients.

The infection rate of YEZV was low (1/402) in tick-bitten patients in northeastern China, compared with YEZV patients in Japan (5/248). To date, no severe YEZV-infected patient has been reported, and the patients in the 2 countries recovered completely. Thus, active surveillance should be performed on the tick-bitten populations to evaluate the prevalence and clinical characteristics of YEZV infection in the studied regions.

YEZV RNA has been detected in *H. megaspinosa*, *I. ovatus*, and *I. persulcatus* ticks in Hokkaido, Japan, showing a prevalence of 0.0%–5.7% (*5*). In this study, YEZV was detected only in *I. persulcatus* ticks, showing a prevalence of 0.5% (95% CI 0.2%–1.0%), and other tick species, such as *H. japonica*, *H. concinna*, and *D. silvarum*, were negative for YEZV RNA. Those results indicate that *I. persulcatus* ticks might serve as a potential vector for YEZV in northeastern China.

YZEV was identified in a tick-bitten patient who had febrile illness and *I. persulcatus* tick bites in northeastern China. Phylogenetic analysis confirmed the association between febrile illness and the virus. To date, there are ≥8 pathogenetic tickborne viruses in humans and animals found in northeastern China: tickborne encephalitis virus (*7*), severe fever with thrombocytopenia syndrome virus (*8*), Nairobi sheep disease virus (*9*), Alongshan virus (*10*), Jingmen tick virus (*11*), Songling virus (*3*), Beiji nairovirus (*4*), and YEZV. Differential diagnosis of these tickborne viruses should be conducted in for febrile patients who have a history of tick bites in northeastern China.

This study was supported by the National Key Research and Development Program of China (2022YFC2601900), the National Natural Science Foundation of China (82002165 and 32072887), the Outstanding Young Scholars Cultivating Plan of the First Hospital of Jilin University (2021-YQ-01), the Medical and Health Talent Special Project in Jilin Province of China (JLSWSRCZX2021-002), the Pearl River Talent Plan in Guangdong Province of China (2019CX01N111), and the Medical Innovation Team Project of Jilin University (2022JBGS02).

About the Author

Mr. Lv is a scientist at the Second Affiliated Hospital of Inner Mongolia University for the Nationalities, Inner Mongolia General Forestry Hospital, Yakeshi, China. His primary research interest is emerging tickborne diseases.

References

1. Walker PJ, Widen SG, Wood TG, Guzman H, Tesh RB, Vasilakis N. A global genomic characterization of nairoviruses identifies nine discrete genogroups with distinctive structural characteristics and host-vector associations. Am J Trop Med Hyg. 2016;94:1107–22. https://doi.org/10.4269/ajtmh.15-0917
2. Liu X, Zhang X, Wang Z, Dong Z, Xie S, Jiang M, et al. A tentative Tamdy orthonairovirus related to febrile illness in northwestern China. Clin Infect Dis. 2020;70:2155–60. https://doi.org/10.1093/cid/ciz602
3. Ma J, Lv XL, Zhang X, Han SZ, Wang ZD, Li L, et al. Identification of a new orthonairovirus associated with human febrile illness in China. Nat Med. 2021;27:434–9. https://doi.org/10.1038/s41591-020-01228-y
4. Wang YC, Wei Z, Lv X, Han S, Wang Z, Fan C, et al. A new nairo-like virus associated with human febrile illness in China. Emerg Microbes Infect. 2021;10:1200–8. https://doi.org/10.1080/22221751.2021.1936197
5. Kodama F, Yamaguchi H, Park E, Tatemoto K, Sashika M, Nakao R, et al. A novel nairovirus associated with acute febrile illness in Hokkaido, Japan. Nat Commun. 2021;12:5539. https://doi.org/10.1038/s41467-021-25857-0
6. Tomazatos A, von Possel R, Pekarek N, Holm T, Rieger T, Baum H, et al. Discovery and genetic characterization of a novel orthonairovirus in *Ixodes ricinus* ticks from Danube Delta. Infect Genet Evol. 2021;88:104704. https://doi.org/10.1016/j.meegid.2021.104704
7. Sun RX, Lai SJ, Yang Y, Li XL, Liu K, Yao HW, et al. Mapping the distribution of tick-borne encephalitis in mainland China. Ticks Tick Borne Dis. 2017;8:631–9. https://doi.org/10.1016/j.ttbdis.2017.04.009
8. Zhang X, Wang N, Wang Z, Che L, Chen C, Zhao WZ, et al. First fatal infection and phylodynamic analysis of severe fever with thrombocytopenia syndrome virus in Jilin Province, northeastern China. Virol Sin. 2021;36:329–32. https://doi.org/10.1007/s12250-020-00228-z
9. Gong S, He B, Wang Z, Shang L, Wei F, Liu Q, et al. Nairobi sheep disease virus RNA in ixodid ticks, China, 2013. Emerg Infect Dis. 2015;21:718–20. https://doi.org/10.3201/eid2104.141602
10. Wang ZD, Wang B, Wei F, Han SZ, Zhang L, Yang ZT, et al. A new segmented virus associated with human febrile illness in China. N Engl J Med. 2019;380:2116–25. https://doi.org/10.1056/NEJMoa1805068
11. Jia N, Liu HB, Ni XB, Bell-Sakyi L, Zheng YC, Song JL, et al. Emergence of human infection with Jingmen tick virus in China: a retrospective study. EBioMedicine. 2019;43:317–24. https://doi.org/10.1016/j.ebiom.2019.04.004

Address for correspondence: Zedong Wang, Department of Infectious Diseases, Center of Infectious Diseases and Pathogen Biology, State Key Laboratory of Zoonotic Diseases, First Hospital of Jilin University, Changchun 130122, Jilin, China; email: wangzedong@jlu.edu.cn

Effects of Seasonal Conditions on Abundance of Malaria Vector *Anopheles stephensi* Mosquitoes, Djibouti, 2018–2021

Alia Zayed, Manal Moustafa, Reham Tageldin, James F. Harwood

We describe the influence of seasonal meteorologic variations and rainfall events on *Anopheles stephensi* mosquito populations during a 40-month surveillance study at a US military base in Djibouti. Focusing surveillance and risk mitigation for *An. stephensi* mosquitoes when climatic conditions are optimal presents an opportunity for malaria prevention and control in eastern Africa.

Anopheles stephensi mosquitoes, an urban malaria vector, have established robust populations in the Horn of Africa. Since the mosquito's detection in 2012 (*1*), malaria cases in Djibouti increased 42.9-fold during 2013–2021, reaching ≈72,300 cases (*2*). Before introduction of *An. stephensi* mosquitoes, Djibouti was approaching the preelimination phase for malaria (*3*). Because *An. stephensi* mosquitoes are competent vectors for *Plasmodium falciparum* and *P. vivax* parasites (*3*), WHO considers this mosquito species a major threat to malaria elimination in Africa (*4*). *An. stephensi* mosquitoes have also been detected in Sudan, Ethiopia, and Somalia (*5*–*8*). Understanding *An. stephensi* mosquito adaptation to environmental conditions affecting population dynamics in urban settings is crucial in Africa. *An. stephensi* mosquitoes abundance (number of mosquitoes collected per trap night) changed from seasonal during fall–spring 2013–2016 to year-round in 2017 (*3*). Since *An. stephensi* mosquitoes were introduced, malaria cases have increased among military personnel, some immunologically naive, deployed as members of multinational militaries in Djibouti (*9*). Camp Lemonnier (CLDJ), a US naval base, has urban characteristics similar to the city of Djibouti, in which it is located. For this study, we monitored vector dynamics on the base, providing data to help inform health protection strategies among both military and civilian populations.

Author affiliations: US Naval Medical Research Unit No. 3, Cairo Detachment, Cairo, Egypt (A. Zayed, M. Moustafa, R. Tageldin); US Naval Medical Research Unit No. 3, Sigonella, Italy (J. Harwood); Cairo University, Cairo, Egypt (A. Zayed)

DOI: https://doi.org/10.3201/eid2904.220549

The Study

In coordination with the CLDJ Expeditionary Medical Facility, during January 2018–April 2021, we conducted weekly mosquito surveillance at 32 on-base sites covering 2 km^2 and stored information in dataset A. In October 2019, we began identifying monthly captures of *An. stephensi* mosquitoes specifically (i.e., identified at the species level) (dataset B). We set US Centers for Disease Control and Prevention (CDC) CO_2-baited Miniature Light traps (https://www.cdc.gov/mosquitoes/guidelines/west-nile/surveillance/environmental-surveillance.html) and Woodstream Mosquito Magnet (MM) propane-generated CO_2 traps (https://www.woodstream.com) overnight near dwellings, dining areas, sport facilities, and other areas frequented by humans. We identified *Anopheles* species on the basis of criteria published elsewhere (*10*,*11*). We analyzed abundance data in the context of specific weather events and seasonal climatic trends at the time of collection. We obtained meteorologic data from several sources (Appendix, https://wwwnc.cdc.gov/EID/article/29/4/22-0549-App1.pdf), using latitude 11.54733 N and longitude 43.15948 E (0.6–1.2 km from study sites) for location and a locally appropriate meteorologic calendar to determine seasons. We assessed the effects on *An. stephensi* mosquito abundance of monthly mean temperatures and rainfall amounts at time of precipitation and at 2-week, and 1- and 2-month lag times (i.e., time after rainfall). We did not consider longer lag times because of the likely effects of evaporation.

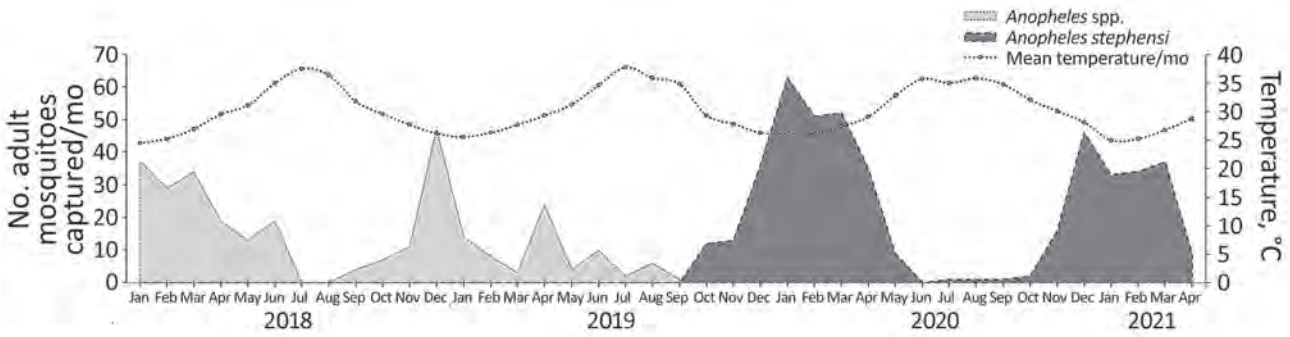

Figure 1. Associations between numbers of adult mosquitoes captured and mean temperature, by month, US military base, Djibouti, September 2019–August 2020. (We began identifying *Anopheles stephensi* mosquitoes specifically in October 2019.

We used the Shapiro-Wilk test to check normal distribution of *An. stephensi* mosquito data and Pearson correlation coefficient to evaluate relationships between mosquito abundance and climatic variables. We categorized temperatures as either above or equal to or below median annual temperature (30°C). We

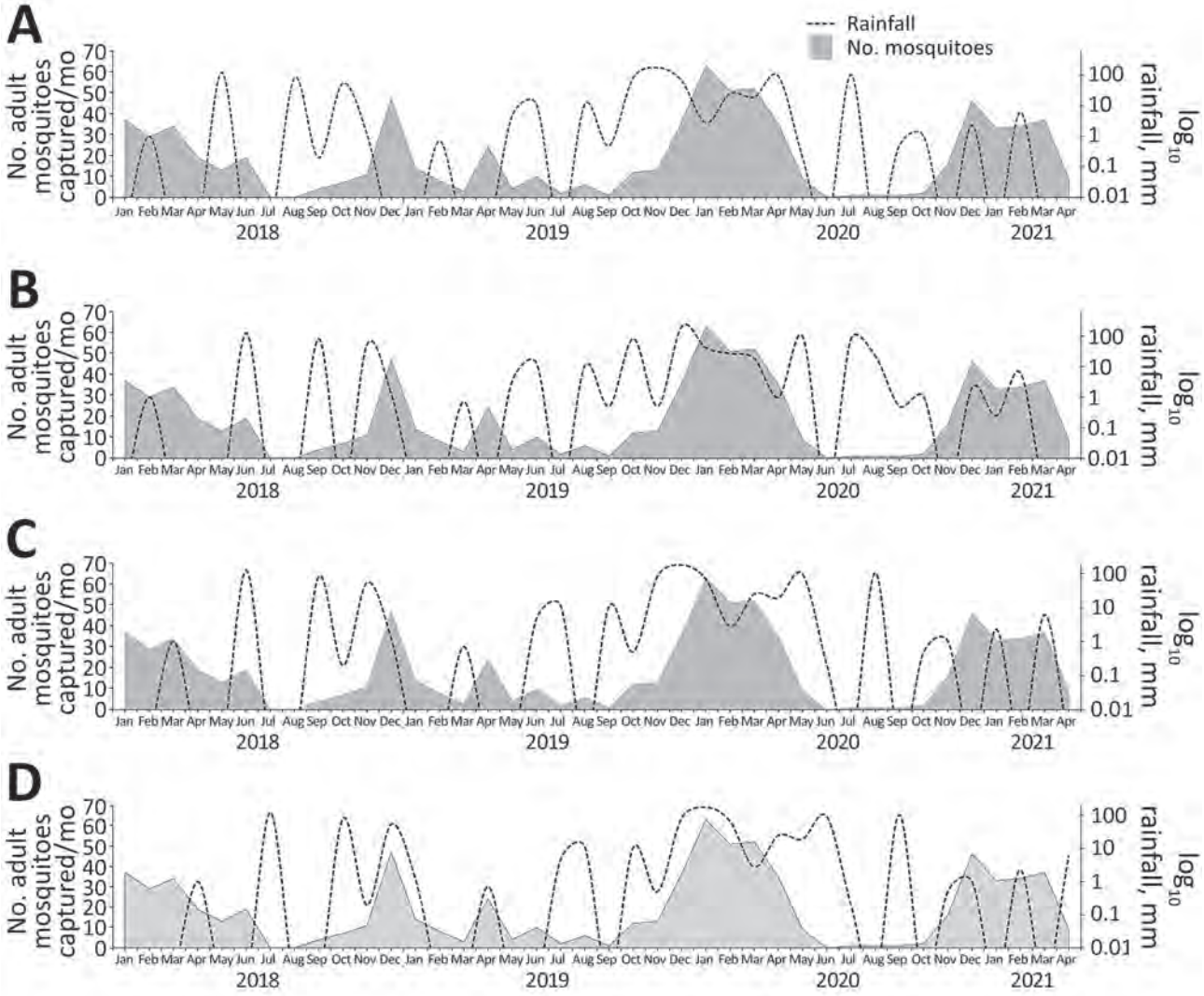

Figure 2. Associations between monthly collected numbers of *Anopheles stephensi* mosquitoes captured and precipitation rates, US military base, Djibouti, September 2019–August 2020. A) At time of rainfall; B) 2 weeks after rainfall; C) 1 month after rainfall; D) 2 months after rainfall.

Table 1. Univariate Poisson regression analysis of lagged effects of rainfall on abundance of *Anopheles stephensi* mosquitoes 2 weeks, 1 month, and 2 months after rainfall periods, US military base, Djibouti, September 2019–August 2020*

Time after rainfall	Rainfall level, mm/wk	Regression analysis		Abundance
		IRR (95% CI)	p value	
2 wk	40–155	0.56 (0.3–1.1)	0.09	2.3
	21.1–39.9	2.4 (1.7–3.4)	<0.0001	9.6
	5–21	1.5 (0.9–2.5)	0.11	6
	0.2–4.9	2.59 (2–3.4)	<0.0001	10.4
	0	Referent		4
1 mo	40–155	1.86 (0.9–2.2)	0.009	7
	21.1– 39.9	2.99 (2–3.8)	<0.0001	11.3
	5–21	1.13 (0.9–2.4)	0.6	4.3
	0.2–4.9	2.58 (1.5–2.7)	<0.0001	9.8
	0	Referent		3.8
2 mo	40–155	1.37 (1.2–3)	0.17	5.5
	21.1–39.9	2.75 (2.1–4.2)	<0.0001	11
	5–21	1.42 (0.7–1.9)	0.18	5.7
	0.2–4.9	2 (1.9–3.5)	<0.0001	8
	0	Referent		4

*Abundance is the average number of mosquitoes per trap night. IRR, incidence rate ratio.

grouped rainfall data according to frequency at each of 5 levels: 0, 0.2–4.9, 5–21, 21.1–39.9, and 40–155 mm/week. We used Poisson regression for univariate and multivariate analyses to determine associations between mosquito abundance and predictor variables, and used PROC GENMOD in SAS version 9.4 (SAS Institute, Inc., https://www.sas.com) to perform logistic regression. We expressed results in incidence rate ratios (IRR) and used p = 0.05 as the cutoff for statistical significance.

An. stephensi represented 95.6% of all *Anopheles* spp. mosquitoes we identified. Using dataset B to compare effectiveness of trap types, we found that MM traps captured 25.6% more *An. stephensi* mosquitoes than did CDC traps (IRR 2.3; p<0.0001) (Appendix Table, Figure). Univariate regression analysis of datasets A and B (Appendix Table) demonstrated that *An. stephensi* mosquito populations persisted year-round. Related to seasonal distribution, in dataset A, winter accounted for 56.4% of *Anopheles* spp. mosquito captures; spring, 28.1%; fall, 9.8%; and summer, 5.7%. In dataset B, winter accounted for 55.2% of *An. stephensi* mosquito captures; spring, 37.1%; fall, 6.9%; and summer, 0.8%. Associations between *An. stephensi* mosquito abundance and monthly mean temperatures (Figure 1) were positive for temperatures ≤30 (IRR 5.5 for dataset A, 7.4 for dataset B; p<0.0001). In dataset A, 85% of *Anopheles* spp. mosquitoes were collected at temperatures ≤30°C; for dataset B, the percentage was 94% of *An. stephensi* mosquitoes (Appendix Table).

Mosquito abundance increased 4–8 weeks after flooding in November 2019 (Figure 2). We also analyzed data on mosquito abundance 2 weeks and 1 and 2 months after rainfall throughout September 2019–August 2020, during which time 2 floods occurred (Table 1). Regression analysis showed significant associations between rainfall and *Anopheles* mosquito abundance recorded 2 weeks (IRR 2.4), 1 month (IRR 2.99), and 2 months (IRR 2.75) after periods of rainfall 21.1–39.9

Table 2. Multivariate Poisson regression analysis of seasonal and climatic factors associated with *Anopheles stephensi* mosquito abundance with and without lag effect after rainfall periods, US military base, Djibouti, September 2019–August 2020*

Variable	No lag effect		1-mo lag effect	
	IRR (95% CI)	p value	IRR (95% CI)	p value
Seasons				
Winter	4.2 (2.7–6.3)	<0.0001	4.12 (2.7–6.2)	<0.0001
Spring	2.8 (1.9–4.2)	<0.0001	2.86 (1.9–4.2)	<0.0001
Fall	1.3 (0.8–1.9)	0.3	1.19 (0.8–1.8)	0.42
Summer	Referent		Referent	
Temperature, °C				
≤30	2.4 (1.9–3.1)	<0.0001	2.2 (1.7–2.9)	<0.0001
>30	Referent		Referent	NA
Rain amounts, mm/wk				
40–155	0.33 (0.2–0.7)	0.004	1.2 (0.8–1.8)	0.4
21.1–39.9	1.1 (0.8–1.5)	0.6	1.5 (1.2–2.1)	0.0024
5–21	0.9 (0.6–1.3)	0.53	0.9 (0.6–1.5)	0.7
0.2–4.9	0.7 (0.6–0.9)	0.005	1.4 (1.2–1.7)	0.0002
0	Referent		Referent	

*NA, not applicable; IRR, incidence rate ratio.

mm/week ($p<0.0001$), corresponding to average mosquito counts of 9.6 (2 weeks), 11.3 (1 month), and 11.0 (2 months) after the rainfall. Unexpectedly, mosquito abundance also increased significantly 2 weeks (IRR 2.59), 1 month (IRR 2.58), and 2 months (IRR 2.00; $p<0.0001$) after periods of rainfall of just 0.2–4.9 mm/week. Multivariate analysis indicated that season and temperature were the variables most significantly associated with mosquito abundance when analyzed with no lag or 1-month rainfall lag effect. Winter (IRR 4.2 [no lag], 4.1 [1-month lag]; $p<0.0001$) and spring (IRR 2.8 [no lag], 2.9 [1-month lag]; $p<0.0001$) were the factors most associated with increases in *Anopheles* mosquitoes, followed by temperatures ≤30°C (IRR 2.4 [no lag], 2.2 [1-month lag]; $p<0.0001$) (Table 2).

Conclusions

We speculate that the slow continuous release of CO_2 of MM traps contributed to higher captures of *An. stephensi* mosquitoes than for CDC traps. In a study in Malaysia, MM traps performed 3-fold better than CDC traps for capturing *Anopheles* spp. mosquitoes (*12*), demonstrating the suitability of MM traps for *An. stephensi* mosquito surveillance in urban settings and areas with limited or no access to dry ice (*13*).

An. stephensi mosquitoes were present year-round but at substantially higher populations during winter (mean temperature 26°C, average rainfall 2.3 mm/week) and spring (mean temperature 29°C, average rainfall 7.3 mm/week). A previous study observed a similar link between temperature and *An. stephensi* mosquito populations, with 29°C assessed as optimal (*14*). We linked the bionomics of *An. stephensi* mosquito abundance in urban areas to human-modified conditions, such as air conditioning–produced condensation, water storage tanks, open jerry cans, and water-filled tires following rainfall, all of which increased favorable mosquito habitats (*1*) and in which we observed larval habitats around CLDJ. Flash flooding in Djibouti did not increase *An. stephensi* mosquito abundance. In fact, flooding might have destroyed laid eggs, hatched larvae, and temporary larval habitats, as was reported in China (*15*), possibly explaining higher population growth after periods of rainfall of 21.1–39.9 mm/week than 40–155 mm/week. Because breeding sites in urban areas depend as much on human-generated water sources as rainfall, adult mosquitoes were able to persist even during periods of low precipitation (*14*). We found that periods of rainfall at 21.1–39.9 mm/week and temperatures slightly <30°C were optimal for adult *An. stephensi* mosquito abundance. Therefore, surveillance and control efforts should be most intense during times of the year when these conditions are common. However, because *An. stephensi* mosquitoes are present year-round, prevention and control measures cannot be relaxed during any season (Appendix).

Although our study was set at CLDJ facilities, conditions were comparable to other urban settings in Djibouti, which should encourage local health authorities to benefit from our data. The persistence of mosquito populations at CLDJ, which regularly monitors and employs control efforts, should raise the alarm for increased malaria risk in densely populated city areas with fewer public health and disease control resources. Given limited resources, we recommend targeted reduction of *An. stephensi* larval habitat in this area.

Acknowledgments

We are greatly indebted to Expeditionary Medical Facility HM1 (hospital corpsman first class) Bicomong, HM2 Fletcher, HM2 McClinton, HM2 Foley, HM3 Begley, J. Flores, and Camp Lemonnier Djibouti for support in collecting and identifying mosquitoes.

This work was financially supported by Armed Forces Health Surveillance Division, Global Emerging Infections Surveillance (GEIS) Branch: P0137_20_N3_05.02 and P0042_21_N3.

Views expressed in this article reflect the results of research conducted by the author and do not necessarily reflect official policies or positions of the US Department of the Navy, Department of Defense, or federal government. Authors are military service members or federal/contracted employees of the US government. This work was prepared as part of official duties. Title 17 U.S.C. 105 provides that copyright protection under this title is not available for any work of the US government. Title 17 U.S.C. 101 defines a US government work as work prepared by a military service member or employee of the US government as part of that person's official duties.

About the Author

Dr. Zayed is an entomologist at the US Naval Medical Research Unit-3, Cairo, with academic and research involvement in Middle Eastern countries. Her primary research interests are vector surveillance and control.

References

1. Faulde MK, Rueda LM, Khaireh BA. First record of the Asian malaria vector *Anopheles stephensi* and its possible role in the resurgence of malaria in Djibouti, Horn of Africa. Acta Trop. 2014;139:39–43. https://doi.org/10.1016/j.actatropica.2014.06.016

2. World Health Organization. World malaria report 2021 [cited 2022 Dec 1]. https://www.who.int/teams/global-malaria-programme/reports/world-malaria-report-2021
3. Seyfarth M, Khaireh BA, Abdi AA, Bouh SM, Faulde MK. Five years following first detection of *Anopheles stephensi* (Diptera: Culicidae) in Djibouti, Horn of Africa: populations established-malaria emerging. Parasitol Res. 2019;118:725–32. https://doi.org/10.1007/s00436-019-06213-0
4. World Health Organization. Vector alert: *Anopheles stephensi* invasion and spread [cited 2022 March 26]. https://www.who.int/publications/i/item/WHO-HTM-GMP-2019.09
5. Takken W, Lindsay S. Increased threat of urban malaria from *Anopheles stephensi* mosquitoes, Africa. Emerg Infect Dis. 2019;25:1431–3. https://doi.org/10.3201/eid2507.190301
6. Balkew M, Mumba P, Yohannes G, Abiy E, Getachew D, Yared S, et al. Correction to: An update on the distribution, bionomics, and insecticide susceptibility of *Anopheles stephensi* in Ethiopia, 2018–2020. [Erratum for Malar J. 2021;20:263.] PubMed https://doi.org/10.1186/s12936-021-03852-6
7. Ahmed A, Khogali R, Elnour MAB, Nakao R, Salim B. Emergence of the invasive malaria vector *Anopheles stephensi* in Khartoum State, Central Sudan. Parasit Vectors. 2021;14:511. https://doi.org/10.1186/s13071-021-05026-4
8. Ali S, Samake JN, Spear J, Carter TE. Morphological identification and genetic characterization of *Anopheles stephensi* in Somaliland. Parasit Vectors. 2022;15:247. https://doi.org/10.1186/s13071-022-05339-y
9. de Santi VP, Khaireh BA, Chiniard T, Pradines B, Taudon N, Larréché S, et al. Role of *Anopheles stephensi* mosquitoes in malaria outbreak, Djibouti, 2019. Emerg Infect Dis. 2021;27:1697–700. https://doi.org/10.3201/eid2706.204557
10. Gillies MT, Coetzee MA. A supplement to the Anophelinae of Africa south of the Sahara. East London, South Africa: South African Institute for Medical Research; 1987.
11. Coetzee M. Key to the females of Afrotropical *Anopheles* mosquitoes (Diptera: Culicidae). Malar J. 2020;19:70. https://doi.org/10.1186/s12936-020-3144-9
12. Jeyaprakasam NK, Pramasivan S, Liew JWK, Van Low L, Wan-Sulaiman WY, Ngui R, et al. Evaluation of Mosquito Magnet and other collection tools for *Anopheles* mosquito vectors of simian malaria. Parasit Vectors. 2021;14:184. https://doi.org/10.1186/s13071-021-04689-3
13. Johansen CA, Montgomery BL, Mackenzie JS, Ritchie SA. Efficacies of the mosquito magnet and counterflow geometry traps in North Queensland, Australia. J Am Mosq Control Assoc. 2003;19:265–70.
14. Sinka ME, Pironon S, Massey NC, Longbottom J, Hemingway J, Moyes CL, et al. A new malaria vector in Africa: predicting the expansion range of *Anopheles stephensi* and identifying the urban populations at risk. Proc Natl Acad Sci U S A. 2020;117:24900–8. https://doi.org/10.1073/pnas.2003976117
15. Wu Y, Qiao Z, Wang N, Yu H, Feng Z, Li X, et al. Describing interaction effect between lagged rainfalls on malaria: an epidemiological study in south-west China. Malar J. 2017;16:53. https://doi.org/10.1186/s12936-017-1706-2

Address of correspondence: Alia Zayed, US Naval Medical Research Unit No. 3, Cairo Detachment, Cairo, Egypt; email: alia.m.zayed.ln@health.mil

Tularemia in Pregnant Woman, Serbia, 2018

Milena Saranovic, Marija Milic, Ivan Radic, Natasa Katanic, Mirjana Vujacic, Milos Gasic, Ivan Bogosavljevic

Tularemia was diagnosed for a 33-year-old pregnant woman in Serbia after a swollen neck lymph node was detected at gestation week 18. Gentamicin was administered parenterally (120 mg/d for 7 d); the pregnancy continued with no complications and a healthy newborn was delivered. Treatment of tularemia optimizes maternal and infant outcomes.

Tularemia is a systemic, potentially serious zoonotic disease caused by *Francisella tularensis* bacteria (*1*). Interhuman transmission of tularemia has not been reported. Transmission is primarily by Ixodidae ticks (*2*,*3*); the second most frequent vectors are mosquitoes in restricted areas (e.g., Sweden and Finland) (*4*). Contact with live infected animals can be a source of human infection. Many tularemia cases also occur through contact with contaminated aquatic environments (e.g., swimming, canyoning, fishing) (*5*,*6*). Incubation period is 1–10 days, and clinical signs depend on the route of infection. Direct contact with animals or tick bites leads to a skin lesion with satellite lymphadenopathy. Ingesting contaminated food or drinking contaminated water leads to pharyngitis and cervical lymphadenopathy. Clinical signs are ulceroglandular disease with cutaneous ulcerations and marked lymphadenopathy; glandular disease with no ulcers but marked lymphadenopathy; oculoglandular disease with preauricular lymphadenopathy and conjunctivitis; oropharyngeal disease with pharyngitis and cervical lymphadenopathy; gastrointestinal disease with vomiting, abdominal discomfort, and diarrhea; respiratory disease (pneumonia or pleuritis); and typhoid tularemia (fever without early signs/symptoms) (*7*). If not treated adequately, tularemia can spread to the lungs, pleura, gastrointestinal tract, or central nervous system (*8*,*9*).

There are 2 subspecies of *F. tularensis*: type A, which is almost completely restricted to North America, and type B, which is found in Europe (*1*). Type A strains are highly virulent. Before the advent of effective antimicrobial drugs, mortality rate for both types was 5%–10% (*10*). Current mortality rates are 2%–3% for type A and <1% for type B tularemia but vary according to type of infection and *F. tularensis* genotype. Mortality rates among patients with bilateral type A acute pneumonia are ≥30% (*7*).

After 2000, the annual incidence rate of tularemia in Europe was highest in Kosovo (>5 cases/100,000 population), followed by Sweden, Finland, Slovakia, Czech Republic, Norway, Serbia, Hungary, Bulgaria, and Croatia (*1*). Tularemia is more common in men than in women and extremely rare in pregnant women (*2*,*3*). To date, at least 12 cases of tularemia during pregnancy have been described in the literature (Appendix, https://wwwnc.cdc.gov/EID/article/29/4/22-1318-App1.pdf). We report the case of a pregnant woman with tularemia in Serbia.

The Case

In 2018, a 33-year-old woman in the second trimester of pregnancy (18 weeks' gestation) was referred to the Gynecology Department of the Policlinic for Students' Healthcare, University of Pristina, for a painless lymphadenopathy on the left side of her neck. The woman denied having a fever or other signs/symptoms of infection. She lived in the urban area of Kosovska Mitrovica and reported no contact with known reservoirs of *F. tularensis*, although she did mention having gone for a walk and spending some time in natural areas, but not swimming, a few days before symptom onset. She denied drinking nonpotable water (e.g., spring water) and confirmed that she drank only bottled water.

Author affiliations: University of Pristina, (temporarily in) Kosovska Mitrovica, Serbia (M. Saranovic, M. Milic, I. Radic, N. Katanic, M. Gasic, I. Bogosavljevic); Clinic for Infectious Disease, Health Center, Kosovska Mitrovica (N. Katanic, M. Vujacic)

DOI: https://doi.org/10.3201/eid2904.221318

Three months before pregnancy, cervical screening (including smear test and microbiology) detected no abnormalities. She had no previous pregnancies or remarkable medical or surgical history. During week 7 of gestation, a viable, eutopic, singleton pregnancy was confirmed, and at week 12, gynecologic and ultrasonography examinations and double marker, blood, urine, and biochemical testing were performed. Fetal growth corresponded with the length of the amenorrhea, and all results were within the normal range for pregnancy. Double marker testing indicated low risk for trisomies. The patient was asymptomatic. The next appointment was at week 16 of gestation, when uneventful pregnancy with constant growth velocity was confirmed.

The painless lymphadenopathy was detected at week 18. The lymph node was mobile, ≈2 cm in diameter, and painless. Blood analysis results, including leukocytes, were within reference limits and showed no evidence of bacteremia. Nose and throat swab sample cultures showed no microbial growth.

For biopsy of the swollen lymph node, we referred the patient to the Clinic for Otorhinolaryngology and Maxillofacial Surgery at the Clinical Centre of Serbia, University of Belgrade. At the time of the transfer, she was 19 weeks pregnant, febrile, but clinically stable. Fetal growth corresponded to gestational age. Immunologic analyses, blood count, and peripheral blood smear performed by the hematologist ruled out blood disorders and systemic diseases (antinuclear antibodies were negative). Serologic analyses excluded infection caused by Epstein-Barr virus, cytomegalovirus, HIV, herpes simplex virus, and hepatitis B and C viruses. Toxoplasmosis and brucellosis were excluded by relevant testing.

The enlarged neck node was excised with local anesthesia at week 19 of gestation. Histopathologic findings confirmed histolytic necrotizing lymphadenitis (also called Kikuchi-Fujimoto disease), which can be induced by an infectious disease. Serum was sent to SYNLAB (Augsburg, Germany) for *F. tularensis* testing, and after 2 weeks, enzyme immunoassay showed increased IgM against *F. tularensis* (16.1 U/mL, cutoff<10 U/mL) but not IgG, which correlated with the clinical signs and indicated acute infection.

The patient was hospitalized for 2 weeks; she was febrile for 2 days (temperature not >39°C) and treated symptomatically. Ultrasonography for fetal anomaly performed at the Institute for Gynaecology and Obstetrics "Visegradska," Belgrade, detected no abnormality, and fetal growth velocity was maintained. Blood analysis remained within reference limits, with no evidence of bacteremia. After receiving gentamicin (120 mg intramuscularly 1×/d) for 7 days, the patient was discharged at week 22 of gestation.

At term, the woman vaginally delivered a healthy boy, weighing 3,860 g, with Apgar scores of 9 at 1 minute and 10 at 5 minutes. Histopathologic examination of the placenta revealed no evidence of pathology. Newborn hearing screening on day 3 was normal bilaterally. At examinations performed 1 and 4 months after delivery, both mother and baby were healthy, with no complications, and all blood test results were within reference limits. The newborn was not tested further for infectious diseases.

Conclusions

According to the available literature, tularemia in pregnancy is rare; at least 12 cases have been described (Appendix). Although gentamicin, ciprofloxacin, and doxycycline are not recommended as the first-line treatment for pregnant women, the World Health Organization recommends ciprofloxacin and gentamicin for treatment of tularemia during pregnancy (*11*–*14*). Use of gentamicin, ciprofloxacin, and doxycycline is not associated with increased risk for birth defects, stillbirth, premature birth, or low birth weight (*12*,*13*). A previous case indicated that during pregnancy, dacryocystitis and abscess on the neck with pharyngitis did not affect the pregnancy outcome after surgical and antimicrobial treatment (*15*). The gradient of symptoms and clinical manifestations of tularemia in pregnant women differ and depend on the mode of transmission of the infection, the amount and virulence of the pathogen, and the host immunity. Mild clinical signs/symptoms can be expected in healthy young pregnant women without other comorbidities who acquire infection in the second or third trimester, as did the patient we report.

Tularemia is extremely rare during pregnancy; mild disease can appear during the second and third trimesters, and adequate treatment can be administered without consequences to the fetus. Therefore, in a pregnant woman with lymphadenopathy, with or without signs/symptoms, infections such as tularemia should be considered in the differential diagnosis, especially in areas where tularemia still circulates at a high incidence rate. To optimize maternal and infant outcomes, tularemia can and should be adequately and effectively treated during pregnancy.

About the Author

Dr. Saranovic is an assistant professor of anatomy and a researcher at the Faculty of Medicine, University of Pristina. Her research interests are gynecology and obstetrics, specifically sterility and infertility.

References

1. Stone RM. Harrison's principles of internal medicine. 15th edition. In: Braunwald E., Fauci AS, Kasper DL, Hauser SL, Longo DL, Jameson JL, editors. New York, NY: McGraw-Hill 2004. p. 991–3.
2. Hubálek Z, Treml F, Halouzka J, Juricová Z, Hunady M, Janík V. Frequent isolation of *Francisella tularensis* from *Dermacentor reticulatus* ticks in an enzootic focus of tularaemia. Med Vet Entomol. 1996;10:241–6. https://doi.org/10.1111/j.1365-2915.1996.tb00737.x
3. Gurycová D, Výrosteková V, Khanakah G, Kocianová E, Stanek G. Importance of surveillance of tularemia natural foci in the known endemic area of Central Europe, 1991–1997. Wien Klin Wochenschr. 2001;113:433–8.
4. Eliasson H, Bäck E. Tularaemia in an emergent area in Sweden: an analysis of 234 cases in five years. Scand J Infect Dis. 2007;39:880–9. https://doi.org/10.1080/ 00365540701402970
5. Berdal BP, Mehl R, Meidell NK, Lorentzen-Styr AM, Scheel O. Field investigations of tularemia in Norway. FEMS Immunol Med Microbiol. 1996;13:191–5. https://doi.org/10.1111/j.1574-695X.1996.tb00235.x
6. Abd H, Johansson T, Golovliov I, Sandström G, Forsman M. Survival and growth of *Francisella tularensis* in *Acanthamoeba castellanii.* Appl Environ Microbiol. 2003;69:600–6. https://doi.org/10.1128/AEM.69.1.600-606.2003
7. Snowden J, Simonsen KA. Tularemia. Treasure Island (FL): StatPearls Publishing; 2022.
8. Maurin M, Gyuranecz M. Tularaemia: clinical aspects in Europe. Lancet Infect Dis. 2016;16:113–24. https://doi.org/10.1016/S1473-3099(15)00355-2
9. Gürcan S. Epidemiology of tularemia. Balkan Med J. 2014; 31:3–10. https://doi.org/10.5152/balkanmedj.2014.13117
10. Tärnvik A, Berglund L. Tularaemia. Eur Respir J. 2003;21:361–73. https://doi.org/10.1183/09031936.03.00088903
11. World Health Organization. WHO guidelines on tularemia. Geneva: The Organization; 2007.
12. Yu PA, Tran EL, Parker CM, Kim HJ, Yee EL, Smith PW, et al. Safety of antimicrobials during pregnancy: a systematic review of antimicrobials considered for treatment and postexposure prophylaxis of plague. Clin Infect Dis. 2020;70(Suppl 1):S37–50. https://doi.org/10.1093/cid/ciz1231
13. Ziv A, Masarwa R, Perlman A, Ziv D, Matok I. Pregnancy outcomes following exposure to quinolone antibiotics—a systematic-review and meta-analysis. Pharm Res. 2018;35:109. https://doi.org/10.1007/s11095-018-2383-8
14. Boui M, Errami E. Tularemia outbreak in Kosovo [in French]. Ann Dermatol Venereol. 2007;134:839–42. https://doi.org/10.1016/S0151-9638(07)92827-6
15. Kosker M, Celik T, Yuksel D. Treatment of tularemia during pregnancy. J Infect Dev Ctries. 2015;9:118–9. https://doi.org/10.3855/jidc.5245

Address for correspondence: Milena Saranovic, Faculty of Medicine, University of Pristina temporarily settled in Kosovska Mitrovica, Anri Dinana bb, 38228, Kosovska Mitrovica, Serbia; email: milena.saranovic@gmail.com

Ocular Trematodiasis in Children, Sri Lanka

Chandana H. Mallawarachchi, Mangala M. Dissanayake, Sidesh R. Hendavitharana, Saman Senanayake, Nisayuri Gunathilaka, Nilmini T.G.A. Chandrasena, Thishan C. Yahathugoda, Susiji Wickramasinghe, Nilanthi R. de Silva

Using histopathology and phylogenetic analysis of the internal transcribed spacer 2 gene, we found ≥2 distinct trematode species that caused ocular trematode infections in children in Sri Lanka. Collaborations between clinicians and parasitologists and community awareness of water-related contamination hazards will promote diagnosis, control, and prevention of ocular trematode infections.

Helminths are major etiologic agents of human blindness in low-income countries (*1*). Adult, juvenile, and larval stages of nematodes, cestodes, and trematodes have been recovered from ocular and periocular tissues. Some helminths are natural parasites of humans, although most are zoonotic (*2*). Most eye helminthiases are accidental, resulting from aberrant migration of immature worms in host tissues. Ocular helminthiases reported in Sri Lanka have been mainly caused by nematode species such as ascarids, filariids, and strongylids (*3*–*7*). Adult avian trematodes (*Philophthalmus* spp.) causing accidental subconjunctival infection in humans have also been reported in Sri Lanka (*5*,*6*). Rare occurrences of trematode-induced conjunctival and anterior chamber granulomas have been reported in South India and Egypt (*8*,*9*). Although adult flukes were not identified in those cases, histologic analysis of excised nodules suggested trematode etiology (*8*,*9*), and molecular methods confirmed a trematode etiology in Egypt (*9*). In the cases from South India, trematode DNA with high sequence similarity to *Procerovum varium* flukes (family Heterophyidae) from fish-eating birds was detected (*10*).

Anterior chamber nodules of the eye of suspected helminth etiology have been noted for almost a decade in the North Central Province of Sri Lanka, and clinical outcomes have varied from complete cures to cataracts and blindness. We report 3 cases of episcleral nodules with confirmed trematode etiology in the Eastern and North Central Provinces of Sri Lanka and describe clinical manifestations, histopathology, and phylogeny of the causative trematode species.

The Study

We conducted a retrospective study with tissue samples from 3 pediatric patients in Sri Lanka. The samples were referred from the ophthalmology units of the District General Hospital in Trincomalee, National Hospital in Kandy, and Base Hospital in Kantale for molecular analysis at the Department of Parasitology, Faculty of Medicine, University of Peradeniya, Peradeniya, Sri Lanka, during 2020–2021. The Ethics Review Committee of the Medical Research Institute, Colombo, Sri Lanka, approved this study (project no. 26/2020).

In case 1, a 13-year-old male child with a 3-week history of a red right eye in which a nodular lesion developed sought care at the District General Hospital in Trincomalee in September 2020. Examination revealed a dome-shaped, whitish, 3-mm episcleral nodule situated inferonasal ≈3 mm from the limbus (Figure 1). The eye was mildly inflamed, but the patient's visual acuity was normal. Slit lamp examination did not reveal signs of inflammation in the anterior chamber, and the rest of the affected eye and left eye were normal. The patient was healthy otherwise and had complete blood cell

Author affiliations: Medical Research Institute, Colombo, Sri Lanka (C.H. Mallawarachchi); District General Hospital, Trincomalee, Sri Lanka (M.M. Dissanayake, N. Gunathilaka); Base Hospital, Kantale, Sri Lanka (S.R. Hendavitharana); National Hospital, Kandy, Sri Lanka (S. Senanayake); University of Kelaniya, Kelaniya, Sri Lanka (N.T.G.A. Chandrasena, N.R. de Silva); University of Ruhuna, Galle, Sri Lanka (T.C. Yahathugoda); University of Peradeniya, Peradeniya, Sri Lanka (S. Wickramasinghe)

DOI: https://doi.org/10.3201/eid2904.221517

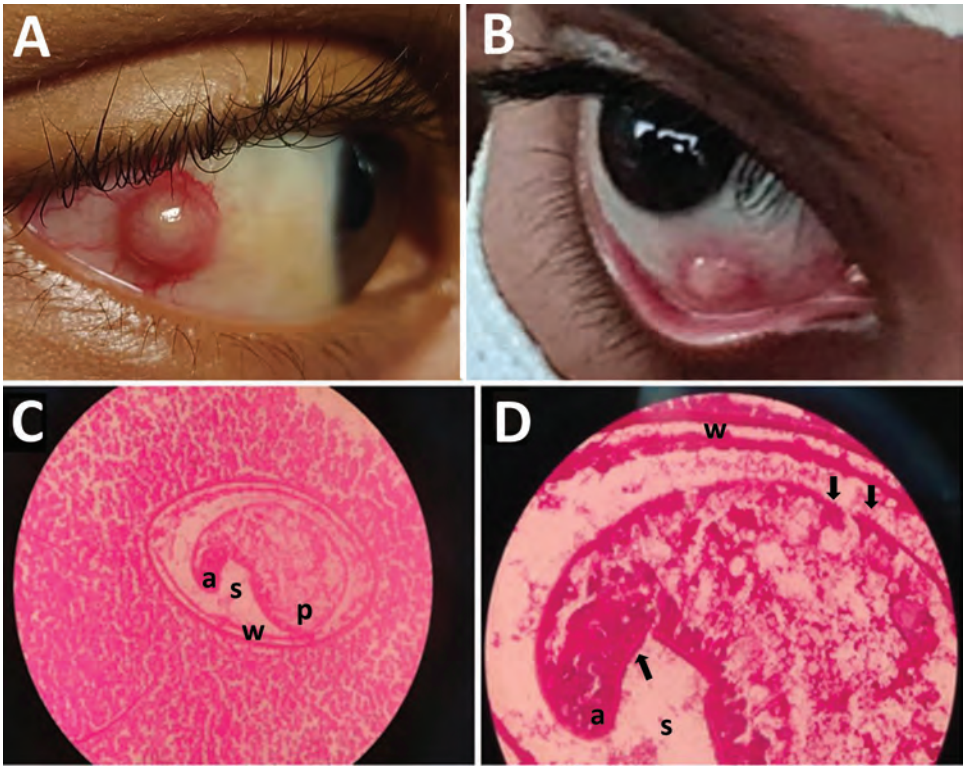

Figure 1. Trematode infection in the eyes of 2 pediatric patients in a study of ocular trematodiasis in children, Sri Lanka. A, B) Episcleral nodules found in eyes of 2 male pediatric patients. C, D) Metacercarial stage of a trematode in hematoxylin/eosin-stained tissue section of an excised episcleral nodule from a 12-year old boy. a, anterior end; p, posterior end; s, space between the larva and cyst wall; w, double layer cyst wall. Arrows in panel D indicate possible spines on surface tegument. Original magnification ×40 for panel C, ×100 for panel D.

counts and C-reactive protein levels within normal ranges. Several other children living in the neighborhood and 2 siblings of the index case-patient had similar complaints. All affected children had bathed in an irrigation canal connected to the Kantale reservoir.

The nodule was excised under general anesthesia, placed in 10% neutral-buffered formalin, and sent to the pathology laboratory for histopathological assessment, which showed a nodular-shaped granulated tissue fragment with a central cystic area. The cystic area had a micro-abscess with many neutrophils, some eosinophils, and a cross-section of an encysted helminth that was 0.2 mm in diameter (Figure 1). Morphology of the helminth was consistent with the metacercaria stage of a trematode, showing a cyst wall, surface tegument with possible minute surface spines, and a sucker (Figure 1) (2). The patient's recovery was uneventful, and no new lesions were observed at a 6-month follow-up examination.

In case 2, a 12-year-old male child from Hingurakgoda in the Polonnaruwa District sought care in April 2021 at the National Hospital in Kandy for a scleral nodule in the right eye that gradually enlarged over a 3-month period (Table). Nodule-associated pain, tenderness, redness, tearing, or impaired vision did not occur. The patient was treated with ocular antimicrobial drugs and steroids but had no improvement. None of his family members had similar complaints. He lived near an irrigation canal connected to the Minneriya reservoir, where he bathed daily. Examination revealed a scleral nodule that was 2 mm in diameter and medial to the limbus of the right eye.

Table. Clinical history of 3 male patients with confirmed ocular trematode infections in study of ocular trematodiasis in children, Sri Lanka*

Case no.	Age, y	Infection site	Clinical manifestations	Trematode identification
1	13	Right eye	A 3-wk history of redness in right eye followed by formation of an episcleral nodule. Examination revealed a dome-shaped, whitish, 3-mm episcleral nodule situated inferonasal ≈3 mm from the limbus.	Trematode metacercaria and histologic diagnosis (Figure 1, panels A, B)
2	12	Right eye	A 3-mo history of episcleral nodule in right eye. Examination revealed a scleral nodule, 2 mm in diameter, medial to the limbus.	Unknown trematode isolate 1 and *ITS2* sequencing (Figure 2)
3	11	Right eye	A 3–4-wk history of redness and irritation in right eye and formation of an episcleral nodule. Examination revealed a scleral nodule, 4 mm in diameter, medial to the limbus.	Unknown trematode isolate 2 and *ITS2* sequencing (Figure 2)

**ITS2*, internal transcribed spacer 2 gene.

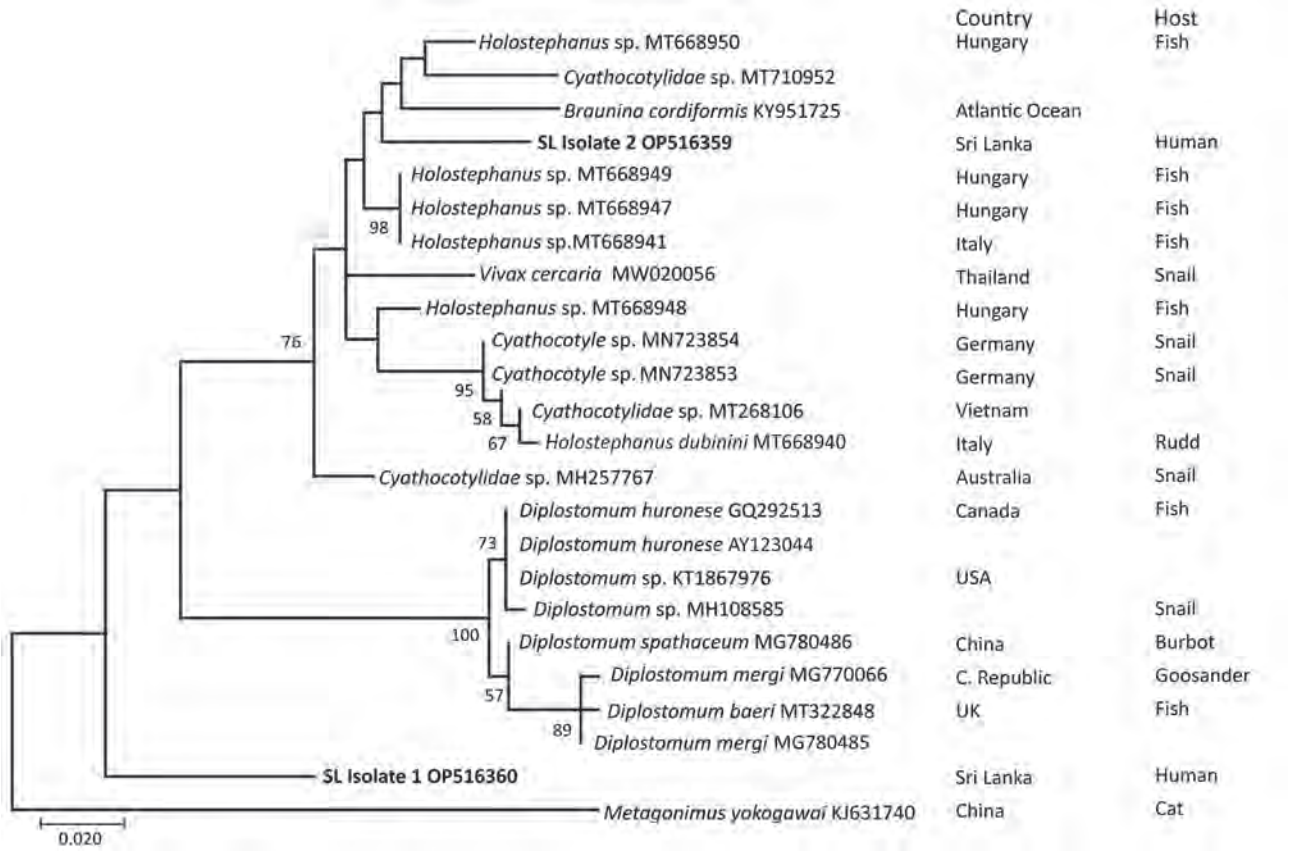

Figure 2. Phylogenetic analysis of isolates from 2 episcleral nodule isolates from the eyes of pediatric patients in study of ocular trematodiasis in children, Sri Lanka. Genomic DNA was isolated from biopsy samples from 2 patients. PCR was used to target the trematode internal transcribed spacer 2 (*ITS2*) gene, which was then sequenced. Maximum-likelihood analysis was used to construct a phylogenetic tree containing partial sequences of isolate 1 and 2 (bold font) from Sri Lanka and 24 taxa from GenBank. Partial *ITS2* gene sequences were aligned by using MEGA version 10.2.4 software (https://www.megasoftware.net). Numbers near nodes indicate the percentages of 1,000 nonparametric bootstrap pseudoreplicates (>50). GenBank accession numbers are provided for *ITS2* gene reference sequences. The sequences for the 2 isolates from this study were deposited in GenBank (accession nos. OP516360 and OP516359). *Metagonimus yokogawai* (KJ631740) isolated from a cat is included as the outgroup. SL, Sri Lanka. Scale bar indicates nucleotide substitutions per site.

The ocular adnexae were normal. A whitish corneal opacity was noted near the limbal border of the nodule (Figure 1).

In case 3, an 11-year-old male child from Kantale sought care at the Base Hospital in Kantale for redness and irritation in the right eye in which a nodular lesion developed over a 3–4-week period in December 2020. His visual acuity was normal. A 4-mm episcleral nodule situated medial to the limbus was noted (Table). He also bathed in an irrigation canal connected to the Kantale reservoir.

We extracted genomic DNA from tissue biopsies (from patients 2 and 3) fixed in 70% ethanol by using the PureLink Genomic DNA Mini Kit (ThermoFisher Scientific, https://www.thermofisher.com). We performed PCR to amplify the internal transcribed spacer 2 (*ITS2*) and 28S rRNA gene regions and mitochondrial *COX1* gene (Appendix, https://wwwnc.cdc.gov/EID/article/29/4/22-1517-App1.pdf). Isolates 1 (patient 2) and 2 (patient 3) were *ITS2*-positive but negative for 28S rRNA and *COX1* by PCR. We performed Sanger sequencing of the *ITS2*-positive samples (Appendix) and constructed a phylogenetic tree by using MEGA-X version 10.2.4 software (https://www.megasoftware.net) and the maximum-likelihood statistical method (Figure 2). The 2 sequences from Sri Lanka that we submitted to GenBank were 487 bp (accession no. OP516359) and 427 bp (accession no. OP516360). Isolate 1 was basal to *Diplostomum* sp., whereas isolate 2 clustered with *Braunina cordiformis* (GenBank accession no. KY951725) (4.4% nt divergence), *Cyathocotylidae* sp. (GenBank accession no. MT710952) (3.8% nt divergence), and *Holostephanaus* sp. (GenBank accession no. MT668950) (1.8% nt divergence) (Figure 2).

Conclusions

Humans appear to be an accidental intermediate host of the trematodes isolated in Sri Lanka, whereas genomic sequences from trematodes in different countries indicate other hosts, such as snails, fish, birds, and cats. On the basis of our molecular and phylogenetic analyses, we suggest that different trematode species are responsible for ocular trematodiasis in Sri Lanka.

Isolated cases of adult trematode infections of the eye caused by *Philophthalmus* spp., *Fasciola hepatica*, and schistosomes have been reported in other countries (*5*,*6*,*11*–*14*). Trematode cercaria of *Procerovum varium* was proposed as the etiologic agent of ocular inflammatory lesions among children bathing in village ponds in South India (*10*). The route of entry of those cercariae was either oral or by direct penetration of the eye during exposure in snail-infested waters (*10*). *Alaria mesocercaria* trematodes have been reported as a cause of neuroretinitis (*15*). However, infections of human tissues with metacercaria have not been well documented. Our report provides evidence of trematode metacercariae in human ocular tissues. The sequence data indicate that the trematode species found in the isolates from Sri Lanka do not belong to any previously known (or sequenced) species that cause eye infections. The immune-privileged status of the eye might promote cercaria development of the unidentified trematode species in humans.

Excision of the inflamed nodules was curative and enabled extraction of the worm for identification. Establishing the identity of larval helminths in tissue sections is difficult because of rapid tissue degradation caused by substantial inflammation and the requirement for specialist assistance for histopathologic analysis (*7*). Molecular diagnostic methods have overcome these issues, enabling the species-level identification of helminths in tissue sections (*9*,*10*).

In summary, trematode metacercariae might occur in the ocular tissues of children exposed to freshwater reservoirs and their aquatic fauna, posing a water-related public health burden. Ocular trematode infections were caused by ≥2 distinct trematode species in Sri Lanka. Creating awareness among clinicians and the community and active collaboration with parasitologists will promote diagnosis, control, and prevention of ocular trematode infections.

Acknowledgments

We thank the Centers for Disease Control and Prevention, Center for Global Health, Division of Parasitic Diseases and Malaria, for the diagnostic assistance provided by the DPDx website (https://www.cdc.gov/dpdx) and Lakmali Bandara for performing DNA extractions and PCR.

This research received no specific grant support from the public, commercial, or not-for-profit funding agencies.

About the Author

Dr. Mallawarachchi was a clinical parasitologist from the Medical Research Institute, Colombo, Sri Lanka. Unfortunately, he passed away while pursuing postgraduate training in the United Kingdom.

References

1. Sabrosa NA, Cunningham ET Jr, Arevalo JF. Ocular nematode and trematode infections in the developing world. Int Ophthalmol Clin. 2010;50:71–85. https://doi.org/10.1097/IIO.0b013e3181d2d915
2. Otranto D, Eberhard ML. Zoonotic helminths affecting the human eye. Parasit Vectors. 2011;4:41. https://doi.org/10.1186/1756-3305-4-41
3. Iddawela D, Ehambaram K, Wickramasinghe S. Human ocular dirofilariasis due to *Dirofilaria repens* in Sri Lanka. Asian Pac J Trop Med. 2015;8:1022–6. https://doi.org/10.1016/j.apjtm.2015.11.010
4. Iddawela D, Ehambaram K, Bandara P. Prevalence of *Toxocara* antibodies among patients clinically suspected to have ocular toxocariasis: a retrospective descriptive study in Sri Lanka. BMC Ophthalmol. 2017;17:50. https://doi.org/10.1186/s12886-017-0444-0
5. Dissanaike AS, Bilimoria DP. On an infection of a human eye with *Philophthalmus* sp. in Ceylon. J Helminthol. 1958;32:115–8. https://doi.org/10.1017/S0022149X00019519
6. Rajapakse RDK, Wijerathne KMTN, S de Wijesundera MS. Ocular infection with an avian trematode (*Philophthalmus* sp). Ceylon Med J. 2009;54:128–9. https://doi.org/10.4038/cmj.v54i4.1454
7. Wariyapola D, Goonesinghe N, Priyamanna TH, Fonseka C, Ismail MM, Abeyewickreme W, et al. Second case of ocular parastrongyliasis from Sri Lanka. Trans R Soc Trop Med Hyg. 1998;92:64–5. https://doi.org/10.1016/S0035-9203(98)90956-7
8. Rathinam S, Fritsche TR, Srinivasan M, Vijayalakshmi P, Read RW, Gautom R, et al. An outbreak of trematode-induced granulomas of the conjunctiva. Ophthalmology. 2001;108:1223–9. https://doi.org/10.1016/S0161-6420 (01)00604-2
9. Amin RM, Goweida MB, El Goweini HF, Bedda AM, Lotfy WM, Gaballah AH, et al. Trematodal granulomatous uveitis in paediatric Egyptian patients: a case series. Br J Ophthalmol. 2017;101:999–1002. https://doi.org/10.1136/bjophthalmol-2017-310259
10. Arya LK, Rathinam SR, Lalitha P, Kim UR, Ghatani S, Tandon V. Trematode fluke *Procerovum varium* as cause of ocular inflammation in children, South India. Emerg Infect Dis. 2016;22:192–200. https://doi.org/10.3201/eid2202.150051
11. Waikagul J, Dekumyoy P, Yoonuan T, Praevanit R. Conjunctiva philophthalmosis: a case report in Thailand. Am J Trop Med Hyg. 2006;74:848–9. https://doi.org/10.4269/ajtmh.2006.74.848
12. Sato C, Sasaki M, Nabeta H, Tomioka M, Uga S, Nakao M. A philophthalmid eyefluke from a human in Japan. J Parasitol. 2019;105:619–23. https://doi.org/10.1645/19-53

13. Dalimi A, Jabarvand M. *Fasciola hepatica* in the human eye. Trans R Soc Trop Med Hyg. 2005;99:798–800. https://doi.org/10.1016/j.trstmh.2005.05.009
14. Newton JC, Kanchanaranya C, Previte LR Jr. Intraocular *Schistosoma mansoni*. Am J Ophthalmol. 1968;65:774–8. https://doi.org/10.1016/0002-9394(68)94397-3
15. McDonald HR, Kazacos KR, Schatz H, Johnson RN. Two cases of intraocular infection with *Alaria mesocercaria* (Trematoda). Am J Ophthalmol. 1994;117:447–55. https://doi.org/10.1016/S0002-9394(14)70003-0

Address for correspondence: Susiji Wickramasinghe, Department of Parasitology, Faculty of Medicine, University of Peradeniya, Peradeniya, 20400, Sri Lanka; email: susiji.wickramasinghe@med.pdn.ac.lk

April 2022

Zoonotic Infections

- Citywide Integrated *Aedes aegypti* Mosquito Surveillance as Early Warning System for Arbovirus Transmission, Brazil
- *Shewanella* spp. Bloodstream Infections in Queensland, Australia
- Increasing Antimicrobial Resistance in World Health Organization Eastern Mediterranean Region, 2017–2019
- Phylogenetic Analysis of Spread of Hepatitis C Virus Identified during HIV Outbreak Investigation, Unnao, India
- SARS-CoV-2 IgG Seroprevalence among Blood Donors as a Monitor of the COVID-19 Epidemic, Brazil
- Diminishing Immune Responses against Variants of Concern in Dialysis Patients 4 Months after SARS-CoV-2 mRNA Vaccination
- Genomic Epidemiology of Early SARS-CoV-2 Transmission Dynamics, Gujarat, India

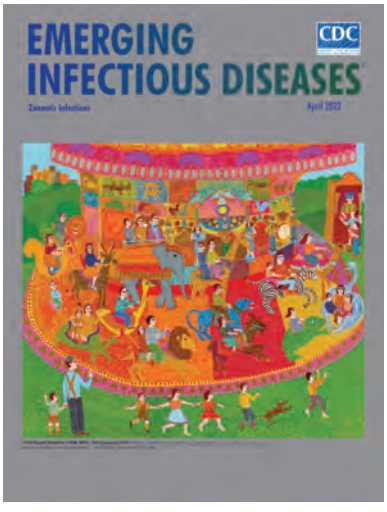

- Reassessing Reported Deaths and Estimated Infection Attack Rate during the First 6 Months of the COVID-19 Epidemic, Delhi, India
- Isolation of Heartland Virus from Lone Star Ticks, Georgia, USA, 2019
- *Bordetella hinzii* Pneumonia in Patient with SARS-CoV-2 Infection
- Fatal Human Alphaherpesvirus 1 Infection in Free-Ranging Black-Tufted Marmosets in Anthropized Environments, Brazil, 2012–2019

- Molecular Surveillance for Imported Antimicrobial Resistant *Plasmodium falciparum*, Ontario, Canada
- Unique Clinical, Immune, and Genetic Signature in Patients with Borrelial Meningoradiculoneuritis
- Durability of Antibody Response and Frequency of SARS-CoV-2 Infection 6 Months after COVID-19 Vaccination in Healthcare Workers
- SARS-CoV-2 Outbreak among Malayan Tigers and Humans, Tennessee, USA, 2020
- Vehicle Windshield Wiper Fluid as Potential Source of Sporadic Legionnaires' Disease in Commercial Truck Drivers
- Increased Attack Rates and Decreased Incubation Periods in Raccoons with Chronic Wasting Disease Passaged through Meadow Voles
- Infectious Toscana Virus in Seminal Fluid of Young Man Returning from Elba Island, Italy

EMERGING INFECTIOUS DISEASES

To revisit the April 2022 issue, go to: https://wwwnc.cdc.gov/eid/articles/issue/28/4/table-of-contents

Serial Intervals and Incubation Periods of SARS-CoV-2 Omicron and Delta Variants, Singapore

Kangwei Zeng, Santhya, Aijia Soong, Nitika Malhotra, Dhanushanth Pushparajah, Koh Cheng Thoon, Benny Yeo, Zheng Jie Marc Ho, Mark Chen I-Cheng

We compared serial intervals and incubation periods for SARS-CoV-2 Omicron BA.1 and BA.2 subvariants and Delta variants in Singapore. Median incubation period was 3 days for BA.1 versus 4 days for Delta. Serial interval was 2 days for BA.1 and 3 days for BA.2 but 4 days for Delta.

The World Health Organization declared the SARS-CoV-2 Omicron variant a variant of concern on November 26, 2021 (*1*), and Omicron rapidly displaced Delta as the dominant variant. After detecting the first local Omicron case on December 9, 2021, the Singapore Ministry of Health performed rigorous contact tracing for the initial cases, which enabled us to compare serial interval and incubation periods of Omicron with similar investigations performed earlier for the Delta variant.

The Study

We obtained case linkages, source exposure date, and date of first COVID-19–related symptom onset from the Ministry of Health contact tracing team for PCR-confirmed cases on the basis of previously described procedures for epidemiologic investigations (*2*). We also determined whether initially asymptomatic case-patients' symptoms were subsequently reported through medical chart review.

Author affiliations: National Centre for Infectious Diseases, Singapore (K. Zeng, Santhya, A. Soong, M. Chen I-Cheng); Ministry of Health, Singapore (K. Zeng, N .Malhotra, D. Pushparajah, Z.J.M. Ho, M.C. I-Cheng); KK Women's and Children's Hospital, Singapore (K.C. Thoon); National University of Singapore, Singapore (K.C. Thoon); National Technological University, Singapore (K.C. Thoon); National Public Health Laboratory, Singapore (B. Yeo)

DOI: https://doi.org/10.3201/eid2904.220854

We identified Delta variant cases from selected clusters with epidemiologic investigations during April 27, 2021–July 2, 2021, when Delta was dominant; 95% (n = 103) were confirmed by whole-genome sequencing (WGS). Omicron BA.1 cases were based on investigations beginning December 9, 2021. Of those, 67% (n = 66) were WGS-confirmed; 23% (n = 22) were not sequenced but exhibited spike (S) gene target failure on PCR, whereas 10% (n = 10) were presumed to be BA.1 on the basis of epidemiologic links. Omicron BA.2 cases were identified in investigations beginning January 3, 2022. Of those, 18% (n = 8) were WGS-confirmed; 26% (n = 12) were not sequenced but did not exhibit S gene target failure, whereas 50% (n = 23) were presumed to be BA.2 on the basis of epidemiologic links.

Among potential transmission pairs, we identified pairs with clear infector–infectee relationships where onset dates for both were available. Analysis of incubation period (time from exposure to onset) included only case-patients who acquired infection from a known source with exposure limited to 1 day. We based serial interval on the difference in onset dates within each transmission pair. We excluded transmission pairs with multiple possible transmission pathways within the household or social network and pairs (n = 17, 8%) with zero or negative serial interval because epidemiologic investigations suggest several of those pairs involved questionable onset dates. Serial interval was further stratified by whether transmission pairs originated from a household or nonhousehold setting. We report medians and interquartile ranges (IQRs) and assessed statistically significant differences using the Wilcoxon rank-sum test (Figure). We also estimated means and 95% CIs of serial interval and incubation period for each variant by fitting a Gamma and Weibull model using the maximum-likelihood method (Appendix,

https://wwwnc.cdc.gov/EID/article/29/4/22-0854-App1.pdf).

Based on data for 36 transmission pairs for the Omicron BA.1 subvariant and 42 transmission pairs for the Delta variant (Table), the incubation period for BA.1 was shorter by ≈1 day, a median of 3 (IQR 2–4) days, compared with 4 (IQR 3–7) days for Delta (Figure). Incubation period could not be calculated for BA.2 because many cases lacked clear exposure dates.

For serial interval, we identified 76 transmission pairs for Omicron BA.1, 38 for BA.2, and 88 for Delta. BA.1 transmission pairs included 2 large clusters originating in a fitness center (n = 20 pairs) and a restaurant (n = 16), in addition to subsequent transmission chains to household members, social contacts, and coursemates in a training session. Other local BA.1 transmission pairs originated either from imported cases (n = 27) or unlinked local primary cases (n = 13) who then infected household and social or work contacts. BA.2 transmission pairs (n = 38) included 4 clusters from preschools/childcare centers and 14 household transmission pairs. Delta transmission pairs were selected from various clusters: of 2 social (n = 11), 3 workplace (n = 27), 2 nosocomial (n = 24), and 1 preschool (n = 26).

For BA.1, the median serial interval of 2 (IQR 2–4) days was shorter than its incubation period of 3 days and shorter than the serial interval for Delta (median 4 [IQR 3–6] days). For Delta, serial interval was similar to its incubation period (Figure). Of note, the difference in serial interval between BA.1 and Delta was greater for nonhousehold transmission. Moreover, although serial interval for BA.1 was shorter in the nonhousehold setting than the household transmission setting, the reverse was true for Delta. One possible explanation is that transmission of BA.1 to nonhousehold contacts occurs during presymptomatic and early symptomatic phases, before a person self-isolates, whereas some BA.1 patients recovering at home would continue to infect other household members over multiple days after symptom onset. In contrast, the Delta case-patients included in our analyses were isolated from household members upon diagnosis, which would reduce household transmission in the days after onset. As for BA.2, the median serial interval of 3 (IQR 2–3) days was significantly shorter than the Delta serial interval and slightly but not significantly longer than the serial interval for BA.1. Median nonhousehold serial interval of 3 (IQR 2–3) days for BA.2 was significantly longer than for BA.1. Whether this difference reflects changes such as reduced contact tracing for Omicron subvariants after January 2022 is unclear.

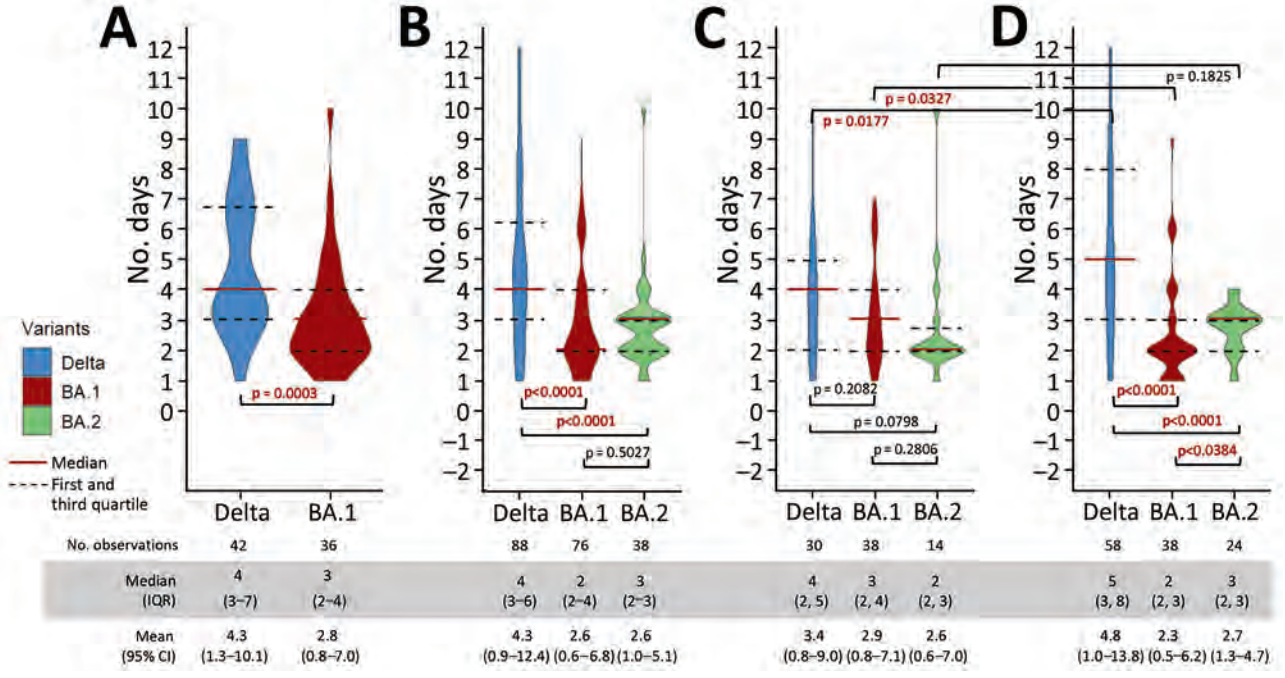

Figure. Comparative analysis of serial interval of SARS-CoV-2 Delta and Omicron variants, Singapore. A) Incubation period using only transmission pairs with clear epidemiological links and single-day source exposure to primary case. B) Serial interval of all symptomatic transmission pairs. C) Serial interval of all symptomatic transmission pairs with transmissions within households. D) Serial interval of all symptomatic transmission pairs with transmissions outside of households (workplace, social events). Means and 95% CIs are based on fitting a Gamma distribution using the maximum-likelihood method. p values were calculated using Wilcoxon rank-sum test.

Table. Demographic data for SARS-CoV-2 Omicron and Delta variants case-patients in study of incubation periods and serial intervals, Singapore*

	Incubation period cases		Serial interval cases		
Characteristic	Delta, n = 42	BA.1, n = 36	Delta, n = 88	BA.1, n = 76	BA.2, n = 38
Age group, y					
Median (IQR)	24 (9–34)	26 (21–38)	32 (21–41)	27 (20–42)	4 (3–33)
0–21	15 (35.7)	10 (27.7)	23 (26.1)	23 (30.3)	25 (65.8)
22–39	20 (47.6)	18 (50.0)	39 (44.3)	30 (39.5)	7 (18.4)
40–59	3 (7.1)	7 (19.4)	14 (15.9)	16 (21.1)	5 (13.2)
≥60	4 (9.5)	1 (2.8)	12 (13.6)	7 (9.2)	1 (2.6)
Sex					
M	33 (78.6)	23 (63.9)	56 (63.6)	43 (56.6)	16 (42.1)
F	9 (21.4)	13 (36.1)	32 (36.4)	33 (43.4)	22 (57.9)
Ethnicity					
Chinese	26 (61.9)	21 (58.3)	51 (58.0)	35 (46.1)	21 (55.3)
Malay	13 (31.0)	1 (2.8)	26 (29.5)	7 (9.2)	10 (7.9)
Indian	1 (2.4)	4 (11.1)	1 (1.1)	15 (19.7)	3 (26.3)
Others	2 (4.8)	10 (27.8)	10 (11.4)	19 (25.0)	4 (10.5)
Vaccination status					
Unvaccinated	38 (90.5)	1 (2.8)	76 (86.4)	12 (15.8)	25 (65.8)
Partially vaccinated	1 (2.4)	0	4 (4.5)	0	0
Fully vaccinated	3 (7.1)	27 (75.0)	8 (9.1)	45 (59.2)	6 (15.8)
Boosted	0	8 (22.2)	0	19 (25.0)	7 (18.4)
Type of transmission					
Household	0	1 (2.8)	30 (34.1)	38 (50.0)	14 (36.8)
Nonhousehold	42 (100)	35 (97.2)	58 (65.9)	38 (50.0)	24 (63.2)

*Values are no. (%) except as indicated.

Conclusions

The serial interval we observed for BA.1 is corroborated by other international data, including 1.5–3.2 days in England (S. Abbott et al., unpub. data, https://www.medrxiv.org/content/10.1101/2022.01.08.22268920v1; H. Allen et al., unpub. data, https://www.medrxiv.org/content/10.1101/2022.02.15.22271001v1) and 2.22 days in South Korea (*3*). Norway reported a similar median Omicron incubation period of 3 days (*4*). A study from Hong Kong, despite a small sample size (n = 13), similarly reported the estimated mean serial interval of BA.2 as 2.7 days (median 2.5 [SD 1.5] days) (*5*), although a study from Spain reported an incubation period of 3.1 days and longer serial interval of 4.8 days (*6*). Relaxing nonpharmaceutical interventions would cause longer serial intervals and might explain some of these differences. Given a serial interval shorter than its incubation period, Omicron might be more predisposed to causing transmission before symptom onset than Delta. As a consequence, isolation after symptom onset would be less effective at preventing transmission. The short serial interval also poses challenges for contact tracing to identify and isolate secondary cases before they become infectious. Strategies such as preevent testing and regular testing of at-risk persons must also be performed at shorter intervals to remain effective.

The first limitation of our study is that most BA.1 case-patients (87%) were fully vaccinated, whereas most BA.2 and Delta case-patients were not (BA2, 65% unvaccinated; Delta, 80% unvaccinated). More than half of BA.2 cases were from preschool or school clusters, so many case-patients were younger and unvaccinated. We therefore could not determine whether differences in serial interval and incubation periods were caused by vaccination status rather than an intrinsic property of the virus. Selection bias caused by cluster control strategies might also result in overrepresentation of cases from larger clusters and thus more cases from superspreading events, which might also be associated with shorter serial interval and incubation period. However, other than vaccination status, most of those biases apply to both Delta and Omicron and are therefore unlikely explanations for differences between Delta and the 2 Omicron subvariants.

Mean serial intervals of 2–3 days have been reported for some other human coronaviruses and influenza A, which are also predominantly infections of the upper respiratory tract (*7*). The short serial interval is hence consistent with laboratory experiments demonstrating that Omicron grows more rapidly than Delta in human nasal epithelial cultures (T.P. Peacock et al., unpub. data, https://www.biorxiv.org/content/10.1101/2021.12.31.474653v2).

In conclusion, Omicron BA.1 and BA.2 had shorter serial intervals than the Delta variant, which could partially explain Omicron's more rapid epidemic trajectory. The shorter serial interval could also have rendered public health interventions for earlier COVID-19 variants less effective for Omicron subvariants.

Acknowledgments

We thank the Ministry of Health, National Centre for Infectious Diseases, National Public Health Laboratory, and Severe Illness and Death from Possibly Infectious Causes (SIDPIC) members, Ng Oon Tek, Paul Anantharajah Tambyah, Ooi Say Tat, Surinder Kaur M S Pada, Jade Soh Xiao Jue, Helen Oh May Lin, Thoon Koh Cheng, Li Jiahui, Anson Wong Hei Man, Chettiaiah S Chelvi, Emily Yeo Xier, Vankayalapati Priyanka, Manisha Menon, Vijaya Alalageri, Yelen, Yang Yong, and Alifa Khairunnisa Binte Johari, for their support in this study.

About the Author

Mr. Zeng is an epidemiologist at the National Centre for Infectious Diseases, Singapore. His primary research interests are infectious disease surveillance and epidemiology.

References

1. World Health Organization. Classification of Omicron (B.1.1.529): SARS-CoV-2 variant of concern [cited 2022 May 27]. https://www.who.int/news/item/26-11-2021-classification-of-omicron-(b.1.1.529)-sars-cov-2-variant-of-concern
2. Pung R, Chiew CJ, Young BE, Chin S, Chen MI, Clapham HE, et al.; Singapore 2019 Novel Coronavirus Outbreak Research Team. Investigation of three clusters of COVID-19 in Singapore: implications for surveillance and response measures. Lancet. 2020;395:1039–46. https://doi.org/10.1016/S0140-6736(20)30528-6
3. Kim D, Ali ST, Kim S, Jo J, Lim JS, Lee S, et al. Estimation of serial interval and reproduction number to quantify the transmissibility of SARS-CoV-2 Omicron variant in South Korea. Viruses. 2022;14:533. https://doi.org/10.3390/v14030533
4. Brandal LT, MacDonald E, Veneti L, Ravlo T, Lange H, Naseer U, et al. Outbreak caused by the SARS-CoV-2 Omicron variant in Norway, November to December 2021. Euro Surveill. 2021;26:2101147. https://doi.org/10.2807/1560-7917.ES.2021.26.50.2101147
5. Mefsin YM, Chen D, Bond HS, Lin Y, Cheung JK, Wong JY, et al. Epidemiology of infections with SARS-CoV-2 Omicron BA.2 variant, Hong Kong, January–March 2022. Emerg Infect Dis. 2022;28:1856–8. https://doi.org/10.3201/eid2809.220613
6. Del Águila-Mejía J, Wallmann R, Calvo-Montes J, Rodríguez-Lozano J, Valle-Madrazo T, Aginagalde-Llorente A. Secondary attack rate, transmission and incubation periods, and serial interval of SARS-CoV-2 Omicron variant, Spain. Emerg Infect Dis. 2022;28:1224–8. https://doi.org/10.3201/eid2806.220158
7. Vink MA, Bootsma MC, Wallinga J. Serial intervals of respiratory infectious diseases: a systematic review and analysis. Am J Epidemiol. 2014;180:865–75. https://doi.org/10.1093/aje/kwu209

Address for correspondence: Mark Chen I-Cheng, National Public Health and Epidemiology Unit, National Centre for Infectious Diseases, 16 Jln Tan Tock Seng, 308442, Singapore; email: mark_ic_chen@ncid.sg

Serial Interval and Incubation Period Estimates of Monkeypox Virus Infection in 12 Jurisdictions, United States, May–August 2022

Zachary J. Madewell,[1] Kelly Charniga,[1] Nina B. Masters, Jason Asher, Lily Fahrenwald, William Still, Judy Chen, Naama Kipperman, David Bui, Meghan Shea, Katharine Saunders, Lori Saathoff-Huber, Shannon Johnson, Khalil Harbi, Abby L. Berns, Taidy Perez, Emily Gateley, Ian H. Spicknall, Yoshinori Nakazawa, Thomas L. Gift, 2022 Mpox Outbreak Response Team[2]

Using data from 12 US health departments, we estimated mean serial interval for monkeypox virus infection to be 8.5 (95% credible interval 7.3–9.9) days for symptom onset, based on 57 case pairs. Mean estimated incubation period was 5.6 (95% credible interval 4.3–7.8) days for symptom onset, based on 35 case pairs.

Since May 6, 2022, mpox (formerly monkeypox) cases have been reported across the globe. According to the Centers for Disease Control and Prevention (CDC), 85,115 confirmed mpox cases and 182 deaths have occurred in 110 locations across historically endemic and nonendemic regions as of January 25, 2023 (*1*). Mpox symptoms usually start within 3 weeks of exposure to monkeypox virus (MPXV) and may include fever, headache, chills, swollen lymph nodes, and exhaustion (*2*). A rash usually develops within 1–4 days after onset of symptoms. MPXV is transmitted through close contact with infectious rash, scabs, or body fluids; respiratory droplets during prolonged face-to-face contact; and fomites such as clothing, towels, or bedding (*1*). Transmission in the current outbreak has occurred primarily through close physical contact associated with sexual activities among gay, bisexual, and other men who have sex with men. Transmission of MPXV is possible from the time of symptom onset until all scabs have fallen off and fully healed (*3*).

The serial interval is defined as the time between symptom onset in a primary case-patient and symptom onset in the secondary case-patient and depends on the incubation period (the time from a person's infection to the onset of signs and symptoms) (*4*), epidemic phase, and population contact patterns. The serial interval is critical for estimating the effective reproduction number (R_t) and forecasting incidence, both of which are important for understanding the course of an outbreak and the effect of interventions (e.g., antiviral drugs and vaccines). In the current outbreak, many patients report multiple anonymous sex partners or attendance at large events, such as festivals, in the 3 weeks before symptom onset, which has complicated efforts to identify primary and secondary case pairs. By using

Author affiliations: Centers for Disease Control and Prevention, Atlanta, Georgia, USA (Z.J. Madewell, K. Charniga, N.B. Masters, J. Asher, I.H. Spicknall, Y. Nakazawa, T.L. Gift); Chicago Department of Public Health, Chicago, Illinois, USA (L. Fahrenwald); District of Columbia Department of Health, Washington, DC, USA (W. Still); New York City Department of Health and Mental Hygiene, New York, New York, USA (J. Chen, N. Kipperman); California Department of Public Health, Sacramento, California, USA (D. Bui); Colorado Department of Public Health and Environment, Denver, Colorado, USA (M. Shea); Florida Department of Health, Tallahassee, Florida, USA (K. Saunders); Illinois Department of Public Health, Springfield, Illinois, USA (L. Saathoff-Huber); Michigan Department of Health and Human Services, Lansing, Michigan, USA (S. Johnson); North Carolina Department of Health and Human Services, Raleigh, North Carolina, USA (K. Harbi); Rhode Island Department of Health, Providence, Rhode Island, USA (A.L. Berns); South Carolina Department of Health and Environmental Control, Columbia, South Carolina, USA (T. Perez); Tennessee Department of Health, Nashville, Tennessee (E. Gateley)

DOI: https://doi.org/10.3201/eid2904.221622

[1]These first authors contributed equally to this article.

[2]Additional members of 2022 Mpox Outbreak Response Team who contributed data are listed at the end of this article.

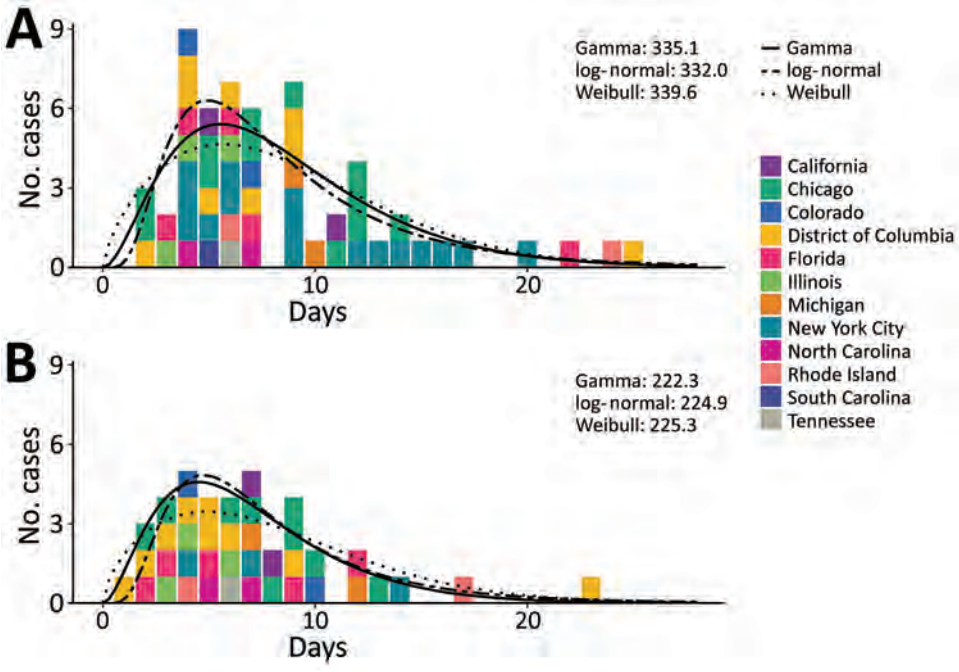

Figure 1. Empirical and fitted distributions of the serial intervals of rash onset (A) (n = 40 cases) and symptom onset (B) (n = 57 cases) for monkeypox virus, 12 jurisdictions, United States, May–August 2022. Leave-one-out information criterion values for each model are shown inside the plots in the upper right-hand corner.

preliminary data from 17 mpox case pairs in the United Kingdom, researchers estimated the mean serial interval to be 9.8 days with high uncertainty (95% credible interval [CrI] 5.9–21.4 days) (*5*). An investigation of 16 primary and secondary case pairs in Italy indicated the estimated mean generation time, or time between infection of primary and secondary cases, to be 12.5 (95% CrI 7.5–17.3) days (*6*). In this report, we estimate the serial interval and incubation period for symptom onset and rash onset for MPXV infection in the United States.

The Study

Data on self-reported symptom and rash onset dates for primary and secondary case pairs, including the type of contact that occurred between pairs, were compiled by 12 state and local health departments. We examined serial interval for both earliest symptom onset and rash onset because the latter may be more specific to mpox than the other signs. Earliest symptom onset included any mpox symptom as defined by CDC (*2*), including rash. We only included cases if there was a high degree of certainty that the secondary case-patient was infected by the primary case-patient (Appendix, https://wwwnc.cdc.gov/EID/article/29/4/22-1622-App1.pdf).

For each case pair, we calculated days between onset of any mpox symptoms and days between rash onset in the primary and secondary case-patients. We used the EpiEstim package version 4.1.2 in R software (The R Foundation for Statistical Computing, https://www.r-project.org) to estimate the distribution of the serial interval for known primary and secondary case pairs using Bayesian methods for symptom and rash onset (Appendix) (*7*). We did not adjust for right-truncation of the data because we included cases during the stable or declining phase of the outbreak (*8*).

We received data for 120 case pairs from 13 jurisdictions (Appendix Figures 1, 2). Fifty-seven case pairs met the inclusion criteria (Figure 1; Appendix). Dates of symptom onset among primary case-patients ranged from May 11 to August 13, 2022 (Appendix Figure 3). Forty of the 57 pairs included rash onset dates for primary and secondary case-patients. We also considered in our analysis the type of contact for the case pairs (Appendix Table 1). The gamma distribution provided the best fit to the serial interval data. The overall mean estimated serial interval for symptom onset was 8.5 (95% CrI 7.3–9.9) days (SD 5.0 [95% CrI 4.0–6.4] days) and for rash onset was 7.0 (95% CrI 5.8–8.4) days (SD 4.2 [95% CrI 3.2–5.6] days) (Table; Appendix Tables 2, 3).

Table. Estimated incubation period and serial interval of monkeypox virus infection, 12 jurisdictions, United States, May–August 2022*

	Incubation period, d			Serial interval, d		
Onset	Mean (95% CrI)	SD (95% CrI)	No. cases	Mean (95% CrI)	SD (95% CrI)	No. case pairs
Symptom onset	5.6 (4.3–7.8)	4.4 (2.8–8.7)	36	8.5 (7.3–9.9)	5.0 (4.0–6.4)	57
Rash onset	7.5 (6.0–9.8)	4.9 (3.2–8.8)	35	7.0 (5.8–8.4)	4.2 (3.2–5.6)	40

*CrI, credible interval.

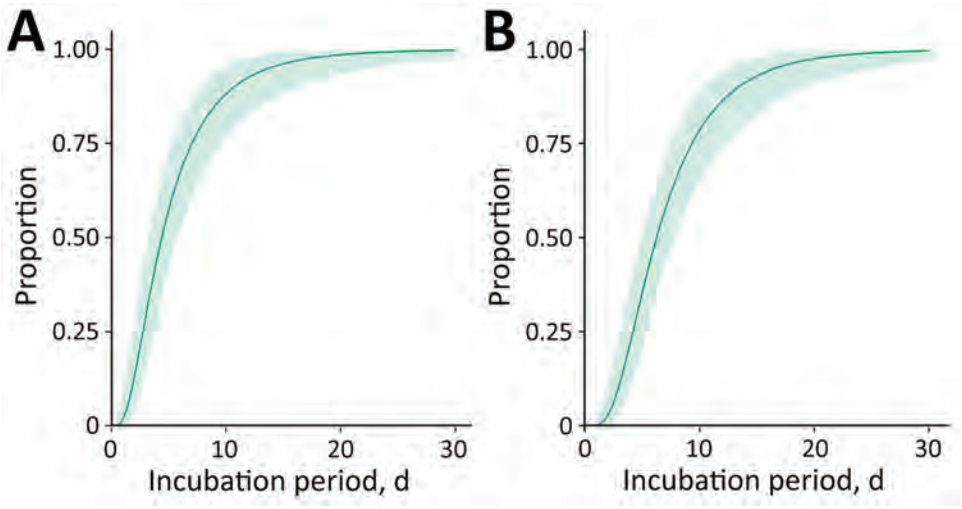

Figure 2. Updated estimated cumulative density functions according to a log-normal distribution of monkeypox virus incubation periods, by symptom onset (A) (n = 36 cases) and rash onset (B) (n = 35 cases), 12 jurisdictions, United States, May–August 2022.

We estimated the incubation period using 22 US mpox cases reported in an earlier study (K. Charniga et al., unpub. data, https://doi.org/10.1101/2022.06.22.22276713) plus 14 cases from our dataset (Appendix). Of the new case-patients, 10 were exposed during a single day. The mean incubation period from exposure to symptom onset for 36 case-patients was 5.6 (95% CrI 4.3–7.8) days (SD 4.4 [95% CrI 2.8–8.7] days), whereas the mean incubation period from exposure to rash onset for 35 case-patients was 7.5 (95% CrI 6.0–9.8) days (SD 4.9 [95% CrI 3.2–8.8] days) (Figure 2; Appendix Figure 4).

Conclusions

Determining the serial interval of a pathogen can inform our understanding of the timing of transmission relative to symptom onset. The serial interval of 8.5 days for symptom onset was similar to an estimate from the United Kingdom of 9.8 days after correcting for right-truncation (*5*) but shorter than the generation time of 12.5 days reported from Italy (*6*). The serial interval correlates with human behavior and can decrease with increasing awareness among men who have sex with men or interventions, a pattern similar to that observed among the general population during the COVID-19 pandemic (*9*). The Italy estimates were from the initial period of the epidemic (May–June 2022), whereas our study was for July–August 2022. Serial interval changes can be very rapid (*10*). We also found a serial interval of 7.0 days for rash onset. The estimated serial interval for symptom onset was longer than that for the incubation period (5.6 days), suggesting most transmission occurred after the onset of symptoms in the primary case-patient. Conversely, the serial interval for rash onset (7.0 days) was slightly shorter than that for the rash incubation period (7.5 days), which may suggest some prerash transmission; indeed, there were instances in the observed data where secondary case-patients were exposed before onset of reported rash in the primary case-patient. However, the credible intervals for the estimates overlap. The serial interval for symptom onset ranged from 2 to 25 days. This wide range may be attributable in part to variability in the nature and intensity of contact.

The first limitation of this study is that precise ascertainment of symptom and rash onset dates is critical for serial interval estimation, but initial mpox symptoms are often nonspecific and may be unrelated to MPXV infection. Second, despite careful selection of linked primary and secondary case pairs, exposure from additional unknown sources may have occurred. Third, social desirability bias may have factored into the self-reported exposures before infection. Fourth, serial interval may vary by age, underlying conditions, vaccination status, or contact type (route of exposure); we did not stratify our analysis by these factors because of limited data. Fifth, we excluded secondary case-patients who had symptom onset on the same day as or before the primary case-patient to ensure a high degree of confidence linking case pairs; however, the serial interval could be negative (*11*). Sixth, the serial interval for rash onset could be biased if rash is more quickly identified in the secondary case-patient because of case finding and investigation of the primary case-patient.

Notwithstanding those limitations, our estimate of the serial interval for MPXV infection includes more case pairs than have been reported previously from the United Kingdom (*5*) and Italy (*6*). We also provide estimates for rash onset, which may be more reliable than initial symptom onset for determining serial interval.

2022 Mpox Outbreak Response Team, by affiliation: CDC (Julia Shaffner); California Department of Public Health (Shua J. Chai, Marisa A.P. Donnelly, Robert E. Snyder, Cameron Stainken, Eric C. Tang, Akiko Kimura, Jason Robert C. Singson, and Philip Peters); Colorado Department of Public Health and Environment (Robyn Weber and Erin Youngkin); District of Columbia Department of Health (Sarah Gillani, Karla Miletti, and Allison Morrow); Tennessee Department of Health (Caleb Wiedeman); Florida Department of Health (Danielle Stanek and Joshua Moore); Chicago Department of Public Health (Bridget Brassil, Isaac Ghinai, Janna Kerins, Aaron Krusniak, Sarah Love, Peter Ruestow, and Emma Weber); North Carolina Department of Health and Human Services (Erin Ricketts); Rhode Island Department of Health (Emma Creegan, Karen Luther, and Patricia McAuley); Will County Health Department Mpox Investigation Team; Kendall County Health Department Mpox Investigation Team.

Acknowledgments

We thank mpox response teams from state and local health departments in the following jurisdictions: California, Chicago, Colorado, District of Columbia, Hawaii, Florida, Illinois, Michigan, New York City, North Carolina, Rhode Island, South Carolina, and Tennessee. Hawaii contributed data, but the case pairs did not meet the inclusion criteria. We also thank the CDC Center for Forecasting and Outbreak Analytics for technical assistance, the Mpox Task Force in the CDC Center for State, Tribal, Local, and Territorial Support for outreach and liaison, and the Data, Analytics, and Visualization Task Force Informatics Team, CDC, for data management and support.

This activity was reviewed by CDC and was conducted consistent with applicable federal law and CDC policy (45 C.F.R. part 46, 21 C.F.R. part 56; 42 U.S.C. Sect. 241(d); 5 U.S.C. Sect. 552a; 44 U.S.C. Sect. 3501 et seq).

About the Author

Dr. Madewell is a fellow in the Public Health Analytics and Modeling Track of the CDC Steven M. Teustch Prevention Effectiveness Fellowship. His primary research interests include epidemiologic study and modeling of infectious diseases. Dr. Charniga is a fellow in the Public Health Analytics and Modeling Track of the CDC Steven M. Teustch Prevention Effectiveness Fellowship. Her primary research interests include outbreak analysis and zoonotic diseases.

References

1. Centers for Disease Control and Prevention. Monkeypox. 2022 [cited 2022 Sep 19]. https://www.cdc.gov/poxvirus/monkeypox
2. Centers for Disease Control and Prevention. Monkeypox: signs and symptoms. 2022 [cited 2022 Nov 22]. https://www.cdc.gov/poxvirus/monkeypox/symptoms/index.html
3. Delaney KP, Sanchez T, Hannah M, Edwards OW, Carpino T, Agnew-Brune C, et al. Strategies adopted by gay, bisexual, and other men who have sex with men to prevent monkeypox virus transmission—United States, August 2022. MMWR Morb Mortal Wkly Rep. 2022;71:1126–30. https://doi.org/10.15585/mmwr.mm7135e1
4. Reynolds MG, Yorita KL, Kuehnert MJ, Davidson WB, Huhn GD, Holman RC, et al. Clinical manifestations of human monkeypox influenced by route of infection. J Infect Dis. 2006;194:773–80. https://doi.org/10.1086/505880
5. UK Health Security Agency. Investigation into monkeypox outbreak in England: technical briefing 1. 2022 [cited 2022 Aug 25]. https://www.gov.uk/government/publications/monkeypox-outbreak-technical-briefings/investigation-into-monkeypox-outbreak-in-england-technical-briefing-1#:~:text=Without%20correcting%20for%20right%2Dtruncation,8.9)%2C%20see%20Figure%202a
6. Guzzetta G, Mammone A, Ferraro F, Caraglia A, Rapiti A, Marziano V, et al. Early estimates of monkeypox incubation period, generation time, and reproduction number, Italy, May–June 2022. Emerg Infect Dis. 2022;28:2078–81. https://doi.org/10.3201/eid2810.221126
7. Cori A, Cauchemez S, Ferguson NM, Fraser C, Dahlqwist E, Demarsh PA, et al. EpiEstim: estimate time varying reproduction numbers from epidemic curves. 2020 [cited 2022 Nov 23]. https://cran.r-project.org/web/packages/EpiEstim/index.html
8. Ward T, Christie R, Paton RS, Cumming F, Overton CE. Transmission dynamics of monkeypox in the United Kingdom: contact tracing study. BMJ. 2022;379:e073153. https://doi.org/10.1136/bmj-2022-073153
9. Ali ST, Wang L, Lau EHY, Xu X-K, Du Z, Wu Y, et al. Serial interval of SARS-CoV-2 was shortened over time by nonpharmaceutical interventions. Science. 2020;369:1106–9. https://doi.org/10.1126/science.abc9004
10. Xin H, Wang Z, Feng S, Sun Z, Yu L, Cowling BJ, et al. Transmission dynamics of SARS-CoV-2 Omicron variant infections in Hangzhou, Zhejiang, China, January–February 2022. Int J Infect Dis. 2023;126:132–5. https://doi.org/10.1016/j.ijid.2022.10.033
11. Du Z, Xu X, Wu Y, Wang L, Cowling BJ, Meyers LA. Serial interval of COVID-19 among publicly reported confirmed cases. Emerg Infect Dis. 2020;26:1341–3. https://doi.org/10.3201/eid2606.200357

Address for correspondence: Zachary J. Madewell, Centers for Disease Control and Prevention, 1600 Clifton Rd NE, Mailstop H21-9, Atlanta, GA 30329-4027, USA; email: ock0@cdc.gov

Two-Year Cohort Study of SARS-CoV-2, Verona, Italy, 2020–2022

Zeno Bisoffi,[1] Nicoletta De Santis,[1] Chiara Piubelli, Michela Deiana, Francesca Perandin, Pietro Girardi, Luca Heller, Natalia Alba, Carlo Pomari,[2] Massimo Guerriero[2]

We performed a follow-up of a previously reported SARS-CoV-2 prevalence study (April–May 2020) in Verona, Italy. Through May 2022, only <1.1% of the city population had never been infected or vaccinated; 8.8% was the officially reported percentage. Limiting protection measures and vaccination boosters to elderly and frail persons seems justified.

In Italy at the beginning of 2022, a large part of the population >10 years of age was vaccinated against SARS-CoV-2 (*1*). Nevertheless, a high number of new infections occurred in the following months, largely caused by increasing contagiousness of new virus variants. Reliable data on the proportion of the population that remains naive (unvaccinated and no history of infection) are crucial to improve SARS-CoV-2 infection control policies. Relying only on reported cases caused a gross underestimation of the true prevalence in the early stages of the pandemic, both in Italy (*2*–*5*) and elsewhere (*6*–*9*).

In April and May 2020, at the end of the first pandemic wave in Italy, we performed a prevalence survey on a random sample in Verona, Italy, and showed that ≈3% of the population had acquired the infection, 5 times the official figures (*4*). We then performed a follow-up of this cohort, ending May 31, 2022, to monitor the cumulative incidence of the infection and to estimate the proportion of the city population that had never had the infection or had been vaccinated, thus remaining fully susceptible or naive.

Authors affiliations: Istituto di Ricovero e Cura a Carattere Scientifico Sacro Cuore Don Calabria Hospital, Verona, Italy (Z. Bisoffi, N. De Santis, C. Piubelli, M. Deiana, F. Perandin, C. Pomari, M. Guerriero); AULDSS 9 Scaliger Regione del Veneto, Verona (P. Girardi, L. Heller, N. Alba)

DOI: https://doi.org/10.3201/eid2904.221268

The Study

The study population has been described in detail (*4*). The initial cohort had 1,515 persons randomly selected from the city population (Figure 1; Appendix Figure, https://wwwnc.cdc.gov/EID/article/29/4/22-1268-App1.pdf). Mean age was 49.1 years, and most (54%) persons were women. Ten (0.7%) persons were positive for SARS-CoV-2 RNA, 40 (2.6%) were positive for IgG against nucleocapsid protein of SARS-CoV-2, and 1,465 (96.7%) tested negative. Using latent class analysis, we estimated a 3% prevalence of infection (*4*). We also summarize follow-up studies of the initial cohort (Figure 1).

We performed 3 follow-up surveys. The first survey was a telephone survey during June–July 2021. The second survey, during November 2021, was in-person interviews on previous infections and vaccination status, and molecular (reverse transcription PCR) and antibody testing. The third survey was a telephone survey during January 2022.

On May 31, 2022, those persons who were still naive in January were interviewed again. Survey data were then compared with reported data from the city's health authority (Figure 2).

During June–July 2021, of the initial cohort of 1,515 persons, 1,182 (78.0%) responded, of whom 134 (11.3%) reported having had SARS-CoV-2 laboratory-confirmed infection at least once. Of those who had been vaccinated (897, 75.9%), a total of 563 (62.8%) had already received the second dose. A total of 242 (20.5%) persons did not report vaccination or previous infection.

During November 2021, a total of 897 persons (59.2% of the initial cohort) consented to participate. All were administered a questionnaire, and we

[1]These first authors contributed equally to this article.

[2]These senior authors contributed equally to this article.

obtained nasal and pharyngeal swab specimens and blood samples from all consenting persons. We performed reverse transcription PCR of swab specimens as described (*4*) to detect active infections; only 1 (0.1%) specimen showed a positive result.

We analyzed serum samples by using the SARS-CoV-2 IgG-N Assay (Abbott, https://www.ie.abbott) to detect IgG against nucleocapsid protein, as described (*4*). We also used the SARS-CoV-2 IgG II Quant Assay (Abbott) for the quantitative measure of IgG against spike (receptor-binding domain) protein according to the manufacturer's procedure by using the ARCHITECT I System (Abbott). We also performed this test on biobank samples from the initial 2020 cohort, when the test was not yet available, to make it possible to compare 2020 results with 2021 results.

We compared the results of antibody tests from the survey with 2020 data (Table). A total of 160 (17.8%) of 897 persons tested positive for nucleocapsid IgG, (which is unaffected by vaccination), and 831 (92.7%) of 896 persons (1 missing value) tested positive for antibody against spike (receptor-binding domain) protein, which reacts to vaccination and natural infection. Of the 34 persons who had tested positive for nucleocapsid IgG during 2020, half had negative results at the following survey.

At the interview, of the 897 persons, 820 (91.4%) reported being vaccinated, of whom 735 (89.6%) had already received their second dose; 128 (14.3%) reported being infected at least 1 time. There were only 36 (4.0%) naive persons (no antibodies and no history of infection or vaccination).

During January 2022, of the 1,193 persons (78.7% of the initial cohort) who responded, 254 (21.3%) reported previous infections, and 1,123 (94.1%) had been vaccinated, including 322 (28.7%) with 2 doses and 764 (68.0%) with 3 doses. A total of 36 (3.0%) reported no infection or vaccination, of whom 6 were

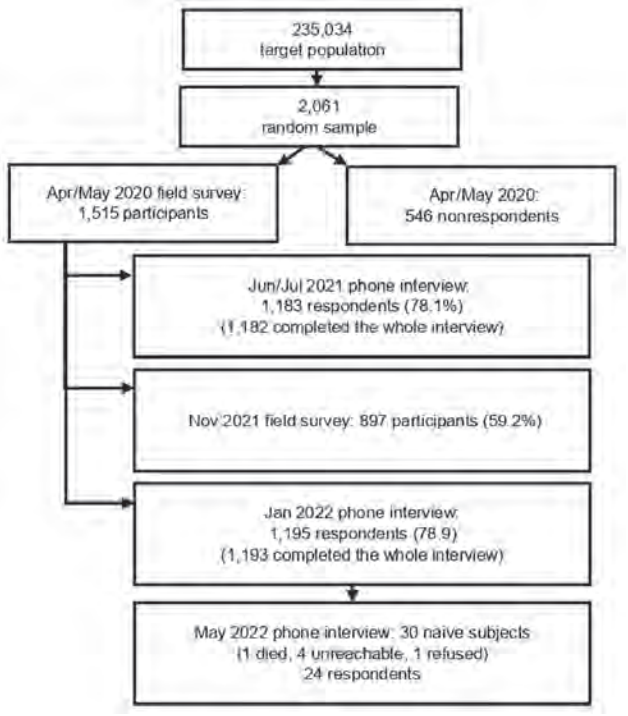

Figure 1. Flow chart for study of reported and sampling data for SARS-CoV-2, Verona, Italy, May 2020–2022, starting from the initial sample of 1,515 persons who participated in the first study.

antibody positive in the previous survey. We classified the remaining 30 (2.5%) persons as naive and listed them for another interview on May 31, 2022.

During May 2022, of the 30 persons from the previous survey, 1 had died, 4 were unreachable, and 1 refused to answer. Of the remaining 24 persons, 8 were infected and remained unvaccinated, 2 were vaccinated and not infected, and 1 was vaccinated and infected. A total of 13 (1.1%) of 1,187 persons presumably remained naive. Thus, at the end May 2022, the best estimate from the study population was that 98.9% of persons >10 years of age in Verona had been infected, vaccinated, or both.

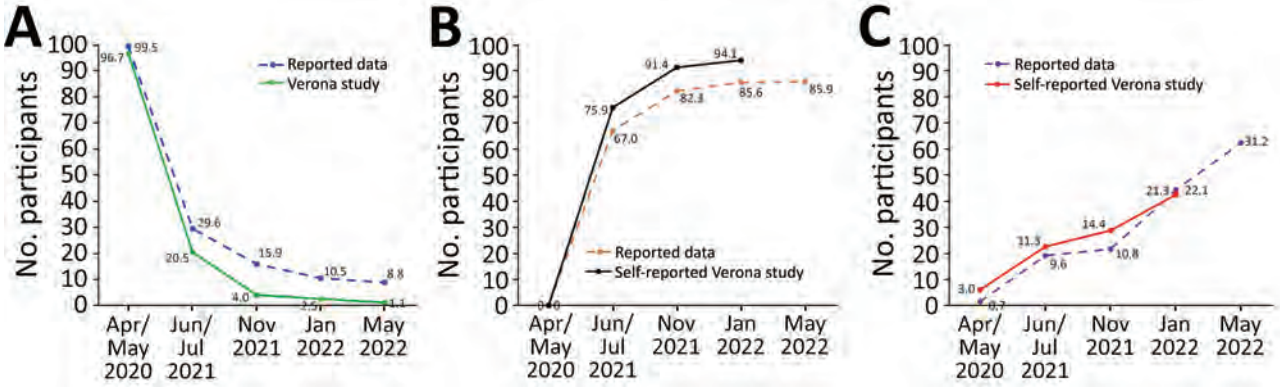

Figure 2. Reported and sampling data for SARS-CoV-2, Verona, Italy, May 2020–2022. Comparison is shown between official (reported) and Verona study proportions of naive (A), vaccinated (B), and infected (C) persons. Values along data lines indicate cumulative incidence.

Table. Comparison of antibody test results in 2 field surveys for SARS-CoV-2, Verona, Italy, May 2020 and November 2021

Characteristic	2021			
	Negative, no. (%)	Positive, no. (%)	Total, no. (%)	p value
IgG against nucleocapsid				
2020				<0.0001
Negative, no. (%)	720 (83.4)	143 (16.6)	863 (100.00)	
Positive, no. (%)	17 (50.0)	17 (50.0)	34 (100.0)	
Total, no.(%)	737 (82.2)	160 (17.8)	897 (100.0)	
IgG against spike protein				
2020				
Negative, no. (%)	65 (7.6)	796 (92.4)	861 (100.0)	
Positive, no. (%)	0 (0)	35 (100.0)	35 (100.0)	0.170*
Total, no. (%)	65 (7.3)	831 (92.7)	896 (100.0)	

*By Fisher exact test.

We compared data resulting from the random sample analysis (Figure 2) with reported data available up to May 31, 2022. The reported initial prevalence was much lower; the data had practically coincided in January 2022.

During May 2022 the cumulative reported incidence reached 31.2%, and the proportion of naive population was 8.8%, versus the 1.1% we found in our study (Figure 2). The actual percentage might be even lower, considering that results for IgG against nucleocapsid tend to become negative over time. Thus, we might have failed to detect some previous infections in the last field survey and, in any case, we did not perform further antibody investigations in the later stages.

Conclusions

According to the survey data, almost the entire population of Verona had some degree of protection in May 2022 against the severe forms of the disease. After a natural infection, the risk for severe forms of COVID-19 is much attenuated, even for nonvaccinated persons (*10*–*13*). The 3 doses of vaccine confer a long-term protection against severe disease, and hybrid immunity is more effective (*14*). Because immunity tends to wane over time, our finding that almost the whole population had been infected or vaccinated does not mean that all persons are protected. Moreover, immunity against new infections is much less effective and is short lasting, especially for the Omicron variants (*11*,*15*). The high contagiousness of these variants will predictably lead to continued circulation of the virus, which will act as a booster for most persons.

The first limitation of this study is that a not negligible proportion of the initial cohort were not able to be followed up. A selection bias cannot be excluded because persons who participated in the follow-up might be more health-conscious and more likely to adhere to vaccination. Only in November 2021 was it possible to repeat the molecular and serologic study. However, even with those limitations, we were able to reconstruct the trend of the pandemic in Verona and compare research results with reported data. Our estimate of the population that is still completely naive is lower than the official figures.

In Verona, the pandemic seems to have entered a phase in which we can be cautiously optimistic about its future course. It remains crucial to protect the frail and elderly persons, including those given booster vaccinations when indicated, but a cautious relaxation of restrictions for the general population seems justified, and repeated boosters for nonfrail persons might not be necessary.

Acknowledgments

We thank the study participants for their cooperation; the CEO of the Istituto di Ricovero e Cura a Carattere Scientifico Sacro Cuore Don Calabria Hospital Mario Piccinini for providing support; Stefano Tais, Monica Degani, and Eleonora Rizzi for coordinating laboratory work; Dora Buonfrate and Concetta Castilletti for critically reading the manuscript; hospital staff for providing assistance with swabs and blood sampling; and administrative staff for performing interviews.

This study was supported by the Italian Ministry of Health under Fondi Ricerca Corrente – Linea 1 and by European Union funding within the NextGenerationEU-MUR PNRR Extended Partnership initiative on Emerging Infectious Diseases (Project no. PE00000007, INF-ACT).

About the Author

Dr. Bisoffi is scientific director and director of the Department of Infectious, Tropical Diseases and Microbiology at the Istituto di Ricovero e Cura a Carattere Scientifico Sacro Cuore Don Calabria Hospital, Negrar di Valpolicella, Verona, Italy. He is the coordinator of TropNet, the European Network for Tropical Medicine and Travel Health. His primary research interests are surveillance and diagnosis of imported tropical and infectious diseases and clinical decision-making in tropical medicine.

References

1. Task force COVID-19 del Dipartimento Malattie Infettive e Servizio di Informatica, Istituto Superiore di Sanità. COVID-19 epidemic. Country update: January 5, 2022 [in Italian] [cited 2023 Jan 19]. https://www.epicentro.iss.it/coronavirus/bollettino/Bollettino-sorveglianza-integrata-COVID-19_5-gennaio-2022.pdf
2. Albani V, Loria J, Massad E, Zubelli J. COVID-19 underreporting and its impact on vaccination strategies. BMC Infect Dis. 2021;21:1111. https://doi.org/10.1186/s12879-021-06780-7
3. Bassanello M, Pasini L, Senzolo M, Gambaro A, Roman M, Coli U, et al. Epidemiological study in a small rural area of Veneto (Italian region) during SARS-CoV-2 pandemia. Sci Rep. 2021;11:23247. https://doi.org/10.1038/s41598-021-02654-9
4. Guerriero M, Bisoffi Z, Poli A, Micheletto C, Conti A, Pomari C. Prevalence of SARS-CoV-2, Verona, Italy, April–May 2020. Emerg Infect Dis. 2021;27:229–32. https://doi.org/10.3201/eid2701.202740
5. Melotti R, Scaggiante F, Falciani M, Weichenberger CX, Foco L, Lombardo S, et al. Prevalence and determinants of serum antibodies to SARS-CoV-2 in the general population of the Gardena valley. Epidemiol Infect. 2021;149:e194. https://doi.org/10.1017/S0950268821001886
6. Angulo FJ, Finelli L, Swerdlow DL. Estimation of US SARS-CoV-2 infections, symptomatic infections, hospitalizations, and deaths using seroprevalence surveys. JAMA Netw Open. 2021;4:e2033706–2033706. https://doi.org/10.1001/jamanetworkopen.2020.33706
7. Chamberlain AT, Toomey KE, Bradley H, Hall EW, Fahimi M, Lopman BA, et al. Cumulative incidence of SARS-CoV-2 infections among adults in Georgia, United States, August to December 2020. J Infect Dis. 2022;225:396–403. https://doi.org/10.1093/infdis/jiab522
8. Irons NJ, Raftery AE. Estimating SARS-CoV-2 infections from deaths, confirmed cases, tests, and random surveys. Proc Natl Acad Sci U S A. 2021;118:e2103272118. https://doi.org/10.1073/pnas.2103272118
9. Maley JH, Sandsmark DK, Trainor A, Bass GD, Dabrowski CL, Magdamo BA, et al. Six-month impairment in cognition, mental health, and physical function following COVID-19–associated respiratory failure. Crit Care Explor. 2022;4:e0673. https://doi.org/10.1097/CCE.0000000000000673
10. Nordström P, Ballin M, Nordström A. Risk of SARS-CoV-2 reinfection and COVID-19 hospitalisation in individuals with natural and hybrid immunity: a retrospective, total population cohort study in Sweden. Lancet Infect Dis. 2022;22:781–90. https://doi.org/10.1016/S1473-3099(22)00143-8
11. Altarawneh HN, Chemaitelly H, Hasan MR, Ayoub HH, Qassim S, AlMukdad S, et al. Protection against the Omicron variant from previous SARS-CoV-2 infection. N Engl J Med. 2022;386:1288–90. https://doi.org/10.1056/NEJMc2200133
12. Goldberg Y, Mandel M, Bar-On YM, Bodenheimer O, Freedman LS, Ash N, et al. Protection and waning of natural and hybrid immunity to SARS-CoV-2. N Engl J Med. 2022;386:2201–12. https://doi.org/10.1056/NEJMoa2118946
13. Abu-Raddad LJ, Chemaitelly H, Ayoub HH, AlMukdad S, Yassine HM, Al-Khatib HA, et al. Effect of mRNA vaccine boosters against SARS-CoV-2 Omicron infection in Qatar. N Engl J Med. 2022;386:1804–16. https://doi.org/10.1056/NEJMoa2200797
14. Feikin DR, Higdon MM, Abu-Raddad LJ, Andrews N, Araos R, Goldberg Y, et al. Duration of effectiveness of vaccines against SARS-CoV-2 infection and COVID-19 disease: results of a systematic review and meta-regression. Lancet. 2022;399:924–44. https://doi.org/10.1016/S0140-6736(22)00152-0
15. Suarez Castillo M, Khaoua H, Courtejoie N. Vaccine-induced and naturally-acquired protection against Omicron and Delta symptomatic infection and severe COVID-19 outcomes, France, December 2021 to January 2022. Euro Surveill. 2022;27:2200250. https://doi.org/10.2807/1560-7917.ES.2022.27.16.2200250

Address for correspondence: Zeno Bisoffi, Istituto di Ricovero e Cura a Carattere Scientifico Sacro Cuore Don Calabria Hospital, Via Sempreboni 5, 37024 Negrar di Valpolicella, Verona, Italy; email: zeno.bisoffi@sacrocuore.it

Chikungunya Outbreak in Country with Multiple Vectorborne Diseases, Djibouti, 2019–2020

Emilie Javelle, Franck de Laval, Guillaume André Durand, Aissata Dia, Cécile Ficko, Aurore Bousquet, Deborah Delaune, Sébastien Briolant, Audrey Mérens, Constance Brossier, Hervé Pommier, Florian Gala, Alain Courtiol, Quentin Savreux, Sébastien Sicard, Jean-Philippe Sanchez, Francis Robin, Fabrice Simon, Xavier de Lamballerie, Gilda Grard, Isabelle Leparc-Goffart, Vincent Pommier de Santi

During 2019–2020, a chikungunya outbreak occurred in Djibouti City, Djibouti, while dengue virus and malaria parasites were cocirculating. We used blotting paper to detect arbovirus emergence and confirm that it is a robust method for detecting and monitoring arbovirus outbreaks remotely.

Djibouti is a semi-arid country bordered by Eritrea, Somalia, and Ethiopia. In the region, the main vector of chikungunya virus (CHIKV) and dengue virus (DENV) is the *Aedes aegypti* mosquito. The French Armed Forces are stationed in Djibouti City, where 70% of the country's population live (total population ≈900,000). Military bases and housing are located in the urban area, and the entire French Defense Community (FDC), including service members, families, and civilian employees, comprise a population of 2,700.

During July–October 2019, a large-scale chikungunya outbreak (41,162 suspected cases, 16 laboratory-confirmed cases, attack rate 12.3%) occurred in Dire Dawa, Ethiopia, 260 km from Djibouti City (Appendix Figure, https://wwwnc.cdc.gov/EID/article/29/4/22-1850-App1.pdf) (*1*). In a 2010–2011 survey in Djibouti City, although no epidemic has been reported since, 2.6% of the population had serologic evidence of CHIKV infection (*2*). Given the road, rail, and air connections between the 2 cities and the CHIKV-naive local populations, we estimated the likelihood of a CHIKV outbreak in Djibouti City to be highly probable. Patient management was challenging because dengue fever and malaria are endemic to Djibouti (*3*).

We describe the comprehensive response implemented by the FDC to these multiple vectorborne diseases and evaluated the use of blood on blotting paper for arboviral diagnosis. With the consent of patients, we collected and anonymized epidemiologic and clinical data for diagnostic purposes. According to French regulations, because this outbreak was considered an immediate threat to public health, ethics approval was not required for this investigation.

The Study

In October 2019, we strengthened epidemiologic surveillance in the FDC to detect CHIKV emergence. We defined a suspected case of arboviral-like disease (ALD) as fever or chills and/or acute arthralgia and/or rash and/or vomiting and diarrhea. Symptomatic patients were encouraged to seek medical care for systematic testing for dengue, chikungunya, and malaria. From each person with ALD signs/symptoms, we collected venous blood, spotted it onto Whatman 3MM blotting paper (Sigma-Aldrich, https://www.sigmaaldrich.com), dried the samples at room temperature, and stored them in a sealed plastic pouch

Author affiliations: French Aix Marseille University, Marseille, France (E. Javelle, G.A. Durand, S. Briolant, F. Simon, X. de Lamballerie, G. Grard, I. Leparc-Goffart, V. Pommier de Santi); French Armed Forces Biomedical Research Institute, Marseille (E. Javelle, G.A. Durand, S. Briolant, G. Grard, I. Leparc-Goffart); University Hospital Institute-Méditerranée Infection, Marseille (E. Javelle, S. Briolant); French Armed Forces Center for Epidemiology and Public Health, Marseille (F. de Laval, A. Dia, C. Brossier, S. Sicard, V. Pommier de Santi); Bégin Military Teaching Hospital, Saint Mandé, France (C. Ficko, A. Bousquet, A. Mérens, A. Courtiol); Armed Forces Biomedical Research Institute, Brétigny-Sur-Orge, France (D. Delaune); French Military Health Service, Djibouti City, Djibouti (H. Pommier, F. Gala, Q. Savreux, J.-P. Sanchez, F. Robin)

DOI: https://doi.org/10.3201/eid2904.221850

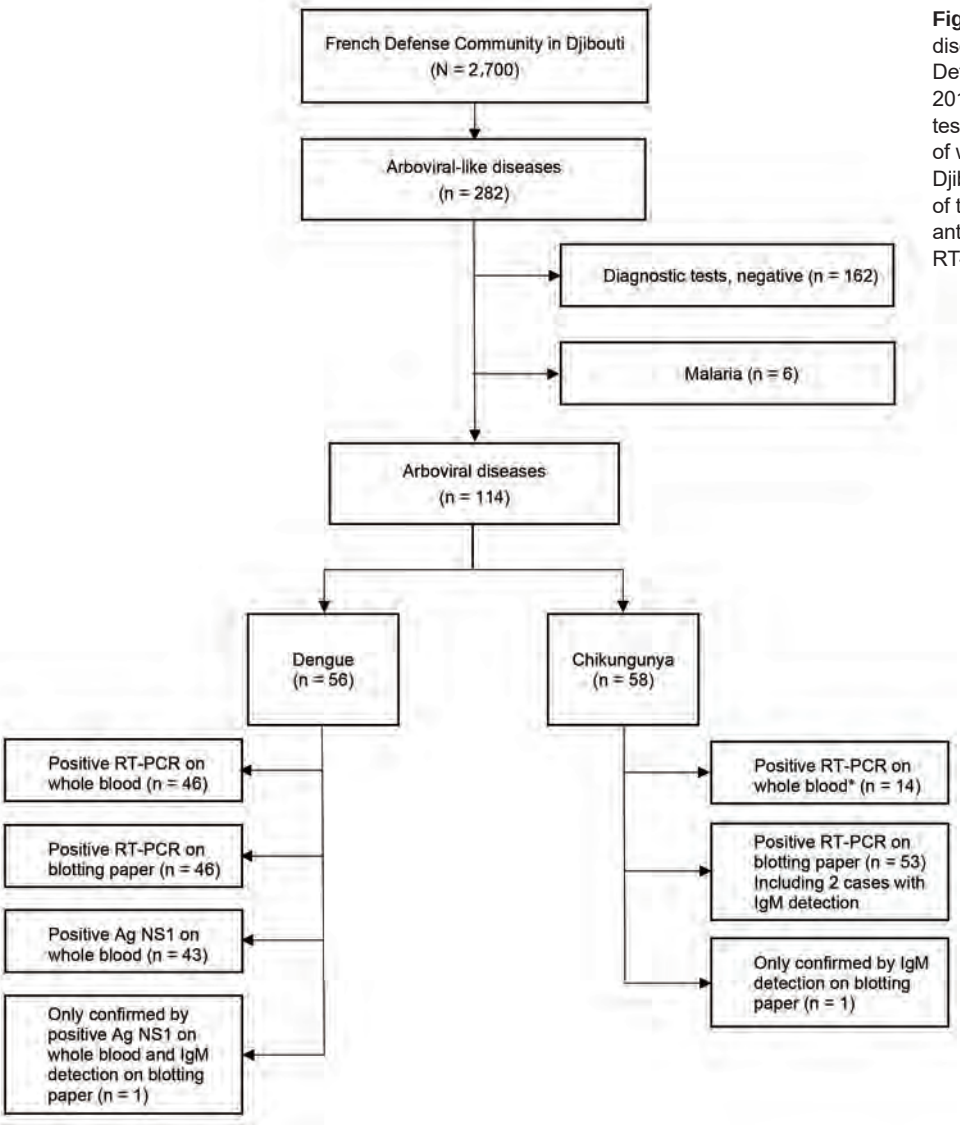

Figure 1. Flowchart for arboviral-like disease diagnoses among French Defense Community in Djibouti, 2019–2020. *Number of samples tested was limited because RT-PCR of whole blood was introduced in Djibouti City 1 month after the start of the chikungunya outbreak. Ag, antigen; NS1, nonstructural protein 1; RT-PCR, reverse transcription PCR.

for preservation and transport (*4*). The National Reference Center for arboviruses in France performed reverse transcription PCR (RT-PCR) and serologic testing for CHIKV and DENV on blotting paper as described elsewhere (*5*). In January, equipment was set up locally to perform in-house RT-PCR for DENV and CHIKV on whole-blood samples (Figure 1) (*6*,*7*). Chikungunya cases were confirmed by positive RT-PCR on whole blood or blotting paper or by detection of CHIKV IgM on blotting paper. Dengue cases were confirmed by a positive DENV RT-PCR on whole blood or blotting paper or a positive nonstructural protein 1 (NS1) antigen rapid diagnostic test (RDT) (Bioline Dengue Duo; Abbott, https://www.abbott.com). We provided care according to the French National Recommendations (*8*) and World Health Organization guidelines (*9*). Concurrently, we strengthened the following in the FDC vector-control measures and personal protection: larval source management, long clothing, insect repellents, and long-lasting insecticidal nets.

We compared clinical presentations of dengue and chikungunya by using R version 3.5.1 software (The R Project for Statistical Computing, https://www.r-project.org) for statistical analyses. Overall, among the 2,700 persons in the FDC, we included 282 with ALD. Through March 2020, we confirmed 120 cases of vectorborne disease (attack rate 42.6%, 120/282): 58 chikungunya (2.1%, 58/2,700), 56 dengue (2.1%), 6 malaria (5 *Plasmodium falciparum* and 1 *P. vivax*), and no co-infections (Figure 2). We also documented 2 concomitant influenza A virus and arbovirus infections. Among patients with vectorborne diseases, 67.5% (81/120) were male, and 73.3%

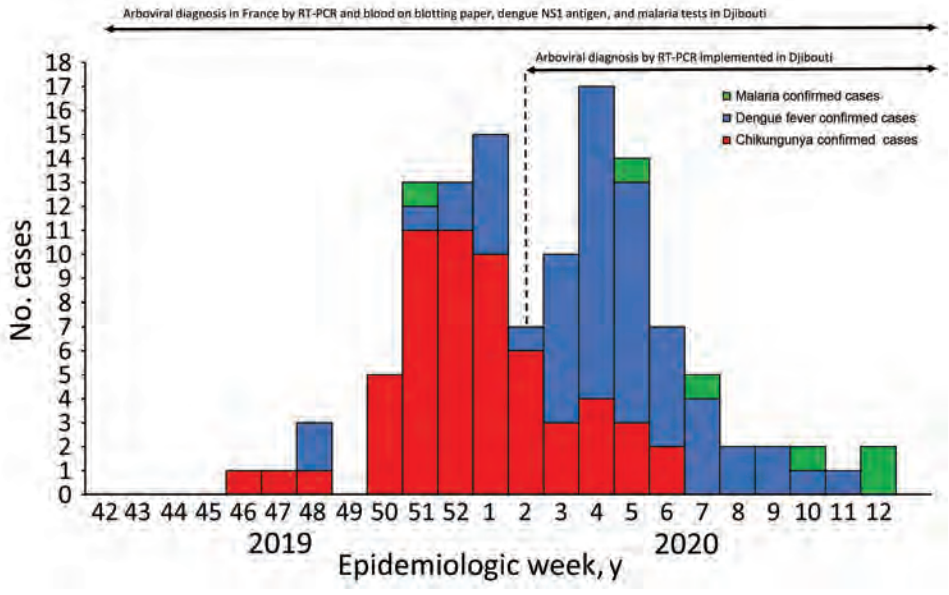

Figure 2. Vectorborne diseases among the French Defense Community in Djibouti: epidemic curve and availability of diagnostic tools, 2020 (chikungunya = 58, dengue = 56, and malaria = 6 cases). NS1, nonstructural protein 1; RT-PCR, reverse transcription PCR.

(88/120) were service members. The median age was 34.5 (range 8.3–79.6, interquartile range 27.1–40.0) years, and 92.5% (111/120) of persons sought care within 48 hours of symptom onset (median 1, range 0–7, interquartile range 0–1 days).

We confirmed the first chikungunya case among persons in the FDC in November 2019. The outbreak started in December and lasted 13 weeks. The CHIKV strain belonged to the Indian lineage of the East/Central/South African genotype (*10*). The dengue outbreak peaked in late January and was linked to DENV-1 with a unique serotype, confirmed for 36/56 dengue cases (Figure 2). CHIKV and DENV co-circulated for 16 weeks. One chikungunya case was diagnosed by CHIKV IgM on blotting paper alone; all others (57/58, 98%) were confirmed by RT-PCR. One dengue case was diagnosed by positive NS1 antigen RDT with positive DENV IgM on blotting paper; all others (55/56, 98%) were confirmed by RT-PCR (Figure 1). The National Reference Center received blotting paper samples for 93.0% (106/114) of the DENV and CHIKV infections and confirmed 97.2% (103/106) of the diagnoses, 93.4% (99/106) by RT-PCR and 3.8% (4/106) by serology (1 DENV and 3 CHIKV). DENV and CHIKV RT-PCR testing were performed both on whole blood and on blotting paper for 44.7% (51/114) (Tables 1, 2). Compared with RT-PCR of whole blood, no RT-PCR of blotting paper produced false-positive results.

Samples from ALD patients were locally tested with NS1 antigen RDT, and 43 (43/120, 36%) results were positive. Results were negative for 13/56 (23%) persons with dengue, all tested within a mean delay of 1.5 (range 0–3) days from symptom onset. Among the 46 with DENV infection confirmed by whole-blood RT-PCR, 36 (78%) had concomitant positive RDT results.

The main ALD sign was fever (90.8%, 109/120). Headaches and digestive disorders were more associated with dengue fever (odds ratio [OR] 7.2, 95% CI 2.3–22.8) than chikungunya (OR 5.9, 95% CI 1.8–19.6) (Appendix Table). Highly predictive of chikungunya were arthralgia of the toe (OR 29.97, 95% CI 3.19–195.61), ankle (OR 18.28, 95% CI 6.14-54.71), finger (OR 12.47, 95% CI 3.93–39.61), and wrist (OR 18.27, 95% CI 5.71–58.52). Secondary infection developed in 4 patients with chikungunya (1 case each of pneumonia, dysentery, herpetic recurrence, and gingivitis with oral candidiasis). Among

Table 1. Chikungunya cases confirmed by RT-PCR (n = 57/58) of blood samples, WB or BP, among 114 confirmed cases of arboviral disease, Djibouti*

Results	Positive on BP, no. (%)	Negative on BP, no. (%)	NA for BP, no. (%)	Total
Positive on WB	10 (72)	2 (14)	2 (14)	14
Negative on WB	0	39 (85)	7 (15)	46
NA for WB	43 (80)	11 (20)	0	54
Total	53 (46)	52 (46)	9 (8)	114

*RT-PCR tests were performed from October 2019 on dried blood spots stored on BP at the French National Reference Center for arboviruses in France. From January 2020, RT-PCR tests were also locally performed on WB samples at the French military medical center in Djibouti. BP, blotting paper; NA, not available (samples or result missing); RT-PCR, reverse transcription PCR; WB, whole blood.

Table 2. Dengue cases confirmed by RT-PCR (n = 55/56) of blood samples, WB or BP, among 114 confirmed cases of arboviral disease, Djibouti*

Results	Positive on BP, no. (%)	Negative on BP, no. (%)	NA for BP, no. (%)	Total
Positive on WB	37 (81)	2 (4)	7 (15)	46
Negative on WB	0	12 (86)	2 (14)	14
NA for WB	9 (17)	45 (83)	0	54
Total	46 (40)	59 (52)	9 (8)	114

*RT-PCR tests were performed from October 2019 on dried blood spots stored on BP at the French National Reference Center for arboviruses in France. From January 2020, RT-PCR tests were also locally performed on WB samples at the French military medical center in Djibouti. BP, blotting paper; NA, not available (samples or result missing; RT-PCR, reverse transcription PCR; WB, whole blood.

dengue patients, 4 had hepatic cytolysis (maximum transaminases elevation 12 times the upper limit), and 3 had secondary infections including acute pneumonia, *Escherichia coli* pyelonephritis, and intestinal amoebiasis. No patient met criteria for having severe dengue. No ALD patient required intensive care. All malaria patients recovered after a 3-day course of artenimol/piperaquine and secondary treatment with primaquine treatment for the patient with *P. vivax* infection. Treatment of arboviral disease relied essentially on analgesics, antihistamines, and hydration. The prescription of nonsteroidal anti-inflammatory drugs, aspirin, or corticosteroids was formally contraindicated during the first days of any infection. For patients with confirmed chikungunya, we carefully assessed the benefit-risk balance of introducing nonsteroidal anti-inflammatory drugs.

Conclusions

Despite recent improvement in diagnostic tools, chikungunya outbreaks in Africa are probably underreported (*11*). During 2019–2020, a large-scale chikungunya outbreak occurred in Djibouti City (*12*). However, because of lack of diagnostic tests and dedicated reporting, no data are available to estimate its extent. The chikungunya outbreak remained limited (attack rate 2.1%) in the FDC but was followed by a dengue outbreak. We found that clinical features are helpful but not sufficient to discriminate between chikungunya and dengue (*13*,*14*). Biological confirmation remains necessary for determining appropriate care. The use of blood samples on blotting paper has been described as a field method for detecting arboviruses (*4*,*5*), routinely used in the French Armed Forces when deployed in Africa (*15*). In this study, we used blood samples on blotting paper to detect emergence of CHIKV and monitor the course of the outbreaks. Blotting paper provided a robust method for blood sampling and transport to a reference laboratory, making it possible to confirm 90% of the arboviral diagnoses. We recommend blotting paper as a field tool to detect and monitor arboviral epidemics remotely.

Acknowledgments

We thank Patrick Gravier, David Fery, Pierre Blanco de Torre, Christophe Bodelot, Sandrine Duron, Olivier Cabre, Olivier Merle, Madjid Mokrane, Christelle Tong, Marion Fossier, Diane Houssin, and Jérôme Desplans for their help with this study.

About the Author

Dr. Javelle is a military physician and infectious diseases specialist at the Laveran Military Teaching Hospital and conducts research at the French Armed Forces Biomedical Research Institute and at the University Hospital Institute Méditerranée-Infection, in Marseille, France. She has clinical and scientific experience in vector-borne diseases and travel medicine.

References

1. Geleta D, Tesfaye N, Ayigegn H, Waldetensai A, Gemechu F, Amare H. Epidemiological description of chikungunya virus outbreak in Dire Dawa Administrative City, western Ethiopia, 2019. Int J Clin Exp Med Sci. 2020;6:41. https://doi.org/10.11648/j.ijcems.20200603.13
2. Andayi F, Charrel RN, Kieffer A, Richet H, Pastorino B, Leparc-Goffart I, et al. A sero-epidemiological study of arboviral fevers in Djibouti, Horn of Africa. PLoS Negl Trop Dis. 2014;8:e3299. https://doi.org/10.1371/journal.pntd.0003299
3. de Santi VP, Khaireh BA, Chiniard T, Pradines B, Taudon N, Larréché S, et al. Role of *Anopheles stephensi* mosquitoes in malaria outbreak, Djibouti, 2019. Emerg Infect Dis. 2021;27:1697–700. PubMed https://doi.org/10.3201/eid2706.204557
4. Andriamandimby SF, Heraud JM, Randrianasolo L, Rafisandratantsoa JT, Andriamamonjy S, Richard V. Dried-blood spots: a cost-effective field method for the detection of chikungunya virus circulation in remote areas. PLoS Negl Trop Dis. 2013;7:e2339. https://doi.org/10.1371/journal.pntd.0002339
5. Matheus S, Huc P, Labeau B, Bremand L, Enfissi A, Merle O, et al. The use of serum spotted onto filter paper for diagnosing and monitoring chikungunya virus infection. J Clin Virol. 2015;71:89–92. https://doi.org/10.1016/j.jcv.2015.08.008
6. Pastorino B, Bessaud M, Grandadam M, Murri S, Tolou HJ, Peyrefitte CN. Development of a TaqMan RT-PCR assay without RNA extraction step for the detection and quantification of African chikungunya viruses. J Virol Methods. 2005;124:65–71. https://doi.org/10.1016/j.jviromet.2004.11.002

7. Leparc-Goffart I, Baragatti M, Temmam S, Tuiskunen A, Moureau G, Charrel R, et al. Development and validation of real-time one-step reverse transcription-PCR for the detection and typing of dengue viruses. J Clin Virol. 2009;45:61–6. https://doi.org/10.1016/j.jcv.2009.02.010
8. Simon F, Javelle E, Cabie A, Bouquillard E, Troisgros O, Gentile G, et al. French guidelines for the management of chikungunya (acute and persistent presentations). November 2014. Med Mal Infect. 2015;45:243–63. https://doi.org/10.1016/j.medmal.2015.05.007
9. World Health Organization. Dengue: guidelines for diagnosis, treatment, prevention and control: new edition. Geneva: The Organization; 2009 [cited 2022 Nov 5]. https://apps.who.int/iris/handle/10665/44188
10. Fourié T, Dia A, Savreux Q, Pommier de Santi V, de Lamballerie X, Leparc-Goffart I, et al. Emergence of Indian lineage of ECSA chikungunya virus in Djibouti, 2019. Int J Infect Dis. 2021;108:198–201. https://doi.org/10.1016/j.ijid.2021.03.090
11. Bettis AA, L'Azou Jackson M, Yoon IK, Breugelmans JG, Goios A, Gubler DJ, et al. The global epidemiology of chikungunya from 1999 to 2020: a systematic literature review to inform the development and introduction of vaccines. PLoS Negl Trop Dis. 2022;16:e0010069. https://doi.org/10.1371/journal.pntd.0010069
12. News Desk. Chikungunya epidemic in Djibouti: "Unprecedented", according to media report. Outbreak News Today. 2020 Jan 18. [cited 2022 Jan 25]. http://outbreaknews-today.com/chikungunya-epidemic-in-djibouti-unprecedented-according-to-media-report-32763
13. Bonifay T, Vesin G, Bidaud B, Bonnefoy C, Dueymes M, Nacher M, et al. Clinical characteristics and predictive score of dengue vs. chikungunya virus infections. Med Mal Infect. 2019;49:250–6. https://doi.org/10.1016/j.medmal.2018.09.010
14. Thiberville S-D, Boisson V, Gaudart J, Simon F, Flahault A, de Lamballerie X. Chikungunya fever: a clinical and virological investigation of outpatients on Reunion Island, South-West Indian Ocean. PLoS Negl Trop Dis. 2013;7:e2004. https://doi.org/10.1371/journal.pntd.0002004
15. Tong C, Javelle E, Grard G, Dia A, Lacrosse C, Fourié T, et al. Tracking Rift Valley fever: from Mali to Europe and other countries, 2016. Euro Surveill. 2019;24:1800213. https://doi.org/10.2807/1560-7917.ES.2019.24.8.1800213

Address for correspondence: Vincent Pommier de Santi, Centre d'épidémiologie et de santé publique des armées, GSBdD Marseille Aubagne—CESPA—BP 40029, Marseille 13568, France; email: v.pommierdesanti@gmail.com

EID Podcast A Worm's Eye View

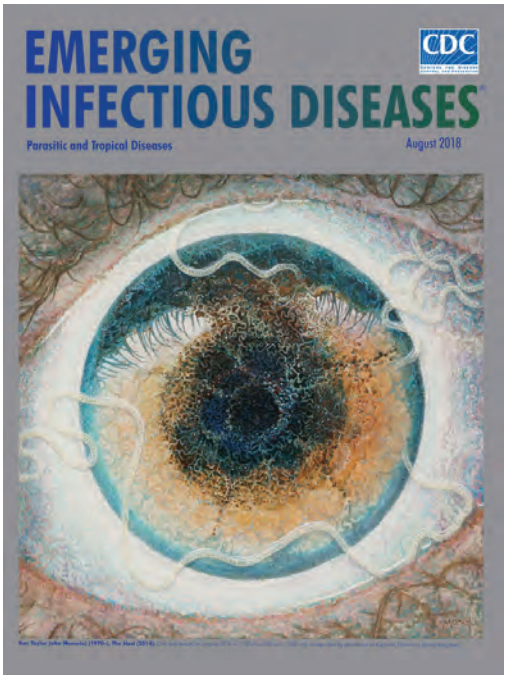

Seeing a several-centimeters-long worm traversing the conjunctiva of an eye is often the moment when many people realize they are infected with *Loa loa*, commonly called the African eyeworm, a parasitic nematode that migrates throughout the subcutaneous and connective tissues of infected persons. Infection with this worm is called loiasis and is typically diagnosed either by the worm's appearance in the eye or by a history of localized Calabar swellings, named for the coastal Nigerian town where that symptom was initially observed among infected persons. Endemic to a large region of the western and central African rainforests, the *Loa loa* microfilariae are passed to humans primarily from bites by flies from two species of the genus *Chrysops*, *C. silacea* and *C. dimidiate*. The more than 29 million people who live in affected areas of Central and West Africa are potentially at risk of loiasis.

Ben Taylor, cover artist for the August 2018 issue of EID, discusses how his personal experience with the *Loa loa* parasite influenced this painting.

Visit our website to listen:
https://tools.cdc.gov/medialibrary/index.aspx#/media/id/392605

EMERGING INFECTIOUS DISEASES®

Blackwater Fever Treated with Steroids in Nonimmune Patient, Italy

Anna Rita Di Biase, Dora Buonfrate, Francesca Stefanelli, Giorgio Zavarise, Erica Franceschini, Cristina Mussini, Lorenzo Iughetti, Federico Gobbi

Author affiliations: University of Modena and Reggio Emilia, Modena, Italy (A.R. Di Biase, F. Stefanelli, C. Mussini, L. Iughetti); IRCCS Sacro Cuore don Calabria Hospital, Negrar, Verona, Italy (D. Buonfrate, G. Zavarise, F. Gobbi); Azienda Ospedaliero-Universitaria of Modena, Modena (E. Franceschini)

DOI: http://doi.org/10.3201/eid2904.221267

Causes of blackwater fever, a complication of malaria treatment, are not completely clear, and immune mechanisms might be involved. Clinical management is not standardized. We describe an episode of blackwater fever in a nonimmune 12-year-old girl in Italy who was treated with steroids, resulting in a rapid clinical resolution.

On May 9, 2022 (day 1), a 12-year-old girl was admitted to the pediatric emergency department of Modena Hospital, Modena, Italy, for persistent fever (>2 days) and lethargy. She had returned to Italy from a family excursion to Nigeria 11 days prior to admission. She did not take malaria prophylaxis. Her initial hospital evaluations revealed severe thrombocytopenia, increased total bilirubin, and lactate dehydrogenase (Table). Hemoglobin was within normal range. A rapid diagnostic test for malaria was positive, and blood smears confirmed high *Plasmodium falciparum* parasitemia (26%).

The girl was admitted to the intensive care unit, where she received 4 doses of 2.4 mg/kg intravenous artesunate. Therapy was then switched to artemether/lumefantrine (80/480 mg dose, administered orally in 6 doses). Blood smears were negative for *P. falciparum* starting on day 4. Because the girl's hemoglobin levels had dropped steadily from the time of admission (Table), she received a blood transfusion on day 4. On day 5, she was discharged from the intensive care unit in good clinical condition and moved to the pediatric ward, where hyperchromic urine samples were observed. Empiric antibiotic treatment was started (ceftriaxone first, then piperacillin/tazobactam) to treat her persistent fever. Result of blood and urine cultures were negative, as were investigations for SARS-CoV-2 and other respiratory viruses. Chest radiographs and brain computed tomography scans (the latter performed to investigate additional causes of lethargy) had unremarkable results. Ultrasound examination revealed biliary sludge. Because the patient's hemoglobin level continued to drop, she received additional blood transfusions on days 10 and 12.

Our team suspected blackwater fever (BWF), a complication of *P. falciparum* infection, and colleagues from a referral center for tropical diseases confirmed the diagnosis and recommended administration of steroids. We prescribed a 5-day treatment course of oral prednisone (1.3 mg/kg), starting on day 13. We tapered off the dose over the next 15 days and administered another blood transfusion on day 16. Symptoms cleared completely the day after steroid treatment began, and urine samples became normochromic 7 days later. The patient was discharged in good clinical condition on Day 23. One month later, blood test results were unremarkable (Table). No

Table. Laboratory exams during hospitalization for a 12-year-old girl with blackwater fever, Modena, Italy*

Parameter	Day 1	Day 2	Day 4	Day 7	Day 10	Day 13	Day 23	Follow-up
Labwork								
Hemoglobin, g/dL	12.3	9.1	7.8	10.2	7.9	9.9	10.1	12.6
Platelets, 10^3/mmc	27	45	96	79	354	379	451	301
Bilirubin, mg/dL	1.96	1.53	1.21	1.06	1.57	2.25	0.61	0.42
ALT, U/L	77	79	389	446	260	124	62	12
AST, U/L	NA	NA	1398	1435	254	128	35	NA
LDH, U/L	1870	1732	7676	7200	5147	5646	1715	513
PCR, mg/dL	23.8	15.2	24.3	11.6	1.5	1.8	<0.2	<0.2
Hemoglobinuria	N	N	Y	Y	Y	Y	N	N
Treatment								
Artesunate	×	×	–	–	–	–	–	–
Artemether/lumefantrine	–	–	×†	–	–	–	–	–
Blood transfusion	–	–	×	–	×‡	–	–	–
Steroids	–	–	–	–	–	×§	–	–

*ALT, alanine aminotransferase; AST, aspartate aminotransferase; LDH, lactate dehydrogenase; N, no; NA, not applicable; PCR, polymerase chain reaction; Y, yes; ×, administered; –, not administered.
†Days 3–5.
‡Days 10, 12 and 16.
§Days 13–17.

abnormal hemoglobin or glucose-6-phosphate-dehydrogenase results were noted.

BWF is a condition characterized by massive hemolysis after treatment for acute malaria, with clinical symptoms that include hemoglobinuria, anemia, jaundice, and fever (*1*–*3*). The name of the syndrome relates to the presence of dark urine noted in affected patients. An apparent decrease in cases of BWF was noted when artemisinin compounds replaced quinine as first-line treatment for malaria (*3*,*4*). However, a randomized, controlled trial comparing quinine versus artesunate for treatment of severe malaria in children and found frequency of BWF did not differ significantly between the 2 study arms (p = 0.076) (*5*).

Artesunate has been associated with hemolytic anemia, a condition that differs from BWF in that hemolysis is delayed (usually starting from 2 to 3 weeks following initiation of artesunate therapy, although some cases can occur earlier); most important, hemoglobinuria is not reported. Another differentiating factor between the 2 conditions is that hemolysis due to artesunate is extravascular and, in BWF, hemolysis is intravascular (*6*).

The pathophysiologic mechanisms causing BWF are not completely understood, and no definitive evidence has emerged from investigations into the role of antimalarial drugs (mostly quinine, with some reports about halofantrine and mefloquine), characteristics of the human host (e.g., glucose-6-phosphate-dehydrogenase deficiency), and parasite type (e.g., different *Plasmodium* strains) (*1*,*7*,*8*). No relationship has been reported between high levels of parasitemia and development of BWF. Because most cases of BWF arise in nonimmune persons, immune mechanisms have been suspected to cause the hemolysis (*8*). Nevertheless, many cases have been observed in children >5 years of age who resided in malaria-endemic areas and were suspected to carry at least partial immunity against *Plasmodium* spp. (*8*). Studies suggest that those children failed to attain protective immunity against malaria and, indeed, showed an immune profile similar to expatriates in Europe. Different mechanisms have been speculated to be involved in activating the immune response leading to BWF, including excessive complement activation and presence of a malaria immune complex antigen-antibody (*8*).

Treatment with steroids, as was determined for this patient, has been previously instituted in a malaria-endemic setting (*9*). Although evidence is not sufficient to recommend this therapeutic approach, it seems reasonable from a pathophysiologic standpoint and deserves further evaluation. Besides steroids, the 2 pillars of BWF management are blood transfusion and refraining from drugs possibly causing the syndrome (*9*). Because of the rarity (and neglect) of BWF (*3*), randomized controlled trials comparing treatment options are not currently feasible. Nonetheless, the disease is a serious consequence for children who are susceptible; there is a 3-fold higher risk of death for children with severe anemia and BWF than for children with severe anemia and no BWF (*2*). Considering that statistic and the poor outcomes observed in the 6 months following a BWF episode (*2*), evidence in support of clinical management is clearly needed.

This work was partly supported by the Italian Ministry of Health "Fondi Ricerca Corrente" to IRCCS Sacro Cuore Don Calabria Hospital–Linea 1.

About the Author

Dr Anna Rita di Biase is an MD specialist in Pediatrics and Pediatric Immunology. She is chief of the pediatric emergency unit at the University Hospital of Modena, Modena, Italy.

References

1. Shanks GD. The multifactorial epidemiology of blackwater fever. Am J Trop Med Hyg. 2017;97:1804–7. https://doi.org/10.4269/ajtmh.17-0533
2. Opoka RO, Waiswa A, Harriet N, John CC, Tumwine JK, Karamagi C. Blackwater fever in Ugandan children with severe anemia is associated with poor postdischarge outcomes: a prospective cohort study. Clin Infect Dis. 2020;70:2247–54. https://doi.org/10.1093/cid/ciz648
3. Bodi JM, Nsibu CN, Longenge RL, Aloni MN, Akilimali PZ, Tshibassu PM, et al. Blackwater fever in Congolese children: a report of clinical, laboratory features and risk factors. Malar J. 2013;12:205. https://doi.org/10.1186/1475-2875-12-205
4. Rodriguez-Valero N, Castro P, Martinez G, Marco Hernandez J, Fernandez S, Gascon J, et al. Blackwater fever in a non-immune patient with *Plasmodium falciparum* malaria after intravenous artesunate. J Travel Med. 2018;25. https://doi.org/10.1093/jtm/tax094
5. Dondorp AM, Fanello CI, Hendriksen IC, Gomes E, Seni A, Chhaganlal KD, et al.; AQUAMAT group. Artesunate versus quinine in the treatment of severe falciparum malaria in African children (AQUAMAT): an open-label, randomised trial. Lancet. 2010;376:1647–57. https://doi.org/10.1016/S0140-6736(10)61924-1
6. Jauréguiberry S, Thellier M, Ndour PA, Ader F, Roussel C, Sonneville R, et al.; French Artesunate Working Group. Delayed-onset hemolytic anemia in patients with travel-associated severe malaria treated with artesunate, France, 2011-2013. Emerg Infect Dis. 2015;21:804–12. https://doi.org/10.3201/eid2105.141171
7. Chau TTH, Day NPJ, Van Chuong L, Mai NTH, Loc PP, Phu NH, et al. Blackwater fever in southern Vietnam: a prospective descriptive study of 50 cases. Clin Infect Dis. 1996;23:1274–81. https://doi.org/10.1093/clinids/23.6.1274
8 Bodi JM, Nsibu CN, Hirayama K. Immunogenetic mechanisms of black water fever: article review.

Gene Technol. 2021;10:160 [cited 2022 Aug 5]. https://www.walshmedicalmedia.com/open-access/immunogenetic-mechanisms-of-black-water-fever-article-review-62849.html
9. Gobbi F, Audagnotto S, Trentini L, Nkurunziza I, Corachan M, Di Perri G. Blackwater fever in children, Burundi. Emerg Infect Dis. 2005;11:1118–20. https://doi.org/10.3201/eid1107.041237

Address for correspondence: Federico Gobbi, Department of Infectious Tropical Diseases and Microbiology, IRCCS Sacro Cuore don Calabria Hospital, via Sempreboni 5, 37024 Negrar, Verona, Italy; email: federico.gobbi@sacrocuore.it

Helicobacter ailurogastricus in Patient with Multiple Refractory Gastric Ulcers, Japan

Masaya Sano, Emiko Rimbara, Masato Suzuki, Hidenori Matsui, Miwa Hirai, Sae Aoki, Tsuyoshi Kenri, Keigo Shibayama, Hidekazu Suzuki

Author affiliations: Tokai University School of Medicine, Kanagawa, Japan (M. Sano, M. Hirai, H. Suzuki); National Institute of Infectious Diseases, Tokyo, Japan (E. Rimbara, M. Suzuki, H. Matsui, S. Aoki, T. Kenri); Nagoya University Graduate School of Medicine, Aichi, Japan (K. Shibayama)

DOI: https://doi.org/10.3201/eid2904.221807

We report the isolation of *Helicobacter ailurogastricus*, a *Helicobacter* species that infects cats and dogs, from a person with multiple refractory gastric ulcers. In addition to *H. suis*, which infects pigs, *Helicobacter* species that infect cats and dogs should be considered as potential gastric pathogens in humans.

A 61-year-old man in Japan had multiple ulcers diagnosed on esophagogastroduodenoscopy (EGD) performed during his annual health check-up and was referred to Tokai University Hospital (Kanagawa, Japan) because of an inadequate therapeutic response. Histologic examination of tissue from the ulcer site showed inflammatory cells and few findings suggestive of malignancy. Hematoxylin and eosin staining showed spiral bacteria resembling a *Helicobacter* species.

Test results for *H. pylori* serum antibodies and stool antigen were negative. The patient had onset of epigastric discomfort after his work became busy but attributed his symptoms to his work burden and did not seek medical care. Although he had not taken nonsteroidal antiinflammatory drugs or aspirin, he did not respond to therapy, even with the administration of the antisecretory agent vonoprazan (20 mg), and had multiple refractory gastric ulcers diagnosed.

After obtaining informed consent, we enrolled the patient in a clinical trial investigating the effects of non–*H. pylori Helicobacter* (NHPH) infections on intractable ulcers and gastric mucosa–associated lymphoid tissue lymphoma. On August 24, 2021, we assessed the patient for NHPH by using culture and PCR of gastric biopsy samples collected during EGD (Appendix, https://wwwnc.cdc.gov/EID/article/29/4/22-1807-App1.pdf). EGD showed no atrophy in the background gastric mucosa, healing of the ulcers observed previously, multiple erosions, and residual ulcers in the antrum (Figure, panel A). The PCR test result for NHPH was positive, but the bacterial culture result was negative. On November 30, 2021, a repeat EGD to assess ulcer healing status showed further healing. Repeat culture and PCR tests for NHPH were both positive. We isolated *Helicobacter* spp. strain NHP21-4376 from the greater curvature of the gastric antrum and NHP21-4377 from the lesser curvature.

The microorganisms had a corkscrew-like spiral form (Figure, panel B) resembling that of *Helicobacter suis*, the most prevalent NHPH species in the human stomach. We performed whole-genome sequencing of the NHP21-4376 and NHP21-4377 strains by using the Illumina platform (Illumina, https://www.illumina.com) (Appendix). We assembled the Illumina reads de novo by using Shovill 1.1.0 (https://github.com/tseemann/shovill) with the default parameters. We determined the bacterial species by calculating the average nucleotide identity (ANI) using pyani 0.2.12 (https://github.com/widdowquinn/pyani). Strains NHP21-4376 and NHP21-4377 had >98% identity with *H. ailurogastricus* strains, including the type strain ASB7^T, indicating that they were *H. ailurogastricus* (Appendix Figure 1).

Phylogenetic analysis based on 342 core genes among gastric *Helicobacter* species also confirmed that NHP21-4376 and NHP21-4377 are in the same clade as *H. ailurogastricus* strains ASB7^T and ASB9 and are distinct from *H. suis* strains (Appendix Figure 2). We deposited draft genome sequences of *H.*

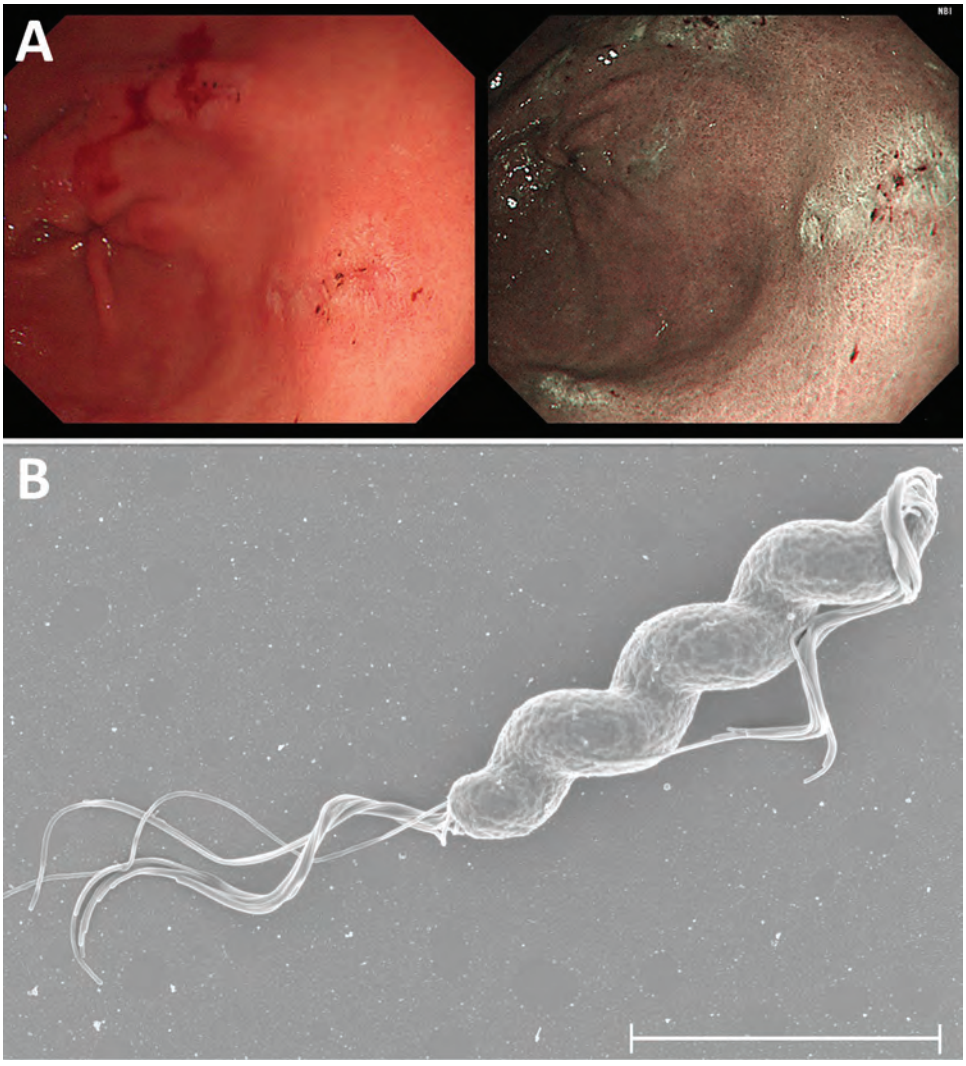

Figure. Endoscopic images from a gastric ulcer patient infected with *Helicobacter ailurogastricus* and morphologic observation and genomic comparison of isolated *H. ailurogastricus* NHP21-4376 and NHP21-4377 strains, Japan. A) Multiple linear erosions and small ulcers on the background mucosa with no evidence of atrophy in the gastric antral area. B) Scanning electron micrograph of *Helicobacter ailurogastricus* strain NHP21-4377. Scale bar indicates 2 μm.

ailurogastricus into GenBank (NHP21-4376 accession nos. BSCV01000001–64 and NHP21-4377 accession nos. BSCW01000001–66).

Antimicrobial susceptibility tests showed that *H. ailurogastricus* NHP21-4376 had a high MIC for levofloxacin (Table) and that the NHP21-4376 strain had a Ser to Arg mutation at position 78 in the quinolone resistance–determining region of DNA gyrase A (Appendix Figure 3). This position corresponds to Asn at position 87, where its mutation is responsible for fluoroquinolone resistance in *H. pylori* (*1*).

H. suis, which is the most prevalent NHPH species in humans, is believed to originate in pigs. Virulence-associated features were recently shown in *H. suis* isolates obtained from human stomachs (*2*); gastric ulcer recurrence was not observed in the patient infected with *H. suis* after *H. suis* eradication (*2*). Furthermore, *H. ailurogastricus* and *H. heilmannii* are 2 of the most prevalent NHPH strains infecting the human stomach, after *H. suis* (*3*,*4*). *H. ailurogastricus* was formerly classified as *H. heilmannii*. *H. heilmannii* and *H. ailurogastricus* are prevalent *Helicobacter* species that infect the stomachs of cats (*5*). Moreover, *H. ailurogastricus* is shown to be the prevalent gastric *Helicobacter* species infecting the stomach of cats and dogs in Japan (Appendix Table, Figure 4).

In this case, the patient was strongly suspected to have acquired the infection from his cats, although the stool of his pets could not be analyzed because the

Table. Antimicrobial susceptibilities of *Helicobacter ailurogastricus* strains ASB7^T and NHP21-4376 isolated from patient, Japan, 2021

Strain	Host	MIC, mg/L					
		Amoxicillin	Clarithromycin	Metronidazole	Minocycline	Gentamicin	Levofloxacin
ASB7^T	Cat	0.25	≤0.25	16	≤2	≤4	≤0.5
NHP21-4376	Human	1	≤0.25	16	≤2	≤4	4

patient's consent was not obtained. The patient has not had a recurrence of multiple ulcers but remains positive for *H. ailurogastricus*. The limitation of this case report is that, although we succeeded in culturing *H. ailurogastricus* in the stomach of this patient and the drug-susceptibility test has determined the regimen for eradication, we have not yet been able to perform eradication therapy. Therefore, the efficacy of eradication in *H. ailurogastricus* infections has not been confirmed. *H. ailurogastricus* eradication therapy will be administered at the next patient visit to prevent ulcer recurrence.

The clinical importance of NHPH infection in the human stomach has been increasing in the post–*H. pylori* era. Because NHPH species such as *H. suis* and *H. ailurogastricus* cannot be detected by most *H. pylori* diagnostic tests, such as the urea breath test and stool antigen test, NHPH infections should be considered when routine *H. pylori* tests are negative, despite the presence of inflammatory findings in the gastric mucosa.

This work was supported by MEXT/JSPS KAKENHI (grant no. 20H03667, awarded to H.S.), and by AMED (grant no. JP20fk0108148, awarded to E.R. and H.S.).

About the Author

Dr. Sano is an instructor at the Division of Gastroenterology and Hepatology, Tokai University School of Medicine. His primary research interests are endoscopic treatment of gastrointestinal diseases and elucidation of pathological mechanisms.

References

1. Nishizawa T, Suzuki H. Mechanisms of *Helicobacter pylori* antibiotic resistance and molecular testing. Front Mol Biosci. 2014;1:19. https://doi.org/10.3389/fmolb.2014.00019
2. Rimbara E, Suzuki M, Matsui H, Nakamura M, Morimoto M, Sasakawa C, et al. Isolation and characterization of *Helicobacter suis* from human stomach. Proc Natl Acad Sci U S A. 2021;118:e2026337118. https://doi.org/10.1073/pnas.2026337118
3. Nakamura M, Øverby A, Michimae H, Matsui H, Takahashi S, Mabe K, et al. PCR analysis and specific immunohistochemistry revealing a high prevalence of non–*Helicobacter pylori* Helicobacters in *Helicobacter pylori*–negative gastric disease patients in Japan: high susceptibility to an Hp eradication regimen. Helicobacter. 2020;25:e12700. https://doi.org/10.1111/hel.12700
4. Shafaie S, Kaboosi H, Peyravii Ghadikolaii F. Prevalence of non *Helicobacter pylori* gastric Helicobacters in Iranian dyspeptic patients. BMC Gastroenterol. 2020;20:190. https://doi.org/10.1186/s12876-020-01331-x
5. Joosten M, Lindén S, Rossi M, Tay AC, Skoog E, Padra M, et al. Divergence between the highly virulent zoonotic pathogen *Helicobacter heilmannii* and its closest relative, the low-virulence "*Helicobacter ailurogastricus*" sp. nov. Infect Immun. 2015;84:293–306. https://doi.org/10.1128/IAI.01300-15

Address for correspondence: Hidekazu Suzuki, Division of Gastroenterology and Hepatology, Department of Internal Medicine, Tokai University School of Medicine, 143 Shimokasuya, Isehara, Kanagawa, 259-1193, Japan; email: hsuzuki@tokai.ac.jp

Harbor Porpoise Deaths Associated with *Erysipelothrix rhusiopathiae*, the Netherlands, 2021

Lonneke L. IJsseldijk, Lineke Begeman, Birgitta Duim, Andrea Gröne, Marja J.L. Kik, Mirjam D. Klijnstra, Jan Lakemeyer, Mardik F. Leopold, Bas B. Oude Munnink, Mariel ten Doeschate, Linde van Schalkwijk, Aldert Zomer, Linda van der Graaf-van Bloois, Els M. Broens

Author affiliations: Utrecht University, Utrecht, the Netherlands (L.L. IJsseldijk, B. Duim, A. Gröne, M.J.L. Kik, J. Lakemeyer, M. ten Doeschate, L. van Schalkwijk, A. Zomer, L. van der Graaf-van Bloois, E.M. Broens); Erasmus University Medical Center, Rotterdam, the Netherlands (L. Begeman, B.B. Oude Munnink); Wageningen Food Safety Research, Wageningen, the Netherlands (M.D. Klijnstra); Wageningen Marine Research, Den Helder, the Netherlands (M.F. Leopold)

DOI: https://doi.org/10.3201/eid2903.221698

In August 2021, a large-scale mortality event affected harbor porpoises (*Phocoena phocoena*) in the Netherlands. Pathology and ancillary testing of 22 animals indicated that the most likely cause of death was *Erysipelothrix rhusiopathiae* infection. This zoonotic agent poses a health hazard for cetaceans and possibly for persons handling cetacean carcasses.

Erysipelothrix bacteria cause infections in humans and other species after contact with infected animals or environmental sources (*1*). Illness ranges from mild to systemic, which can include septicemia and endocarditis. *Erysipelothrix* can survive for long periods in the environment, including marine ecosystems (*1*) associated with marine fish, mollusks, and crustaceans. *Erysipelothrix* infection affects captive and

free-ranging crustaceans and is linked to fatal sepsis (*2*). To our knowledge, reports of large-scale mortality events caused by *Erysipelothrix* infection in marine mammals are absent from the literature, and *Erysipelothrix* has not been detected in stranded porpoises along the Netherlands coastline since the start of our harbor porpoise stranding research program in 2008.

At the end of August 2021, a total of 190 dead harbor porpoises (*Phocoena phocoena*) were found on Dutch Wadden islands; the annual average for stranded harbor porpoises on the entire Dutch coastline is 600. No anthropogenic activities in the southern or central North Sea that could explain this mortality event were reported to the government of the Netherlands in the 4–6 weeks before the event.

Most porpoises were found in an advanced state of decomposition. Twenty-two animals were collected for examination at the Faculty of Veterinary Medicine of Utrecht University (Appendix Table 1, https://wwwnc.cdc.gov/EID/article/29/4/22-1698-App1.pdf). We immediately necropsied 2, and the rest were temporarily frozen pending postmortem investigation and ancillary testing.

Because of advanced decomposition, we could perform only gross pathologic examinations and sampling for ancillary testing, following a standardized international protocol (*3*). Adult female porpoises were mostly in good to moderate nutritional condition with mild to moderate parasitic infections of various organs and had been reproductively active (Appendix Table 1). Of the 21 stomachs examined (1 was not examined because of gross damage caused by scavengers), none contained marine debris; 10 contained the remains of a few prey, reflecting nonrecent food intake, and the remaining stomachs were empty.

Samples from 3 porpoises with gross changes (mammary gland, lung, spinal cord) were cultured on blood agar (bioTrading, https://biotrading.com) at 37°C for 48 h. Culture results were positive for *Erysipelothrix rhusiopathiae*. Subsequently, we tested liver samples from 21 animals for *E. rhusiopathiae*; and 16 were positive (Appendix Table 2). To investigate the relatedness of isolates, genomes of 18 isolates were sequenced by using Illumina NextSeq (https://www.illumina.com) and assembled by using SPAdes version 3.14.1 (*4*); we included 11 publicly available reference genomes from different *E. rhusiopathiae* clades (*5*). A core genome alignment was made with Parsnp version 1.2 (*6*) and visualized by using iTol version 4 (*7*).

Genomes from this study were phylogenetically positioned between clade 2 *E. rhusiopathiae* reference genomes and formed 2 distinct clusters showing ≈3,400 single-nucleotide polymorphism (SNP) differences and limited diversity of <6 SNPs within the clusters (Figure). That pattern suggests dissemination of 2 clonal lineages of *E. rhusiopathiae*, either through exposure to a common source or contact between individuals.

Virology tests on 14 fecal, 15 blood, and 17 spleen samples and metagenomic sequencing with VirCapSeq-VERT (*8*) revealed no virus sequences of

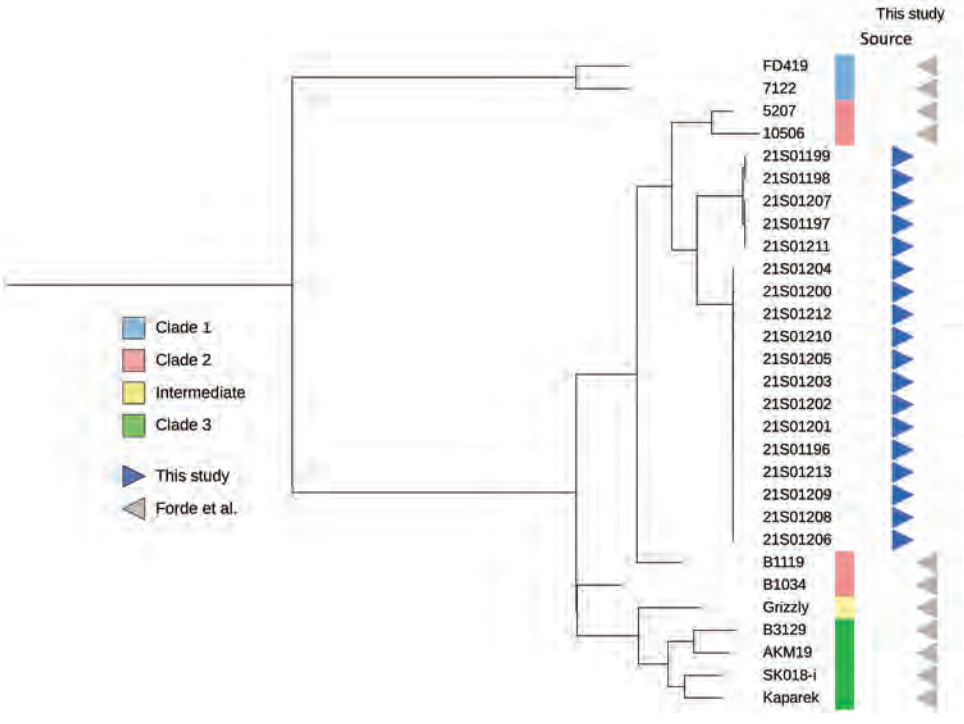

Figure. Phylogenetic tree of *Erysipelothrix rhusiopathiae* from stranded harbor porpoises, the Netherlands, 2021, compared with reference genomes described by Forde et al. (*5*). Branches are square root transformed. Detailed information for each sample is provided in Appendix Table 3 (https://wwwnc.cdc.gov/EID/article/29/4/22-1698-App1.pdf).

interest. In addition, we tested 20 lung and 20 brain samples for influenza A virus, paramyxoviruses (including morbilliviruses), coronaviruses (including SARS-CoV-2), and herpesviruses. Only 2 brain samples tested positive for *P. phocoena* alphaherpesvirus (Appendix Table 1), described as an incidental cause of death in porpoises (*9*). Our results indicate that viruses were an unlikely factor in this mortality event.

We pooled 20 stomach content samples and 21 liver samples in triplicate and analyzed them with a Liquid Chromatograph Triple Quadrupole Mass Spectrometer (LC-MS/MS) (McCrone Associates, https://www.mccrone.com) for domoic acid, saxitoxins, tetrodotoxin, and lipophilic marine toxins. Only saxitoxin was detected; it was in 1 pooled liver sample (estimated concentration 15 μg/kg). Subsequently, we analyzed livers individually, and saxitoxin was not confirmed in any of the individual samples. We therefore conclude that harmful algae were an unlikely factor in this mortality event.

Gross pathologic assessment revealed a moderate to good body condition for most porpoises, but none had recently fed. This finding suggests a subacute cause of death from sudden and excessive disease. No clinically relevant viruses were detected. Phycotoxins were detected in a limited number of porpoises. In contrast, *E. rhusiopathiae* was isolated from most investigated porpoises. Therefore, we consider *E. rhusiopathiae* to be the most likely cause of death. Advanced autolysis of the carcasses made detection of distinctive lesions associated with *Erysipelothrix* infection impossible. The low number of SNPs differing between isolates suggests common exposure, possibly a food source, transmission between porpoises, or both.

Our results draw attention to possibly increased cetacean susceptibility to *E. rhusiopathiae*, to new or emerging sources of *Erysipelothrix* in the marine environment, or both. *Erysipelothrix* remains viable in a carcass up to 12 days in direct sunlight, up to 4 months in putrefied flesh, and up to 9 months in a buried carcass (*10*). This new emerging source and the long survival time in carcasses demonstrates a need for having only trained personnel handle stranded animals, proper disposal of carcasses, and increased awareness for the potential presence and transmission of this zoonotic bacterium among cetaceans.

Acknowledgments

We thank all volunteers and organizations of the Dutch Stranding Network for their tremendous efforts and work to document stranded porpoises during the event. Necropsies were assisted by Louis van den Boom, Natashja Ennen-Buijs, Olle Juch, Darryl Leydekkers, Immelie Coenen Morales, Jan Mosterd, Eva Schotanus, and Ruby Wagensveld. We also thank Judith van den Brand for her input in the discussions of the ancillary testing. Virology was conducted at Erasmus MC, with special thanks to Marco van de Bildt, Irina Chestakova, Marjan Boter, Babette Weller, Reina Sikkema, and Marion Koopmans. Bacteriology was conducted at the Veterinary Microbiological Diagnostic Center, for which we thank all staff involved. Stomach investigations were conducted at Wageningen Marine Research with the help of Guido Keijl and Eva Schotanus. Algae toxin research was carried out by Wageningen Food Safety Research with the help of Domenique van der Horst.

The research was financed by the Ministry of Agriculture, Nature and Food Quality (project no. 1400012118), for which we are especially grateful for the help of Anne-Marie Svoboda and Sandra van der Graaf.

About the Author

Dr. IJsseldijk is assistant professor at the Division of Pathology, Department of Biomolecular Health Sciences, Faculty of Veterinary Medicine, Utrecht University. Her primary research interests focus on marine mammal health and conservation.

References

1. Wang Q, Chang BJ, Riley TV. Erysipelothrix rhusiopathiae. Vet Microbiol. 2010;140:405–17. https://doi.org/10.1016/j.vetmic.2009.08.012
2. Ceccolini ME, Wessels M, Macgregor SK, Deaville R, Perkins M, Jepson PD, et al. Systemic *Erysipelothrix rhusiopathiae* in seven free-ranging delphinids stranded in England and Wales. Dis Aquat Organ. 2021;145:173–84. https://doi.org/10.3354/dao03609
3. IJsseldijk LL, Brownlow AC, Mazzariol S, editors. Best practice for cetacean post mortem investigation and tissue sampling. Joint ACCOBAMS and ASCOBANS document. Stralsund, Germany: Agreement for the Conservation of Cetaceans of the Baltic Sea, Mediterranean Sea and Contiguous Atlantic Area (ACCOBAMS); Agreement on the Conservation of Small Cetaceans of the Baltic, North East Atlantic, Irish and North Seas (ASCOBANS); 2019 [cited 2022 Nov 7]. https://www.ascobans.org/sites/default/files/document/ascobans_ac25_inf3.2_rev1_best-practice-cetacean-post-mortem-investigation.pdf
4. Bankevich A, Nurk S, Antipov D, Gurevich AA, Dvorkin M, Kulikov AS, et al. SPAdes: a new genome assembly algorithm and its applications to single-cell sequencing. J Comput Biol. 2012;19:455–77. https://doi.org/10.1089/cmb.2012.0021
5. Forde T, Biek R, Zadoks R, Workentine ML, De Buck J, Kutz S, et al. Genomic analysis of the multi-host pathogen *Erysipelothrix rhusiopathiae* reveals extensive recombination as well as the existence of three generalist clades with wide geographic distribution. BMC Genomics. 2016;17:461. https://doi.org/10.1186/s12864-016-2643-0
6. Treangen TJ, Ondov BD, Koren S, Phillippy AM. The Harvest suite for rapid core-genome alignment and visualization of

thousands of intraspecific microbial genomes. Genome Biol. 2014;15:524. https://doi.org/10.1186/s13059-014-0524-x
7. Letunic I, Bork P. Interactive Tree Of Life (iTOL) v4: recent updates and new developments. Nucleic Acids Res. 2019;47(W1):W256–9. https://doi.org/10.1093/nar/gkz239
8. Briese T, Kapoor A, Mishra N, Jain K, Kumar A, Jabado OJ, et al. Virome capture sequencing enables sensitive viral diagnosis and comprehensive virome analysis. MBio. 2015;6:e01491–15. https://doi.org/10.1128/mBio.01491-15
9. van Elk C, van de Bildt M, van Run P, de Jong A, Getu S, Verjans G, et al. Central nervous system disease and genital disease in harbor porpoises (*Phocoena phocoena*) are associated with different herpesviruses. Vet Res (Faisalabad). 2016;47:28. https://doi.org/10.1186/s13567-016-0310-8
10. Brooke CJ, Riley TV. *Erysipelothrix rhusiopathiae*: bacteriology, epidemiology and clinical manifestations of an occupational pathogen. J Med Microbiol. 1999;48:789–99. https://doi.org/10.1099/00222615-48-9-789

Address for correspondence: Els M. Broens, Department of Biomolecular Health Sciences, Faculty of Veterinary Medicine, Utrecht University, Yalelaan 1, 3584 TD, Utrecht, the Netherlands; email: e.m.broens@uu.nl

Powassan Virus Infection Detected by Metagenomic Next-Generation Sequencing, Ohio, USA

Marjorie Farrington,[1] Jamie Elenz, Matthew Ginsberg, Charles Y. Chiu, Steve Miller, Scott F. Pangonis

Author affiliations: Children's Hospital Medical Center of Akron, Akron, Ohio, USA (M. Farrington, M. Ginsberg, S.F Pangonis); Columbiana County Health District, Lisbon, Ohio, USA (J. Elenz); University of California, San Francisco, California, USA (C.Y. Chiu, S. Miller)

DOI: https://doi.org/10.3201/eid2904.221005

We describe a 4-year-old male patient in Ohio, USA, who had encephalitis caused by Powassan virus lineage 2. Virus was detected by using metagenomic next-generation sequencing and confirmed with IgM and plaque reduction neutralization assays. Clinicians should recognize changing epidemiology of tickborne viruses to enhance encephalitis diagnosis and management.

1Current affiliation: St. Louis Children's Hospital, St. Louis, Missouri, USA.

Powassan virus (POWV) is a tickborne flavivirus that causes encephalitis with severe neurologic sequelae (*1*). In the United States, POWV infections occur primarily in the Northeast and Great Lakes regions (2). We report a case of human POWV infection in Ohio.

A 4-year-old boy was brought to the emergency department because of fever, vomiting, and convulsive status epilepticus. He had no neurologic history or developmental delays. Mosquito and tick exposure history was substantial, although no engorged ticks were recently removed. The patient had not traveled outside of Ohio.

Results of a computed tomography scan of the head were unremarkable. We initiated intravenous vancomycin, ceftriaxone, and acyclovir. Magnetic resonance imaging showed left temporal pulvinar and thalamic T2-weighted fluid attenuated inversion recovery hyperintensity and restricted diffusion; an electroencephalogram showed lateralized periodic discharges. Cerebrospinal fluid (CSF) was collected by lumbar puncture, revealing a leukocyte count of 44 cells/μL (reference range <10 cells/μL) of which 85% were lymphocytes; glucose and protein levels were normal. The patient's BIOFIRE FILMARRAY Meningitis/Encephalitis PCR panel (bioMérieux, https://www.biomerieux-diagnostics.com) was negative (Table). He was admitted to the pediatric intensive care unit, and seizures were controlled with anticonvulsants. Tests for infectious and noninfectious causes of meningitis and encephalitis were negative (Table). Antimicrobial drugs were discontinued after negative bacterial cultures were observed. Acyclovir was discontinued after PCR of CSF for herpes simplex virus was negative.

On hospitalization day 5, severe neurologic decline developed, and brain magnetic resonance imaging was repeated. New areas of T2 hyperintensity and restricted diffusion and thalamic microhemorrhages in a rhombencephalitis pattern were identified. Lumbar puncture was repeated, revealing considerable lymphocytic pleocytosis and elevated protein (156 mg/dL). Leading diagnoses were autoimmune encephalitis and acute necrotizing encephalopathy of childhood (ANEC). The patient exhibited severe encephalopathy, nystagmus, right hemiparesis, and diffuse hypertonia. He was treated with high dose methylprednisolone, plasmapheresis, and intravenous immunoglobulins.

Genetic testing for familial ANEC type 1 was negative. We sent CSF obtained on hospital day 5 to the University of California San Francisco for metagenomic

Table. Test results for infectious and noninfectious causes of meningitis and encephalitis in study of Powassan virus infection detected by metagenomic next-generation sequencing, Ohio, USA*

Tests	Results
Infectious causes	
CSF meningitis encephalitis PCR panel†	No organisms detected
CSF bacterial culture	Negative
Lyme disease serology	Negative
Serum arbovirus IgG and IgM panel, reference range <1:10‡	<1:10
EBV viral capsid antigen IgM and IgG, antibody index <0.2‡	Negative
EBV nuclear antigen IgG, antibody index <0.2‡	Negative
Bartonella henselae and *B. quintana* antibodies	
IgG, <1:128	Negative
IgM, <1:20	Negative
Noninfectious causes	
Serum antinuclear antibody	Negative
Serum myelin oligodendrocyte glycoprotein	Negative

*CSF, cerebrospinal fluid; EBV, Epstein-Barr virus.
†BIOFIRE FILMARRAY Meningitis/Encephalitis PCR panel (bioMérieux, https://www.biomerieux-diagnostics.com). Panel included *Streptococcus pneumoniae, S. agalactiae, Haemophilus influenzae, Neisseria meningitidis, Listeria monocytogenes, Escherichia coli*, *Cryptococcus neoformans/gattii*, varicella-zoster virus, cytomegalovirus, herpes simplex virus types 1 and 2, *Enterovirus*, human herpesvirus 6, and *Parechovirus*.
‡Acute and convalescent serum samples were sent to Mayo Clinic Laboratories (https://www.mayocliniclabs.com) for arbovirus and EBV analysis. Arbovirus panel included La Crosse encephalitis virus, eastern equine encephalitis virus, western equine encephalitis virus, West Nile encephalitis virus, and St. Louis encephalitis virus.

next-generation sequencing (mNGS), which detected a single 140-nt POWV sequence (Appendix, https://wwwnc.cdc.gov/EID/article/29/4/22-1005-App1.pdf). We performed phylogenetic analysis of the sequence and assigned the patient's virus to lineage 2 (Figure, panel A); the sequence mapped to the nonstructural *NS3* gene (Figure, panel B). We performed BLAST (*3*) sequence alignments in GenBank, which yielded matches to POWV genomes (Figure, panel C). CSF samples obtained before the patient received intravenous Igs were sent for confirmatory testing to the CDC Arbovirus Diagnostic Laboratory, Division of Vector-Borne Diseases, National Center for Emerging and Zoonotic Infectious Diseases (https://www.cdc.gov/ncezid/dvbd/specimensub), which showed IgM against POWV (capture ELISA), negative POWV-specific PCR, and a positive plaque reduction neutralization test at 1:8 dilution (reference range <1:2), confirming the final diagnosis was ANEC caused by POWV. The patient continued having severe neurologic sequalae requiring a tracheostomy, gastrostomy tube, and inpatient rehabilitation. At follow-up 1 year after admission, he had been decannulated, was able to orally ingest liquids and solids, and ambulated independently, but he had substantial language and cognitive deficits.

Diagnostic yield for patients with encephalitis from any cause is 37% (*4*); mNGS enables detection of nearly all pathogens in a single assay and can improvwe diagnostic yield for patients with CNS infections (*5*). We identified 1 nucleotide sequence aligning to POWV, which is below the preestablished reporting threshold for a positive result of ≥3 reads spanning ≥3 regions of the viral genome (*5*). Thus, our finding was potentially a false positive, especially because POWV is not endemic to Ohio. However, POWV has never been a contaminant in clinical mNGS analyses of >4,000 CSF samples at the University of California San Francisco laboratory, and our result was confirmed as a true positive by a plaque reduction neutralization test**.** Of note, a case of POWV encephalitis identified by mNGS from 10 genomic sequencing reads has been reported (*6*). Furthermore, POWV-specific PCR of our patient's CSF was negative, consistent with a low viral titer near the limit of detection by molecular assays. Patients with POWV encephalitis are often PCR negative because viremia precedes CNS disease development (*7*).

The number of POWV cases reported has increased over the past few decades (*2*), likely because of tick range expansion. *Ixodes scapularis* is the only tick species in northeastern Ohio that can transmit POWV (*8*). Tick range expansion might be caused by increasing temperatures from climate change (*9*), migration of animal hosts, and changes in land use or host populations (*10*). Ticks carrying POWV lineage 2 were not identified on the family's property. However, healthcare and public health workers should be aware of changing epidemiology and potential emerging tickborne infections in nonendemic regions.

In conclusion, we identified a POWV infection in Ohio by using mNGS. Tests for autoimmune etiologies, familial ANEC (type 1), and other viral agents were negative, excluding alternative diagnoses. Our case highlights the ability of mNGS to identify rare or unexpected pathogens that cause encephalitis. Providers should recognize

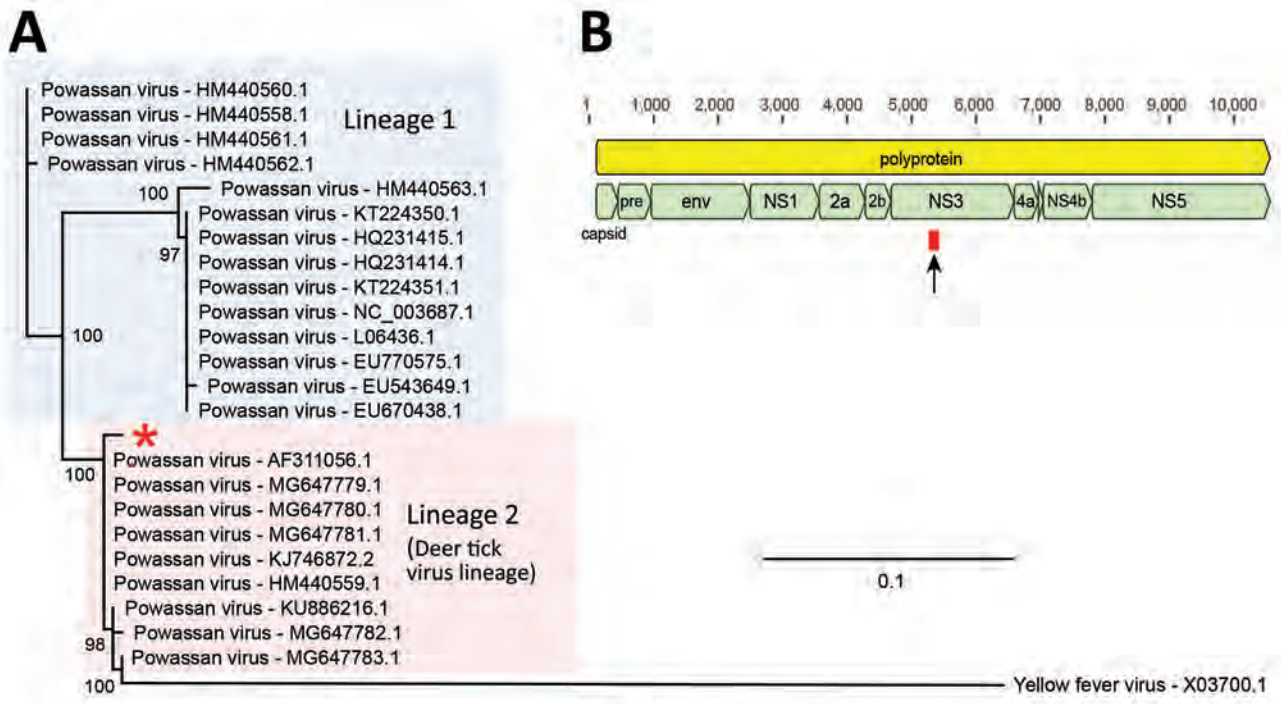

C

Description	Query coverage	E-value	% Identity	Accession no.
Powassan virus isolate RTS92 polyprotein gene, complete cds	100%	1E-61	98.6%	MG647781.1
Powassan virus isolate RTS82 polyprotein gene, complete cds	100%	1E-61	98.6%	MG647780.1
Powassan virus isolate RTS81 polyprotein gene, complete cds	100%	1E-61	98.6%	MG647779.1
Powassan virus isolate LI-1 polyprotein gene, complete cds	100%	1E-61	98.6%	KJ746872.2
Powassan virus isolate 17103-1037, complete genome	100%	1E-61	98.6%	OL704372.1
Powassan virus isolate 18103-167-010, complete genome	100%	1E-61	98.6%	OL704348.1
Powassan virus isolate 19103-41-001, complete genome	100%	1E-61	98.6%	OL704334.1
Powassan virus isolate 19103-37-004, complete genome	100%	1E-61	98.6%	OL704333.1
Powassan virus isolate 19103-37-002, complete genome	100%	1E-61	98.6%	OL704332.1
Powassan virus isolate 19103-14-001, complete genome	100%	1E-61	98.6%	OL704329.1

Figure. Identification and phylogenetic analysis of Powassan virus found in cerebrospinal fluid of 4-year-old boy detected by metagenomic next-generation sequencing, Ohio, USA. A) Phylogenetic analysis of the 140-bp region in the Powassan virus genome corresponding to the single sequence read detected by metagenomic next-generation sequencing. Single read from the patient in this study was aligned with sequences from 23 representative Powassan virus genomes from lineage 1 (blue shaded box) and lineage 2 (deer tick virus lineage, pink shaded box) and 1 yellow fever virus sequence as an outgroup by using MAFFT v7.388 (Appendix reference *11*, https://wwwnc.cdc.gov/EID/article/29/4/22-1005-App1.pdf). Phylogenetic tree was constructed by using the maximum-likelihood method and PhyML 3.0 software (Appendix reference *12*); support values for the main branches are shown. Powassan virus from our patient (red asterisk) belongs to lineage 2. GenBank accession numbers are shown for each sequence. Scale bar indicates nucleotide substitutions per site. B) Powassan virus genome showing major capsid and nonstructural genes. Single sequence read from the patient mapped to the *NS3* gene (arrow and red box). C) List of top 10 GenBank reference sequences matching the patient's 140-nt read after using MegaBLAST (https://blast.ncbi.nlm.nih.gov) alignment as default setting, each showing 98.6% sequence identity. If Powassan virus sequences were excluded from the reference database, no other matches in GenBank were found. Cds, coding sequence; env, envelope protein; NS, nonstructural; pre, M protein precursor peptide.

changing epidemiology of tickborne viruses, such as POWV, to enhance encephalitis diagnosis and management. When cases are identified, local public health departments should complete comprehensive entomological and epidemiologic studies to determine virus prevalence.

About the Author

Dr. Farrington recently completed her pediatrics residency at the Children's Hospital Medical Center of Akron in 2022. She is currently working as a pediatric hospitalist at the St. Louis Children's Hospital–Washington University.

References

1. Kemenesi G, Bányai K. Tick-borne flaviviruses, with a focus on Powassan virus. Clin Microbiol Rev. 2018;32:e00106-17. https://doi.org/10.1128/CMR.00106-17
2. Centers for Disease Control and Prevention. Powassan virus [cited 2022 May 3]. https://www.cdc.gov/powassan/statistics.html
3. Altschul SF, Gish W, Miller W, Myers EW, Lipman DJ. Basic local alignment search tool. J Mol Biol. 1990;215:403–10. https://doi.org/10.1016/S0022-2836(05)80360-2
4. Glaser CA, Honarmand S, Anderson LJ, Schnurr DP, Forghani B, Cossen CK, et al. Beyond viruses: clinical profiles and etiologies associated with encephalitis. Clin Infect Dis. 2006;43:1565–77. https://doi.org/10.1086/509330
5. Miller S, Naccache SN, Samayoa E, Messacar K, Arevalo S, Federman S, et al. Laboratory validation of a clinical metagenomic sequencing assay for pathogen detection in cerebrospinal fluid. Genome Res. 2019;29:831–42. https://doi.org/10.1101/gr.238170.118
6. Piantadosi A, Kanjilal S, Ganesh V, Khanna A, Hyle EP, Rosand J, et al. Rapid detection of Powassan virus in a patient with encephalitis by metagenomic sequencing. Clin Infect Dis. 2018;66:789–92. https://doi.org/10.1093/cid/cix792
7. Hermance ME, Thangamani S. Powassan virus: an emerging arbovirus of public health concern in North America. Vector Borne Zoonotic Dis. 2017;17:453–62. https://doi.org/10.1089/vbz.2017.2110
8. Eisen RJ, Eisen L, Beard CB. County-scale distribution of *Ixodes scapularis* and *Ixodes pacificus* (Acari: Ixodidae) in the continental United States. J Med Entomol. 2016;53:349–86. https://doi.org/10.1093/jme/tjv237
9. Bouchard C, Dibernardo A, Koffi J, Wood H, Leighton PA, Lindsay LR. N increased risk of tick-borne diseases with climate and environmental changes. Can Commun Dis Rep. 2019;45:83–9 https://doi.org/10.14745/ccdr.v45i04a02
10. Diuk-Wasser MA, VanAcker MC, Fernandez MP. Impact of land use changes and habitat fragmentation on the eco-epidemiology of tick-borne diseases. J Med Entomol. 2021;58:1546–64. https://doi.org/10.1093/jme/tjaa209

Address for correspondence: Scott F Pangonis, Children's Medical Center of Akron, 1 Perkins Sq, Akron, OH 44321, USA; email: spangonis@akronchildrens.org

Rickettsia conorii Subspecies *israelensis* in Captive Baboons

Giovanni Sgroi, Roberta Iatta, Grazia Carelli, Annamaria Uva, Maria Alfonsa Cavalera, Piero Laricchiuta, Domenico Otranto

Author affiliations: Experimental Zooprophylactic Institute of Southern Italy, Portici, Italy (G. Sgroi); University of Bari Aldo Moro, Bari, Italy (G. Sgroi, R. Iatta, G. Carelli, A. Uva, M.A. Cavalera, D. Otranto); Zoosafari Park Fasano, Brindisi, Italy (P. Laricchiuta); Bu-Ali Sina University, Hamedan, Iran (D. Otranto)

DOI: https://doi.org/10.3201/eid2904.221176

Hamadryas baboons (*Papio hamadryas*) may transmit zoonotic vector-borne pathogens to visitors and workers frequenting zoological parks. We molecularly screened 33 baboons for vector-borne pathogens. Three (9.1%) of 33 animals tested positive for *Rickettsia conorii* subspecies *israelensis*. Clinicians should be aware of potential health risks from spatial overlapping between baboons and humans.

Papio hamadryas baboons (order Primates, family Cercopithecidae) are frequently hosted in zoological gardens worldwide. The natural susceptibility of baboons to many zoonotic agents (*1*) may present a potential risk for transmission of emerging infectious diseases to humans. Nevertheless, few data are available on vector-borne pathogens of human concern that are hosted by baboons (e.g., *Rickettsia africae*, *Babesia microti*–like parasites, and *Anaplasma phagocytophilum*) (*1*). Data are likewise scarce on the role of *P. hamadryas* baboons in circulating arthropod vectors in zoological gardens and the resulting risk for transmitting vector-borne pathogens to persons frequenting such areas. We aimed to determine the occurrence of zoonotic vector-borne pathogens in a zoopark in the Apulia region of southern Italy and assess baboons' potential roles as reservoirs of emerging pathogens. Our study was approved by the University of Bari Aldo Moro ethics committee (Prot. Uniba 176/19).

During February–December 2020, we anesthetized baboons in the zoopark and housed them in cages for blood sampling. For each baboon, we recorded age, sex, weight, and body condition score (1–5); we obtained peripheral blood samples by cephalic vein puncture. To determine complete blood count and for molecular analysis, we collected 2 mL blood

samples in Vacutainer K3-EDTA tubes. For biochemical analysis, we collected an additional 5 mL blood in Vacutainer clot activator serum tubes and centrifuged (15 min at 1,500 × *g* at room temperature), then delivered it to the University of Bari Department of Veterinary Medicine (Bari, Italy). We extracted DNA using QIAGEN QIAamp DNA Blood and Tissue kits (https://www.qiagen.com) and molecularly tested for vector-borne pathogens (Table) (*2*–*4*). We purified and sequenced amplicons in both directions using a Big Dye Terminator v3.1 Cycle Sequencing Kit in an Applied Biosystems 3130 Genetic Analyzer (ThermoFisher, https://www.thermofisher.com), then edited and analyzed them using Geneious version 9.0 (https://www.geneious.com). We then compared resulting sequences with those in GenBank. We performed complete blood counts using CELL-DYN 3700 Hematology Analyzer (Abbott, https://www.abbott.com), biochemical profile using a KPM Analytics SAT 450 random access analyzer (https://www.kpmanalytics.com), and protein electrophoresis analyses using Sebia Hydrasys 2 Scan Focusing (https://www.sebia.com). We calculated 95% CIs for proportions and χ^2 and odds ratios (OR) to assess differences in prevalence and infection risk stratified by age and sex. We used *t*-tests to compare mean laboratory values between baboons positive and negative for vector-borne pathogens. We considered p values <0.05 statistically significant.

We included 33 baboons: 21 male, 12 female; 13 juvenile, 16 adult, and 4 elderly. Blood samples from 3/33 (9.1%, 95% CI 3.1%–23.4%; 1 adult male, 1 adult female, 1 juvenile male) were positive for *R. conorii* subsp. *israelensis* by the *glt*A gene; all samples were negative by *omp*A and *omp*B genes. The only sequence type we identified showed 99%–100% nucleotide identity with *R. conorii* subsp. *israelensis* from GenBank; we deposited our sequence in GenBank (accession no. OQ360110). All baboons tested negative for other vector-borne pathogens.

Although we found adult and male baboons at higher risk for infection (OR 2.6), we found no significant difference by age or sex (p = 0.439). No baboon showed ectoparasitic infestation or clinical signs of vector-borne diseases, and all displayed good physical status (mean complete blood count 3, average bodyweight 17.5 kg). Hematologic and serum chemistry values were within normal ranges (Appendix Tables 1, 2, https://wwwnc.cdc.gov/EID/article/29/4/22-1176-App1.pdf) for both *R. conorii*–negative and –positive baboons (p >0.05).

Our study revealed a nonnegligible prevalence (9.1%, 3/33) of *R. conorii* subsp. *israelensis* in *P. hamadryas* baboons, representing a pathogen–host association previously demonstrated only among asymptomatic dogs and cats from Portugal (*5*) and in severe cases among symptomatic humans from Italy (*6*). This survey confirms circulation of rickettsiae among baboons, also reported in 1 study of *R. africae* in *P. cynocephalus* yellow baboons from Zambia (*1*).

Despite routine treatment of baboons (orally administering 0.4 mg/kg ivermectin every 15 days by ground bait), presence of ticks in the zoopark was supported by a previous finding of tickborne pathogens (*A. phagocytophilum*, *Coxiella burnetii*, and *Rickettsia* spp.) in a lion (*7*). Given the baboon grooming behavior of removing ectoparasites from their bodies, lack of *Rhipicephalus sanguineus* sensu lato ticks, a vector of rickettsiae (*8*), was not surprising (*9*). However, association between zoopark-dwelling baboons and *Rhipicephalus* spp. ticks, including *R. sanguineus* s.l., is well known (*9*). Because this tick species is prevalent in the study area in all developmental stages, exposure very likely occurs (*10*).

Taken together, the high density of *P. hamadryas* baboons, their close proximity to the zoopark, and the anthropophilic behavior of *R. sanguineus* s.l. ticks (*10*) highlight the threat to park visitors and workers from *R. conorii* subsp. *israelensis* infection. Absence of clinical signs in positive baboons and lack of

Table. PCR protocols used in study of vector-borne pathogens among baboons, Italy, 2020

Pathogen	Target gene	Primer	Sequence, 5′ →3′	Fragment length, bp	Reference
Babesia/*Theileria* spp.	18S rRNA	RLB-F	GAGGTAGTGACAAGAAATAACAATA	460–520	(*2*)
		RLB-R	TCTTCGATCCCCTAACTTTC		
Ehrlichia/*Anaplasma* spp.	16S rRNA	EHR-16SD	GGTACCYACAGAAGAAGTCC	345	(*2*)
		HER-16SR	TAGCACTCATCGTTTACAGC		
Rickettsia spp.	*glt*A	CS-78F	GCAAGTATCGGTGAGGATGTAAT	401	(*2*)
		CS-323R	GCTTCCTTAAAATTCAATAAATCAGGAT		
Spotted fever group Rickettsiae	*omp*A	Rr190.70F	ATGGCGAATATTTCTCCAAAA	632	(*2*)
		Rr190.701R	GTTCCGTTAATGGCAGCATCT		
	*omp*B	120–2788	AAACAATAATCAAGGTACTGT	600	(*3*)
		120–3599	TACTTCCGGTTACAGCAAAGT		
Leishmania infantum	kDNA minicircle	Leish-1	AACTTTTCTGGTCCTCCG GGTAG	120	(*4*)
		Leish-2	ACCCCCAGTTTCCCGCC		

differences in hematological and biochemical parameters between negative and positive animals indicate the asymptomatic features of infection and make clarifying the baboons' role as a potential reservoir more urgent. Measures to control tick circulation should be established to reduce risk for transmission of *R. conorii* subsp. *israelensis* to zoopark visitors and workers.

Acknowledgments

The authors are grateful to the staff of Fasano Zoopark involved in field activities.

R.I. and D.O. were partially supported by EU funding within the NextGeneration EU-MUR PNRR Extended Partnership initiative on Emerging Infectious Diseases (Project no. PE00000007, INF-ACT).

About the Author

Mr. Sgroi has a PhD in animal health and zoonosis from the University of Bari Aldo Moro. His main research activities focus on biology, epidemiology, and control of vector-borne pathogens of zoonotic concern.

References

1. Nakayima J, Hayashida K, Nakao R, Ishii A, Ogawa H, Nakamura I, et al. Detection and characterization of zoonotic pathogens of free-ranging non-human primates from Zambia. Parasit Vectors. 2014;7:490. https://doi.org/10.1186/s13071-014-0490-x
2. Sgroi G, Iatta R, Lia RP, D'Alessio N, Manoj RRS, Veneziano V, et al. Spotted fever group rickettsiae in *Dermacentor marginatus* from wild boars in Italy. Transbound Emerg Dis. 2021;68:2111–20. https://doi.org/10.1111/tbed.13859
3. Roux V, Raoult D. Phylogenetic analysis of members of the genus *Rickettsia* using the gene encoding the outer-membrane protein rOmpB (ompB). Int J Syst Evol Microbiol. 2000;50:1449–55. https://doi.org/10.1099/00207713-50-4-1449
4. Sgroi G, Iatta R, Veneziano V, Bezerra-Santos MA, Lesiczka P, Hrazdilová K, et al. Molecular survey on tick-borne pathogens and *Leishmania infantum* in red foxes (*Vulpes vulpes*) from southern Italy. Ticks Tick Borne Dis. 2021;12:101669. https://doi.org/10.1016/j.ttbdis.2021.101669
5. Maia C, Cristóvão JM, Pereira A, Parreira R, Campino L. Detection of *Rickettsia conorii israelensis* DNA in the blood of a cat and a dog from southern Portugal. Top Companion Anim Med. 2019;36:12–5. https://doi.org/10.1053/j.tcam.2019.06.001
6. Guccione C, Colomba C, Rubino R, Bonura C, Anastasia A, Agrenzano S, et al. A severe case of Israeli spotted fever with pleural effusion in Italy. Infection. 2022;50:269–72. https://doi.org/10.1007/s15010-021-01693-8
7. Torina A, Naranjo V, Pennisi MG, Patania T, Vitale F, Laricchiuta P, et al. Serologic and molecular characterization of tickborne pathogens in lions (*Panthera leo*) from the Fasano Safari Park, Italy. J Zoo Wildl Med. 2007;38:591–3. https://doi.org/10.1638/2007-0043R1.1
8. Rovery C, Brouqui P, Raoult D. Questions on Mediterranean spotted fever a century after its discovery. Emerg Infect Dis. 2008;14:1360–7. https://doi.org/10.3201/eid1409.071133
9. Akinyi MY, Tung J, Jeneby M, Patel NB, Altmann J, Alberts SC. Role of grooming in reducing tick load in wild baboons (*Papio cynocephalus*). Anim Behav. 2013;85:559–68. https://doi.org/10.1016/j.anbehav.2012.12.012
10. Otranto D, Dantas-Torres F, Giannelli A, Latrofa MS, Cascio A, Cazzin S, et al. Ticks infesting humans in Italy and associated pathogens. Parasit Vectors. 2014;7:328. https://doi.org/10.1186/1756-3305-7-328

Address for correspondence: Domenico Otranto, University of Bari Aldo Moro, strada provinciale per Casamassima km3, 70010 Valenzano, Italy; email: domenico.otranto@uniba.it

Prevention of *Thelazia callipaeda* Reinfection among Humans

Marija Trenkić, Suzana Tasić-Otašević, Marcos Antonio Bezerra-Santos, Marko Stalević, Aleksandar Petrović, Domenico Otranto

Author affiliations: Ophthalmology Clinic University Clinical Center, Niš, Serbia (M. Trenkić); University of Niš, Niš (M. Trenkić, S. Tasić-Otašević, M. Stalević, A. Petrović); Public Health Institute, Niš (S. Tasić-Otašević); University of Bari Aldo Moro, Bari, Italy (M.A. Bezerra-Santos, D. Otranto); Bu-Ali Sina University, Hamedan, Iran (D. Otranto)

DOI: https://doi.org/10.3201/eid2904.221610

Thelazia callipaeda is a zoonotic vector-borne nematode that infects and causes eye disease among a wide range of domestic and wild mammals, including humans. We describe an unusual case of reinfection by this nematode in Serbia and call for a focus on preventive measures in endemic areas.

The genus *Thelazia* (order Spirurida, family Thelaziidae) comprises several species of nematode that cause ocular infections in different host mammals, including humans (*1*). Over the past 20 years, the *T. callipaeda* eyeworm has gained interest among

Table. Morphometry of 11 specimens (6 female, 5 male) of *Thelazia callipaeda* from a naturally infected human in Serbia

Measurement	Male	Female
Body length, mm	9.58–12.7 (mean 11.05; SD ±1.16)	13.5–16.5 (mean 14.96; SD ±1.23)
Body width, μm	310–390 (mean 343; SD ±31.14)	360–490 (mean 434; SD ±56.83)
Buccal capsule length, μm	26.4	29.6
Buccal capsule width, μm	25.1	26.4
Nerve-ring from anterior extremity, μm	267.5	373.7
Esophagus length, μm	665.4	719.9
Vulva from anterior extremity, μm	Not applicable	663.2
Left spicule length, μm	1,648	NA
Right spicule length, μm	157.2	NA
Tail length, μm	62.8	72.4

the scientific community because several human cases have been reported in countries in Asia and Europe, making this parasite an agent of public health concern (*1*). Adult and larval forms of *T. callipaeda* eyeworms infect the ocular apparatus of a wide range of both domestic (e.g., dogs, cats) and wild (e.g., red foxes, wolves, jackals, bears, lagomorphs) animal species, including humans (*1*–*3*). In Europe, 2 species of drosophilid fruit flies were confirmed to act as vectors of *T. callipaeda* eyeworms: *Phortica variegata*, tested under laboratory and natural conditions (*4*), and *P. oldenbergi* only experimentally (*5*). Thelaziosis should be expected among humans in areas where *T. callipaeda* infection is endemic in animal reservoirs. Absence of preventive measures could be a factor influencing human reinfections in endemic areas. We describe a case of *T. callipaeda* reinfection in a human patient and call for focus on prevention in areas where the parasite and its vectors thrive.

A man, 41 years of age, living in a small village in the southern part of Serbia contacted an ophthalmologist at the University Clinical Center in Nis, Serbia, because of ocular discomfort. The patient reported a history of clinical thelaziosis caused by *T. callipaeda* infection 5 years earlier. Ophthalmic manifestations were conjunctivitis with increased lacrimation, itching, and sensation of a foreign body in his left eye. During ophthalmologic examination, we removed 11 eyeworms (6 female, 5 male) from the eye and subsequently identified them morphologically as *T. callipaeda* according to an identification key (*6*). The nematodes had a filariform body type with a transversally striated cuticle and a buccal capsule of hexagonal shape. Among female worms, the vulva was located anterior to the esophagus-intestinal junction; male worms had a curved caudal end with 2 asymmetric spicules and precloacal and postcloacal papillae (Table; Figure).

To confirm morphologic identification, we extracted genomic DNA from individual worms using a QIAGEN DNeasy Blood & Tissue Kit (https://www.qiagen.com), and performed PCR analysis using the primers NTF (5′-TGATTGGTGGTTTTGGTAA-3′) and NTR (5′-ATAAGTACGAGTATCAATATC-3′), which amplify a 689-bp portion of the mitochondrial

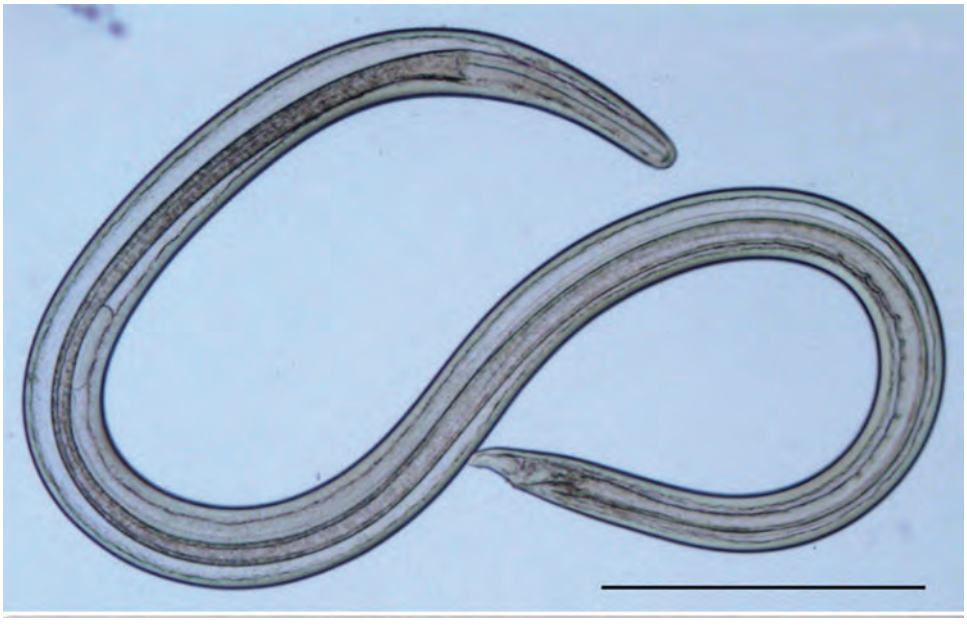

Figure. *Thelazia callipaeda* eyeworms collected from the left eye of a man in Serbia. A) Female worm; B) anterior end of adult female; C) posterior end of adult female; D) posterior end of adult male.

cytochrome *c* oxidase subunit 1 (*cox*1) gene. We purified amplified DNA products and sequenced them in both directions using ThermoFisher Big Dye Terminator version 3.1 chemistry in an Applied Biosystems 3130 genetic analyzer with an ABI-PRISM 377 automated sequencer (https://www.thermofisher.com). We analyzed sequences using MEGA version 7 software (https://www.megasoftware.net) and compared them with those available in GenBank using BLAST (https://blast.ncbi.nlm.nih.gov/Blast.cgi). Nucleotide sequences had 100% identity with *T. callipaeda* (GenBank accession no. AM042549.1). In addition, phylogenetic analysis performed by using the maximum-likelihood method based on the Tamura-Nei model showed the representative sequence from our study clustered with other sequences of *T. callipaeda* belonging to haplotype 1 (Appendix, https://wwwnc.cdc.gov/EID/article/29/4/22-1610-App1.pdf), the only haplotype thus far described in Europe. We deposited the nucleotide sequence in GenBank (accession no. OP696980).

We treated the patient with topical antimicrobials and corticosteroids (rinsing with 3% boric acid 5×/d and topical tobramicin/deksametazon 5×/d). At clinical follow-up 7 and 14 days later, we found no signs or symptoms of eye infection.

T. callipaeda eyeworm prevalence in humans and animals has increased throughout Europe in recent decades (*1*). To date, human thelaziosis has been described in 12 patients from Europe, including a case-patient in Serbia (*7*) reinfected by *T. callipaeda* eyeworms 5 years after an initial case, as in the case we describe here. A related study called for implementing preventive measures, such as vector control and treatment of domestic reservoirs (e.g., dogs), to avoid zoonotic human infection (*8*). In addition, wild carnivore reservoirs, such as red foxes and wolves, should be considered as sources of infection for humans who frequent the same forest areas (*9*). The patient in our study reported that he spent long periods picking mushrooms in the forest, and he exhibited clinical manifestations of thelaziosis during the summer (July), when outdoor activities are most common and the *P. variegata* fruit fly, a *T. callipaeda* eyeworm vector, is most abundant.

Reinfection in this patient highlights that *T. callipaeda* eyeworms can cause recurrent infection in human hosts, which suggests the potential usefulness of implementing prevention and control strategies in the Balkan Peninsula, where this parasite and its vector and animal reservoirs are spreading (*10*). Moreover, it indicates that inspecting for *T. callipaeda* eyeworms should be part of routine periodic examinations in endemic areas, even among asymptomatic persons.

Acknowledgments

The authors thank Riccardo Paolo Lia for his support on morphologic identification and Giada Annoscia for her support on molecular analysis.

About the Author

Dr. Trenkić is an assistant professor in the medical faculty, Department of Ophthalmology, University of Niš. She performs ophthalmologic research.

References

1. Otranto D, Mendoza-Roldan JA, Dantas-Torres F. *Thelazia callipaeda*. Trends Parasitol. 2021;37:263–4. https://doi.org/10.1016/j.pt.2020.04.013
2. Papadopoulos E, Komnenou A, Karamanlidis AA, Bezerra-Santos MA, Otranto D. Zoonotic *Thelazia callipaeda* eyeworm in brown bears (*Ursus arctos*): a new host record in Europe. Transbound Emerg Dis. 2022;69:235–9. https://doi.org/10.1111/tbed.14414
3. Bezerra-Santos MA, Moroni B, Mendoza-Roldan JA, Perrucci S, Cavicchio P, Cordon R, et al. Wild carnivores and *Thelazia callipaeda* zoonotic eyeworms: a focus on wolves. Int J Parasitol Parasites Wildl. 2022;17:239–43. https://doi.org/10.1016/j.ijppaw.2022.03.005
4. Otranto D, Brianti E, Cantacessi C, Lia RP, Máca J. The zoophilic fruitfly *Phortica variegata*: morphology, ecology and biological niche. Med Vet Entomol. 2006;20:358–64. https://doi.org/10.1111/j.1365-2915.2006.00643.x
5. Bezerra-Santos MA, Bernardini I, Lia RP, Mendoza-Roldan JA, Beugnet F, Pombi M, et al. *Phortica oldenbergi* (Diptera: Drosophilidae): a new potential vector of the zoonotic *Thelazia callipaeda* eyeworm. Acta Trop. 2022;233:106565. https://doi.org/10.1016/j.actatropica.2022.106565
6. Otranto D, Lia RP, Traversa D, Giannetto S. *Thelazia callipaeda* (Spirurida, Thelaziidae) of carnivores and humans: morphological study by light and scanning electron microscopy. Parassitologia. 2003;45:125–33.
7. Tasić-Otašević S, Gabrielli S, Trenkić-Božinović M, Petrović A, Gajić B, Colella V, et al. Eyeworm infections in dogs and in a human patient in Serbia: a One Health approach is needed. Comp Immunol Microbiol Infect Dis. 2016;45:20–2. https://doi.org/10.1016/j.cimid.2016.01.003
8. Bezerra-Santos MA, Mendoza-Roldan JA, Sgroi G, Lia RP, Venegoni G, Solari Basano F, et al. Efficacy of a formulation of sarolaner/moxidectin/pyrantel (Simparica Trio®) for the prevention of *Thelazia callipaeda* canine eyeworm infection. Parasit Vectors. 2022;15:370. https://doi.org/10.1186/s13071-022-05501-6
9. Čabanová V, Miterpáková M, Oravec M, Hurníková Z, Jerg S, Nemčíková G, et al. Nematode *Thelazia callipaeda* is spreading across Europe. The first survey of red foxes from Slovakia. Acta Parasitol. 2018;63:160–6. https://doi.org/10.1515/ap-2018-0018
10. Hodžić A, Latrofa MS, Annoscia G, Alić A, Beck R, Lia RP, et al. The spread of zoonotic *Thelazia callipaeda* in the Balkan area. Parasit Vectors. 2014;7:352. https://doi.org/10.1186/1756-3305-7-352

Address for correspondence: Domenico Otranto, University of Bari Aldo Moro, Strada provinciale per Casamassima km3, 70010 Valenzano, Italy; email: domenico.otranto@uniba.it

Mpox in Young Woman with No Epidemiologic Risk Factors, Massachusetts, USA

Mark J. Siedner, John Trinidad, Cesar G. Berto, Catherine M. Brown, Lawrence C. Madoff, Ellen H. Lee, Maryam Iqbal, Olivia Samson, John Albin, Sarah E. Turbett, Olivia Davies, Daniela Kroshinsky, David Hooper, Elizabeth Hohmann, Kevin Ard, Erica S. Shenoy

Author affiliations: Masschussetts General Hospital and Harvard Medical School, Boston, Massachusetts, USA (M.J. Siedner, J. Trinidad, C.G. Berto, J. Albin, S.E. Turbett, O. Davies, D. Kroshinsky, D. Hooper, E. Hohmann, K. Ard, E. Shenoy); Massachusetts Department of Public Health, Boston (C.M. Brown, L.C. Madoff), New York City Department of Health and Mental Hygiene, Long Island City, New York, USA (E.H. Lee, M. Iqbal, O. Samson)

DOI: https://doi.org/10.3201/eid2904.221921

We describe a case of mpox characterized by a circularly distributed facial rash but no identified risk factors. Fomite transmission of monkeypox virus from contaminated linen at a massage spa was suspected. Clinicians should consider mpox in patients with consistent clinical syndromes, even in the absence of epidemiologic risk factors.

During the 2022 global outbreak, ≈95% of mpox cases, caused by monkeypox virus infection, were attributed to close physical contact, and >98% were reported among men (*1*,*2*). We describe a case of a young woman who had no sexual or close physical contact with a nyone suspected of having mpox during the 2 months before she had a confirmed monkeypox virus infection.

A woman in the United States, in her late 20s who had hypothyroidism after curative thyroidectomy for medullary thyroid cancer 7 years before, sought care in July 2022 at a hospital emergency department 8 days after a facial rash developed. The rash was initially pruritic, and erythematous macules were located on the bilateral infraorbital and malar areas, lower cutaneous lip, and chin, which progressed to vesicles followed by pustules. She was prescribed doxycycline and valacyclovir. She experienced subjective fevers, myalgias, bilateral cervical lymphadenopathy, and scattered papules that developed bilaterally on her legs and arms, prompting her to return to the emergency department (Figure). She also had tender cervical lymphadenopathy and scattered erythematous macules on her limbs. Laboratory tests were negative for HIV, syphilis, gonorrhea, *Chlamydia* sp., herpes simplex virus, and varicella zoster virus. PCR for orthopoxvirus was positive and had a cycle threshold of 21.2. The patient was started on tecovirimat. Facial swelling and lymphadenopathy resolved within the next 48 hours, and no new lesions were noted thereafter (Figure).

The patient resided alone in New York and had traveled to California and Massachusetts for business and leisure during the 3 weeks before her rash developed. She described herself as a woman who has sex with men only. She reported no sexual activity or any close intimate contact with anyone during the 3 months before her rash developed and had no contact with anyone suspected of having mpox disease. She had a history of acne but had not used new skin products in the preceding weeks. She reported receiving 2 massages in the preceding weeks, 1 at a hotel spa 13 days before rash developed and another at a private day spa 4 days before rash developed. On both occasions,

Figure. Progression of facial rash during mpox in a young woman in the absence of epidemiologic risk factors, Massachusetts, USA. Days since rash onset or beginning tecovirimat therapy are indicated. The rash began with pruritic erythematous macules on the bilateral infraorbital and malar areas, lower cutaneous lip, and chin and, by day 4, had progressed to vesicles followed by pustules on day 6 (top row, left cheek; bottom row, right cheek). On day 8 after rash onset, the patient had multiple confluent ulcers; macerated rolled borders were observed on the left cheek, and a single, large, deep-seated ulcer that had raised borders and a central hemorrhagic crust was observed on the right cheek. Satellite blisters and papules were present at early stages of ulcer development. The patient was started on tecovirimat on day 11 after rash onset, after which her lesions continued to evolve and had eventual loss of central eschar but persistent exudative, macerated borders by day 12 of tecovirimat therapy (day 22 after rash onset). Smaller lesions were treated with mupirocin ointment and dressed with loose gauze coverings. Toward the end of her 14-day treatment course (day 22), the escharotic ulcers developed granulated tissue. Ulcers had abundant granulated tissue and no central eschar and had begun to reepithelialize ≈2 weeks after completion of therapy (day 37).

she laid face down on a massage table on top of a circular pillow covered by thin linen or a towel. She had a dentist appointment 6 days before and a dermatologist appointment 3 days before rash developed. On both occasions, the clinicians donned clean disposable gloves before contact.

Because of the physical location of the patient's lesions and lack of sexual encounters during the incubation period, an ensuing public health investigation focused on the spa visits. No other mpox cases among staff or clientele of either spa were identified during a review of cases by the New York City Department of Health and Mental Hygiene or Massachusets Department of Health or by matching staff and client lists with electronically reported mpox results (New York City Department of Health and Mental Hygiene only). Both spas reported that they changed coverings on the massage tables between clients, used freshly laundered linens and towels, and used a disinfectant that has efficacy against enveloped viruses. Environmental sampling at the spas was not performed because of the amount of time that had passed between the spa visits and mpox diagnosis. No mpox cases after visits to the dentist were identified.

We report an mpox case in a woman who had no epidemiologic risk factors for this disease. Although the transmission source in this case could not be confirmed, the rash locations and pattern suggest inoculation through fomites from contaminated facial towels or other linens, as has been reported for monkeypox virus and other poxviruses (*6*,*7*). In a cluster of 20 cases linked to a tattoo establishment, where monkeypox virus was recovered on piercing equipment (*5*), persons visiting the establishment were infected >2 weeks after the suspected index case, suggesting prolonged virus viability on surfaces. Surface contamination by viable monkeypox virus has also been reported in hospital rooms and community settings (*8*). Viable virus is more recoverable from porous materials, such as linens and towels, than nonporous materials, such as metals and plastics (*9*). The Centers for Disease Control and Prevention provides comprehensive sterilization recommendations for both linens and hard nonporous materials (*10*). The rash in this case was characterized by large deep wounds that did not begin to granulate until ≈5 weeks after rash onset, indicating the need to elucidate viral shedding duration from these types of ulcers.

In conclusion, as in recent reports of persons who had mpox without intimate contact (*3*–*5*), this case highlights the importance of maintaining clinical suspicion of mpox for persons who do not meet known epidemiologic criteria. This case also supports the possibility of fomite-based transmission of monkeypox virus.

Acknowledgments

We thank the Massachusetts Department of Health, New York City Department of Health and Mental Hygiene, Massachusetts General Hospital Microbiology Laboratory staff, and nursing staff for their contributions to the care of this patient and John Brooks for his expertise and advice on clinical care and public health considerations for this case.

The patient in this case report provided written informed consent to have her clinical case and photographs shared for the purpose of medical care and academic publication.

About the Author

Dr. Siedner is a clinical epidemiologist and infectious disease clinician at Massachusetts General Hospital and Harvard Medical School. His research focuses on improving healthcare delivery for people with HIV and other infectious diseases in resource-limited settings.

References

1. Philpott D, Hughes CM, Alroy KA, Kerins JL, Pavlick J, Asbel L, et al; CDC Multinational Monkeypox Response Team. Epidemiologic and clinical characteristics of monkeypox cases—United States, May 17–July 22, 2022. MMWR Morb Mortal Wkly Rep. 2022;71:1018–22. https://doi.org/10.15585/mmwr.mm7132e3
2. Centers for Disease Control and Prevention. Monkeypox cases by age and gender, race/ethnicity, and symptoms. 2022 [cited 2022 Sep 1]. https://www.cdc.gov/poxvirus/monkeypox/response/2022/demographics.html
3. Karan A, Styczynski AR, Huang C, Sahoo MK, Srinivasan K, Pinsky BA, et al. Human monkeypox without viral prodrome or sexual exposure, California, USA, 2022. Emerg Infect Dis. 2022;28:2121–3. https://doi.org/10.3201/eid2810.221191
4. Xia J, Huang CL, Chu P, Kroshinsky D. Eczema monkeypoxicum: report of monkeypox transmission in a patient with atopic dermatitis. JAAD Case Rep. 2022;29:95–9. https://doi.org/10.1016/j.jdcr.2022.08.034
5. Del Río García V, Palacios JG, Morcillo AM, Duran-Pla E, Rodríguez BS, Lorusso N. Monkeypox outbreak in a piercing and tattoo establishment in Spain. Lancet Infect Dis. 2022;22:1526–8. https://doi.org/10.1016/S1473-3099(22)00652-1
6. Vaughan A, Aarons E, Astbury J, Brooks T, Chand M, Flegg P, et al. Human–to–human transmission of monkeypox virus, United Kingdom, October 2018. Emerg Infect Dis. 2020;26:782–5. https://doi.org/10.3201/eid2604.191164
7. Lederman E, Miramontes R, Openshaw J, Olson VA, Karem KL, Marcinak J, et al. Eczema vaccinatum resulting from the transmission of vaccinia virus from a smallpox vaccinee: an investigation of potential fomites in the home environment. Vaccine. 2009;27:375–7. https://doi.org/10.1016/j.vaccine.2008.11.019
8. Pfeiffer JA, Collingwood A, Rider LE, Minhaj FS, Matheny AM, Kling C, et al. High-contact object and surface contamination in a household of persons with monkeypox virus infection—Utah, June 2022. MMWR Morb Mortal Wkly Rep. 2022;71:1092–4. https://doi.org/10.15585/mmwr.mm7134e1

9. Morgan CN, Whitehill F, Doty JB, Schulte J, Matheny A, Stringer J, et al. Environmental persistence of monkeypox virus on surfaces in household of person with travel-associated infection, Dallas, Texas, USA, 2021. Emerg Infect Dis. 2022;28:1982–9. https://doi.org/10.3201/eid2810.221047
10. Centers for Disease Control and Prevention. Cleaning and disinfecting your home, workplace, and other community settings [cited 2023 Jan 3]. https://www.cdc.gov/poxvirus/monkeypox/if-sick/cleaning-disinfecting.html

Address for correspondence: Mark J. Siedner, Medical Practice Evaluation Center, Massachusetts General Hospital, Boston, MA 02114, USA; email: msiedner@mgh.harvard.edu

Retrospective Screening of Clinical Samples for Monkeypox Virus DNA, California, USA, 2022

Caitlin A. Contag, Jacky Lu, Zachary T. Renfro, Abraar Karan, Jorge L. Salinas, Michelle Khan, Daniel Solis, Malaya K. Sahoo, Fumiko Yamamoto, Benjamin A. Pinsky

Authors affiliation: Stanford University School of Medicine, Stanford, California, USA

DOI: https://doi.org/10.3201/eid2904.221576

We retrospectively screened oropharyngeal and rectal swab samples originally collected in California, USA, for *Chlamydia trachomatis* and *Neisseria gonorrhoeae* testing for the presence of monkeypox virus DNA. Among 206 patients screened, 17 (8%) had samples with detectable viral DNA. Monkeypox virus testing from mucosal sites should be considered for at-risk patients.

Monkeypox virus (MPXV) is an enveloped, double-stranded DNA virus in the family *Poxvirus*, genus *Orthopoxvirus*, and is related to variola, the causative agent of smallpox. In 2022, MPXV transmission caused a large global mpox disease outbreak that disproportionately affected male persons who identified as gay, bisexual, and men who have sex with men (MSM) and persons who identified as transgender (*1*). The clinical manifestations of MPXV infection also evolved from prior outbreaks; more patients in 2022 had anogenital rash and proctitis, rather than disseminated cutaneous lesions (*1*). During prior mpox outbreaks, asymptomatic or subclinical MPXV infection was thought to be rare, but evidence from the 2022 outbreak suggests that infected patients can have minimal symptoms (*2*,*3*). To identify persons with subclinical MPXV infection, we retrospectively analyzed oropharyngeal and rectal swab samples submitted for *Chlamydia trachomatis* and *Neisseria gonorrhoeae* (CT/NG) testing at a tertiary academic medical center.

Swab samples were collected at Stanford Health Care by using the Aptima Multitest Swab Specimen Collection Kit for the Aptima Combo 2 Assay (Hologic, https://www.hologic.com). We included all samples collected during July 7–September 6, 2022 that had sufficient residual volume. The study was approved by the Stanford University institutional review board (protocol no. 66786).

We extracted total nucleic acids from 300 μL of Aptima Specimen Transport Medium (Hologic) by using the Chemagic instrument (PerkinElmer, https://www.perkinelmer.com), according to the manufacturer's recommendations. To test for MPXV DNA, we used 2 laboratory-developed quantitative PCR (qPCR) assays modified from Centers for Disease Control and Prevention published assays (*4*,*5*). The first qPCR targeted viral DNA polymerase sequence conserved throughout nonvariola orthopoxviruses, including MPXV. The second qPCR targeted the viral tumor necrosis factor (TNF) receptor sequence specific for MPXV clade II (formerly West African clade). We performed qPCR reactions as previously described (*6*), except we used the CFX96 thermal cycler (Bio-Rad, https://www.bio-rad.com). We tested all specimens with both qPCR assays and interpreted samples with concordant MPXV as mpox-positive and samples without detected MPXV as mpox-negative. When there was discordance between viral DNA polymerase and the viral TNF receptor targets, we repeated both reactions from the eluate and interpreted the sample as positive only if MPXV was reproducibly detected. We excluded 3 concordant negative samples in which the internal control (β-globin gene) failed in one or both reactions.

A total of 347 swab samples submitted for CT/NG testing from 206 patients met the inclusion criteria: 195 (56%) oropharyngeal and 152 (44%) rectal swab specimens. Patients ranged in age from 7 days–77 years (mean 35 years). Most (176/206; 85%) patients were male; 1 patient was assigned male at birth but identified as genderqueer. Twelve patients

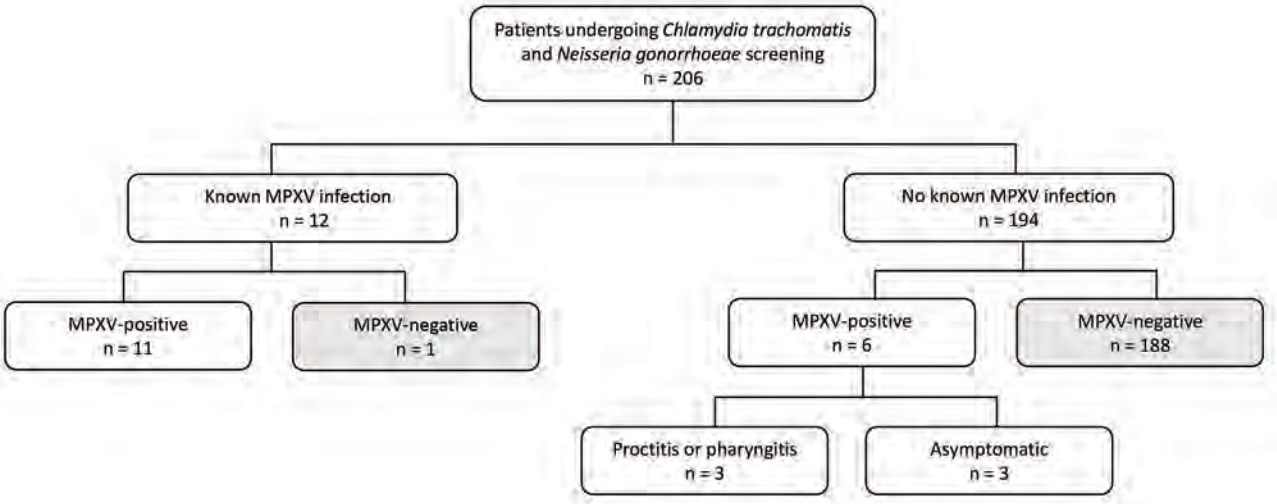

Figure. Flowchart of retrospective quantitative PCR screening for MPXV in oropharyngeal and rectal swab samples submitted for *Chlamydia trachomatis* and *Neisseria gonorrhoeae* testing, California, USA, 2022. Patients with known MPXV infection (n = 12) were diagnosed by quantitative PCR of cutaneous lesions. Patients without known mpox did not have MPXV-positive tests or cutaneous lesions at the time of specimen collection for *C. trachomatis* and *N. gonorrhoeae* testing. MPXV, monkeypox virus.

in this cohort had known MPXV infection diagnosed via lesion qPCR.

Overall, we detected viral DNA in 24/347 (7%) samples, including 11/195 oropharyngeal and 13/152 rectal swab specimens, representing 17/206 (8%) patients (Figure). Among 17 patients who tested MPXV-positive, 6 (35%) had received an mpox vaccine. No patients received a vaccine >14 (range 4–12) days before their positive test. Of 12 persons with known mpox who underwent CT/NG testing, 11 (91.7%) had detectable MPXV DNA from swab samples, comprising 16 positive samples. Six patients without lesions or diagnosed mpox had detectable MPXV DNA from CT/NG swabs, comprising 8 positive samples (Table). Of those patients, 3 (50%) were asymptomatic and 3 (50%) symptomatic; 2 had proctitis and 1 had pharyngitis. Like patients with known mpox, all 6 patients with newly diagnosed mpox were MSM. In addition, 50% (3/6) of patients with new mpox diagnoses were co-infected with another sexually transmitted infection compared with 42% (5/12) of patients with known MPXV infections, 33% (2/6) were HIV-positive (vs. 42%; 5/12), and 33% (2/6) were on HIV preexposure prophylaxis (vs. 58%, 7/12).

Our findings demonstrate that patients without cutaneous lesions can be MPXV-positive, which is

Table. Patients with newly diagnosed mpox via retrospective qPCR of oropharyngeal or rectal swab samples, California, USA, 2022*

Age, y/sex	Sample type, Ct values†		Clinical manifestations and history	History of HIV or PrEP	Concurrent STI
	Oropharyngeal	Rectal			
55/M	ND/ND	28.6/29.4	Asymptomatic; sought CT/NG testing after notification of STI exposure 2 wks before at a sex club in Europe; specific sexual practice unknown	PrEP	Syphilis
30/M	ND/ND	35.5/35.1	Asymptomatic; undergoing routine CT/NG screening; exposure unknown	PrEP	None diagnosed
17/M	37.5/38.2	22.0/24.0	Asymptomatic; undergoing STI screening after recent vaginal sex and receptive and insertive oral and anal sex with male and female partners; timing of exposure unknown; MPXV-positive cutaneous lesions subsequently developed	HIV-1–negative; not on PrEP	Chlamydia, gonorrhea, syphilis
31/M	29.6/29.8	Not collected	Sore throat, tonsillar exudates, and lymphadenopathy 4 d after sexual encounter with a male partner 11 d before testing	Unknown	None diagnosed
29/M	ND/ND	17.2/17.9	Hematochezia; reported receptive anal sex 4 wk before testing	HIV-1–positive	None diagnosed
46/M	34.2/34.7	19.1/19.2	Hematochezia and rectal pain; reported recent receptive anal sex	HIV-1–positive	Chlamydia, gonorrhea

*Ct, cycle threshold; CT/NG, *Chlamydia trachomatis* and *Neisseria gonorrhoeae*; MPXV, monkeypox virus; ND, not detected; PrEP, preexposure prophylaxis; qPCR, quantitative PCR; STI, sexually transmitted infection.
†Results indicate Ct for viral DNA polymerase/viral tumor necrosis factor receptor.

consistent with observations reported in similarly designed studies in Europe (*7*,*8*). Occult infection with oropharyngeal and rectal viral shedding might have contributed to the scale of the 2022 mpox outbreak, which spread through sexual networks. All but 1 patient with known MPXV infection in our cohort had detectable viral DNA in oropharyngeal or rectal swab samples, suggesting that the new infections we detected are likely true positives. Furthermore, all newly identified mpox patients in our study had >1 sample for which both qPCR targets were detected.

Current MPXV tests cleared for emergency use are indicated only for use on lesion samples (*9*). Further studies are needed to characterize viral shedding dynamics, particularly related to symptom onset and duration of infectivity. As data demonstrating mucosal viral shedding in mpox emerge, expanding testing to allow broader sample collection and expedite diagnostic validation of samples from various anatomic sites will be crucial.

In conclusion, during the ongoing mpox outbreak, clinicians should consider oropharyngeal and rectal MPXV qPCR testing for at-risk patients with pharyngitis or proctitis. In addition, asymptomatic screening in high-risk populations might be warranted if community prevalence is high or rising.

About the Author

Dr. Contag is an infectious diseases fellow at Stanford University, Stanford, California, USA. Her primary research interests are emerging and reemerging infectious diseases and the management of critical illness in low-resource settings.

References

1. Thornhill JP, Barkati S, Walmsley S, Rockstroh J, Antinori A, Harrison LB, et al.; SHARE-net Clinical Group. Monkeypox virus infection in humans across 16 countries—April–June 2022. N Engl J Med. 2022;387:679–91. https://doi.org/10.1056/NEJMoa2207323
2. Abbasi J. Reports of asymptomatic monkeypox suggest that, at the very least, some infections go unnoticed. JAMA. 2022;328:1023–5. https://doi.org/10.1001/jama.2022.15426
3. Jezek Z, Marennikova SS, Mutumbo M, Nakano JH, Paluku KM, Szczeniowski M. Human monkeypox: a study of 2,510 contacts of 214 patients. J Infect Dis. 1986;154:551–5. https://doi.org/10.1093/infdis/154.4.551
4. Li Y, Olson VA, Laue T, Laker MT, Damon IK. Detection of monkeypox virus with real-time PCR assays. J Clin Virol. 2006;36:194–203. https://doi.org/10.1016/j.jcv.2006.03.012
5. Li Y, Zhao H, Wilkins K, Hughes C, Damon IK. Real-time PCR assays for the specific detection of monkeypox virus West African and Congo Basin strain DNA. J Virol Methods. 2010;169:223–7. https://doi.org/10.1016/j.jviromet.2010.07.012
6. Karan A, Styczynski AR, Huang C, Sahoo MK, Srinivasan K, Pinsky BA, et al. Human Monkeypox without viral prodrome or sexual exposure, California, USA, 2022. Emerg Infect Dis. 2022;28:2121–3. https://doi.org/10.3201/eid2810.221191
7. Ferré VM, Bachelard A, Zaidi M, Armand-Lefevre L, Descamps D, Charpentier C, et al. Detection of monkeypox virus in anorectal swabs from asymptomatic men who have sex with men in a sexually transmitted infection screening program in Paris, France. Ann Intern Med. 2022;175:1491–2. https://doi.org/10.7326/M22-2183
8. De Baetselier I, Van Dijck C, Kenyon C, Coppens J, Michiels J, de Block T, et al.; ITM Monkeypox study group. Retrospective detection of asymptomatic monkeypox virus infections among male sexual health clinic attendees in Belgium. Nat Med. 2022;28:2288–92. https://doi.org/10.1038/s41591-022-02004-w
9. US Food and Drug Administration. FDA monkeypox response: FDA's role in mpox preparedness and response, and information about mpox (formerly referred to as monkeypox) [cited 2023 Jan 7]. https://www.fda.gov/emergency-preparedness-and-response/mcm-issues/fda-monkeypox-response

Address for correspondence: Caitlin Contag, Stanford University, Department of Medicine, Division of Infectious Diseases and Geographic Medicine, 300 Pasteur Dr, L-134, Stanford, CA 94305, USA; email: cacontag@stanford.edu

Human Metapneumovirus Infections during COVID-19 Pandemic, Spain

Maria L. García-García, Elena Pérez-Arenas, Pedro Pérez-Hernandez, Iker Falces-Romero, Sara Ruiz, Francisco Pozo, Inmaculada Casas, Cristina Calvo

Author affiliations: Severo Ochoa University Hospital Leganés, CIBERINFEC ISCIII, Madrid, Spain (M.L. García-García, S. Ruiz); La Paz University Hospital, Madrid, Spain (E. Pérez-Arenas, P. Pérez-Hernandez); La Paz University Hospital, IdiPaz Foundation, CIBERINFEC ISCIII, Madrid (I. Falces-Romero, C. Calvo); Severo Ochoa University Hospital Leganés, Madrid (S. Ruiz); National Center Microbiology, CIBEREST, Madrid (F. Pozo, I. Casas)

DOI: https://doi.org/10.3201/eid2904.230046

We describe an unusual outbreak of respiratory infections caused by human metapneumovirus in children during the sixth wave of COVID-19 in Spain, associated with the Omicron variant. Patients in this outbreak were older than usual and showed more hypoxia and pneumonia, longer length of stay, and greater need for intensive care.

Respiratory infections caused by human metapneumovirus (hMPV) are typically epidemic during February–April. hMPV infections cause bronchiolitis and recurrent wheezing episodes and are responsible for hospitalizations mainly in children <2 years of age (*1*). The COVID-19 pandemic has changed the epidemiology of respiratory viral infections, modifying the classic seasonality of respiratory syncytial virus (RSV), influenza, and other viruses (*2*–*4*). In Spain, an outbreak of pediatric hMPV infections was identified in November–December 2021, coinciding with the sixth wave of COVID-19 in the country. This study aimed to describe this outbreak and to compare it with previous hMPV outbreaks, before the COVID-19 pandemic.

We retrospectively collected data from respiratory hMPV infections requiring hospitalization in children <18 years of age during October–December 2021 in La Paz University Hospital (Madrid, Spain) and analyzed clinical characteristics. We performed multiple PCR respiratory panels as standard clinical practice in children in whom infection by RSV, influenza, and SARS-CoV-2 had previously been ruled out by rapid test or PCR.

We obtained data from a systematic prospective study conducted over 15 years in all hospitalized children with respiratory infections in Severo Ochoa University Hospital (Madrid) using multiple PCR panels performed at the National Center for Microbiology. This study was approved by the hospital ethics committee. We compared clinical data from hospitalized patients in 2021 with our historical series of hMPV infections collected during 2005–2020, before the COVID-19 pandemic.

We analyzed data from 48 patients with hMPV infection during October–December 2021; of those, 56.3% were male and 54% were >2 years of age, and median age was 22.7 (interquartile range [IQR] 7.1–34.9) months. Twenty-nine (60%) of the cases were detected in December and 1 in October. In 19 cases (39%), we detected co-infection with other viruses, mainly adenoviruses and human coronaviruses. A total of 34 (70.8%) case-patients had fever >38°C; in addition, 41 (85.4%) had hypoxia, and 34 (70.8%) had an infiltrate visible in their chest radiograph; radiography was not performed in 11 cases. The most frequent diagnoses were pneumonia (35%), bronchiolitis (27%), and episodes of wheezing (16%). Antimicrobial drugs were prescribed in 26 cases (54%). Seven patients (14%) required pediatric intensive care unit (PICU) admission; 2 needed mechanical ventilation. The median duration of fever was 3 (IQR 2.7–5)

Table. Comparison of the clinical characteristics of children with human metapneumovirus respiratory infections requiring hospitalization during the COVID-19 pandemic (2021) and previous seasons, Spain

Clinical data	2021, n = 48	2005–2020, n = 498	OR (95% CI)	p value
Age, mo	22 ±15.9	13 ±17.2	NA	0.002
Sex, no. (%)				
M	27 (56.2)	289 (58.0)	NA	0.875
F	21 (43.8)	209 (42.0)	NA	
Temperature >37.9ºC	34 (70.8)	342 (68.7)	NA	0.734
Highest temperature	**39.0 ±0.5**	**38.7 ±0.6**		**0.008**
Hypoxia, oxygen saturation <93%, no. (%)	**41 (85.4)**	**331 (66.5)**	**3.9 (1.4–9.0)**	**0.002**
Chest infiltrate, no. (%)	**34 (70.8)**	**184 (36.9)**	**10.2 (3.1–32.9)**	**<0.001**
Antimicrobial treatment, no. (%)	**26 (54.2)**	**123 (24.7)**	**3.2 (1.8–5.6)**	**<0.001**
Viral co-infection, no. (%)	19 (39.6)	208 (41.8)	NA	0.632
Time of illness, Nov–Dec, no. (%)	**47 (97.9)**	**9 (1.8)**	NA	**<0.001**
Diagnosis, no. (%)				<0.001
Wheezing episode	8 (16.7)	288 (57.8)	NA	NA
Bronchiolitis	13 (27.1)	144 (28.9)	NA	NA
Pneumonia	17 (35.4)	44 (8.8)	NA	NA
Blood tests				
Leucocytes, cells/mm^3	11,140 ±5,530	12,112 ±4,620	NA	0.589
C-reactive protein	40 ±44	37 ±54	NA	0.698
Outcome				
Duration of stay, d	**6.8 ±4.8**	**4.6 ±7.1**	NA	**0.004**
Duration of fever, d	**3.9 ±2.4**	**2.7 ±1.8**	NA	**0.001**
Duration of hypoxia, d	**6.2 ±4.2**	**2.9 ±2.1**	NA	**<0.001**
PICU admission, no. (%)	**7 (14.6)**	**13 (2.6)**	**5.1 (1.8–8.0)**	**0.004**

*Values are mean (SD) except as indicated. Bold text indicates statistically significant differences. NA, not applicable; OR, odds ratio; PICU, pediatric intensive care unit.

days, hypoxia 5 (IQR 3.5–7.5) days, and admission, 6 (IQR 4–8) days.

We compared the data from those recent patients with data from 498 cases of hMPV infection at the hospital during 2005–2020. During that period, 9 (1.8%) cases were detected in November–December and 453 (90.9%) during February–May. Patients in the 2021 season were older than those from the previous 15-year period and had significantly higher rates of hypoxia, pneumonia, antimicrobial drug treatment; they also had longer durations of fever, hypoxia, hospital admission, and PICU admission (Table 1).

In November–December 2021, during the sixth wave of COVID-19 in Spain, the country experienced an extemporaneous hMPV outbreak at the time when RSV epidemic was usually observed. This outbreak of hMPV infections affected children older than were usually affected in previous years; we also observed a more severe clinical course and higher rates of hypoxia, pneumonia, and admission to PICU than historically.

We considered that there may have been competition between respiratory viruses that could justify the delay in the RSV outbreak (*5*), which occurred in summer (June–July) 2021 in Spain; such competition was not the case for the hMPV outbreak, which coincided with spread of the Omicron variant of SARS-CoV-2. One possible explanation is relaxation of social distancing measures or the extreme contagiousness of Omicron. The increased severity of illness could be partly explained by the absence of hMPV infections in the previous 2 years, resulting in a susceptible population of older children who had not had previous hMPV infections and therefore had no immunity. In previous seasons, children >1 year of age were immunized by previous infections or even through residual maternal protection; this protection did not exist in 2021, and older children were infected. In conclusion, this outbreak illustrates that clinicians should be aware of potential differences in the epidemiology of other viral respiratory infections during and after the COVID-19 pandemic.

This study was partially funded by FIS (Fondo de Investigaciones Sanitarias—Spanish Health Research Fund), grant nos. PI06/0532, PI09/0246, PI12/0129, PI-18CIII/00009, PI21CIII/00019, and PI21/00377 .

About the Author

Dr. García-García is the head of the pediatrics department at Severo Ochoa Hospital, Leganés, Spain. She is an expert in respiratory viral infections and pediatric pneumology.

References

1. García-García ML, Calvo C, Rey C, Díaz B, Molinero MD, Pozo F, et al. Human metapnuemovirus infections in hospitalized children and comparison with other respiratory viruses. 2005–2014 prospective study. PLoS One. 2017;12:e0173504. https://doi.org/10.1371/journal.pone.0173504
2. Yeoh DK, Foley DA, Minney-Smith CA, Martin AC, Mace AO, Sikazwe CT, et al. Impact of coronavirus disease 2019 public health measures on detections of influenza and respiratory syncytial virus in children during the 2020 Australian winter. Clin Infect Dis. 2021;72:2199–202. https://doi.org/10.1093/cid/ciaa1475
3. Flores-Pérez P, Gerig N, Cabrera-López MI, de Unzueta-Roch JL, Del Rosal T, Calvo C; COVID-19 Study Group in Children. Acute bronchiolitis during the COVID-19 pandemic. Enferm Infecc Microbiol Clin (Engl Ed). 2022;40:572–5. https://doi.org/10.1016/j.eimc.2021.06.012
4. Torres-Fernandez D, Casellas A, Mellado MJ, Calvo C, Bassat Q. Acute bronchiolitis and respiratory syncytial virus seasonal transmission during the COVID-19 pandemic in Spain: a national perspective from the pediatric Spanish Society (AEP). J Clin Virol. 2021;145:105027. https://doi.org/10.1016/j.jcv.2021.105027
5 Dee K, Goldfarb DM, Haney J, Amat JAR, Herder V, Stewart M, et al. Human rhinovirus infection blocks severe acute respiratory syndrome coronavirus 2 replication within the respiratory epithelium: implications for COVID-19 epidemiology. J Infect Dis. 2021;224:31–8. https://doi.org/10.1093/infdis/jiab147

Address for correspondence: Cristina Calvo, Pediatrics and Infectious Diseases Dept, Hospital Universitario La Paz, P° Castellana, 261, 28046 Madrid, Spain; email: ccalvorey@gmail.com

Highly Pathogenic Avian Influenza A(H5N1) Virus in a Harbor Porpoise, Sweden

Elina Thorsson, Siamak Zohari, Anna Roos, Fereshteh Banihashem, Caroline Bröjer, Aleksija Neimanis

Author affiliations: National Veterinary Institute (SVA), Uppsala, Sweden (E. Thorsson, S. Zohari, F. Banihashem, C. Bröjer, A. Neimanis); Swedish Museum of Natural History, Stockholm, Sweden (A. Roos)

DOI: https://doi.org/10.3201/eid2904.221426

We found highly pathogenic avian influenza A(H5N1) virus clade 2.3.4.4b associated with meningoencephalitis in a stranded harbor porpoise (*Phocoena phocoena*). The virus was closely related to strains responsible for a concurrent avian influenza outbreak in wild birds. This case highlights the potential risk for virus spillover to mammalian hosts.

Europe and, more recently, the Americas are experiencing unprecedented mortality in wild and domestic birds because of the highly pathogenic avian influenza virus (HPAI) A(H5N1) virus clade 2.3.4.4b (*1*). Infections in tens of thousands of wild birds representing at least 112 species, including large numbers of seabirds, have been documented (*1*,*2*). Since December 2021, HPAI H5N1 has dominated infections in wild birds in Sweden, other countries in Europe, and the Americas, and it has spilled over into wild mammals, such as red foxes and mustelids (*1*). Increased mortality in harbor seals (*Phoca vitulina*) and gray seals (*Halichoerus grypus*) in eastern North America has been associated with HPAI H5N1 infection (*3*). Although influenza A virus (IAV) infections in seals have been repeatedly documented, reports in cetaceans are scarce (*4*). We are aware of only 2 cases where IAV in a cetacean might have been associated with disease (*4*,*5*). We report HPAI H5N1 infection in a harbor porpoise (*Phocoena phocoena*) in Sweden.

In late June 2022, an immature male harbor porpoise became stranded in shallow water off the west coast of Sweden (58.64817 N, 11.28973 E). It swam in circles, was unable to right itself, and drowned shortly after discovery. The carcass was stored frozen until necropsy examination at the National Veterinary Institute (Uppsala, Sweden). Macroscopic findings were minimal and included pulmonary edema consistent with drowning. Microscopically, we detected moderate lymphoplasmacytic meningoencephalitis with neuronal necrosis, gliosis, perivascular cuffing, and vasculitis in the brain (Figure 1, panel A). The lung contained few areas of mild, mononuclear septal thickening and increased numbers of alveolar macrophages.

Stranded porpoises in Sweden are screened routinely for cetacean morbilliviruses, which can be neurotropic in cetaceans, and IAV, which can be neurotropic in other species (*4*,*6*). We analyzed pooled lung, spleen, and brain samples for cetacean morbilliviruses by using real-time reverse transcription PCR (*6*) with the addition of an in-house designed hydrolysis probe (6FAM-TGG TTC CAA CAG GYA G-MGB) for detection. No morbilliviral RNA was found. We detected IAV genome from lung and bronchial swab specimens (*7*) and subtyped the virus as HPAI H5N1; viral genome sequences were determined directly from tissue samples. Phylogenetic analysis of the complete genome sequences (GISAID accession nos. EPI2150621–8) classified the virus as H5N1 clade 2.3.4.4b. The genome contained no genetic motif of mammalian adaptation besides those already described for H5 clade 2.3.4.4 (HA-H5 172A-Airborne transmission, M1 N30D, Y215A-Virulence// NS1 P42S, L103F and I106M-Virulence) (*8*). Detecting IAV

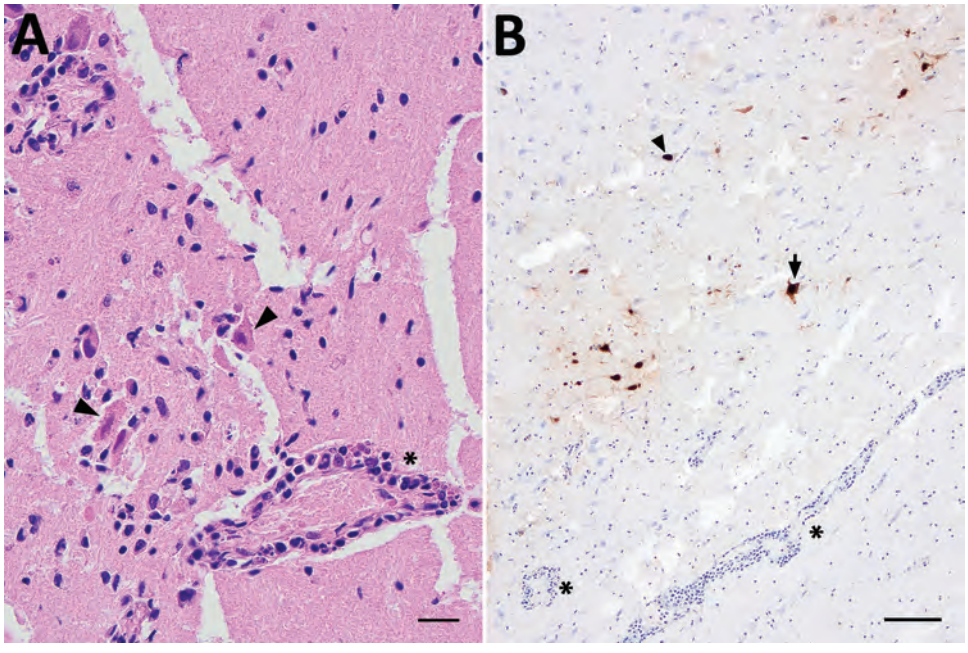

Figure 1. Microscopic analyses of tissue samples from a harbor porpoise (*Phocoena phocoena*) infected with highly pathogenic avian influenza virus H5N1 clade 2.3.4.4b, Sweden. A) Brain tissue showing neuronal necrosis (arrowheads) and perivascular lymphoplasmacytic cuffing of vessels and vasculitis (asterisk). Scale bar represents 20 μm. B) Immunohistochemical labeling of influenza A nucleoprotein in neuronal nuclei (arrowhead) and cytoplasm (arrow), as well as glial cells. Perivascular cuffing (asterisks) is seen in close association to influenza A immunolabeling. Scale bar represents 100 μm.

in respiratory tract swab specimens prompted us to analyze other organs. We detected the highest IAV loads in the brain (cycle threshold [Ct] value 20.57) and smaller loads in the lungs (Ct 30.72), kidney (Ct 31.37), liver (Ct 32.75), and spleen (Ct 33.43). We detected no virus in the intestine, muscle, or blubber.

We performed immunohistochemical analysis using a commercial influenza A nucleoprotein primary monoclonal antibody (EBS-I-238; Biologicals Limited, https://biologicals-ltd.com) as previously described (*9*) on all organs containing IAV genome to examine viral antigen distribution and the relationship to pathological lesions. We noted multifocal areas of moderate immunolabelling in the brain in nuclei and cytoplasm of neurons (Figure 1, panel B), glial cells, and epithelial cells of the choroid plexus. Scant intranuclear and intracytoplasmic viral antigen was in scattered cells in alveoli (macrophages or sloughed epithelium). We did not observe any viral antigen in other tissues examined.

IAV infection in a harbor porpoise represents expanding viral host range. Infections in cetaceans can result in animal death, as demonstrated by the abnormal behavior and subsequent drowning caused by the meningoencephalitis associated with infection. Virus was found predominantly in the brain, a finding consistent with H5N1 clade 2.3.4.4b infection in other mammals (*10*). Routine examination of the brain is warranted in cetacean disease surveillance, and IAV infection should be considered in animals demonstrating abnormal behavior or neuropathology. The virus detected in this porpoise was most closely related to viruses circulating in wild birds at the same time and location (Figure 2, https://wwwnc.cdc.gov/EID/article/29/4/22-1426-F2.htm), indicating likely spillover from wild birds. The route of transmission is unknown but includes contact with infected birds or indirect contact through contaminated water, suggesting that infection pressure in the ecosystem was high.

Although the genome of the detected HPAI H5N1 virus did not contain any known genetic marker of mammal adaptation, the clinical manifestations and presence of virus in diverse organs, including the brain, indicate the potential risk of HPAI viruses to mammalian hosts even without adaptation. This risk is a consideration for persons in close contact with infected animals. In addition, extensive circulation of the HPAI H5Nx virus clade 2.3.4.4b in wild and domestic bird populations and sporadic transmission to humans and other mammals enables the virus to evolve, increasing the risk of it becoming more transmissible or pathogenic for mammals. Understanding the epidemiology and host–pathogen environmental ecology of IAVs among wildlife, coupled with continuous surveillance, developing better tools for risk assessments, and updating public and animal health countermeasures and intervention strategies, are essential for reducing the threats of zoonotic influenza.

Acknowledgments

We thank Ulrika Larsson Pettersson for laboratory assistance with the histology and immunohistochemistry and SLU Aqua for practical help in the field. We gratefully acknowledge the authors from the laboratories responsible for obtaining influenza A virus specimens and the submitting laboratories where genetic sequence data were generated and shared via GISAID (https://www.gisaid.org), on which this research is based.

Health and disease surveillance of marine mammals in Sweden is funded by the Swedish Agency for Marine and Water Management as part of Sweden's environmental monitoring.

About the Author

Dr. Thorsson is a wildlife pathologist at the National Veterinary Institute and a resident of the European College of Veterinary Medicine, Wildlife Population Health. Her primary research interests are veterinary pathology, infectious diseases of wildlife, and wildlife population health.

References

1. European Food Safety Authority; European Centre for Disease Prevention and Control; European Union Reference Laboratory for Avian Influenza; Adlhoch C, Fusaro A, Gonzales JL, Kuiken T, Marangon S, Niqueux É, et al. Avian influenza overview March–June 2022. EFSA Journal. 2022;20:e07415.
2. Istituto Zooprofilattico Sperimentale delle Venezie. Highly pathogenic avian influenza (HPAI) in Europe: update. Wild birds: species affected [cited 2022 Sep 12]. https://izsvenezie.com/documents/reference-laboratories/avian-influenza/europe-updates/HPAI/2021-1/wild-birds.pdf
3. National Oceanic and Atmospheric Administration Fisheries. Recent increase in seal deaths in Maine linked to avian flu [cited 2022 Sep 12]. https://www.fisheries.noaa.gov/feature-story/recent-increase-seal-deaths-maine-linked-avian-flu
4. Runstadler JA, Puryear W. A brief introduction to influenza a virus in marine mammals. In: Spackman E, editor. Animal influenza virus. Methods in molecular biology, vol. 2123. New York: Humana; 2020. p. 429–450. https://doi.org/10.1007/978-1-0716-0346-8_33
5. University of Florida, College of Veterinary Medicine. A first: Avian influenza detected in American dolphin [cited 2022 Sep 12]. https://www.vetmed.ufl.edu/2022/09/07/a-first-avian-influenza-detected-in-american-dolphin

6. Yang W-C, Wu B-J, Sierra E, Fernandez A, Groch KR, Catão-Dias JL, et al. A simultaneous diagnosis and genotyping method for global surveillance of cetacean morbillivirus. Sci Rep. 2016;6:30625. https://doi.org/10.1038/srep30625
7. Grant M, Bröjer C, Zohari S, Nöremark M, Uhlhorn H, Jansson DS. Highly pathogenic avian influenza (HPAI H5Nx, clade 2.3.4.4.b) in poultry and wild birds in Sweden: synopsis of the 2020–2021 season. Vet Sci. 2022;9:344. https://doi.org/10.3390/vetsci9070344
8. Yamaji R, Saad MD, Davis CT, Swayne DE, Wang D, Wong FYK, et al. Pandemic potential of highly pathogenic avian influenza clade 2.3.4.4 A(H5) viruses. Rev Med Virol. 2020;30:e2099. https://doi.org/10.1002/rmv.2099
9. Bröjer C, Ågren EO, Uhlhorn H, Bernodt K, Mörner T, Jansson DS, et al. Pathology of natural highly pathogenic avian influenza H5N1 infection in wild tufted ducks (*Aythya fuligula*). J Vet Diagn Invest. 2009;21:579–87. https://doi.org/10.1177/104063870902100501
10. Rijks JM, Hesselink H, Lollinga P, Wesselman R, Prins P, Weesendorp E, et al. Highly pathogenic avian influenza A (H5N1) virus in wild red foxes, the Netherlands, 2021. Emerg Infect Dis. 2021;27:2960–2. https://doi.org/10.3201/eid2711.211281

Address for correspondence: Aleksija Neimanis, Department of Pathology and Wildlife Diseases, National Veterinary Institute (SVA), SE-751 89 Uppsala, Sweden; email: aleksija.neimanis@sva.se

SARS-CoV-2 Omicron Replacement of Delta as Predominant Variant, Puerto Rico

Gilberto A. Santiago, Hannah R. Volkman, Betzabel Flores, Glenda L. González, Keyla N. Charriez, Limari Cora Huertas, Steven M. Van Belleghem, Vanessa Rivera-Amill, Chelsea Major, Candimar Colon, Rafael Tosado, Laura E. Adams, Melissa Marzán, Lorena Hernández, Iris Cardona, Eduardo O'Neill, Gabriela Paz-Bailey, Riccardo Papa, Jorge L. Muñoz-Jordan

Author affiliations: Centers for Disease Control and Prevention, San Juan, Puerto Rico (G.A. Santiago, H.R. Volkman, B. Flores, G.L. González, K.N. Charriez, C. Major, C. Colon, R. Tosado, L.E. Adams, G. Paz-Bailey, J.L. Muñoz-Jordan); University of Puerto Rico Molecular Sciences and Research Center, San Juan (L.C. Huertas, S.M. Van Belleghem, R. Papa); Ponce Research Institute, Ponce Health Sciences University, Ponce, Puerto Rico (V. Rivera-Amill); Puerto Rico Department of Health, San Juan (M. Marzán, L. Hernández, I. Cardona); Centers for Disease Control and Prevention, Atlanta, Georgia, USA (E. O'Neill)

DOI: https://doi.org/10.3201/eid2904.221700

We reconstructed the SARS-CoV-2 epidemic caused by Omicron variant in Puerto Rico by sampling genomes collected during October 2021–May 2022. Our study revealed that Omicron BA.1 emerged and replaced Delta as the predominant variant in December 2021. Increased transmission rates and a dynamic landscape of Omicron sublineage infections followed.

Since the arrival of SARS-CoV-2 in Puerto Rico in March 2020, epidemic waves of COVID-19 have occurred on the island during the emergence of several variants of concern. Genomic surveillance conducted by partnered public health and academic groups reported an epidemic wave caused by the Alpha variant in April 2021, which coincided with the vaccination campaign for adults (*1*). Despite the detection of other variants of interest or concern, circulation of most of those variants was limited. According to the Puerto Rico Department of Health, the Delta variant has caused >49,000 confirmed cases since June 2021 (Appendix 1, https://wwwnc.cdc.gov/EID/article/29/4/22-1700-App1.pdf). The epidemic wave began to decline in August 2021, reaching its lowest rate since the beginning of the Delta wave in December 2021. This decline was possibly associated with the successful COVID-19 vaccination program, in which 83% of the eligible population of Puerto Rico had received the initial series of COVID-19 vaccines by October 31, 2021 (*2*,*3*).

The first confirmed case of the Omicron variant in Puerto Rico was reported on November 29, 2021, and within a week, Omicron had replaced Delta to become the dominant circulating variant. The relatively low circulation of Delta, combined with Omicron's high transmissibility and the waning of protective immunity before the vaccine booster campaign, might all have contributed to the rapid spread of this variant (*4*). The first Omicron peak was 9.1 times higher than any previous SARS-CoV-2 epidemic peak documented in Puerto Rico (Appendix Figure 1). By May 31, 2022, epidemic waves of the Omicron variant had caused ≈494,200 cases, peaking appreciably around January and May 2022.

We analyzed the Delta and Omicron sublineage turnover dynamics by using all the SARS-CoV-2

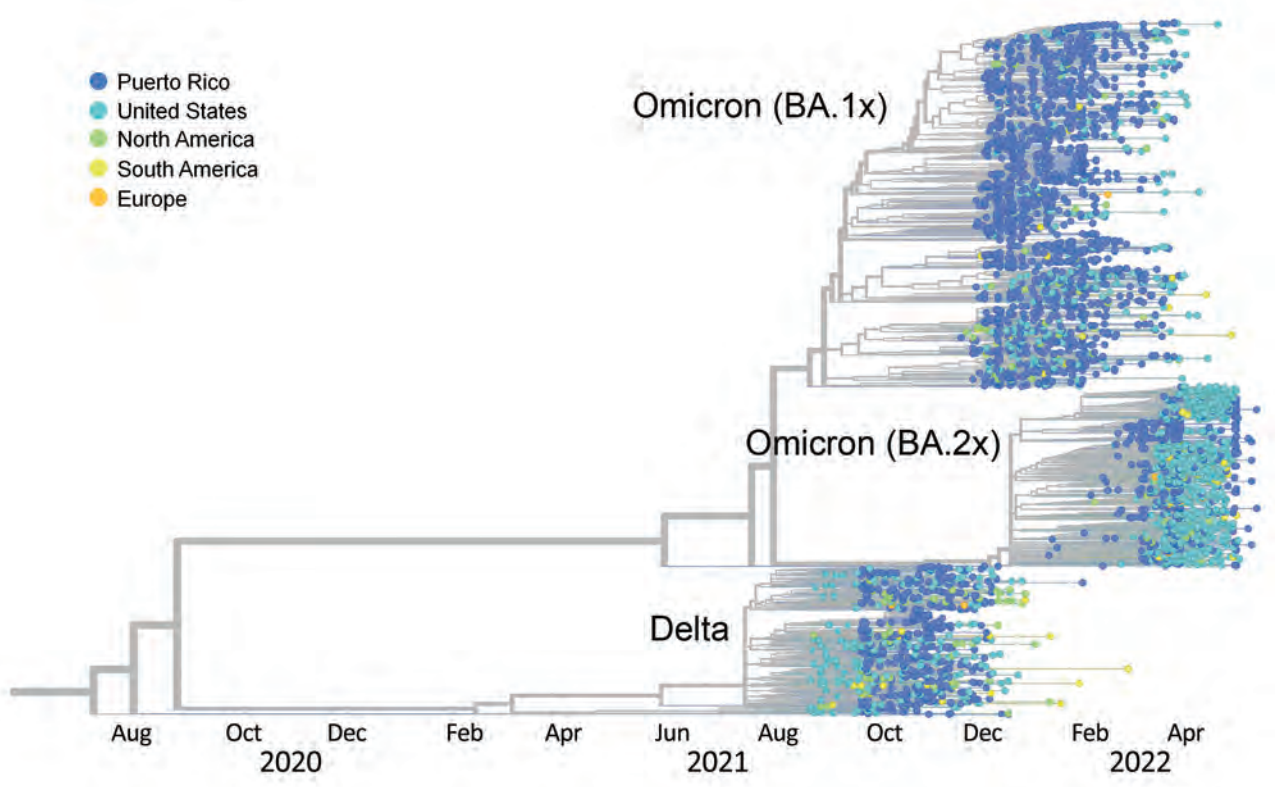

Figure. Decline of SARS-CoV-2 Delta variant and emergence of Omicron sublineages BA.1 and BA.2, illustrated by time-calibrated phylogenetic tree inferred with ncov augur/auspice workflow to represent the molecular evolution of the Delta variant in Puerto Rico since October 1, 2021, and subsequent expansion of the Omicron variant through May 30, 2022. Taxa labels are color-coded by geographic region of sampling to present the phylogenetic relatedness of viruses from Puerto Rico (dark blue) to viruses from the United States (light blue) and other regions of the world.

genomes from Puerto Rico sampled during October 2021–May 2022 available in GISAID (https://www.gisaid.org) as of June 8, 2022. By the end of December 2021, the Omicron sublineage BA.1 accounted for >60% of the sampled genomes, and the BA.1.1 sublineage dominated circulation until late March 2022 (Appendix Figure 2). Sublineage BA.2 began cocirculating with BA.1 sublineages in late January 2022 and remained at a low level until late March 2022, when it replaced BA.1.1 as the dominant sublineage. Subsequently, sublineage BA.2 caused another epidemic wave that peaked in mid-April 2022 (Appendix Figure 2). A period of sustained high transmission characterized the second Omicron wave; positive test rates for both antigen and molecular tests remained at >10% during April–August 2022.

To elucidate the emergence of the Omicron variant and subsequent replacement of Delta as the predominant variant, we used a phylogenetic approach to reconstruct the SARS-CoV-2 epidemic in Puerto Rico (Figure). We sequenced 2,377 SARS-CoV-2 complete genomes directly from reverse transcription PCR–positive diagnostic samples collected in Puerto Rico during the study period (*1*). We conducted time-calibrated phylogenetic analyses locally using the ncov augur/auspice pipeline (https://docs.nextstrain.org/projects/ncov/en/latest/index.html) with a custom subsample from the Puerto Rico dataset in GISAID and a custom subsample of contextual genomes derived from the GISAID NextRegion-North America dataset representative of the Americas, with an emphasis on the United States and the Caribbean region (Appendix). Our analysis demonstrates that the rapid emergence and expansion of the Omicron BA.1 sublineage during the decline of Delta is concordant with the epidemiologic trends reported during the same period (Figure; Appendix). Most genomes from Puerto Rico are closely related to genomes sampled in the United States, suggesting frequent virus introductions by infected travelers, as previously observed for other SARS-CoV-2 variants on the island (*1*). Tree topology shows the genomes from Puerto Rico grouping in multiple monophyletic clusters, suggesting that multiple importations propelled the expansion of subvariants. Our analysis also demonstrates the cumulative increase and subsequent expansion of BA.2

while it cocirculated with BA.1.1. We observed 2 distinct clusters of BA.2 genomes in the tree, suggesting 2 waves of BA.2 sublineage expansion. The first wave, detected in late March 2022, consisted of a variety of BA.2 sublineages, whereas the second wave in mid-May 2022 was caused by sublineage BA.2.12.1, which replaced all other sublineages (Figure).

Our findings show that Omicron BA.1 seems to have emerged in a scenario favorable for rapid expansion, in which rates of transmission for Delta were low and protection from the vaccine or natural infection was waning in the population (*3*,*5*). An effective booster vaccination campaign by late 2021 could possibly have mitigated the BA.1 epidemic wave, although the occurrence of a second wave of BA.2 suggests this sublineage is more resistant to mRNA vaccines (*6*,*7*). The SARS-CoV-2 genomic epidemiology trends observed in Puerto Rico during the period of circulation of the Delta and Omicron variants resemble the trends reported in the United States (*8*). Additional increases in positive cases could be expected upon introduction of the BA.4 and BA.5 sublineages.

Acknowledgments

We thank our partners from the Puerto Rico Department of Health, especially the staff from the Institute of Public Health Laboratories and the Biological and Chemical Emergencies Laboratory for their contribution to the genomic surveillance framework and sample procurement. We acknowledge all healthcare workers and authors submitting data to GISAID.

This project was partially funded by the Centers for Disease Control and Prevention's Advanced Molecular Detection Program and the COVID-19 Laboratory Task Force, the Puerto Rico Science, Technology and Research Trust (V.R.-A.), NIMHD U54MD007579 (VRA), and CDC U01CK000580 (V.R.-A.). Additional funding for this study was provided by the National Institute of General Medical Sciences of the National Institute of Health under award number U54GM133807 (NoA: 5U54GM133807-02 to R.P.. Some of the sequencing work was conducted at the University of Puerto Rico Sequencing and Genomics facility funded by INBRE Grant P20 GM103475 from the National Institute for General Medical Scienced (NIGMS), a component of the National Institutes of Health (NIH), and the Bioinformatics Research Core of the INBRE. The content is solely the responsibility of the authors and does not necessarily represent the official views of the National Institutes of Health. This project was also supported by UPR COVID-19 emergency funds (#2020-2488 to R.P.).

All genome sequences and associated metadata in this dataset are published in GISAID's EpiCoV database, EPI_SET_220930nq. To view the contributors of each individual sequence with details such as accession number, virus name, collection date, originating lab and submitting lab, and the list of authors, please visit https://epicov.org/epi3/epi_set/220930nq for contextual genomes and list of genomes generated by this study.

About the Author

Dr. Santiago is a lead research microbiologist at the Centers for Disease Control and Prevention, National Centers for Emerging and Zoonotic Infectious Diseases, Division of Vector Borne Diseases, Dengue Branch, San Juan, Puerto Rico. His research is focused on the development of molecular diagnostic tests and genomic epidemiology of dengue virus, Zika virus, and SARS-CoV-2.

References

1. Santiago GA, Flores B, González GL, Charriez KN, Huertas LC, Volkman HR, et al. Genomic surveillance of SARS-CoV-2 in Puerto Rico enabled early detection and tracking of variants. Commun Med (Lond). 2022;2:100. https://doi.org/10.1038/s43856-022-00168-7
2. Centers for Disease Control and Prevention. COVID-19 vaccinations in the United States, county. 2022 [cited 2022 Aug 31]. https://data.cdc.gov/Vaccinations/COVID-19-Vaccinations-in-the-United-States-County/8xkx-amqh/data
3. Cuadros DF, Moreno CM, Musuka G, Miller FD, Coule P, MacKinnon NJ. Association between vaccination coverage disparity and the dynamics of the COVID-19 Delta and Omicron waves in the US. Front Med (Lausanne). 2022;9:898101. https://doi.org/10.3389/fmed.2022.898101
4. Gram MA, Emborg HD, Schelde AB, Friis NU, Nielsen KF, Moustsen-Helms IR, et al. Vaccine effectiveness against SARS-CoV-2 infection or COVID-19 hospitalization with the Alpha, Delta, or Omicron SARS-CoV-2 variant: a nationwide Danish cohort study. PLoS Med. 2022;19:e1003992. https://doi.org/10.1371/journal.pmed.1003992
5. Chaguza C, Coppi A, Earnest R, Ferguson D, Kerantzas N, Warner F, et al. Rapid emergence of SARS-CoV-2 Omicron variant is associated with an infection advantage over Delta in vaccinated persons. Med (N Y). 2022;3:325–334.e4. https://doi.org/10.1016/j.medj.2022.03.010
6. Yamasoba D, Kimura I, Nasser H, Morioka Y, Nao N, Ito J, et al.; Genotype to Phenotype Japan (G2P-Japan) Consortium. Virological characteristics of the SARS-CoV-2 Omicron BA.2 spike. Cell. 2022;185:2103–2115.e19. https://doi.org/10.1016/j.cell.2022.04.035
7. Garcia-Beltran WF, St Denis KJ, Hoelzemer A, Lam EC, Nitido AD, Sheehan ML, et al. mRNA-based COVID-19 vaccine boosters induce neutralizing immunity against SARS-CoV-2 Omicron variant. Cell. 2022;185:457–466.e4. https://doi.org/10.1016/j.cell.2021.12.033
8. Centers for Disease Control and Prevention. COVID data tracker. 2022 [cited 2021 Nov 16]. https://covid.cdc.gov/covid-data-tracker/#variants-genomic-surveillance

Address for correspondence: Gilberto A. Santiago, Centers for Disease Control and Prevention, 1324 Cañada St, San Juan 00920, Puerto Rico; email: GSantiago@cdc.gov

Experimental Infection of North American Deer Mice with Clade I and II Monkeypox Virus Isolates

Yvon Deschambault, Levi Klassen, Geoff Soule, Kevin Tierney, Kimberly Azaransky, Angela Sloan, David Safronetz.

Author affiliations: Public Health Agency of Canada, Winnipeg, Manitoba, Canada (Y. Deschambault, L. Klassen, G. Soule, K. Tierney, K. Azaransky, A. Sloan, D. Safronetz); Canadian Mennonite University, Winnipeg (L. Klassen); University of Manitoba, Winnipeg (D. Safronetz)

DOI: https://doi.org/10.3201/eid2904.221594

The global spread of monkeypox virus has raised concerns over the establishment of novel enzootic reservoirs in expanded geographic regions. We demonstrate that although deer mice are permissive to experimental infection with clade I and II monkeypox viruses, the infection is short-lived and has limited capability for active transmission.

Monkeypox virus (MPXV; genus *Orthopoxvirus*, *Poxviridae*), which causes mpox disease, is a zoonotic pathogen that is endemic in Central Africa (clade I) and Western Africa (clade II) (*1*). In mid-May 2022, the World Health Organization first reported an increasing number of mpox cases in nonendemic countries, most of which had no established travel links to endemic regions (*2*). By October 2022, the outbreak encompassed >100 countries with reported confirmed mpox cases (*3*).

The global spread of MPXV outside of regions in which this virus was known to be endemic raises concerns over reverse zoonotic events resulting in the establishment of novel wildlife reservoirs. Small mammals, including rodents, have previously been implicated as enzootic reservoirs of MPXV. In North America, studies have shown that prairie dogs are susceptible to MPXV infection and may serve as a potential reservoir, but data on other wild rodents are limited (*4*). *Peromyscus* species rodents have an extensive and geographically diverse host range spanning most regions across North America and are well-established reservoirs for several zoonotic pathogens (*5*).

We evaluated the competency of deer mice (*Peromyscus maniculatus rufinus*) as a potential zoonotic reservoir for MPXV by using representative isolates from both clades. We infected groups of 12 adult (>6 weeks of age) deer mice with 1 of 3 MPXV isolates through intranasal instillation. The isolates included a clade II human isolate from the 2022 outbreak (MPXV/SP2833) (challenge dose 10^6 PFU); a second clade II virus isolated directly from a North American prairie dog (USA-2003) (challenge dose 10^6 PFU); and a historical clade I isolate (MPXV/V79-1-005) (challenge dose 10^4 PFU). For each virus preparation, we administered the maximum challenge dose based on titration on Vero cells. On days 4 and 10 postinfection, we euthanized 3 male and 3 female mice and collected selected solid organs for analysis of viral titers using molecular assays targeting of envelope protein gene (B6R) (*6*) and infectious viral quantification assays. In addition, we collected oral and rectal swab specimens and tested them similarly to assess the potential for shedding.

We conducted animal studies in accordance with the Canadian Council of Animal Care guidelines and following an animal use document approved by an institutional Animal Care and Use Committee, in a Biosafety Level 4 laboratory of the Public Health Agency of Canada. We conducted fully validated molecular assays in accordance with Public Health Agency of Canada special pathogens diagnostic procedures.

Throughout the course of the study, we observed no obvious signs of disease in any of the infected deer mice. We did not record daily weights because of the requirement for anesthetizing animals before any hands-on manipulation. Analysis of tissue samples from mice infected with the 2022 Canada isolate (MPXV/SP2833) revealed limited and sporadic spread of MPXV beyond the sites of inoculation (nasal turbinates and lungs) (Table). By comparison, USA-2003 appeared to disseminate beyond the respiratory tract, resulting in uniform detection of MPXV DNA in liver and spleen specimens collected at 4 days postinfection (dpi). The clade I virus (MPXV/V79-1-005) yielded results more similar to those for USA-2003; nasal turbinate, lung, liver and spleen samples were positive at 4 dpi. By day 10 dpi, organ specimens from most mice across the 3 infection groups were trending toward clearance (Table). Infectious titers conducted on lung and nasal turbinate specimens collected at both timepoints from the 3 challenge groups corroborated these findings and demonstrated decreasing viral titers between the 2 timepoints (Figure).

Of note, the clade I virus did not achieve high titers in either organ, even when analyzed at 4 dpi. Although this finding may suggest the MPXV/V79-1-005 isolate does not replicate as efficiently in deer mice, the apparent low viral titers observed may be

Table. Summary of PCR results of selected organs collected from deer mice experimentally infected with 3 different MPXV isolates*

		MPXV/SP2833		USA-2003		MPXV/V79-1-005	
Tissue	Sex	4 dpi	10 dpi	4 dpi	10 dpi	4 dpi	10 dpi
Nasal turbinate	M	3/3 (100)	1/3 (33)	3/3 (100)	3/3 (100)	2/3 (67)	2/3 (67)
	F	3/3 (100)	3/3 (100)	3/3 (100)	2/3 (67)	3/3 (100)	2/3 (67)
	Total	6/6 (100)	4/6 (67)	6/6 (100)	5/6 (83)	5/6 (83)	4/6 (67)
Lung	M	3/3 (100)	0/3 (0)	3/3 (100)	3/3 (100)	3/3 (100)	2/3 (67)
	F	3/3 (100)	1/3 (33)	3/3 (100)	1/3 (33)	3/3 (100)	2/3 (67)
	Total	6/6 (100)	1/6 (17)	6/6 (100)	4/6 (67)	6/6 (100)	4/6 (67)
Heart	M	1/3 (33)	0/3 (0)	2/3 (67)	0/3 (0)	1/3 (33)	0/3 (0)
	F	0/3 (0)	0/3 (0)	0/3 (0)	0/3 (0)	0/3 (0)	0/3 (0)
	Total	1/6 (17)	0/6 (0)	2/6 (33)	0/6 (0)	1/6 (17)	0/6 (0)
Liver	M	0/3 (0)	0/3 (0)	3/3 (100)	0/3 (0)	2/3 (67)	0/3 (0)
	F	0/3 (0)	0/3 (0)	3/3 (100)	2/3 (67)	3/3 (100)	0/3 (0)
	Total	0/6 (0)	0/6 (0)	6/6 (100)	2/6 (33)	5/6 (83)	0/6 (0)
Spleen	M	1/3 (33)	0/3 (0)	3/3 (100)	1/3 (33)	2/3 (67)	0/3 (0)
	F	0/3 (0)	0/3 (0)	3/3 (100)	1/3 (33)	3/3 (100)	0/3 (0)
	Total	1/6 (17)	0/6 (0)	6/6 (100)	2/6 (33)	5/6 (83)	0/6 (0)
Small intestine	M	1/3 (33)	0/3 (0)	1/3 (33)	0/3 (0)	0/3 (0)	0/3 (0)
	F	0/3 (0)	0/3 (0)	2/3 (67)	0/3 (0)	0/3 (0)	0/3 (0)
	Total	1/6 (17)	0/6 (0)	3/6 (50)	0/6 (0)	0/6 (0)	0/6 (0)
Oral swab	M	3/3 (100)	1/3 (33)	3/3 (100)	1/3 (33)	1/3 (33)	0/3 (0)
	F	2/3 (67)	1/3 (33)	3/3 (100)	2/3 (67)	1/3 (33)	0/3 (0)
	Total	5/6 (83)	2/6 (33)	6/6 (100)	3/6 (50)	2/6 (33)	0/6 (0)
Rectal swab	M	3/3 (100)	1/3 (33)	3/3 (100)	2/3 (67)	0/3 (0)	1/3 (33)
	F	2/3 (67)	1/3 (33)	1/3 (33)	2/3 (67)	0/3 (0)	0/3 (0)
	Total	5/6 (83)	2/6 (33)	4/6 (67)	4/6 (67)	0/6 (0)	1/6 (17)

*Values are no. (%). dpi, days postinfection; MPXV, monkeypox virus.

attributable to the lower inoculum dose. A similar challenge dose of this strain resulted in lethal infection in CAST/EiJ mice (*7*). Further, subsequent cell culture propagations of MPXV/V79-1-005 resulted in similar titers as the clade II isolates used previously, suggesting that all 3 replicate to a similar extent on Vero cells. Nevertheless, follow-up studies with other clade I viruses are warranted.

We collected oral and rectal swab specimens to assess shedding and the potential for transmission of

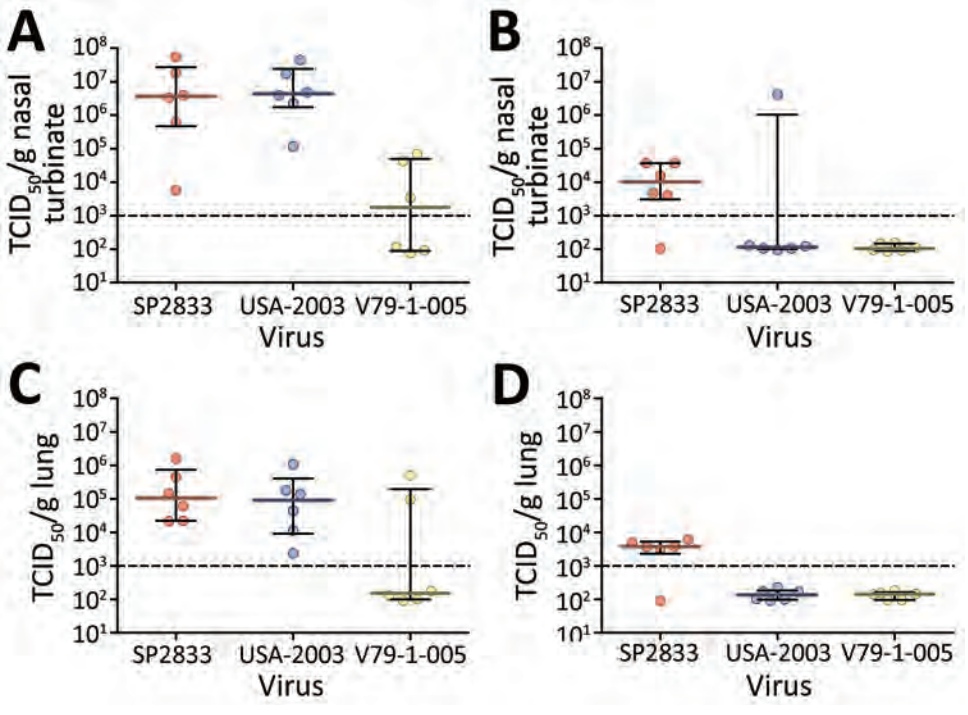

Figure. Monkeypox virus infectious titers from lung and nasal turbinate samples from experimentally infected deer mice. Groups of 12 deer mice (6 male, 6 female) were experimentally infected with monkeypox virus isolates SP2833, USA-2003 (both clade II), or V79-1-005 (clade II) through the intranasal route. Lung and nasal turbinates were collected from 3 male and 3 female rodents at days 4 and 10 postinfection and infectious titers assessed using standard tissue culture methods. Shown are the infectious titers for individual specimens (dots) or median values (solid lines) and interquartile ranges (error bars) for nasal turbinate specimens collected at day 4 (A) and day 10 (B) postinfection and lung specimens collected at day 4 (C) and day 10 (D) postinfection. Dotted line represents the lower limit of detection of the assay. $TCID_{50}$, median tissue culture infectious dose.

MPXV from infected deer mice. Overall, shedding, as suggested by the presence of MPXV DNA in swab extracts, was readily detectable in deer mice inoculated with either clade II virus at day 4, but we noted decreasing levels of positivity by day 10. Shedding of MPXV/V79-1-005 (clade 1) was far less than that of either of the clade II viruses we evaluated (Table).

Our study suggests that these rodents may support a short-term but abortive infection with at least clade II MPXV isolates, although with limited capacity to spread. Given the short duration of infection, these animals probably do not represent a viable enzootic reservoir for MPXV. Further studies should be conducted on other rodents in North America and Europe to assess their competency as vectors or reservoirs of MPXV. Particular interest should be given to *Rattus* species rodents that may frequently come into contact with medical waste containing viable MPXV.

This work was funded by the Public Health Agency of Canada. We obtained the MPXV USA-2003 reagent NR-2500 through the BEI Resources Repository, National Institute of Allergy and Infectious Diseases, National Institutes of Health.

All authors declare no conflict of interest.

About the Author

Mr. Deschambault is a senior laboratory technician in the Special Pathogens Program of the Public Health Agency of Canada. His research interests include disease modeling and vaccine development for emerging and high-consequence viral pathogens.

References

1. Likos AM, Sammons SA, Olson VA, Frace AM, Li Y, Olsen-Rasmussen M, et al. A tale of two clades: monkeypox viruses. J Gen Virol. 2005;86:2661–72. https://doi.org/10.1099/vir.0.81215-0
2. Velavan TP, Meyer CG. Monkeypox 2022 outbreak: an update. Trop Med Int Health. 2022;27:604–5. https://doi.org/10.1111/tmi.13785
3. Centers for Disease Control and Prevention. 2022 monkeypox outbreak global map [cited 2022 Oct 18]. https://www.cdc.gov/poxvirus/monkeypox/response/2022/world-map.html
4. Parker S, Buller RM. A review of experimental and natural infections of animals with monkeypox virus between 1958 and 2012. Future Virol. 2013;8:129–57. https://doi.org/10.2217/fvl.12.130
5. Barbour AG. Infection resistance and tolerance in *Peromyscus* spp., natural reservoirs of microbes that are virulent for humans. Semin Cell Dev Biol. 2017;61:115–22. https://doi.org/10.1016/j.semcdb.2016.07.002
6. Li Y, Olson VA, Laue T, Laker MT, Damon IK. Detection of monkeypox virus with real-time PCR assays. J Clin Virol. 2006;36:194–203. https://doi.org/10.1016/j.jcv.2006.03.012
7. Warner BM, Klassen L, Sloan A, Deschambault Y, Soule G, Banadyga L, et al. In vitro and in vivo efficacy of tecovirimat against a recently emerged 2022 monkeypox virus isolate. Sci Transl Med. 2022;14:eade7646. https://doi.org/10.1126/scitranslmed.ade7646

Address for correspondence: David Safronetz, Special Pathogens Program, National Microbiology Laboratory Branch, Public Health Agency of Canada, 1015 Arlington St, Winnipeg, MB R3E 3R2, Canada; email: david.safronetz@phac-aspc.gc.ca

Orf Nodule with Erythema Multiforme during a Monkeypox Outbreak, France, 2022

Charlotte Cavalieri, Anne-Sophie Dupond, Audrey Ferrier-Rembert, Olivier Ferraris, Timothée Klopfenstein, Souheil Zayet

Author affiliations: Nord Franche-Comté Hospital, Trévenans, France (C. Cavalieri, A.-S. Dupond, T. Klopfenstein, S. Zayet); Institut de Recherche Biomédicale des Armées, Brétigny-sur-Orge, France (A. Ferrier-Rembert, O. Ferraris)

DOI: https://doi.org/10.3201/eid2904.230058

A 26-year-old patient in France who worked as a butcher sought care initially for erythema multiforme. Clinical examination revealed a nodule with a crusty center, which upon investigation appeared to be an orf nodule. Diagnosis was confirmed by PCR. The patient was not isolated and had a favorable outcome after basic wound care.

Orf nodule is a rare viral zoonosis attributable to an infection caused by a parapoxvirus (*1*). It is transmitted to humans by contact with sheep or goats that are affected by contagious ecthyma. The term orf is used to designate contagious ovine pustular dermatitis. In infected sheep and goats, infection most often results in perioral and perinasal ulcerations but occasionally also in a generalized pustular rash.

The most at risk for exposure are persons working in the meat sector, such as farmers or butchers (*1*). Farmers and those who maintain animal herds are often familiar with the condition and do not seek

medical attention. Clinical visits for orf may therefore be more common among nonfarmers. Incidence often peaks at the time of religious festivals, when sheep are traditionally sacrificed, and the incubation time is approximately 1 week (*2*). The diagnosis is basically clinical and can be confirmed with PCR (*3*). Orf nodules may resemble mpox lesions, but unlike mpox, orf is not transmitted from human to human. Routine precautions in clinical settings are sufficient, and patients are not recommended to isolate.

In August 2022, a 26-year-old man with no notable medical history visited an emergency department for disseminated skin lesions predominantly in acral areas. The patient lives with his wife and children in Franche-Comté, France, and works as a butcher. He denied extraconjugal sex, including sex with men, and using illicit drugs, and he had not traveled recently. Neither fever nor contagion was reported. His attending physician prescribed local antibiotics (fucidin acid) and oral antibiotic drugs (amoxicillin/clavulanate), with no effect.

Clinical examination revealed symmetric maculopapular lesions predominantly on the palms and foot, with purplish center and pinkish halo (target shaped lesions), typical of erythema multiforme (Figure, panel A, B). Results of respiratory and neurologic examinations were unremarkable. A nodule with a necrotic pustule center was surrounded by a grayish-white edematous crown on the left index finger, suggesting a lesion of orf nodule more than a monkeypox infection (Figure, panel C). This lesion appeared 72 hours before the disseminated cocoon lesions, according to the patient.

Laboratory findings showed white cell count of 9.2 G/L (reference range 4–10 G/L) but lymphopenia of 880/mm^3 (reference range 1,500–4,000/mm^3). C-reactive protein was moderately high at 10 mg/L (reference range <5 mg/L); liver function was normal. Results of PCR for herpes simplex viruses 1 and 2 on skin biopsy were negative, as were serologic tests for *Mycoplasma pneumoniae*, HIV, and hepatitis B and C viruses. Because of the ongoing mpox outbreak, PCR for monkeypox virus was, performed after simple swabbing on the pustule, but results were negative.

Parapoxvirus PCR was performed by swab of nodule (on the left index finger) (Figure, panel C). The sample was sent to the National Reference Center for Orthopoxvirus Expert Laboratory (*3*). The laboratory used 2 real-time PCRs to confirm the diagnosis of orf nodule. The first assay detected parapoxvirus on the basis of the B2L and J6R genes; the second assay detected orf virus on the basis of the V22R and J6R genes. The patient was discharged with basic wound care, discontinuation of antibiotics, and a follow-up appointment 1 week later. At follow-up, erythema multiforme had disappeared and the nodule clinical regressed.

In typical forms, orf nodule is a skin lesion, unique to the area of inoculation, in particular the right fingers and forearm. A macular lesion appears and rapidly becomes papulovesicular, then nodular, surrounded by an inflammatory halo. Other forms include botriomycoid, angiomatous, or keratoacanthoma-like. The lesion generally heals without complication with antiseptic treatment in 4–6 weeks but in rare cases, erythema multiforme develops (*2*,*4*,*5*).

How orf virus induces erythema multiforme is not clearly understood. Other viral infections like herpes simplex viruses can also trigger hypersensitivity reaction because of release of T cells triggered by ether viral mimicry of host proteins or release of viral proteins from cells containing viral DNA fragments (*1*).

In this case, the patient experienced inaugural erythema multiforme and secondarily a suspected lesion of orf nodule in a period when monkeypox virus infection was endemic (i.e., >4,000 orthopoxvirus infections have been reported in France since May 2022) (*6*). Lesions of monkeypox and orf can be similar, but the manifestations are sufficiently distinctive (*7*,*8*). In this

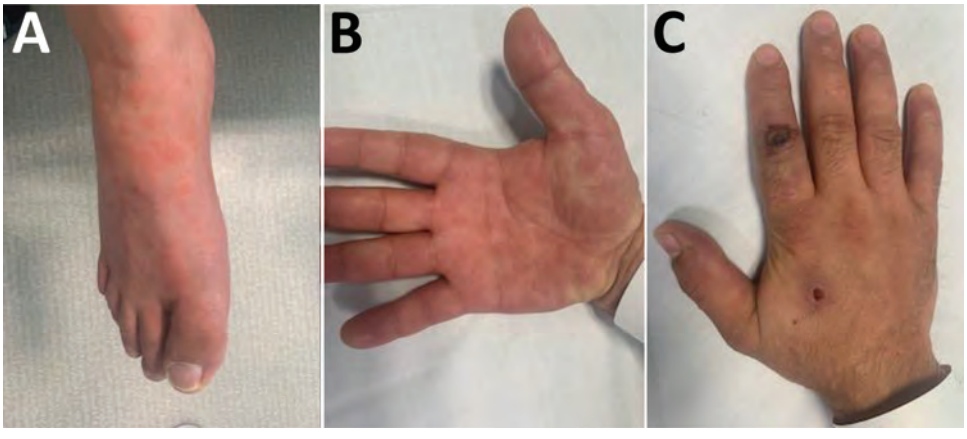

Figure. Orf virus infection in a 26-year-old man after contact with slaughtered sheep and goats, France, 2022. A, B) Target lesion characteristic of erythema multiforme predominant on the foot (A) and hand (B). C) Nodule caused with a necrotic pustule center surrounded by a grayish-white edematous crown on the left index finger. Lesion was swabbed and tested by using a parapoxvirus PCR test.

case, orf virus infection was suspected because of the patient's occupational exposure and clinical compatible skin lesions (e.g., single pustular lesion and erythema multiforme aspect on the rest of the body and the absence of systemic symptoms) (*9*); infection was diagnosed with positive parapoxvirus PCR test (*3*). However, an unusual recent case in Portugal involved monkeypox infection after a needle stick injury (*10*). The patient had a solitary pustular lesion of the finger, similar to our patient, but that lesion was painful, and the clinical picture was completed with the appearance of diffuse vesicles and systemic symptoms.

This case highlights the importance of collecting a careful history at the time of patient care, including collection of exposures to possible zoonoses. Those measures are warranted to avoid unnecessary isolation and treatment and to enable appropriate infection control measures.

C.C. and S.Z. were the major contributors in writing the manuscript and performing the literature review. A.S.D. provided the pictures and the legend. A.F.R. and O.F. conducted the microbiologic study. T.K. revised the manuscript. Both lead authors have read and agreed to the published version of the manuscript. The data presented in this case study are available on request from the corresponding author.

This research did not receive any specific grant from funding agencies in the public, commercial, or not-for-profit sectors. The authors declare no conflicts of interest.

About the Author

Dr. Zayet is a specialist in the Infectious Diseases Department of Nord Franche-Comte Hospital, Trevenans, France. His primary research interests focus on hepatitis and tuberculosis, especially in HIV-infected patients and COVID-19 patients.

References

1. Haig DM, McInnes C, Deane D, Reid H, Mercer A. The immune and inflammatory response to orf virus. Comp Immunol Microbiol Infect Dis. 1997;20:197–204. https://doi.org/10.1016/S0147-9571(96)00045-8
2. Ghislain PD, Dinet Y, Delescluse J. Orf in urban surroundings and religious practices: a study over a 3-year period [in French]. Ann Dermatol Venereol. 2001;128:889–92.
3. Delaune D, Iseni F, Ferrier-Rembert A, Peyrefitte CN, Ferraris O. The French Armed Forces Virology Unit: a chronological record of ongoing research on orthopoxvirus. Viruses. 2017;10:3. https://doi.org/10.3390/v10010003
4. Joseph RH, Haddad FA, Matthews AL, Maroufi A, Monroe B, Reynolds M. Erythema multiforme after orf virus infection: a report of two cases and literature review. Epidemiol Infect. 2015;143:385–90. https://doi.org/10.1017/S0950268814000879
5. Maman M, Medhioub Y. A case of Orf disease complicated by erythema multiforme [in French]. Arch Pediatr. 2017;24:1241–3.
6. Santé Publique France. Cas de variole du singe : point de situation au 15 novembre 2022 [cited 2023 Jan 10]. https://www.santepubliquefrance.fr/les-actualites/2022/cas-de-variole-du-singe-point-de-situation-au-15-novembre-2022
7. Peñuelas Leal R, Labrandero Hoyos C, Grau Echevarría A, Martínez Domenech Á, Lorca Sprohnle J, Casanova Esquembre A, et al. Dory flop sign in monkeypox: 2 cases. Sex Transm Dis. 2022;49:858–9. https://doi.org/10.1097/OLQ.0000000000001706
8. Pourriyahi H, Aryanian Z, Afshar ZM, Goodarzi A. A systematic review and clinical atlas on mucocutaneous presentations of monkeypox: with a comprehensive approach to all aspects of the new and previous monkeypox outbreaks. J Med Virol. 2022 Oct 17 [Epub ahead of print].
9. Eisenstadt R, Liszewski WJ, Nguyen CV. Recognizing minimal cutaneous involvement or systemic symptoms in monkeypox. JAMA Dermatol. 2022;158:1457–8. https://doi.org/10.1001/jamadermatol.2022.4652
10. Caldas JP, Valdoleiros SR, Rebelo S, Tavares M. Monkeypox after occupational needlestick injury from pustule. Emerg Infect Dis. 2022;28:2516–9. https://doi.org/10.3201/eid2812.221374

Address for correspondence: Souheil Zayet, Department of Infectious Disease, Nord Franche-Comté Hospital, 100 Route de Moval, 90400 Trevenans, France; email: souhail.zayet@gmail.com or souheil.zayet@hnfc.fr

SARS-CoV-2 Molecular Evolutionary Dynamics in the Greater Accra Region, Ghana

Bright Adu,[1] Joseph H.K. Bonney,[1] Beverly Egyir, Isaac Darko Otchere, Prince Asare, Francis E. Dennis, Evelyn Yayra Bonney, Richard Akuffo, Ivy A. Asante, Evangeline Obodai, Selassie Kumordjie, Joyce Appiah-Kubi, Quaneeta Mohktar, Hilda Opoku Frempong, Franklin Asiedu-Bekoe, Mildred A. Adusei-Poku, James O. Aboagye, Bright Agbodzi, Clara Yeboah, Seyram B. Agbenyo, Peace O. Uche, Keren O. Attiku, Bernice Twenewaa Sekyere, Dennis Laryea, Kwame Buabeng, Helena Lamptey, Anita Ghansah, Dorothy Yeboah-Manu, Abraham K. Anang, William K. Ampofo, George B. Kyei, John K. Odoom

[1]These authors contributed equally to this article.

Author affiliations: Noguchi Memorial Institute for Medical Research, University of Ghana College of Health Sciences, Legon, Ghana (B. Adu, J.H.K. Bonney, B. Egyir, I.D. Otchere, P. Asare, F.E. Dennis, E.Y. Bonney, R. Akuffo, I.A. Asante, E. Obodai, S. Kumordjie, J. Appiah-Kubi, Q. Mohktar, H. Opoku Frempong, J.O. Aboagye, B. Agbodzi, C. Yeboah, S.B. Agbenyo, P.O. Uche, K.O. Attiku, B.Twenewaa Sekyere, D. Laryea, K. Buabeng, H. Lamptey, A. Ghansah, D. Yeboah-Manu, A.K. Anang, W.K. Ampofo, G.B. Kyei, J.K. Odoom); Ghana Health Service, Accra, Ghana (F. Asiedu-Bekoe); University of Ghana Medical School, Accra (M.A. Adusei-Poku); University of Ghana Medical Centre, Legon (G.B. Kyei)

DOI: https://doi.org/10.3201/eid2904.221410

To assess dynamics of SARS-CoV-2 in Greater Accra Region, Ghana, we analyzed SARS-CoV-2 genomic sequences from persons in the community and returning from international travel. The Accra Metropolitan District was a major origin of virus spread to other districts and should be a primary focus for interventions against future infectious disease outbreaks.

The emergence of SARS-CoV-2 variants with superior transmissibility or immune evasion advantages may cause outbreaks and dominate transmission in a population (*1*). Thus, keeping track of the dynamics of variant transmissions in a population is crucial for developing timely and appropriate responses to outbreaks.

In Ghana, whereas the entire population experienced the COVID-19 pandemic, most infections were primarily recorded in the Greater Accra Region (GAR), the most densely populated region in Ghana with the smallest landmass (*2*). The genetic diversity of SARS-CoV-2 infections in Ghana during early (*3*) and recent (*4*) transmissions showed initial transmission driven by multiple lineages of the virus, after which the Alpha, Delta, and Omicron variants dominated. To gain information about the dynamics of SARS-CoV-2 spread within the GAR, the epicenter of the COVID-19 outbreak in Ghana, we performed a detailed analysis of variants.

We analyzed 1,163 SARS-CoV-2 genomic sequences from 834 community samples collected from 14 of the 21 districts in the GAR and 329 from returning international travelers (Table) during March 2020–February 2022. We extracted RNA from oro/nasopharyngeal swab samples of patients by using a QIAamp Viral RNA Mini Kit (QIAGEN, https://www.qiagen.com).

We prepared complementary DNA by using the LunaScript RT Super Mix Kit (New England BioLabs, https://www.neb.com). For amplicon generation, we used either the ARTIC nCoV-2019 version 3 primers (Artic Network, https://artic.network) (batch 1 samples, collected before July 2021) or the Midnight RT PCR Expansion kit (Oxford Nanopore Technologies, https://www.nanoporetech.com) (batch 2 samples, collected after July 2021). We sequenced batch 1 samples on Illumina MiSeq after library preparation with an Illumina DNA prep kit (https://www.illumina.com) and batch 2 samples on GridION after library preparation with SQK-RBK110.96 kit (Oxford Nanopore Technologies).

Table. Distribution of SARS-CoV-2 sequences analyzed by district of Ghana and origin of international travelers

Origin of travelers	Sequences, no. (%)
Ghana, n = 834	
Accra Metropolitan District	421 (50.5)
Ashaiman Municipal	1 (0.1)
Adenta Municipal	41 (4.9)
Ga East	19 (2.3)
Ga Central	8 (1.0)
Ga South	6 (0.7)
Ga West	21 (2.5)
Kpone Katamanso	1 (0.1)
La-Dade Kotopon	21 (2.5)
La-Nkwantanang Madina	9 (1.1)
Ledzokuku Krowor	6 (0.7)
Ningo Prampram	1 (0.1)
Shai Osudoku	12 (1.4)
Tema Municipal	25 (3.0)
Unnamed district*	242 (29.0)
World, n = 329	
Africa	159 (48.3)
Asia	85 (25.8)
Europe	57 (17.3)
North America	28 (8.5)

*Samples from within the Greater Accra Region but with no clear indication of the specific district.

For both batches of samples, we analyzed reads by using the ARTIC version 1.2 field bioinformatics pipeline (https://github.com/artic-network/fieldbioinformatics). We assigned Lineages by using Pangolin version 4.1.3 with pangolin-data version 1.17 (*5*).

For the phylogenetic analysis, we first aligned sequences in MAFFT version 7.490 (*6*). We inferred the maximum-likelihood tree topology of the variable positions with 1,000 bootstraps by using IQ-TREE version 2.0.7 (*7*) with the general time reversible nucleotide substitution model. We populated the maximum-likelihood tree with sampling dates by using TreeTime version 0.8.6 (*8*) and assuming a mean constant nucleotide substitutions per site per year rate of 8.0×10^{-4} (*9*) after excluding outlier sequences. We then rerooted the final dated tree with 936 sequences to the initial wild-type SARS-CoV-2 strain (GenBank accession no. NC_045512.2) and visualized in R version 4.1.2 (https://www.r-project.org) by using ggtree version 3.2.1 and ggtreeExtra version 1.4.2 packages (*10*). For the import–export analysis, we labeled the internal nodes and external

leaves of the dated phylogeny with the location/district of sample origin by using TreeTime. We inferred the number of state changes from one location/district to another and time of event by using a python script developed by Wilkinson Lab (https://github.com/CERI-KRISP/africa-covid19-genomics/tree/main/python_scripts).

Of the 152,896 SARS-CoV-2 infections reported in Ghana by February 28, 2022, the GAR alone contributed 90,267 (59.04%) (Appendix Table 1, https://wwwnc.cdc.gov/EID/article/29/4/22-1410-App1.pdf). Of the 21 districts in the GAR, the Accra Metropolitan District (AMD) consistently contributed ≈50% of reported SARS-CoV-2 infections in the region since the outbreak began in Ghana (https://ghs.gov.gh/covid19/archive.php). This finding mirrors our finding of 50.5% of sequences from the region being from the AMD (Table). Although all analyzed sequences (Appendix Table 2) came from the GAR, representative metadata for some samples were not indicated by all districts. Those districts were grouped as "Unnamed District" and accounted for 29% of the sequences, most of which were the Alpha variant (Appendix Figure 1).

Because different lineages have dominated SARS-CoV-2 transmission in Ghana at different periods, we categorized the data into the main SARS-CoV-2 variants (Alpha, Beta, Delta, Eta, Omicron, and others). From the phylogenetic analysis, the SARS-CoV-2 variants circulating in the districts of the GAR and those from returning international travelers resolved into 5 major clusters corresponding to defined categories (Appendix Figure 2, panel A). Sequences from the returning international travelers colocalized with the GAR samples, suggesting minimal divergence. We found that an estimated 77 SARS-CoV-2 variant introduction events occurred in the AMD, mainly from other parts of Africa and other districts (Appendix Figure 2, panel B). In contrast, there were an estimated 185 SARS-CoV-2 variant exportation events from the AMD, mainly to the other districts of the GAR and to relatively fewer to countries outside Ghana (Appendix Figure 2, panels C, D). Of those variant exportation events, 153 were to other districts in the GAR, making the AMD a prime district for targeted interventions aimed at reducing the spread of SARS-CoV-2 and other infectious pathogens.

In conclusion, SARS-CoV-2 genomic surveillance in the GAR of Ghana revealed the pattern of spread of variants among districts of the region, demonstrating the role of the AMD in the spread of SARS-CoV-2 in the GAR. We propose that the AMD should be a primary focus in public health interventions aimed at controlling SARS-CoV-2 and other future infectious disease outbreaks in the GAR.

Acknowledgments

We thank all the study participants; clinicians; and field, laboratory, and data teams from the Noguchi Memorial Institute for Medical Research of the University of Ghana and the Ghana Health Service.

Funding was received from the African Society for Laboratory Medicine subaward INV018978 through Africa CDC Africa Pathogen Genomics Initiative and the Department of Health and Social Care and managed by the Fleming Fund and performed under the auspices of the SEQAFRICA project. The Fleming Fund is a £265 million UK aid program supporting up to 24 low- and middle-income countries, which generates, shares, and uses data on antimicrobial resistance and works in partnership with Mott MacDonald, the management agent for the Country and Regional Grants and Fellowship Programme.

Contributions were conceptualization by B. Adu, J.H.K.B., B.E., W.K.A., J.K.O; methodology by B. Adu, F.E.D., E.Y.B., R.A., I.A.A., E.O., S.K., J.A.K., Q.M., H.O.F., B. Agbodzi, M.A.P., J.O.A., C.Y., S.B.A., P.O.U., K.O.A., B.T.S., K.B., H.L., F.A.B., D.L., D.Y.M., A.K.A., G.B.K.; investigation: by B. Adu, J.H.K.B, B.E., I.D.O., F.E.D., R.A., P.A., F.A.B., D.L., A.G., W.K.A., J.K.O.; visualization by B. Adu, I.D.O., P.A.; funding by B. Adu, B.E., A.G., D.Y.M., A.K.A.; writing original draft by B. Adu, I.D.O., P.A.; and editing by all authors. All authors agreed on the final version.

About the Author

Dr. Adu is a senior research fellow at the Noguchi Memorial Institute for Medical Research of the University of Ghana and the coordinator for the Next Generation Sequencing Core Facility of the Institute. His research interests include pathogen genomics and immunology.

References

1. Johns Hopkins University, Coronavirus Resources Centre. Cumulative cases by days since 50th confirmed case [cited 2021 May 8]. https://coronavirus.jhu.edu/data/cumulative-cases
2. Ghana Health Service. COVID-19: regional distribution of active cases [cited 2022 Mar 15]. https://www.ghs.gov.gh/covid19/dashboardm.php
3. Ngoi JM, Quashie PK, Morang'a CM, Bonney JH, Amuzu DS, Kumordjie S, et al. Genomic analysis of SARS-CoV-2 reveals local viral evolution in Ghana. Exp Biol Med (Maywood). 2021;246:960–70. https://doi.org/10.1177/1535370220975351
4. Morang'a CM, Ngoi JM, Gyamfi J, Amuzu DSY, Nuertey BD, Soglo PM, et al. Genetic diversity of SARS-CoV-2 infections in Ghana from 2020–2021. Nat Commun. 2022;13:2494. https://doi.org/10.1038/s41467-022-30219-5
5. Rambaut A, Holmes EC, O'Toole Á, Hill V, McCrone JT, Ruis C, et al. A dynamic nomenclature proposal for SARS-CoV-2 lineages to assist genomic epidemiology. Nat Microbiol. 2020;5:1403–7. https://doi.org/10.1038/s41564-020-0770-5

6. Katoh K, Standley DM. MAFFT multiple sequence alignment software version 7: improvements in performance and usability. Mol Biol Evol. 2013;30:772–80. https://doi.org/10.1093/molbev/mst010
7. Minh BQ, Schmidt HA, Chernomor O, Schrempf D, Woodhams MD, von Haeseler A, et al. IQ-TREE 2: new models and efficient methods for phylogenetic inference in the genomic era. Mol Biol Evol. 2020;37:1530–4. https://doi.org/10.1093/molbev/msaa015
8. Sagulenko P, Puller V, Neher RA. TreeTime: maximum-likelihood phylodynamic analysis. Virus Evol. 2018;4:vex042. https://doi.org/10.1093/ve/vex042
9. Giovanetti M, Slavov SN, Fonseca V, Wilkinson E, Tegally H, Patane JSL, et al. Genomic epidemiology of the SARS-CoV-2 epidemic in Brazil. Nat Microbiol. 2022;7:1490–1500.
10. Xu S, Dai Z, Guo P, Fu X, Liu S, Zhou L, et al. ggtreeExtra: compact visualization of richly annotated phylogenetic data. Mol Biol Evol. 2021;38:4039–42. https://doi.org/10.1093/molbev/msab166

Address for correspondence: Bright Adu, Department of Immunology, Noguchi Memorial Institute for Medical Research, College of Health Sciences, University of Ghana, PO Box LG 581, Legon, Ghana; email: badu@noguchi.ug.edu.gh

Genomic Characterization of Respiratory Syncytial Virus during 2022–23 Outbreak, Washington, USA

Stephanie Goya, Jaydee Sereewit, Daniel Pfalmer, Tien V. Nguyen, Shah A.K. Mohamed Bakhash, Elizabeth B. Sobolik, Alexander L. Greninger

Author affiliations: University of Washington, Seattle, Washington, USA (S. Goya, J. Sereewit, D. Pfalmer, T.V. Nguyen, S.A.K. Mohamed Bakhash, E.B. Sobolik, A.L. Greninger); Fred Hutchinson Cancer Research Center, Seattle (A.L. Greninger)

DOI: https://doi.org/10.3201/eid2904.221834

We sequenced 54 respiratory syncytial virus (RSV) genomes collected during 2021–22 and 2022–23 outbreaks in Washington, USA, to determine the origin of increased RSV cases. Detected RSV strains have been spreading for >10 years, suggesting a role for diminished population immunity from low RSV exposure during the COVID-19 pandemic.

Annual seasonality of respiratory syncytial virus (RSV) in Washington, USA, has been limited primarily to late autumn and winter (*1*). However, an RSV outbreak was not detected during the 2020–21 season because of the COVID-19 pandemic. After lockdowns were relaxed in the summer of 2021, an early RSV season began in August (Figure, panel A). The 2022–23 outbreak also began earlier, but the number of RSV cases was unexpectedly higher than in 2021, alarming public health authorities and the general community (*2*).

Increased severity of the 2022–23 RSV outbreak might have been caused by diminished protective immunity in the population from prolonged low exposure to this virus (*3*). Furthermore, selective pressure because of low transmission in 2020 might have caused emergence of new viral strains with improved fitness. We evaluated whether RSV causing the 2022–23 outbreak had genomic characteristics different from strains from previous seasons.

We performed hybridization capture-based, metagenomic next-generation sequencing of 54 RSV genomes (14 RSV strains from 2021–22 and 40 from 2022–23) isolated during outbreaks in King County, Washington. In brief, we extracted virus RNA from excess nasal or nasopharyngeal swab specimens collected from persons seeking care at University of Washington Medicine COVID-19 collection sites, clinics, emergency rooms, and inpatient facilities who tested positive for RSV by PCR with a cycle threshold <30 (Table) (*4*). All persons were outpatients except for 2 hospitalized patients from 2021. For phylogenetic analyses, we downloaded complete genomes of RSV-A and RSV-B subtypes from GenBank and GISAID (https://www.gisaid.org) databases. We performed genome alignments by using MAFFT software (https://mafft.cbrc.jp/alignment/software) and constructed phylogenetic trees by using IQ-TREE (*5*) (Appendix, https://wwwnc.cdc.gov/EID/article/29/4/22-1834-App1.pdf).

Among sequenced specimens, we detected 1 RSV-A and 13 RSV-B subtypes from 2021–22 and 30 RSV-A and 10 RSV-B subtypes from 2022–23 (Table). We did not detect co-infections with other respiratory viruses (Appendix) or differences in subtype predominance by patient age group or sex during the 2022–23 outbreak ($p>0.1$ by Fisher exact test). We genotyped the RSV *G* gene and found that 7 RSV-A sequences were GA2.3.5 and 24 were GA2.3.6b genotypes (both comprising ON1 strains), and all RSV-B sequences were the GB5.0.5.a genotype (BA strains) (*6*) (Appendix). We found that Washington RSV (WA-RSV) sequences were closely related to contemporary viruses by

using complete genome phylogenetic analysis with all historical and recent RSV sequences in public databases up to December 2022 (Appendix). We then constructed reduced phylogenetic trees with RSV genomes from public databases collected during 2017–2022 (Figure, panels B, C; Appendix Figures 1, 2); the trees showed the WA-RSV sequences from 2021–22 and 2022–23 outbreaks were closely related to those genomes. However, WA-RSV sequences from 2018 and 2019 were not phylogenetically close to database-derived RSV genomes collected during 2017–2022. Some WA-RSVs from 2022 were individually associated with viruses from France, Spain, Argentina, Brazil, Netherlands, Israel, Australia, and northern Macedonia, isolated in 2019, 2021, or early 2022, suggesting multiple viral introductions within Washington. Nevertheless, most WA-RSVs were within statistically supported monophyletic clades (Figure, panels B, C; Appendix Figures 1, 2), indicating the 2022–23 outbreak in King County has been mainly caused by the same RSV-A and RSV-B lineages observed globally for ≈1 decade. We observed no phylogenetic relationship between clade and patient age.

Analysis of all viral genes from 2022–23 WA-RSVs showed no specific nonsynonymous changes compared with other RSV strains collected globally since 2017. Furthermore, WA-RSVs contained amino acid changes previously identified in sequences isolated before the COVID-19 pandemic. For example, the amino acid constellation A103T and T122A in the RSV-A fusion protein was also detected in 14 other RSV genomes, including a 2019 sequence from the

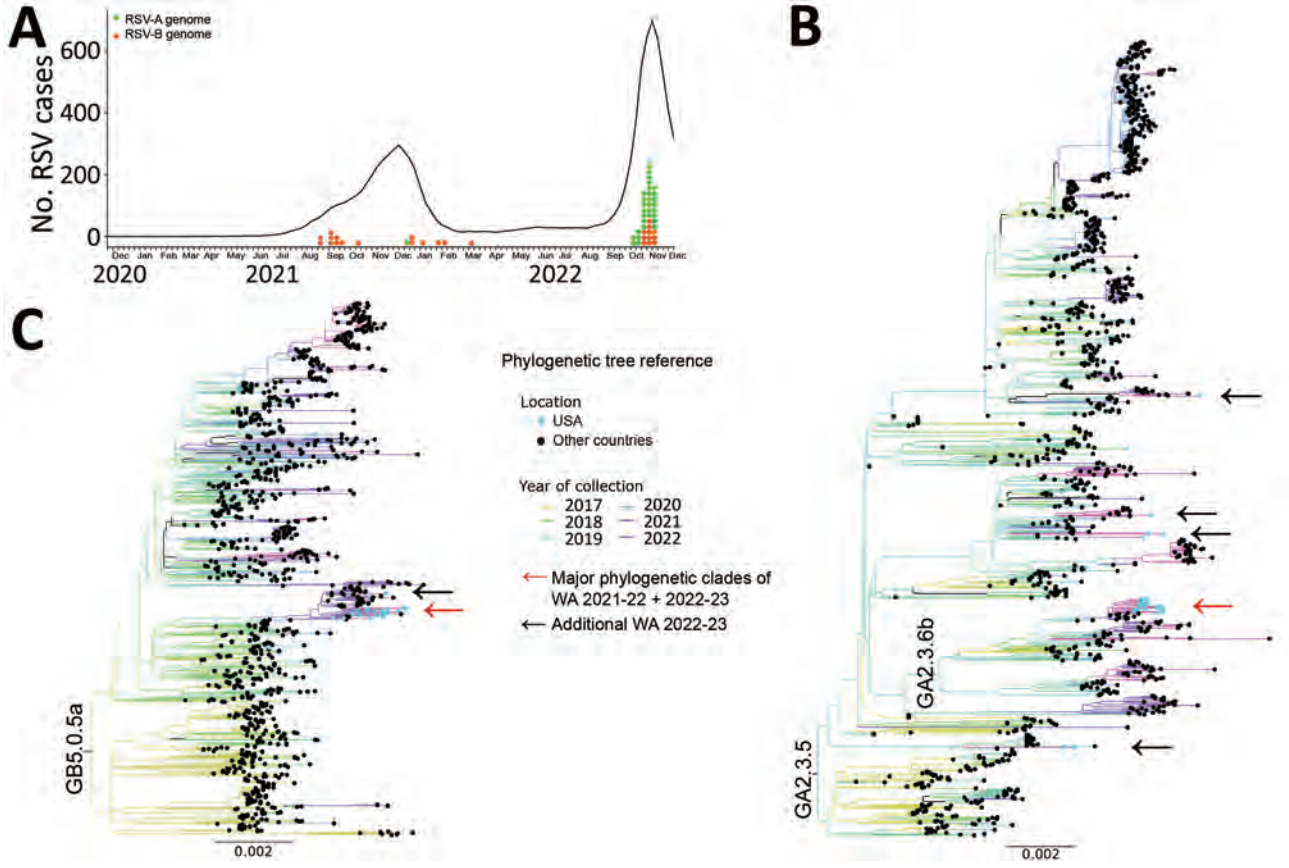

Figure. Molecular epidemiology and genomic characterization of RSV during 2021–22 and 2022–23 outbreaks, Washington, USA. A) Number of patients positive for RSV-A and RSV-B during 2021–22 and 2022–23 outbreaks. Graph shows 5-week averages of RSV-positive cases in Washington detected by PCR; data were taken from The National Respiratory and Enteric Virus Surveillance System (https://www.cdc.gov/surveillance/nrevss/index.html) through December 7, 2022. Tick marks indicate weeks for each month beginning on November 28, 2020, and ending on December 3, 2022. Orange and green dots show collection dates for RSV genomes analyzed in this study. B, C) Maximum-likelihood phylogenetic trees of complete genomes of RSV-A (B) and RSV-B (C) collected during 2017–2022. Collection years for specimens are depicted by tree branch color. RSV genomes from the United States are highlighted with light blue circles at branch tips. Red arrow indicates the location of the major phylogenetic clade comprising most of the sequences from Washington during 2021–22 and 2022–23; black arrows indicate locations of other sequences from Washington during 2022–23. Scale bar indicates nucleotide substitutions per site. Complete phylogenetic trees are provided in the Appendix (https://wwwnc.cdc.gov/EID/article/29/4/22-1834-App1.pdf). RSV, respiratory syncytial virus; RSV-A, RSV subtype A; RSV-B, RSV subtype B.

Table. Number of sequenced respiratory syncytial virus genomes according to different patient characteristics during 2021–22 and 2022–23 virus outbreaks in Washington, USA*

Characteristics	2021–22 outbreak			2022–23 outbreak		
	RSV-A	RSV-B	Total	RSV-A	RSV-B	Total
No. complete genomes	1	13	14	30	10	40
Patient sex						
M	0	6	6	13	7	20
F	1	7	8	16	4	20
Clinical status						
Inpatient	1	1	2	0	0	0
Outpatient	0	12	12	30	10	40
Patient age, y						
<3	0	5	5	10	6	16
3–18	0	3	3	10	2	12
19–65	1	4	5	8	1	9
>65	0	2	2	2	1	3

*RSV, respiratory syncytial virus; RSV-A, RSV subtype A; RSV-B, RSV subtype B.

Netherlands (GenBank accession no. MZ515825.1), suggesting a bottleneck effect caused by low transmission during 2020 that reduced virus diversity (*7*). Alternating prevalence of RSV subtypes between outbreaks might also lead to high levels of RSV spread (Table). Further analyses of RSV sequences from Washington and globally are needed to confirm those hypotheses.

The first limitation of our study is that few RSV genomes from Washington were available before the COVID-19 pandemic. Second, we conducted convenience sampling from excess clinical specimens and had limited access to clinical metadata. Nonetheless, Washington is comparatively a well-sampled state for RSV sequences, because only 2 other RSV genomes have been isolated from the rest of the United States since 2017. RSV genomics is also currently limited by a lack of consensus on genotyping classification.

In conclusion, effects of COVID-19 pandemic lockdown measures on the RSV ecosystem have been reported (*8*–*10*). Real-time genomic surveillance of RSV outbreaks in Washington did not reveal specific changes in RSV since the COVID-19 pandemic began that would account for increased viral spread. Our data suggest that RSV reemergence in King County is likely because of diminished protective immunity in the population from low RSV exposure, a consequence of pandemic mitigation measures. With likely future widespread availability of RSV vaccines, continued real-time RSV genomic surveillance will be required to monitor the evolution and emergence of new viral strains.

This study was approved by the University of Washington Institutional Review Board with a consent waiver (protocol no. STUDY00000408).

A.L.G. reports contract testing for Abbott, Cepheid, Novavax, Pfizer, Janssen, and Hologic and research support from Gilead and Merck, outside of the described work.

About the Author

Dr. Goya is a postdoctoral researcher in the Department Laboratory of Medicine and Pathology at the University of Washington Medical Center. Her work focuses on respiratory virus evolution and interactions with the immune system.

References

1. Jackson ML, Scott E, Kuypers J, Nalla AK, Roychoudury P, Chu HY. Epidemiology of respiratory syncytial virus across five influenza seasons among adults and children one year of age and older—Washington state, 2011/2012–2015/2016. J Infect Dis. 2021;223:147–56. https://doi.org/10.1093/infdis/jiaa331
2. Schrier K, Sperring J. The Seattle Times. Declaration of public health emergency is urgently needed for RSV. December 4, 2022 [cited 2022 Dec 7]. https://www.seattletimes.com/opinion/declaration-of-public-health-emergency-is-urgently-needed-for-rsv
3. Hatter L, Eathorne A, Hills T, Bruce P, Beasley R. Respiratory syncytial virus: paying the immunity debt with interest. Lancet Child Adolesc Health. 2021;5:e44–5. https://doi.org/10.1016/S2352-4642(21)00333-3
4. Greninger AL, Waghmare A, Adler A, Qin X, Crowley JL, Englund JA, et al. Rule-out outbreak: 24-hour metagenomic next-generation sequencing for characterizing respiratory virus source for infection prevention. J Pediatric Infect Dis Soc. 2017;6:168–72. https://doi.org/10.1093/jpids/pix019
5. Minh BQ, Schmidt HA, Chernomor O, Schrempf D, Woodhams MD, von Haeseler A, et al. IQ-TREE 2: new models and efficient methods for phylogenetic inference in the genomic era. Mol Biol Evol. 2020;37:1530–4. https://doi.org/10.1093/molbev/msaa015
6. Goya S, Galiano M, Nauwelaers I, Trento A, Openshaw PJ, Mistchenko AS, et al. Toward unified molecular surveillance of RSV: a proposal for genotype definition. Influenza Other Respir Viruses. 2020;14:274–85. https://doi.org/10.1111/irv.12715
7. Sanjuán R, Domingo-Calap P. Genetic diversity and evolution of viral populations. In: Bamford D, Zuckerman M, editors. Encyclopedia of virology. 4th ed. Cambridge: Elsevier Academic Press; 2021. p. 53–61.
8. Dolores A, Stephanie G, Mercedes S NJ, Érica G, Mistchenko AS, Mariana V. RSV reemergence in Argentina since the SARS-CoV-2 pandemic. J Clin Virol. 2022;149:105126. https://doi.org/10.1016/j.jcv.2022.105126

9. Fourgeaud J, Toubiana J, Chappuy H, Delacourt C, Moulin F, Parize P, et al. Impact of public health measures on the post-COVID-19 respiratory syncytial virus epidemics in France. Eur J Clin Microbiol Infect Dis. 2021;40:2389–95. https://doi.org/10.1007/s10096-021-04323-1
10. Foley DA, Yeoh DK, Minney-Smith CA, Martin AC, Mace AO, Sikazwe CT, et al. The interseasonal resurgence of respiratory syncytial virus in Australian children following the reduction of coronavirus disease 2019-related public health measures. Clin Infect Dis. 2021;73:e2829–30. https://doi.org/10.1093/cid/ciaa1906

Address for correspondence: Alexander L. Greninger, Department of Laboratory Medicine and Pathology, University of Washington, 850 Republican St, Seattle, WA 98109, USA; email: agrening@uw.edu

EID journal

Want to stay updated on the latest news in *Emerging Infectious Diseases*? Let us connect you to the world of global health. Discover groundbreaking research studies, pictures, podcasts, and more by following us on Twitter at @CDC_EIDjournal.

Infectious: Pathogens and How We Fight Them

John S. Tregoning, PhD

**Oneworld Publications, New York, New York, 2021
ISBN13: 9780861541225; Pages: 384; Price: US $25.95 (hardcover), $30.62 (audiobook: Dreamscape Media, LLC; Mike Cooper, narrator; 9 h, 35 min)**

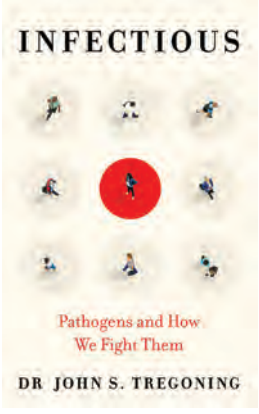

Infectious disease outbreaks can have profound societal ramifications (*1*), as underscored by the ongoing COVID-19 pandemic (*2*). *Infectious: Pathogens and How We Fight Them*, by John S. Tregoning, celebrates the research dedicated to understanding and controlling harmful microbes. An immunologist at Imperial College, London, Tregoning writes an accessible, authoritative primer, covering such topics as microbiology, epidemiology, and therapeutic solutions. He describes advances in techniques for identifying etiologic agents that have influenced scientific approaches to controlling, preventing, and even eliminating pathogens. He acknowledges pioneers such as Linnaeus and Gram and their work in categorizing organisms and differentiating bacteria (*3*). He also sheds light on the subject of pathogen–host interactions and genetic change: "Most mutations lead to nonsense… a minuscule number… [help] pathogens escape from the immune response and adapt to drugs."

The book provides readers a succinct description of innate and adaptive immunity, including how specific immune memory occurs when adaptive cells recognize, for example, a SARS-CoV-2 viral spike protein. Tregoning reviews how antibodies and T and B cells orchestrate immune responses and discusses how lifelong immunity can occur after recovery from certain diseases, such as measles. He shares a moving tribute to Brigitte Askonas for her contributions to our understanding of immune memory, made after she was forced to leave her homeland in 1938 because of her Jewish heritage. Tregoning also emphasizes that science thrives with diversity and inclusion, acknowledging trailblazers such as Alice Ball, an African American, for the first treatment of leprosy, and Tu Youyou, the Chinese Nobel laureate, for her discovery of artemisinin, an antimalarial drug.

Tregoning convincingly explains why accurate diagnosis is crucial to epidemiologic investigations and therapeutic interventions. He provides examples of how causes of mysterious illnesses were determined, including *Chlamydia psittaci*–associated pneumonia among US sailors in 1929 and recent clusters of SARS-CoV-2 infections transmitted by asymptomatic persons. His optimistic assumption that we will continue to prevail against pathogenic microbes is bolstered by descriptions of breakthroughs in research on antimicrobials, smallpox, malaria, and COVID-19. He offers upbeat predictions of future advances, such as elucidation of the host-specific response to infections and using artificial intelligence to detect outbreaks. The author's bright outlook is, nonetheless, tempered by recognition of undesirable consequences of inappropriate use of antimicrobial drugs.

Discussions of the threatening aspects of pathogens are countered by humorous observations and heartfelt vignettes. Tregoning jokingly describes Félix d'Hérelle's "rather striking beard/moustache combo" in one moment and later describes crying uncontrollably after his son's recovery from respiratory syncytial virus. Regarding how Barry Marshall identified the cause of gastric ulcers, he notes: "[He] proved the link by deliberately infecting himself with *Helicobacter pylori*, giving himself an ulcer and a Nobel Prize."

The book's focus on "ologies" and therapeutics does not fully address social drivers of pathogens or grapple with barriers to science-based interventions (*5*). Tregoning also missed an opportunity to emphasize the need for strengthening the global mechanism for outbreak reporting and an enhanced integrated One Health approach to evolving threats (*6*,*7*).

Infectious will appeal to diverse audiences including biomedical trainees and policy makers because it transforms the discussion about harmful microbes into an engaging narrative. The book is an enjoyable and enlightening celebration of humanity's achievements in the unending struggle with pathogens. Delivered with clarity, the book's audio version is rewarding.

Nkuchia M. M'ikanatha

Author affiliation: Pennsylvania Department of Health, Harrisburg, Pennsylvania, USA; Pennsylvania State University College of Agriculture, University Park, Pennsylvania, USA

Acknowledgements

I am grateful to Stephen M. Ostroff and David P. Welliver for providing excellent feedback on drafts of this review.

DOI: https://doi.org/10.3201/eid2904.221820

References

1. Dobson AP, Carper ER. Infectious diseases and human population history: throughout history the establishment of disease has been a side effect of the growth of civilization. BioScience. 1996;46:115–26. https://doi.org/10.2307/1312814
2. WHO Director-General's opening remarks at the media briefing on COVID-19, 11 March 2020 [cited 2022 Dec 20]. https://www.who.int/director-general/speeches/detail/who-director-general-s-opening-remarks-at-the-media-briefing-on-covid-19---11-march-2020
3. Coico R. Gram staining. Curr Protoc Microbiol. 2005;3 (Appendix):3C.
4. O'Garra A. Brigitte Askonas (1923–2013). Nature. 2013;494:37. https://doi.org/10.1038/494037a
5. Janes CR, Corbett KK, Jones JH, Trostle J. Emerging infectious diseases: the role of social sciences. Lancet. 2012;380:1884–6. https://doi.org/10.1016/S0140-6736(12)61725-5
6. Phelan AL, Carlson CJ. A treaty to break the pandemic cycle. Science. 2022;377:475–7. 10.1126/science.abq5917 https://doi.org/10.1126/science.abq5917
7. National Academies of Sciences, Engineering, and Medicine. Systematizing the One Health approach in preparedness and response efforts for infectious disease outbreaks: proceedings of a workshop. Washington: The National Academies Press; 2022. https://doi.org/10.17226/26301

Address for correspondence: Nkuchia M. M'ikanatha, Commonwealth of Pennsylvania Department of Health, Division of Infectious Disease Epidemiology, Health and Welfare Bldg, 7th and Forster St, Rm 933, Harrisburg PA 17120, USA; email: nmikanatha@pa.gov, nmikanatha@gmail.com

etymologia revisited

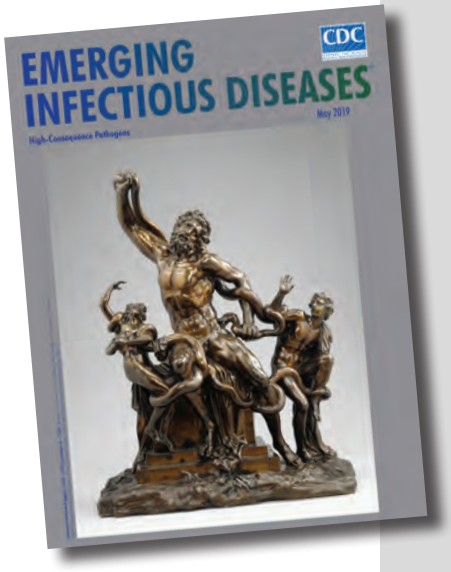

Originally published in May 2019

Nipah Virus

[ne´-pə vī´-rəs]

In 1994, a newly described virus, initially called equine morbillivirus, killed 13 horses and a trainer in Hendra, a suburb of Brisbane, Australia. The reservoir was subsequently identified as flying foxes, bats of the genus *Pteropus* (Greek pteron ["wing"] + *pous* ["foot"]). In 1999, scientists investigated reports of febrile encephalitis and respiratory illness among workers exposed to pigs in Malaysia and Singapore. (The pigs were believed to have consumed partially eaten fruit discarded by bats.)

The causative agent was determined to be closely related to Hendra virus and was later named for the Malaysian village of Kampung Sungai Nipah. The 2 viruses were combined into the genus *Henipavirus*, in the family *Paramyxoviridae*. Three additional species of *Henipavirus*—Cedar virus, Ghanaian bat virus, and Mojiang virus—have since been described, but none is known to cause human disease. Outbreaks of Nipah virus occur almost annually in India and Bangladesh, but *Pteropus* bats can be found throughout the tropics and subtropics, and henipaviruses have been isolated from them in Central and South America, Asia, Oceania, and East Africa.

Sources:

1. Centers for Disease Control and Prevention. Outbreak of Hendra-like virus—Malaysia and Singapore, 1998–1999. MMWR Morb Mortal Wkly Rep. 1999;48:265–9.
2. Selvey LA, Wells RM, McCormack JG, Ansford AJ, Murray K, Rogers RJ, et al. Infection of humans and horses by a newly described morbillivirus. Med J Aust. 1995;162:642–5.

https://wwwnc.cdc.gov/eid/article/25/5/et-2505_article

Attributed to O. Grin (active 1919), *The typhus louse shaking hands with Death*, 1919 (detail). Color lithograph, image and border 42.5 in x 28.8 in/100 × 73.2 cm. Wellcome Collection, London, United Kingdom. Permanent link: https://wellcomecollection.org/works/gx47fn2a

Specter of Epidemic Typhus

Byron Breedlove

Typhus fevers—including scrub typhus, murine typhus, and epidemic typhus—are vectorborne rickettsial diseases spread to humans by chiggers, fleas, and lice, respectively. Epidemic typhus, sometimes called louse-borne typhus, is caused by the bacterium *Rickettsia prowazekii, and* this form of typhus is transmitted to humans by the body louse *Pediculus humanus humanus.*

Though now considered an uncommon disease, epidemic typhus outbreaks resulted in millions of deaths during previous centuries in Europe, Mexico, South America, and Central America. Such outbreaks were prevalent among people living in poverty, displaced and homeless populations, prisoners, and military troops. According to infectious disease researchers Emmanouil Angelakis, Yassina Bechah, and Didier Raoult, "Epidemic typhus has accompanied disasters that impact humanity and has arguably determined the outcome of more wars than have soldiers and generals." Now, new concerns exist about possible outbreaks of epidemic typhus in war-torn areas, such as parts of Ukraine.

In 1909, French physician and microbiologist Charles Nicolle discovered the mode of transmission for epidemic typhus. Myron Schultz and David Morens wrote that Nicolle "was well aware of

Author affiliation: Centers for Disease Control and Prevention, Atlanta, Georgia, USA

DOI: https://doi.org/10.3201/eid2904.AC2904

the clinical presentation of typhus—its triad of fever, rash, and stupor—and of its link to poverty" and that he "reasoned that lice on patients' clothes were most likely the vectors." Medical historian K. David Patterson noted that "the Russian term *platyanaya vosh'*, clothes louse, is more accurate that the English term" body louse because these insects live in the inner folds of clothing, from where they make frequent forays onto their host's skin for blood meals. Although Nicolle did not determine the infectious agent that causes epidemic typhus, his discovery of the vector proved instrumental in helping control its outbreaks.

In 1916, Brazilian physician Henrique da Rocha Lima established that the disease was caused by a bacterium he named *Rickettsia prowazekii*. That name honors the legacy of American pathologist Howard T. Ricketts and Czech bacteriologist Stanislaus Joseph Mathias von Prowazek, Rocha Lima's colleague, both of whom contracted fatal cases of typhus during their research. In 1920, S. Burt Wolbach conducted ensuing research that confirmed that lice were the vectors for *R. prowazekii*.

Patterson wrote, "Typhus was a major health problem in late 19th and 20th century Russia, and great epidemics flared up whenever war or famine produced hardship and massive population movements. Major typhus epidemics took place late in World War I and in the years of civil war following the Bolshevik Revolution. Typhus claimed some 2 to 3 million lives from 1918 to 1922."

Reaching at-risk populations in crowded cities and remote communities with information about diseases, including typhus, was challenging. Visually arresting public health posters directed at both civilian and military populations provided a relatively inexpensive way to reach large numbers of people, many of whom were illiterate. Communications professor David Serlin noted, "Although the war was hardly the cause of the epidemical public health poster, the authoritarian conditions of wartime and the extensive use of posters for recruiting were favorable to it."

This month's cover image shows a Russian public health poster from 1919, the third year of the Russian civil war, and the year Vladimir Lenin declared that "Either the louse will defeat socialism, or socialism will defeat the lice." It is cataloged in the Wellcome Collection with the title *The typhus louse shaking hands with Death*.

Embodied as a leering skeleton, Death sits on a black bench, a well-used scythe slung over its shoulder, an hourglass resting at its feet, and empty eye sockets fixated on a grotesque, engorged, enlarged louse. Death clasps the front leg of the louse as the pair seal a mortal contract, visually communicating the peril posed by louse infestations and typhus infection. Featured prominently along the top of the poster in Cyrillic script (translated here into English) is the exhortation, "The Louse and Death are friends and comrades. Kill all lice that carry infection." No accompanying information sheds details about O. Grin, credited with creating this poster, nor has anything come to light after sleuthing via internet searches for this moniker.

Outbreaks of epidemic typhus still occur in the Andes regions of South America and some parts of Africa. Sporadic cases are reported in the United States when people are exposed to flying squirrels or their nests. However, conflict and disasters raise the specter of reemergence of epidemic typhus, and it is still considered a public health threat. Modern medicine provides diagnostic tools and the antibiotic doxycycline to mitigate *R. prowazekii* infection outbreaks, but early detection remains essential.

Bibliography

1. Alilio P. The louse manifesto. Alpha Omega Alpha Society [cited 2023 Feb 1]. https://www.alphaomegaalpha.org/wp-content/uploads/2021/03/19_Autumn_Alilio.pdf
2. Angelakis E, Bechah Y, Raoult D. The history of epidemic typhus. Microbiol Spectr. 2016;4:4.4.51. https://doi.org/10.1128/microbiolspec.PoH-0010-2015
3. Bechah Y, Capo C, Mege JL, Raoult D. Epidemic typhus. Lancet Infect Dis. 2008;8:417–26. https://doi.org/10.1016/S1473-3099(08)70150-6
4. Bernardes Filho F, Avelleira JC. Henrique da Rocha Lima. An Bras Dermatol. 2015;90:363–6. https://doi.org/10.1590/abd1806-4841.20153945
5. Centers for Disease Control and Prevention. Epidemic typhus [cited 2023 Jan 23]. https://www.cdc.gov/typhus/epidemic/index.html
6. Famous Scientists. The art of genius. Charles Nicolle [cited 2023 Jan 20]. https://www.famousscientists.org/charles-nicolle
7. Newton PN, Fournier PE, Tappe D, Richards AL. Renewed risk for epidemic typhus related to war and massive population displacement, Ukraine. Emerg Infect Dis. 2022;28:2125–6. https://doi.org/10.3201/eid2810.220776
8. Patterson KD. Typhus and its control in Russia, 1870–1940. Med Hist. 1993;37:361–81. https://doi.org/10.1017/S0025727300058725
9. Schultz MG, Morens DM. Photo quiz (Charles-Jules-Henri Nicolle). Emerg Infect Dis. 2009;15:1519–22 .https://doi.org/10.3201/eid1509.090891
10. Serlin D. Imagining illness: public health and visual culture. Minneapolis (MN): University of Minnesota Press; 2010. p. 183–4.

Address for correspondence: Byron Breedlove, EID Journal, Centers for Disease Control and Prevention, 1600 Clifton Rd NE, Mailstop H16-2, Atlanta, GA 30329-4027, USA; email: wbb1@cdc.gov

EMERGING INFECTIOUS DISEASES®

Upcoming Issue

- Recurrent *Clostridioides difficile* Infection, New Haven County, Connecticut, USA, 2015–2020
- Phylogenetic Analysis of Transmission Dynamics of Dengue in Large and Small Population Centers, Northern Ecuador
- Use of High-Resolution Geospatial and Genomic Data to Characterize Recent Tuberculosis Transmission, Botswana
- Environmental, Occupational, and Demographic Risk Factors for Clinical Scrub Typhus, Bhutan
- *Leishmania donovani* Transmission Cycle Associated with Human Infection, *Phlebotomus alexandri* Sand Flies, and Hare Blood Meals, Israel
- Emergence of Erythromycin-Resistant Invasive Group A *Streptococcus*, West Virginia, USA
- Misdiagnosis of *Clostridioides difficile* Infections by Standard-of-Care Specimen Collection and Testing for Hospitalized Adults, Louisville, Kentucky, USA, 2019–2020
- Case-Control Study of Long COVID, Sapporo, Japan
- Poor Prognosis for Puumala Virus Infections Predicted by Lymphopenia and Dyspnea
- Fatal Case of Heartland Virus Disease Acquired in the Mid-Atlantic Region, United States
- Case Report and Literature Review of Occupational Transmission of Monkeypox Virus to Healthcare Workers, South Korea
- Cutaneous Leishmaniasis Caused by *Leishmania infantum*, Israel, 2018–2021
- Novel Circovirus in Blood from Intravenous Drug Users, Yunnan, China
- Characteristics and Treatment of *Gordonia bacteraemias*, France
- Comparative Aerosol and Surface Stability of SARS-CoV-2 Variants of Concern
- No Substantial Histopathologic Changes in *Mops condylurus* Bats Naturally Infected with Bombali Ebolavirus, Kenya
- Spatiotemporal Evolution of SARS-CoV-2 Alpha and Delta Variants during Large Nationwide Outbreak, Vietnam, 2021
- Norovirus GII.3[P25] in Patients and Produce, Chanthaburi, Thailand, 2022
- Panton-Valentine Leukocidin–Positive CC398 MRSA in Urban Clinical Settings, the Netherlands
- New Genotype of *Coxiella burnetii* Causing Epizootic Q Fever Outbreak in Rodents, Northern Senegal
- Cystic Echinococcosis in Northern New Hampshire, United States
- *Burkholderia pseudomallei* Laboratory Exposure, Arizona, USA
- Epizootic Hemorrhagic Disease Virus Serotype 8, Italy, November 2022

Complete list of articles in the April issue at https://wwwnc.cdc.gov/eid/#issue-298

Earning CME Credit

To obtain credit, you should first read the journal article. After reading the article, you should be able to answer the following, related, multiple-choice questions. To complete the questions (with a minimum 75% passing score) and earn continuing medical education (CME) credit, please go to http://www.medscape.org/journal/eid. Credit cannot be obtained for tests completed on paper, although you may use the worksheet below to keep a record of your answers.

You must be a registered user on http://www.medscape.org. If you are not registered on http://www.medscape.org, please click on the "Register" link on the right hand side of the website.

Only one answer is correct for each question. Once you successfully answer all post-test questions, you will be able to view and/or print your certificate. For questions regarding this activity, contact the accredited provider, CME@medscape.net. For technical assistance, contact CME@medscape.net. American Medical Association's Physician's Recognition Award (AMA PRA) credits are accepted in the US as evidence of participation in CME activities. For further information on this award, please go to https://www.ama-assn.org. The AMA has determined that physicians not licensed in the US who participate in this CME activity are eligible for AMA PRA Category 1 Credits™. Through agreements that the AMA has made with agencies in some countries, AMA PRA credit may be acceptable as evidence of participation in CME activities. If you are not licensed in the US, please complete the questions online, print the AMA PRA CME credit certificate, and present it to your national medical association for review.

Article Title

Pediatric Invasive Meningococcal Disease, Auckland, New Zealand (Aotearoa), 2004–2020

CME Questions

1. Which one of the following statements regarding the global epidemiology, outcomes, and prevention of invasive meningococcal disease (IMD) is most accurate?

A. IMD most commonly affects adolescents
B. Nearly two thirds of children have disabling sequelae of IMD
C. Aotearoa New Zealand has the highest prevalence of meningitis B (MenB) disease in the world
D. The 4CMenB vaccine can reduce carriage of Neisseria meningitidis, but not IMD

2. Which one of the following statements regarding the epidemiology of IMD in the current study set in Aotearoa New Zealand is most accurate?

A. There was a steady increase in the incidence of IMD during the study period
B. Most cases presented in fall
C. Incidence rates were highest among Māori and Pacific people and in low-income neighborhoods
D. The median age at pres entation was 2 months

3. Which one of the following statements regarding clinical and laboratory features of IMD in the current study is most accurate?

A. The median duration of illness before presentation was 5 days
B. More than 60% of cases had meningitis
C. 8% of cases were admitted to the ICU
D. One quarter of children underwent surgical procedures

4. Which one of the following statements regarding the outcomes of IMD in the current study is most accurate?

A. The case-fatality rate was 10%
B. More than 90% of deaths occurred in Māori or Pacific children
C. Most deaths occurred in children older than 1 year
D. The rate of recorded follow-up audiometry after IMD was 92%

Earning CME Credit

To obtain credit, you should first read the journal article. After reading the article, you should be able to answer the following, related, multiple-choice questions. To complete the questions (with a minimum 75% passing score) and earn continuing medical education (CME) credit, please go to http://www.medscape.org/journal/eid. Credit cannot be obtained for tests completed on paper, although you may use the worksheet below to keep a record of your answers.

You must be a registered user on http://www.medscape.org. If you are not registered on http://www.medscape.org, please click on the "Register" link on the right hand side of the website.

Only one answer is correct for each question. Once you successfully answer all post-test questions, you will be able to view and/or print your certificate. For questions regarding this activity, contact the accredited provider, CME@medscape.net. For technical assistance, contact CME@medscape.net. American Medical Association's Physician's Recognition Award (AMA PRA) credits are accepted in the US as evidence of participation in CME activities. For further information on this award, please go to https://www.ama-assn.org. The AMA has determined that physicians not licensed in the US who participate in this CME activity are eligible for AMA PRA Category 1 Credits™. Through agreements that the AMA has made with agencies in some countries, AMA PRA credit may be acceptable as evidence of participation in CME activities. If you are not licensed in the US, please complete the questions online, print the AMA PRA CME credit certificate, and present it to your national medical association for review.

Article Title

Nocardia pseudobrasiliensis Co-infection in SARS-CoV-2 Patients

CME Questions

1. Your patient is a 54-year-old woman receiving corticosteroid therapy for rheumatoid arthritis who is admitted for worsening pneumonia despite nirmatrelvir-ritonavir treatment after a positive polymerase chain reaction test for COVID-19. On the basis of a case report of a 52-year-old man with SARS-CoV-2 coinfection with pulmonary *Nocardia pseudobrasiliensis*, hypoxia, and pneumonia, and a literature review (total, 10 patients) by Stamos and colleagues, which one of the following statements about clinical features and predisposing factors for nocardiosis and COVID-19 coinfection is correct?

A. Central nervous system (CNS) nocardiosis was the most common site of infection, occurring in 6 of 10 patients
B. All 10 patients had steroid treatment and other risk factors predisposing them to infection with *Nocardia* spp.
C. Most patients developed nocardiosis between 1 and 5 days after SARS-CoV-2 diagnosis
D. *N. pseudobrasiliensis* was the most frequently isolated species

2. According to the case report of SARS-CoV-2 coinfection with pulmonary N. pseudobrasiliensis and a literature review by Stamos and colleagues, which one of the following statements about course and treatment of nocardiosis and COVID-19 coinfection, based on a case report of SARS-CoV-2 coinfection with pulmonary *N. pseudobrasiliensis*, is correct?

A. Sulfonamide-carbapenem combinations are used as empiric therapy for nocardiosis
B. Nocardia spp. do not differ widely in antibiotic susceptibility
C. The case patient responded well to trimethoprim-sulfamethoxazole (TMP-SMX), as is nearly always the case with *N. pseudobrasiliensis*
D. Despite worsening hypoxia on day 5, the case patient's chest computed tomography scan (CT) was unremarkable

3. On the basis of the case report of SARS-CoV-2 coinfection with pulmonary *N. pseudobrasiliensis* and a literature review by Stamos and colleagues, which one of the following statements about clinical implications of the features, course, treatment and predisposing factors for nocardiosis and COVID-19 coinfection is correct?

A. Overall risk for all-cause coinfection in patients with COVID-19 is moderately high
B. The study proves that SARS-CoV-2 infection is an independent risk factor for nocardiosis
C. Nocardiosis is usually acquired as a nosocomial infection
D. Differential diagnosis for severe pneumonia in immunosuppressed patients should include nocardiosis, even if they have COVID-19

DAVID J. SENCER CDC MUSEUM

History·Legacy·Innovation

Dr. David J. Sencer, Mrs. Mountin and Jim Collins celebrate CDC's 25th anniversary, 1961.

CDC at 75

January 9, 2023–July 28, 2023

TEMPORARY EXHIBITIONS GALLERY

Opening January 9, *CDC at 75* is a commemorative exhibition that tells unique stories about the work of this fabled agency and provides a glimpse into the breadth and depth of CDC's history and vast accomplishments. It features rarely seen objects, documents, and media taken from the CDC Museum's rich collections and archives.

Hours

Monday–Wednesday: 9 a.m.–5 p.m.
Thursday: 9 a.m.–7 p.m.
Friday: 9 a.m.–5 p.m.
Closed weekends and federal holidays

Location

1600 Clifton Road, NE
Atlanta, GA
30329-4021
Phone (404) 639-0830

Admission and parking free • Vehicle inspection required
Government-issued photo ID required for adults over the age of 18
Passport required for non-U.S. citizens